CHEMICAL & PHARMACEUTICAL BULLETIN

Vol. 35, No. 4 April 1987

Regular Articles

[Chem. Pharm. Bull. 35(4)1327—1333(1987)]

Adsorption of Catecholamines on a Gold Electrode Surface Studied by Specular Reflection Measurement

KIYOKO TAKAMURA,* KUNIO ITO and FUMIYO KUSU

Tokyo College of Pharmacy, 1432-1 Horinouchi, Hachioji, Tokyo 192-03, Japan

(Received August 4, 1986)

The adsorption of catecholamines including norepinephrine, epinephrine, isoproterenol, dopamine, dopa and homocatechol on a gold electrode surface was studied in phosphate buffer of pH 6.9 by specular reflection measurement. Norepinephrine is oxidized at potentials more positive than +0.1 V *vs.* saturated calomel electrode (SCE) and adsorbed at the potential range from −0.7 to −0.05 V. Its antagonists, phenoxybenzamine, tolazoline, ergotamine, oxprenolol and propranolol, are also adsorbed on the electrode, more strongly than norepinephrine. The adsorption behavior of catecholamines on the electrode surface may reflect electrostatic interactions between adrenergic transmitter substances and their receptors.

Keywords——catecholamine; adsorption; gold electrode; specular reflectivity; adrenergic receptor; electrode-solution interface

Catecholamines, including norepinephrine, dopamine and epinephrine, are of considerable biological and pharmacological importance owing to their involvement in chemical neurotransmission processes and their usefulness as drugs for treating various clinical disorders such as hypertension, shock, cardiac failure and arrhythmia, asthma, allergy and anaphylaxis.

Norepinephrine is the transmitter of most sympathetic postganglionic fibers and certain tracts in the central nervous system. Dopamine is the predominant transmitter of the mammalian extrapyramidal system and several mesocortical and mesolimbic neuronal pathways.[1] In an adrenergic neurotransmission system, neurotransmitter substances such as norepinephrine and dopamine travel by convective or diffusive mass transport in the synaptic gap and reach receptor sites on the postsynaptic membrane. Interaction between transmitter substances and receptors results in the generation of new electrical signals to cause neurotransmission.

Hirono *et al.*[2] calculated the electrostatic potential at the molecular surface of a dopamine targeting dopamine receptor, using Cartesian coordinates and Mulliken net atomic charges obtained by the semiempirical molecular orbital method. The electrostatic potential image indicated that a small absolute potential region (−2—2 kcal/mol) exists perpendicular to the catechol ring plane, on one side of which there is a positive potential region

(>2 kcal/mol) and on the other side, a nitrogen atom lone pair (<−2 kcal/mol). The electrostatic potential of most of the molecular surface was within ±6 kcal/mol. Thus, the dopamine molecule may be capable of interacting electrostatically with surfaces charged within ±0.3 eV. In our preliminary experiment on the adsorption of catecholamines, the electrosorption of dopamine seemed to occur in the potential region within about ±300 mV *vs.* point of zero charge (pzc), which is in fair agreement with the above charge. This implies that the adsorption behavior of transmitters on an electrode surface may reflect the electrostatic interactions between transmitters and the receptor surface.

Therefore, we carried out a study on the adsorption of adrenergic transmitters and related substances onto a gold electrode surface as a model of a certain type of interactions between transmitter substances and receptors. Since an electrode surface may be regarded as a very simplified biosurface charged negatively or positively and in contact with an electrolyte solution, an understanding of the surface behavior of these substances should help to elucidate the electrostatic interactions involved in their neurochemical behavior at receptor sites. Specular reflection was used to detect trace amounts of adsorbed species on electrode surfaces with high sensitivity.

Experimental

Reagents——L-Epinephrine, DL-isoproterenol hydrochloride, ergotamine tartrate, oxprenolol hydrochloride and tolazoline hydrochloride were obtained from Sigma Chemical Company. L-Norepinephrine and phenoxybenzamine hydrochloride were from Tokyo Kasei Industries Ltd. and dopamine hydrochloride from Wako Pure Chemical Industries Ltd. L-Dopa and propranolol hydrochloride were purchased from Nakarai Chemicals Ltd. All reagents were used without further purification.

Phosphate solutions (0.067 M, pH 6.9 and pH 9.3) served as supporting electrolytes and were prepared from phosphate salts (NaH_2PO_4, K_2HPO_4, Na_3PO_4) and freshly purified water by using a Barnsted D-27942 three-module system.

Instruments——The apparatus for specular reflectivity measurements, coupled with a Hokuto Denko HA-101 potentiostat and Hokuto Denko HB-107A function generator, was the same as that in the previous papers.[3,4]

Electrodes——A gold plate (99.99% pure, 25 × 19 mm) served as the working electrode. It was polished with a 0.3 μm α-alumina slurry on a nylon cloth (Buehler Ltd.) and thoroughly rinsed with freshly purified water. A saturated calomel electrode (SCE) and gold plate were used as the reference and counter electrodes, respectively.

Procedures——The procedures used to obtain reflectivity (R/R_0)-potential (E) and R/R_0-time (t) curves were the same as described in the previous paper.[3] All measurements were carried out using a light beam at a wavelength of 500 nm and perpendicular polarization at an incident angle of 15°. Before making an actual measurement, a sufficient amount of pure argon gas was bubbled through the electrolyte solution to expel dissolved oxygen.

Results and Discussion

Current–Potential and Reflectivity–Potential Curves

On a current (i)–E curve of norepinephrine in a phosphate buffer solution (pH 6.9) at the potential range from −0.8 to 0.5 V, an anodic peak appeared at +0.2 V. This was due to a two-electron oxidation of norepinephrine followed by the chemical reactions shown below.[5]

In these reactions, some products such as noradrenochrome absorb light near 500 nm; this is undesirable for specular reflection measurement. Consequently, the potential examined was restricted to the range from −0.8 to −0.05 V. The i–E curve of norepinephrine in this potential range is given in the upper half of Fig. 1 and shows no redox wave.

The R/R_0–E curves measured simultaneously with the i–E curves are shown in the lower half of Fig. 1. The R/R_0–E curve of gold in a phosphate buffer solution (pH 6.9) had two approximately linear portions with different slopes intersecting at about −0.25 V (see curve c). This potential value appeared to be the pzc for gold in the solution.

The addition of norepinephrine to the solution caused no change in the R/R_0 value at potentials between −0.8 and −0.7 V, but a marked decrease in R/R_0 was observed in

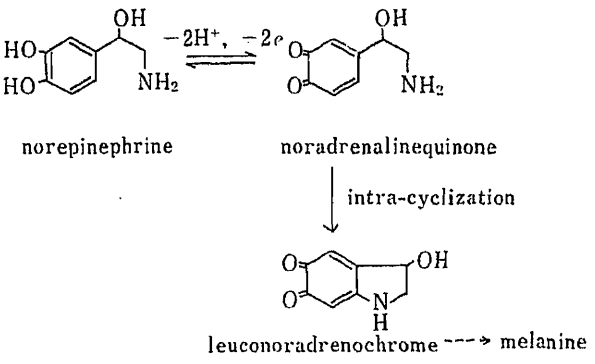

Chart 1

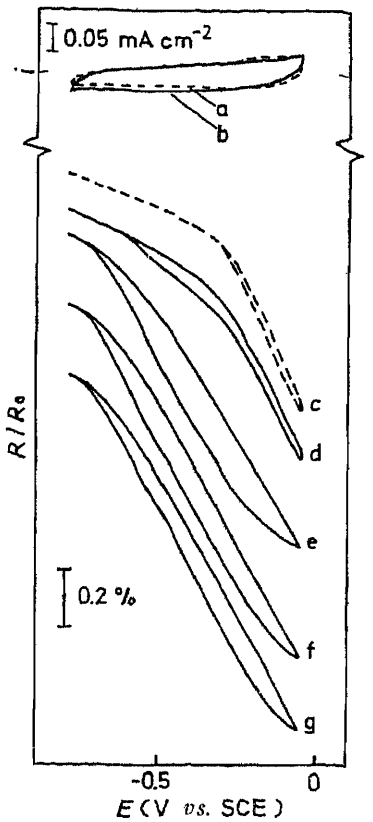

Fig. 1. Current-Potential (Upper) and Reflectivity-Potential (Lower) Curves of Gold in 0.067 M Phosphate Buffer (pH 6.9) in the Absence (a, c) and Presence of Norepinephrine

Norepinephrine concentration: a and c, 0; d, 3.0×10^{-6}; e, 2.1×10^{-5}; b and f, 6.6×10^{-5}; g, 1.5×10^{-4} M. Potential sweep rate: $100\,mV\,s^{-1}$. Wavelength: 500 nm.

potential regions more positive than about −0.7 V (Fig. 1, curves d—g). The reflectivity change was enhanced by increasing the norepinephrine concentration but tended to saturate, reaching a limiting value at *ca.* 1×10^{-4} M. These observations suggest that adsorption of norepinephrine takes place on the gold electrode surface, since a decrease in reflectivity was often found to result from adsorption of organic compounds,[6] and it was explained in terms of the following linear approximation equation.[7]

$$(\Delta R/R_0)_{\perp,\theta=1}=-\frac{8\pi d n_s\cos\phi}{\lambda}\cdot\frac{\varepsilon''_{ad}(n_s^2-\varepsilon'_M)+\varepsilon''_M(\varepsilon'_{ad}-n_s^2)}{(n_s^2-\varepsilon'_M)^2+\varepsilon''^2_M} \quad (1)$$

where $\Delta R/R_0$ denotes the reflectivity change at monolayer coverage ($\theta=1$) observed by the perpendicularly polarized light ($\perp$), ϕ is the incidence angle, λ the wavelength, n_s the refractive index of the bulk electrolyte solution, and ε' and ε'' are the real and imaginary parts of the complex dielectric constants, respectively. The subscripts ad and M represent the adsorbed layer and metal surface, respectively. When an optically transparent layer of an organic compound is formed on the substrate in water, $\varepsilon''_{ad}\simeq0$ and $\varepsilon''_{ad}>n_s^2$, and therefore, $\Delta R/R_0$ is always negative.

Potential and Concentration Dependence of Adsorption

The relationship between reflectivity change $\Delta R/R_0$ and surface coverage θ of an

electrode by an adsorbate was derived as follows,

$$(\Delta R/R_0)_{\perp,\theta}=\theta(\Delta R/R_0)_{\perp,\theta=1} \quad (2)$$

provided that the thickness of the monolayer, d, and the optical constants of the adsorbed layer and metal surface are not altered during the adsorption process.[7]

Measurements for other catecholamines such as epinephrine, dopamine, dopa, isoproterenol and homocatechol, were also carried out. All compounds were found to be adsorbed on the gold electrode surface.

The $\Delta R/R_0$ values due to adsorption of the catecholamines were obtained by the potential-step method using solutions of different catecholamine concentrations. The potential was first set at -0.8 V, where no adsorption occurs, and then stepped to more positive potentials, and the R/R_0 *vs.* t curves were recorded until the R/R_0 no longer decreased. The same procedure was also applied to the supporting electrolyte solution. Reflectivity changes at equilibrium in the presence and absence of catecholamines at the same potential were obtained. By subtracting the latter from the former at the same potential, the net change in R/R_0 due to the adsorption, denoted as $\Delta R/R_0$, was obtained. Each curve in Fig. 2 has a maximum $|\Delta R/R_0|$[8] at a potential near the pzc and $|\Delta R/R_0|$ decreases with deviation from the potential, suggesting that each catecholamine behaves as a neutral organic compound in the adsorption. However, the potentials of the $|\Delta R/R_0|$ maxima were actually somewhat more positive than the pzc of gold in the supporting electrolyte. This can be ascribed to the contact of a negatively charged part, perhaps the catechol moiety, of an adsorbed molecule with the gold electrode surface.

The smooth $|\Delta R/R_0|$–E curves of norepinephrine suggest that no orientational change takes place, at least in the potential region from -0.8 to -0.2 V. Supposing that the limiting value of $|\Delta R/R_0|=0.78\%$ in Fig. 2, A corresponds to the reflectivity change at monolayer coverage of norepinephrine, θ values can be obtained by the use of Eq. 2. In Fig. 3, θ values are plotted against norepinephrine concentrations, and Langmuir-like adsorption isotherms were obtained. They were analyzed by using Eq. 3, initially derived by Bockris and Swinkles[9]

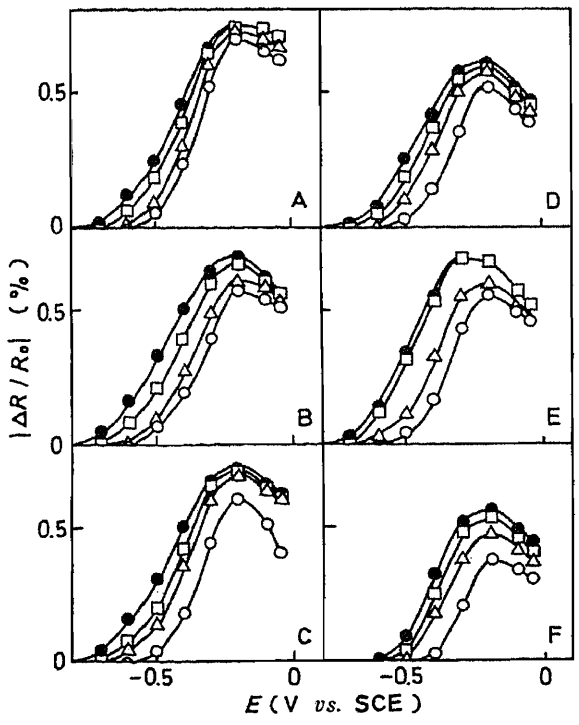

Fig. 2. Potential Dependence of Reflectivity Change Obtained for (A) Norepinephrine, (B) Epinephrine, (C) Isoproterenol, (D) Dopamine hydrochloride, (E) Dopa and (F) Homocatechol

Concentration: A (○) 3.0×10^{-6}, (△) 8.0×10^{-6}, (□) 3.0×10^{-5}, (●) 1.5×10^{-4}; B (○) 3.0×10^{-6}, (△) 8.0×10^{-6}, (□) 3.0×10^{-5}, (●) 1.5×10^{-4}; C (○) 2.0×10^{-6}, (△) 7.0×10^{-6}, (□) 2.6×10^{-5}, (●) 1.4×10^{-4}; D (○) 3.0×10^{-6}, (△) 2.0×10^{-5}, (□) 6.5×10^{-5}, (●) 1.5×10^{-4}; E (○) 2.0×10^{-6}, (△) 2.7×10^{-5}, (□) 1.4×10^{-4}, (●) 2.3×10^{-4}; F (○) 5.1×10^{-6}, (△) 3.5×10^{-5}, (□) 1.5×10^{-4}, (●) 3.7×10^{-4} M.

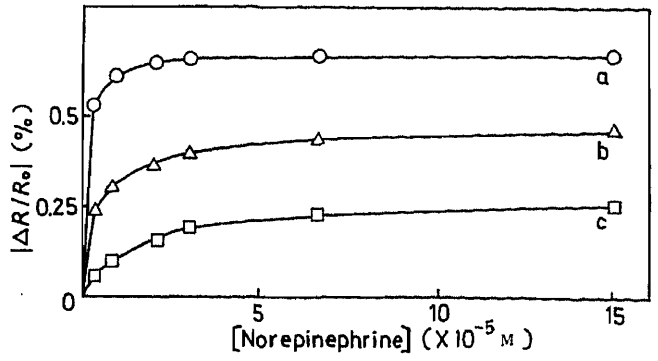

Fig. 3. Concentration Dependence of the Reflectivity Change for Norepinephrine at a, −0.3 V; b, −0.4 V; c, −0.5 V.

for the adsorption of organic molecules in solution, and applied to certain cases by Dahms and Green.[10]

$$\theta/(1-\theta)^p = cK \tag{3}$$

where p is the number of water molecules replaced by one molecule of the adsorbed species, and c, the concentration of organic molecule, used in place of activity in a dilute solution. The constant K is the adsorption coefficient. For norepinephrine adsorption at potentials ranging from −0.8 to −0.2 V, the plot of $\log(\theta/c)$ *vs.* $\log(1-\theta)$ gave a straight line, indicating that Eq. 3 holds for the adsorption isotherm of norepinephrine. Similar adsorption isotherms were also obtained for other catecholamines, but not dopa.

From these results, it can be noted that most of the catecholamines exhibit a rather simple pattern of adsorption behavior as a neutral molecule with no orientational change on the electrode surface.

Adsorption of Adrenergic Receptor-Blocking Drugs

To determine if the surface behavior of neurotransmitters, such as norepinephrine and epinephrine, would shed some light on their interactions with receptor sites, we investigated the adsorption behavior of adrenergic receptor-blocking drugs,[11] which offset the action of catecholamines by occupying receptors.

The following five adrenergic receptor-blocking drugs were examined: as α-blockers, phenoxybenzamine, tolazoline and ergotamine; as β-blockers, oxprenolol and propranolol. None of these compounds participated in redox reactions in the potential range from −0.8 to 0 V in the phosphate buffer solution (pH 6.9). All, except phenoxybenzamine, gave a reflectivity decrease in the R/R_0–E curves obtained in the solution throughout the potential range examined. It is clear that tolazoline, ergotamine, oxprenolol and propranolol are adsorbed at all potentials examined.

Because of hydrogen evolution on a gold electrode, observation in the negative potential region is limited up to −0.8 V at pH 6.9. To obtain the $|\Delta R/R_0|$–E curves for the above drugs, phosphate solution of pH 9.3 was used and the data thus obtained are shown in Fig. 4. In Fig. 4, B and C, the $|\Delta R/R_0|$–E curves for tolazoline and ergotamine (α-blocker) are bell-shaped with maxima at ≃0.4 V (*i.e.*, the pzc of gold in the phosphate solution of pH 9.3). Figure 4, D and E, shows the $|\Delta R/R_0|$–E curves of oxprenolol and propranolol (β-blockers). These drugs may be adsorbed on the electrode surface even from a fairly dilute solution (*ca.* 10^{-5} M), but their adsorption isotherms did not obey the Langmuir-like adsorption described by Eq. 3. This probably is due to orientational changes depending on potential and/or mutual interactions of the adsorbed molecules.

The adsorption behavior of these antagonists was compared qualitatively with that of norepinephrine. It can be seen from their adsorption dependence on concentration and electrode potential that the adsorptivity of the antagonists is stronger than that of

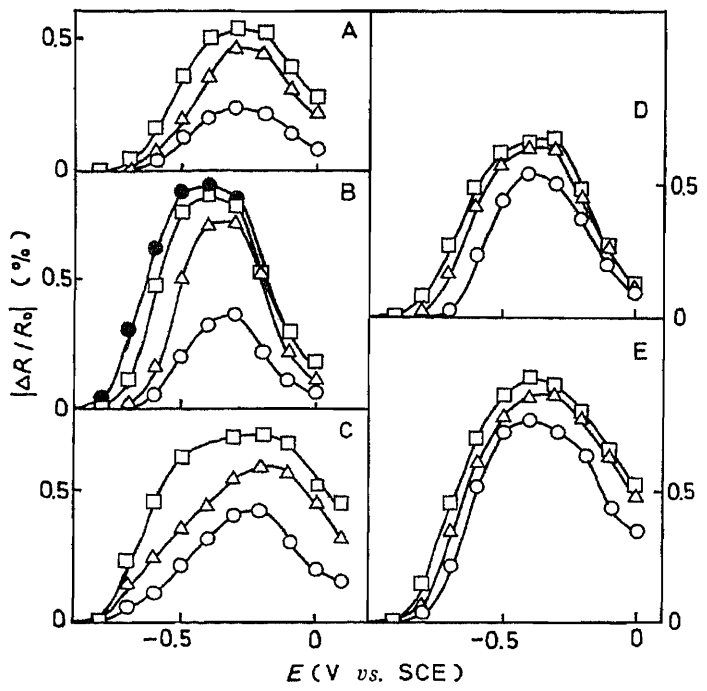

Fig. 4. Potential Dependence of Reflectivity Change Obtained in a Phosphate Solution (pH 6.9 (A) and 9.3 (B)—(E)) for (A) Phenoxybenzamine Hydrochloride, (B) Tolazoline Hydrochloride, (C) Ergotamine Tartrate, (D) Oxprenolol Hydrochloride and (E) Propranolol Hydrochloride

Concentration: A (○) 4.7×10^{-6}, (△) 8.8×10^{-6}, (□) 2.9×10^{-5}; B (○) 9.9×10^{-7}, (△) 7.4×10^{-5}, (□) 3.5×10^{-5}, (●) 1.3×10^{-4}; C (○) 7.4×10^{-7}, (△) 1.5×10^{-6}, (□) 2.8×10^{-6}; D (○) 1.5×10^{-6}, (△) 1.4×10^{-5}, (□) 3.5×10^{-5}; E (○) 1.7×10^{-6}, (△) 7.9×10^{-6}, (□) 3.7×10^{-5} M.

norepinephrine, especially in the potential region more negative than −0.3 V. That is, the antagonist drugs are readily adsorbed on a negatively charged electrode surface.

Electrochemical Approach to Adrenergic Chemical Neurotransmission Processes

In chemical neurotransmission, a neurotransmitter present in the synaptic gap may initially be attracted to the post synaptic membrane through electrostatic interactions and then bind to the receptor site in a particular orientation. Pilla[12] pointed out the similarities of electrical behavior between a biomembrane surface/biological fluid interface and an electrode/electrolyte solution interface. Although biomembranes have relatively complex structure, they are charged because of the presence of polar groups such as phospholipid head, and they are in contact with biological fluid which contains electrolytes. Furthermore, the biomembrane surface is regarded as being directly covered in the first sphere with a structured water layer whose properties are different from those of bulk water. Such features resemble those of an electrical double layer of electrode/solution interface.[13] Thus, the adsorption behavior of neurotransmitters at the electrode/solution interface is expected to reflect the electrostatic interactions between a neurotransmitter and its receptor site.

Based on the adsorption isotherm given by Eq. 3, the value of p for norepinephrine was obtained to be 4.1 ± 0.4 from the slope of log (θ/c)*vs.* log $(1-\theta)$. The area occupied by one adsorbed norepinephrine molecule can be estimated from p by comparison with the area of an adsorbed water molecule, using the CPK molecular model. Assuming a water molecule to occupy an area of 0.09 nm^2, the area occupied by norepinephrine was calculated to be 0.37 nm^2. Comparing this value with the surface area of the norepinephrine molecule based on the crystal structure,[14] the most probable orientation of adsorbed norepinephrine is that the

catechol moiety and hydroxy groups at the β-position may be in contact with the electrode surface in a flat orientation.

The activity of norepinephrine is due to its complexation with adrenergic receptors such as α-adrenergic and β-adrenergic receptors. From QSAR experiments, the following model of drug-receptor interaction is proposed.[15] Phenolic hydroxy groups assist in the fixation to the β-adrenergic-receptor site through electrostatic forces. The aromatic ring, attaching itself to the receptor by van der Waals' forces, is also essential for β-adrenergic activity. The alcoholic hydroxy group allows other electrostatic bonding with the receptor. The presence of an amino group is essential, especially for α-adrenergic activity, owing to its interaction in cationic form with the receptor's anionic phosphate groups. Comparing the possible orientation of norepinephrine at the electrode surface with that at the receptor based on the drug-receptor model, interactions between norepinephrine and the electrode surface may reflect mainly drug-receptor interactions on the β-receptor.

A study of the electrosorption behavior of norepinephrine and adrenergic blocking drugs may provide basic information concerning the competitive inhibitory effects of antagonists on the interactions of the agonist with solvated and charged surfaces.

References and Notes

1) N. Weiner, "The Pharmacological Basis of Therapeutics," 7th ed., ed. by A. G. Gilman, L. S. Goodman and A. Gilman, Macmillan, New York, 1980, pp. 145—180.
2) S. Hirono, H. Umeyama and I. Moriguchi, *Chem. Pharm. Bull.*, **32**, 3061 (1984).
3) F. Kusu and K. Takamura, *Denki Kagaku*, **53**, 361 (1985).
4) F. Kusu and K. Takamura, *J. Electroanal. Chem.*, **161**, 169 (1984).
5) G. Dryhurst, K. M. Kadish, F. Scheller and R. Renneberg, "Biological Electrochemistry," Vol. 1, Academic Press, Inc., New York, 1982, p. 116.
6) F. Kusu and K. Takamura, *Surf. Sci.*, **158**, 633 (1985).
7) J. D. E. McIntyre, "Advances in Electrochemistry and Electrochemical Engineering," Vol. 9, ed. by P. Delahay and C. W. Tobias, John Wiley and Sons, Inc., New York, 1973, p. 61.
8) The magnitude of net reflectivity change is given in terms of $|\Delta R/R_0|$ in the present paper, since all the $\Delta R/R_0$ values experimentally obtained are negative.
9) J. O'M. Bockris and D. A. J. Swinkels, *J. Electrochem. Soc.*, **111**, 736 (1964).
10) H. Dahms and M. J. Green, *J. Electrochem. Soc.*, **110**, 1075 (1963).
11) N. Weiner, "The Pharmacological Basis of Therapeutics," 7th ed., ed. by A. G. Gilman, L. S. Goodman and A. Gilman, Macmillan, New York, 1980, pp. 181—214.
12) A. A. Pilla, *Bioelectrochem. Bioenerg.*, **1**, 227 (1974).
13) M. N. Berry, A. R. Grivell and P. G. Wallace, "Comprehensive Treatise of Electrochemistry," Vol. 10, ed. by S. Srinivasan, Y. A. Chizmadzhev, J. O'M. Bockis, B. E. Conway and E. Yeager, Plenum Press, New York, 1985, pp. 347—356.
14) J. P. Tollenaere, H. Moereels and L. A. Raymaekers, "Atlas of the Three-Dimensional Structure of Drugs," Elsevier/North-Holland Biomedical Press, Amsterdam, 1979, p. 62.
15) A. Korolkovas, "Essentials of Molecular Pharmacology," John Wiley and Sons, Inc., New York, 1970, pp. 231—241.

[Chem. Pharm. Bull. 35(4)1334—1338(1987)]

Studies on the Hydroalkylation of Benzene and Methylbenzenes in the Presence of a Combination Catalyst of $Pd–Al_2O_3$ and $NaCl–AlCl_3$

TSUTOMU KAMIYAMA,* SABURO ENOMOTO, and MASAMI INOUE

Faculty of Pharmaceutical Sciences, Toyama Medical and Pharmaceutical University, Sugitani, Toyama 930-01, Japan

(Received September 22, 1986)

The mechanism of the hydroalkylation of benzene and methylbenzenes to cyclohexylbenzenes was studied in the presence of a palladium-fused salt ($NaCl–AlCl_3$) catalyst under hydrogen pressure. The activities of the hydrogenation catalyst and the alkylation catalyst were each estimated kinetically. The activity of the fused salt was compared with that of anhydrous aluminum chloride for the alkylation of aromatic compounds. The rate constants and Arrhenius parameters of the hydrogenation on palladium and the alkylation on the fused salt supported the presence of the cyclohexyl cation as an intermediate species in the hydroalkylation.

Keywords——hydroalkylation; mechanism; palladium catalyst; fused salt; benzene; cyclohexene; cyclohexylbenzene

The hydroalkylation reaction, giving cyclohexylbenzene (**4**) from benzene (**1**) in one step, was found by Truffault,[1] using $Ni–P_2O_5$ catalyst. Several reports[2-4] and patents[5-9] have been published on the hydroalkylation of **1**. Most of them refer to a bifunctional catalyst system of a Group VIII metal such as Ni, Pt, Pd, Ru, and Rh supported on solid acids. Several authors have studied the reaction of **1** and suggested cyclohexene (**2**) to be the key intermediate,[2-4] though the details of the mechanism are not known.

We previously prepared the combination catalyst of palladium and the fused salt ($NaCl–AlCl_3$).[10] The catalyst was applied for the hydroalkylation of **1** to **4**,[11] aniline to *p*-cyclohexylaniline[12] and phenol to *p*-cyclohexylphenol.[13] We have now successfully separated the intermediate olefins from the reaction products and confirmed the reaction pathway for the hydroalkylation of **1** and methylbenzenes. In this paper, the characterization of the combination catalyst, the palladium catalyst and the fused salt, is described. A reaction mechanism is proposed on the basis of the kinetics of hydrogenation and alkylation of **1** and methylbenzenes.

Results and Discussion

1) Isolation of the Reaction Intermediates from the Hydroalkylation Products

For the hydroalkylation of **1** to **4**, several possible reaction intermediates were considered (Chart 1). One is a partial hydrogenation product of biphenyl (**7**), formed by the condensation of two molecules of **1** on the fused salt. However, with our catalyst, **7** was not detected by gas-liquid chromatography (GLC) on heating **1** (30 g) with the fused salt (4 g) and 0.25% $Pd–Al_2O_3$ (1 g) at 120 °C for 5 h in the absence of hydrogen. Another one is the cyclohexyl cation, formed by the abstraction of a hydride ion from cyclohexane (**3**) on palladium. When **3** was heated at 120 °C for 10 h in the presence of 0.24% $Pd–Al_2O_3$ (1 g) and the fused salt (4 g) in the absence of hydrogen, no **2** or high-boiling-point products such as bicyclohexyl were detected.

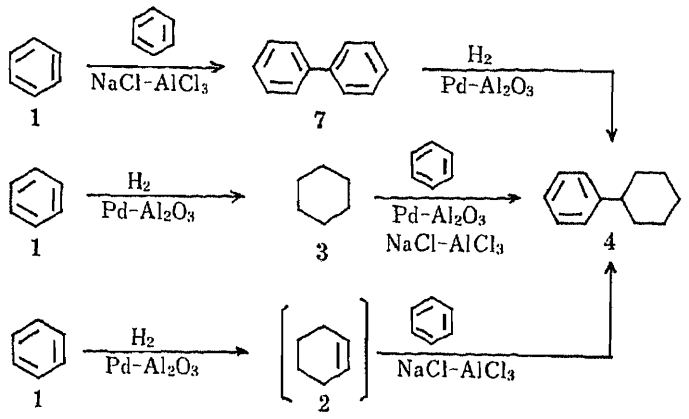

Chart 1

TABLE I. Formation of Olefins in the Hydroalkylation Using 1% $Pd-Al_2O_3$ and $AlCl_3 \cdot 6H_2O$

Hydrocarbon	Temp. (°C)	Time (h)	Conv. (%)	Product (yield, %)
	120	0.5	15.7	 (0)
	120	0.5	11.6	 (0.2)
	130	1.0	8.1	 (0.7)
	130	1.5	12.3	 (0.4)
	130	1.5	14.9	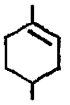 (0.5)

Hydrocarbon (20 ml), 1% $Pd-Al_2O_3$ (1 g), and $AlCl_3 \cdot 6H_2O$ (1 g) were used. The initial H_2 pressure was 130 kg/cm^2.

Therefore, among the reaction intermediates, **2** was the most probable key intermediate in the hydroalkylation of benzene, as already suggested by Slaugh and Leonard.[2] We tried to separate **2** from the hydroalkylation products of **1**, and found that the hydrogenation was retarded by the addition of $AlCl_3 \cdot 6H_2O$, and corresponding olefins were obtained from methylbenzenes, although the yields were poor (Table I). However, under these conditions, **2** was not obtained. If the hydrogenation of **1** proceeds in a stepwise manner, it is plausible that **3** is produced by way of **2**.[14] Therefore, it was suggested that the reduction of **2** was so rapid that the intermediate could not be isolated.

Among methylbenzenes examined, the yields of dimethylcyclohexenes were higher than that of 1-methylcyclohexene (**6**). The highest yield (0.7%) was obtained for 1,2-dimethylcyclohexene; presumably the two adjacent methyl groups stabilized the olefin. These results showed that easily reducible olefins are formed as intermediate compounds during the hydrogenation of methylbenzenes to cyclohexanes.

2) The Catalytic Behavior of the Fused Salt of NaCl–$AlCl_3$

To study the role of NaCl–$AlCl_3$ in the hydroalkylation, the kinetics of alkylation of **1** or methylbenzenes with **2** were examined. The results obtained were compared with the activity of $AlCl_3$ alone. The initial rate of alkylation of benzenes with **2** increased with increase in the relative basicity of the aromatic compounds.[15] A linear relationship between the logarithm of

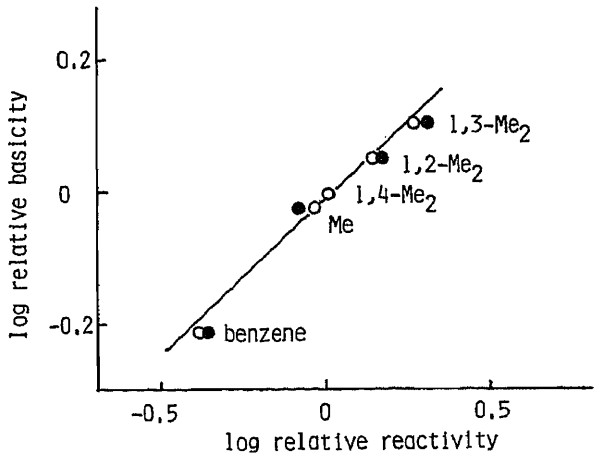

Fig. 1. Relationship between Relative Basicity and Relative Rate of Alkylation with Cyclohexene

○, catalyzed by $AlCl_3$; ●, catalyzed by NaCl–$AlCl_3$.

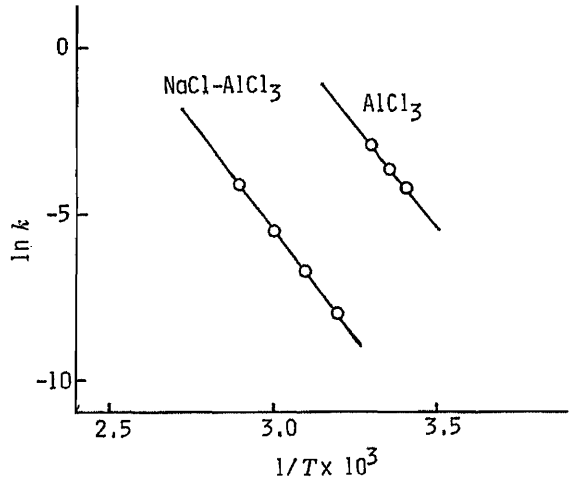

Fig. 2. Arrhenius Plots for the Alkylation of Benzene with Cyclohexene in the Presence of the Fused Salt or $AlCl_3$

Benzene (11.25 M), cyclohexene (0.19 M), and NaCl–$AlCl_3$ (1:1) (0.40 M) were used for the fused salt-catalyzed reaction. $E_a = 24.8$ kcal·mol^{-1}. Benzene (11.25 M), cyclohexene (0.19 M), and $AlCl_3$ (0.007 M) were used for the $AlCl_3$-catalyzed reaction. $E_a = 24.5$ kcal·mol^{-1}.

TABLE II. Relative Basicity, Initial Rate Constant and Relative Reactivity

Hydrocarbon	Rel. basicity[a]	Initial rate constant		Rel. reactivity[d]	
		NaCl–$AlCl_3$[b] ($\times 10^{-5}$ mol/l·min)	$AlCl_3$[c] ($\times 10^{-3}$ mol/l·min)	NaCl–$AlCl_3$	$AlCl_3$
	0.61	0.97	0.61	0.42	0.41
	0.92	1.89	1.37	0.82	0.91
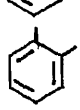	1.13	3.33	2.05	1.44	1.37
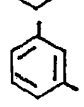	1.26	4.58	2.77	1.99	1.85
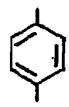	1.00	2.30	1.50	1.00	1.00

a) See ref. 15. *b*) Hydrocarbon (2.33 M), cyclohexene (2.33 M), NaCl–$AlCl_3$ (1:1) (0.54 M), and cyclohexane were used. The reaction was carried out at 60 °C. *c*) Hydrocarbon (0.89 M), cyclohexene (0.89 M), $AlCl_3$ (0.41 M), and cyclohexane were used. The reaction was carried out at 0 °C. *d*) Relative reactivities were recalculated on the basis of *p*-xylene = 1.00.

the relative rate of the alkylation and the logarithm of the relative basicity was obtained (Fig. 1).

The alkylation of *o*-xylene proceeded approximately 4.5 times faster than that of **1** (Table II). These results are typical of Friedel–Crafts catalysts. The activation energies obtained from the Arrhenius plots of the initial rate in the presence of NaCl–$AlCl_3$ and $AlCl_3$ were 24.8 and 24.5 kcal·mol^{-1}, respectively (Fig. 2). These results also indicated that NaCl–$AlCl_3$ catalyzed the alkylation through a similar mechanism to $AlCl_3$.

Therefore, a plausible reaction path is as follows: **1** is hydrogenated to **2** on Pd–Al_2O_3, and then **2** migrates from palladium to the fused salt to form the cyclohexyl cation. In the case of toluene (**5**), both the 1-methylcyclohexyl cation (**6—1**) and the 2-methylcyclohexyl cation (**6—2**) can be considered as candidates for the intermediate species. The former seems more probable than the latter since a tertiary carbonium ion is more stable than a secondary one. Therefore, **6—1** attacked the electron-rich carbon of the phenyl ring (*p*-position) to give 4,1′-dimethylcyclohexylbenzene as the major product. However, substitution at the *ortho* position did not take place owing to the steric effect of the methyl group on **5**.

3) Kinetics of Hydrogenation and Alkylation of Benzene

In the hydroalkylation, the relative rates of hydrogenation and alkylation affected the yield of **4**. We measured the rate of the hydrogenation of **2** using 0.25% Pd–Al_2O_3 (1 g) in the presence of the fused salt (NaCl–$AlCl_3$, 4 g). The rate constants (k_{hydro}) were calculated according to the following equation.[16]

$$\log P_0/P = k_{hydro}t/2.303$$

P_0: initial H_2 pressure; P: H_2 pressure at time t

The Arrhenius plots for the hydrogenation of **2** in the presence of NaCl–$AlCl_3$ are shown in Fig. 3.

The values of the activation energy and the rate constant for the hydrogenation at 120 °C were 5.95 kcal·mol^{-1} and 0.24 min^{-1}. The rate constant for the alkylation at 120 °C (k_{alk} = 1.56 min^{-1}) was obtained by extrapolation of the Arrhenius plots (Fig. 2). In the hydroalkylation of **1** at 120 °C, the yields of **3** and **4** were 8.4 and 16.4%, respectively. From kinetic data, k_{alk} was 6.5 times faster than k_{hydro}. If the hydrogenation and the alkylation of **2** are competitive, the yield of **4** may also reach 6.5 times that of **3**. This discrepancy was explained by considering the delayed desorption of **2** from the palladium surface. Thus, the successive hydrogenation of **2** on the palladium catalyst took place to give **3**. On the other hand, a part of **2** migrated from the surface of Pd–Al_2O_3 onto the surface of NaCl–$AlCl_3$ and

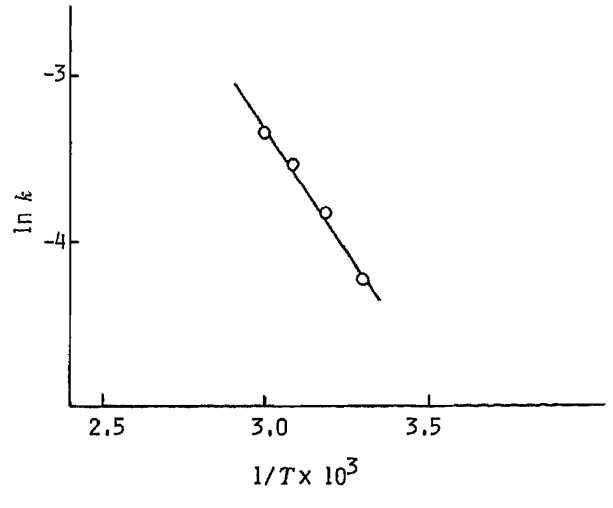

Fig. 3. Arrhenius Plots for the Hydrogenation of Cyclohexene in the Presence of the Fused Salt

Benzene (30 ml), cyclohexene (0.024 mol), NaCl–$AlCl_3$ (4 g), and 0.25% Pd–Al_2O_3 (1 g) were used. The initial H_2 pressure was 130 kg/cm^2. Only a trace amount of cyclohexylbenzene was detected. E_a = 5.95 kcal·mol^{-1}.

was swiftly alkylated with **1** to give **4**.

Experimental

Gas-liquid chromatography (GLC) for the analyses of benzene, methylbenzenes, olefins, and hydrogenated products was carried out on a Shimadzu GC-3BF gas chromatograph by using a column packed with 25% Apiezon grease M on C-22 (30—60 mesh, 1 m)–20% polyethylene glycol (PEG) on Chromosorb W (60—80 mesh, 2 m).[17] Hydroalkylated products were also analyzed by GLC (Hitachi 063; column packing, 2% silicone OV-17 on Chromosorb W, 60—80 mesh, 2 m). Proton nuclear magnetic resonance (^{1}H-NMR) spectra were recorded on a Hitachi R-600 (60 MHz) or JEOL GX-270 (270 MHz) instrument in $CDCl_3$. Carbon-13 nuclear magnetic resonance (^{13}C-NMR) spectra were obtained on a Varian XL-200 spectrometer. Chemical shifts are given in δ-values referred to internal tetramethylsilane.

Preparation of Catalysts——Palladium on alumina and the fused salt were prepared according to the previously reported method.[11] The palladium catalyst was activated before use (200 °C, 1 h in an H_2 stream).

General Procedures——Hydrogenations and hydroalkylations were carried out in a stainless steel autoclave (SR-10, 100 ml). The substrate, Pd–Al_2O_3, and the fused salt were put in the autoclave. The air in the autoclave was displaced with hydrogen, the autoclave was heated to the desired temperature, and then hydrogen was introduced to 130 kg/cm^2. The reaction was started by magnetic stirring. The partially hydrogenated olefins were isolated by preparative GLC on a column packed with a 20% PEG 20 M (2 m)–25% Apiezon grease M (2 m).

Physical Properties of Hydroalkylation Products and Olefins——The physical data for hydroalkylation products were previously reported.[11] NMR data for olefins are as follows. For 1-methylcyclohexane: ^{1}H-NMR δ: 1.25—2.35 (m, 7H), 1.89 (s, 3H), 5.38 (s, 1H). For 1,2-dimethylcyclohexene; ^{1}H-NMR δ: 1.24—2.30 (m, 8H), 1.72 (s, 6H). For 1,3-dimethylcyclohexene; ^{1}H-NMR δ: 0.89 (d, 3H, J=7.2 Hz), 1.03—2.34 (m, 7H). 1.76 (s, 3H), 5.23 (s, 1H). ^{13}C-NMR δ: 21.90, 22.03, 30.02, 30.34, 31.19, 127.80, 133.34.[18] For 1,4-dimethylcyclohexene; ^{1}H-NMR δ: 0.93 (d, 3H, J=6.2 Hz), 1.21—2.03 (m, 7H), 1.70 (s, 3H), 5.34 (s, 1H).

References and Notes

1) R. Truffault, *Bull. Soc. Chim. Fr.*, **1**, 3941 (1934).
2) L. H. Slaugh and J. A. Leonard, *J. Catal.*, **13**, 385 (1969).
3) J. J. Louver and A. Francoy, *J. Catal.*, **16**, 62 (1970).
4) Y. Yamazaki, A. Masuda, K. Kawai, and S. Kimura, *Bull. Jpn. Pet. Inst.*, **18**, 25 (1976).
5) A. Arkell, J. M. Crone, and P. M. Suggitt, U. S. Patent 3760017 (1973) [*Chem. Abstr.*, **80**, 14710*v* (1974)].
6) E. A. Zuech and B. Okla, U. S. Patent 3829514 (1974) [*Chem. Abstr.*, **81**, 104951*z* (1974)].
7) M. Yasuhara, M. Nishino, and S. Matsuhisa, Japan. Patent 7601445 (1976) [*Chem. Abstr.*, **84**, 150254*j* (1976)].
8) E. A. Zuech and B. Okla, U. S. Patent 3956183 (1976) [*Chem. Abstr.*, **85**, 77838*s* (1976)].
9) I. Mikami *et al.*, Japan. Patent 7762253 (1977) [*Chem. Abstr.*, **87**, 184179*r* (1977)].
10) T. Kamiyama, S. Enomoto, and M. Inoue, *Chem. Lett.*, **1979**, 261.
11) T. Kamiyama, S. Enomoto, and M. Inoue, *Chem. Pharm. Bull.*, **29**, 15 (1981).
12) T. Kamiyama, S. Enomoto, and M. Inoue, *Chem. Pharm. Bull.*, **30**, 777 (1982).
13) T. Kamiyama, S. Enomoto, and M. Inoue, *Chem. Pharm. Bull.*, **34**, 450 (1986).
14) G. P. Pez and R. K. Crissey, *J. Catal.*, **21**, 393 (1983).
15) H. C. Brown and B. J. Brady, *J. Am. Chem. Soc.*, **74**, 3570 (1952).
16) H. A. Smith, D. M. Alderman, and F. W. Nadig, *J. Am. Chem. Soc.*, **67**, 272 (1945).
17) H. Yamamoto, M. O'hara, and T. Kwan, *Chem. Pharm. Bull.*, **12**, 959 (1964).
18) R. A. Benkeser, F. G. Belmonte, and J. Kang, *J. Org. Chem.*, **48**, 2796 (1983).

[Chem. Pharm. Bull. 35(4)1339—1346(1987)]

Ring-Chain Tautomerism and Some Reactions of 2-Hydroxyindoline Derivatives

TOMOMI KAWASAKI, HIROAKI OHTSUKA, CHUN-SHENG CHIEN, MITSUGU OMATA, and MASANORI SAKAMOTO*

Meiji College of Pharmacy, 1-35-23, Nozawa, Setagaya-ku, Tokyo 154, Japan

(Received June 30, 1986)

The spectral (proton and carbon-13 nuclear magnetic resonance) and chemical properties of the 1-acetyl-2-hydroxyindolines **1**—**5**, which can exist in the ring (A) and chain (B) tautomers, have been investigated. The methylation and acetylation of the 2-hydroxy-3-indolinones **1**—**3** gave the ring tautomeric methyl ether and acetyl esters of **1**—**3**, while the reaction with *o*-phenylenediamine (**9**) gave the quinoxalines **10** and **11** as the chain tautomeric products. The reactions of **1**—**3** with the phosphonium ylide **12** gave the 2-methoxycarbonylmethyl-3-indolinones **14** (R=Ph) and **16** (R=Me) and/or the 2-hydroxy-3-methoxycarbonylmethyleneindolines **15** (R=Ph) and **18** (R=H), respectively, depending on the nature of the substituent (R) at the 2-position in **1**—**3**. The acetylation and reaction of the 2,3-dihydroxyindoline **4** with **12** are also described.

Keywords——2-hydroxyindoline; tautomerism; Wittig reaction; acetylation; methylation; ^{13}C-NMR; quinoxaline; furo[3,2-*b*]indole.

It is known that 1-acetyl-2-hydroxyindolines can exist in equilibrium with their open-chain tautomers.[1] Previously, we have reported the preparation of the 1-acetyl-2-hydroxy-3-indolinones **1**—**3** and the 1-acetyl-2,3-dihydroxyindolines **4** and **5** by the oxidation of 1-acetylindoles with an oxodiperoxomolybdenum comound.[2] Since the 2-hydroxyindolines **1**—**5** may possess two or more reactive sites which are interrelated by their ring-chain tautomerism, they are expected to be attractive synthetic intermediates to heterocyclic compounds.[3] We have now examined some reactions of the 2-hydroxyindolines **1**—**4**, and also reinvestigated the spectral properties of **1**—**5** in order to understand their ring-chain tautomerism.

Spectral Properties

Since Harrison[1g] had established the ring-chain tautomerism of 2-hydroxyindolines by examination of their ^{13}C-nuclear magnetic resonance (^{13}C-NMR) spectra, we first reexamined

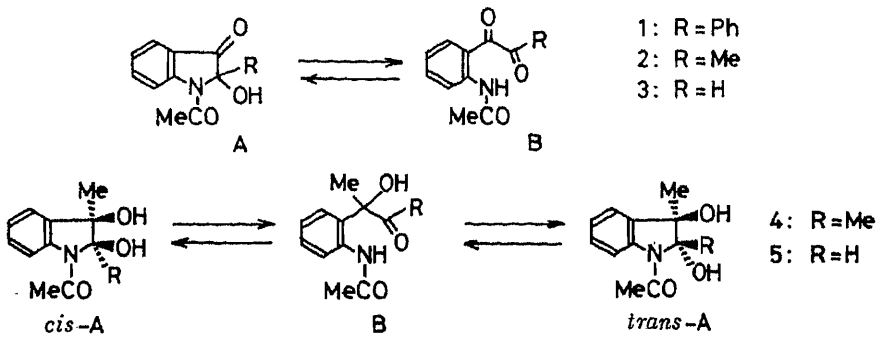

Chart 1

TABLE I. ^{1}H- and ^{13}C-NMR Data for 2-Hydroxyindolines **1**—**5**

Compd. No.	Solv.	Tautomeric form	^{1}H-NMR δ		^{13}C-NMR δ				
			N–COMe	Others	C=O	N–C=O	2-C of A	Me (q)	Others
1	$CDCl_3$	A and B	2.27,[a] 2.02[b]	11.33 (OH), 5.23 (NH)	196.23, 198.84, 192.97	171.32, 169.87	90.35	24.67, 25.45	
	DMSO-d_6	A	1.92	8.04 (OH)	195.01	170.69	94.84	24.23	
2	DMSO-d_6	A	2.49	1.62 (Me)	198.59	169.87	88.02	22.68, 23.91	
3	DMSO-d_6	A	2.33	7.35 (OH), 5.46 (d, J= 8 Hz, 2-H)	196.71	169.69	81.53 (d)	23.54	
4	$CDCl_3$	A and B	2.21,[c] 2.16[d]	1.45,[c] 1.55,[c] 1.74,[d] 1.91[d] (4 Me)	211.39	171.00, 168.49	96.02	18.86, 22.03, 23.75, 24.14, 24.69	77.20,[j] 80.13[k]
	DMSO-d_6	A and B	2.36,[e,f] 1.97[g]	1.34,[e] 1.36,[f] 1.44,[f] 1.52,[e] 1.63,[g] 1.94[g] (6 Me)	208.91	169.53, 169.84, 167.86	95.51, 97.51	19.60, 21.84, 22.21, 23.74, 23.91, 23.96, 23.19, 24.39, 24.55	75.68,[j] 79.52,[k] 79.64[k]
5	DMSO-d_6	A	2.30,[h] 2.28[i]	1.35,[i] 1.49[h] (2 Me), 5.22 (2-H)		169.31, 169.77	89.02 (d), 92.34 (d)	20.45, 23.19, 23.36, 28.03	75.56,[k] 77.28[k]

s, singlet; d, doublet; q, quartet. The ratio of peaks: *a*):*b*)=1:2, *c*):*d*)=1:1.8, *e*,*f*):*g*)=3:1, *e*):*f*)=1:1.4, *h*):*i*)=1:3. *j*) (s, HO–C–CO– of B). *k*) (s, 3-C of A).

the ^{1}H- and ^{13}C-NMR spectra of the 2-hydroxyindolines **1**—**5** in detail. The results are presented in Table I.

In $CDCl_3$, 1-acetyl-2-hydroxy-2-phenyl-3-indolinone (**1**) exists as a mixture of ring (**1A**) and chain (**1B**) tautomers. Thus, the ^{13}C-NMR spectrum showed signals due to C-2 (δ 90.35), C-3 (196.23) and amido carbonyl carbons (171.32) of **1A**, and the two keto (192.97, 198.84) and amido carbonyl carbons (169.87) of **1B**, and the ^{1}H-NMR spectrum showed signals due to the two acetamido protons at δ 2.27 and 2.02, in the ratio of *ca.* 1 : 2. When the spectra were recorded in dimethylsulfoxide (DMSO)-d_6, there was a striking change in the ratio of **1A** and **1B**; only the signals due to **1A** were observed, while no signal due to **1B** was seen.[4] It was found that the ratio of **1A** and **1B** depends on the nature of the solvent; **1** tends to exist as the ring form **1A** in a polar solvent.

Similarly, the 2-methyl- **2** and 2-unsubstituted 2-hydroxy-3-indolinones **3** were found to exist in DMSO-d_6 as the ring tautomers **2A** and **3A**, respectively.[4] It is known[1b-f] that the ring-chain tautomerism of 2-hydroxyindolines is dependent on the substituent at the 2-position; in DMSO-d_6, 2-unsubstituted derivatives exist preferentially as the ring forms, while 2-substituted ones exist as the chain forms. In the case of **1**—**3**, however, the ring tautomers A are predominant in DMSO-d_6. This predominance can be explained on the basis of the participation of the carbonyl group at the 3-position in the stabilization of the ring tautomer A, while is analogous to the finding that carbonyl compounds with electron-withdrawing groups tend to form their hydrates, *e.g.*, 1,2,3-indantrione, glyoxal, and so on.[5]

The ^{13}C-NMR spectrum of 1-acetyl-2,3-dihydroxy-2,3-dimethylindoline (**4**) in $CDCl_3$ was identical to that reported by Harrison,[1g] corresponding to a mixture of ring (**4A**) and chain (**4B**) tautomers. Although the ring of **4A** can exist in two stereoisomers, the ^{1}H- and ^{13}C-NMR spectra of **4** in $CDCl_3$ show no evidence for their existence. When the spectra were recorded in DMSO-d_6, the signals due to the *cis*- and *trans*-isomers of **4A** appeared; the ^{13}C-NMR spectrum showed the 2-C (δ 95.51, 97.51) and 3-C (79.52, 79.64) signals of two isomers of **4A**. In this case, solvent dependence of the ratio of the equilibrium constituents was observed; in $CDCl_3$ the ratio of **4A** and **4B** was *ca.* 1 : 1.8, while in DMSO-d_6 it was *ca.* 3 : 1, and the ratio of the two stereoisomers of **4A** was *ca.* 1 : 1.4.

In the case of 1-acetyl-2,3-dihydroxy-3-methylindoline (**5**), the NMR spectra in DMSO-d_6 show that **5** is a mixture of *cis*-and *trans*-isomers of the ring tautomer 5A, and no peak due to the chain tautomer 5B was detected.[4]

Chemical Properties

Next, we examined some reactions of **1**—**4**; methylation, acetylation, and reaction with *o*-phenylenediamine (**9**) and with a phosphonium ylide **12**.

Treatment of the 2-hydroxy-3-indolinone **1** with methyl iodide and potassium *tert*-butoxide gave the 2-methoxy-3-indolinone **6** in 71% yield; the structure was assigned on the basis of the analytical and spectral data. The isomeric structure **6'** was readily ruled out by the appearance of the signal due to 2-C (δ 94.84) of **6** in the ^{13}C-NMR spectrum. The methylation of **2** was carried out similarly to give only a complex mixture.[6]

Acetylation of **1** and **3** gave the O-acetates **7** and **8**, respectively, whose structures were confirmed by spectral evidence; the ^{13}C-NMR spectrum of **7** showed a signal at δ 90.85 due to 2-C of **7**, and the ^{1}H-NMR spectrum of **8** showed a singlet peak at δ 6.33 due to 2-H of **8**.

The reaction of **1** and **2** with **9** afforded the quinoxalines **10** and **11** in 98% and 97% yields, respectively. The reaction may proceed *via* the condensation of their open-chain tautomers B as α-diketones with **9**; this is similar to the well-known reaction used for the synthesis of quinoxalines.[8]

Next, we examined the reactions of **1**—**3** with the phosphonium ylide **12**, and found clear differences. Thus, the reaction of **1** with **12** gave the 2-methoxycarbonylmethyl-3-indolinone

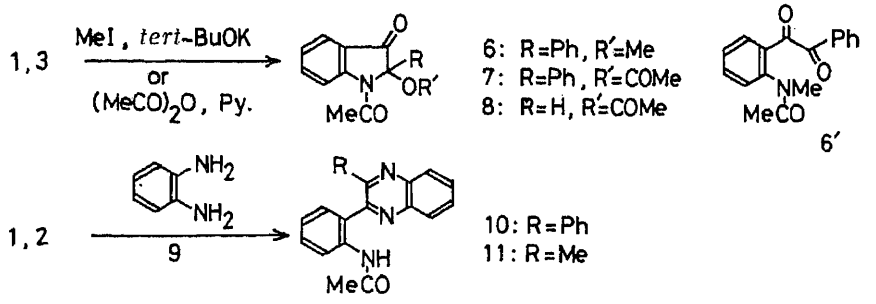

py. = pyridine

Chart 2

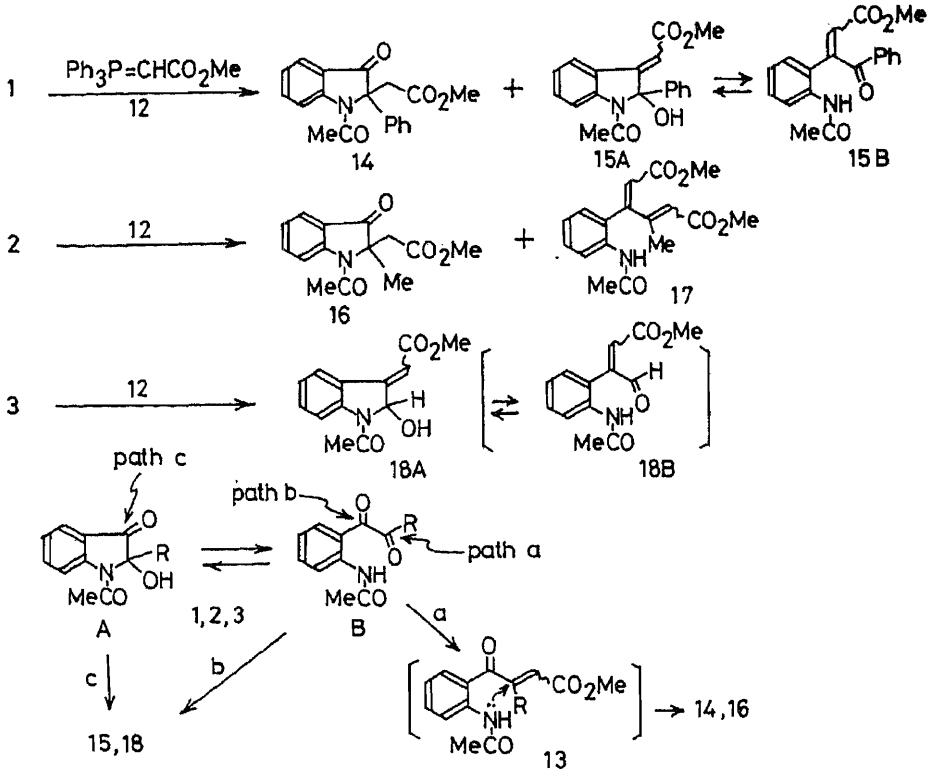

Chart 3

14 and the 2-hydroxy-3-methoxycarbonylmethyleneindoline **15** in 29% and 52% yields, respectively. The structures of **14** and **15** were determined on the basis of their analytical and spectral data; the parent ions in the mass spectra (MS) each appeared at *m/z* 323, indicating that **14** and **15** are isomeric. The infrared (IR) spectrum of **14** showed three carbonyl bands at 1742, 1736, and 1680 cm^{-1}, and in the ^{1}H-NMR spectrum two doublets (J=16 Hz) due to methylene protons were observed at δ 3.68 and 4.02. On the other hand, the ^{1}H-NMR spectrum of **15** in $CDCl_3$ showed two singlets at δ 5.82 and 6.36 (one proton in total) due to the olefinic protons and two singlets at δ 1.82 and 2.12 (three protons) due to the amidomethyl protons. The spectrum indicated that, at least in $CDCl_3$, the product **15** exists in two forms, the ring and chain tautomers, **15A** and **15B**, as well as **1**. Thus, in the ^{13}C-NMR spectrum ($CDCl_3$), there were four singlets due to ester and amido carbonyl carbons at δ 165.13, 166.87, 168.63, and 171.60, and two doublets due to olefinic carbons of **15A** and **15B** at δ 113.96 and 116.58, and further a singlet due to the keto carbonyl carbon of **15B** at δ 196.29 and a singlet due to 2-C of **15A** at δ 94.63. However, we could not clarify the *E* and *Z* stereochemistries of

15A and **15B**. The formation of **14** may be understood in terms of attack of the ylide **12** on the benzoyl carbonyl of **1B**, leading to **13**, followed by cyclization (path a), while the formation of **15** may occur by attack of **12** either on the other benzoyl carbonyl of **1B** (path b) or on the carbonyl of **1A** (path c) as shown in Chart 3.

When **2** was allowed to react with **12**, the 2-methoxycarbonylmethyl-3-indolinone **16** was obtained in 76% yield, together with **17** in 9% yield. The structures were confirmed by the analytical and spectral data (see Experimental). The preferential formation of **16** may be explained as follows; since the chain form **2B** may exist in a small amout under the reaction conditions, the ylide **12** may attack the acetyl carbonyl group of **2B** (path a), which is more reactive than the benzoyl of **2B** and the 3-keto carbonyl of **2A**.

In contrast, the reaction of **3** with **12** preferentially gave the 2-hydroxy-3-methoxycarbonylmethyleneindoline **18** in 81% yield; the structure of **18** was assigned on the basis of its spectral data (see Experimental). In this case, no evidence was found for the existence of the open-chain form **18B** in DMSO-d_6.[4] The formation of **18** may proceed *via* attack of **12** on the carbonyl of **3A** (path c), since, if **12** reacts with **3B**, it would attack not the benzoyl carbonyl of **3B**, but the more reactive aldehyde carbonyl of **3B** (path a) to form another type of product such as **16**.

These results show that the reaction course is dependent on the substituent at the 2-position of **1**—**3**, since it affects the ring-chain tautomerism.

Finally, we examined the acetylation and reaction of the 2,3-dihydroxyindoline **4** with the ylide **12**. Treatment of **4** with acetic anhydride in pyridine gave the 2-acetoxymethyl-3-methyl- and 3-acetoxymethyl-2-methylindoles, **20** and **21**, in 41% and 15% yields, respectively; the structures of these products were confirmed by the spectra data (see Experimental). The formation of **20** and **21** can be explained by the acetylation of the ring form **4A**, leading to the diacetate **19**, followed by elimination and rearrangement of the acetoxy groups, as shown in Chart 4.

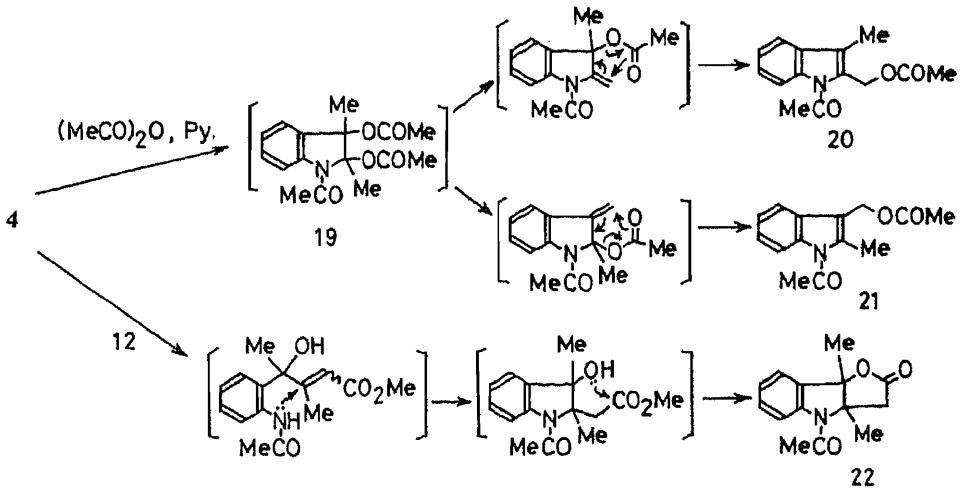

Chart 4

The reaction of **4** with **12** gave the furo[3,2-*b*]indole **22** in 31% yield. A plausible mechanism for the formation of **22** is shown in Chart 4.

Experimental

All melting points are uncorrected. IR spectra were recorded on a Hitachi 270-30 spectrophotometer. ^{1}H- and ^{13}C-NMR spectra were measured with JEOL JNM-PMX 60 and GX-400 spectrometers using tetramethylsilane as an

internal standard. MS were obtained with a JEOL D-300 spectrometer operating at 70 eV. Column chromatography was carried out on silica gel (80—100 mesh, Kanto Chemical Co., Inc.).

Methylation of 1-Acetyl-2-hydroxy-2-phenyl-3-indolinone (1)——A solution of **1** (0.267 g, 1 mmol) and potassium *tert*-butoxide (0.168 g, 1.5 mmol) in dry tetrahydrofuran (THF) (10 ml) was stirred at room temperature for 2 h, then a solution of methyl iodide (0.71 g, 5 mmol) in dry THF (10 ml) was added at room temperature. The mixture was stirred at the same temperature overnight, and concentrated under reduced pressure to give a residue, which was purified by column chromatography on silica gel with C_6H_6 as an eluent to give 1-acetyl-2-methoxy-2-phenyl-3-indolinone (**6**) (0.199 g, 71%), mp 101.5—103 °C (from C_6H_6). *Anal.* Calcd for $C_{17}H_{15}NO_3$: C, 72.58; H, 5.37; N, 4.98. Found: C, 72.42; H, 5.28; N, 4.99. IR $\nu_{max}^{CHCl_3}$ cm^{-1}: 1734 (C=O), 1683 (N–C=O). ^{1}H-NMR ($CDCl_3$) δ: 2.00 (3H, s, NCOMe), 3.37 (3H, s, –OMe), 7.05—8.0 (8H, m, Ar-H), 8.77 (1H, d, J=9 Hz, Ar-H). ^{13}C-NMR ($CDCl_3$) δ: 24.20 (q, COMe), 51.74 (q, –OMe), 94.84 (s, C-2), 118.08, 124.65, 124.67, 125.22, 128.94, 128.96, 129.00, 129.29, 138.29 (each d, Ar-C), 120.95, 135.56, 153.83 (each s, Ar-C), 170.69 (s, N–C=O), 195.00 (s, C-3).

Acetylation of 1——A solution of **1** (0.80 g, 3 mmol) and acetic anhydride (0.765 g, 7.5 mmol) in dry pyridine (14 ml) was allowed to stand at room temperature for 1 d. The reaction mixture was diluted with $CHCl_3$ (100 ml) and washed with 10% HCl (80 ml) and water. The $CHCl_3$ layer was dried over $MgSO_4$ and concentrated *in vacuo* to give a residue. The residue was purified by column chromatography on silica gel with $CHCl_3$ as an eluent to give 2-acetoxy-1-acetyl-2-phenyl-3-indolinone (**7**) (0.38 g, 41%), together with recovered **1** (0.44 g, 56%).

7: mp 219—220 °C (from C_6H_6–pet. ether) [lit.[1a] mp 205—206 °C]. *Anal.* Calcd for $C_{18}H_{15}NO_4$: C, 69.89; H, 4.89; N, 4.53. Found: C, 69.96; H, 4.75; N, 4.48. IR $\nu_{max}^{CHCl_3}$ cm^{-1}: 1770, 1744 (–COO–, C=O), 1688 (N–C=O). ^{1}H-NMR ($CDCl_3$) δ: 2.03, 2.26 (each 3H, each s, NCOMe, OCOMe), 7.26 (1H, d, J=8 Hz, Ar-H), 7.35—7.45 (5H, m, Ar-H), 7.65—7.75 (2H, m, Ar-H), 8.68 (1H, d, J=8 Hz, Ar-H). ^{13}C-NMR ($CDCl_3$) δ: 20.51, 24.78 (each q, Me), 90.85 (s, C-2), 117.87, 124.79, 123.94, 125.06, 129.42, 137.46 (each d, Ar-C), 121.12, 133.51, 137.46 (each s, Ar-C), 168.09, 169.57 (each s, O–C=O, N–C=O), 191.52 (s, C-3). MS *m/z*: 309 (M^+).

Acetylation of 1-Acetyl-2-hydroxy-3-indolinone (3)——Using a procedure similar to that described above for the acetylation of **1**, **3** (0.35 g, 1 mmol) was treated with acetic anhydride (0.47 g, 4.6 mmol) in dry pyridine (5 ml) for 4 d to give 2-acetoxy-1-acetyl-3-indolinone (**8**) (0.34 g, 81%), mp 93—95 °C (from ether). *Anal.* Calcd for $C_{12}H_{11}NO_4$: C, 61.80; H, 4.75; N, 6.01. Found: C, 61.70; H, 4.62; N, 5.97. IR $\nu_{max}^{CHCl_3}$ cm^{-1}: 1762, 1740 (–COO–, C=O), 1696 (N–C=O). ^{1}H-NMR ($CDCl_3$) δ: 2.18, 2.30 (each 3H, each s, NCOMe, OCOMe), 6.33 (1H, s, N–CH–O), 7.0—7.85 (3H, m, Ar-H), 8.41 (1H, d, J=8 Hz, Ar-H). MS *m/z*: 233 (M^+).

Reaction of 1 with *o*-Phenylenediamine (9)——A solution of **1** (0.765 g, 3 mmol) and **9** (0.324 g, 3 mmol) in acetic acid (10 ml) was heated at 100 °C for 1 h. After removal of the solvent under reduced pressure, the residue was purified by column chromatography on silica gel with $CHCl_3$–ethyl acetate (50:1) as an eluent to give 2-(2-acetylaminophenyl)-3-phenylquinoxaline (**10**) (1.00 g, 98%), mp 165—168 °C (from C_6H_6–*n*-hexane). *Anal.* Calcd for $C_{22}H_{17}N_3O$: C, 77.85; H, 5.05; N, 12.38. Found: C, 77.69; H, 4.84; N, 12.42. IR $\nu_{max}^{CHCl_3}$ cm^{-1}: 3400 (NH), 1688 (C=O). ^{1}H-NMR (DMSO-d_6) δ: 1.73 (3H, s, NCOMe), 7.0—8.4 (13H, m, Ar-H), 9.35 (1H, br s, NH, exchangeable with D_2O). MS *m/z*: 339 (M^+).

Reaction of 1-Acetyl-2-hydroxy-2-methyl-3-indolinone (2) with 9——By using a procedure similar to that described above for the reaction of **1** with **9**, **2** (0.615 g, 3 mmol) was treated with **9** (0.324 g, 3 mmol) to give 2-(2-acetylaminophenyl)-3-methylquinoxaline (**11**) (0.81 g, 97%), mp 180—182 °C (from C_6H_6). *Anal.* Calcd for $C_{17}H_{15}N_3O$: C, 73.63; H, 5.45; N, 15.15. Found: C, 73.91; H, 5.33; N, 15.23. IR $\nu_{max}^{CHCl_3}$ cm^{-1}: 3400 (NH), 1691 (C=O). ^{1}H-NMR (DMSO-d_6) δ: 1.80 (3H, s, NCOMe), 2.53 (3H, s, Me), 7.3—8.3 (8H, m, Ar-H), 9.45 (1H, br, NH, exchangeable with D_2O).

Reaction of 1 with Methoxycarbonylmethylenetriphenylphosphorane (12)——A solution of **1** (0.563 g, 2.1 mmol) and **12** (1.20 g, 3.6 mmol) in dry toluene (20 ml) was refluxed for 17 h. The reaction mixture was concentrated *in vacuo* and the crude material was subjected to column chromatography on silica gel with $CHCl_3$ as an eluent to give 1-acetyl-2-methoxycarbonylmethyl-2-phenyl-3-indolinone (**14**) (0.199 g, 29%) and 1-acetyl-2-hydroxy-3-methoxycarbonylmethylene-2-phenylindoline (**15**) (0.357 g, 52%) successively, in that order.

14: mp 174—176 °C (from C_6H_6). *Anal.* Calcd for $C_{19}H_{17}NO_4$: C, 70.57; H, 5.30; N, 4.33. Found: C, 70.33; H, 5.18; N, 4.31. IR $\nu_{max}^{CHCl_3}$ cm^{-1}: 1742, 1736, 1680 (C=O). ^{1}H-NMR ($CDCl_3$) δ: 2.18 (3H, s, NCOMe), 3.47 (3H, s, COOMe), 3.68, 4.02 (each 1H, each d, J=16 Hz, $-CH_2COO-$), 7.15—8.0 (8H, m, Ar-H), 8.67 (1H, br, Ar-H). MS *m/z*: 323 (M^+).

15: mp 158—163 °C (dec.) (from ether–*n*-hexane). *Anal.* Calcd for $C_{19}H_{17}NO_4$: C, 70.57; H, 5.30; N, 4.33. Found: C, 70.74; H, 5.21; N, 4.28. IR $\nu_{max}^{CHCl_3}$ cm^{-1}: 3594 (OH), 1715, 1665, 1637 (C=O). ^{1}H-NMR ($CDCl_3$) δ: 1.82, 2.12 (together 3H, each s, NCOMe), 3.59, 3.63 (together 3H, each s, COOMe), 5.08 (*ca.* 0.8H, br s, OH or NH), 5.82, 6.36 (together 1H, each s, C=CH–), 7.1—8.0 (m, Ar-H), 8.40, 8.74 (each 0.8H, each s, Ar-H). ^{13}C-NMR ($CDCl_3$) δ: 24.42, 24.55 (each q, NCOMe), 51.56, 52.10 (each q, OMe), 94.63 (s, C-2 of **15A**), 113.96, 116.58 (each d, =CH–), 165.13, 166.81, 168.63, 171.60 (each s, N–C=O, O–C=O 196.29 (s, Ph–C=O of **15B**). MS *m/z*: 323 (M^+).

Reaction of 2 with 12——A solution of **2** (0.87 g, 4.24 mmol) and **12** (3.12 g, 9.32 mmol) in $CHCl_3$ (50 ml) was refluxed for 7 h. After removal of the solvent under reduced pressure, the residue was chromatographed on a silica gel column. Elution with CH_2Cl_2 gave 1-acetyl-2-methoxycarbonylmethyl-2-methyl-3-indolinone (**16**) (0.84 g, 76%).

Elution with CH_2Cl_2–ethyl acetate (50:1) gave dimethyl 2-(2-acetylaminophenyl)-3-methyl-2,4-hexadienedioate (**17**) (0.125 g, 9%).

16: mp 102—103 °C (from C_6H_6). *Anal.* Calcd for $C_{14}H_{15}NO_4$: C, 64.36; H, 5.79; N, 5.36. Found: C, 64.44; H, 5.75; N, 5.43. IR $\nu_{max}^{CHCl_3}$ cm^{-1}: 1730, 1668 (C=O). ^{1}H-NMR ($CDCl_3$) δ: 1.55 (3H, s, Me), 2.51 (3H, s, NCOMe), 3.10, 3.90 (each 1H, each d, J=17 Hz, $-CH_2COO-$), 3.45 (3H, s, COOMe), 7.0—8.0 (4H, m, Ar-H). MS *m/z*: 261 (M^+).

17: mp 118—119.5 °C (from C_6H_6–ether). *Anal.* Calcd for $C_{17}H_{19}NO_5$: C, 63.34; H, 6.04; N, 4.41. Found: C, 64.13; H, 5.92; N, 4.37. IR $\nu_{max}^{CHCl_3}$ cm^{-1}: 3450 (NH), 1717 (C=O), 1615 (C=C). ^{1}H-NMR ($CDCl_3$) δ: 2.02 (3H, s, Me), 2.38 (3H, s, NCOMe), 3.55, 3.63 (each 3H, each s, COOMe), 5.65, 6.45 (each 1H, each s, C=CH–) 6.8—8.2 (5H, m, Ar-H, NH). MS *m/z*: 317 (M^+).

Reaction of 3 with 12——A solution of **3** (1.00 g, 5.2 mmol) and **12** (2.10 g, 6.3 mmol) in $CHCl_3$ (58 ml) was stirred at room temperature for 6 h. After removal of the solvent under reduced pressure, the residue was purified by column chromatography on silica gel with $CHCl_3$–ethyl acetate (9:1) as an eluent to give 1-acetyl-2-hydroxy-3-methoxycarbonylmethyleneindoline (**18**) (1.04 g, 81%), mp 143—144 °C (from ether). *Anal.* Calcd for $C_{13}H_{13}NO_4$: C, 63.15; H, 5.30; N, 5.67. Found: C, 63.22; H, 5.27; N, 5.51. IR $\nu_{max}^{CHCl_3}$ cm^{-1}: 3500 (OH), 1690 (O–C=O), 1640 (N–C=O). ^{1}H-NMR (DMSO-d_6) δ: 2.36 (3H, s, NCOMe), 3.74 (3H, s, COOMe), 6.57 (1H, d, J=1.5 Hz, C=CH–), 6.60 (1H, d, J=8 Hz, O–CH–C=), 6.98 (1H, d, J=8 Hz, OH, exchangeable with D_2O), 7.12, 7.43 (each 1H, each t, J=8 Hz, Ar-H), 7.84, 8.14 (each 1H, each d, J=8 Hz, Ar-H). ^{13}C-NMR (DMSO-d_6) δ: 23.19 (q, NCOMe), 51.26 (q, OMe), 82.25 (d, C-2), 110.28 (d, =CH–), 116.12, 122.37, 123.51, 132.56 (each d, Ar-C), 125.22, 144.41, 152.72 (each s, Ar-C, C-3), 165.35, 168.97 (each s, N–C=O, O–C=O). MS *m/z*: 247 (M^+).

Acetylation of 1-Acetyl-2,3-dihydroxy-2,3-dimethylindoline (4)——By using a procedure similar to that described above for the acetylation of **1**, **4** (0.443 g, 2 mmol) was treated with acetic anhydride (1.74 g, 17 mmol) in dry pyridine (4 ml) at 50 °C for 2 d. The reaction mixture was purified by column chromatography on silica gel with CH_2Cl_2 as an eluent to give 2-acetoxymethyl-1-acetyl-3-methylindole (**20**) (0.202 g, 41%) and 3-acetoxymethyl-1-acetyl-2-methylindole (**21**) (0.075 g, 15%).

20: mp 65—66 °C (from ether–*n*-hexane). *Anal.* Calcd for $C_{14}H_{15}NO_3$: C, 68.55; H, 6.16; N, 5.71. Found: C, 68.43; H, 6.09; N, 5.65. IR $\nu_{max}^{CHCl_3}$ cm^{-1}: 1738 (O–C=O), 1703 (N–C=O). ^{1}H-NMR ($CDCl_3$) δ: 2.05 (3H, s, OCOMe), 2.32 (3H, s, Me), 2.75 (3H, s, NCOMe), 5.47 (2H, s, $-CH_2OCO-$), 7.1—8.0 (4H, m, Ar-H). MS *m/z*: 245 (M^+).

21: mp 102—103 °C (from ether–*n*-hexane). *Anal.* Calcd for $C_{14}H_{15}NO_3$: C, 68.55; H, 6.16; N, 5.71. Found: C, 68.45; H, 6.19; N, 5.61. IR $\nu_{max}^{CHCl_3}$ cm^{-1}: 1736 (O–C=O), 1708 (N–C=O). ^{1}H-NMR ($CDCl_3$) δ: 2.03 (3H, s, OCOMe), 2.63 (3H, s, Me), 2.70 (3H, s, NCOMe), 5.25 (2H, s, $-CH_2OCO-$), 7.1—8.1 (4H, m, Ar-H). MS *m/z*: 245 (M^+).

The introduction of the acetoxy groups in **20** and **21** was confirmed by comparison of the chemical shifts of the methyl groups at the 2- and 3-positions with those of 1-acetyl-3-methoxymethyl-2-methyl- (δ 2.58) and 1-acetyl-2-methoxymethyl-3-methylindole (δ 2.26).[9]

Reaction of 4 with 12——By using a procedure similar to that described above for the reaction of **1** with **12**, **4** (0.663 g, 3 mmol) was treated with **12** (1.10 g, 3.3 mmol) in dry toluene (30 ml) for 7 h. The reaction mixture was purified by column chromatography on silica gel with CH_2Cl_2 as an eluent to give 4-acetyl-3,3a,4,8b-tetrahydro-3a,8b-dimethylfuro[3,2-*b*]indol-2(H)-one (**22**) (0.229 g, 31%), mp 208—210 °C (from C_6H_6). *Anal.* Calcd for $C_{14}H_{15}NO_3$: C, 68.55; H, 6.16; N, 5.71. Found: C, 68.45; H, 6.15; N, 5.67. IR $\nu_{max}^{CHCl_3}$ cm^{-1}: 1770 (O–C=O), 1662 (N–C=O). ^{1}H-NMR ($CDCl_3$) δ: 1.53, 1.73 (each 3H, each s, Me), 2.47 (3H, s, NCOMe), 2.83, 3.83 (each 1H, each d, J=19 Hz, $-CH_2COO-$), 7.0—7.7 (4H, m, Ar-H). MS *m/z*: 245 (M^+).

Acknowledgement The authors wish to thank the staff of the Analysis Center of this college for elemental analysis (Miss A. Koike), and measurements of NMR (Miss Y. Takeuchi) and MS (Mr. K. Sato).

References and Notes

1) *a*) C. W. Rees and C. R. Sabet, *J. Chem. Soc.*, **1965**, 870; *b*) O. Buchardt and C. Lohse, *Tetrahedron Lett.*, **1966**, 4355; *c*) O. Buchardt, J. Becher, and C. Lohse, *Acta Chem. Scand.*, **20**, 2467 (1966); *d*) O. Buchardt, B. Jensen, and I. K. Larsen, *ibid.*, **21**, 1841 (1967); *e*) O. Buchardt, P. L. Kumler, and C. Lohse, *ibid.*, **23**, 159 (1969); *f*) *Idem, ibid.*, **23**, 1155 (1969); *g*) D. M. Harrison, *Tetrahedron Lett.*, **1984**, 6063; *h*) For reviews dealing with the ring-chain tautomerism; P. R. Jones, *Chem. Rev.*, **63**, 461 (1963); R. Valters, *Russ. Chem. Rev.*, **43**, 665 (1974).

2) *a*) T. Kawasaki, C.-S. Chien, and M. Sakamoto, *Chem. Lett.*, **1983**, 855; *b*) C.-S. Chien, T. Suzuki, T. Kawasaki, and M. Sakamoto, *Chem. Pharm. Bull.*, **32**, 3945 (1984); *c*) C.-S. Chien, T. Takanami, T. Kawasaki, and M. Sakamoto, *ibid.*, **33**, 1843 (1985).

3) The know reactions of 1-acetyl-2-hydroxyindolines are dehydration,[3a] acetylation,[1a] oxidations,[3a,b] and rearrangements[1a,3b–e]; *a*) O. Buchardt, J. Becher, C. Lohse, and J. Moller, *Acta Chem. Scand.*, **20**, 262 (1966); *b*) C. M. Atkinson, J. W. Kershaw, and A. Taylor, *J. Chem. Soc.*, **1962**, 4426; *c*) B. Witkop, *J. Am. Chem. Soc.*, **72**, 614 (1950); *d*) J. B. Patrick and B. Witkop, *ibid.*, **72**, 633 (1950); *e*) J. W. Kershaw and A. Taylor, *J. Chem. Soc.*, **1964**, 4320.

4) The cyclic tautomer B, if present, may exist only at very low concentrations under the conditions employed.
5) S. H. Pine, J. B. Hendrickson, D. J. Cram, and G. S. Hammond, "Organic Chemistry," 4th ed., McGraw-Hill, Inc., Tokyo, 1981, pp. 253—256.
6) The methylation of **2** was achieved by the use of diazomethane.[7]
7) C.-S. Chien, A. Hasegawa, T. Kawasaki, and M. Sakamoto, *Chem. Pharm. Bull.*, **34**, 1493 (1986).
8) A. E. A. Porter, "Comprehensive Heterocyclic Chemistry," Vol. 3, ed. by A. R. Katritzky, Pergamon Press, New York, 1984, pp. 157—197.
9) S. F. Vice and G. I. Dmitrienko, *Can. J. Chem.*, **60**, 1233 (1982).

[Chem. Pharm. Bull. 35(4)1347—1352(1987)]

Studies on Fungal Products. XI.[1] Isolation and Structures of Novel Cyclic Pentapeptides from *Aspergillus* sp. NE-45

REIJI KOBAYASHI,[a] YUJI SAMEJIMA,[a] SHOICHI NAKAJIMA,[a]
KEN-ICHI KAWAI*,[a] and SHUN-ICHI UDAGAWA[b]

Faculty of Pharmaceutical Sciences, Hoshi University,[a] Ebara 2-4-41, Shinagawa-ku, Tokyo 142, Japan and National Institute of Hygienic Sciences,[b] Kamiyoga 1-18-1, Setagaya-ku, Tokyo 158, Japan

(Received July 24, 1986)

Three new compounds designated as cycloaspeptides A (**1**), B (**2**), and C (**3**) were isolated along with ergosterol from the mycelial chloroform extract of *Aspergillus* sp. NE-45. The structures of cycloaspeptides A, B, and C were established on the basis of chemical and spectroscopic evidence as **1**, **2**, and **3**, respectively. Cycloaspeptides are new cyclic pentapeptides containing an anthranilic acid residue and two *N*-methyl amino acid residues.

Keywords——*Aspergillus*; cyclic peptide; cycloaspeptide A; cycloaspeptide B; cycloaspeptide C; anthranylic acid; *N*-methyl amino acid; amino acid analysis

Aspergillus sp. NE-45 is a fungus isolated from soil of the forest between Chumro and Kuldi Ghar, Gandaki, Western Development Region in Nepal, collected by S. Udagawa in 1980.[2] Three new compounds, which were designated cycloaspeptides A (**1**), B (**2**), and C (**3**), along with ergosterol, were isolated from the mycelial chloroform extract of this fungus. The structural elucidation of the above compounds (**1**—**3**) is reported in this paper.

Cycloaspeptide A (**1**), mp 270—272 °C, $[\alpha]_D$ −228°, gave a molecular ion at *m/z* 641 on field desorption (FD) and electron impact ionization (EI) mass spectrometry, and elemental analysis confirmed its empirical formula as $C_{36}H_{43}N_5O_6$. The absorptions at 1680 and 1650 cm^{-1} in the infrared (IR) spectrum of **1**, and the positive chlorine–tolidine test (blue),[3] suggested the presence of amides, but not esters, in its structure. The carbon-13 nuclear magnetic resonance (^{13}C-NMR) signals at δ 168.03, 168.13, 169.51, 169.59, and 174.13 were assigned to five amide carbonyls. On acetylation, **1** afforded a monoacetate (**4**), mp 178—180 °C, $[\alpha]_D$ −138°, $C_{38}H_{45}N_5O_7$, which showed a proton nuclear magnetic resonance (^{1}H-NMR) signal at δ 2.266 (3H, s), assigned to the methyl protons of an aromatic acetoxy group. No other significant changes were observed at **4** compared with **1**. Thus it is clear that the remaining one oxygen in **1** is a phenolic hydroxyl. On methylation with methyl iodide and sodium hydride, **1** gave a penta-*N*-methyl-*O*-methyl derivative (**5**), mp 166—168 °C, $C_{40}H_{51}N_5O_6$, which showed five *N*-methyl signals (δ 2.590, 2.616, 2.818, 3.075, and 3.621) and one aromatic *O*-methyl signal (δ 3.786). No IR absorption due to a hydroxyl, amino, or imino group was observed in the molecule of **5**. The negative reactivity in the ninhydrin test indicated the absence of an amino group in **1**. The above results suggested that **1** was a cyclic pentapeptide.

The homonuclear ^{1}H-{^{1}H} decoupling experiments and the analysis of the ^{13}C-NMR spectrum of **1** (Fig. 1) suggested the presence of alanine (Ala), leucine (Leu), *N*-methylphenylalanine (MePhe), *N*-methyltyrosine (MeTyr), and anthranilic acid (*o*-aminobenzoic acid, ABA) as amino acid residues. Me-L-Phe and Me-L-Tyr were synthesized from L-phenylalanine (Phe) and L-tyrosine (Tyr), respectively, in accordance with the method of

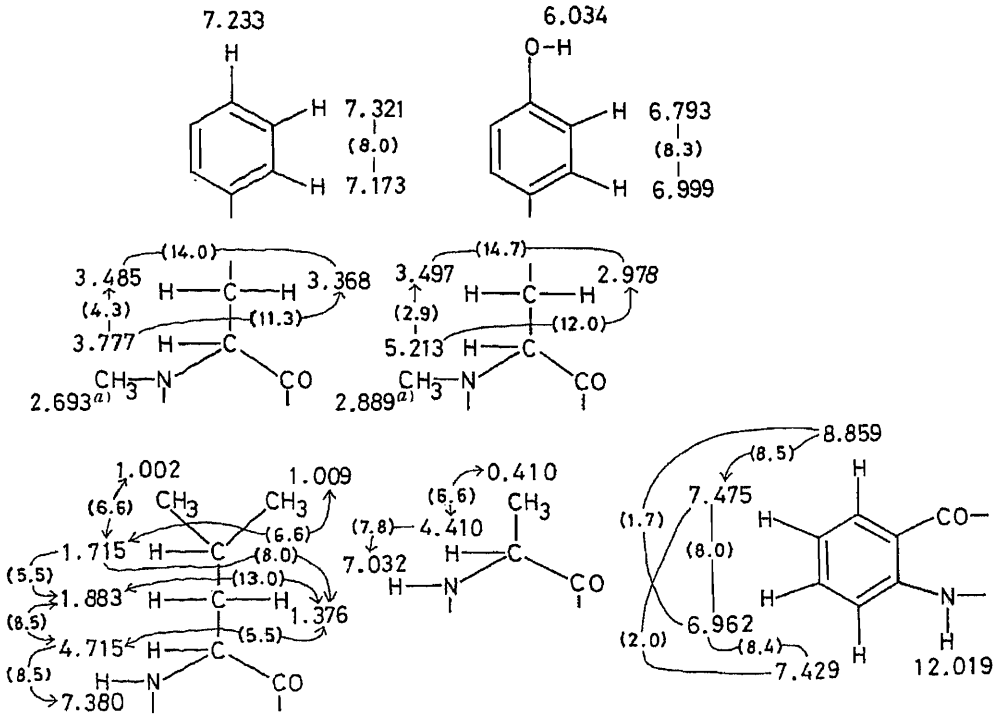

Fig. 1. ^{1}H-NMR Chemical Shift Assignments of Cycloaspeptide A (1)

An arrow ($H_a \rightarrow H_b$) indicates that proton b was decoupled when proton a was irradiated. The coupling constants are given in parentheses.
a) The assignments may be reversed.

TABLE I. Amino Acid Components of Complete Hydrolysates of Cycloaspeptides A (1), B (2), and C (3)

Hydrolysates	Amino acid components[a]				
1	Ala[b]	MePhe[c]	Leu[b]	MeTyr[c]	ABA[c]
2	Ala[b]	MePhe[c]	Leu[b]	Tyr[b]	ABA[c]
3	Ala[b]	Phe[b]	Leu[b]	MeTyr[c]	ABA[c]

a) Detected by cellulose TLC with ninhydrin reagent. *b*) Also detected by amino acid analysis. *c*) Also detected by HPLC with detection at 254 nm.

Coggins and Benoiton[4] for use as standard samples in amino acid analysis. L-Phe and *O*-benzyl-L-Tyr (L-Tyr was benzylated preliminarily[5]) were reacted with benzyloxycarbonyl chloride, methylated with methyl iodide and sodium hydride, and then hydrolyzed and hydrogenated to give Me-L-Phe and Me-L-Tyr. The acid hydrolysates of **1** were analyzed by cellulose thin layer chromatography (TLC), and Ala, MeTyr, Leu, and MePhe were detected with ninhydrin reagent (Table I). In addition, at the top of the TLC plate, a strong blue fluorescent spot, which showed no coloration with ninhydrin, was detected under ultraviolet (UV) light. This compound was shown to be identical with authentic ABA on silica gel TLC after extraction with chloroform. The result of the amino acid analysis and high performance liquid chromatography (HPLC) also confirmed that **1** was composed of Ala, Leu, MePhe, MeTyr, and ABA.

It was necessary to obtain a linear peptide by the partial hydrolysis of **1** in order to determine the arrangement of the amino acid residues, because **1** has neither a C-terminal nor an N-terminal. Partial acid hydrolyses under various conditions were examined in order to get

TABLE II. Amino Acid Components of Partial Acid Hydrolysates Derived from Cycloaspeptide A (1)

Peptide	Amino acid components[a]			
IA	Ala[b]	MePhe[c]	Leu[b]	
IB	MePhe[c]	Leu[b]	MeTyr[c]	
IC	Ala[b]	MePhe[c]	ABA[c]	
ID	Ala[b]	MePhe[c]	Leu[b]	ABA[c]

a) Detected by cellulose TLC with ninhydrin reagent. *b*) Also detected by amino acid analysis. *c*) Also detected by HPLC with detection at 254 nm.

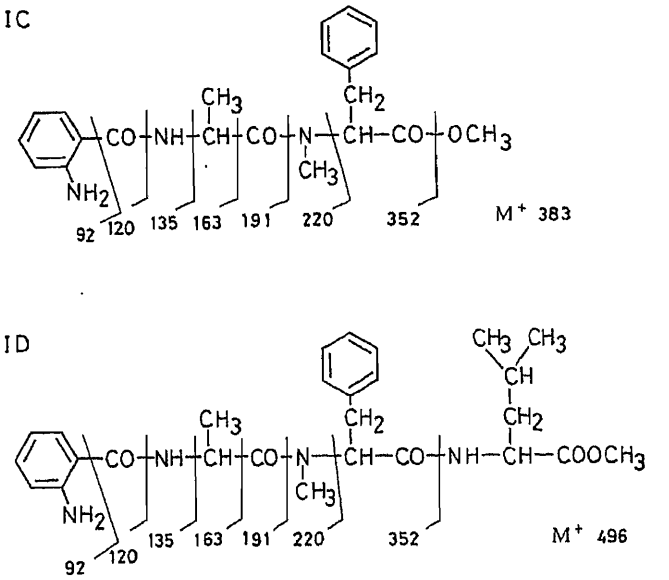

Fig. 2. Mass Fragmentation of Methyl Esters of Peptides IC and ID (*m/z*)

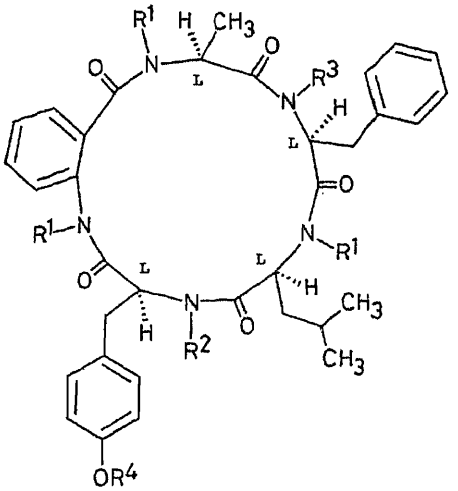

1: $R^1=R^4=H$, $R^2=R^3=CH_3$
2: $R^1=R^2=R^4=H$, $R^3=CH_3$
3: $R^1=R^3=R^4=H$, $R^2=CH_3$
4: $R^1=H$, $R^2=R^3=CH_3$, $R^4=COCH_3$
5: $R^1=R^2=R^3=R^4=CH_3$

Chart 1

a single peptide, but two or more peptides were obtained in each experiment. Thus the best partial hydrolysate (with 12 N HCl–AcOH at 27 °C for 48 h) was analyzed by amino acid analysis, HPLC, and cellulose TLC. The results are shown in Table II. The C-terminals of the peptide fragments, IC and ID, were methylated with diazomethane, and the mass spectra (MS) of the methyl esters prepared from peptides IC and ID showed favorable fragmentation (Fig. 2). The structures of the methyl esters of IC and ID were determined as H–ABA–Ala–MePhe–OH and H–ABA–Ala–MePhe–Leu–OH, respectively. The above results confirmed the structure of cycloaspeptide A to be **1**.

Cycloaspeptides B (**2**), mp 250—252 °C, $[\alpha]_D$ −138° [tetrahydrofuran (THF)–dimethylformamide (DMF)], and C (**3**), mp 281—283 °C, $[\alpha]_D$ −168° (THF–DMF), were confirmed to have the molecular formula $C_{35}H_{41}N_5O_6$. Both compounds were positive in the chlorine–tolidine test (blue) and negative in the ninhydrin test. The ^{1}H-NMR spectra of **2** and **3** were closely similar to that of **1** except for the absence of one *N*-methyl group in **2** and **3**. The ^{1}H-NMR signals assigned to *N*-methyl groups were observed at δ2.693 and 2.889 in **1**, whereas signals were observed at δ2.797 in **2** and at δ2.552 in **3**. The permethylation of **2** and **3** gave the same compound (**5**) as that of **1**. Thus, it is clear that **2** and **3** are cyclic pentapeptides identical with **1**, except for the number of *N*-methyl groups. On complete acid hydrolysis (Table I), **2** gave Tyr and MePhe, and **3** gave MeTyr and Phe, whereas **1** afforded

MeTyr and MePhe. Compounds **2** and **3** are thus the demethyl derivatives at MeTyr and MePhe in the structure of **1**, respectively. The above results confirmed the structures of cycloaspeptides B and C as **2** and **3**, respectively.

In order to determine the stereochemistry of **1**, each amino acid separated after the complete acid hydrolysis of **1** was converted to the 2,4-dinitrophenyl (DNP) derivative.[6] Comparison of the circular dichroism (CD) curves[7] of these compounds with those of the standard derivatives, prepared from L-amino acids, confirmed that the stereochemistry of the amino acid components of **1** was L-ala, Me-L-Phe, L-Leu, and Me-L-Tyr. Consequently the structure of **1** was determined as cyclo (L-alanyl-*N*-methyl-L-phenylalanyl-L-leucyl-*N*-methyl-L-tyrosyl-*o*-aminobenzoyl) as shown in **1**, including its absolute stereochemistry.

Anthranilic acid (ABA) derivatives have been isolated from various fungi, and cyclopenin[8] and its derivatives, dioxopiperazines including an ABA residue, were isolated from *Penicillium cyclopium*, but cyclic peptides containing ABA in the molecule are very rate. Cycloaspeptide A (**1**) had no antifungal or antibacterial activity[9] at concentrations lower than 100 μg/disc. Since many of the cyclic peptides isolated from fungi and known to be toxic, cycloaspeptides may have some biological activity. Further tests are planned.

Experimental

Melting points are uncorrected. IR and UV spectra were taken with a Hitachi 215 spectrophotometer and a Hitachi 124 spectrophotometer, respectively. EI, FD, and chemical ionization (CI) MS were obtained on a JEOL JMS-D 300 spectrometer. ^{1}H- and ^{13}C-NMR spectra were measured with a JEOL JNM-GX 400 spectrometer at 399.78 and 100.43 MHz, respectively, using tetramethylsilane as an internal standard. The coupling patterns are indicated as follows: singlet=S or s, doublet=D or d, Triplet=T or t, quarter=Q or q, multiplet=m, and broad=br. Capital letters refer to the pattern resulting from directly bonded coupling ($^1J_{C,H}$). Optical rotations were measured with a JASCO DIP-181 spectrometer. CD curves were determined on a JASCO J-40 spectrophotometer. Amino acid analyses were performed on a JEOL JLC-5AH automatic amino acid analyzer equipped with a Shimadzu Chromatopac C-RIB, on a Nihon Seimitsu NSLC-100 HPLC, and/or Merck HPTLC precoated cellulose plates.

Isolation of Cycloaspeptides A (1), B (2), and C (3)——*Aspergillus* sp., strain NE-45, was cultivated at 27 °C for 14—17 d in Czapek-Dox medium using 300 Roux flasks containing 250 ml of the above medium in each flask. The dried mycelia (980 g) were pulverized, defatted with hexane, and extracted with chloroform at room temperature. The evaporated residue (19 g) was chromatographed on silica gel successively with benzene–acetone (10 : 1) to obtain ergosterol (180 mg), with benzene–acetone (5 : 1) to give cycloaspeptide A (**1**) (700 mg), with benzene–acetone (3 : 1) to obtain cycloaspeptide B (**2**) (36 mg), and finally with benzene–acetone (2 : 1) to afford cycloaspeptide C (**3**) (27 mg).

Cycloaspeptide A (**1**): Colorless needles with violet fluorescence under UV, mp 270—272 °C from MeOH. $[\alpha]_D^{20}$ −228° (c=1.01, $CHCl_3$). IR ν_{max}^{KBr} cm^{-1}: 3300 (OH, NH), 1680, 1650 (amide), 1630, 760. UV λ_{max}^{EtOH} nm (log ε): 223 (4.62), 242 (4.29), 248 (4.29), 254 (4.37), 260 (4.30), 286 (3.65), 308 (3.76). EI-MS m/z(%): 641 (M^+, 6), 497 (14), 352 (11), 351 (10), 285 (51), 184 (80), 134 (98), 120 (100), 113 (40), 107 (73), 91 (55), 44 (58). FD-MS m/z (%): 680 [$(M+K)^+$, 11], 664 [$(M+Na)^+$, 56], 641 (M^+, 100). *Anal.* Calcd for $C_{36}H_{43}N_5O_6 \cdot H_2O$: C, 65.53; H, 6.88; N, 10.62. Found: C, 65.67; H, 6.73; N, 10.34. ^{1}H-NMR ($CDCl_3$) δ: 0.410 (3H, d, J=6.6 Hz), 1.002 (3H, d, J=6.6 Hz), 1.009 (3H, d, J=6.6 Hz), 1.376 (1H, ddd, J=13.0, 8.0, 5.5 Hz), 1.715 (1H, m), 1.883 (1H, ddd, J=13.0, 8.5, 5.5 Hz), 2.693 (3H, s, NMe), 2.889 (3H, s, NMe), 2.978 (1H, dd, J=14.7, 12.0 Hz), 3.368 (1H, dd, J=14.0, 11.3 Hz), 3.485 (1H, dd, J=14.0, 4.3 Hz), 3.497 (1H, dd, J=14.7, 2.9 Hz), 3.777 (1H, dd, J=11.3, 4.3 Hz), 4.410 (1H, qd, J=6.6, 7.8 Hz), 4.715 (1H, ddd, J=8.5, 8.5, 5.5 Hz), 5.213 (1H, dd, J=12.0, 2.9 Hz), 6.034 (1H, s, OH), 6.793 (2H, d, J=8.3 Hz), 6.962 (1H, br dd, J=8.4, 8.0 Hz), 6.999 (2H, d, J=8.3 Hz), 7.032 (1H, d, J=7.8 Hz, –CONH–), 7.173 (2H, br d, J=8.0 Hz), 7.233 (1H, t-like), 7.321 (2H, t-like), 7.380 (1H, d, J=8.5 Hz, –CONH–), 7.429 (1H, dd, J=8.4, 2.0 Hz), 7.475 (1H, ddd, J=8.5, 8.0, 2.0 Hz), 8.859 (1H, dd, J=8.5, 1.7 Hz), 12.019 (1H, s, –CONH–). ^{13}C-NMR ($CDCl_3$) δ: 16.02 (Q), 21.84 (Q), 23.26 (Q), 24.76 (D), 30.02 (Q, NMe), 31.98 (T), 33.97 (T), 39.04 (Q, NMe), 41.12 (T), 44.15 (D), 48.84 (D), 63.29 (D), 69.94 (D), 114.90 (S), 115.63 (D×2), 120.72 (D), 122.18 (D), 126.83 (D), 127.14 (D), 129.07 (D×2), 129.28 (D×2), 130.19 (D×2), 130.23 (S), 134.22 (D), 137.46 (S), 141.25 (S), 154.90 (S), 168.03 (S, CON), 168.13 (S, CON), 169.51 (S, CON), 169.59 (S, CON), 174.13 (S, CON). CD (c=8.97×10^{-4}, MeOH) $[\theta]^{20}$ (nm): −9.14×10^3 (231), −4.46×10^3 (254), −3.79×10^3 (262), +0.45×10^3 (297).

Cycloaspeptide B (**2**): Colorless needles with violet fluorescence under UV, mp 250—252 °C from MeOH. $[\alpha]_D^{15}$ −138° (c=0.10, THF–DMF). IR ν_{max}^{KBr} cm^{-1}: 3480, 3360, 3280 (OH, NH), 1660, 1630 (amide). UV λ_{max}^{EtOH} nm (log ε): 222 (3.84), 257 (3.82), 278 (3.75). EI-MS m/z (%): 627 (M^+, 0.5), 497 (10), 368 (11), 271 (15), 134 (57), 120 (40), 113 (38), 107 (30), 91 (37), 44 (100). FD-MS m/z (%): 666 [$(M+K)^+$, 12], 650 [$(M+Na)^+$, 25], 627 (M^+, 100). *Anal.* Calcd

for $C_{35}H_{41}N_5O_6 \cdot 2H_2O$: C, 63.83; H, 6.83; N, 10.55. Found: C, 63.67; H, 6.89; N, 10.52. ^{1}H-NMR (Me_2SO-d_6) δ: 0.258 (3H, d, J=6.6 Hz), 0.749 (3H, d, J=6.6 Hz), 0.776 (3H, d, J=6.6 Hz), 1.023 (1H, m), 1.352 (2H, m), 2.797 (3H, s, NMe), 2.843 (1H, dd, J=14.0, 3.3 Hz), 2.857 (1H, dd, J=14.2, 12.1 Hz), 3.320 (1H, dd, J=14.2, 3.7 Hz), 3.330 (1H, dd, J=14.0, 2.9 Hz), 4.334 (2H, m), 4.694 (1H, dd, J=10.6, 4.0 Hz), 5.222 (1H, dd, J=12.1, 3.7 Hz), 6.663 (2H, d, J=8.4 Hz), 7.011 (2H, d, J=8.4 Hz), 7.155 (1H, ddd, J=7.9, 7.4, 1.1 Hz), 7.289 (5H, m), 7.558 (1H, ddd, J=8.4, 7.4, 1.4 Hz), 7.883 (1H, dd, J=7.9, 1.4 Hz), 8.070 (1H, br d, J=8.5 Hz, -CONH-), 8.450 (1H, br d, J=8.9 Hz, -CONH-), 8.660 (1H, br d, J=8.4 Hz), 8.713 (1H, br d, J=3.0 Hz, -CONH-), 9.373 (1H, s, OH), 11.877 (1H, s, -CONH-).

Cycloaspeptide C (**3**): Colorless needles with violet fluorescence under UV, mp 281—283 °C from MeOH. $[\alpha]_D^{15}$ −168° (c=0.09, THF-DMF). IR ν_{max}^{KBr} cm^{-1}: 3350, 3240 (OH, NH), 1665, 1630 (amide). UV λ_{max}^{EtOH} nm (log ε): 222 (4.27), 257 (4.17), 263 sh (4.16), 278 sh (4.01). FD-MS m/z (%): 628 [(M+H)$^+$, 100], 627 (M$^+$, 53). *Anal.* Calcd for $C_{35}H_{41}N_5O_6 \cdot 11/3H_2O$: C, 64.68; H, 6.75; N, 10.75. Found: C, 64.49; H, 6.45; N, 10.62. ^{1}H-NMR (Me_2SO-d_6) δ: 0.866 (3H, d, J=6.7 Hz), 0.902 (3H, d, J=6.4 Hz), 1.079 (3H, d, J=7.2 Hz), 1.179 (1H, ddd, J=13.3, 7.8, 5.7 Hz), 1.511 (1H, m), 1.694 (1H, ddd, J=13.3, 7.8, 5.7 Hz), 2.552 (3H, s, NMe), 2.806 (1H, dd, J=12.7, 11.5 Hz), 2.918 (1H, dd, J=12.7, 4.4 Hz), 3.086 (1H, m), 3.330 (1H, m), 3.810 (1H, qd, J=7.2, 4.8 Hz), 4.127 (1H, dd, J=9.3, 5.8 Hz), 4.345 (1H, ddd, J=8.5, 7.8, 5.7 Hz), 4.418 (1H, ddd, J=11.5, 10.5, 4.4 Hz), 6.666 (2H, d, J=8.2 Hz), 6.934 (2H, d, J=8.2 Hz), 7.113 (1H, br t, J=7.8 Hz), 7.139 (2H, br d, J=7.8 Hz), 7.196 (1H, br t, J=7.8 Hz), 7.258 (2H, br t, J=7.8 Hz), 7.527 (1H, br dd, J=8.5, 7.8 Hz), 7.773 (1H, d, J=10.5 Hz, -CONH-), 7.897 (1H, br d, J=7.8 Hz), 8.224 (1H, d, J=8.5 Hz, -CONH-), 8.802 (1H, br d, J=8.5 Hz), 8.842 (1H, d, J=4.8 Hz, -CONH-), 9.232 (1H, s, OH), 11.424 (1H, s, -CONH-).

Acetylation of 1——Compound **1** (50 mg) was dissolved in pyridine (0.5 ml) containing acetic anhydride (1.0 ml), and the solution was kept overnight at room temperature. Then the reaction mixture was poured into ice-water and extracted with chloroform. The evaporated extract was chromatographed on silica gel with benzene–acetone (10 : 1) to give a monoacetate (**4**) (34 mg). Colorless needles with violet fluorescence under UV, mp 178—180 °C from MeOH. $[\alpha]_D^{15}$ −138° (c=0.10, $CHCl_3$). IR ν_{max}^{KBr} cm^{-1}: 3500, 3300 (NH), 1760 (COO), 1660, 1630 (amide). UV λ_{max}^{EtOH} nm (log ε): 257 (4.39), 264 sh (4.37), 282 (4.12). EI-MS m/z (%): 683 (M$^+$, 12), 540 (12), 421 (7), 352 (15), 315 (14), 308 (7), 192 (26), 189 (23), 134 (100), 120 (32). CI-MS m/z (%): 684 [(M+1)$^+$, 20], 195 (100). *Anal.* Calcd for $C_{38}H_{45}N_5O_7 \cdot CH_3OH$: C, 65.43; H, 6.90; N, 9.78. Found: C, 65.66; H, 6.75; N, 9.85. ^{1}H-NMR (Me_2SO-d_6) δ: 0.233 (3H, d, J=6.6 Hz), 0.879 (3H, d, J=6.6 Hz), 0.908 (3H, d, J=6.6 Hz), 1.275 (1H, m), 1.531 (1H, m), 1.668 (1H, m), 2.266 (3H, s, OAc), 2.659 (3H, s, NMe), 2.688 (3H, s, NMe), 2.860 (1H, dd, J=14.4, 12.0 Hz), 3.20—3.42 (3H, m), 4.283 (1H, m), 4.445 (2H, m), 5.306 (1H, dd, J=11.5, 2.9 Hz), 7.061 (2H, d, J=8.5 Hz), 7.065 (1H, m), 7.202 (2H, d, J=8.5 Hz), 7.275 (5H, m), 7.514 (1H, br dd, J=8.4, 7.3 Hz), 7.979 (1H, br d, J=7.3 Hz), 8.763 (1H, d, J=8.4 Hz), 8.770 (1H, d, J=8.4 Hz, -CONH-), 8.839 (1H, d, J=5.1 Hz, -CONH-), 11.952 (1H, s, -CONH-).

Permethylation of 1——Compound **1** (50 mg) was dissolved in anhydrous THF (10 ml) and added to a suspension of sodium hydride (300 mg) in anhydrous THF (10 ml). The mixture was stirred at room temperature for 3 h. After addition of methyl iodide (5 ml), the mixture was further stirred at room temperature for 24 h, and the solvent was evaporated off. The residue was chromatographed on silica gel with chloroform–methanol (50 : 1) to give a penta-*N*-methyl-*O*-methyl derivative (**5**) (27 mg). Colorless crystalline powder, mp 166—168 °C from *n*-hexane. IR ν_{max}^{KBr} cm^{-1}: 1650 sh, 1630 (amide). EI-MS m/z (%): 697.3825 (M$^+$, 24) (697.3837 Calcd for $C_{40}H_{51}N_5O_6$), 596 (58), 563 (23), 507 (17), 449 (16), 379 (32), 296 (31), 219 (48), 134 (70), 111 (100). ^{1}H-NMR ($CDCl_3$) δ: 0.663 (3H, d, J=6.7 Hz), 0.809 (3H, d, J=6.6 Hz), 0.819 (3H, d, J=6.6 Hz), 1.314 (1H, m), 1.825 (2H, m), 2.567 (1H, m), 2.590 (3H, s, NMe), 2.616 (3H, s, NMe), 2.812 (1H, m), 2.818 (3H, s, NMe), 3.075 (3H, s, NMe), 3.095 (2H, m), 3.621 (3H, s, NMe), 3.725 (1H, m), 3.786 (3H, s, OMe), 4.583 (1H, q, J=6.7 Hz), 4.920 (1H, dd, J=11.7, 2.3 Hz), 5.236 (1H, dd, J=11.0, 3.4 Hz), 5.582 (1H, dd, J=6.3, 2.1 Hz), 6.903 (2H, d, J=8.7 Hz), 7.227 (2H, d, J=8.7 Hz), 7.20—7.37 (7H, m), 7.473 (1H, br t, J=8.1 Hz), 8.964 (1H, br d, J=8.1 Hz).

Permethylation of 2 and 3——Compounds **2** (5 mg) and **3** (5 mg) were methylated with sodium hydride and methyl iodide in the same manner as described above to give a permethylate (**5**) (3 mg and 2.5 mg, respectively). The products were identical with that derived from **1** (TLC and IR comparison, and mixed melting point determination).

Complete Acid Hydrolysis of 1, 2, and 3——The compound (**1**, **2**, or **3**) (1 mg each) was hydrolyzed with 5.7 N HCl (0.3 ml) at 110 °C for 24 h in a sealed tube. The hydrolysate was analyzed on cellulose TLC using the solvent system of *n*-butanol–acetic acid–pyridine–water (3 : 3 : 3 : 1). Detection was done with ninhydrin reagent, by using an amino acid analyzer, and/or by HPLC system which consisted of a 70×2.1-mm guard column packed with Co:Pell ODS (Whatman Inc., Clifton, N.J.) in series with a 100×4.6-mm Spherisorb ODS-2 column (particle size: 3 μm, Senshu Scientific Co., Tokyo) using the solvent system of acetonitrile–0.1% trifluoroacetic acid (22 : 78) at a flow rate of 1 ml/min, with monitering at 254 nm. The results are summarized in Table I. ABA was also detected by silica gel TLC using the solvent system of chloroform–methanol (10 : 1).

Partial Acid Hydrolysis of 1——Compound **1** (10 mg) was hydrolyzed with a mixture of 12 N HCl (0.3 ml) and acetic acid (0.2 ml) at 27 °C for 48 h in a sealed tube. The hydrolyzed mixture was separated by preparative cellulose TLC with *n*-butanol–acetic acid–pyridine–water (3 : 3 : 3 : 1) to afford the fragment peptides IA, IB, IC, and ID. These peptide fragments were hydrolyzed with 5.7 N HCl at 110 °C by the same procedure as described above, and the hydrolysates were analyzed by cellulose TLC, amino acid analyzer, and/or HPLC. The results are summarized in

Table II.

Methylation of Fragment Peptides IC and ID——An ether solution of diazomethane was added to a methanol solution of peptide IC or ID. The solvent was removed by evaporation, and the reaction mixture was purified by HPLC. The MS of purified peptides IC and ID were measured.

Peptide IC: EI-MS *m/z* (%): 383 (M^+, 12), 352 (0.5), 221 (6), 220 (1.4), 194 (3), 191 (7), 190 (5), 163 (32), 135 (1.4), 134 (11), 120 (100), 92 (12).

Peptide ID: EI-MS *m/z* (%): 496 (1.3), 425 (4), 352 (1.5), 351 (3), 263 (9), 233 (11), 221 (13), 220 (3), 201 (9), 192 (6), 191 (5), 163 (18), 162 (100), 147 (13), 135 (4), 134 (34), 120 (46), 92 (15), 91 (11), 44 (40).

2,4-Dinitrophenylation of Amino Acids——The DNP-derivatives were synthesized by the procedure of Sanger,[6] and purified by column chromatography using chloroform–methanol–acetic acid (95:5:1). The CD curve of each DNP-amino acid between 280—430 nm was measured. CD (MeOH) $[\theta]^{20}$ (nm): DNP-L-Ala: −2500 (328), +2100 (390). DNP-Me-L-Phe: +13400 (316), +12800 (404). DNP-L-Leu: −2000 (328), +1800 (385). DNP-Me-L-Tyr: +18300 (320), +11500 (400). DNP-Ala from **1**: −2800 (328), +1900 (390). DNP-MePhe from **1**: +14600 (318), +12300 (402). DNP-Leu from **1**: −1700 (324), +1800 (384). DNP-MeTyr from **1**: +19700 (320), +11600 (397).

Acknowledgement The authors are grateful to Dr. M. Kubo of Tsumura Institute for FD mass measurements. We also thank Miss Y. Aoki, Mrs. M. Yuyama, and Miss T. Tanaka of this university for amino acid analyses, and NMR and mass measurements. We also thank Mrs. T. Ogata of this university for elemental analyses.

References and Notes

1) Part X: K. Nozawa, H. Seya, S. Nakajima, S. Udagawa and K. Kawai, *J. Chem. Soc., Perkin Trans. 1*, accepted.
2) Y. Ohtani (ed.), "Reports on the Cryptogamic Study in Nepal, March 1982," Miscellaneous Publication of the National Science Museum, Tokyo, 1982.
3) C. G. Greig and N. L. Leeback, *Nature* (London), **188**, 310 (1960).
4) J. R. Coggins and N. L. Benoiton, *Can. J. Chem.*, **49**, 1968 (1971).
5) B. W. Erickson and R. D. Merrifield, *J. Am. Chem. Soc.*, **95**, 3750 (1973).
6) F. Sanger, *Biochem. J.*, **39**, 507 (1945).
7) U. Nagai, M. Kawai, M. Katsumi, Y. Kani, R. Ueki and A. Tanaka, Symposium Papers for 21st Symposium on the Chemistry of Natural Products, Sapporo, 1978, p. 80.
8) A. Bracken, A. Pocker and H. Raistrick, *Biochem. J.*, **57**, 587 (1954).
9) The methods of determination of the antibacterial and antifungal activities were described in the following papers: H. Seya, K. Nozawa, S. Nakajima, K. Kawai and S. Udagawa, *J. Chem. Soc., Perkin Trans. 1*, **1986**, 109; H. Seya, K. Nozawa, S. Udagawa, S. Nakajima and K. Kawai, *Chem. Pharm. Bull.*, **34**, 2411 (1986).

[Chem. Pharm. Bull. 35(4)1353—1359(1987)]

Studies on the Conformation of 1-Aryl-1-nitrosoureas and Related Compounds

MASAYUKI TANNO* and SHOKO SUEYOSHI

National Institute of Hygienic Sciences, 1-18-1 Kamiyoga, Setagaya-ku, Tokyo 185, Japan

(Received July 31, 1986)

The carbon-13 nuclear magnetic resonance spectra of 1-aryl-3,3-dialkyl-1-nitrosoureas and related compounds were measured at about −40 °C, and their chemical shifts were assigned. The conformations of the *N*-nitroso compounds having the 1-aryl-1-nitrosoureido group were established through comparisons with *N*-alkyl-*N*-nitrosoanilines, and the decomposition mechanism of 1-aryl-3,3-dialkyl-1-nitrosoureas is discussed on the basis of the results.

Keywords——1-aryl-3,3-dialkyl-1-nitrosourea; 1-aryl-1-nitrosourea; *N*-nitrosourea; *N*-nitrosoacetanilide; *N*-nitrosoaniline; triazene; nitrosyl radical; *E*–*Z* conformation; ^{13}C-NMR

In an investigation of the decomposition of 1-aryl-3,3-dialkyl-1-nitrosoureas (**1**) at room temperature, we have found a difference in decomposition between 3,3-diethyl-1-(2-tolyl)-1-nitrosourea (**1a**) and its 4-tolyl isomer (**1b**) in chloroform or carbon tetrachloride. While the 2-tolyl derivative (**1a**) decomposed to afford the triazene (**11a**), the positional isomer (**1b**) gave mainly the nitro compound (**12**) and the urea (**13b**) besides the triazene (**11b**).[1] We considered that the structural features of these *N*-nitrosoureas would be related to the reactivity differences. Although the assignment of the carbon-13 nuclear magnetic resonance (^{13}C-NMR) spectra of 1-aryl-1-nitrosoureas (**1a, b**) has already been reported,[1] we did not discuss the structural features in detail, including the assignment of the *E*–*Z* isomers. This paper describes studies on the structural features of 1-aryl-1-nitrosoureas and related compounds.

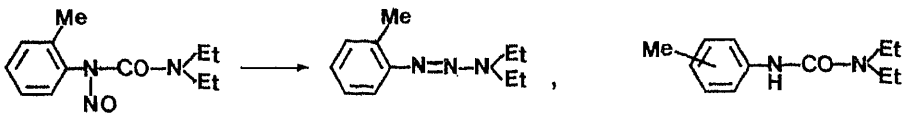

1a 11a 13a, b

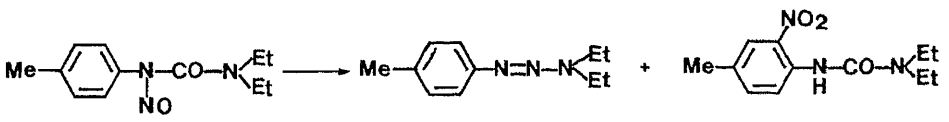

1b 11b 12

Chart 1

Results and Discussion

The carbon chemical shifts of the *N*-nitroso compounds are collected in Tables I and II. The spectra of the nitrosoureas (**1—3, 5, 6**) and the nitrosoacetanilides (**4**) were measured at about −40 °C, since the compounds are unstable at room temperature.

The conformational analysis of *N*-alkyl-*N*-nitrosoanilines has already been studied by proton nuclear magnetic resonance (^{1}H-NMR spectroscopy).[2] However, the nature of the conjugation between the amine nitrogen and the phenyl ring in these nitrosoanilines has not been clarified from the ^{1}H-NMR data. In order to elucidate the conformation of the *N*-nitrosoureas (**1**—**3**, **5**, **6**) and the *N*-nitrosoacetanilides (**4**), we first assigned the carbon chemical shifts of the phenyl ring carbons of *N*-alkyl-*N*-nitrosoanilines (**7**—**10**). As shown in Table II, the carbon signals of the *N*-alkyl-*N*-nitrosoanilines (**7**—**10**) indicated the presence of an equilibrium mixture of *Z* and *E* isomers, though the *tert*-butyl derivative (**9**) existed only as the *E* isomer. The chemical shifts of C^1 of the *E* isomers were always observed at higher field than those of the corresponding *Z* isomers.

A study of the electronic spectra of *N*-alkyl-*N*-nitrosoanilines[3] indicated that *N*-ethyl-*N*-nitrosoaniline (**7c**) and *N*-nitrosoindoline (**10**) exist almost wholly in the *Z* form and take a planar or near-planar conformation. In other words, it appears that a conjugated system is present between the aryl ring and the amine nitrogen. The *N*-nitrosoanilines (**7a**, **8**, **9**) having a bulky group at the nitrogen or possessing an *ortho* methyl group on the aryl ring are highly twisted.[3] In fact, the conjugation effects are reflected in the chemical shifts at C^2 of the aryl ring. The C^2 signal of the *Z* form of **7b** appears at higher field as compared with that of **9b** (only *E* form). This may be attributed to the contribution of the resonance form in the *Z* isomer, as shown in Chart 2. On the other hand, the *N*-alkyl carbon chemical shifts of the *Z* isomers of *N*-nitrosoamides or *N*-nitrosoanilines have been observed at higher field than those of the corresponding *E* isomers.[4]

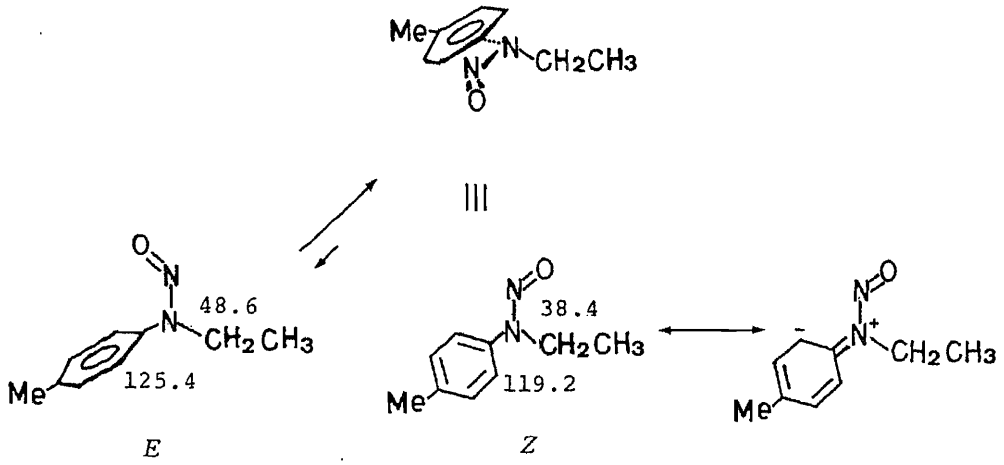

7b

Chart 2

From the assignments for the *N*-nitrosoanilines (**7**—**10**), the *E*–*Z* conformations of the aliphatic *N*-nitrosoureas (**5**, **6**) can be deduced, and the results are shown in Table II. Consequently, it was revealed that the carbonyl carbon of the *E* form of **6** resonated at lower field than that of the *Z* form. On the basis of the data for compounds **5**—**10**, the chemical shifts of the *N*-nitrosoureas of aryl type (**1**—**4**) could also be assigned as summarized in Table I. The chemical shifts of C^2 (or C^6) and the carbonyl are noted in Chart 3.

The disubstituted *N*-nitrosoureas (**2**, **3**) and the *N*-nitrosoacetanilides (**4**) exist only in the *E* conformer, in which the NO group is located anti to the CO group, in the range of about −40 °C to 10 °C. The possible conformations are shown as forms I—V in Chart 4. In forms II and V, the NO group interacts unfavorably with the X group and the CO group, respectively. The NO group and the CO group should be hindered in form IV if an *ortho*-substituent is

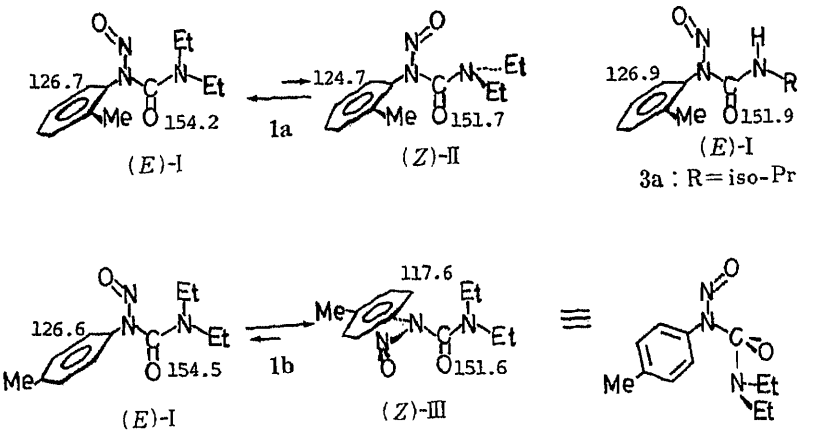

Chart 3

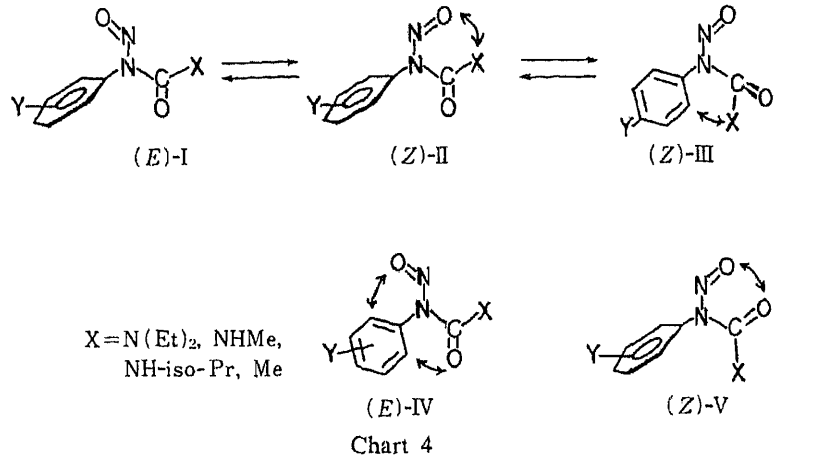

Chart 4

present on the phenyl ring. Consequently, the preferred conformer of the disubstituted nitrosoureas (**2**, **3**) and the nitrosoacetanilides (**4**) should be form I.[5]

On the other hand, observation of the two sets of signals of the trisubstituted *N*-nitrosoureas (**1**) indicates a possible conformational equilibrium involving forms I—III. Conformer I (major form) and conformer II[6] (minor form) are observed for the (2-tolyl)nitrosourea (**1a**). In the 4-tolyl isomer (**1b**), conformer I and conformer III[7] are observed, and the latter is predominant.

As the substituent X is larger in the trisubstituted nitrosoureas (**1b—d**) than in the disubstituted nitrosoureas (**2**, **3**), the NO group in **1b—d** is subject to steric repulsion by the two ethyl groups at the N^3 position. The hindrance between the NO group and the X group in form II may permit the coexistence of conformer III. Actually, the carbon signals of the alkyls at the N^3 position in the trisubstituted nitrosoureas show broad peaks as compared with those in the disubstituted derivatives. This phenomenon seems to be due to restricted rotation about the CO–N^3 bond. In conformer III, the Ph–N–NO part is approximately coplanar, and the N^1–CO bond is twisted. The C^2 or C^6 signal of the (4-tolyl)nitrosoureas (**1b—d**) appears at higher field in the planar form III than in the nonplanar form I. However, the nonplanar form I is preferred to form III in the 2-tolyl compound (**1a**) due to the increase of steric hindrance between the *ortho* methyl group and the X group.

Next we will discuss the nature of the decomposition of the *N*-nitroso compounds, using the above information on their conformations. 1-Methyl-3,3-(pentamethylen)-1-nitrosourea (**5**), which exists only as the *E* form, was stable at room temperature during 10 d. In contrast, the isopropyl derivative (**6**), consisting of a mixture of *Z* and *E* conformers, decomposed to generate CO_2 under the same conditions. This feature was confirmed by the appearance of the CO_2 stretching vibration at 2320 cm^{-1} with the passage of time. In the intramolecular rearrangement to the diazoester intermediate,[8] the presence of the *Z* form (like conformer II) having a coplanar O=N–N–C=O moiety in the ground state may be of importance, as shown in Chart 3. The trisubstituted (2-tolyl)nitrosourea (**1a**) containing the *Z* form of the coplanar O=N–N–C=O (conformer II) decomposed rapidly to the triazene (**11a**) with the evolution of CO_2 at room temperature. On the other hand, the (4-tolyl)nitrosourea (**1b**) adopts mainly a different *Z* form (conformer III). Thus, the 4-tolyl derivative (**1b**) gave the corresponding triazene (**11b**) in lower yield than the 2-tolyl isomer (**1a**).[1]

TABLE I. ^{13}C-NMR Chemical Shifts[a] (ppm) of *N*-Nitrosoureas (**1—3**) and *N*-Nitroacetanilides (**4**)

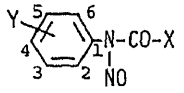

1: X=N(Et)$_2$ **3**: X=NH-iso-Pr
2: X=NHMe **4**: X=Me

Compd.	Y	Form[g]	C-1	C-2	C-3	C-4	C-5	C-6	CO	Y	X[c] N^3–C		X[c] C–Me	
1a[1]	2-Me	I[e]	134.0	136.4	130.9	127.3	129.9	126.7	154.2	18.0	40.8,	42.2	13.4,	13.6
		II	[d]	136.8	132.0	126.9	129.1	124.7	151.7	18.6	40.9,	[d]	12.8,	[d]
1b[1]	4-Me	I	131.4	126.6	129.9	139.7	129.9	126.6	154.5	21.2	41.2,	[d]	13.6,	[d]
		III[e]	135.3	117.6	130.3	137.6	130.3	117.6	151.6	21.0	41.4,	42.7	12.3,	13.7
1c	H	I	134.1	126.9	129.3	129.6	129.3	126.9	154.4		[d]			
		III[e]	137.7	117.4	129.8	127.6	129.8	117.4	151.5		41.5,	42.8	12.4,	13.7
1d	4-Cl	I	132.4	128.6	129.5	135.4	129.5	128.6	154.1		[d]			
		III[e]	136.3	118.7	129.9	133.0	130.0	118.7	151.1		41.6,	42.8	12.4,	13.9
2b	4-Me	I	129.5	127.6	130.0	140.2	130.0	127.6	153.9	21.3	27.2			
2e	4-MeO	I	124.3	129.0	114.5	160.2	114.5	129.0	154.0	55.4	27.3			
3a	2-Me	I	131.8	136.3	130.3[b]	128.0	130.8[b]	126.9	151.9	17.4	43.1		22.8	
3b	4-Me	I	129.4	127.5	130.0	140.0	130.0	127.5	152.2	21.3	43.1		22.7	
3c	H	I	132.1	127.8	129.3	130.0	129.3	127.8	152.1		43.2		22.7	
3e	4-MeO	I	124.3	129.0	114.5	160.1	114.5	129.0	152.3	55.4	43.8		22.8	
4a	2-Me	I	131.5	135.7	130.8[b]	127.8	130.4[b]	127.0	174.0	17.2			22.9	
4b	4-Me	I	129.0	127.4	130.2	140.3	130.2	127.4	174.5	23.1[f]			23.1[f]	
4d	4-Cl	I	130.0	129.2	129.7	135.9	129.7	129.2	174.0				23.0	

a) Measured in $CDCl_3$ at −40 °C. *b*) Assignments may be reversed. *c*) Et groups in **1a—d** show broad signals. *d*) Not observable under the experimental conditions. *e*) The intensities of the signals are overwhelmingly stronger than those of the other isomer.[15] *f*) Coincidences. *g*) Forms I—III are shown in Chart 4.

Conclusion

From these results, the effective conformer for the diazoester intermediate formation by *N*-nitroso compounds of aryl type (**1**—**4**) seems to be conformer II, in which the O=N–N–C=O part is coplanar. The disubstituted *N*-nitrosoureas of aryl type (**2**, **3**) and the *N*-

TABLE II. ^{13}C-NMR Chemical Shifts[a] (ppm) of *N*-Nitrosoureas (**5**, **6**) and *N*-Nitrosoanilines (**7**—**10**)

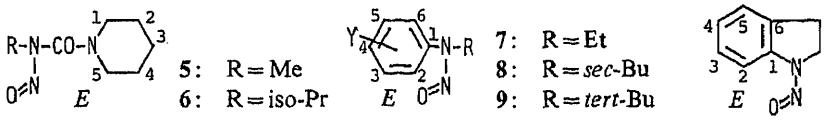

Compd.	Y	Form[g]	C-1	C-2	C-3	C-4	C-5	C-6	CO	Y	R N-C	R C-CH_2-	R C-Me
5		*E*	49.4[b,c]	25.9	24.3	25.9	46.0		154.2		29.8		
6		*E*[e]	48.8[b,c]	26.3	24.3	25.6	45.2		153.1		45.4		18.6
		Z	46.6[b,c]	26.1	24.0	25.4	44.2		151.6		53.3		22.9, 20.6
7a	2-Me	*E*	137.5	135.9	130.9	126.8[f]	129.3	126.2		17.8[f]	48.8		14.1
		Z	140.2	134.9	131.5	126.8[f]	129.1	127.7		17.8[f]	41.7		11.0
7b	4-Me	*E*	[d]	125.4	129.1	[d]	129.1	125.5		20.4	48.6		14.2
		Z	138.5	119.2	129.5	136.5	129.5	119.1		20.1	38.4		11.6
7c	H	*E*	[d]	126.2	129.3	128.8	129.3	126.2			48.6		14.2
		Z	141.5	119.5	129.4	127.1	129.4	119.5			38.8		11.6
8a	2-Me	*E*	136.5	136.2	131.5	126.6[f]	130.8	126.5		18.2[f]	62.2	29.5	20.0, 10.9
		Z	138.8	136.0	130.8	126.6[f]	129.1	126.4		18.2[f]		27.3	18.8, 11.0
8b	4-Me	*E*	134.2	127.2	129.9	139.0	129.5	127.2		21.0	62.0	28.6	20.0, 10.9
		Z	138.3	126.3	129.6	137.6	129.6	126.3		20.9	51.9	27.1	17.6, 11.1
9a	2-Me	*E*	137.4	136.5	130.6	127.2	129.0	126.4		18.2	61.7		30.2
9b	4-Me	*E*	134.6	128.2	129.8	138.9	129.8	128.2		21.0	61.1		29.9
10		*E*	[d]	117.4	126.2	126.5	127.5	[d]			59.9	26.8	
		Z	140.8	118.8	128.0	126.1	126.8	132.0			45.4	26.0	

a) Measured in $CDCl_3$ at −40 °C for **5** and **6**, and at room temperature for **7**—**10**. *b*) Assignments for C^1 and C^5, or for C^2 and C^3 may be reversed. *c*) The carbon signals of the piperidine ring are broad except for C^3. *d*) Not observable under the experimental conditions. *e*) The intensities of the signals are overwhelmingly stronger than those of the other isomer.[15] *f*) Coincidences. *g*) Form *E* has the NO group located anti to the CO group or syn to the aryl ring.

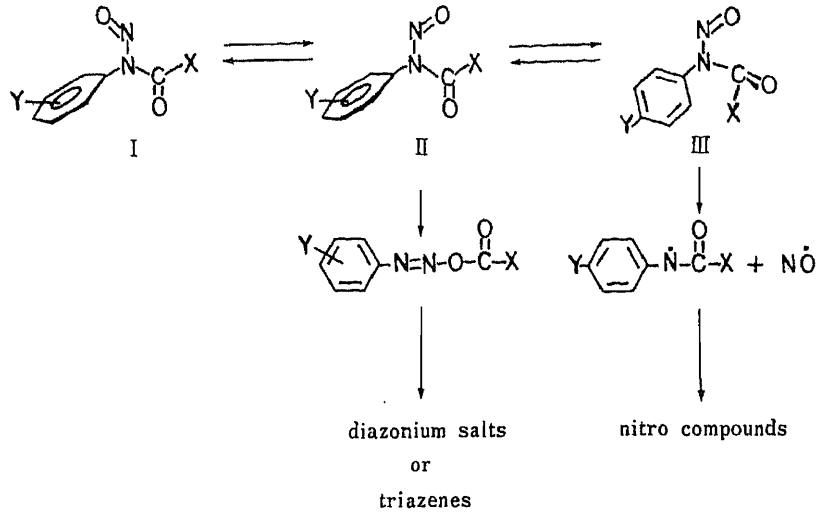

Chart 5

nitrosoacetanilides (**4**) were observed to adopt only conformer I. However, **2**—**4** may adopt conformer II or a similar form at the decomposition temperature, since these compounds decompose to generate a diazonium ion in carbon tetrachloride.[9,10]

The rearrangement of this type in the (4-tolyl)nitrosourea (**1b**) competes with liberation of a nitrosyl radical as a source of the formation of the nitro compound (**12**),[1] as indicated in Chart 5. The 1-aryl-1-nitrosoureas readily form the NO radical in carbon tetrachloride at 33 °C,[1,10,11] though the N–NO bond cleavage of the aliphatic *N*-nitroso compounds proceeds by photolysis.[12] The generation of the NO radical is probably due to the contribution of conformer III, which has the partially conjugated system of Ph⋯N⋯N⋯O, and the neighboring CO group, which accelerates the fission of the N–NO bond owing to the electrostatic repulsion between the NO group and the CO group. This partial conjugated structure is supposed to be advantageous for moving one electron from the conjugated system of the aromatic ring to the NO group.

It is known that *N*-nitrosocarbazoles and *N*-nitrosodiphenylamines generate a nitrosyl radical under reflux in xylene or benzene, and give the corresponding nitro compounds.[13] These *N*-nitroso compounds also have a planar conformation with conjugation of the aromatic ring and the NO group.[14] If a conformation of this type is involved in the activation of N–NO bond cleavage in nonpolar solvents, one may utilize this character to carry out nitrosation or nitration under mild conditions.

Experimental

^{13}C-NMR spectra were measured with a JEOL FX-200 spectrometer with tetramethylsilane as an internal standard. The spectra were recorded under the following conditions; ^{13}C-NMR at a frequency of 50.10 MHz with a spectral width of 10000 Hz; pulse width 4 μs; acquisition time 0.8192 s; number of data points 16384; temperature of about 35 °C for compounds **7**—**10** and −40 °C for compounds **1**—**6**. Chemical shifts are accurate to ±0.05 ppm. The concentration used was 1.0—10 × 10^{-5} mol/ml of $CDCl_3$ in each case.

Infrared (IR) spectra were taken with a JASCO A-102 spectrometer.

Materials——1-Aryl-1-nitrosoureas (**1**, **5**, **6**) were prepared by nitrosation of the corresponding ureas according to the method described in a previous paper.[1]

The ureas used as starting materials for nitrosation were as follows. 1-Phenyl-3,3-diethylurea: mp 89—90 °C. IR $\nu_{max}^{CHCl_3}$ cm^{-1}: 3460 (NH), 1650 (CO). ^{13}C-NMR ($CDCl_3$) δ: 155.1 (CO), 139.8, 120.3, 128.5, 122.6 (phenyl-C^1, C^2 and C^6, C^3 and C^5, C^4), 51.5, 13.8 (Et). 1-(4-Chlorophenyl)-3,3-diethylurea: mp 120—121 °C. IR $\nu_{max}^{CHCl_3}$ cm^{-1}: 3460 (NH), 1650 (CO). ^{13}C-NMR ($CDCl_3$) δ: 154.7 (CO), 138.3, 121.5, 128.5, 127.6 (phenyl-C^1, C^2 and C^6, C^3 and C^5, C^4), 41.5, 13.8 (Et). 1-Methyl-3,3-(pentamethylen)urea: mp 76—77 °C. IR $\nu_{max}^{CHCl_3}$ cm^{-1}: 3475, 3380^{br} (free and associated NH), 1620 (CO). ^{13}C-NMR ($CDCl_3$) δ: 158.9 (CO), 27.5 (*N*-Me), 44.8, 25.7, 24.5 (piperidino-C^1 and C^5, C^2 and C^4, C^3). 1-Isopropyl-3,3-(pentamethylen)urea: mp 134—135 °C. IR $\nu_{max}^{CHCl_3}$ cm^{-1}: 3465, 3400^{br} (free and associated NH), 1625 (CO). ^{13}C-NMR ($CDCl_3$) δ: 157.3 (CO), 42.4, 23.3 (*N*-iso-Pr), 44.8, 25.7, 24.5 (piperidino-C^1 and C^5, C^2 and C^4, C^3).

Nitrosoureas: 1-Phenyl-3,3-diethyl-1-nitrosourea (**1c**): Oil. IR $\nu_{max}^{CHCl_3}$ cm^{-1}: 1695 (CO). *Anal.* Calcd for $C_{11}H_{15}N_3O_2$: C, 59.71; H, 6.83; N, 18.99. Found: C, 59.95; H, 6.92; N, 12.95. 1-(4-Chlorophenyl)-3,3-diethyl-1-nitrosourea (**1d**): mp 45 °C (dec.). IR $\nu_{max}^{CHCl_3}$ cm^{-1}: 1695 (CO). *Anal.* Calcd for $C_{11}H_{14}ClN_3O_2$: C, 51.67; H, 5.52; N, 16.43. Found: C, 52.19; H, 5.62; N, 16.81. 1-Methyl-3,3-(pentamethylen)-1-nitrosourea (**5**): mp 31 °C (dec.) (hygroscopic). IR $\nu_{max}^{CHCl_3}$ cm^{-1}: 1680 (CO). *Anal.* Calcd for $C_7H_{13}N_3O_2 \cdot 1/6H_2O$: C, 48.26; H, 7.72; N, 24.12. Found: C, 48.32; H, 7.73; N, 24.21. 1-Isopropyl-3,3-(pentamethylen)-1-nitrosourea (**6**): Oil. IR $\nu_{max}^{CHCl_3}$ cm^{-1}: 1680 (CO). *Anal.* Calcd for $C_9H_{17}N_3O_2$: C, 54.25; H, 8.60; N, 21.09. Found: C, 53.98; H, 8.64; N, 20.89. The analytical data for the disubstituted nitrosoureas (**2b**, **2e**, **3a**—**c**) were reported in a separate paper.[10]

N-Nitrosoacetanilides[9,16] and *N*-nitrosoanilines[2] were prepared by the procedures cited. These compounds were chromatographed on silica gel with a mixture of *n*-hexane, ether and $CHCl_3$. All of the purified nitroso compounds were yellow oils except for **9b**. *N-tert*-Butyl-*N*-nitroso-4-toluidine (**9b**): mp 53—54 °C. *Anal.* Calcd for $C_{11}H_{16}N_2O$: C, 68.72; H, 8.39; N, 14.57. Found: C, 68.56; H, 8.49; N, 14.62.

Decomposition of 1-Aryl-3,3-(pentamethylen)-1-nitrosoureas (5, 6) in $CHCl_3$——About 5.0 × 10^{-5} mol of 1-isopropyl-3,3-(pentamethylen)-1-nitrosourea (**6**) in 1 ml of $CHCl_3$ was sealed in a KBr cell and the IR spectrum was taken at room temperature. The absorption intensity at 2320 cm^{-1} due to CO_2 increased with the passage of time.[1] 1-Methyl-3,3-(pentamethylen)-1-nitrosourea (**5**) remained intact during 10 d under the same conditions.

References and Notes

1) S. Sueyoshi and M. Tanno, *Chem. Pharm. Bull.*, **33**, 488 (1984).
2) C. E. Looney, W. D. Phillips, and E. L. Reilly, *J. Am. Chem. Soc.*, **79**, 6136 (1957); G. J. Karabatsos and R. A. Taller, *ibid.*, **86**, 4373 (1964).
3) J. T. D'Agostino and H. H. Jaffe, *J. Am. Chem. Soc.*, **92**, 5160 (1970).
4) P. S. Pregosin and E. W. Randall, *J. Chem. Soc., Chem. Commun.*, **1971**, 399.
5) The location of alkyl groups of the disubstituted nitrosoureas is favorable in the *Z* form with respect to the CO group. *Cf.*, J. K. Snyder and L. M. Stock, *J. Org. Chem.*, **45**, 886 (1980); C. N. R. Rao, K. G. Rao, A. Goel, and K. Balasubramanian, *J. Chem. Soc. A*, **1973**, 3077.
6) In the case of conformer II, it may be energetically advantageous to locate the NO group between the two ethyl groups at the N^3 position.
7) The proton at the C^2 or C^6 position in conformer III is located between the X group and the CO group.
8) R. Huisgen and L. Krause, *Justus Liebigs Ann. Chem.*, **574**, 157 (1951); M. Miyahara and S. Kamiya, *Chem. Pharm. Bull.*, **30**, 3466 (1982); S. S. Singer, *J. Org. Chem.*, **47**, 3839 (1982).
9) D. H. Hey, T. Stuart-Webb, and G. H. Williams, *J. Chem. Soc.*, **1952**, 4657; C. Rüchardt and C. C. Tan, *Chem. Ber.*, **103**, 1774 (1970).
10) M. Tanno and S. Sueyoshi, *Chem. Pharm. Bull.*, **35**, 1360 (1987).
11) The formation of the nitro compounds was depressed by a radical inhibitor. S. Sueyoshi and M. Tanno, Abstracts of Papers, 12th Symposium on Progress in Organic Reactions and Syntheses, November 1985, p. 111.
12) J. N. S. Tam, R. W. Yip, and Y. L. Chow, *J. Am. Chem. Soc.*, **96**, 4543 (1974).
13) P. Welzel, *Chem. Ber.*, **104**, 808 (1971).
14) L. Forlani, L. Lunazzi, D. Macciantelli, and B. Minguzzi, *Tetrahedron Lett.*, **1079**, 1451.
15) The isomer ratios could not be determined by integration of the ^{1}H-NMR spectrum because of overlapping signals.
16) P. Miles and H. Suschitzky, *Tetrahedron*, **18**, 1369 (1962).

[Chem. Pharm. Bull. 35(4)1360—1371(1987)]

Preparation and Properties of 3-Alkyl-1-arylnitrosoureas and Related Compounds

MASAYUKI TANNO* and SHOKO SUEYOSHI

National Institute of Hygienic Sciences, 1–18–1 Kamiyoga, Setagaya-ku, Tokyo 185, Japan

(Received July 31, 1986)

Nitrosation of 3-alkyl-1-arylureas was investigated with sodium nitrite in 99% formic acid or with isoamyl nitrite in chloroform. The preparation of 3-alkyl-1-aryl-1-nitrosoureas was effectively performed by using isoamyl nitrite in the absence of acids, since the 1-nitrosoureas were isomerized to the 3-nitroso isomers by acids. The carbon-13 nuclear magnetic resonance and infrared spectral properties of the products were examined and their structural features are discussed.

It was found that 3-alkyl-1-aryl-1-nitrosoureas decomposed to form alkyl isocyanates and 3-alkyl-1-(2-nitroaryl)ureas in carbon tetrachloride. 1,3-Rearrangement and transnitrosation also took place in this solvent.

Keywords——3-alkyl-1-arylnitrosourea; 3,3-diethyl-1-tolyl-1-nitrosourea; *N*-nitrosourea; nitrosation; 1,3-rearrangement; isomerization; transnitrosation; nitration

We recently reported[1] on the chemical properties of novel trisubstituted *N*-nitrosoureas. 3,3-Diethyl-1-(4-tolyl)-1-nitrosourea (**1b**) decomposed to give the triazene (**2b**) and the nitro compound (**3**) in chloroform or carbon tetrachloride at room temperature, while the 2-tolyl derivative (**1a**) gave mainly the triazene (**2a**) under similar conditions. The reaction of nitrosoureas to give the triazenes is of interest because several derivatives of 3-alkyl-1-phenyltriazenes and 3,3-dialkyl-1-phenyltriazenes have been reported to show antitumor activity.[2] Therefore, we examined whether 3-alkyl-1-aryltriazenes were produced or not by the decomposition of 3-alkyl-1-arylnitrosoureas (**4**, **5**).

A number of reports have dealt with the antitumor activities and the chemical properties of 1,3-dialkylnitrosoureas.[3–5] In a study of the nitrosation of 3-alkyl-1-phenylureas, Johnston *et al.*[5] obtained a mixture of 1-nitrosoureas and the 3-nitroso isomers. Kamiya and co-workers[6–8] described the synthesis and decomposition of 1,3-diaryl-1-nitrosoureas and related compounds. However, there are few data on the chemical properties of 3-alkyl-1-aryl-1-nitrosoureas, especially 3-methyl-1-phenyl-1-nitrosourea (**4c**), because of the difficulty of its isolation. In the nitrosation of 3-methyl-1-phenylurea (**9c**), the 3-nitrosourea (**6c**) is produced overwhelmingly and the desired 1-nitrosourea (**4c**) can not be obtained by the ordinary method using sodium nitrite and acids. In this paper, we wish to present the preparation and properties of 3-alkyl-1-aryl-1-nitrosoureas and related compounds.

Preparation of Nitrosoureas

N-Nitrosoureas (**4**—**7**) and *N*-nitrosoacetanilides (**8**) were prepared by nitrosation of the corresponding ureas (**9**, **10**) and acetanilides, respectively. The ureas (**9**, **10**) as starting materials were prepared by the reaction of aryl isocyanates with alkylamines or anilines with alkyl isocyanates in ether. Since the nitroso compounds were unstable at room temperature, they were quickly purified by silica gel column chromatography with a mixture of *n*-hexane and ether under cooling.[1]

The nitrosation of 1-aryl-1-isopropylureas (**10**) with sodium nitrite and 99% formic acid

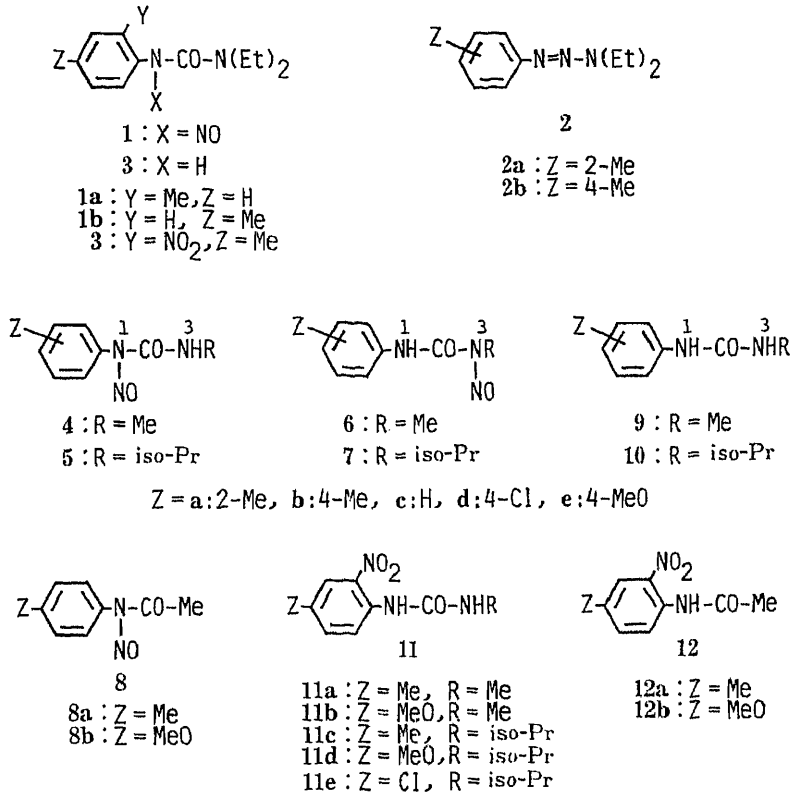

Chart 1

at 5 °C, followed by neutralization with sodium carbonate, gave a mixture of 1-aryl-3-isopropyl-1-nitrosoureas (**5**) and their 3-nitroso isomers (**7**). The yields of the nitrosoureas (**5**, **7**), prepared by nitrosation using sodium nitrite and formic acid (method A), are shown in Table I. Method A gave **5** and **7** in 15—65% and 18—78% yields, respectively. On the other hand, the similar nitrosation of 1-aryl-3-methylureas (**9**) by method A gave only the 3-nitrosoureas (**6**) in over 90% yields and virtually did not give the corresponding 1-nitroso isomers (**4**). This observation seems to reflect a difference of electron density at the ureido nitrogens and the steric effect of the N^3-alkyl group. The NO group attached to the ureido nitrogen undergoes 1,3-rearrangement in the presence of an acid.[5,9] The produced nitrosoureas also rearrange to their positional isomers during this nitrosation. The 1,3-rearrangement, which proceeds *via* two steps of denitrosation and isomerization (re-nitrosation), may be thermodynamically controlled.

We have tried, therefore, to prepare 3-alkyl-1-aryl-1-nitrosoureas (**4**, **5**) in the absence of an acid. The results of nitrosation with isoamyl nitrite in chloroform at 5 °C are shown in Table I (method B). The yields of 1-nitrosoureas (**6**) obtained by method B were higher than those in method A. The new compounds (**4**) were isolated in very low yields, though **4e** was obtained in fairly good yield. Physical and analytical data for the nitrosoureas (**4**—**7**) are listed in Table I.

The influence of the acid is very great in nitrosation. For instance, in the nitrosation of **9e** by method A, the 1-nitrosourea (**4e**) was observed in an appreciable amount by thin layer chromatography during the first 10 min at the beginning of the reaction, but the amount of **4e** gradually decreased and that of its 3-nitroso isomer (**6e**) increased with time. Therefore, the nitrosation of **4e** for the first 10 min may be kinetically controlled and the rearrangement to **6e** seems to be thermodynamically controlled.

Thus, 3-alkyl-1-(4-tolyl)nitrosoureas (**4b**—**7b**) were treated with formic acid in order to

TABLE I. Physicochemical Properties and Analytical Data of 3-Alkyl-1-aryl-1-nitrosoureas (**4**, **5**) and Their 3-Nitroso Isomers (**6**, **7**)

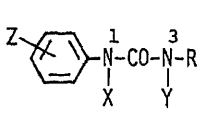

4: X=NO, Y=H R=Me
5: X=NO, Y=H, R=iso-Pr
6: X=H, Y=NO, R=Me
7: X=H, Y=NO, R=iso-Pr

Compd.	Z	Method	Yield[a] (%)	mp[b] (°C)	Formula	Analysis (%) Calcd (Found) C	H	N	IR $\nu_{max}^{CHCl_3}$ cm^{-1} NH Ring[d]	CO
4a	2-Me	A	1	87—88	$C_9H_{11}N_3O_2$	55.95	5.74	21.75	3440	1720
		B	2			(56.11	5.74	21.76)	1600 (vw)	
4b	4-Me	A	—	101.5—102.5	$C_9H_{11}N_3O_2$	55.95	5.74	21.75	3430	1720
		B	2			(56.09	5.75	21.64)	1590 (vw)	
4c	H	A	—	96—97	$C_8H_9N_3O_2$	53.62	5.06	23.45	3440	1725
		B	1			(53.70	5.06	23.32)	1590 (vw)	
4d[c]	4-Cl	A	—	102—103	$C_8H_8ClN_3O_2$	44.60	3.84	19.51	3430	1720
		B	1		$1/10\,H_2O$	(45.10	3.80	18.96)	1590 (w)	
4e	4-MeO	A	—	106—107	$C_9H_{11}N_3O_3$	51.67	5.30	20.09	3430	1720
		B	77			(51.42	5.27	19.97)	1600 (m)	
5a	2-Me	A	65	90.5—91.5	$C_{11}H_{15}N_3O_2$	59.71	6.83	18.99	3420	1720
		B	76			(60.10	6.94	18.76)	1600 (vw)	
5b	4-Me	A	15	101.5—102.5	$C_{11}H_{15}N_3O_2$	59.71	6.83	18.99	3425	1720
		B	56			(60.28	6.98	18.56)	1600 (vw)	
5c	H	A	—	61.5—62.5	$C_{10}H_{13}N_3O_2$	57.96	6.32	20.28	3420	1720
		B	36			(58.11	6.34	20.28)	1590 (vw)	
5d	4-Cl	A	—	66—67	$C_{10}H_{12}ClN_3O_2$	49.69	5.00	17.39	3430	1720
		B	27			(49.71	5.00	17.00)	1590 (w)	
5e	4-MeO	A	26	83—84	$C_{11}H_{15}N_3O_3$	55.68	6.37	17.71	3420	1710
		B	57			(55.87	6.41	17.77)	1590 (s)	
6a	2-Me	A	90	69—70	$C_9H_{11}N_3O_2$	55.95	5.74	21.75	3410	1730
		B	87			(55.91	5.75	21.74)	1585 (m)	
6b	4-Me	A	97	102.5—103.5[4]					3390	1725
		B	95						1590 (m)	
6c	H	A	95	84—85[4]					3390	1725
		B	85						1590 (s)	
6d	4-Cl	A	95	110—111[4]					3390	1725
		B	93						1595 (m)	
6e	4-MeO	A	92	98.5—99.5[4]					3400	1725
		B	10						1595 (m)	
7a	2-Me	A	18	45.5—46.5	$C_{11}H_{15}N_3O_2$	59.71	6.83	18.99	3420	1720
		B	5			(59.45	6.78	18.69)	1585 (m)	
7b	4-Me	A	37	71.5—72.5	$C_{11}H_{15}N_3O_2$	59.71	6.83	18.99	3400	1720
		B	9			(59.84	6.88	18.94)	1590 (m)	
7c	H	A	78	84—85	$C_{10}H_{13}N_3O_2$	57.96	6.32	20.28	3390	1720
		B	17			(58.10	6.33	20.30)	1590 (m)	
7d	4-Cl	A	40	88—89	$C_{10}H_{12}ClN_3O_2$	49.69	5.00	17.39	3390	1720
		B	2			(49.93	4.99	17.09)	1585 (s)	
7e	4-MeO	A	27	56.5—57.5	$C_{11}H_{15}N_3O_3$	55.68	6.37	17.71	3390	1720
		B	1			(55.68	6.29	17.75)	1590 (m)	

a) Isolation yields. *b*) Decomposition points (recrystallized from a mixture of *n*-hexane and ether). *c*) Hygroscopic. *d*) vw, very weak; w, weak; m, moderate; s, strong.

examine their 1,3-rearrangement. As shown in Fig. 1, both the 3-isopropyl derivatives (**5b** and **7b**) were converted smoothly to their isomers (**7b** and **5b**) in the presence of an excess of formic acid. The 1,3-rearrangement in each case is first-order within the first 15 min. The rate

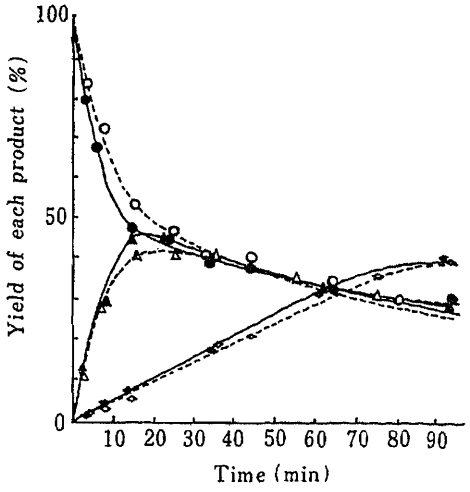

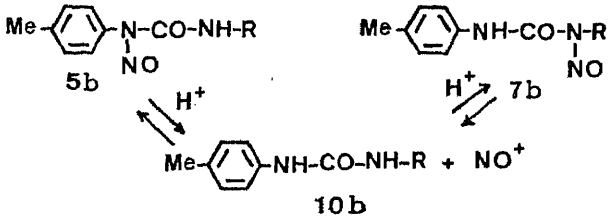

Fig. 1. 1,3-Rearrangement and Denitrosation of 3-Isopropyl-1-(4-tolyl)-1-nitrosourea (**5b**) and Its 3-Nitroso Isomer (**7b**)

Solid line: starting **5b** (●), produced **7b** (▲) and **10b** (◆). Broken line: starting **7b** (○), produced **5b** (△) and **10b** (◇).

constants are $k_1 = 3.3 \times 10^{-4}\,s^{-1}$ (**5b**→**7b**) and $k_2 = 2.1 \times 10^{-4}\,s^{-1}$ (**7b**→**5b**), and the equilibrium constant (k_1/k_2) is about 1.6 at 14 °C. On the other hand, the isomerization of **4b** to **6b** was extremely fast and the reverse reaction (**6b** to **4b**) was not observed under the experimental conditions used. These data indicate that the presence of acid is likely to decrease the yields of 1-aryl-1-nitrosoureas, that is, the preparation of this type of nitrosoureas is best performed by mild nitrosation using isoamyl nitrite in the absence of acids.

Properties of 1-Aryl-1-nitrosoureas

The spectroscopic data for 1-aryl-1-nitrosoureas (**4**, **5**) and their 3-nitroso isomers (**6**, **7**) are listed in Tables I and II. The infrared (IR) spectra in chloroform showed the CO stretching vibration in the range of 1710—1730 cm^{-1} and the NH absorption in the range of 3390—3440 cm^{-1}. The NH bands for 1-(4-substituted phenyl)-1-nitrosoureas (**4b—e**, **5b—e**) appeared at higher frequencies than those of the corresponding 3-nitroso isomers (**6b—d**, **7b—e**) except for **6e**. In contrast, a reverse relationship was observed in the 2-tolyl derivatives (**4a—7a**). The characteristic difference between the 1-nitrosoureas (**4**, **5**) and the 3-nitrosoureas (**6**, **7**) in the IR spectra lies in the range of 1585—1600 cm^{-1} except for the compounds having an MeO group (**4e—7e**). The 3-nitrosoureas show a moderate or strong absorption around 1600 cm^{-1}, while the 1-nitroso isomers show a weak band in this range. The absorption around 1600 cm^{-1} in the nitrosoureas can be regarded as a vibration of the skeleton of the aromatic ring,[10] because it was not shifted, though the amide II band at 1510—1580 cm^{-1} moved toward lower frequencies in dilute solution. The intensity of this absorption is related to the extent of the conjugated interaction between the aromatic ring and the 4-substituent.[11] In the cases of **4e** and **5e** having a powerful electron-releasing group, a relatively strong absorption at 1590—1600 cm^{-1} can be attributed to the band arising from conjugation between the aromatic ring and the MeO group, since the conjugation between the aromatic ring and the N^1-ureido nitrogen in the compounds (**4e**, **5e**) was shown not to be strong from the carbon-13 nuclear magnetic resonance (^{13}C-NMR) data.[12]

The weak absorption of the 1-nitrosoureas (**4**, **5**) at around 1600 cm^{-1} suggests that the

TABLE II. ^{13}C-Chemical Shifts[a] (ppm) of Nitrosoureas (**4**—**7**), Ureas (**9**, **10**), Nitro Compounds (**11**, **12**) and Carbamates (**21**)

Compd.	Z	R	C-1	C-2	C-3	C-4	C-5	C-6	CO	Z	R
4b[b]	2-Me	Me	129.5	127.6	130.0	140.2	130.0	127.6	153.9	21.3	27.2
5b[b]	4-Me	iso-Pr	129.4	127.5	130.0	140.0	130.0	127.5	152.2	21.3	43.1, 22.7
6a	2-Me	Me	129.6	134.8	130.7	125.6	127.0	122.7	150.8	17.6	26.5
6b	4-Me	Me	134.6[c]	120.4	129.7	134.2[c]	129.7	120.4	150.6	20.8	26.4
6c	H	Me	136.6	120.2	129.2	124.9	129.2	120.2	150.6		26.4
6d	4-Cl	Me	130.2	121.4	129.4	135.3	129.4	121.4	150.6		26.5
6e	4-MeO	Me	129.7	122.3	114.5	159.1	114.5	122.3	150.8	55.5	26.5
7a	2-Me	iso-Pr	129.1	134.7	130.6	125.3	126.9	122.3	150.9	17.8	44.4, 19.0
7b	4-Me	iso-Pr	134.1[c]	120.1	129.6	134.2[c]	129.6	120.1	150.7	20.9	44.2, 18.9
7c	H	iso-Pr	136.5	119.9	129.1	124.6	129.1	119.9	150.6		44.2, 18.9
7e	4-MeO	iso-Pr	129.5	122.0	114.0	156.4	114.0	122.0	150.9	55.4	44.3, 19.0
9a	2-Me	Me	133.0	136.2	131.1	126.2	127.2	126.8	157.2	17.8	27.1
9b	4-Me	Me	134.0	122.1	129.9	136.0	129.9	122.1	157.1	20.8	27.0
9c	H	Me	138.5	121.8	129.4	124.2	129.4	121.8	156.5		27.1
9d	4-Cl	Me	139.6	117.3	128.3	124.8	128.3	119.3	155.9		26.2
9e	4-MeO	Me	131.0	125.3	114.8	157.4[c]	114.8	125.3	157.3[c]	55.6	27.1
10a	2-Me	iso-Pr	132.8	136.3	131.1	126.0	127.2	125.6	155.7	17.8	42.3, 23.3
10b	4-Me	iso-Pr	132.7	120.9	129.6	136.5	129.6	120.9	156.1	20.7	42.0, 23.2
10c	H	iso-Pr	139.5	120.0	128.9	122.7	128.9	120.0	156.3		41.9, 23.1
10d	4-Cl	iso-Pr	139.6	119.0	128.3	124.4	128.3	119.0	154.3		40.9, 22.9
10e	4-MeO	iso-Pr	131.4	123.5	114.5	156.4[d]	114.5	123.5	156.4[d]	55.6	42.0, 23.3
11a	4-Me	Me	131.4	135.4	125.3	134.9	137.0	121.5	164.9	20.3	27.2
11b	4-MeO	Me	131.1	136.1	108.0	153.8[c]	123.2	124.3	155.0[c]	55.9	27.2
11c	4-Me	iso-Pr	131.2	135.6	125.2	134.9	136.8	121.7	153.9	20.4	42.7, 23.0
11d	4-MeO	iso-Pr	131.2	136.7	107.9	153.7[d]	123.4	124.1	153.7[d]	55.9	42.8, 23.1
11e	4-Cl	iso-Pr	136.0	135.5	125.1	126.4	135.8	122.8	153.1		42.9, 23.1
12a[14]	4-Me	Me	132.5	136.4	125.3	133.3	136.6	122.2	168.7	20.4	25.4
12b	4-MeO	Me	128.5	137.3	108.7	155.1	124.0[d]	124.0[d]	168.7	56.0	25.3
21a	4-Me	iso-Am	132.7	119.1	135.7[d]	135.7[d]	135.7[d]	119.1	154.2	20.7	[e]
21b	4-Cl	iso-Am	136.9	120.1	128.9	128.3	128.9	120.1	153.9		[e]
21c	4-Cl	Et	136.9	120.2	128.9	128.4	128.9	120.2	153.8		61.3, 14.5

a) Measured in $CDCl_3$ except for **12d** and **13d** (in DMSO-d_6) with TMS as an internal standard. Temperature of −40 °C for **4**, **5** and **7**, −10 °C for **6** and room temperature for other compounds. *b*) The chemical shifts of other 1-nitrosoureas are reported in reference 12. *c*) Assignments may be reversed. *d*) Coincidences. *e*) Isoamyl group: **21a**: 63.8 (C^1), 37.8 (C^2), 25.0 (C^3), 22.5 (C^4); **21b**: 64.1 (C^1), 37.7 (C^2), 25.0 (C^3), 22.5 (C^4).

conformation preferentially adopted is a form twisted between the aromatic ring and the N^1-ureido nitrogen. This suggestion is supported by the ^{13}C-NMR data. We have determined the conformation of the 1-aryl-1-nitrosoureas at low temperature by using ^{13}C-NMR.[12] These compounds have a conformation in which the aryl ring is twisted against the ureido group and the NO group is in the *E* relationship to the C=O moiety.

The C^2 or C^6 signal of the phenyl ring in the 3-nitrosoureas (**6**, **7**) appears at higher field than those of the 1-nitrosoureas (**4**, **5**), as shown in Table II. The ^{13}C-NMR data indicate that the phenyl–N^1 bond is more highly conjugated in the 3-nitrosoureas than in the 1-nitroso isomers, in agreement with the IR data. Further, the chemical shifts of the CO carbon in the 3-nitrosoureas are also observed at higher field than those of the corresponding 1-nitrosoureas. The conformation of the nitrosoureas (**4**—**7**) was identified by comparing the chemical shifts with those of 1-methyl-3,3-(pentanediyl)-1-nitrosourea (only *E* form) and 1-isopropyl-3,3-(pentanediyl)-1-nitrosourea (a mixture of *E* and *Z* forms).[12] The NO group is in the *E* relationship to the CO group in both the 1-nitrosoureas and the 3-nitroso isomers, in other

words, the NO group of the 1-nitrosoureas is directed toward the aryl ring and that of the 3-nitroso isomers is directed toward the N^3-alkyl group.

Decomposition of 1-Aryl-1-nitrosoureas

3,3-Dialkyl-1-aryl-1-nitrosoureas (**1**) decomposed in chloroform or carbon tetrachloride to give the triazenes (**2**) and the nitro compounds (**3**). When the trisubstituted nitrosoureas (**1**) decomposed to form the triazenes, the evolution of CO_2 was detectable as absorption at 2320 cm^{-1} in the IR spectra.[1] 3-Alkyl-1-aryl-1-nitrosoureas (**4**, **5**) and *N*-nitrosoacetanilides (**8**) gave mainly the (2-nitroaryl)ureas (**11**) and 2-nitroacetanilides (**12**), respectively. The formation of CO_2 and the corresponding triazenes (**13**) was not confirmed in the case of the disubstituted nitrosoureas (**4**, **5**).

N-Nitrosoacetanilides are known to decompose to a diazonium ion. The diazonium ion can be isolated as its acetate in carbon tetrachloride and trapped as an azo compound with 2-naphthol in sodium hydroxide solution.[13] In the decomposition of the nitrosoureas (**4**, **5**), the formation of a diazonium salt (**15**) *via* a diazoester intermediate (**14**) is predictable by analogy, as shown in Chart 2. However, no intermediates could be isolated, and the trapping of the diazonium ion by the preceding method using 2-naphthol in the alkaline solution seemed to be unsuitable in our experiment, since there is a possibility of producing the diazonium hydroxide (**17**) without passing through the diazonium carbamate (**15**) by attack of hydroxide ion on the CO group of nitrosoureas to form a tetrahedral intermediate or by abstraction of the ureido proton by hydroxide ion.[4] Thus, in order to confirm the mechanism of the decomposition of the 1-aryl-1-nitrosoureas, we examined an azo coupling reaction with 3-methyl-1-phenyl-5-pyrazolone in carbon tetrachloride. The azo coupling products (**19a**, **b**) were obtained from 3-(2-tolyl)-1-nitrosourea (**5a**) and 3-(4-tolyl)-1-nitrosourea (**5b**) in 20% and 35% yields, respectively. These results suggest the formation of the diazoester intermediate (**14**) in this reaction. When a chloroform solution of the nitrosoureas (**4**, **5**) was allowed to stand at room temperature, the solution showed strong absorption at 2250 cm^{-1} in

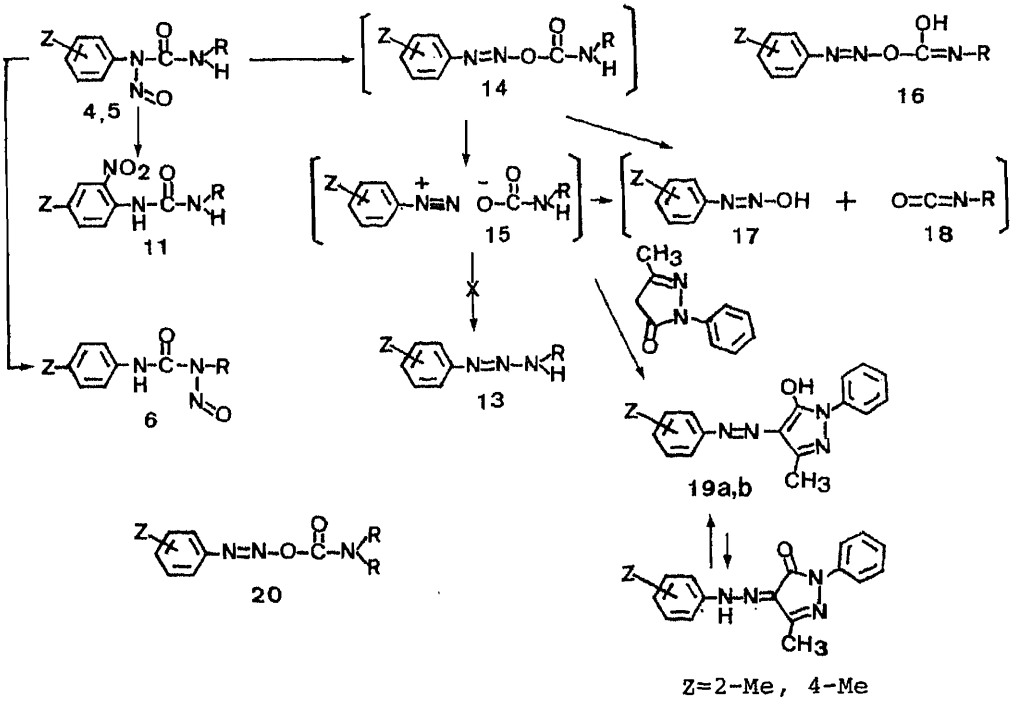

Chart 2

the IR spectrum. This absorption is due to the alkyl isocyanate (**18**), for the urea (**10e**) was obtained by the decomposition of **5b** in the presence of 4-anisidine. There seem to be two possible pathways for the formation of the alkyl isocyanate (**18**) (Chart 2). However, it was not proved whether **18** was produced directly from **14** or through the other intermediate (**15**).

The disubstituted nitrosoureas differ from the trisubstituted derivatives with respect to the mode of decomposition of the intermediate derived from the nitrosoureas. The mobile N^3H-proton of the intermediate (**14** or **15**) in the decomposition of disubstituted nitrosoureas migrates to the carbonyl oxygen to yield the diazohydroxide (**17**) and the isocyanate (**18**). Then, the tautomer (**16**) of **14** is also permitted as an intermediate in the decomposition to **18**. On the other hand, the intermediate (**20**) produced from the trisubstituted nitrosoureas (**1**) evolves CO_2 by breaking of the CO–N^3 bond in the absence of the N^3H-proton, consequently yielding the triazenes.

In the nitrosation of the ureas (**10b, d**) with isoamyl nitrite at room temperature, isoamyl 4-substituted phenylcarbamates (**21a, b**) were obtained in 24—37% yields. Further, 3-isopropyl-1-(4-substituted phenyl)-3-nitrosoureas (**7b, d**) gave the corresponding carbamates (**21a, b**) in isoamyl alcohol. The formation of the aryl isocyanates is predictable in these reactions; they would be trapped by isoamyl alcohol to give the carbamates (Chart 3). Diphenyl-*N*-nitrosourea gives phenyl isocyanate on refluxing in benzene.[8] The chloroform solution of 1-aryl-3-isopropyl-3-nitrosoureas (**7**) showed a strong absorption due to the NCO group at 2260 cm^{-1} after standing at room temperature. These results are evidence that the disubstituted 3-nitrosoureas also decompose to the isocyanates *via* the diazoester intermediate.

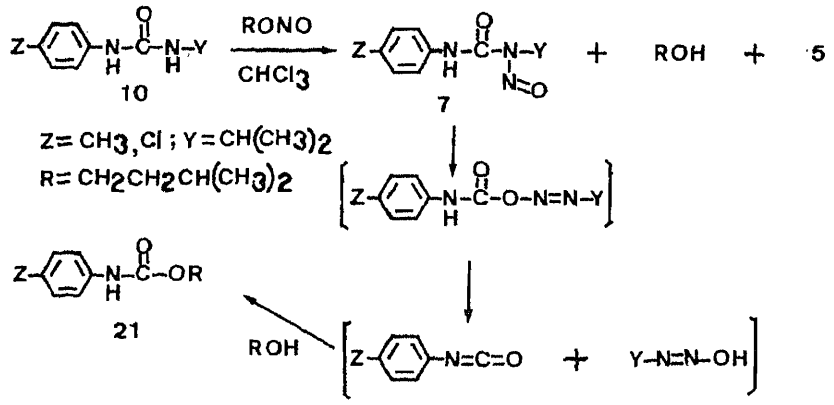

Chart 3

Nitration and Isomerization

The disubstituted 1-nitrosoureas (**4, 5**) and the *N*-nitrosoacetanilides (**8**) afforded the corresponding 2-nitroaryl compounds (**11, 12**) similarly to the trisubstituted nitrosoureas (**1**). The nitration yields are shown in Table III. The nitrated products (**12**) were obtained in low yields, though the starting materials (**8a, b**) were destroyed rapidly in carbon tetrachloride. The nitrosoureas (**4, 5**) decomposed more slowly. The 4-methoxyphenyl derivatives (**4e, 5e**) were obtained in better yields than the 4-tolyl derivatives (**4b, 5b**), perhaps because of their strongly electron-releasing MeO group.

Although it is not proven, the following mechanism may be considered for the formation of the nitro compounds. The nitroso compound will probably dissociate into the nitric oxide and the arylureidyl (or arylacetaminyl) radical. The nitric oxide is oxidized by oxygen, and the generated nitrogen dioxide may combine with the arylureidyl (or arylacetaminyl) radical to give the nitro compound. It is unlikely that the *C*-nitroso compound is formed from the *N*-

nitroso compound, followed by oxidation to give the nitro compound, under mild experimental conditions in the absence of a powerful oxidizing agent. We are still seeking to establish the pathway in detail.

We found that the decomposition of the nitroso compounds was a competitive reaction[12] with the nitration due to the N–NO bond cleavage and the formation of diazoester due to the attack of NO at the CO group. The difference of nitration between the nitrosoacetanilides and the nitrosoureas may reflect the difference of polarization of the CO group which is closely related to the formation of the diazoester intermediate (**14**) described in the preceding section. The nitration seems to be advantageous in the nitrosoureas, for the attack of NO at the ureido carbonyl is depressed relative to that at the amido carbonyl, and consequently the N–NO bond cleavage proceeds preferentially in the nitrosoureas as compared with the nitrosoacetanilides.

3-Alkyl-1-(2-tolyl)-1-nitrosoureas (**4a**, **5a**) are stable as compared with the corresponding 4-tolyl isomers. This may be because the phenyl–N^1 bond is more twisted[12] in the 2-tolyl derivatives than in the 4-tolyl isomers and the localization of the lone pair at the N^1 position stabilizes the N–NO bond.

The 3-methyl-1-nitrosoureas (**4b**, **e**) isomerized to the 3-nitrosoureas (**6b**, **e**) in carbon tetrachloride. Such a 1,3-shift of the NO group attached to the ureido group has never

TABLE III. Yields of Nitration and 1,3-Rearrangement in the Decomposition of 3-Alkyl-1-nitrosoureas (**4**, **5**) and *N*-Nitrosoacetanilides (**8**) in CCl_4 at 33 °C

Compd.	React. time[b] (min)	Product (%)[a]	
		Nitro compd.	3-Nitrosourea
4b	180	**11a** (2)	**6b** (22)
4b[c]	160	**11a** (14)	**6b** (32)
4e	250	**11b** (8)	**6e** (27)
5b	230	**11c** (1)	—
5b[c]	130	**11c** (3)	**7b** (14)
5b[d]	180	**11c** (3)	**7b** (5)
5e	230	**11d** (10)	
8a	34	**12a** (0.3)	
8b	44	**12b** (0.8)	

a) Product yields were determined by HPLC (see experimental section). *b*) One-half of the initial amount of nitroso compound is reduced at this time. *c*) 0.1 eq mol of 99% formic acid was added. *d*) Equimolar 99% formic acid was added.

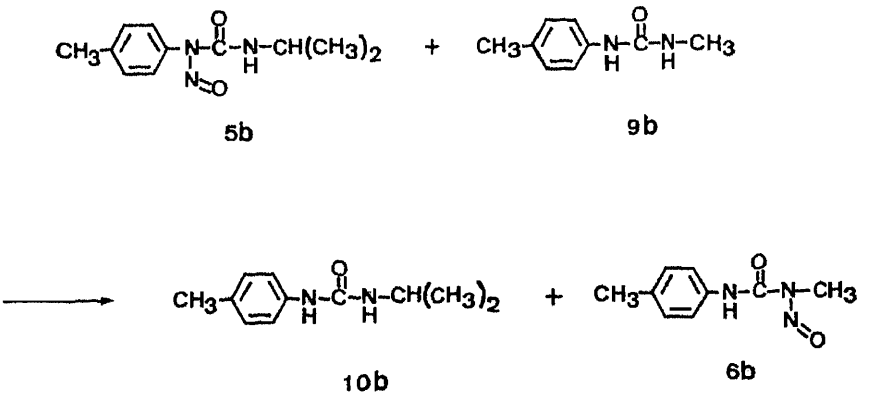

Chart 4

TABLE IV. Physicochemical Properties and Analytical Data of Nitro Compounds (**11**, **12**), Azo Compounds (**19**) and Carbamates (**21**)

Compd.	Yield (%)	mp (°C) Recrystn. solvent	Formula	Analysis (%) Calcd (Found)			IR $\nu_{max}^{CHCl_3}$ cm^{-1} NH CO
				C	H	N	
11a	40	205.5—206.5 (Ether–acetone)	$C_9H_{11}N_3O_3$	51.67 (51.59	5.30 5.29	17.71 19.92)	3450, 3340 1690
11b	45	180—181 (Ether–acetone)	$C_{11}H_{15}N_3O_3$	55.68 (55.50	6.37 6.40	17.71 17.78)	3425, 3350 1685
11c	45	198—199 (Ether–acetone)	$C_9H_{11}N_3O_3$	48.00 (47.88	4.92 4.90	18.66 18.72)	3450, 3350 1640
11d	35	205—206 (Ether–acetone)	$C_{11}H_{15}N_3O_4$	52.17 (51.84	5.97 5.96	16.59 16.60)	3440, 3350 1685
11e	24	192—193 (Acetone)	$C_{10}H_{12}ClN_3O_3$	46.61 (46.32	4.69 4.61	16.31 16.23)	3425, 3350 1690
12b	30	119.5—120.5 (Ether–acetone)	$C_4H_{10}N_2O_4$	51.42 (51.29	4.80 4.78	13.33 13.41)	3375 1685
19a	32	191—192 ($CHCl_3$)	$C_{17}H_{16}N_4O$	69.84 (69.73	5.52 5.49	19.17 19.19)	
19b	10	143.5—144.5 ($CHCl_3$)	$C_{17}H_{16}N_4O$	69.84 (69.56	5.52 5.53	19.17 19.16)	
21b	24	61—62 (*n*-Hexane–ether)	$C_{12}H_{16}ClNO_2$	59.62 (59.38	6.67 6.55	5.79 5.75)	3440 1718
21c	12	68.5—69.5 (*n*-Hexane–ether)	$C_9H_{10}ClNO_2$	54.14 (54.05	5.05 4.98	7.02 6.99)	3430 1717

TABLE V. ^{13}C-Chemical Shifts[a] (ppm) of Azo Compounds (**19**)

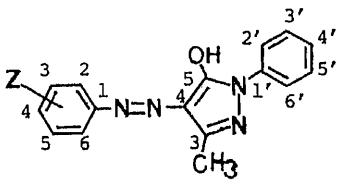

Compd.	Z	Phenyl						Pyrazolyl			Me	Z
		C-1 C-1′	C-2 C-2′	C-3 C-3′	C-4 C-4′	C-5 C-5′	C-6 C-6′	C-3	C-4	C-5		
19a	2-Me	140.5 158.0	125.4 118.8	131.1 128.9	125.5 125.2	127.5 128.9	114.6 118.8	139.5[b]	129.3	138.1[b]	11.8	16.8
19b	4-Me	148.4 157.9	115.8 118.5	130.2 128.9	135.8 125.9	130.2 128.9	115.8 118.5	139.0[b]	128.0	138.2[b]	11.7	21.0

a) Measured in $CDCl_3$ at room temperature with TMS as an internal standard. *b*) Assignments may be reversed.

previously been found in nonpolar solvents, though a similar rearrangement in acids was reported.[5,9] In the case of carbon tetrachloride containing a small amount of formic acid, the yields of the nitro compounds and 1,3-rearrangement products were increased (Table III).

Moreover, transnitrosation occurred from 3-isopropyl-1-(4-tolyl)-1-nitrosourea (**5b**) to 3-methyl-1-(4-tolyl)urea (**12b**) to give 3-methyl-1-(4-tolyl)-3-nitrosourea (**6b**) (Chart 4). The mechanisms of 1,3-rearrangement and transnitrosation of compounds having the *N*-

nitrosoureido group in nonpolar solvents are under investigation.

Experimental

All melting points were determined with a Yanagimoto melting point apparatus and are uncorrected. IR spectra were measured with a JASCO A-102 spectrophotometer. Ultraviolet (UV) spectra were recorded with a Shimadzu UV-240 spectrophotometer. High performance liquid chromatography (HPLC) was performed on a JASCO TWINCLE chromatograph and UV detector (Toyo Soda UV-8) operating at 254 nm, using a TSK-Gel LS 310K column (4 × 300 mm i.d., Toyo Soda) with *n*-hexane–ethyl acetate (4:1, v/v) as a mobile phase. Peak areas were determined with a Shimadzu C-R3A Chromatopack. The internal standard employed was 4-methyl-2-nitroacetanilide (**12a**).[14,15] Proton nuclear magnetic resonance (^{1}H-NMR) spectra were measured with a Varian EM 360-A spectrometer and ^{13}C-NMR spectra were measured with a JEOL FX-200 spectrometer with tetramethylsilane (TMS) as an internal standard. The abbreviations are as follows: s, singlet; d, doublet; m, multiplet; br, broad; sh, shoulder.

3-Alkyl-1-arylureas (9, 10)——Methyl isocyanate or isopropyl isocyanate (75 mmol) was added to a solution of arylamine (75 mmol) in ether (300 ml) at −5 °C with stirring. The resulting crystals (after concentration, if necessary) were filtered off, and recrystallized from a mixture of ether and acetone. Colorless pillars or plates. The yields of all products were over 70%. ^{13}C-NMR spectral data are shown in Table II and IR data and melting points are listed in Table VI.

Nitrosoureas (4—7)——3-Alkyl-1-arylureas (**9, 10**) were nitrosated by methods A or B. Method A is exemplified by the nitrosation of **10b** and method B is exemplified by that of **9b**.

Method A: 3-Isopropyl-1-(4-tolyl)urea (**10b**) (1.92 g, 10 mmol) was dissolved in 99% formic acid (10 ml). Sodium nitrite (0.75 g, 11 mmol) was added to the solution at 0—5 °C and the mixture was stirred for 30 min while maintaining the temperature below 5 °C. The reaction mixture was poured into $CHCl_3$, a small quantity of cold water was added, and the whole was extracted with $CHCl_3$. The $CHCl_3$ layer was washed with saturated sodium bicarbonate solution and cold water until the washings were neutral. The $CHCl_3$ layer was filtered through a silicon-treated filter paper (1 ps phase separator, Whatman Ltd.) and evaporated under reduced pressure in an ice-water bath. The residue was chromatographed on a column of silica gel with a mixture of *n*-hexane and ether under cooling as described in the preceding paper.[1] The first fraction gave 0.8 g (37%) of 3-isopropyl-1-(4-tolyl)-3-nitrosourea (**7b**). Pale yellow needles, mp 71.5—72.5 °C (dec.). UV $\lambda_{max}^{CHCl_3}$ nm (log ε): 241 (4.10), 278 (3.60), 286 (3.59), 396 (2.09), 413 (2.03). ^{1}H-NMR ($CDCl_3$) δ: 1.34 (6H, d, J=7 Hz, $CH(C\underline{H}_3)_2$), 2.35 (3H, s, CH_3), 5.50 (1H, m, J=7 Hz, $C\underline{H}(CH_3)_2$), 7.17 and 7.47 (4H, dd, J=9 Hz, phenyl), 8.70 (1H, br, NH). The second fraction gave 0.2 g (15%) of 3-isopropyl-1-(4-tolyl)-1-nitrosourea (**5b**). Yellow pillars, mp 101.5—102.5 °C (dec.). UV $\lambda_{max}^{CHCl_3}$ nm (log ε): 242 (3.98), 402 (2.38), 420 (2.08). ^{1}H-NMR ($CDCl_3$) δ: 1.32 (6H, d, J=7 Hz, $CH(C\underline{H}_3)_2$), 2.37 (3H, s, CH_3), 4.27 (1H, m, J=7 Hz, $C\underline{H}(CH_3)_2$), 6.60 (1H, br, NH), 6.85 and 7.29 (4H, dd, J=8 Hz, phenyl).

Method B: Isoamyl nitrite (7.0 g, 0.06 mol) was added dropwise to a suspension of 3-methyl-1-(4-tolyl)urea (**9b**) (6.6 g, 0.04 mol) in $CHCl_3$ (200 ml) at 0—5 °C and stirred for 10 h. The unreacted urea was filtered off and the filtrate was evaporated to dryness under reduced pressure in an ice-water bath. The residue was chromatographed as described in method A. The first fraction gave 7.3 g (95%) of 3-methyl-1-(4-tolyl)-3-nitrosourea (**6b**). Pale yellow

TABLE VI. IR Data and Melting Points of Ureas (**9, 10**)

Compd.	mp (°C)	IR $\nu_{max}^{CHCl_3}$ [a] cm^{-1}	
		NH	CO
9a	173—174	3430, 3450^{sh}	1660
9b[4]	181—182	3425, 3350^{sh}	1660
9c[4]	154—155	3430, 3350^{sh}	1665
9d[4]	209.5—210.5	3320, 3330^{sh}	1630
9e[4]	168—169	3425, 3350^{sh}	1650
10a	181.5—182.5	3425, 3325^{sh}	1650
10b	159—160	3350, 3425^{sh}	1650
10c	160.5—161.5	3425, 3350^{sh}	1650
10d	220.5—221.5	3320	1620
10e	156—157	3425, 3350^{sh}	1655

a) The spectra of **9b** and **10b** were measured in Nujol.

plates, mp 102–103 °C (dec.).[4] UV $\lambda_{max}^{CHCl_3}$ nm (log ε): 241 (4.10), 277 (3.64), 285 (3.64), 392 (1.94), 410 (1.83). The second fraction gave 0.15 g (2%) of 3-methyl-1-(4-tolyl)-1-nitrosourea (**4b**). Yellow plates, mp 101.5—102.5 °C (dec.). UV $\lambda_{max}^{CHCl_3}$ nm (log ε): 240 (3.69), 402 (2.54), 420 (2.43). ^{1}H-NMR ($CDCl_3$) δ: 2.38 (3H, s, CH_3), 3.04 (3H, d, J=5 Hz, $NHCH_3$), 6.84 and 7.28 (4H, dd, J=8 Hz, phenyl), 6.90 (1H, br, NH).

Nitrosation of other ureas were carried out according to in the methods A or B. Physicochemical, analytical and spectral data are listed in Tables II and IV.

3-Alkyl-1-(2-nitroaryl)ureas (11)——A typical experiment is described here for **11a**. Fuming nitric acid (*d*: 1.52, 2 ml) was added to a solution of 3-methyl-1-(4-tolyl)urea (**9a**) (1.1 g, 7 mmol) in acetic acid (10 ml) at 0—5 °C with stirring, and the mixture was stirred for 20 min at room temperature. The reaction mixture was poured into crushed ice and extracted with CH_2Cl_2. The CH_2Cl_2 layer was washed with saturated $NaHCO_3$ solution and dried over anhydrous Na_2SO_4. The solvent was evaporated off and the residue was purified by silica gel column chromatography with a mixture of *n*-hexane, ether and $CHCl_3$ as an eluting solvent. 3-Methyl-1-(2-nitro-4-tolyl)urea (**11a**) was obtained. Yellow prisms (from ether and acetone), mp 205.5—206.5 °C. Yield, 0.56 g (40%).

The other nitro compounds (**11b—e, 12b**) were prepared in a similar manner. Physicochemical, analytical and spectral data are shown in Tables II and IV.

Isoamyl Arylcarbamates (21)[16]——4-Chlorophenyl isocyanate (0.4 g, 2.6 mmol) in $CHCl_3$ (1 ml) was added to isoamyl alcohol (0.7 g, 8 mmol) and the solution was left overnight at room temperature. The resulting crystals were filtered off and recrystallized from ether. Isoamyl 4-chlorophenylcarbamate (**21b**) was obtained. Colorless needles, mp 61—62 °C. Yield, 0.6 g (95%).

Isoamyl 4-tolylcarbamate (**21a**) was also obtained from 4-tolyl isocyanate and isoamyl alcohol after chromatography of the reaction mixture on silica gel with a mixture of *n*-hexane and ether (10 : 1). A pale yellow oily product. Yield, 1.1 g (68%). Analytical data and spectral data are given in Tables II and IV.

The Reaction of 3-Alkyl-1-arylureas (13b, d) with Isoamyl Nitrite——Isoamyl nitrite (1.4 g, 12 mmol) was added to a suspension of 3-isopropyl-1-(4-chlorophenyl)urea (**10d**) (2.1 g, 10 mmol) in $CHCl_3$ (100 ml), and the mixture was stirred overnight at room temperature. The reaction mixture was filtered and the filtrate was concentrated under reduced pressure. The residue was chromatographed on a column of silica gel with a mixture of *n*-hexane and ether (10 : 1) under cooling. The first fraction gave 0.15 g (24%) of isoamyl 4-chlorophenylcarbamate (**21b**) which was identical with an authentic sample described above. The second fraction gave 0.2 g (12%) of ethyl 4-chlorophenylcarbamate (**21c**).[17] Colorless needles (from ether), mp 68.5—69.5 °C. The third fraction gave 0.05 g (2%) of 1-(4-chloro-2-nitrophenyl)-3-isopropylurea (**11e**) which was identical with an authentic sample described above.

3-Isopropyl-1-(4-tolyl)urea (**10b**) was also treated with isoamyl nitrite in a similar manner. Isoamyl 4-tolylcarbamate (**21a**) and 3-isopropyl-1-(2-nitro-4-tolyl)urea (**11b**) were obtained in 37% and 5% yields, respectively. These products were identified by comparison with authentic samples as described above.

Reaction of the 3-Nitrosoureas (6b, d) and Isoamyl Alcohol——1-(4-Chlorophenyl)-3-isopropyl-3-nitrosourea (**6d**) (0.2 g, 0.83 mmol) in $CHCl_3$ (2 ml) was added to a solution of isoamyl alcohol (0.1 g, 1.2 mmol) and the solution was allowed to stand overnight at room temperature. The reaction mixture was chromatographed on a column of silica gel with a mixture of *n*-hexane and ether (10 : 1). The eluate gave isoamyl 4-chlorophenylcarbamate (**21b**), which was identical with an authentic sample. Yield, 0.18 g (90%).

3-Isopropyl-1-(4-tolyl)-3-nitrosourea (**6b**) gave isoamyl 4-tolylcarbamate (**21a**) in a similar manner. Yield, 0.2 g (50%).

Formation of Azo Compounds (19) from the 1-Nitrosoureas (5a, b)——3-Methyl-1-phenyl-5-pyrazolone (0.7 g, 4 mmol) was added to a solution of 3-isopropyl-1-(4-tolyl)-1-nitrosourea (**5b**) (0.44 g, 2 mmol) in CCl_4 (10 ml) and the mixture was allowed to stand for 2 d. The solvent was evaporated off and the residue was chromatographed on a column of silica gel. The first fraction eluted with a mixture of *n*-hexane and ether (5 : 1) gave 5-hydroxy-3-methyl-1-phenyl-4-(4-tolyl)azopyrazole (**19b**). Reddish needles (from $CHCl_3$), mp 144.5—145.5 °C. Yield, 0.19 g (32%).

5-Hydroxy-3-methyl-1-phenyl-4-(2-tolyl)azopyrazole (**19a**) was similarly prepared from 3-isopropyl-1-(2-tolyl)-1-nitrosourea (**5a**). Reddish needles (from $CHCl_3$), mp 191—192 °C. Yield, 10%. Analytical and spectral data are shown in Tables IV and V.

Decomposition of 3-Alkyl-1-aryl-1-nitrosoureas (4, 5)——1) Formation of Alkyl Isocyanates: 3-Isopropyl-1-(4-tolyl)-1-nitrosourea (**5b**) was dissolved in $CHCl_3$ and left overnight at room temperature. The solution showed a strong absorption at 2250 cm^{-1}. When 4-anisidine was added to the solution and the mixture was allowed to stand for 2 h, 3-isopropyl-4-methoxyphenylurea (**10e**) was obtained after purification by silica gel column chromatography with a mixture of *n*-hexane and ether (7 : 3).

2) Formation of the 2-Nitroaryl Compounds (**11**) and the 3-Nitrosoureas (**6, 7**): 3-Alkyl-1-aryl-1-nitrosoureas (**4, 5**) were dissolved in CCl_4 (exactly 10 ml) containing **10a** as an internal standard. Each solution was kept at 33±0.5 °C and aliquots were subjected periodically to HPLC under the conditions described above. The amounts of 3-alkyl-1-(2-nitroaryl)ureas (**11**) and 3-alkyl-1-aryl-3-nitrosoureas (**6**) increased with time. The yields of **6** and **11** at the half-life period of the starting nitrosoureas are shown in Table III. A similar experiment was carried out in the presence of formic acid in CCl_4 and the results are also shown in Table III.

4-Methyl-*N*-nitrosoacetanilide (**8a**) and 4-methoxy-*N*-nitrosoacetanilide (**8b**) were also treated similarly. They

gave 4-methyl-2-nitroacetanilide (**12a**) and 4-methoxy-2-nitroacetanilide (**10b**), respectively (Table III).

1,3-Rearrangement of 3-Alkyl-1-(4-tolyl)-1-nitrosoureas (4b, 5b) and Their 3-Nitroso Isomers (6b, 7b) in the Presence of Formic Acid——3-Isopropyl-1-(4-tolyl)-1-nitrosourea (**5b**) or its 3-nitroso isomer (**7b**) (38 mg, 0.17 mmol) was dissolved in cooled 99% formic acid (2 ml) and the solution was kept at 14 °C (it coagulated at temperatures below 7 °C). A sample (2 ml) of the reaction mixture was taken every 3 min, and each sample was neutralized with $NaHCO_3$ (0.6 g) then dissolved in water (4 ml). The mixture was extracted with $CHCl_3$ (4 ml) and the $CHCl_3$ layer was diluted to a volume of exactly 10 ml. Each solution was subjected to HPLC under the conditions described above. The amounts of the components are plotted *vs.* time in Fig. 1. The rearrangement within the first 15 min was a pseudo first-order reaction and the rate constants were $k_1 = 3.30 \times 10^{-4}\,s^{-1}$ (**5b**→**7b**) and $k_2 = 2.05 \times 10^{-4}\,s^{-1}$ (**7b**→**5b**); the formation of the urea (**10b**) was not more than 10%.

3-Methyl-1-(4-tolyl)nitrosoureas (**4b, 6b**) were similarly treated. However, the rate constants for the 3-methyl derivatives (**4b, 6b**) could not be measured under the experimental conditions used, because **4b** rearranged to its 3-nitroso isomer (**6b**) immediately and **6b** did not change to **4b**.

Transnitrosation of 3-Isopropyl-1-(4-tolyl)-1-nitrosourea (5b) to 3-Methyl-1-(4-tolyl)urea (9b) in CCl_4——The 1-nitrosourea (**5b**) (9.75 mg, 0.04 mmol) and the urea (**9b**) (8.3 mg, 0.04 mmol) were dissolved in CCl_4 (10 ml) and the solution was kept at 33±0.5 °C for 7 h. The yield of 3-methyl-1-(4-tolyl)-3-nitrosourea (**6b**) was determined by HPLC. Yield, 43%.

Acknowledgement We are grateful to Mrs. H. Kitamura, the Analytical Center, Shizuoka College of Pharmacy, for elemental analyses.

References and Notes

1) S. Sueyoshi and M. Tanno, *Chem. Pharm. Bull.*, **33**, 488 (1985).
2) D. E. V. Wilman and P. M. Goddard, *J. Med. Chem.*, **23**, 1052 (1980); T. Girldi, C. Nisi, T. A. Connars, and P. M. Goddard, *ibid.*, **20**, 850 (1977).
3) V. A. Levin and C. W. Wilson, *Cancer Treat. Rep.*, **60**, 719 (1976); J. A. Montgomery, *ibid.*, **60**, 651 (1976); J. W. Lown and S. M. S. Chuhn, *J. Org. Chem.*, **46**, 2479 (1981) *etc.*
4) K. Yoshida and K. Yano, *Bull. Chem. Soc. Jpn.*, **55**, 2200 (1982).
5) T. P. Johnston, G. S. McCaleb, P. S. Opliger, and J. A. Montgomery, *J. Med. Chem.*, **9**, 892 (1966).
6) S. Kamiya, *Chem. Pharm. Bull.*, **23**, 2744 (1975).
7) S. Kamiya and S. Sueyoshi, *Chem. Pharm. Bull.*, **31**, 1738 (1983).
8) M. Miyahara and S. Kamiya, *Chem. Pharm. Bull.*, **30**, 3466 (1982); M. Miyahara, S. Kamiya, and M. Nakadate, *ibid.*, **30**, 41 (1983).
9) S. Sueyoshi and S. Kamiya, *Chem. Pharm. Bull.*, **29**, 1267 (1981).
10) C. G. Cannon and G. B. M. Sutherland, *Spectrochim. Acta*, **4**, 373 (1951).
11) N. B. Colthup, *J. Opt. Soc. Am.*, **40**, 397 (1950).
12) M. Tanno and S. Sueyoshi, *Chem. Pharm. Bull.*, **35**, 1353 (1987).
13) C. Rüchardt and C. C. Tan, *Chem. Ber.*, **103**, 1774 (1970).
14) S. Sueyoshi and M. Tanno, *Eisei Shikensho Hokoku*, **102**, 108 (1986).
15) The experiments on 4-methyl-*N*-nitrosoacetanilide (**8a**) employed 4-methoxy-2-nitroacetanilide (**12b**) as an internal standard.
16) Commercial isoamyl alcohol contains a small amount of 2-methylbutyl alcohol. Therefore, 2-methylbutyl arylcarbamates were always contained in the crude products. 2-Methylbutyl 4-tolylcarbamate: ^{13}C-NMR ($CDCl_3$) δ: 10.8, 25.7, 34.2, 69.4 (butyl), 16.0 (C-CH_3), 20.3 (Ph-CH_3), 132.2, 118.9, 129.0, 135.6 (Ph-C^1–C^4), 154.1 (CO). 2-Methylbutyl 4-chlorophenylcarbamate: ^{13}C-NMR ($CDCl_3$) δ: 10.8, 25.7, 34.2, 69.7 (butyl), 16.0 (C-CH_3), 127.9, 120.0, 128.5, 137.0 (Ph-C^1–C^4), 154.1 (CO).
17) Commercial ethyl phenylcarbamate: IR $\nu_{max}^{CHCl_3}$ cm^{-1}: 3430 (NH), 1720 (CO). ^{13}C-NMR ($CDCl_3$) δ: 14.5, 61.1 (CH_2CH_3), 138.3, 119.0, 128.9, 123.3 (Ph-C^1–C^4), 154.0 (CO).

[Chem. Pharm. Bull. 35(4)1372—1377(1987)]

Reactivity of Phthalimide-*N*-oxyl: A Kinetic Study

CHIHIRO UEDA, MASAHITO NOYAMA, HIDENOBU OHMORI, and MASAICHIRO MASUI*

Faculty of Pharmaceutical Sciences, Osaka University, 1-6 Yamadaoka, Suita, Osaka 565, Japan

(Received July 31, 1986)

The reactivity of phthalimide-*N*-oxyl radical (**2**), which is produced by an electrochemical one-electron oxidation of *N*-hydroxyphthalimide (**1**), was investigated. The self-decomposition of **2** obeyed second-order kinetics with respect to itself and the rate was little affected by changing the temperature or the concentration of dissolved oxygen, water or added base. In the reaction between **2** and benzhydrol or its α-deuterated derivative, the decay of the radical was first-order with respect to each component. The observed large deuterium isotope effect ($k_H/k_D = 10.6$ at 25 °C) is attributed to the rate-limiting hydrogen abstraction. Rate measurements were performed on the reaction with 24 other substrates which have one or more hydrogen atoms on a benzylic or allylic position or on a carbon adjacent to a hetero atom.

Keywords——*N*-hydroxyphthalimide; phthalimide-*N*-oxyl; hydrogen abstraction; indirect electrochemical oxidation; EC catalytic process

In our laboratory it has been shown that *N*-hydroxyphthalimide (**1**) can act as an effective electrochemical mediator in a variety of oxidation reactions. Many sorts of compounds including alcohols,[1] those having a benzylic carbon or α-carbon to a hetero atom,[2] olefins,[3] amides and lactams,[4] ketals,[5] and aldehyde acetals[6] were found to be substrates for the mediation. The reaction mechanism has been considered to be as shown in Chart 1, in which the phthalimide-*N*-oxyl radical (**2**) acts as the oxidant. However, chemical characterization of the radical has not yet been carried out, though it would be useful for a precise understanding of the process. This paper reports the results of quantitative evaluation

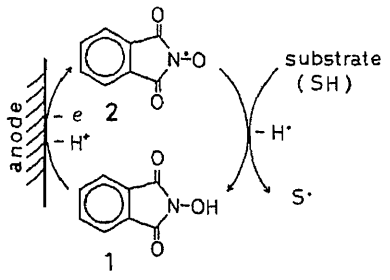

Chart 1

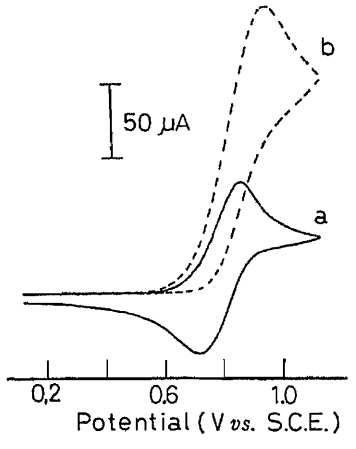

Fig. 1. Cyclic Voltammograms of **1**

In acetonitrile containing 0.1 M $NaClO_4$ and 10 mM pyridine: (a) without, (b) with 50 mM isochroman. Glassy carbon electrode (area = 0.071 cm^2); voltage sweep rate, 50 mV s^{-1}; concentration of **1**, *ca.* 5 mM.

of the reactivity of **2** in self-decomposition and in the reaction with substrates.

Results and Discussion

Nature of 2 in the Absence of the Substrates

On cyclic voltammetry in acetonitrile containing 0.1 M sodium perchlorate and an excess of pyridine,[7] **1** showed a nearly reversible redox couple at 0.78 V *vs.* S.C.E. (Fig. 1a). The normalized peak current, 15.6 μA/mM, for the oxidation wave was comparable with those of 4-substituted 2-cyano-2-phenylvinylamines, the electrode process of which was shown to be a one-electron transfer.[8] The formation and the decay of **2** were found to be synchronized with spectral changes at around 400 nm. As shown in Fig. 2, the absorbance at that wavelength was monitored during a macro scale electrolysis and the following open circuit relaxation.[9] Since constant current electrolysis was used, a linear dependence between the increasing optical density and time (*i.e.*, consumed electricity) was observed at the earlier part of the run. From the slope, the apparent absorptivity of **2** could be estimated.[10] An electron spin resonance (ESR) spectrum was also obtained from the solution, and the data (A_N=4.77 G (1N), A_H= 0.4 G (2H), g=2.0070) were close to the reported values.[11]

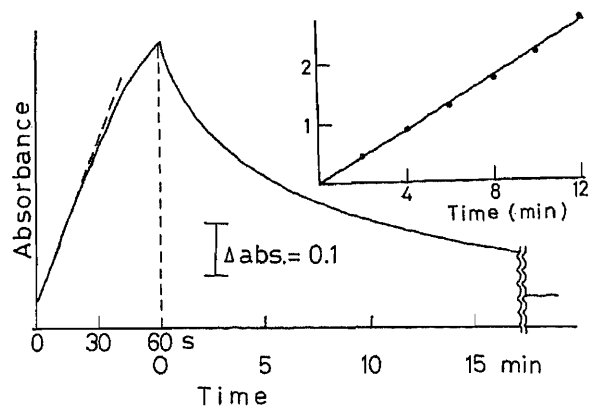

Fig. 2. Absorption–Time Curve for the Generation and Decay of **2** and the Second-Order Plot for the Self-Decomposition

Conditions were as follows: concentration of **1**, 5 mM; pyridine, 5 mM; constant current electrolysis (5 mA); monitored wavelength, 400 nm; temperature, 25 °C. The ordinate of the second-order plot corresponds to $(A_0-A)/A_0A$, where A_0 and A are the absorbance at t=0 and t, respectively.

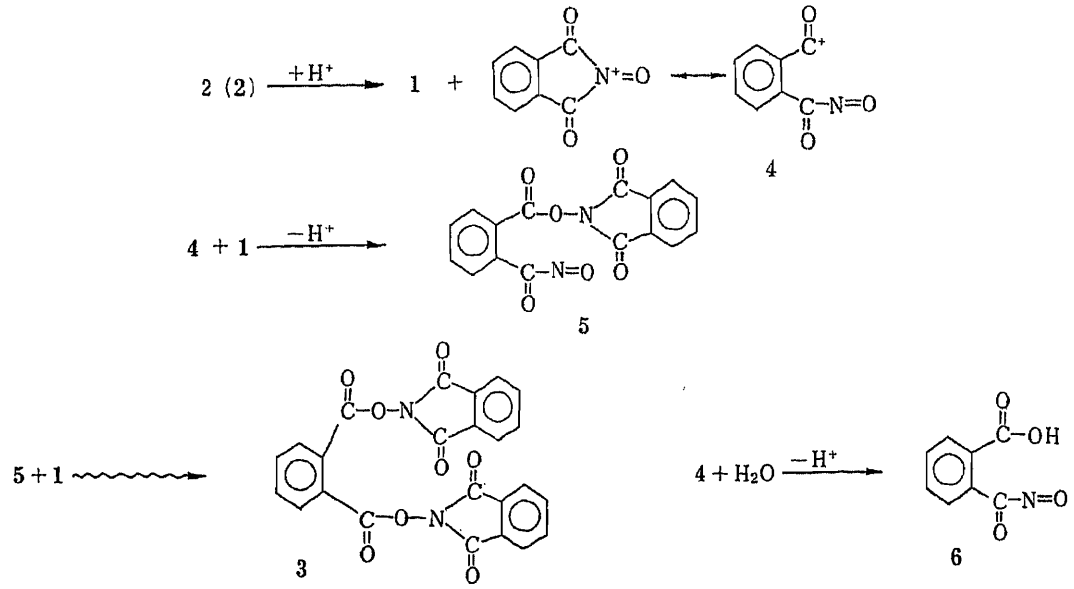

Chart 2

From the right half of the absorbance–time curve in Fig. 2, a good second-order relationship to the radical itself was shown with a rate constant of 24.1 $1\,mol^{-1}\,s^{-1}$. Similar measurements were carried out by changing the following variables; initial concentration of **2**, presence and absence of dissolved oxygen, temperature (15—35 °C) and the base concentration. All the observed rate constants were scattered in the range of $\pm 10\%$, so that a simple bimolecular reaction with a very small activation energy was suggested.

To investigate the products of the self-decomposition of **2**, exhaustive electrolysis of the solution of **1** was carried out at 0.90 V. The consumed electricity was 2.4 F/mol and the trimer (**3**) was isolated from the resulting solution in 71% yield. Phthalic acid (2.5%), phthalic anhydride (8%), phthalimide (trace) and recovered **1** (3.5%) were also detected by high-performance liquid chromatography (HPLC). As judged from the kinetic data, disproportionation of the radical **2**, probably including the formation of a molecule of **1** and an *N*-oxonium cation or its equivalent, can be presumed. While little information about the subsequent processes is available, the pathway in Chart 2 can be deduced from the results on oxidation of hydroxamic acids to form *N*,*O*-diacylhydroxylamines.[12] Since the acyl cation **4** can be considered as an acylating agent, **5** will be produced by reaction with **1**. One more nucleophilic attack of **1** on the other carbonyl carbon in **5** is necessary to form **3**, but the details of the process are not clear at present. If a water molecule contaminating the medium reacts with **4** as a nucleophile, a carboxylic acid **6** will be produced instead of **5**. The minor products, phthalic acid and phthalic anhydride may be formed through **6** by reaction with another molecule of water or by intramolecular cyclization, respectively.

Nature of 2 in the Presence of the Substrates

Figure 1b shows a voltammogram of **1** in the presence of isochroman, which was chosen because of its highest reactivity toward **2** among the substrates tested in the present study (see Table II). A remarkable increase in the anodic peak current with complete disappearance of the cathodic counterpart was demonstrated. The additive alone did not show any redox wave in the potential region, so this behavior is attributable to an EC catalytic process[13] in which the turnover of **2** to **1** by isochroman takes place at an appreciable rate even in the diffusion layer.

To investigate the reaction process in the bulk solution, benzhydrol was chosen, mainly because of its moderate reactivity toward **2** and the ease of obtaining the α-deuterated derivative. The procedures were similar to those of the self-decomposition, but a stopped-flow technique was used. With a large excess of the alcohol a good first-order decay of **2** was demonstrated. The observed rate constants, k_{obs}, for the substrate and its α-deuterated derivative under various conditions are listed in Table I. The values in the last column correspond to the second-order rate constants obtained by dividing the k_{obs} by the substrate concentration. The constancy of the values in runs 1—3 indicates that the reaction is also first-order with respect to the substrate. These rates were little affected by changing the pyridine concentration (run 4). A remarkably large deuterium isotope effect, $k_H/k_D = 10.6$, which falls into a theoretical maximum region,[14] was observed (runs 2 and 8), indicating that the reaction rate is controlled by the α-C-H (or D) bond cleavage. The activation energies were estimated to be 4.8 and 6.7 kcal mol^{-1} for α-H and α-D substrates, respectively. The difference between the two values is comparable with that obtained theoretically (1.21 ± 0.04 kcal mol^{-1}).[15] On the other hand, the activation energies seem appreciably smaller than those reported in the analogous hydrogen abstraction from cumene by benzoyl *tert*-butyl nitroxide (17.9 kcal mol^{-1}),[16] and by di-*tert*-butyliminoxyl (16.8 kcal mol^{-1}).[17] However, it is generally known that the magnitude of the value in this type of reaction depends not only on the dissociation energies of the bonds to be cleaved and formed, but also on the structures of the substrates and the radicals.[15,18] The smaller value in the present case may be attributed to

the structural characteristics of the radical **2**, in which the nitrogen atom is fixed on the ring and flanked by the two carbonyl groups.

It has been reported that benzhydrol is oxidized in the mediating system, yielding benzophenone with good efficiency.[1] Since the consumed electricity based on the substrate was 2 F/mol, participation of another molecule of **2** has been claimed for this indirect oxidation. However, no information concerning the latter process could be obtained from the present results.

Table II summarizes the second-order rate constants obtained for a variety of substrates. Most of these compounds were chosen because their oxidation products in the mediating system have been at least partly elucidated. From the data, we may make the following generalizations, though only qualitatively. First, all the substrates tested here have one or more hydrogen atoms on a benzylic or allylic position or on carbon adjacent to a hetero atom. Such activation seems to be essential for exhibiting reactivity toward **2**, and duplication is more effective. Some examples of the latter case are found in the following pairs: ethylbenzene < benzylmethylether ($\simeq$benzyl alcohol), tetralin < isochroman, isopropanol < benzhydrol.

Second, cyclic substrates show faster rates than the corresponding acyclic ones. Cyclohexanol, tetralin and isochroman are more reactive than isopropanol, ethylbenzene and benzylmethylether, respectively.

TABLE I. Rate Data for the Reactions of the Radical **2**[a] with Benzhydrol and Its α-Deuterated Derivative

Run	Substrate	Concentration (mM)	Temperature (°C)	k_{obs} (s^{-1})[b]	k ($l\,mol^{-1}\,s^{-1}$)
1	Ph–CH(OH)–Ph	10	25	0.384	38.4
2		50	25	1.95	38.9
3		100	25	3.32	33.2
4[c]		50	25	1.66	33.2
5		50	15	1.23	24.6
6		50	35	2.13	42.6
7	Ph–CD(OH)–Ph	50	15	0.127	2.54
8		50	25	0.182	3.64
9		50	35	0.270	5.40

a) Initial concentrations, *ca.* 0.5 mM. *b*) Average value of at least three different runs. *c*) Pyridine concentration, 50 mM (others were 5 mM).

TABLE II. Second-Order Rate Constants[a] of the Reaction of the Radical **2** with Various Substrates

Substrate	k ($l\,mol^{-1}\,s^{-1}$)	Substrate	k ($l\,mol^{-1}\,s^{-1}$)
Isopropanol	1.89	Cyclohexene[c,d]	20.2
Cyclohexanol[b]	4.52	*trans*-4-Octene[d]	12.8
β-Phenethyl alcohol	0.776	2,3-Dimethyl-2-butene[d]	77.6
Benzyl alcohol	15.6	Tetrahydrofuran[c]	2.88
Anise alcohol	51.8	Tetrahydropyran	Very slow[f]
p-Nitrobenzyl alcohol	10.3	Dibutyl ether	1.50
Ethylbenzene[c]	1.85	Dibutyl sulfide	36.3
Benzylmethylether[c]	10.9	Tetrahydrothiophene[c]	96.2
Isochroman[c]	156	Tetrahydrothiopyran	15.3
Fluorene[c]	26.2	*N*-Acetylpyrrolidine[e]	47.6
Tetralin[c]	43.2	*N*-Benzoylpyrrolidine[e]	26.2
Cyclopentene[d]	28.4	*N*-Benzoylpiperidine[e]	0.576

a) Determined from at least three different kinetic runs. *b*—*e*) The products of the indirect oxidation were reported in refs. 1, 2, 3 and 4, respectively. *f*) Less than 0.2 $l\,mol^{-1}\,s^{-1}$.

Third, higher reactivity of five-membered-ring substrates compared to the corresponding six-membered ones, except for the case of cycloalkene, is also suggested. These results account for the poor efficiencies of the six-membered substrates in the mediating system. Tetrahydrothiopyran and *N*-benzoylpiperidine gave the oxidation products in only 8 and 9% yields, respectively,[19] while the corresponding five-membered analogs gave the products in 30 and 79% yields, respectively.[2,4] Furthermore, tetrahydropyran was practically not oxidizable in the system but tetrahydrofuran gave the lactone in 11% yields.[2]

Although quantitative treatment of the structure–reactivity relationship of the substrate toward **2** was not successful, the chemical characterization of the reaction has been achieved. Advantages of **2** as a reagent for the hydrogen abstraction reaction have also been revealed. It shows reactivity with a wide range of compounds, its generation can be easily controlled electrochemically in terms of the rate and the amount, and the direct determination of the radical concentration is possible by spectrophotometric measurements.

Experimental

Materials——*N*-Hydroxyphthalimide was obtained from Tokyo Kasei Kogyo Co. (>99%). α-Deuterated benzhydrol was prepared from benzophenone by $LiAlD_4$ (Merck; >98%) reduction in tetrahydrofuran followed by recrystallization from methanol–water, MS *m/z*: 185 (M^+). Acetonitrile was purified as described previously.[20] All other chemicals were from commercial sources and were used with or without appropriate purification.

Apparatus——Cyclic voltammetry and controlled potential electrolysis were carried out essentially as described previously.[8] Kinetic experiments were carried out using JASCO UVIDEC-1 double beam and Union Giken RA-601 stopped-flow spectrophotometers and a Hokuto Denko HA-104 potentiostat-galvanostat. A Union Giken RA-405 kinetic data processor was used for monitoring the fast reactions.

Kinetic Measurements of the Self-Decomposition of 2——A Pyrex cylindrical vessel (diameter; 2.6 cm, volume; 20 ml) fixed on a magnetic stirrer was placed in the double beam spectrophotometer so that the light would cross the center. The light-path length (2.60 cm) was determined optically. A glassy carbon plate (anode) and a platinum wire (cathode) were placed in the cell. The constant current electrolysis of the solution of **1** was carried out for an appropriate duration followed by circuit opening. The absorption at the selected wavelength was recorded throughout the run.

Product Analysis of the Self-Decomposition of 2——A typical example is described.

A solution of **1** (326 mg) dissolved in 50 ml of acetonitrile containing 0.1 M $NaClO_4$ and pyridine (790 mg; 5 eq) was subjected to electrolysis at 0.90 V at a glassy carbon plate anode in an H-type cell. Up to the time when the current became <2% of the initial value, 455 C (2.4 e per molecule) had been consumed. The electrolytic solution was evaporated and the residue was washed with ether and water. The resulting solid was recrystallized from acetonitrile and identified as *O,O'*-(1,2-phenylenedicarbonyl)-bis-*N*-hydroxyphthalimide (**3**), (216 mg, 71%), mp 229—233 °C. *Anal.* Calcd for $C_{24}H_{12}N_2O_8$: C, 63.16; H, 2.65; N, 6.14%. Found: C, 63.25; H, 2.54; N, 6.20. IR ν_{max}^{Nujol} cm^{-1}: 1780, 1740, 1180, 1130, 990, 875, 790, 700. NMR ($CDCl_3$) δ: 7.5—8.3. MS *m/z*: 457 ($M^+ + 1$). The above ether washings were collected and evaporated. The resulting residue was dissolved in methanol and adjusted to 20.0 ml in a volumetric flask, then subjected to HPLC measurements. A Waters 6000-A solvent delivery system, a Shimadzu SPD-2A spectrophotometric detector and a Bondapack C_{18}-Corasil column were used, with 50% aqueous methanol as the solvent. Identification of minor products was performed by comparing the retention time in HPLC and the *Rf* values in silica gel thin layer chromatography with those of authentic samples. To confirm the structure of **3**, the following derivatization was also carried out. The trimer (1.51 g) was suspended in 30 ml of 40% aqueous ethanol containing 10% NaOH and refluxed for 24 h. The solution was acidified with HCl and extracted with ethyl acetate (20 ml × 7). The extract was dried over Na_2SO_4 and evaporated. Practically pure phthalic acid (83% from **3**) was obtained by washing the residue with chloroform.

Kinetic Measurements of the Reaction with the Substrates——In one of the two reservoirs of the sample mixing unit of the stopped-flow spectrophotometer, platinum wire working and counter electrodes were attached so that the accumulation of **2** under appropriate electrolytic conditions could be achieved. Then, a part of the solution was mixed rapidly with a solution which was stored in the other reservoir containing the substrate to be examined. The standard reaction conditions were as follows (concentrations are those after mixing): **1**, 5 mM; pyridine, 5 mM; substrate, 50 mM; radical concentration generated from **1**, *ca.* 0.5 mM; temperature, 25 °C. The decay of the absorption at 400 nm was followed.

Acknowledgment We are grateful to Professor H. Sayo of Kobe-Gakuin University for the ESR measurements.

References and Notes

1) M. Masui, T. Ueshima, and S. Ozaki, *J. Chem. Soc., Chem. Commun.*, **1983**, 479.
2) M. Masui, S. Hara, T. Ueshima, T. Kawaguchi, and S. Ozaki, *Chem. Pharm. Bull.*, **31**, 4209 (1983).
3) M. Masui, K. Hosomi, K. Tsuchida, and S. Ozaki, *Chem. Pharm. Bull.*, **33**, 4798 (1985).
4) M. Masui, S. Hara, and S. Ozaki, *Chem. Pharm. Bull.*, **34**, 975 (1986).
5) M. Masui, T. Kawaguchi, and S. Ozaki, *J. Chem. Soc., Chem. Commun.*, **1985**, 1484.
6) M. Masui, T. Kawaguchi, S. Yoshida, and S. Ozaki, *Chem. Pharm. Bull.*, **34**, 1837 (1986).
7) It has been confirmed that **1** shows a lower oxidation potential and high turnover number with high current efficiency in the presence of an added base such as pyridine (see reference 1). Therefore, all the electrochemical experiments on **1** in this paper were carried out with an excess of base.
8) M. Masui, C. Ueda, T. Moriguchi, T. Michida, M. Kataoka, and H. Ohmori, *Chem. Pharm. Bull.*, **32**, 1392 (1984).
9) T. Kuwana and N. Winograd, "Electroanalytical Chemistry," Vol. 7, ed. by A. J. Bard, Marcel Dekker, New York, 1974, pp. 1—78 and references cited therein; E. Ahlberg, J. Halvorsen, and V. D. Parker, *Acta Chem. Scand., Ser. B*, **33**, 781 (1979).
10) The slope in Fig. 2 has dimensions of absorbance unit/sec, which can be converted to mol/l by using the known constants such as the light-path length, the cell volume and the current intensity, assuming quantitative efficiency. The absorptivities were 1460, 1330, 929 and 557 $1\,mol^{-1}\,cm^{-1}$ at 380, 400, 420 and 440 nm, respectively.
11) H. Lemaire and A. Rassat, *J. Chim. Phys.*, **61**, 1580 (1964); A. Mackor, Th. A. J. W. Wajer, and Th. J. deBoer, *Tetrahedron*, **24**, 1623 (1968).
12) T. R. Oliver and W. A. Waters, *J. Chem. Soc.(B)*, **1971**, 677; S. Ozaki and M. Masui, *Chem. Pharm. Bull.*, **25**, 1179 (1977).
13) A. J. Bard, L. R. Faulkner, "Electrochemical Methods," Wiley, New York, 1980, Chapter 11.
14) For example, L. P. Hammett, "Physical Organic Chemistry," McGraw-Hill, New York, 1970, Chapter 5.
15) P. Gray, A. A. Herod, and A. Jones, *Chem. Rev.*, **71**, 279 (1971).
16) S. A. Hussain, T. C. Jenkins, M. J. Perkins, and N. P. Y. Siew, *J. Chem. Soc., Perkin Trans. 1*, **1979**, 2803.
17) G. D. Mendenhall and K. U. Ingold, *J. Am. Chem. Soc.*, **95**, 2963 (1973).
18) For example, A. F. Trotman-Dickenson: "Advances in Free-Radical Chemistry," Vol. I, ed. by G. H. Williams, Academic Press, London, 1965.
19) Unpublished data.
20) H. Ohmori, A. Matsumoto, and M. Masui, *J. Chem. Soc., Perkin Trans. 2*, **1980**, 347.

[Chem. Pharm. Bull. 35(4)1378—1382(1987)]

Studies on *as*-Triazine Derivatives. IX.[1] Synthesis of 5-Substituted 1,2,4-Triazine Derivatives through an Addition Reaction and Subsequent Oxidation

SHOETSU KONNO, SETSUYA OHBA, MATAICHI SAGI, and HIROSHI YAMANAKA*

Pharmaceutical Institute, Tohoku University, Aobayama, Sendai 980, Japan

(Received July 31, 1986)

The addition reactions of various nucleophiles to 6-methyl-3-phenyl-1,2,4-triazine (**1**) were investigated and a practical preparation of **1** was developed. The reactions showed many similarities to those of quinazoline (at the 4-position) and acridine (at the 9-position). The hitherto unknown compounds 5-cyano- (**3**), 5-carbamoyl- (**5**) and 5-phenacyl-6-methyl-3-phenyl-1,2,4-triazines (**11c**) were synthesized.

Keywords——1,2,4-triazine; nucleophilic addition; aromatization; active methylene compound; catalytic reduction

The most reactive position of a 1,2,4-triazine (*as*-triazine) ring is position 5, where nucleophiles can attack very easily.[2] For example, 3,5,6-trichloro-*as*-triazine reacts with 1 mol eq of sodium methoxide to give 3,6-dichloro-5-methoxy-*as*-triazine exclusively.[3] Furthermore, the combined electron-attracting effects of three ring nitrogen atoms suggest position 5 to be highly susceptible to nucleophilic addition, when there is no leaving group at this position.[4] The present paper deals with the synthesis of 5-substituted *as*-triazine derivatives from 6-methyl-3-phenyl-*as*-triazine (**1**).

The reaction of **1** with nucleophiles came up to our expectation, as shown in Chart 1. Compound **1** reacted with sodium bisulfite in methanol to give 6-methyl-3-phenyl-2,5-dihydro-*as*-triazine-5-sulfonic acid (**2**). When a current of sulfur dioxide was bubbled through an aqueous methanolic solution of **1**, the same sulfonic acid (**2**) was obtained. On treatment with sodium cyanide in dimethylformamide (DMF) at room temperature, **2** was converted into 6-methyl-3-phenyl-*as*-triazine-5-carbonitrile (**3**) together with a small amount of **1**. The nitrile (**3**) was alternatively obtained by passing hydrogen cyanide into a solution of **1** in DMF. In this case, air oxidation is considered to be responsible for the direct formation of **3**, although there is no direct evidence for this.

On the other hand, the reaction of **1** with sodium cyanide in DMF resulted in the dimerization of **1**, and the bi-triazine (**4**) was isolated mainly, together with 6-methyl-3-phenyl-*as*-triazine-5-carboxamide (**5**). The by-product (**5**) was identical with an authentic specimen derived from **3** by treatment with hydrogen peroxide in an alkaline medium.

Furthermore, 5-hydrazino-6-methyl-3-phenyl-*as*-triazine (**6**) and 6-methyl-5-oxo-3-phenyl-2,5-dihydro-*as*-triazine (**7**)[5] were obtained by treatment of **1** with hydrazine and with hydrogen peroxide, respectively. In connection with this result, the addition of hydrazine to quinazoline has been reported to give 4-hydrazinoquinazoline, in which the oxidizing reagent for the aromatization of the intermediate was suggested to be hydrazine itself.[6]

The addition of carbon nucleophiles to **1** was also successful. Namely, methylmagnesium iodide reacted with **1** at room temperature to give 5,6-dimethyl-3-phenyl-2,5-dihydro-*as*-

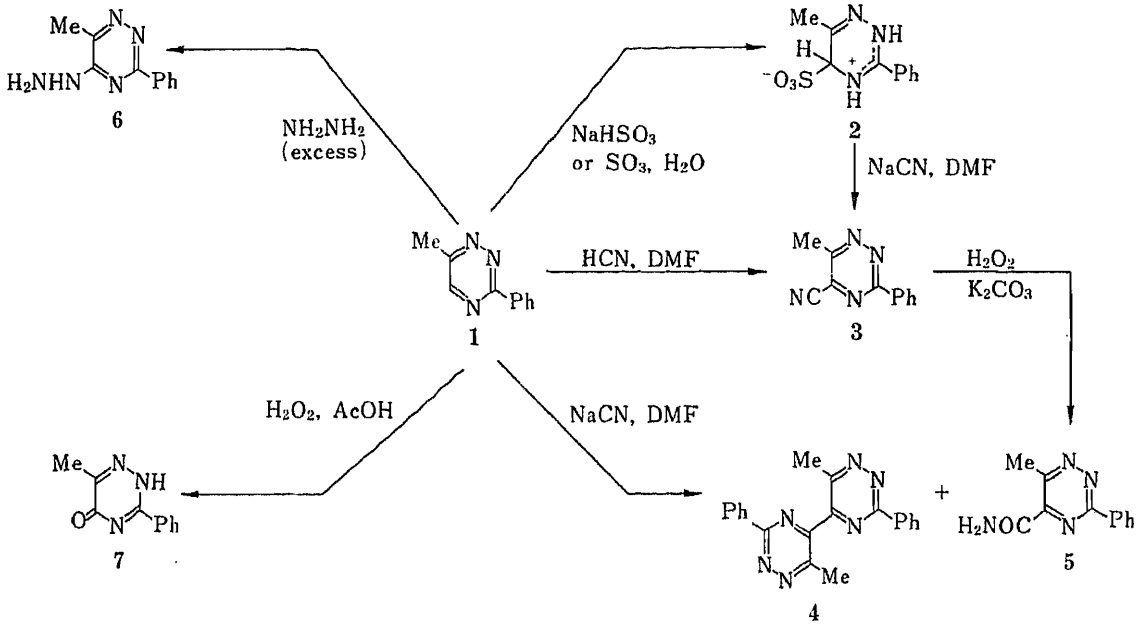

Chart 1

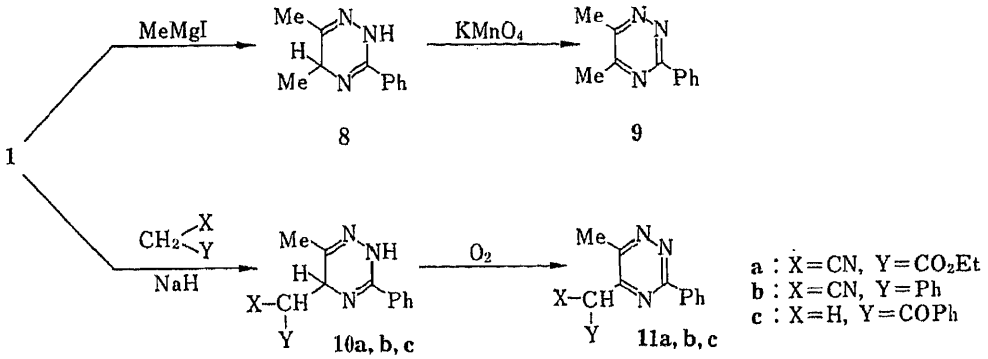

Chart 2

triazine (**8**), which was smoothly aromatized to 5,6-dimethyl-3-phenyl-*as*-triazine (**9**) by potassium permanganate oxidation. Herein, the 2,5-dihydro-structure is adopted tentatively according to the common practice.[7]

In the presence of sodium hydride, compounds containing an active methylene or methyl group such as ethyl cyanoacetate, phenylacetonitrile, and acetophenone added smoothly to the 5-position of **1** to give the corresponding adducts (**10a—c**). Although these adducts were too unstable for purification, subsequent oxidation of the crude materials with molecular oxygen gave the aromatic compounds (**11a—c**), as expected.

We also developed a convenient synthesis of **1**. When **7** was treated with phosphoryl chloride and diethylaniline, the reaction proceeded at room temperature, and 5-chloro-6-methyl-3-phenyl-*as*-triazine (**12**) was obtained in good yield. It is possible to control the catalytic reduction of **12** over palladium charcoal to give **1** without concomitant formation of by-products. In connection with these experiments, the following findings should be mentioned.

1) The reaction of methylglyoxal with benzamidrazone has been reported to give a mixture of **1** and 5-methyl-3-phenyl-*as*-triazine, the separation of which was unsuccessful.[8] In

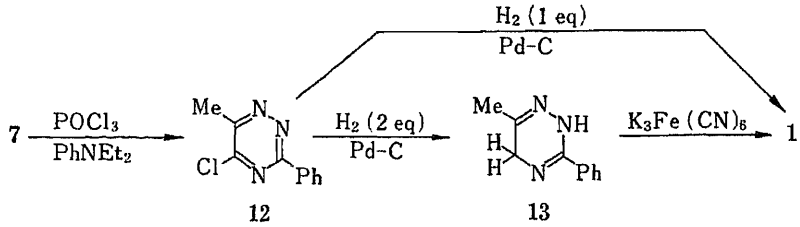

Chart 3

contrast, the condensation of pyruvic acid with benzamidrazone gave **7** regio-selectively.

2) On heating **7** with phosphoryl chloride alone, the reaction resulted in the recovery of **7**, although the reaction mixture turned dark brown. Therefore the addition of diethylaniline is essential for the dehydroxy-chlorination of **7**.

3) The exhaustive reduction of **12** under these conditions gave 6-methyl-3-phenyl-2,5-dihydro-*as*-triazine (**13**), although the oxidation of **13** with potassium ferricyanide in an alkaline medium afforded **1**.

The present results confirm[9] that the reactivity of *as*-triazines at the 5-position resembles that of quinazoline (at the 4-position)[10] or acridine (at the 9-position).[11]

Experimental

All melting points are uncorrected. Infrared (IR) spectra were measured with a JASCO IRA-1 spectrometer. Mass spectra (MS) were taken with a Hitachi M-52G spectrometer. Proton nuclear magnetic resonance (^{1}H-NMR) spectra were taken at 60 MHz with a JEOL JNM-PMX 60 spectrometer. Chemical shifts are expressed in δ values. The following abbreviations are used: s=singlet, d=doublet, t=triplet, q=quartet, m=multiplet, and br=broad.

Reaction of 1 with $NaHSO_3$——SO_2 was bubbled into a solution of NaOH (8 g) in H_2O (25 ml) and the resulting precipitate was filtered off. Compound **1** was added to the above filtrate and the mixture was stirred for 10 min at room temperature. The resulting precipitate was collected by filtration and washed with cold H_2O. Recrystallization from H_2O gave 7.35 g (87%) of 6-methyl-3-phenyl-2,5-dihydro-*as*-triazine-5-sulfonic acid monohydrate (**2**), mp 198 °C (dec.), as colorless prisms. ^{1}H-NMR (DMSO-d_6): 2.32 (3H, s), 4.96 (1H, s), 7.7—8.0 (6H, m, exchangeable with D_2O for 1H), 11.0—13.5 (1H, br, exchangeable with D_2O). *Anal.* Calcd for $C_{10}H_{11}N_3O_3S \cdot H_2O$: C, 44.27; H, 4.83; N, 15.49; S, 11.81. Found: C, 44.37; H, 4.80; N, 15.59; S, 11.92.

Reaction of 1 with SO_2——SO_2 was bubbled into a solution of **1** (5.1 g, 0.03 mol) in 50% aq. MeOH (30 ml). The resulting precipitate was collected by filtration and washed with cold H_2O. Recrystallization from H_2O gave 7.56 g (90%) of **2**, mp 198 °C (dec.), as colorless prisms. This compound was identical with the sample obtained above.

Reaction of 2 with NaCN——A solution of **2** (1.08 g, 0.004 mol) in DMF (5 ml) was added to a solution of NaCN (0.22 g, 0.0044 mol) in DMF (10 ml) and the mixture was stirred for 2 h at room temperature. After removal of the solvent, the residue was chromatographed on a silica gel column. The first fraction, eluted with benzene, gave 6-methyl-3-phenyl-*as*-triazine-5-carbonitrile (**3**), which was recrystallized from cyclohexane to give yellow prisms, mp 134—135 °C (lit.[1] mp 134—135 °C), in 77% yield (0.65 g). The second fraction, eluted with hexane–Et_2O (9 : 1), gave 6-methyl-3-phenyl-*as*-triazine (**1**), which was recrystallized from hexane–Et_2O to give pale yellow needles, mp 68—69 °C, in 12% yield (0.08 g). These compounds were identical with samples prepared by alternative routes.[1]

Reaction of 1 with HCN——An excess of dry HCN was introduced into a solution of **1** (0.43 g, 0.0025 mol) in DMF (20 ml) and the mixture was allowed to stand for 36 h. After removal of the solvent, the residue was purified by silica gel column chromatography using benzene as an eluent. Recrystallization from cyclohexane gave 0.35 g (71%) of **3**, mp 134—135 °C, as yellow prisms.

Reaction of 1 with NaCN——A solution of **1** (0.86 g, 0.005 mol) in DMF (5 ml) was added to a solution of NaCN (2.5 g, 0.05 mol) in DMF (15 ml), and the mixture was stirred for 36 h at room temperature. H_2O (100 ml) was added to the reaction mixture and the separated crystals were collected by filtration, then washed with H_2O.

After air-drying, the crystals were suspended in DMF (20 ml) and O_2 was bubbled into the mixture for 5 min. After removal of the solvent, the residue was purified by silica gel column chromatography. The fraction eluted with hexane–Et_2O (9 : 1) gave 0.63 g (74%) of 5,5′-bis(6-methyl-3-phenyl-*as*-triazinyl) (**4**), mp 197—199 °C, as orange needles. MS *m/z*: 340 (M^+). The fraction eluted with $CHCl_3$ gave 0.05 g (5%) of 6-methyl-3-phenyl-*as*-triazine-5-carboxamide (**5**), mp 222 °C, as yellow needles.

Hydrolysis of 3 with H_2O_2——A mixture of **3** (0.38 g, 0.002 mol), K_2CO_3 (0.15 g), and 30% H_2O_2 (1 ml) in 80% aq. acetone (30 ml) was stirred for 1 h at room temperature. The precipitate was collected by filtration, and washed

with H_2O. Recrystallization from $CHCl_3$ gave 0.30 g (70%) of **5**, mp 222 °C, as yellow needles.

Reaction of 1 with $NH_2NH_2 \cdot H_2O$——A suspension of **1** (0.86 g, 0.005 mol) in $NH_2NH_2 \cdot H_2O$ (20 ml) was refluxed for 6 h. The mixture was concentrated to dryness under reduced pressure. The residue was washed with H_2O and recrystallized from MeOH to give 0.12 g (12%) of 5-hydrazino-6-methyl-3-phenyl-*as*-triazine (**6**), mp 216 °C (dec.) [lit.[1] mp 216 °C (dec.)], as colorless needles. This compound was identical with a sample prepared by an alternative route.[1]

Reaction of 1 with H_2O_2 in AcOH——A mixture of **1** (0.34 g, 0.002 mol) and 30% H_2O_2 (1 ml) in AcOH (10 ml) was stirred for 5 h at room temperature. After removal of the solvent, the residue was washed with H_2O and recrystallized from EtOH to give 0.31 g (82%) of 6-methyl-5-oxo-3-phenyl-2,5-dihydro-*as*-triazine (**7**), mp 245—247 °C (dec.) (lit.[5] mp 245—247 °C), as colorless needles. This compound was identical with a sample prepared by an alternative route.[5]

Reaction of 1 with Methylmagnesium Iodide——A Grignard solution [prepared from 0.24 g (0.01 g atom) of Mg and 1.39 g (0.01 mol) of MeI in dry ether (35 ml)] was added dropwise to a solution of 1.28 g (0.0075 mol) of **1** in dry ether (35 ml) at room temperature under nitrogen and the mixture was stirred for 10 min. Saturated aq. NH_4Cl was added to the reaction mixture and the organic layer was separated, then dried over Na_2SO_4. After removal of the solvent, the residue was recrystallized from hexane–AcOEt to give 1.2 g (86%) of 5,6-dimethyl-3-phenyl-2,5-dihydro-*as*-triazine (**8**), mp 109—111 °C, as colorless needles. ^{1}H-NMR ($CDCl_3$): 1.34 (3H, d, J=7 Hz), 2.02 (3H, s), 3.97 (1H, q, J=7 Hz), 7.1—8.0 (5H, m), 8.0—8.9 (1H, br, exchangeable with D_2O). *Anal.* Calcd for $C_{11}H_{13}N_3$: C, 70.56; H, 7.00; N, 22.44. Found: C, 70.27; H, 6.85; N, 22.22.

Oxidation of 8 with $KMnO_4$——$KMnO_4$ (2.37 g, 0.015 mol) was added to a solution of **8** (0.94 g, 0.005 mol) in acetone (100 ml) all at once and the mixture was stirred for 12 h. The reaction mixture was filtered and the filtrate was concentrated under reduced pressure. The residue was recrystallized from hexane to give 0.72 g (77%) of 5,6-dimethyl-3-phenyl-*as*-triazine (**9**), mp 78—80 °C (lit.[12] mp 82 °C), as pale yellow needles. This compound was identical with a sample prepared by an alternative route.[12]

Reaction of 1 with Ethyl Cyanoacetate——A mixture of ethyl cyanoacetate (1.13 g, 0.01 mol) and NaH (0.48 g, 50% in oil, 0.01 mol) in dry 1,4-dioxane (20 ml) was refluxed for 30 min. A solution of **1** (0.85 g, 0.005 mol) in dry 1,4-dioxane (30 ml) was added thereto, and the mixture was refluxed for 24 h. After removal of the solvent, 3 N HCl (5 ml) and DMF (30 ml) were added to the residue. O_2 was bubbled into the mixture for 5 min. The reaction mixture was concentrated to dryness under reduced pressure, and the residue was purified by silica gel column chromatography using benzene–AcOEt (9 : 1) as an eluent. Recrystallization from AcOEt gave 0.55 g (39%) of ethyl α-cyano-6-methyl-3-phenyl-*as*-triazine-5-acetate (**11a**), mp 193—194 °C (lit.[1] mp 193—194 °C), as yellow prisms. This compound was identical with a sample prepared by an alternative route.[1]

Reaction of 1 with Phenylacetonitrile——Following the procedure for the preparation of **11a**, treatment of **1** (0.85 g, 0.005 mol) in dry 1,4-dioxane (50 ml) with NaH (0.48 g, 50% in oil, 0.01 mol) and phenylacetonitrile (1.03 g, 0.01 mol) resulted in the formation of a crude product which was oxidized by oxygen. Recrystallization from MeOH gave 0.42 g (31%) of α-phenyl-6-methyl-3-phenyl-*as*-triazine-5-acetonitrile (**11b**), mp 220—221 °C, as yellow needles.

Reaction of 1 with Acetophenone——Following the procedure for the preparation of **11a**, treatment of **1** (0.85 g, 0.005 mol) in dry 1,4-dioxane (50 ml) with NaH (0.48 g, 50% in oil, 0.01 mol) and acetophenone (1.2 g 0.01 mol) resulted in the formation of a crude product which was oxidized by oxygen. Recrystallization from AcOEt gave 0.49 g (34%) of 6-methyl-3-phenyl-5-*as*-triazinylmethyl phenyl ketone (**11c**), mp 134—135 °C (lit.[1] mp 134—135 °C), as yellow prisms. This compound was identical with a sample prepared by an alternative route.[1]

5-Chloro-6-methyl-3-phenyl-*as*-triazine (12)——*N*,*N*-Diethylaniline (4.5 g, 0.03 mol) was added to a suspension of 6-methyl-5-oxo-3-phenyl-2,5-dihydro-*as*-triazine (**7**)[5] (5.61 g, 0.03 mol) in $POCl_3$ (20 ml) and the mixture was stirred at room temperature for 30 min, then diluted with benzene. The benzene solution was washed successively with H_2O, 10% NH_4OH, and sat. aq. NaCl, and dried over Na_2SO_4. After removal of the solvent, the residue was purified by column chromatography on active alumina (Sumitomo, KCG-30) using benzene as an eluent. Recrystallization from hexane–AcOEt gave 5.2 g (84%) of **12**, mp 87—88 °C, as pale yellow prisms.

6-Methyl-3-phenyl-*as*-triazine (1)——i) The catalyst, 10% Pd–C (1.0 g), was added to a solution of **12** (4.11 g, 0.02 mol) and Et_3N (4.04 g, 0.04 mol) in benzene (150 ml) and the mixture was shaken under an H_2 stream (1 atm) at room temperature. After absorption of H_2 (1 l, 2 mol eq), the catalyst was removed by filtration. The filtrate was concentrated to dryness and the residue was recrystallized from hexane–AcOEt to give 2.63 g (76%) of 6-methyl-3-phenyl-2,5-dihydro-*as*-triazine (**13**), mp 119—121 °C, as colorless prisms. IR ($CHCl_3$) cm^{-1}: 3440. ^{1}H-NMR ($CDCl_3$): 2.02 (3H, s), 3.96 (2H, s), 7.4—7.6 (3H, m), 7.7—7.9 (2H, m), 8.4—8.9 (1H, br s, exchangeable with D_2O). *Anal.* Calcd for $C_{10}H_{11}N_3$: C, 69.34; H, 6.40; N, 24.26. Found: C, 69.16; H, 6.25; N, 24.56. A mixture of $K_3Fe(CN)_6$ (5 g, 0.015 mol) and NaOH (1 g) in H_2O (20 ml) was added to a solution of **13** (1.73 g, 0.01 mol) in benzene (20 ml). The mixture was vigorously stirred for 24 h at room temperature. The benzene layer was separated and dried over K_2CO_3. After removal of the solvent, the residue was purified by silica gel column chromatography using hexane–Et_2O (9 : 1) as an eluent. Recrystallization from hexane–Et_2O gave 1.66 g (97%) of **1**, mp 68—69 °C, as pale yellow needles.

ii) Compound **12** (8.22 g, 0.04 mol) was dissolved in benzene (200 ml), and then 5% Pd–C (0.3 g) and Et_3N

TABLE I. Analytical Data and ^{1}H-NMR Spectral Data for All Aromatic *as*-Triazines Synthesized

Compd. No.	Formula or lit. mp (°C)	Analysis (%) Calcd (Found) C	H	N	^{1}H-NMR δ ($CDCl_3$, J=Hz)
1	$C_{10}H_9N_3$	70.18	5.21	24.56	2.63 (s, 3H), 7.3—7.6 (m, 3H), 8.3—8.7 (m, 3H)[a]
		(70.45	5.11	24.56)	
3	134—135[1]				3.01 (s, 3H), 7.5—7.7 (m, 3H), 8.4—8.7 (m, 2H)
4	$C_{20}H_{16}N_6$	70.57	4.74	24.69	2.94 (s), 7.5—7.7 (m), 8.5—8.7 (m), the integrated ratio is 3:3:2
		(70.82	4.63	24.60)	
5	$C_{11}H_{10}N_4O$	61.67	4.71	26.16	2.92 (s, 3H), 3.34 (s, 1H, exchangeable with D_2O), 7.6—7.8 (m, 3H),
		(61.89	4.65	26.43)	7.9—8.3 (br, 1H, exchangeable with D_2O), 8.5—8.8 (m, 2H)[b]
6	216 (dec.)[1]				2.27 (s, 3H), 7.0—7.6 (m, 3H), 7.6—8.1 (m, 2H)[c]
9	82[7]				2.47 (s, 3H), 2.60 (s, 3H), 7.2—7.6 (m, 3H), 8.2—8.6 (m, 2H)[a]
11a	193—194[1]				1.41 (t, 3H, J=7), 2.97 (s, 3H), 4.41 (q, 2H, J=7), 7.3—7.8 (m, 3H), 7.9—8.2 (m, 2H), 14.4—14.9 (br, 1H, exchangeable with D_2O)
11b	$C_{18}H_{14}N_4$	75.50	4.93	19.57	2.46 (s, 3H), 7.0—7.6 (m, 10H)
		(75.79	4.89	19.63)	
11c	134—135[1]				2.62 (s, 3H), 6.16 (s, 1H), 7.4—7.7 (m, 6H), 7.9—8.1 (m, 2H) 8.2—8.4 (m, 2H), 15.6—16.0 (br, 1H, exchangeable with D_2O)
12	$C_{10}H_8ClN_3$	58.41	3.92	20.43	2.42 (s, 3H), 7.3—7.7 (m, 3H), 8.4—8.7 (m, 2H)[a]
		(58.18	3.73	20.41)	

a) Measured in CCl_4. *b*) Measured in DMSO-d_6. *c*) Measured in CF_3CO_2H.

(8.08 g, 0.08 mol) were added. The mixture was shaken under an H_2 stream (1 atm) at room temperature. After absorption of H_2 (1 l, 1 mol eq), the catalyst was filtered off and washed with benzene (50 ml). The filtrate and washing were combined and concentrated to dryness under reduced pressure. The residue was purified as described above. Recrystallization from hexane–Et_2O gave 6.50 g (95%) of **1**, mp 68—69 °C, as pale yellow needles. This compound was identical with the sample obtained above.

Acknowledgement The authors are grateful to the staff of the Central Analysis Room of this Institute for elemental analysis.

References and Notes

1) Part VIII: S. Konno, S. Ohba, M. Agata, Y. Aizawa, M. Sagi, and H. Yamanaka, *Heterocycles*, submitted.
2) H. Neunhoeffer, "Comprehensive Heterocyclic Chemistry," Vol. 3, ed. by A. Katritzky, Pergamon Press, 1984, pp. 385—456.
3) H. Neunhoeffer and B. Lehmann, *Chem. Ber.*, **109**, 1113 (1976).
4) *a*) I. Saikawa and T. Maeda, *Yakugaku Zasshi*, **87**, 1501 (1967); *b*) W. W. Paudler and T.-K. Chen, *J. Heterocycl. Chem.*, **7**, 527 (1970); *c*) D. K. Krass and W. W. Paudler, *ibid.*, **11**, 43 (1974).
5) V. Uchytilová, P. Fiedler, M. Prystas, and J. Gut, *Collect. Czech. Chem. Commun.*, **36**, 1955 (1971).
6) T. Higashino, *Yakugaku Zasshi*, **80**, 245 (1960).
7) *a*) J. Daunis and C. Pigière, *Bull. Soc. Chim. Fr.*, **1973**, 2493; *b*) T. Sasaki, K. Minamoto, and K. Harada, *J. Org. Chem.*, **45**, 4587, 4594 (1980); *c*) S. Konno, M. Sagi, Y. Yūki, and H. Yamanaka, *Heterocycles*, **23**, 2807 (1985).
8) H. Neunhoeffer, L. Motitschke, H. Hennig, and K. Ostheimer, *Justus Liebigs Ann. Chem.*, **760**, 88 (1972).
9) The reported covalent hydration of *as*-triazine derivatives[4b] suggested that *as*-triazines have similar properties to quinazolines and acridines.
10) *a*) E. Hayashi and T. Higashino, *Chem. Pharm. Bull.*, **12**, 1111 (1964); *b*) *Idem, ibid.*, **13**, 291 (1965); *c*) T. Higashino, H. Ito, and E. Hayashi, *ibid.*, **20**, 1544 (1972).
11) *a*) K. Lehmstedt and E. Wirth, *Ber.*, **61**, 2044 (1928); *b*) R. Lehmstedt and F. Dostal, *ibid.*, **72**, 804 (1939); *c*) E. Hayashi, S. Ohsumi, and T. Maeda, *Yakugaku Zasshi*, **79**, 967 (1959); *d*) E. Hayashi, *ibid.*, **79**, 969 (1959); *e*) C. S. Sheppard and R. Levin, *J. Heterocycl. Chem.*, **1**, 67 (1964); *f*) E. Hayashi and T. Nakura, *Yakugaku Zasshi*, **87**, 570 (1967).
12) R. Metze, *Chem. Ber.*, **88**, 772 (1955).

[Chem. Pharm. Bull. 35(4)1383—1387(1987)]

Lipid A and Related Compounds. XI.[1] New, Efficient Synthesis of Lipid X

KIYOSHI IKEDA, TOSHIO TAKAHASHI, CHIKAKO SHIMIZU, SHINICHI NAKAMOTO, and KAZUO ACHIWA*

Shizuoka College of Pharmacy, Oshika 2-2-1, Shizuoka 422, Japan

(Received August 26, 1986)

A new methodology for chemical differentiation of one amino and four hydroxyl groups of glucosamine derivatives and its application for the synthesis of lipid X are described.

Keywords——lipid A; lipid X; glucosamine derivative; chemical differentiation; lipid X synthesis

Lipid A is known to be responsible for most of the biological activities[2] of the lipopolysaccharide (LPS) of gram-negative bacteria, *e.g.*, endotoxicity, adjuvanticity, antitumor activity, and so on. Recent chemical analyses revealed that lipid A contains as a central backbone a 1,6-linked β-D-glucosamine disaccharide substituted by phosphate groups and by ester- and amide-bound fatty acids[3] as indicated in Chart 1. Although many attempts have been made to synthesize lipid A, no generally applicable route for the synthesis of lipid A and related compounds has been developed.[4]

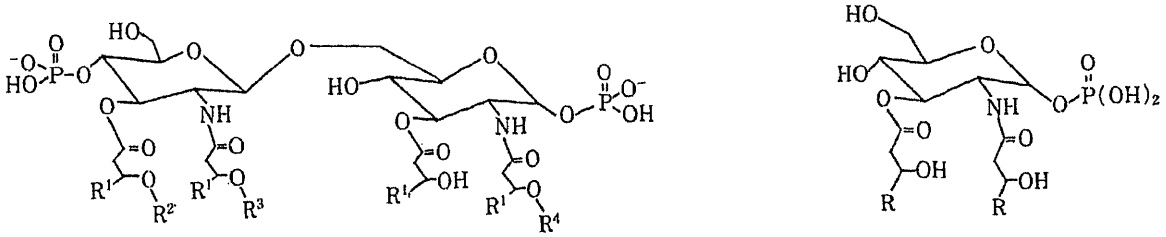

1: $R^1=CH_3(CH_2)_{10}-$, $R^2=CH_3(CH_2)_{12}CO-$, $R^3=CH_3(CH_2)_{10}CO-$, $R^4=H$ (*Escherichia coli*)

2: $R^1=CH_3(CH_2)_{10}-$, $R^2=CH_3(CH_2)_{12}CO-$, $R^3=CH_3(CH_2)_{10}CO-$, $R^4=CH_3(CH_2)_{14}CO-$ (*Salmonella minnesota*)

3: $R^1=CH_3(CH_2)_{10}-$, $R^2=CH_3(CH_2)_{12}CO-$, $R^3=CH_3(CH_2)_{12}CO-$, $R^4=H$ or $CH_3(CH_2)_{14}CO-$ (*Proteus mirabilis*)

5: $R=CH_3(CH_2)_{10}-$ (lipid X)

Chart 1

In a recent communication,[1a] we reported the development of allyl 2-amino-2-deoxy-4,6-isopropylidene-β-D-glucopyranoside (**4**) as a general key intermediate for the synthesis of lipid A and related compounds, and its successful application to the synthesis of lipid X, isolated from phosphatidylglycerol-deficient mutants of *Escherichia coli*.[5] Lipid X has been reported to show significant biological activities such as the activation of B-lymphocytes and macrophages.[6] Our methodology includes a new selective removal of the N-acyl group from the acid-unstable 4,6-isopropylidene compound (**8**) leading to the novel key compound (**4**), whose one amino and four hydroxyl groups can be chemically distinguished from each other

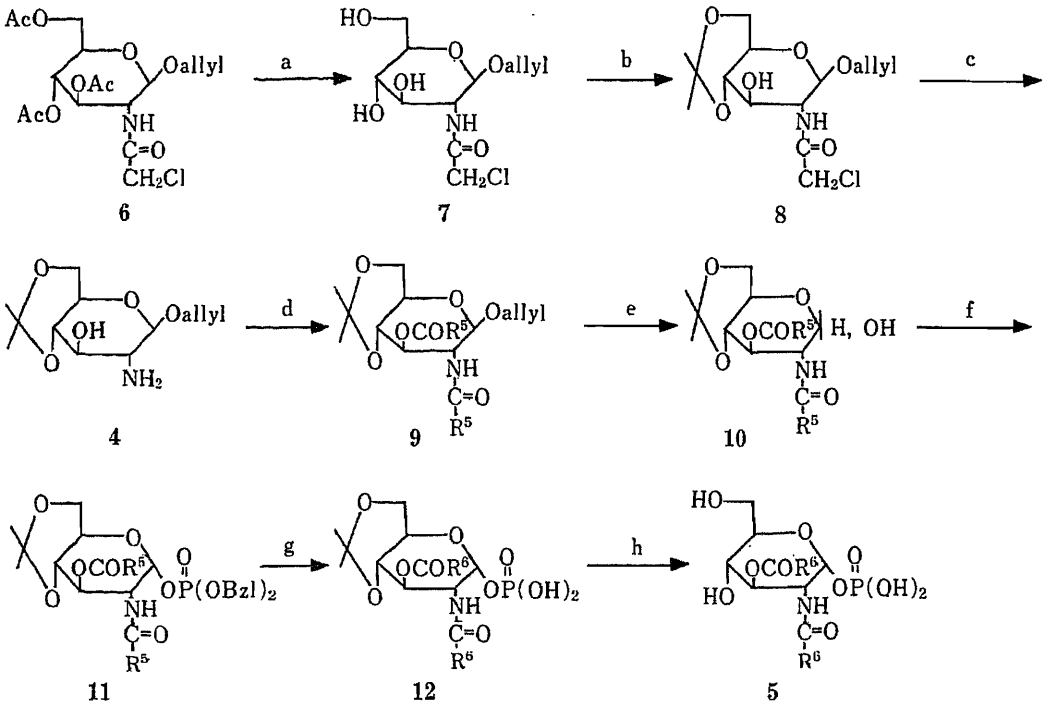

$R^5 = CH_3(CH_2)_{10}\underset{(R)}{\underset{|}{C}HCH_2}-$, $R^6 = CH_3(CH_2)_{10}\underset{(R)}{\underset{|}{C}HCH_2}-$

a) 28% NH_4OH–MeOH (1 : 10); b) $(CH_3)_2C(OCH_3)_2$, *p*-TSA; c) i) pyridine, ii) 5% aqueous NaOH–MeOH (1 : 1); d) R^5CO_2H, *N,N'*-dicyclohexylcarbodiimide, 4-dimethylaminopyridine; e) i) $[Ir(COD)(PMePh_2)_2]PF_6$, ii) I_2; f) *n*-BuLi, $(BzlO)_2POCl$; g) Pd-black/H_2; h) 90% acetic acid

Chart 2

and are easily convertible into the required substituents for lipid A and related compounds. This paper describes in detail the conversion of the key intermediate **4** into lipid X as shown in Chart 2.

The key intermediate **4** was prepared starting from allyl 3,4,6-tri-*O*-acetyl-2-chloroacetamido-2-deoxy-β-D-glucopyranoside (**6**).[7] The latter compound was O-deacetylated and treated with 2,2-dimethoxypropane in dry dimethylformamide (DMF) in the presence of a catalytic amount of *p*-toluenesulfonic acid, to afford compound **8** in 87% yield. The infrared (IR) spectrum of **8** showed characteristic bands of a chloroacetyl group at 1660 cm^{-1} and an isopropylidene group at 854 cm^{-1}. In the proton nuclear magnetic resonance (^{1}H-NMR) spectrum, the presence of a doublet signal due to the anomeric proton (J = 7.9 Hz) at 4.72 ppm in the spectrum of **8** established the configuration of the glycosidic linkage as β.

Several attempts to remove the N-chloroacetyl group of **8** using usual de-N-chloroacetylating reagents such as *ortho*-phenylenediamine in ethanol,[8] thiourea in ethanol,[9] and *N,N*-pentamethylenethiourea in ethanol,[10] resulted in unsatisfactory yields of **4** (trace, 55% and 40%, respectively).

Successful removal of the N-chloroacetyl group of **8** was effected with pyridine[11] as a base, followed by hydrolysis[11] to afford **4** in 90% yield. The structure of **4** was confirmed by the disappearance of the chloroacetyl proton ($ClCH_2CO$–) signal in the ^{1}H-NMR spectrum and the amide absorption in the IR spectrum.

For further conversion of **4** into lipid X, the free amino and hydroxyl groups of **4** were

acylated with optically pure (*R*)-3-benzyloxytetradecanoic acid, dicyclohexylcarbodiimide, and 4-dimethylaminopyridine in CH_2Cl_2 to afford the diacylated **9** in 84% yield. The glycosidic allyl group of **9** was in turn isomerized with an iridium complex $[Ir(COD)(PMePh_2)_2]PF_6$ (5 mol%)[12a] and the resultant 1-propenyl glycosidic compound was treated with I_2 in aqueous tetrahydrofuran (THF)[12b] to afford **10** as a single isomer in 62% yield after purification on a neutral aluminum oxide column (isopropyl ether : acetone = 10 : 1). In the ^{1}H-NMR spectrum of **10**, the anomeric proton appeared as a doublet (J = 3.6 Hz) at 4.98 ppm. In addition, a signal at 92.5 ppm (doublet) in the carbon-13 nuclear magnetic resonance (^{13}C-NMR) spectrum is assigned to the α-anomeric carbon atom. The glycosidic position was then phosphorylated with dibenzyl phosphorochloridate and *n*-butyllithium in THF at −70 °C.[12c] The reaction mixture was directly subjected to hydrogenolysis over Pd-black to afford the 1-phosphate (**12**) in 27% yield from **10**, after purification on a silica gel column ($CHCl_3$: MeOH = 5 : 1). Finally, deprotection of **12** by treatment with 90% acetic acid gave **5** in almost quantitative yield after purification on a silica gel column ($CHCl_3$: MeOH = 1 : 1) followed by lyophilization from dioxane. The diacylated monosaccharide (**5**) showed the characteristic blue color with the phosphate-specific spray reagent.[13] The specific rotation of **5** was in good agreement with that of lipid X reported by Shiba's group.[14] The structures of all compounds were characterized by ^{1}H- and ^{13}C-NMR spectroscopies, as well as IR spectroscopy and elemental analyses.

Further application of this methodology to the synthesis of lipid A is in progress in our laboratory.

Experimental

All melting points are uncorrected. ^{1}H-NMR spectra were recorded on a JEOL JNM-FX-90Q (90 MHz) FT-NMR spectrometer using tetramethylsilane (in $CDCl_3$) as an internal standard. ^{13}C-NMR spectra were recorded on a JEOL JNM-FX90Q (22.5 MHz) FT-NMR spectrometer using tetramethylsilane (in $CDCl_3$) as an internal standard. Abbreviations are as follows: s, singlet; br s, broad singlet; d, doublet; t, triplet; q, quartet; m, multiplet. IR spectra were recorded on a JASCO A-202 infrared spectrophotometer. Optical rotations were determined with a JASCO DIP-140 digital polarimeter.

Column chromatography was carried out on silica gel (Kiesel gel-60, 70—230 mesh, Merck). Thin layer chromatography (TLC) on Kiesel gel 60-F (Merck) was used to monitor the reaction and to ascertain the purity of reaction products. The spots were visualized by spraying with aqueous sulfonic acid followed by heating.

Allyl 2-Chloroacetamido-2-deoxy-β-D-glucopyranoside (7)——Allyl 3,4,6-tri-*O*-acetyl-2-chloroacetamido-2-deoxy-β-D-glucopyranoside (**6**) (3.37 g, 8.0 mmol), prepared as described in the literature,[7] was dissolved in a solution (33 ml) of methanol and 28% aqueous ammonia (10 : 1). The mixture was stirred for 12 h at room temperature and concentrated under reduced pressure. The residue was chromatographed on silica gel with $CHCl_3$–CH_3OH (3 : 1) to give **7** (2.22 g, 94%) as prisms. mp 154—157 °C. $[\alpha]_D^{22}$ −33.3° (c = 1.00, CH_3OH). IR (KBr): 3264 (OH, NH) 1679 cm^{-1} (amide). ^{1}H-NMR (CD_3OD) δ: 4.06 (2H, s, $COCH_2Cl$), 4.53 (1H, d, J = 7.8 Hz, H-1), 5.65—6.14 (1H, m, =CH–), 7.23 (1H, d, J = 8.0 Hz, NH). *Anal.* Calcd for $C_{11}H_{18}ClNO_6 \cdot 1/2H_2O$: C, 43.36; H, 6.28; N, 4.60. Found C, 43.64; H, 6.07; N, 4.65.

Allyl 2-Chloroacetamido-2-deoxy-4,6-isopropylidene-β-D-glucopyranoside (8)——2,2-Dimethoxypropane (6.73 g, 65 mmol) was added to a stirred solution of **7** (6.59 g, 22 mmol) and *p*-toluenesulfonic acid (0.38 g, 2.2 mmol) in DMF (60 ml) at room temperature under nitrogen. After 2 h, the reaction mixture was neutralized with ion exchange resin (Amberlite IRA-400) (5.95 g, 22 mg eq) and then the resin was removed by filtration. The filtrate was evaporated to dryness and the residue was chromatographed on silica gel. Elution with $CHCl_3$–CH_3OH (10 : 1) gave **8** (5.98 g, 76%) as colorless prisms. mp 154—155 °C. $[\alpha]_D^{28}$ −54.2° (c = 1.00, $CHCl_3$). IR (KBr): 3492 (OH), 3316 (NH), 1660 (amide), 854 cm^{-1} (Me_2C). ^{1}H-NMR ($CDCl_3$) δ: 1.35 and 1.50 (each 3H, s, Me_2C), 4.72 (1H, d, J = 7.9 Hz, H-1), 5.64—6.10 (1H, m, =CH), 7.59 (1H, br d, J = 6.4 Hz, NH). *Anal.* Calcd for $C_{14}H_{22}ClNO_6$: C, 50.08; H, 6.60; N, 4.17. Found: C, 49.97; H, 6.58; N, 4.19.

Allyl 2-Amino-2-deoxy-4,6-isopropylidene-β-D-glucopyranoside (4)——A solution of **8** (1.68 g, 5.0 mmol) in pyridine (9 ml) was heated at 90 °C for 2 h. After cooling, the solvent was evaporated off and the residue was dissolved in a solution (15 ml) of 5% aqueous sodium hydroxide and methanol (1 : 1), then stirred at room temperature for 1.5 h. After removal of the solvent, the residue was extracted with two 15 ml portions of $CHCl_3$. The organic extracts were combined and dried ($MgSO_4$). After removal of the solvent, the residue was chromotographed on silica gel with

$CHCl_3$–CH_3OH (15:1) to give **4** (1.25 g, 96%) as colorless prisms, after recrystallization from *n*-hexane. mp 80—81 °C. $[\alpha]_D^{27}$ −72.0° (c=1.04, $CHCl_3$). IR (KBr): 3372 (OH, NH), 1647 (allyl), 855 cm^{-1} (Me_2C). ^{1}H-NMR ($CDCl_3$) δ: 1.43 and 1.51 (each 3H, s, Me_2C), 5.11—5.47 (2H, m, $=CH_2$), 5.68—6.20 (1H, m, =CH–). *Anal.* Calcd for $C_{12}H_{21}NO_5$: C, 55.59; H, 8.15; N, 5.40. Found: C, 55.42; H, 8.13; N, 5.38.

Allyl 2-[(*R*)-3-Benzyloxytetradecanamido]-3-*O*-[(*R*)-3-benzyloxytetradecanoyl]-2-deoxy-4,6-isopropylidene-β-D-glucopyranoside (9)——Dicyclohexylcarbodiimide (0.454 g, 2.2 mmol) was added to a stirred solution of **4** (0.228 g, 0.88 mmol), (*R*)-3-benzyloxytetradecanoic acid (0.735 g, 2.2 mmol) and 4-dimethylaminopyridine (0.035 g, 0.29 mmol) in dry dichloromethane (5 ml) at 0 °C under nitrogen. The mixture was stirred for 5 h at 0 °C, then at room temperature for 12 h. The resulting suspension was filtered through Celite and evaporated. The residue was chromatographed on silica gel with isopropyl ether to give **9** (0.628 g, 80%) as prisms. mp 69—71 °C. $[\alpha]_D^{25}$ −14.0° (c=1.00, $CHCl_3$). IR (KBr): 3340 (NH), 1739 (ester), 1662 (amide), 861 (Me_2C), 700 cm^{-1} (phenyl). ^{1}H-NMR ($CDCl_3$) δ: 0.88 (6H, t, J=5.4 Hz, $(CH_2)_{10}CH_3$ ×2), 1.25 (40H, br s, $(CH_2)_{10}CH_3$ ×2), 1.31 and 1.40 (each 3H, s, Me_2C), 2.36 (2H, d, J=5.6 Hz, $NCOCH_2$), 2.60 (2H, d, J=6.3 Hz, $OCOCH_2$), 4.49—4.57 (4H, m, $PhCH_2$ ×2), 4.98—5.36 (2H, m, CH_2=$CHCH_2$), 5.53—6.02 (1H, m, CH_2=$CHCH_2$), 6.40 (1H, d, J=8.8 Hz, NH), 7.31, 7.74 (10H, s, Ph×2). ^{13}C-NMR ($CDCl_3$) δ: 99.6 (d, C-1), 100.9 (s, Me_2C), 117.1 (t, CH_2=$CHCH_2$), 133.8 (d, CH_2=$CHCH_2$), 171.2 (s, >C=O ×2). *Anal.* Calcd for $C_{54}H_{85}NO_9$: C, 72.69; H, 9.60; N, 1.69. Found: C, 72.44; H, 9.57; N, 1.64.

2-[(*R*)-3-Benzyloxytetradecanamido]-3-*O*-[(*R*)-3-benzyloxytetradecanoyl]-2-deoxy-4,6-isopropylidene-α-D-glucopyranose (10)——Bis-(methyldiphenylphosphine)cycloocta-1,5-diene iridium (I) hexafluorophosphate $[C_8H_{12}Ir(PMePh_2)_2]PF_6$ (13 mg, 0.015 mmol) was added to a stirred solution of **9** (0.280 g, 0.313 mmol) in peroxide-free THF (30 ml) (freshly distilled from sodium and/benzophenone). The stirred solution was degassed, placed under dry and oxygen-free nitrogen, and degassed once more. The catalyst was activated by hydrogen, during which operation the slightly red suspension became colorless. To effect isomerization, the solution was degassed once more, placed under dry and oxygen-free nitrogen and heated at 50 °C for 2 h. The solvent was evaporated off and the residual oil was dissolved in THF–water (10:1) (4.0 ml). To this solution, iodine (0.159 g, 0.628 mmol) and then pyridine (99 mg, 1.3 mmol) were added, and the mixture was stirred at room temperature for 15 min. After removal of the solvent, the residue was chromatographed on neutral aluminum oxide W 200 with isopropyl ether–acetone (10:1) to give **10** (0.163 g, 62%) as a syrup. $[\alpha]_D^{22}$ +10.1° (c=1.76, $CHCl_3$). IR (neat): 3428 (OH, NH), 1738 (ester), 1669 (amide), 858 (Me_2C), 696 cm^{-1} (phenyl). ^{1}H-NMR ($CDCl_3$) δ: 0.88 (6H, t, J=6.3 Hz, $(CH_3)_{10}CH_3$ ×2), 1.25 (40H, br s, $(CH_2)_{10}CH_3$ ×2), 1.31 and 1.41 (each 3H, s, Me_2C), 2.26—2.64 (4H, m, $COCH_2CH$ ×2), 4.25—4.38 (1H, m, H-2), 4.48 (4H, br s, $PhCH_2$ ×2), 4.98 (1H, d, J=3.6 Hz, H-1), 5.13—5.34 (1H, m, H-3), 6.33 (1H, br d, J=8.5 Hz, NH), 7.30 (10H, br s, Ph×2). ^{13}C-NMR ($CDCl_3$) δ: 92.5 (d, C-1), 99.7 (s, Me_2C), 171.5, 171.8 (s, >C=O ×2). *Anal.* Calcd for $C_{51}H_{81}NO_9 \cdot H_2O$: C, 70.34; H, 9.61; N, 1.61. Found: C, 70.14; H, 9.27; N, 1.77.

2-[(*R*)-3-Hydroxytetradecanamido]-3-*O*-[(*R*)-3-hydroxytetradecanoyl]-2-deoxy-4,6-isopropylidene-α-D-glucopyranosyl-1-phosphate (12)——*n*-Butyllithium (1.6 M in hexane) (0.098 ml, 0.16 mmol) was added to a stirred solution of **10** (0.134 g, 0.157 mmol) in dry THF (5.0 ml) at −70 °C under dry nitrogen. After 2 min, dibenzylphosphorochloridate (0.057 g, 0.20 mmol) in dry THF (1.0 ml) was added at the same temperature and the mixture was stirred for a further 5 min at −50 °C. The whole mixture containing **11** was immediately subjected to hydrogenolysis over Pd-black for 20 h at 45—50 °C under 50 atm to give **12** (0.032 g, 27%) as prisms after purification on a silica gel column ($CHCl_3$:CH_3OH=5:1). mp 101—103 °C. $[\alpha]_D^{17}$ +49.4° (c=0.17, $CHCl_3$). IR (KBr): 3300 (OH, NH), 1748 (ester), 1667 (amide), 1238 cm^{-1} (P=O). *Anal.* Calcd for $C_{37}H_{70}NO_{12}P$: C, 59.10; H, 9.38; N, 1.86. Found: C, 58.52; H, 9.04; N, 1.88.

2-[(*R*)-3-Hydroxytetradecanamido]-3-*O*-[(*R*)-3-hydroxytetradecanoyl]-2-deoxy-α-D-glucopyranosyl-1-phosphate (5)——A solution of **12** (0.032 g, 0.043 mmol) in acetic acid and water (9:1) (0.5 ml) was heated at 80 °C for 10 min. After removal of the solvent, the residue was charomatographed on silica gel with $CHCl_3$–CH_3OH (1:1) to give **5** (0.027 g, quant.) as prisms after lyophilization from dioxane. mp 94—96 °C. $[\alpha]_D^{22}$ +14.6° (c=0.14, $CHCl_3$:CH_3OH=1:1). lit.[14] $[\alpha]_D^{15}$ +14.0° (c=0.2, $CHCl_3$). IR (KBr): 3384 (OH, NH), 1734 (ester), 1660 (amide), 1242 cm^{-1} (P=O). *Anal.* Calcd for $C_{34}H_{66}NO_{12}P$: C, 57.37; H, 9.34; N, 1.97. Found: C, 57.67; H, 8.90; N, 2.14.

Acknowledgment The authors are indebted to Dr. K. Narita and the staff of the Analysis Center of this college for microanalysis.

References

1) *a*) T. Takahashi, C. Shimizu, S. Nakamoto, K. Ikeda, and K. Achiwa, *Chem. Pharm. Bull.*, **33**, 1760 (1985); *b*) S. Nakamoto, T. Takahashi, K. Ikeda, and K. Achiwa, *ibid.*, **33**, 4098 (1985); *c*) T. Shimizu, S. Akiyama, T. Masuzawa, Y. Yanagihara, S. Nakamoto, T. Takahashi, K. Ikeda, and K. Achiwa, *ibid.*, **33**, 4621 (1985); *d*) K. Ikeda, S. Nakamoto, T. Takahashi, and K. Achiwa, *Carbohydr. Res.*, **145**, C5 (1986); *e*) T. Takahashi, S. Nakamoto, K. Ikeda, and K. Achiwa, *Tetrahedron Lett.*, **27**, 1819 (1986); *f*) S. Nakamoto and K. Achiwa, *Chem. Pharm. Bull.*, **34**, 2302 (1986); *g*) T. Shimizu, S. Akiyama, T. Masuzawa, Y. Yanagihara, S. Nakamoto, and K. Achiwa, *ibid.*, **34**, 2310 (1986); *h*) T. Shimizu, S. Akiyama, T. Masuzawa, Y. Yanagihara, S. Nakamoto,

T. Takahashi, K. Ikeda, and K. Achiwa, *ibid.*, **34**, 5169 (1986); *i*) T. Shimizu, S. Akiyama, T. Masuzawa, Y. Yanagihara, S. Nakamoto, and K. Achiwa, *ibid.*, **35**, 873 (1987); *j*) K. Ikeda, T. Takahashi, H. Kondo, and K. Achiwa, *ibid.*, (1987) in press.

2) O. Westphal and O. Lüderitz, *Angew. Chem.*, **66**, 407 (1954); O. Lüderitz, C. Galanos, V. Lehmann, H. Mayer, E. T. Rietschel, and J. Weckesser, *Naturwissenschaften*, **65**, 578 (1978).
3) K. Takayama, N. Qureshi, and P. Mascagni, *J. Biol. Chem.*, **258**, 12801 (1983); M. Imoto, S. Kusumoto, T. Shiba, H. Naoki, T. Iwashita, E. Th. Rietschel, H.-W. Wollenweber, C. Galanos, and O. Lüderitz, *Tetrahedron Lett.*, **24**, 4017 (1983); U. Seydel, B. Lindner, H.-W. Wollenweber, and E. T. Rietschel, *Eur. J. Biochem.*, **145**, 505 (1984).
4) C. C. A. van Boeckel, J. P. G. Hermans, P. Westerduin, J. J. Oltvoort, G. A. van der Mavel, and J. H. van Boom, *Tetrahedron Lett.*, **23**, 1951 (1982); M. Imoto, H. Yoshimura, S. Kusumoto, and T. Shiba, *Proc. Jpn. Acad.*, **60B**, 285 (1984); C. Diolez, S. R. Sartati, and L. Szabo, *J. Chem. Soc., Perkin Trans. 1*, **1985**, 57.
5) K. Takayama, N. Qureshi, P. Mascagni, L. Anderson, and C. R. H. Raetz, *J. Biol. Chem.*, **258**, 7379 (1983).
6) C. R. H. Raetz, S. Purcell, and K. Takayama, *Proc. Natl. Acad. Sci. U.S.A.*, **80**, 4624 (1983); M. Nishijima, F. Amano, Y. Akamatsu, K. Akagawa, T. Tokunaga, and C. R. H. Raetz, *ibid.*, **82**, 282 (1985).
7) M. Kiso and L. Anderson, *Carbohydr. Res.*, **72**, C12 (1979).
8) R. W. Holley and A. D. Holley, *J. Am. Chem. Soc.*, **74**, 3069 (1952).
9) M. Masaki, T. Kitahara, H. Kurita, and M. Ohata, *J. Am. Chem. Soc.*, **90**, 4508 (1968).
10) W. Steglich and H.-G. Batz, *Angew. Chem. Int. Ed. Engl.*, **10**, 75 (1971).
11) This de-*N*-chloroacetylating process has been reported only in a simple system: C. H. Gaozza, B. C. Cieri, and S. Lamadan, *J. Heterocycl. Chem.*, **8**, 1079 (1971).
12) *a*) J. J. Oltvoort, C. A. A. van Boeckel, J. H. de Koning, and J. H. van Boom, *Synthesis*, **1981**, 305; *b*) M. A. Nashed and L. Anderson, *J. Chem. Soc., Chem. Commun.*, **1982**, 1274; *c*) M. Inage, H. Chaki, S. Kusumoto, and T. Shiba, *Chem. Lett.*, **1982**, 1281.
13) J. C. Dittmer and R. L. Lester, *J. Lipid Res.*, **5**, 126 (1964).
14) S. Kusumoto, M. Yamamoto, and T. Shiba, *Tetrahedron Lett.*, **25**, 3727 (1984).

[Chem. Pharm. Bull. 35(4)1388—1396(1987)]

Solvolytic Behavior of *O*-(1-Cyclopropylethyl) *S*-Methyl Dithiocarbonate and Related Compounds

KAZUNOBU HARANO, HIDEO KIYONAGA and TAKUZO HISANO*

Faculty of Pharmaceutical Sciences, Kumamoto University, Oe-honmachi 5-1, Kumamoto 862, Japan

(Received September 9, 1986)

O-(1-Cyclopropylethyl) *S*-methyl dithiocarbonate (Ib) was solvolyzed in various solvents to give *S*-(1-cyclopropylethyl) *S*-methyl dithiocarbonate (IIb) quantitatively. The reaction obeyed the first-order rate law and the rates were considerably affected by the polarity of the solvent used. Phenolysis of Ib with *p*-chlorophenol gave IIb and a small amount of the phenol ether. Plots of the logarithm of the reaction rates against *Y* values gave a linear relationship. The reaction was found to be markedly accelerated by phenolic solvents. The rate in *p*-chlorophenol is 509 times faster than that in ethanol. The role of hydrogen-bonding to the thione sulfur in the rearrangement reaction is discussed.

Keywords——1-cyclopropylethanol; thione–thiol rearrangement; solvolysis; phenolysis; kinetics; solvent effect; hydrogen-bonding; homoallylic participation; *O*,*S*-dialkyl dithiocarbonate; *S*,*S*-dialkyl dithiocarbonate

Introduction

Pyrolysis of *O*,*S*-dialkyl dithiocarbonates (xanthates) (I) has been used for the structure determinations of natural products because of the stereoselective formation of olefins by *cis*-elimination (Chugaev reaction) and has also been used as an olefin-forming reaction, which is particularly valuable for the conversion of sensitive alcohols to the corresponding olefins without rearrangement of the carbon skeleton.[1] However, during the past twenty years, the progress in spectroscopic methods has made the former principal role of the Chugaev reaction redundant, and consequently it has become unfamiliar to organic chemists.

On the other hand, xanthates (I) are of interest because of their synthetic utility as precursors of thiols. In this connection, Taguchi and one of the authors have carried out systematic studies[2] on thermal and catalytic rearrangements of xanthates (I) to *S*,*S*-dialkyl

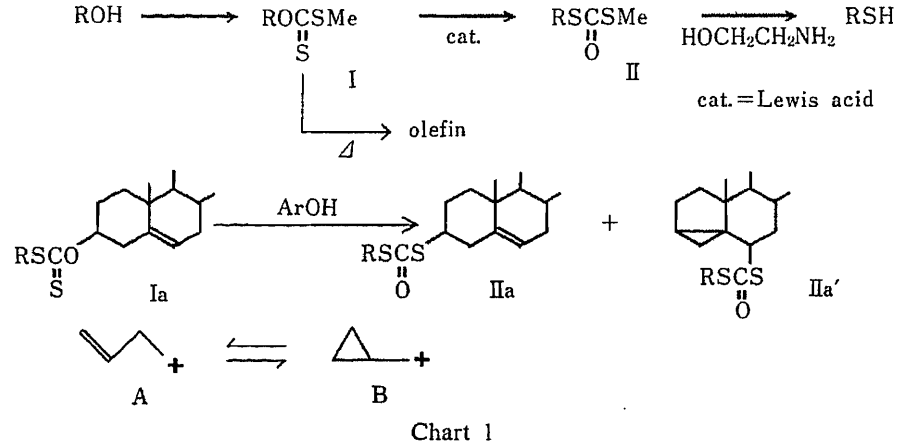

Chart 1

dithiocarbonates (II) and have clarified both the usefulness of the reaction from a synthetic standpoint and the reaction mechanism from a theoretical viewpoint. The rearrangement reactions have been used for synthesis of thiosugars[3] and other synthetic intermediates.[4]

In the previous paper,[5] we reported that phenolysis of *O*-cholesteryl *S*-alkyl dithiocarbonates (Ia) having a homoallylic electron system (A) caused the thiono (-OCSS-)–thiol (-SCOS-) rearrangement to give the corresponding *S*-alkyl *S*-cholesteryl dithiocarbonates (IIa) in high yield. In the reaction, we observed the skeletal rearrangement of cholesteryl (Ia) to *i*-cholesteryl (IIa') with thione–thiol rearrangement, in which the intermolecular hydrogen-bonding to the thione sulfur plays a leading role in the dissociation step. We have anticipated that the cyclopropylmethyl system (B) would show similar reaction behavior.

This paper describes the solvolytic and phenolytic behavior of *O*-(1-cyclopropylethyl) *S*-methyl dithiocarbonate (Ib) and related compounds in comparison with the previous results and with further additional data that we have obtained.

Results and Discussion

Warming Ib in dipolar aprotic solvents gave the corresponding dithiol ester (IIb) quantitatively.[6] When Ib was dissolved in a phenolic solvent at room temperature, Ib was immediately phenolyzed to the dithiol ester (IIb) and 1-(cyclopropylethyl) phenyl ether (III), whereas, in *n*-hexane, it remains unchanged for several months.

The structure of IIb was determined by inspection of the infrared (IR) and proton nuclear magnetic resonance (^{1}H-NMR) spectra and by conversion to the corresponding 2,4-dinitrophenylsulfide (IV). The IR spectrum of IIb shows characteristic bands at 1645 and 870 cm^{-1} due to the -SCOS- moiety. In the ^{1}H-NMR spectrum of the rearranged product (IIb), five protons resonate at considerably high field (0.5—0.9 ppm) as complicated multiplets,[7] reflecting the highly shielded nature of the cyclopropane protons. The spectral pattern is essentially the same as that of the starting material with the exception of the chemical shift of the methine proton adjacent to the -SCOSMe group.

The ^{1}H-NMR spectrum of the crude product showed the absence of the multiplet at 4.0—5.0 ppm which is attributable to olefinic protons, ruling out the formation of an open chain compound, such as *S*-methyl *S*-(3-pentenyl) dithiocarbonate (IIb'). This suggests that skeletal rearrangement of the cyclopropyl system to the homoallylic system did not occur.

The thermal behavior of *O*-(1-cyclopropylethyl) *S*-methyl dithiocarbonate (Ib) was first studied by Overberger and Borchert.[8] They reported yields of 45% of olefins (cyclopropylethylene (V) in the main) and 35% of dithiol esters (IIb and IIb'), of which the major

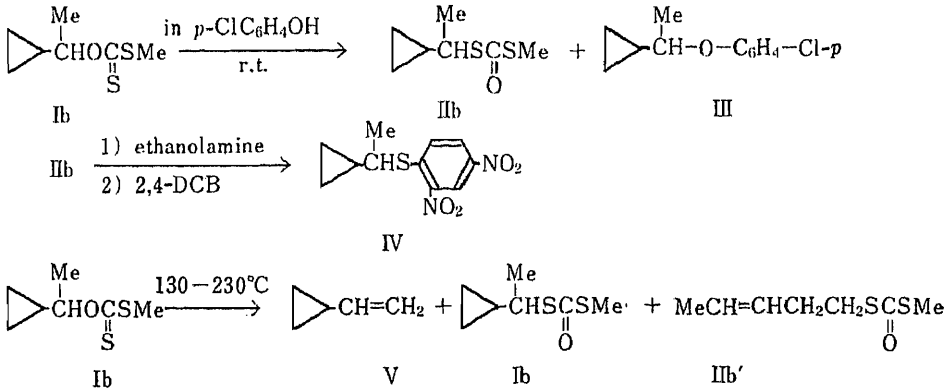

r.t. = room temperature

Chart 2

TABLE I. First-Order Rate Constants for Solvolysis of *O*-(1-Cyclopropylethyl) *S*-Methyl Dithiocarbonate (Ib) in Various Solvents at 47.8±0.1 °C

Solvent	E_T[a] (E_T^N)[b]	Z[a]	Y[a]	δ[c]	$k \times 10^6$ (s^{-1})
$HCONH_2$	56.6 (0.799)		0.604	19.2	11200
Glycol	56.3 (0.790)	81.88		17.05	2890
MeOH	55.5 (0.765)	81.46	−1.09	14.50	454
HCONHMe	54.1 (0.722)			16.1	606
80% EtOH	53.6 (0.767)	84.8	0.0	0.0	1620
EtOH	51.9 (0.654)	78.6	−2.033	12.78	78.4
AcOH	51.9 (0.654)	79.2	−1.639	13.0	114
n-PrOH	50.7 (0.617)	78.3		12.18	38.4
n-BuOH	50.2 (0.602)	77.7		11.6	77.8
iso-PrOH	48.6 (0.552)	76.3		11.44	21.6
iso-AmOH	47.0 (0.503)			11.09	28.0
DMSO	45.0 (0.441)	71.1		13.0	1045
Sulfolane	44.0 (0.410)			12.5	298.6
tert-BuOH	43.9 (0.407)	71.3	−3.26	10.5	5.68
DMF	43.8 (0.404)	68.5		11.79	205
TMU[d]	41.0 (0.318)				24.5
Anisole	37.2 (0.201)			9.0	1.80
p-ClC_6H_5OH					39900
o-ClC_6H_5OH					1460
2,6-Xylenol	47.6				175

a) See ref. 11*c*. *b*) $E_T=[E_T(\text{solvent})-E_T(\text{TMS})]/[E_T(\text{water})-E_T(\text{TMS})]$. *c*) See ref. 14. *d*) Tetramethylurea.

TABLE II. Activation Parameters for Solvolysis of *O*-(1-Cyclopropylethyl) *S*-Methyl Dithiocarbonate (Ib)

Solvent	E_a (kcal/mol)	ΔS^* (e.u.)
HCONHMe	25.2	3.3
EtOH	28.1	8.1
DMSO	22.2	−4.4
DMF	22.8	−6.4
p-ClC_6H_4OH	19.6	−6.0
o-ClC_6H_4OH	16.0	−24

component was identified as *S*-(1-cyclopropylethyl) *S*-methyl dithiocarbonate (IIb). Subsequently, pyrolysis of *O*-(1-cyclopropylethyl) *S*-methyl dithiocarbonate (Ib) has been cited by several researchers as a typical example of a compound which undergoes thermal rearrangement to the corresponding dithiol ester (IIb), although it has four hydrogen atoms at the adjoining carbons.[1,9]

In order to get some information about the nature of the transition state of the rearrangement reaction, we have studied solvent effects on the rate of the solvolytic reaction. The rates of reaction were determined in various solvents by measuring the decrease of the thione chromophore. In all cases, excellent first-order rate plots were obtained to over 70% reaction. The rate constants obtained are given in Table I. The enthalpy and entropy of activation were calculated from these data by using the least-squares method. The values obtained are given in Table II.

The rate of reaction was found to depend significantly on the ionizing power of the solvent, increasing greatly when the solvent was changed from aprotic to protic. As can be

seen in Table I, the rates for the phenolic solvents are larger than those observed for other protic solvents. The largest rate was found in *p*-chlorophenol among all the solvents used. The xanthate solvolyzed about 509 times faster in *p*-chlorophenol than in ethanol. In contrast, the rate acceleration of *o*-chlorophenol is far less than of *p*-chlorophenol, being comparable to that for 80% ethanol. The intermolecular hydrogen-bonding power of *o*-chlorophenol may be reduced by its intramolecular hydrogen-bonding.[10]

When the xanthate (Ib) was treated with *p*-chlorophenol, a considerable amount of phenolysis product (III) was found in the reaction mixture indicating that the reaction

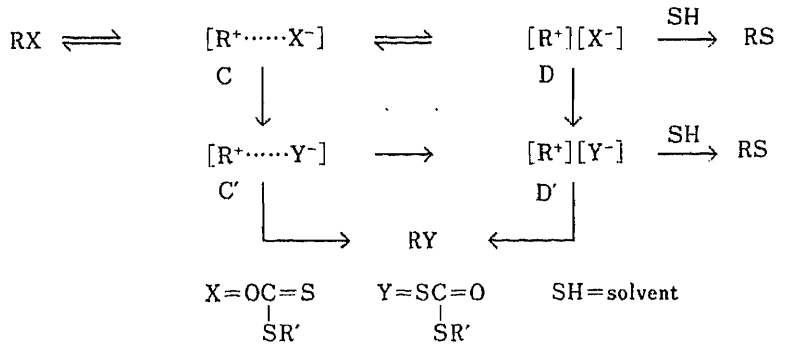

Chart 3

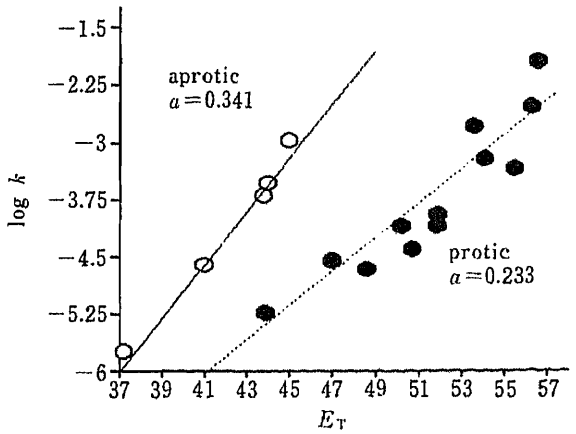

Fig. 1. Plots of k *vs.* E_T Values for the Solvolysis of Ib

TABLE III. Sensitivity of Thione–Thiol Isomerization Reactions to Solvent Ionizing Power (E_T Value)

Substrate[a]	Solvent sensitivity parameter, a[b] × 10^2	Reaction type
O-(2-Diethylaminoethyl) *S*-methyl dithiocarbonate (If)	40.4	c)
O-(1-Cyclopropylethyl) *S*-methyl dithiocarbonate[e] (Ib)	34.1 (aprotic) 23.3 (protic)	c)
O-(2-Methylthioethyl) *S*-methyl dithiocarbonate[e] (Ig)	22.4	c)
O-Cinnamyl *S*-methyl dithiocarbonate (Ie)	12.6	d)
O-Allyl *S*-methyl dithiocarbonate (Ic)	6.31	d)
O-Methallyl *S*-methyl dithiocarbonate[e] (Id)	5.54	d)
O-Allyl thiobenzoate (VI)	4.24	d)

a) See ref. 12 and references cited therein. *b*) $\log k = aE_T + b$. *c*) Solvolysis. *d*) [3,3]-Sigmatropy. *e*) This study.

proceeds through, at least in part, a solvent-separated ion-pair intermediate (D and D′). This is in sharp contrast to the result in the case of *O*-cholesteryl *S*-alkyl dithiocarbonates (Ia) which underwent rearrangement *via* a tight ion-pair intermediate (C and C′).[5]

For an estimate of solvent effects on chemical reactions, a large variety of empirical parameters of solvent polarity[11c,d] have been proposed. In this study, the E_T values of Reichardt,[11] based on the bands of solvatochromism of pyridinium *N*-phenoxide betaine dye were used as a scale of solvent ionizing power in studying the effect of solvents on the rate of reaction.[11e]

As illustrated in Fig. 1, plots of $\log k$ *vs.* E_T values for aprotic and protic solvent systems show roughly linear relationships with slopes $a=0.341$ and 0.233, respectively. The magnitude of the slope a has been successfully used as a measure of the sensitivity of a reaction to the ionizing power of the medium.[2c,12] Values of the least-squares slope a for thione–thiol isomerization reaction are summarized in Table III.

As shown in Table III, the values of a are 6.31×10^{-2} for *O*-allyl *S*-methyl dithiocarbonate (Ic), 5.5×10^{-2} for *O*-(2-methylallyl) *S*-ethyl dithiocarbonate (Id) and 4.24×10^{-2} for *O*-allyl thionbenzoate (VI). These values are very small, indicating that these thione esters may rearrange by a mechanism which involves very little change in charge separation between the ground state and the transition state ([3,3]-sigmatropy). On the other hand, a in the case of Ib is very large and comparable to the value in the case of the allylic rearrangement of *cis*-5-methyl-2-cyclohexenyl acid phthalate (VII) ($a=29.1\times10^{-2}$),[12] the pyrolysis of benzhydryl *S*-phenylthiocarbonate (VIII) to the sulfide (31.2×10^{-2})[12] and the thione-thiol rearrangements of *O*-(2-dimethylaminoethyl) (If) (40.4×10^{-2}) and *O*-(2-methylthioethyl) *S*-methyl (Ig) (22.4×10^{-2}) dithiocarbonates. These values are very large, suggesting that the rearrangement reactions occur through highly polarized transition states, such as an ion-pair.

A plot of the logarithm of the rate constants for Ib *vs.* the Grunwald–Winstein Y values[13] is shown in Fig. 2. It is well known that the classical $SN1$ and $SN2$ mechanisms are only the extremes in a continuous spectrum of mechanisms, and reactions at the $SN2$ end have m-values in the neighborhood of 0.4, while those at the $SN1$ end have m-values of about 1.0. Reactions having intermediate or borderline mechanisms have m-values between these extremes. As can be seen in Fig. 2, m in the case of the concerted reaction for the allylic rearrangement of *O*-allyl *S*-methyl dithiocarbonate (Ic) is only 0.14. On the other hand, m for the present case (Ib) is 0.68. The results are in agreement with the conclusion arrived at from the E_T values, as described above.

For further evaluation of the Fainberg–Winstein Y values[13b] for binary mixtures of 10,

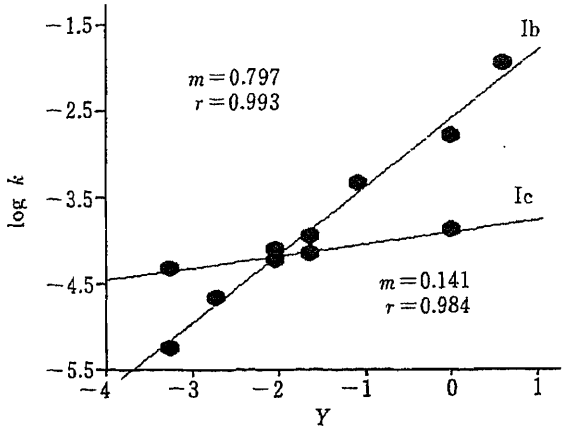

Fig. 2. Plots of k *vs.* Grunwald–Winstein Y Values for the Solvolysis of Ib

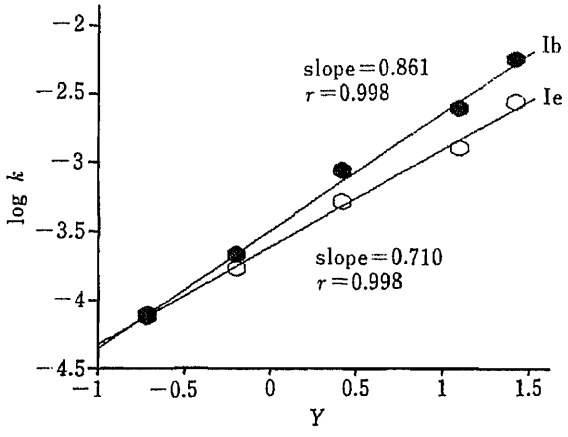

Fig. 3. Plots of k *vs.* Fainberg–Winstein Y Values for the Phenolysis of Ib, e in Phenol–Benzene Solvent

20, 30, 40 and 50% phenol with benzene, the phenolysis rates of Ia and *O*-cinnamyl *S*-methyl dithiocarbonate (Ie) in these solvent systems were also determined at 33.9 °C. The results are presented in Table IV. A plot of the logarithm of the rate constants for Ib, e against the Fainberg–Winstein *Y* values is shown in Fig. 3.

It is noteworthy that plots of k for protic solvents *vs.* δ values[14] (solubility parameters) show a linear relationship, and there is a rough correlation with hydrogen-bonding abilities.

The activation energy for ethanol (protic) is 5 kcal/mol larger than that for dimethylformamide (DMF) (dipolar aprotic), suggesting that the xanthate is stabilized in the ground state by hydrogen-bonding between the thione sulfur and solvent. The activation energies for the phenolic solvents are considerably smaller than that for ethanol (see Table II).

The values of activation entropy vary considerably from −6.0 to 8.1 e. u. on going from DMF to ethanol. The large entropy effect in ethanol is due in part to the highly ordered

TABLE IV. First-Order Rate Constants for Phenolyses of *O*-(1-Cyclopropylethyl) (Ib) and *O*-Cinnamyl (Ie) *S*-Methyl Dithiocarbonates in Phenol–Benzene Solvents at 33.9 °C

PhOH[a] (%)	Y[b]	$k \times 10^5$ (s^{-1})	
		IIb	IIe
90	1.427	557	276
70	1.101	245	126
50	0.425	85.8	51.5
30	−0.192	21.2	16.8
20	−0.711	7.43	7.78

a) First-order constants ($k \times 10^6$) for phenolyses of IIb in *p*-chlorophenol–benzene solvents are as follows: 10%, 33.5; 20%, 170; 30%, 415; 40%, 1002; 50%, 1704. *b*) See ref. 13*b*.

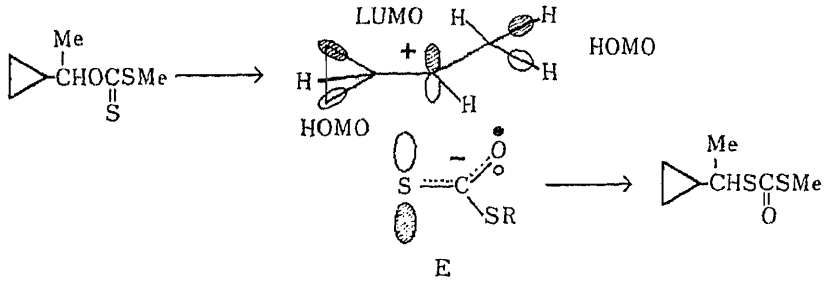

Chart 4

Ib

Ih

PCP=*p*-chlorophenol

Chart 5

structure of the reactants in the ground state. When a phenolic solvent was used, a low entropy of activation was observed, which may be due to its high hydrogen-bonding ability to the leaving group, as well as the steric crowding in solvation. A large negative entropy of activation for *o*-chlorophenol may reflect a crowded transition state in which freedom of motion of the substituents is hindered by the presence of the *o*-chloro group.

O-(1-Methylcyclopropylmethyl) *S*-methyl dithiocarbonate (Ih) reacts about 300 times more slowly than Ib in *p*-chlorophenol at 60 °C. The interaction between the methylium carbon and the cyclopropyl ring can be rationalized by means of the dissection method[15] as illustrated in Chart 4, wherein the cyclopropane ring acts as a donor (HOMO) and the methylium carbon acts as an acceptor (LUMO), resulting in effective anchimeric assistance for ionization of the C–O bond.

In connection with the rearrangement reaction, mention should be made of the alteration of the mechanism of the thione–thiol rearrangement of *S*-(2-alkenyl) *S*-alkyl dithiocarbonates in phenolic solvents. In the phenolysis of *O*-cinnamyl *S*-methyl dithiocarbonate (Ie) in *p*-chlorophenol, the mechanism of the rearrangement reaction changes dramatically from the concerted reaction[2c] to the ionic one. In usual protic solvents such as ethanol, the [3,3]-sigmatropic reaction takes place to give IIe. However, when the same reaction is carried out in a phenolic solvent such as *p*-chlorophenol, a pair of allylic isomers (IIe and IIe′) was obtained as the result of an ionic nucleophilic replacement reaction *via* an intermediate, F.[16] In the reaction, the carbonium ions may be stabilized by the specific solvation[17] of phenols to the extent that the solvent stabilizing energy exceeds the resonance energy of the styrene moiety.

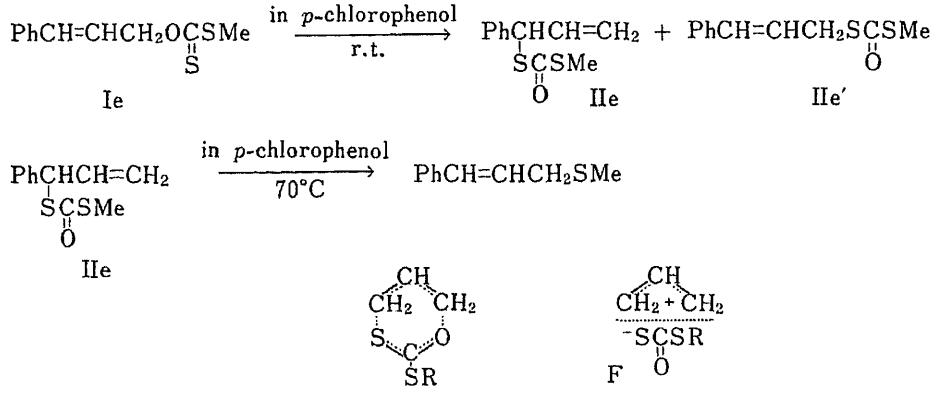

Chart 6

It is concluded that the hydroxyl group is distinctly the center of the reaction in hydroxylic solvents such as alcohols or phenols and they play a role not only as a general solvent but also as a kind of reactant molecule in the ionization process of the S_N1-type solvolysis.[18] The reaction constants in hydroxylic solvents can be used as a measure of the hydrogen-bonding capacity of the solvent with a sulfur atom.

Experimental

The melting points were measured with a Yanagimoto micromelting point apparatus and are uncorrected. The ultraviolet (UV) spectra were determined by Hitachi EPS-3T and JASCO UVIDEC-220B digital spectrophotometers. The ^{1}H-NMR spectra were taken with Hitachi R-600 or JEOL PS-100 and GX-400 spectrophotometers using tetramethylsilane as an internal standard, and the chemical shifts are expressed in δ values. The IR spectra were taken with JASCO IRA-1 and DS-301 grating spectrophotometers.

All the calculations were performed on FACOM M-200 and 382 computers in the computer center of Kyushu University.

Solvents——Solvents were purified by distillation or by recrystallization before use.

***O*, *S*-Dialkyl Dithiocarbonates**——*O*-(1-Cyclopropylethyl) (Ib) and *O*-(1-methylcyclopropylmethyl) (Ih) *S*-methyl dithiocarbonates were prepared according to the reported method.[8] *O*-Allyl (Ic), *O*-(2-methylallyl) (Id), *O*-(3-phenylallyl) (Ie), *O*-(2-diethylaminoethyl) (If) and *O*-(2-methylthioethyl) (Ig) *S*-methyl dithiocarbonates were prepared according to procedures developed in this laboratory.[2c]

The ^{1}H-NMR spectral data for Ib are as follows; ^{1}H-NMR (in CCl_4) of Ib: 0.47, 0.62 (4H, m, $>CH_2$ of cyclopropane ring), 0.90 (1H, m, >CH– of cyclopropane ring), 1.41 (3H, d, J=6 Hz, –Me), 2.53 (3H, s, SMe), 5.18 (1H, dt, J=5.3 Hz, >CH–O).

Compound Ih[19] was obtained as a yellow oil: bp 111 °C (23 mmHg). IR (liquid film) cm^{-1}: 3084 (cyclopropane ring), 1222, 1066 (-OC=SS-). ^{1}H-NMR (in $CDCl_3$, 400 MHz): 0.453 (2H, t, CH_2 of cyclopropane ring), 0.562 (2H, t, CH_2 of cyclopropane ring), 1.198 (3H, s, SMe), 4.377 (2H, s, CH_2–O). *Anal.* Calcd for $C_7H_{12}OS_2$: C, 47.69; H, 6.86. Found: C, 47.80; H, 7.1.

Phenolysis of Ib with *p*-Chlorophenol——Compound I was dissolved in *p*-chlorophenol at room temperature to give immediately the corresponding dithiolester (IIb) and *p*-chlorophenyl 1-cyclopropylethyl ether (III) in 77% and 14% yields, respectively. The products were purified by column chromatography on silica gel with *n*-hexane–benzene. The structure of IIb was determined on the basis of its ^{1}H-NMR spectrum (100 MHz). The data obtained in a double-resonance experiment are as follows; ^{1}H-NMR (in $CDCl_3$): 0.24—0.7 (4H, m, $>CH_2$ of cyclopropane ring), 0.7—1.13 (1H, m, >CH– of cyclopropane ring), 1.45 (3H, d, J=6.9 Hz, Me), 2.41 (3H, s, MeS–), 3.07 (1H, dt, J=7.5 Hz, >CH–S).

The IR spectrum of III was identical with that of an authentic sample (see below).

Rearrangement of Ib to IIb——A solution of Ib (3 g) in an aprotic solvent (5 ml) such as dimethyl sulfoxide (DMSO) was heated at 50 °C for 1 h. After cooling, 10 ml of water was added. The rearranged product (IIb) was extracted with *n*-hexane and distilled under reduced pressure to give IIb, bp 234—236 °C, quantitative yield. Water-soluble solvents such as ethanol gave a similar result.

1-Cyclopropylethyl 3,5-Dinitrobenzoate (IX)——Prepared by the reported method.[20] The ^{1}H-NMR spectral data (400 MHz) are as follows; ^{1}H-NMR (in $CDCl_3$): 0.375 (1H, sextet, $>CH_2$ of cyclopropane ring), 0.495 (1H, sextet, $>CH_2$ of cyclopropane ring), 0.573—0.712 (2H, m, $>CH_2$ of cyclopropane ring), 1.209 (1H, nonet, >CH– of cyclopropane ring), 1.515 (3H, d, J=6.35 Hz, Me), 4.655 (1H, m, octet, >CH–O), 9.174 (2H, d, J=2.4 Hz, H_4), 9.224 (1H, d, J=2.4 Hz, H_2 and H_6). The signals appear as complex multiplets, presumably due to restricted rotation about the bond connecting the cyclopropane ring and C_1 carbon.

***p*-Chlorophenyl 1-Cyclopropylethyl Ether (III)**——1-Cyclopropylethyl 3,5-dinitrobenzoate (IX) was added to a solution of *p*-chlorophenol (6 ml) containing 0.5 g of sodium *p*-chlorophenolate, and the mixture was heated on a water bath for 3 h. The reaction mixture was diluted with 20 ml of benzene and treated with 10% NaOH solution. The benzene layer was separated, washed once with water, dried over anhydrous $MgSO_4$, and evaporated. The residue was chromatographed on silica gel to give a colorless oil, 487 mg. *Anal.* Calcd for $C_{11}H_{13}ClO$: C, 67.18; H, 6.66. Found: C, 67.23; H, 6.66. ^{1}H-NMR (in $CDCl_3$): 0.16—1.23 (5H, m, cyclopropane ring), 1.31 (3H, d, J=6 Hz, –Me), 3.83 (1H, sextet, J=6 Hz, >CH–O), 6.75 (4H, AB quartet, J=9 Hz, *p*-ClC_6H_4O–).

Transformation of IIb to 1-Cyclopropylethyl 2,4-Dinitrophenyl Sulfide (IV)——A solution of IIb (176 mg) and ethanolamine (200 mg) in ethanol (2 ml) was heated on a water bath until the evolution of methanethiol ceased. After cooling, a solution of 2,4-dinitrochlorobenzene (203 mg) in ethanol (2 ml) was added to the reaction mixture and the whole was allowed to stand overnight at room temperature. The precipitates were recrystallized from ethanol to give yellow crystals, mp 71—73.5 °C, identical with the reported sample.[8]

Kinetics——The phenolysis rates were followed at a given temperature by measuring the decrease of the thione absorption at 350 nm, using a 10×10 mm quartz cell which was thermostated with flowing water at constant temperature. The first-order rate constants were calculated from a plot of $\ln(A_t - A_\infty)$ *vs.* time by a least-squares method, where A_t is the absorbance at time t and A_∞ is the absorbance after about 10 half-lives. The absorption data were collected automatically. The results are listed in Tables I—III. All spectra were calculated by means of a nonweighted least-squares program written in FORTRAN.

Acknowledgement We thank Mr. Kouichiro Miyoshi and Miss Kimiko Hamada for experimental assistance. This work was supported in part by a Grant-in-Aid for Scientific Research from the Ministry of Education, Science and Culture.

References and Notes

1) H. R. Nace, "Organic Reactions," Vol. 12, ed. by A. C. Cope, John Wiley and Sons, Inc., New York, 1962, Chapter 2.

2) *a*) T. Taguchi, Y. Kawazoe, K. Yoshihira, H. Kanayama, M. Mori, K. Tabata and K. Harano, *Tetrahedron Lett.*, **1965**, 2717; *b*) T. Kawata, K. Harano and T. Taguchi, *Chem. Pharm. Bull.*, **21**, 604 (1973); *c*) K. Harano and T. Taguchi, *ibid.*, **23**, 467 (1975); *d*) K. Komaki, T. Kawata, K. Harano and T. Taguchi, *ibid.*, **26**, 3807 (1978).

3) M. Kojima, M. Watanabe and T. Taguchi, *Yakugaku Zasshi*, **96**, 905 (1976).
4) K. Harano, N. Ohizumi and T. Hisano, *Tetrahedron Lett.*, **26**, 4203 (1985).
5) K. Harano, K. Miyoshi and T. Hisano, *Chem. Pharm. Bull.*, **33**, 1861 (1985).
6) Bond energy data indicate that isomerization is exothermic by about 24 kcal/mol: E. S. Kooyman, "Organosulfur Chemistry," ed. by M. J. Janssen, Interscience Publishers, New York, 1967, Chapter 1.
7) The complex signals of IIb may be due to restricted rotation of the bond connecting the cyclopropane ring and the carbinyl carbon.
8) C. G. Overberger and A. E. Borchert, *J. Am. Chem. Soc.*, **82**, 4896 (1960).
9) K. G. Rutherford, B. K. Tang, L. K. M. Lam and D. P. C. Fung, *Can. J. Chem.*, **50**, 3288 (1972).
10) C. M. Huggins, G. C. Pimentel and J. N. Shooley, *J. Phys. Chem.*, **60**, 1311 (1956).
11) *a*) K. Dimroth, C. Reichardt, T. Siepmann and F. Bohlmann, *Justus Liebigs Ann. Chem.*, **661**, 1 (1963); *b*) K. Dimroth, C. Reichardt and A. Schweig, *ibid.*, **669**, 95 (1963); *c*) C. Reichardt, *Angew. Chem.*, **77**, 30 (1965); *d*) *Idem, Pure Appl. Chem.*, **54**, 1867 (1982); *e*) The use of the normalized E_N-values has been recently recommended because E_T-values have the dimensions of kcal/mol.[11d]
12) M. Yasuda, K. Harano and K. Kanematsu, *J. Org. Chem.*, **45**, 2368 (1980).
13) *a*) E. Grunwald and S. Winstein, *J. Am. Chem. Soc.*, **70**, 846 (1948); *b*) A. H. Fainberg and S. Winstein, *ibid.*, **78**, 2770 (1956).
14) M. Chastrette, M. Rajzmann, M. Chanon and K. F. Purcell, *J. Am. Chem. Soc.*, **107**, 1 (1985).
15) K. Fukui, "Kagaku Hanno To Densi No Kido (Chemical Reactions and Electron Orbitals)," Maruzen, Tokyo, 1976.
16) K. Harano, N. Ohizumi and T. Hisano, Abstracts of Papers, 106th Annual Meeting of the Pharmaceutical Society of Japan, Chiba, April 1986, p. 374.
17) The pseudo first-order rate constants in the presence of various concentrations of *p*-chlorophenol (5—10%) show a linear relationship against the square of the amounts of *p*-chlorophenol.
18) A referee has suggested that the term "solvolysis" should be used for the displacement reactions by solvents. However, it is generally accepted that carbonium ion reactions in which the attacking nucleophile is a solvent molecule fall into the category of solvolysis.
19) Phenolysis of Ih in *p*-chlorophenol gave the dithiol esters including the skeletally rearranged four-membered ring compound: K. Harano, H. Kiyonaga and T. Hisano, manuscript in preparation.
20) R. V. Volkenburch, K. W. Greenlee, J. M. Derfer and C. E. Boord, *J. Am. Chem. Soc.*, **71**, 3595 (1949).

[Chem. Pharm. Bull. 35(4)1397—1404(1987)]

Synthesis of Chiral 5-Deazaflavin Derivatives and Their Use in Asymmetric Reduction of Ethyl Benzoylformate[1)]

KIYOSHI TANAKA, TEIJI KIMURA, TOMOYA OKADA, XING CHEN and FUMIO YONEDA*

Faculty of Pharmaceutical Sciences, Kyoto University, Sakyo-ku, Kyoto 606, Japan

(Received September 16, 1986)

Some 1,5-dihydro-5-deazaflavin (1,5-dihydropyrimido[4,5-*b*]quinoline-2,4(3*H*,10*H*)-dione) derivatives possessing chiral substituents at the N-3 position were synthesized. Asymmetric reduction of ethyl benzoylformate in the presence of magnesium perchlorate was carried out with these chiral 1,5-dihydro-5-deazaflavin derivatives to give ethyl mandelate in moderate optical and chemical yield. The influence of metal additives other than magnesium upon the asymmetric induction and yield of the reduction was investigated, and it was suggested that intermediate ternary complexation is probably involved in the reaction. No improvement of chiral induction was obtained by changing the metal catalyst.

Keywords——chiral 5-deazaflavin; 1,5-dihydro-5-deazaflavin; asymmetric reduction; ethyl benzoylformate; coenzyme model; metal additive; ethyl mandelate; α-methylbenzylamine

5-Deazaflavin (pyrimido[4,5-*b*]quinoline-2,4(3*H*,10*H*)-dione) derivatives were first synthesized in 1970 by Cheng and co-workers[2)] as part of a search for antagonists of riboflavin. The only structural difference between the flavin (isoalloxazine) and the 5-deazaflavin is the replacement of N-5 of the flavin by CH. This derivation causes the 5-deazaflavins to resemble structurally not only the parent flavins but also nicotinamide nucleotides (NAD) (Chart 1), and this is the reason why 5-deazaflavins are often referred to as "flavin-shaped nicotinamide analogs." In fact, the chemistry of flavin and 5-deazaflavin is fundamentally different[3)] and it has been reported that the chemical behavior of 5-deazaflavin

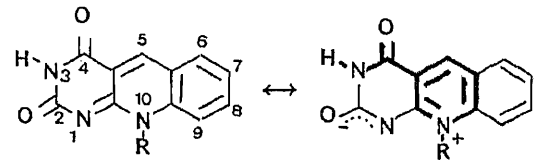

5-deazaflavin

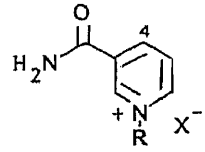

NAD^+

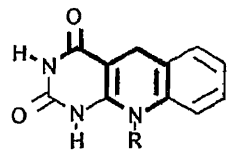

1,5-dihydro-5-deazaflavin

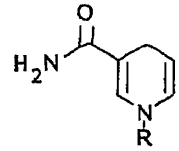

NADH

Chart 1

resembles that of NAD rather than that of flavin.[4] On the other hand, since the discovery of coenzyme F_{420},[5] 5-deazaflavin derivatives have received considerable attention because of their significant roles in redox reactions (anoxybionic metabolism) as well as in the repair of damaged deoxyribonucleic acid (DNA)[6] (DNA photoreactivating function) in biological systems. These findings stimulated extensive work on the chemistry and function of 5-deazaflavin derivatives in both enzymatic and model systems.[7]

Biomimetic reactions using nicotinic acid derivatives have been widely investigated since the pioneering work by Westheimer *et al.*[8] in 1957, in order to provide mechanistic insight into NAD(P)–NAD(P)H catalyzed reactions in the field of bioorganic chemistry.[9] The results of the many investigations have made an important contribution to asymmetric synthesis.[10,11] For example, when a chiral group is substituted on the amide nitrogen of an NADH model compound (Chart 2), asymmetric reduction takes place in the presence of a metal ion. The stereochemical and mechanistic considerations in (net) hydride transfer from and to NAD(P)–NAD(P)H models have also been reported.[12] One of the authors,[13] F. Y., has previously reported that 1,5-dihydro-5-deazaflavin reduced simple carbonyl compounds under acidic conditions to afford the corresponding alcohols, so we turned our attention to asymmetric reduction using chiral 5-deazaflavin derivatives.

In contrast to NADH models, asymmetric hydrogen transfer to and from 5-deazaflavins and flavins had not been examined until our recent communication,[1] and to our knowledge, there are still only a few reports dealing with asymmetric reduction with chiral 5-deazaflavins and flavins.[14]

In this paper, we describe the preparation of chiral 5-deazaflavin derivatives and their use for the asymmetric reduction of ethyl benzoylformate. The influence of metal ions as additives which might influence the rate and stereoselectivity in the reduction will also be discussed briefly.

We designed and synthesized compounds of type (**1**) in which a chiral substituent exists on the N-3 position of the 5-deazaflavin framework. This compound is essentially similar in structure to the above-mentioned NAD(P)H model by which successful asymmetric reduction was achieved (Chart 2). 7-Methyl-5-deazaflavin derivatives were also prepared because the 7-methyl derivatives showed a potential reductive power in "autorecycling reduction."[15]

The use of such 5-deazaflavins in the asymmetric reduction of ethyl benzoylformate was expected to give a comparable degree of stereo (enantio) selectivity due to their structural similarity to NADH models and the greater rigidity of the 5-deazaflavin skeleton.

Treatment of nitrourea[16] with commercially available (*R*)-(+)-α-methylbenzylamine in water gave (*R*)-(+)-*N*-α-methylbenzylurea (**2a**) in good yield. Similar treatment with (*S*)-(−)-α-methylbenzylamine also afforded the corresponding urea (**2b**). These optically active urea derivatives were converted to the barbituric acid derivatives (**3a**, **b**) in 75—80% yield by a conventional method in which the urea derivatives were treated with the mixed anhydride derived from malonic acid and acetic anhydride. Unlike the common barbituric acid

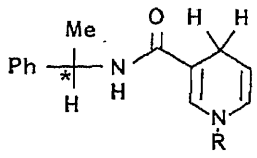

R = $PhCH_2$: BNPH

R = C_3H_7 : PNPH

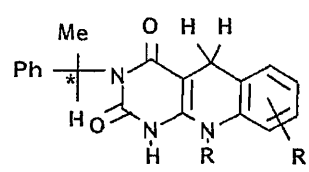

1

Chart 2

derivatives, **3** could not be converted into the chlorides (**4**) with various kinds of reagents. One-carbon extension reaction of 3-(*R*)-(+)- and 3-(*S*)-(−)-α-methylbenzylbarbituric acids with Vilsmeier-type reagent[17] was carried out to yield the corresponding 6-chloro-5-formyluracils (**5a** and **5b**) as oily substances, which were labile on standing and were therefore used for the following cyclization step without purification. Heating of the 6-chloro-5-formyluracil derivatives (**5a, b**) with an appropriate *N*-alkylarylamine or *N*-alkylnaphthylamine in dimethylformamide (DMF) gave the desired optically active 5-deazaflavin derivatives (**6**—**8**) in good yields. These results are summarized in Table I. *N*-Butyl-*p*-toluidine and *N*-butyl-α-naphthylamine were synthesized *via* the corresponding *N*-trifluoroacetyl derivatives from *p*-toluidine and α-naphthylamine, respectively. Of these 5-deazaflavin derivatives, the tetracyclic compound (**8a**) is rather unstable and the yield of this compound was less satisfactory.

Next, we examined asymmetric reduction with the 5-deazaflavin derivatives thus

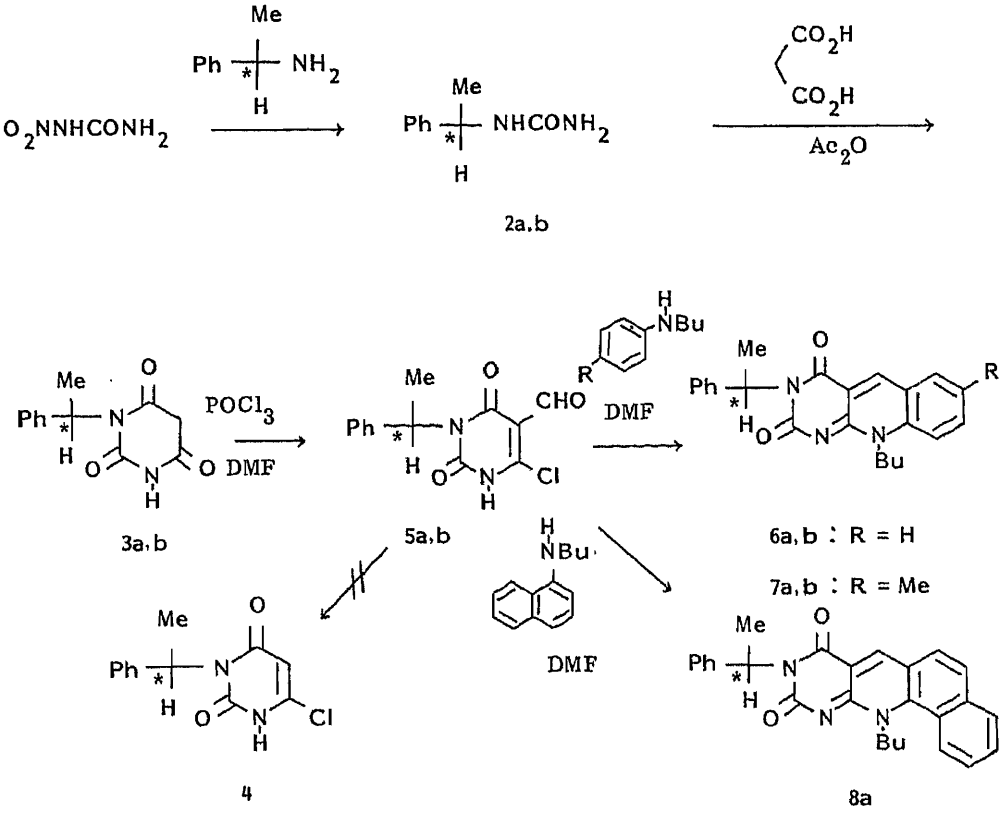

Chart 3

TABLE I. Chiral 5-Deazaflavin Derivatives

5-Deazaflavin	Configuration at N-3 side chain	% Yield[a] from **3**	$[\alpha]_D$ (degree) in chloroform	mp (°C)
6a (R=H)	*R*	55	+147[b]	114—116
6b (R=H)	*S*	53	−147[b]	114—116
7a (R=Me)	*R*	26	+111.5	71—73
7b (R=Me)	*S*	39	−117.4	84—87
8a	*R*	20.5	+205.6	203

a) Isolated yield. *b*) In ethanol.

obtained. Ethyl benzoylformate has been widely used in asymmetric reduction with 1,4-dihydropyridine derivatives,[10-12] as mimics of coenzyme NADH, and is a suitable substrate for the present asymmetric reduction because of its high reactivity and the ease of evaluation of the degree of chiral induction in the product.[18] 5-Deazaflavin derivatives (**6**, **7**) bearing the chiral group at the *N*-3 position were transformed into their reduced form, 1,5-dihydro-5-deazaflavin derivatives (**9**, **10**), quantitatively by reduction with sodium borohydride in methanol or sodium dithionite in water.[19] In this procedure, the 1,5-dihydro-5-deazaflavin derivatives (**9**, **10**) are quite reactive to atmospheric oxygen, and so strict exclusion of oxygen and light was required. Nevertheless, the reaction residue of the reduction was always contaminated by starting 5-deazaflavin (oxidized form) derivatives in the range of 3—15%. Under the highly acidic reaction conditions reported for the reduction of simple ketones by achiral 5-deazaflavin derivatives,[13] racemization of the resulting alcohol might occur, so we employed milder conditions similar to those used for NADH model studies. With equimolar 1,5-dihydro-5-deazaflavin derivative and ethyl benzoylformate, the asymmetric reduction was carried out in the presence of one equivalent amount of magnesium perchlorate in a mixture of acetonitrile–acetic acid (1 : 1) or acetonitrile alone at room temperature under an atmosphere of argon in the dark until most of the 1,5-dihydro-5-deazaflavin derivative had disappeared (checked by thin layer chromatography (TLC)) (Chart 4). The reaction progress can also be monitored by high performance liquid chromatography (HPLC) (μ-Porasil, hexane–ethyl acetate (8 : 1), ultraviolet (UV) 254 nm). After the reaction, the mixture was worked up and the reaction products, ethyl mandelate, recovered ethyl benzoylformate, and

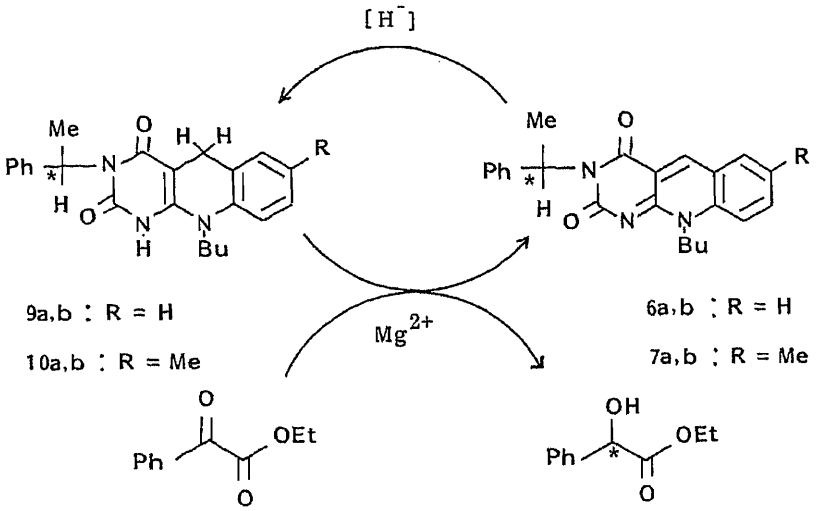

Chart 4

TABLE II. Asymmetric Reduction of Ethyl Benzoylformate

1,5-Dihydro-5-deazaflavin	$[\alpha]_D^{25}$ a)	Ethyl mandelate			
		Chemical yield (%) b)	Configuration	$[\alpha]_D^{25}$ c)	Optical yield (% ee) d)
9a	+125°	12	*S*	+14.2°	14
9b	−127°	15	*R*	−21.8°	21
10b	—	15.4	*R*	−15.1°	14.5

a) In chloroform. b) Isolated yield. c) In ethanol. d) Pure (*R*)-ethyl mandelate[18]: $[\alpha]_D^{24} = -104°$ (in ethanol).

the 5-deazaflavin derivative, were isolated by preparative-TLC (p-TLC) on silica gel. The reaction conditions employed and the results are summarized in Table II. As can be seen, asymmetric induction was observed by using chiral 5-deazaflavin derivatives, but its degree was not so high as had been expected. The optical yield (% ee) was determined on the basis of the reported $[\alpha]_D$ value[18] of ethyl mandelate. Though ethyl mandelate was obtained in moderate chemical and optical yield, the exact chemical yield could not be determined due to the sensitivity of the 1,5-dihydro-5-deazaflavin derivatives to oxygen, and the actual chemical yield might be higher. Since no products other than ethyl mandelate and starting ethyl benzoylformate were isolated, the chemical yield based on the consumed starting ketone may be nearly quantitative. This is a first example of a nonenzymatic, stoichiometric asymmetric reduction using 5-deazaflavin derivatives. The 1,5-dihydro derivative of the compound (**8a**) was not used for reduction because of its poor formation yield and its lability.

In reduction with NADH models, metal ions, especially magnesium ion, play an important role and it was suggested that both rate-enhancement and enantioselectivity depend significantly upon the nature and concentration of the metal ion. The role of the metal ion has been interpreted in terms of electron transfer[20] and complexation[12] between the reductant (mimic model) and metal. In order to improve the asymmetric induction with 1,5-dihydro-5-deazaflavin derivatives, we investigated the reduction of ethyl benzoylformate in the presence of a variety of metal ions under neutral conditions at room temperature. The reaction was carried out in methylene chloride to minimize racemization of the resulting mandelate till no more 1,5-dihydro-5-deazaflavin was detected on a TLC plate. The results and reaction conditions are included in Table III. From the Table III, a higher isolated chemical yield was obtained with aluminum chloride, whereas a better optical yield was

TABLE III. Effect of Metal Additives on Asymmetric Reduction

1,5-Dihydro-5-5-deazaflavin	Metal additive	(eq)	Reaction time (d)	Ethyl mandelate		
				Chemical yield (%)[a]	Configuration	Optical yield (% ee)
9a or **9b**	None	—	7	15—16	—	0
9b	$BF_3 \cdot AcOH$	1	2.5	10.5	*R*	13.6
10b[b]	$Mg(ClO_4)_2$	1	7	15.4	*R*	14.5
10b	$AlCl_3$	1	3	34.5	*R*	5.3
10b	SiO_2	1	4	10.0	*R*	6.0
10b	PPh_3	1	6	13.4	—	0
10b	$CaCl_2$	1	4	3.8	*R*	8.0
10b	$Ga(NO_3)_3$	0.3	4	8.0	—	0
10b	$Eu(fod)_3$	0.1	3	18.5	*R*	4.3

a) Isolated yield. *b*) In $AcOH-CH_3CN$ (1:5).

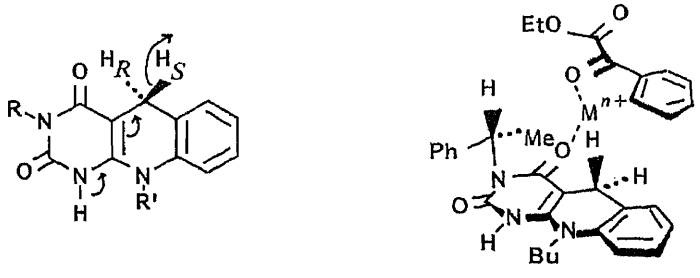

Chart 5

observed with magnesium perchlorate and boron trifluoride–acetic acid. Aluminum chloride probably caused racemization of the alcohol due to its potential Lewis acidity.

In these reductions, (net) hydride transfer might take place from the 1,5-dihydro-5-deazaflavin derivative. Introduction of a chiral substituent into the 5-deazaflavin skeleton at the N-3 position causes the two hydrogens on the achiral carbon atom at the C-5 position in the 1,5-dihydro-5-deazaflavin to be sterically discriminated, and one of the diastereotopic hydrogens (pro-*R* or pro-*S*) is transferred preferentially to the substrate. Furthermore, no asymmetric induction was observed in our present study or in NADH mimic studies in the absence of metal (magnesium) ion. Thus, the transition state for the reduction shown in Chart 5 may be postulated. The moderate or low optical yield observed in our case may be attributable to the flexibility or low degree of participation of the proposed intermediate, a ternary complex.[21] Metal ions having a larger atomic radius such as gallium and europium are not suitable catalysts in terms of this ternary complexation. Racemization by metal additives may not be negligible in our reduction.

Further investigations of asymmetric reduction with 5-deazaflavin derivatives having other types of chiral auxiliary, such as axial (plane) chirality, and reduction in chiral media (chiral catalyst) are in progress.

Experimental

Melting points were determined with a Yanagimoto melting point apparatus and are uncorrected. The infrared (IR ν_{max}) spectra were determined on a Shimadzu IR-400 spectrophotometer in chloroform. The proton nuclear magnetic resonance (^{1}H-NMR) spectra were obtained in dimethyl sulfoxide-d_6 (DMSO-d_6) or chloroform-*d* ($CDCl_3$) at 60 MHz on a JEOL PMX-60 or at 200 MHz on a JEOL FX 200 instrument with chemical shifts being reported in δ units from tetramethylsilane as an internal standard and couplings in hertz. Mass spectra (MS) were taken on a JEOL JMS 01SG-2 instrument by direct insertion at 75 eV. Optical rotation was recorded on a JASCO DIP-360 digital polarimeter. p-TLC was run on 20 × 20 cm plates coated with a 0.1—1.5 mm layer of Merck Silica gel PF_{254} or GF_{254}.

(*R*)-(+)- and (*S*)-(−)-*N*-α-Methylbenzylurea (2a and 2b): General Procedure——α-Methylbenzylamine (13.8 g, 113 mmol) was added to a solution of 10 g (95 mmol) of nitrourea[16] in water (100 ml). The mixture was refluxed for 30 min on a water bath, and cooling of the mixture gave the corresponding *N*-α-methylbenzylurea as colorless needles in 80—90% yield.

(*R*)-(+)-*N*-α-Methylbenzylurea (**2a**): mp 121 °C (from water). ^{1}H-NMR (60 MHz, DMSO-d_6) δ: 1.33 (3H, d, J=7, CH_3), 4.74 (1H, m, CH), 5.44 (2H, s, NH_2), 6.43 (1H, d, J=9, NH), 7.31 (5H, s, Ar). $[\alpha]_D^{24}$ +47.8° (c=2.0, ethanol). *Anal.* Calcd for $C_9H_{12}N_2O$: C, 65.83; H, 7.37; N, 17.06. Found: C, 65.91; H, 7.41; N, 16.87.

(*S*)-(−)-*N*-α-Methylbenzylurea (**2b**): mp 121 °C (from water). ^{1}H-NMR: the same as above. $[\alpha]_D^{24}$ −48.2° (c=2.0, ethanol). *Anal.* Calcd for $C_9H_{12}N_2O$: C, 65.83; H, 7.37; N, 17.06. Found: C, 65.79; H, 7.35; N, 16.90.

3-(*R*)-(+)- and 3-(*S*)-(−)-α-Methylbenzylbarbituric Acid (3a and 3b): General Procedure——Acetic anhydride (3 ml) was added dropwise to a stirred solution of optically active α-methylbenzylurea (2.0 g, 12 mmol) and malonic acid (1.3 g, 12.5 mmol) in acetic acid (10 ml) at 70 °C. Then, the mixture was heated at 80—90 °C for 3 h with stirring. Concentration of the mixture under reduced pressure followed by crystallization of the residue from ethanol afforded the corresponding barbituric acid (**3a** and **3b**) in 75—80% yield as an off-white powder.

3-(*R*)-(+)-α-Methylbenzylbarbituric Acid (**3a**): mp 130 °C. ^{1}H-NMR (60 MHz, DMSO-d_6) δ: 1.73 (3H, d, J=7.5, CH_3), 5.94 (1H, q, J=7.5, CH), 7.33 (5H, s, Ar), 11.3 (1H, s, NH). IR ν_{max} cm^{-1}: 3370, 1725, 1690. $[\alpha]_D^{25}$ +161.5° (c=1.0, ethanol). *Anal.* Calcd for $C_{12}H_{12}N_2O_3$: C, 62.06; H, 5.21; N, 12.06. Found: C, 62.18; H, 5.32; N, 12.15.

3-(*S*)-(−)-α-Methylbenzylbarbituric Acid (**3b**): mp 131 °C. ^{1}H-NMR and IR: the same as those of **3a**. $[\alpha]_D^{24}$ −159.3° (c=1.0, ethanol). *Anal.* Calcd for $C_{12}H_{12}N_2O_3$: C, 62.06; H, 5.21; N, 12.06. Found: C, 62.23; H, 5.28; N, 11.88.

***N*-Butyl-*p*-toluidine**——A mixture of *p*-toluidine (1.07 g), methylene chloride (5 ml), triethylamine (1 ml) and trifluoroacetic anhydride (1.0 ml) was kept standing at 0—5 °C in a refrigerator overnight. The mixture was poured into ice-water and extracted with ether. The ether extract was successively washed with cold diluted hydrochloric acid and brine, and dried over magnesium sulfate. Evaporation of the ether left a crystalline residue. Recrystallization from ether gave 1.1 g of *N*-trifluoroacetyl-*p*-toluidine, mp 114 °C. ^{1}H-NMR (60 MHz, $CDCl_3$) δ: 2.40 (3H, s, CH_3), 7.33 (2H, d, J=8, Ar), 7.67 (2H, d, J=8, Ar), 8.30 (1H, br s, NH). IR ν_{max} cm^{-1}: 3400, 1720.

A mixture of the above *N*-trifluoroacetyl-*p*-toluidine (1.1 g), 1-bromobutane (1.50 g), potassium carbonate (2.0 g)

and acetone (20 ml) was refluxed for 10 h and then concentrated to give a residue containing *N*-butyl-*N*-trifluoroacetyl-*p*-toluidine. Methanol (20 ml) was added to the residue and the mixture was refluxed for 3 h. Concentration of the mixture under reduced pressure gave a residue, which was extracted with ether. The ether layer was washed with water, dried over magnesium sulfate and then concentrated to dryness to give an oily residue. Purification of the residue by short column chromatography on silica gel gave *N*-butyl-*p*-toluidine (730 mg) as a colorless oil. ^{1}H-NMR (60 MHz, $CDCl_3$) δ: 1.10 (3H, brt, J=6, CH_3), 1.36—1.93 (4H, m, 2×CH_2), 2.36 (3H, s, CH_3), 3.15 (2H, br t, J=6, CH_2), 3.53 (1H, s, NH), 6.50 (2H, d, J=8, Ar), 6.97 (2H, d, J=8, Ar). IR ν_{max}cm^{-1}: 3400, 1612.

***N*-Butyl-α-naphthylamine**——Starting from α-naphthylamine (1.43 g, 10 mmol), *N*-trifluoroacetyl-α-naphthylamine (1.60 g) was obtained in the same manner as above, as colorless needles, mp 107 °C. *N*-Trifluoroacetyl-α-naphthylamine: ^{1}H-NMR (200 MHz, $CDCl_3$) δ: 7.30—7.86 (7H, m, Ar), 8.47 (1H, brs, NH). IR ν_{max}cm^{-1}: 3400, 1735, 1598.

By the same procedure as above, 1.60 g of *N*-trifluoroacetyl-α-naphthylamine was converted to 1.27 g of *N*-butyl-α-naphthylamine as an oil. ^{1}H-NMR (200 MHz, $CDCl_3$) δ: 0.94 (3H, d, J=7.5, CH_3), 1.44 (2H, sextet, J=7.5, CH_2), 1.65 (2H, quintet, J=7.5, CH_3), 3.18 (2H, t, J=7.5, CH_2), 4.11 (1H, brs, NH), 6.56 (1H, d, J=7.8, Ar), 7.14—7.80 (6H, m, Ar). IR ν_{max}cm^{-1}: 3420, 1622, 1580.

Optically Active 5-Deazaflavin Derivatives (6a, b, 7a, b and 8a): General Procedure——3α-Methylbenzylbarbituric acid (**3a** or **3b**) (6 mmol) was added a mixture of phosphoryl chloride (5 ml) and DMF (1 ml), and the resulting mixture was heated at 100 °C with stirring for 3 h under an atmosphere of argon. The reaction mixture was concentrated under reduced pressure to give a residue, which was poured into ice-water and then extracted with chloroform. The chloroform extract was washed with water, dried over magnesium sulfate and then evaporated to dryness to give 6-chloro-5-formyl-3α-methylbenzyluracil (**5a** or **5b**) as a brownish oil, which shows absorption bands at 3380, 2760, 2860, 1725, 1700 and 1668 cm^{-1} in the IR spectrum. Because of its instability, this compound was used for the next cyclization step without further purification.

A solution of the above 6-chloro-5-formyluracil and an appropriate amine (*N*-butylaniline, *N*-butyl-*p*-toluidine or *N*-butyl-α-naphthylamine) (6.0 mmol) in 10 ml of dimethylformamide was heated at 90 °C for 3 h with stirring under an atmosphere of argon. Evaporation of dimethylformamide under reduced pressure and purification of the residue by extraction with chloroform followed by column chromatography on silica gel with chloroform gave the corresponding yellow (**6a, b** and **7a, b**) or green (**8a**) optically active 5-deazaflavin derivatives in 20.5—55% yield from the barbituric acid derivatives (**3a** or **3b**) (also see Table I).

(+)-10-Butyl-3-(*R*)-α-methylbenzyl-5-deazaflavin (**6a**): mp 114—117 °C. ^{1}H-NMR (200 MHz, $CDCl_3$) δ: 1.02 (3H, t, J=8, CH_3), 1.94 (3H, d, J=7, CH_3), 4.72 (2H, br t, CH_2), 6.40 (1H, q, J=7, CH), 7.15—7.90 (9H, m, Ar), 8.78 (1H, s, =CH–). IR ν_{max}cm^{-1}: 1695, 1640, 1617, 1568, 1532. $[\alpha]_D^{25}$ +147.0° (c=10, ethanol). *Anal.* Calcd for $C_{23}H_{23}N_3O_2$: C, 73.97; H, 6.21; N, 11.25. Found: C, 73.82; H, 6.40; N, 11.22.

(−)-10-Butyl-3-(*S*)-α-methylbenzyl-5-deazaflavin (**6b**): mp 114—117 °C. ^{1}H-NMR and IR: the same as those of **6a**. $[\alpha]_D^{25}$ −147.0° (c=10, ethanol). *Anal.* Calcd for $C_{23}H_{23}N_3O_2$: C, 73.97; H, 6.21; N, 11.25. Found: C, 73.89; H, 6.32; N, 11.38.

(+)-10-Butyl-7-methyl-3-(*R*)-α-methylbenzyl-5-deazaflavin (**7a**): mp 71—73 °C. ^{1}H-NMR (200 MHz, $CDCl_3$) δ: 1.01 (3H, t, J=7, CH_3), 1.55 (2H, sextet, J=7, CH_2), 1.72 (2H, quintet, J=7, CH_2), 1.94 (3H, d, J=7.5, CH_3), 2.47 (3H, s, CH_3), 4.70 (2H, br t, CH), 6.39 (1H, q, J=7.5, CH_3), 7.18—7.69 (8H, m, Ar), 8.72 (1H, s, =CH–). IR ν_{max}cm^{-1}: 1695, 1641, 1619. $[\alpha]_D^{32}$ +111.5° (c=0.3, chloroform). MS *m/z*: 387 (M^+).

(−)-10-Butyl-7-methyl-3-(*S*)-α-methylbenzyl-5-deazaflavin (**7b**): mp 84—87 °C. ^{1}H-NMR and IR: the same as those of **7a**. $[\alpha]_D^{34}$ −117.4° (c=0.4, chloroform). MS *m/z*: 387 (M^+). *Anal.* Calcd for $C_{24}H_{25}N_3O_2$: C, 74.39; H, 6.50; N, 10.84. Found: C, 74.21; H, 6.71; N, 10.55.

(+)-8,9-Benzo-10-butyl-3-(*R*)-α-methylbenzyl-5-deazaflavin (IUPAC: 12-Butyl-3-(*R*)-α-methylbenzyl-benzo[*h*]pyrimido[4,5-*b*]quinoline-8,10(9*H*, 12*H*)-dione) (**8a**): mp 203 °C, ^{1}H-NMR (200 MHz, $CDCl_3$) δ: 0.97 (3H, t, J=7.2, CH_3), 1.42 (2H, sextet, J=7.2, CH_2), 1.82 (2H, quintet, J=7.2, CH_2), 1.96 (3H, d, J=7.5, CH_3), 4.92 (2H, br t, J=7.2, CH_2), 6.43 (1H, q, J=7.5, CH), 7.20—8.02 (10H, m, Ar), 8.47 (1H, d, J=8, Ar), 8.79 (1H, s, =CH–). IR ν_{max}cm^{-1}: 1693, 1638, 1599. $[\alpha]_D^{25}$ +205.6° (c=0.2, chloroform). MS *m/z*: 423 (M^+). *Anal.* Calcd for $C_{27}H_{25}N_3O_2$: C, 76.56; H, 5.95; N, 9.92. Found: C, 73.02; H, 5.70; N, 9.53.

1,5-Dihydro-5-deazaflavin Derivatives (9a, b and 10a, b): General Procedure——a) A large excess (3—4 eq) of sodium borohydride was added portionwise to a stirred solution of the optically active 5-deazaflavin derivative (**6a, b** or **7a, b**) (1 mmol) in 10 ml of a mixture of methanol and water (10:1) at 0 °C. The mixture was stirred for several minutes at the same temperature under an atmosphere of argon and then poured into an ice-cold aqueous solution of sodium sulfite. Extraction of the mixture with degassed methylene chloride and evaporation of the methylene chloride *in vacuo* under an atmosphere of argon in the dark afforded the 1,5-dihydro-5-deazaflavin quantitatively as a pale-yellow residue. In most cases, this sample was used directly for the asymmetric reduction without further purification due to the ready formation of oxidized 5-deazaflavins. In the cases of **9a, b**, a pure sample was obtained from the residue by careful and quick purification.

(+)-10-Butyl-3-(*R*)-α-methylbenzyl-1,5-dihydro-5-deazaflavin (**9a**): mp 83—84 °C (from ether–hexane). ^{1}H-

NMR (200 MHz, $CDCl_3$) δ: 0.87 (3H, t, $J=8$, CH_3), 1.90 (3H, d, $J=7$, CH_3), 3.66 (2H, m, CH_2), 3.77 (2H, s, CH_2), 6.34 (1H, q, $J=7$, CH), 6.82—7.42 (9H, m, Ar). IR ν_{max} cm^{-1}: 3430, 1690, 1620. MS *m/z*: 375 (M^+). $[\alpha]_D^{25}+125°$ ($c=1.0$, ethanol).

(−)-10-Butyl-3-(*S*)-α-methylbenzyl-1,5-dihydro-5-deazaflavin (**9b**): mp 85 °C. ^{1}H-NMR and IR: the same as those of **9a**. MS *m/z*: 375 (M^+). $[\alpha]_D^{25}-127°$ ($c=2.0$, ethanol).

b) A mixture of optically active 5-deazaflavin (1 mmol) (**6a, b**), sodium dithionite (870 mg, 5 mmol) and 10% aqueous ammonia (5 ml) was heated on a water bath for 1 h. After cooling, the mixture was worked up in the same way as described in procedure a) to give the corresponding 1,5-dihydro-5-deazaflavin (**9a** or **9b**) in quantitative yield.

Asymmetric Reduction of Ethyl Benzoylformate with 1,5-Dihydro-5-deazaflavin Derivatives (9a, b and 10b): General Procedure——a) Ethyl benzoylformate, magnesium perchlorate and the above-mentioned residue of 1,5-dihydro-5-deazaflavin (**9a, b** or **10b**), each 1 mmol, were added to a mixture of acetonitrile and acetic acid (1 : 1). The reaction mixture was stirred at room temperature under an atmosphere of argon in the dark. The progress of the reaction was monitored by TLC or HPLC (μ-Porasil, hexane–ethyl acetate (8 : 1), UV 254 nm). After 7 d, the mixture was poured into ice-water and extracted with chloroform. The chloroform extract was washed with water, dried over magnesium sulfate and then evaporated to give a residue, which was subjected to p-TLC on silica gel with hexane–ethyl acetate (6 : 1). This separation procedure gave recovered ethyl benzoylformate, ethyl mandelate and 5-deazaflavin. Quantitative analysis of the residue by HPLC always showed a higher yield of ethyl mandelate than the isolated one. The optical purity of the resulting ethyl mandelate was determined by comparison of its value of specific rotation with the reported one[18] (see also Table II).

b) Asymmetric reduction of ethyl benzoylformate in the presence of metal catalysts other than magnesium perchlorate was undertaken in the same manner as described for procedure a) except that the solvent used was methylene chloride in place of acetonitrile–acetic acid, and the reaction was terminated when most of the 1,5-dihydro-5-deazaflavin derivatives had disappeared on the TLC plates (see also Table III).

Acknowledgment This work was supported in part by a Grant-in-Aid for Scientific Research from the Ministry of Education, Science and Culture, Japan.

References and Notes

1) A preliminary communication of a part of this work has appeared in *Tetrahedron Lett.*, **25**, 1741 (1984).
2) D. E. O'Brien, L. T. Weinstock and C. C. Cheng, *J. Heterocycl. Chem.*, **7**, 99 (1970).
3) *a*) P. Hemmerich, V. Massey and H. Fenner, *FEBS Lett.*, **84**, 5 (1977); *b*) H.-J. Duchstein, H. Fenner, P. Hemmerich and W. R. Knappe, *Eur. J. Biochem.*, **95**, 167 (1979).
4) F. Yoneda, Y. Sakuma and P. Hemmerich, *J. Chem. Soc., Chem. Commun.*, **1979**, 825.
5) D. Eirich, G. D. Vogels and R. S. Wolfe, *Biochemistry*, **17**, 4583 (1978).
6) A. P. M. Eker, R. H. Dekker, R. H. Berends and W. Berends, *Photochem. Photobiol.*, **33**, 65 (1981).
7) *a*) F. Yoneda, *Yakugaku Zasshi*, **104**, 99 (1984); *b*) K. Tanaka, M. Kawase, M. Okuno, M. Senda, T. Kimachi and F. Yoneda, *Chem. Pharm. Bull.*, **34**, 2265 (1986); *c*) F. Yoneda and K. Tanaka, *Medicinal Research Reviews*, **7**, (1987), in press.
8) R. H. Abeles, R. F. Hutton and F. H. Westheimer, *J. Am. Chem. Soc.*, **79**, 712 (1957).
9) *a*) R. J. Kill and D. A. Widdowson, "Bioorganic Chemistry," Vol. 4, ed. by E. E. van Tamelen, Academic Press, New York, 1982, pp. 239—275; *b*) E. M. Kosower, *ibid.*, Vol. 4, 1982, pp. 293—301; *c*) D. S. Sigman, J. Hajdu and D. J. Creighton, *ibid.*, Vol. 4, 1982, pp. 385—407.
10) *a*) H. B. Kagan and J. C. Fiand, "Topics in Stereochemistry," Vol. 10, ed. by E. L. Eliel and N. L. Allinger, Wiley-Interscience, New York, 1978, pp. 175—285; *b*) K. Drauz, A. Kleeman and J. Martens, *Angew. Chem. Int. Ed. Engl.*, **21**, 584 (1982); *c*) J. W. ApSimon and R. P. Seguin, *Tetrahedron*, **35**, 2797 (1979).
11) A. Ohno, M. Ikeguchi, T. Kimura and S. Oka, *J. Am. Chem. Soc.*, **101**, 7036 (1979).
12) *a*) M. Amano, N. Baba, J. Oda and Y. Inouye, *Bioorganic Chem.*, **12**, 299 (1984); *b*) A. Ohno, M. Kashiwagi and Y. Ishihara, *Tetrahedron*, **42**, 961 (1986).
13) F. Yoneda, Y. Sakuma and Y. Nitta, *Chem. Lett.*, **1978**, 1177.
14) *a*) S. Shinkai, H. Nakao, T. Tsuno, O. Manabe and A. Ohno, *J. Chem. Soc., Chem. Commun.*, **1984**, 849; *b*) S. Shinkai, H. Nakao and O. Manabe, *Tetrahedron Lett.*, **26**, 5183 (1985); *c*) S. Shinkai, T. Yamaguchi, H. Nakao and O. Manabe, *ibid.*, **27**, 1611 (1986).
15) F. Yoneda, K. Kuroda and M. Kamishimoto, *J. Chem. Soc., Chem. Commun.*, **1981**, 1160.
16) T. L. Davis and K. C. Blanchard, *J. Am. Chem. Soc.*, **51**, 1790 (1929).
17) F. Yoneda, Y. Sakuma, S. Mizumoto and R. Ito, *J. Chem. Soc., Perkin Trans. 1*, **1976**, 1805.
18) R. Roger, *J. Chem. Soc.*, **1932**, 2168.
19) F. Yoneda, "Methods in Enzymology," Vol. 66, ed. by D. B. McCormick and L. D. Wright, Academic Press, New York, 1980, pp. 267—277.
20) S. Fukuzumi, S. Kuroda and T. Tanaka, *Chem. Lett.*, **1984**, 417.
21) *Cf.* R. M. Kellogg, *Angew. Chem. Int. Ed. Engl.*, **23**, 782 (1984).

[Chem. Pharm. Bull. 35(4)1405—1412(1987)]

An Efficient, Regiospecific Synthesis of 4-Demethoxydaunomycinone and Daunomycinone

YASUMITSU TAMURA,* MANABU SASHO, SHUJI AKAI, HISAKAZU KISHIMOTO, JUN-ICHI SEKIHACHI, and YASUYUKI KITA

Faculty of Pharmaceutical Sciences, Osaka University, 1-6, Yamada-oka, Suita, Osaka 565, Japan

(Received September 25, 1986)

4-Methoxy and 4-acetoxyhomophthalic anhydrides were prepared by convenient oxidations of homophthalic acid derivatives followed by hydrolysis and dehydrative cyclization. Strong base-induced cycloaddition of these anhydrides to 2-chloro-6,6-ethylenedioxy-5,6,7,8-tetrahydro-1,4-naphthoquinone gave the tetracyclic adducts, which were efficiently converted into 4-demethoxydaunomycinone and daunomycinone.

Keywords——anthracyclinone; 4-demethoxydaunomycinone; daunomycinone; cycloaddition; 4-methoxyhomophthalic anhydride; 4-acetoxyhomophthalic anhydride; ethynylcerium(III) 1,2-addition reagent

The anthracycline antibiotics, daunomycin (**1**), adriamycin (**2**), and 4-demethoxydaunomycin (**3**), are clinically significant drugs for the treatment of a broad spectrum of human cancers.[1] Efficient total synthesis of these anthracyclines, especially regiospecific preparation, has been the subject of intense study[2] due to the lack of an efficient biosynthetic process as well as the search for more active analogs with reduced cardiotoxicity. We have reported[3] a regiocontrolled synthesis of the late-stage intermediates (**7** and **8**) to the anthracyclinones (**4**—**6**) using a strong base-induced cycloaddition of homophthalic anhydrides to 2-chloro-6,6-ethylenedioxy-5,6,7,8-tetrahydro-1,4-naphthoquinone as shown in Chart 1. Although this method is useful for the small-scale preparation of **7** and **8**, the oxidation step of the cycloadducts (**9** and **10**) to the *para*-acetoxylated products (**11** and **12**) with lead tetraacetate (LTA)/acetic acid–methylene chloride remains to be investigated since the yields are quite variable (25—79%) depending on the reaction conditions, especially the purity of the reagent itself, the reaction temperature, and the scale of the reaction. We have previously communicated[4] a greatly improved synthesis of **7** and **8** by using the previously C_4-acetoxylated homophthalic anhydrides (**14** and **15**) and an efficient conversion of **7** and **8** into **4** and **5**. We present here a full account of the work as well as a demonstration of the synthetic utility of C_4-oxygenated homophthalic anhydrides (**13**—**15**) for the preparation of key intermediates (**7** and **8**).

Results and Discussion

The requisite starting materials, 4-methoxy- (**13**) and 4-acetoxyhomophthalic anhydrides (**14** and **15**) were unknown in the literature. Since 2′-oxygenated homophthalic acids seemed to be favorable starting materials for **13**—**15**, we first tried the introduction of some oxygen functions at the C_2-position of dimethyl homophthalate followed by hydrolysis of the esters. Dimethyl homophthalate was converted into the ketene silyl acetal intermediate (i) with

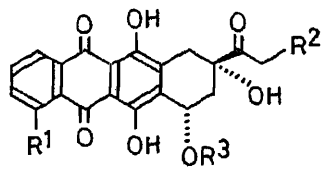

1 : R^1=OMe, R^2=H, R^3=daunosaminyl
2 : R^1=OMe, R^2=OH, R^3=daunosaminyl
3 : R^1=R^2=H, R^3=daunosaminyl
4 : R^1=R^2=R^3=H
5 : R^1=OMe, R^2=R^3=H
6 : R^1=OMe, R^2=OH, R^3=H

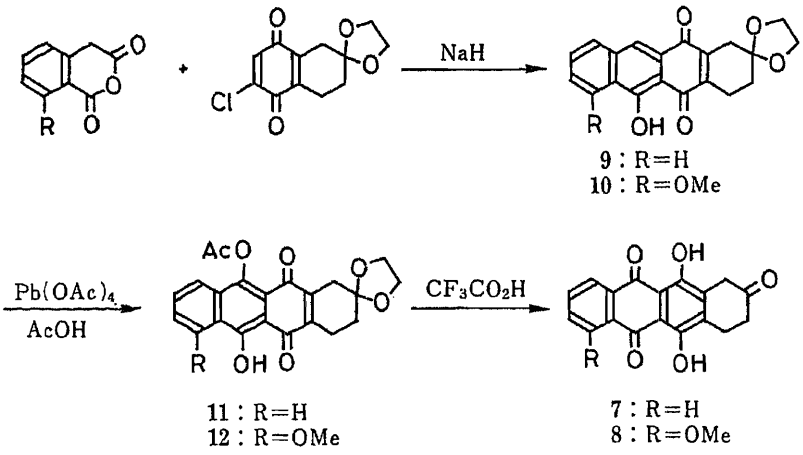

9 : R=H
10 : R=OMe

11 : R=H
12 : R=OMe

7 : R=H
8 : R=OMe

Chart 1

lithium diisopropylamide (LDA)/trimethylsilyl chloride, and (i) was oxidized with LTA[5] or *m*-chloroperbenzoic acid (*m*-CPBA)[6] to give dimethyl 2′-acetoxy- (**16**) or 2′-hydroxyhomophthalate (**17**) in 83% or 44% yield, respectively. 2′-Methoxylation was accomplished by the treatment of dimethyl homophthalate with $PhI(OAc)_2$ [phenyl iodosyl diacetate, PIDA] in methanolic sodium methoxide to give a 50% yield of dimethyl 2′-methoxyhomophthalate (**18**).[7] Although hydrolysis of the ester (**18**) gave the desired 2′-methoxyhomophthalic acid (**19**), other esters (**16** and **17**) gave an unwanted product, phthalide-3-carboxylic acid (**20**) selectively on alkaline hydrolysis followed by careful acidification. After several unsuccessful attempts,[8] the 2′-acetoxyhomophthalic acids (**21** and **22**) were successfully obtained from the homophthalic acids themselves by the most straightforward method: the homophthalic acids were treated with 3.2 eq of LDA in tetrahydrofuran (THF) and quenched with trimethylsilyl chloride to give the ketene silyl acetal intermediates (ii), which were oxidized with LTA in benzene to give quantitatively the corresponding 2′-acetoxyhomophthalic acids. These acids (**19**, **21**, and **22**) were treated with 1.3 eq of trimethylsilylethoxyacetylene[9] in methylene chloride to give, in quantitative yields, the 4-methoxy-(**13**) and 4-acetoxyhomophthalic anhydrides (**14** and **15**), respectively.

Conversion of the anhydrides (**13**—**15**) to the tetracyclic adducts (**23**—**25**) was carried out by our strong base-induced cycloaddition method.[3] Treatment of the sodium salts generated from these anhydrides and 1.0—1.1 eq of NaH in THF with 2-chloro-6,6-ethylenedioxy-5,6,7,8-tetrahydro-1,4-naphthoquinone at room temperature gave the regiospecific naphthacenediones (**23**—**25**) in 65%, 72%, and 62% yields, respectively. The latter two adducts (**24** and **25**) were identical with authentic samples prepared earlier by us [3b] and were readily hydrolyzed quantitatively to **7** and **8** with 80% trifluoroacetic acid. The former adduct was assigned as **23** on the basis of spectral evidence and the following chemical

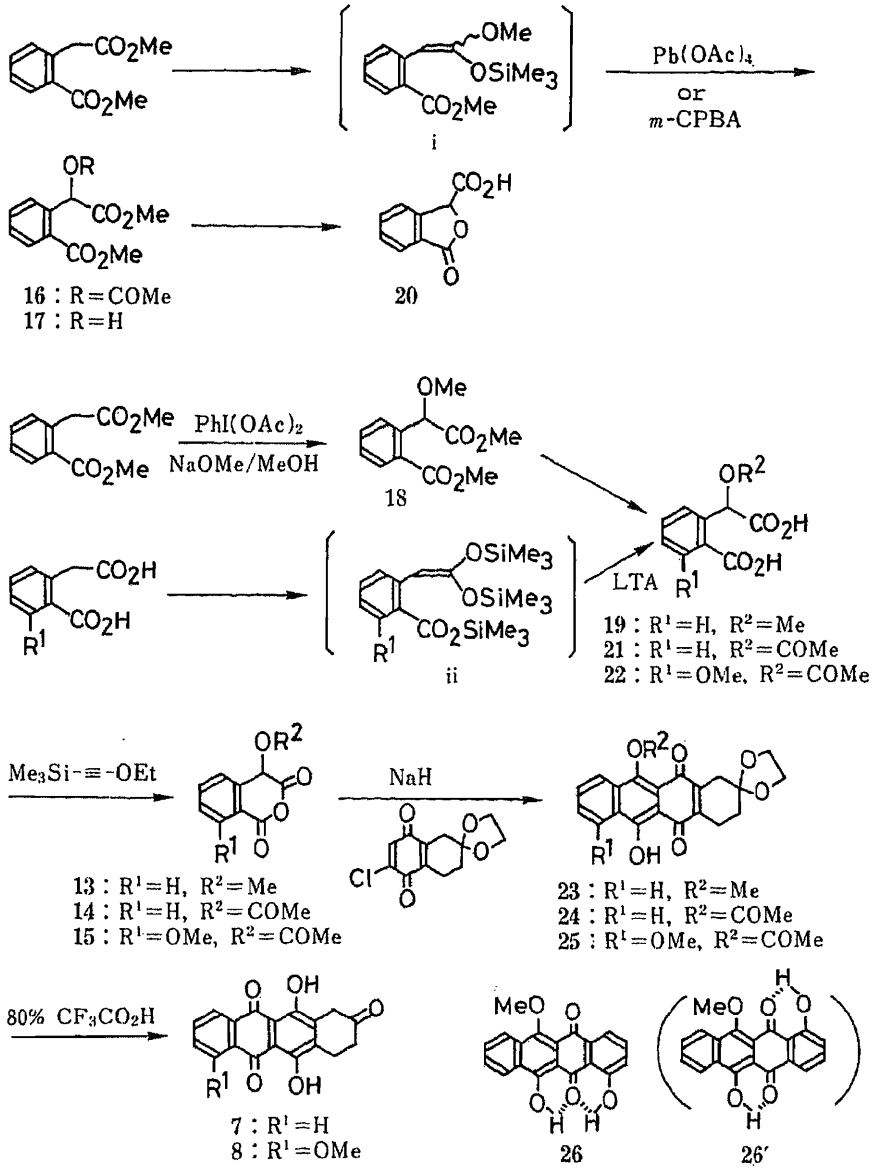

Chart 2

behavior: hydrolysis of **23** with 80% trifluoroacetic acid gave a quantitative yield of **7** and the regiochemistry of the cycloaddition of 4-methoxyhomophthalic anhydride (**13**) was shown to have the same orientation as that of the 4-acetoxyhomophthalic anhydrides (**14** and **15**) in the reaction with 3-bromo-5-hydroxy-1,4-naphthoquinone, giving the single adduct (**26**) [not the regioisomer **26'**].[10] As shown above, the use of C_4-acetoxyhomophthalic anhydrides (**14** and **15**) instead of homophthalic anhydrides was found to be the best method for the preparation of **7** and **8**.

As for the side-chain elaboration of the 9-keto group of these tetracyclic ketones (**7** and **8**), there remains the need for some improvements since the reported side-chain elaboration of the 9-keto group by using ethynylmagnesium bromide gives inadequate yields.[11] All other existing methodologies for the homologation of **7** and **8** using acyl anion equivalents were tried but did not give satisfactory results, probably due to the ready base-catalyzed enolization of the 9-keto group. Recently, we have found[12] that trimethylsilylethynylcerium (III) reagent is quite useful for the conversion of an enolizable ketone into a hydroxyacetone moiety and we

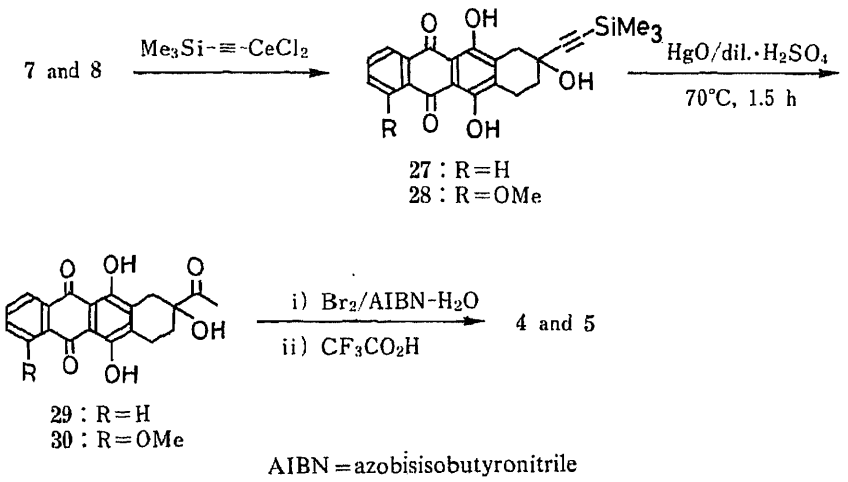

Chart 3

successfully applied this method for the conversion of **7** and **8** to the 9-hydroxyacetone compounds.[13,14] Trimethylsilylethynylation of the tetracyclic ketones (**7** and **8**) with 20 eq of trimethylsilylethynylcerium (III) chloride [prepared from trimethylsilylethynyllithium and cerium (III) chloride in THF] at −78 °C for 3 h gave the 9-trimethylsilylethynyl alcohols (**27** and **28**) in 77% and 69% yields, respectively. Direct transformation of a 2-trimethylsilylethynyl group into a methyl ketone was readily accomplished by a standard method using mercury (II) ion: treatment of the trimethylsilylethynyl alcohols (**27** and **28**) with HgO/dil. H_2SO_4 in refluxing THF gave the 9-hydroxyacetone compounds (**29** and **30**) in 87% and 86% yields, respectively. As conversion of **29** or **30** into **4** or **5** by convenient methods has already been described,[11,15] our approach constitutes a highly convergent synthesis of **4** and **5**.

Experimental

All melting points are uncorrected. Infrared (IR) absorption spectra were recorded on a JASCO HPIR-102 spectrometer and proton nuclear magnetic resonance (^{1}H-NMR) spectra on a Hitachi R-20A (60 MHz), a Hitachi R-22 (90 MHz), or a JEOL JNM-FX 90Q (90 MHz) spectrometer (with tetramethylsilane as an internal standard). Low- and high-resolution mass spectra (MS) were obtained with a JEOL JMS D-300 instrument, with a direct inlet system at 70 eV. Column chromatography was carried out on Merck Silica gel 60.

Methyl 2-Acetoxy-2-(2-methoxycarbonylphenyl)acetate (16)——A solution of *n*-BuLi (1.6 N, 0.75 ml, 1.2 mmol) was added dropwise under nitrogen to a stirred solution of dry diisopropylamine (0.17 ml, 1.2 mmol) in anhydrous THF (3 ml) at 0 °C. The mixture was stirred for a few minutes under the same conditions and then used as a THF solution of LDA. A solution of dimethyl homophthalate (208 mg, 1.0 mmol) in anhydrous THF (3 ml) was added dropwise to the solution of LDA over a few minutes at −78 °C and Me_3SiCl (0.25 ml, 2.0 mmol) was added to the mixture. The whole was stirred at −78 °C for 2 h, allowed to warm to room temperature, and stirred for 30 min. The reaction mixture was concentrated under reduced pressure and pentane (6 ml) was added to the residue. The mixture was filtered rapidly and the filtrate was concentrated *in vacuo* to give the ketene silyl acetal intermediate (i) (282 mg, approximately 100%), which was used in the next oxidation reaction without purification. A solution of the ketene silyl acetal (i) (140 mg, approximately 0.5 mmol) in dry benzene (2 ml) was added to a stirred suspension of LTA (247 mg, 0.5 mmol) in dry benzene (3 ml) at room temperature under nitrogen. The resulting slurry was stirred for 2 h under the same conditions and filtered to remove lead (II) acetate. The filtrate was poured into 5% HCl (15 ml), and extracted with ether (15 ml × 2). The extract was washed with brine, dried over $MgSO_4$, and concentrated *in vacuo* to give a residue, which was subjected to column chromatography on silica gel with hexane : ethyl acetate = 5 : 1 as the eluting solvent to give an 83% yield of **16** (110 mg): colorless oil. IR $\nu_{max}^{CHCl_3}$ cm^{-1}: 1750, 1720. ^{1}H-NMR (10% solution in $CDCl_3$) δ: 2.17 (s, 3H, OCOMe), 3.72 (s, 3H, CO_2Me), 3.91 (s, 3H, CO_2Me), 7.07 (s, 1H, $-CHCO_2Me$), 7.5—7.55 (m, 3H, ArH), 7.9—7.95 (m, 1H, ArH). *Anal.* Calcd for $C_{13}H_{14}O_6$: C, 58.64; H, 5.30. Found: C, 58.81; H, 5.04.

Methyl 2-Hydroxy-2-(2-methoxycarbonylphenyl)acetate (17)——A solution of the ketene silyl acetal (i) (840 mg, approximately 3 mmol), prepared by the procedure described above, in dry hexane (10 ml) was added to a stirred suspension of *m*-CPBA (80%, 647 mg, 3.0 mmol) in dry hexane (10 ml) at 0 °C under nitrogen. The resulting slurry was stirred at room temperature for 30 min and filtered. The filtrate was worked up in the same manner as described

for the preparation of **16** to give a 44% yield of **17** (296 mg): colorless oil. IR $\nu_{max}^{CHCl_3}$ cm^{-1}: 3300, 1725. ^{1}H-NMR (10% solution in $CDCl_3$) δ: 3.48 (s, 3H, CO_2Me), 3.71 (s, 3H, CO_2Me), 5.97 (s, 1H, C<u>H</u>CO_2Me), 7.1—7.8 (m, 4H, ArH). The 2-hydroxy ester (**17**) was acetylated with Ac_2O–pyridine to give the acetate (**16**), which was identical with a sample obtained from dimethyl homophthalate.

Methyl 2-Methoxy-2-(2-methoxycarbonylphenyl)acetate (18)——Dimethyl homophthalate (208 mg, 1.0 mmol) was added to a stirred solution of Na (76 mg, 3.3 mmol) in dry MeOH (3 ml) at room temperature under nitrogen. The mixture was stirred for a few minutes under the same conditions and $C_6H_5I(OAc)_2$ (483 mg, 1.5 mmol) was added. The resulting slurry was stirred at room temperature for 4 d, poured into 10% hydrochloric acid, made neutral, and extracted with CH_2Cl_2 (10 ml × 3). The extract was washed with brine, dried over Na_2SO_4, and concentrated *in vacuo*. The residue was subjected to column chromatography on silica gel with hexane : ethyl acetate = 10 : 1 as the eluting solvent to give a 50% yield of **18** (118 mg): colorless oil. IR $\nu_{max}^{CHCl_3}$ cm^{-1}: 3020, 2950, 2830, 1740, 1720, 1600, 1580. ^{1}H-NMR (10% solution in $CDCl_3$) δ: 3.47 (s, 3H, OMe), 3.70 (s, 3H, CO_2Me), 3.90 (s, 3H, CO_2Me), 5.80 (s, 1H, –C<u>H</u>CO_2Me), 7.3—7.6 (m, 3H, ArH) 7.8—8.0 (m, 1H, ArH). Exact MS Calcd for $C_{12}H_{14}O_5$: 238.0841. Found: 238.0846.

2-Methoxy-2-(2-carboxyphenyl)acetic Acid (19)——A solution of **18** (150 mg, 0.63 mmol) in 7% aqueous KOH (4 ml) and MeOH (2 ml) was heated at reflux for 3 h. The mixture was concentrated *in vacuo* and partitioned between ether (15 ml) and water (5 ml). The solution was adjusted to pH 1 by addition of conc. HCl and extracted with ether. The aqueous layer was saturated with NaCl and extracted with ether (30 ml × 3). The combined extract was washed with brine, dried over $MgSO_4$, and concentrated *in vacuo* to give an 89% yield of **19** (117 mg). Recrystallization from ethyl acetate gave a pure sample as colorless crystals; mp 148—149 °C. *Anal.* Calcd for $C_{10}H_{10}O_5$: C, 57.14; H, 4.80. Found: C, 56.95; H, 4.75.

3-Phthalidecarboxylic Acid (20)——1) From **16**: A solution of **16** (180 mg, 0.68 mmol) in 30% aqueous NaOH (3 ml) and MeOH (3 ml) was heated at reflux for 2 h. The reaction mixture was worked up as described for the preparation of **19** to give a quantitative yield (120 mg) of **20**. Recrystallization from ethyl acetate gave a pure sample: mp 151—153 °C (lit.[16] 149—150 °C). IR ν_{max}^{KCl} cm^{-1}: 2850, 1770, 1710. ^{1}H-NMR (acetone-d_6) δ: 6.11 (s, 1H, CH), 7.75—7.85 (m, 4H, ArH).

2) From **17**: The ester (**17**) (152 mg, 0.68 mmol) was treated with 30% aqueous NaOH under the conditions described above (1) to give a 96% yield (115 mg) of **20**, which was identical with an authentic sample obtained from **16**.

2-Acetoxy-2-(2-carboxyphenyl)acetic Acid (21)——A solution of homophthalic acid (180 mg, 1.0 mmol) in dry THF (3 ml) was added dropwise to a solution of LDA (3.2 mmol) in THF over a few minutes at −78 °C under nitrogen and the mixture was stirred for 30 min under the same conditions. After addition of Me_3SiCl (0.75 ml, 5.9 mmol), the reaction mixture was stirred at −78 °C for 1.5 h, allowed to warm to room temperature, and stirred for an additional 30 min. Work-up in the same manner as described for the preparation of **16** gave the ketene silyl acetal intermediate (ii), which was used in the next oxidation reaction without purification. A solution of the ketene silyl acetal (ii) in dry benzene (4 ml) was added to a stirred suspension of LTA (550 mg, 1.12 mmol) in dry benzene (3 ml) at room temperature under nitrogen. The resulting slurry was worked up in the same manner as described for the preparation of **16** to give a quantitative yield (238 mg) of **21**. Recrystallization from ethyl acetate–hexane gave a pure sample; mp 148—150 °C. IR ν_{max}^{KCl} cm^{-1}: 3070 sh, 3020 sh, 2920, 2850, 2630, 1755, 1720, 1675, 1600, 1580. ^{1}H-NMR (acetone-d_6) δ: 2.12 (s, 3H, OCOMe), 6.80 (br s, 2H, CO_2H × 2), 7.18 (s, 1H, –C<u>H</u>CO_2H), 7.2—7.8 (m, 3H, ArH), 7.9—8.15 (m, 1H, ArH). *Anal.* Calcd for $C_{11}H_{10}O_6$: C, 55.46; H, 4.23. Found: C, 55.39; H, 4.29.

2-Acetoxy-2-(2-carboxy-3-methoxyphenyl)acetic Acid (22)——According to the same procedure as described for the preparation of **21**, a 97% yield (261 mg) of **22** was obtained from 2-carboxy-3-methoxyphenylacetic acid (210 mg, 1.0 mmol). The product was used in the next reaction without purification: colorless syrup. IR $\nu_{max}^{CHCl_3}$ cm^{-1}: 3300—2800, 1760—1710. ^{1}H-NMR (acetone-d_6) δ: 2.09 (s, 3H, OCOMe), 3.87 (s, 3H, OMe), 6.21 (s, 1H, –C<u>H</u>CO_2H), 6.30 (br s, 2H, CO_2H × 2), 6.95—7.55 (m, 3H, ArH). Exact MS Calcd for $C_{12}H_{12}O_7$: 268.0580. Found: 268.0574.

4-Methoxyhomophthalic Anhydride (13)——A solution of **19** (115 mg, 0.55 mmol) and trimethylsilylethoxyacetylene (116 mg, 0.82 mmol) in dry CH_2Cl_2 (2 ml) was stirred at 40 °C for 3.5 h. After removal of insoluble material by filtration, the filtrate was concentrated *in vacuo* to give a 92% yield (97 mg) of **13**. Recrystallization from CH_2Cl_2–hexane gave a pure sample as colorless crystals; mp 122—125 °C. IR $\nu_{max}^{CHCl_3}$ cm^{-1}: 1805, 1765, 1605. ^{1}H-NMR (10% solution in $CDCl_3$) δ: 3.76 (s, 3H, OMe), 5.17 (s, 1H, CH), 7.5—7.85 (m, 3H, ArH), 8.05—8.25 (s, 1H, ArH). *Anal.* Calcd for $C_{10}H_8O_4 \cdot H_2O$; C, 57.14; H, 4.80. Found: C, 57.17; H, 4.78.

4-Acetoxyhomophthalic Anhydride (14)——A solution of **21** (80 mg, 0.34 mmol) and trimethylsilylethoxyacetylene (65 mg, 0.46 mmol) in dry CH_2Cl_2 (1.5 ml) was stirred at room temperature for 4 h. Concentration of the reaction mixture *in vacuo* gave a quantitative yield (74 mg) of **14**: colorless oil. IR $\nu_{max}^{CHCl_3}$ cm^{-1}: 1805, 1765, 1600. ^{1}H-NMR (10% solution in $CDCl_3$) δ: 2.31 (s, 3H, OCOMe), 6.53 (s, 1H, CH), 7.3—7.9 (m, 3H, ArH), 8.05—8.3 (m, 1H, ArH), MS *m/z*: 220 (M^+). Exact MS Calcd for $C_{11}H_8O_5$: 220.0369. Found: 220.0351.

4-Acetoxy-8-methoxyhomophthalic Anhydride (15)——A solution of **22** (80 mg, 0.30 mmol) and trimethylsilylethoxyacetylene (65 mg, 0.46 mmol) in dry CH_2Cl_2 (1.5 ml) was stirred at room temperature for 4 h. Concentration of the reaction mixture *in vacuo* gave a quantitative yield (74 mg) of **15**. Recrystallization from benzene–hexane gave a

pure sample: mp 162—164 °C. IR $\nu_{max}^{CHCl_3}$ cm^{-1}: 1815, 1765, 1600. ^{1}H-NMR (10% solution in $CDCl_3$) δ: 2.32 (s, 3H, OCOMe), 4.00 (s, 3H, OMe), 6.51 (s, 1H, CH), 6.9—7.2 (m, 2H, ArH), 7.70 (t, 1H, J=7.5 Hz, ArH), MS m/z: 250 (M^+). *Anal.* Calcd for $C_{12}H_{10}O_6$: C, 57.60; H, 4.03. Found: C, 57.27; H, 4.01.

General Procedure for the Cycloaddition of Homophthalic Anhydrides (13—15) to 2-Chloro-6,6-ethylenedioxy-5,6,7,8-tetrahydro-1,4-naphthoquinone Leading to Cycloadducts (23—25)——A mixture of the anhydride (0.5 mmol) and NaH (60% in mineral oil, 0.55 mmol) in anhydrous THF (2 ml) was stirred at room temperature for several minutes under nitrogen, then a solution of the quinone (0.5 mmol) in anhydrous THF (4 ml) was added. The reaction mixture was stirred at room temperature for a suitable period (checked by thin layer chromatography (TLC)), then quenched with saturated aqueous NH_4Cl (20 ml) and extracted with CH_2Cl_2 (20 ml × 3). The extract was washed with brine, dried over Na_2SO_4, and concentrated *in vacuo*. The residue was subjected to column chromatography on silica gel with $CHCl_3$: ether = 30 : 1 as the eluting solvent to give the corresponding adduct.

2,2-Ethylenedioxy-6-hydroxy-11-methoxy-1,2,3,4-tetrahydronaphthacene-5,12-dione (23)——This was prepared from **13** (45 mg, 0.23 mmol) and 2-chloro-6,6-ethylenedioxy-5,6,7,8-tetrahydro-1,4-naphthoquinone (59 mg, 0.23 mmol) at room temperature for 3 h in a 65% yield (55 mg). Recrystallization from benzene gave a pure sample: mp 238—240 °C. IR $\nu_{max}^{CHCl_3}$ cm^{-1}: 2925, 2875, 2850 sh, 1650 sh, 1645 sh, 1635, 1600, 1575. ^{1}H-NMR (10% solution in $CDCl_3$) δ: 1.91 (t, 2H, J=7 Hz, CH_2), 2.7—3.1 (m, 4H, CH_2 × 2), 4.00 (s, 4H, OCH_2CH_2O), 4.05 (s, 3H OMe), 7.6—7.9 (m, 2H, ArH), 8.2—8.6 (m, 2H, ArH), 14.80 (s, 1H, OH). *Anal.* Calcd for $C_{21}H_{18}O_6$: C, 68.84; H, 4.95. Found: C, 68.94; H, 4.80.

11-Acetoxy-2,2-ethylenedioxy-6-hydroxy-1,2,3,4-tetrahydronaphthacene-5,12-dione (24)——This was prepared from **14** (74 mg, 0.34 mmol) and 2-chloro-6,6-ethylenedioxy-5,6,7,8-tetrahydro-1,4-naphthoquinone (86 mg, 0.34 mmol) at room temperature for 18 h in a 75% yield (99 mg). Recrystallization from CH_2Cl_2–MeOH gave a pure sample: mp 225—228 °C (lit.[3b] 215—217 °C). This was identical with an authentic sample.

11-Acetoxy-2,2-ethylenedioxy-6-hydroxy-7-methoxy-1,2,3,4-tetrahydronaphthacene-5,12-dione (25)——This was prepared from **15** (86 mg, 0.34 mmol) and 2-chloro-6,6-ethylenedioxy-5,6,7,8-tetrahydro-1,4-naphthoquinone (87 mg, 0.34 mmol) at room temperature for 15 h in a 62% yield (90 mg). Recrystallization from CH_2Cl_2–EtOH gave a pure sample: mp 244.5—246 °C (lit.[3b] 244.5—246 °C). This was identical with an authentic sample.

1,11-Dihydroxy-6-methoxynaphthacene-5,12-dione (26)——A solution of 3-bromo-5-hydroxy-1,4-naphthoquinone (16 mg, 0.06 mmol) in anhydrous THF (1 ml) was added to a stirred suspension of **13** (13 mg, 0.07 mmol) and NaH (60% in mineral oil, 8 mg, 0.20 mmol) in anhydrous THF (2 ml) at room temperature under nitrogen. The reaction mixture was stirred for 2 h under the same conditions, then quenched with saturated aqueous NH_4Cl (10 ml). The aqueous layer was adjusted to pH 2 by addition of 1 N HCl and extracted with CH_2Cl_2 (15 ml × 3). The extract was washed with brine, dried over $MgSO_4$, and concentrated *in vacuo*. The residue was subjected to preparative TLC on silica gel with benzene : hexane = 4 : 1 as the developing solvent to give a 77% yield (16 mg) of **26**. Recrystallization from benzene gave a pure sample: mp 234—236 °C. IR $\nu_{max}^{CHCl_3}$ cm^{-1}: 1660, 1620, 1600, 1580. ^{1}H-NMR (10% solution in $CDCl_3$) δ: 4.07 (s, 3H, OMe), 7.25 (dd, 1H, J=8, 1.5 Hz, ArH), 7.55—8.0 (m, 4H, ArH), 8.3—8.6 (m, 2H, ArH), 12.22 (s, 1H, OH), 14.40 (s, 1H, OH). Exact MS Calcd for $C_{19}H_{12}O_5$: 320.0683. Found: 320.0665.

6,11-Dihydroxy-7,8-dihydronaphthacene-5,9(10*H*),12-trione (7)——1) From **23**: A solution of **23** (20 mg, 0.055 mmol) in CF_3CO_2H (4 ml) and water (1 ml) was heated at 50 °C for 2 h, then concentrated *in vacuo*, and the residue was partitioned between CH_2Cl_2 (10 ml) and water. The aqueous layer was extracted with CH_2Cl_2 (20 ml × 2). The combined extract was washed with brine, dried over Na_2SO_4, and concentrated *in vacuo*. The residue was subjected to column chromatography on silica gel with $CHCl_3$: ethyl acetate = 20 : 1 as the eluting solvent to give a quantitative yield (17 mg) of **7**. Recrystallization from CH_2Cl_2–MeOH gave a pure sample: mp over 300 °C, (lit.[3b] 296—298 °C, lit.[17] 300 °C). This was identical with an authentic sample.

2) From **24**: The experimental details were as reported.[3b]

6,11-Dihydroxy-4-methoxy-7,8-dihydronaphthacene-5,9(10*H*),12-trione (8)——The experimental details were as reported.[3b]

6,9,11-Trihydroxy-9-(2-trimethylsilylethynyl)-7,8,9,10-tetrahydronaphthacene-5,12-dione (27)——The $CeCl_3$–Me_3Si–≡–Li reagent system was used with a modification of the reported method.[18] Anhydrous cerium chloride ($CeCl_3$, 370 mg, 1.5 mmol) was placed in a two-necked flask, heated *in vacuo* (0.1 mmHg) at 140 °C for 2 h and then cooled. Dry THF (3 ml) was added under nitrogen, stirring was continued for 1 h, and the flask was cooled to −78 °C. Then lithium trimethylsilylacetylide [prepared from trimethylsilylacetylene (0.21 ml, 1.5 mmol) and *n*-BuLi (1.6 N, 0.61 ml, 0.97 mmol) in dry THF (2 ml) at −40 °C for 30 min] was added to the cooled suspension with stirring. The mixture was stirred at −78 °C for 1 h and then used as a THF solution of trimethylsilylethynylcerium (III) chloride. To this solution was added a solution of **7** (20 mg, 0.065 mmol) in dry THF (3 ml) at −78 °C under nitrogen. The mixture was stirred for 2 h under the same conditions and then quenched with water (15 ml), made acidic by addition of dil. HCl, and extracted with CH_2Cl_2 (30 ml × 2). The extract was washed with brine, dried over $MgSO_4$, and concentrated *in vacuo*. The residue was purified by column chromatography on silica gel with $CHCl_3$: ethyl acetate = 100 : 1 as the eluting solvent to give a 77% yield (21 mg) of **27** as a red solid. Recrystallization from $CHCl_3$–hexane gave a pure sample: mp 193—195 °C (lit.[14b] 190—191 °C). IR $\nu_{max}^{CHCl_3}$ cm^{-1}: 1620, 1590. ^{1}H-NMR (10% solution in $CDCl_3$) δ: 0.17 (s, 9H, $SiMe_3$), 2.12 (br t, 2H, J=6.0 Hz, CH_2), 2.29 (br s, 1H, OH), 2.97 (br t, 2H,

J=6.0 Hz, CH_2), 3.13 (br s, 2H, CH_2), 7.7—7.9 (m, 2H, ArH), 8.2—8.35 (m, 2H, ArH), 13.35 (s, 1H, OH), 13.36 (s, 1H, OH). Exact MS Calcd for $C_{23}H_{22}O_5Si$: 406.1234. Found: 406.1218.

6,9,11-Trihydroxy-4-methoxy-9-(2-trimethylsilylethynyl)-7,8,9,10-tetrahydronaphthacene-5,12-dione (28)——According to the same procedure as described for the preparation of **27**, a 69% yield (19.5 mg) of **28** was obtained from trimethylsilylacetylene (0.21 ml, 1.5 mmol), *n*-BuLi (1.6 N, 0.61 ml, 0.97 mmol), anhydrous $CeCl_3$ (370 mg, 1.5 mmol) and **8** (22 mg, 0.065 mmol) as a red solid. Recrystallization from $CHCl_3$ gave a pure sample: mp 262—264.5 °C. IR $\nu_{max}^{CHCl_3}$ cm^{-1}: 1605, 1580. ^{1}H-NMR (10% solution in $CDCl_3$) δ: 0.19 (s, 9H, $SiMe_3$), 2.0—2.2 (m, 3H, CH_2 and OH), 3.02 (br t, 2H, J=6.0 Hz, CH_2), 3.15 (br s, 2H, CH_2), 4.10 (s, 3H, OMe), 7.37 (dd, 1H, J=8.5, 1.0 Hz, ArH), 7.76 (t, 1H, J=8.5 Hz, ArH), 8.04 (dd, 1H, J=8.5, 1.0 Hz, ArH), 13.48 (s, 1H, OH), 13.85 (s, 1H, OH). Exact MS Calcd for $C_{24}H_{24}O_6Si$: 436.1339. Found: 436.1322.

9-Acetyl-6,9,11-trihydroxy-7,8,9,10-tetrahydronaphthacene-5,12-dione (4-Demethoxy-7-deoxydaunomycinone) (29)——A solution of **27** (13 mg, 0.032 mmol), HgO (21 mg, 0.097 mmol), and 20% H_2SO_4 (0.5 ml) in THF (2 ml) was heated at reflux for 1.5 h and then cooled to room temperature. The reaction mixture was diluted with 0.5% HCl (10 ml) and extracted with CH_2Cl_2 (15 ml × 3). The extract was washed with brine, dried over $MgSO_4$, and concentrated *in vacuo*. The residue was purified by column chromatography on silica gel with $CHCl_3$: ethyl acetate = 50 : 1 as the eluting solvent to give an 87% yield (9.8 mg) of **29** as a red solid. Recrystallization from CH_2Cl_2–*n*-hexane gave a pure sample: mp 211—213.5 °C (lit.[14a] 212.5—214.5 °C, lit.[11b] 160—162 °C, lit.[19a] 210—212 °C, lit.[15a] 216—218 °C, lit.[19b] 210—211 °C, lit.[19c] 202—203 °C, lit.[19d] 214—216 °C, lit.[19e] 213—215 °C). IR $\nu_{max}^{CHCl_3}$ cm^{-1}: 1705, 1615, 1585. ^{1}H-NMR (10% solution in $CDCl_3$) δ: 1.85—2.1 (m, 2H, CH_2), 2.40 (s, 3H, COMe), 2.9—3.15 (m, 4H, CH_2 × 2), 3.79 (s, 1H, OH), 7.75—7.9 (m, 2H, ArH), 8.2—8.45 (m, 2H, ArH), 13.43 (s, 2H, OH × 2). MS *m/z*: 352 (M^+).

9-Acetyl-6,9,11-trihydroxy-4-methoxy-7,8,9,10-tetrahydronaphthacene-5,12-dione (7-Deoxydaunomycinone) (30)——According to the same procedure as described for the preparation of **29**, an 86% yield (6.6 mg) of **30** was obtained from **28** (8.8 mg, 0.02 mmol), HgO (13 mg, 0.06 mmol), and 20% H_2SO_4 (0.3 ml) as a red solid. Recrystallization from ethyl acetate–THF gave a pure sample: mp 229—233.5 °C (lit.[20a] 229—231 °C, lit.[15b] 230—232 °C, lit.[15c] 228—230 °C, lit.[20b] 228—229 °C). IR $\nu_{max}^{CHCl_3}$ cm^{-1}: 1705, 1605, 1580. ^{1}H-NMR (10% solution in $CDCl_3$) δ: 1.85—2.1 (m, 2H, CH_2), 2.38 (s, 3H, COMe), 2.8—3.2 (m, 4H, CH_2 × 2), 3.78 (s, 1H, OH), 4.08 (s, 3H, OMe), 7.36 (br d, 1H, J=8.0 Hz, ArH), 7.74 (t, 1H, J=8.0 Hz, ArH), 8.02 (br d, 1H, J=8.0 Hz, ArH), 13.43 (s, 1H, OH), 13.87 (s, 1H, OH). MS *m/z*: 382 (M^+).

Acknowledgement We thank Mr. Fumio Fukata for technical assistance.

References and Notes

1) F. Arcamone, *Lloydia*, **40**, 45 (1977); *idem*, "Topics in Antibiotic Chemistry," Vol. 2, ed. by P. G. Sammes, Ellis Horwood, Chichester, England, 1978, pp. 99—239; *idem*, "Doxorubicin Anticancer Antibiotics," Academic Press, in Medicinal Chemistry, Vol. 17, New York, 1981, p. 207, 212, 272, 287, 338; M. B. Naff, J. Plowman, and V. L. Narayanan, "Anthracycline Antibiotics," ed. by H. S. ElKhadem, Academic Press, New York, 1982, pp. 1—57; T. Oki and T. Takeuchi, *Yuki Gosei Kagaku Kyokai Shi*, **40**, 2 (1982).
2) T. R. Kelly, *Ann. Rep. Med. Chem.*, **14**, 288 (1979); W. A. Remers, "The Chemistry of Antitumor Antibiotics," Vol. 1, Chapter 2, Wiley-Interscience, Somerset, NJ, 1979, pp. 63—132; S. Terashima, *Yuki Gosei Kagaku Kyokai Shi*, **40**, 20 (1982); Tetrahedron Symposia-in-Print Number 17, "Recent Aspects of Anthracyclinone Chemistry," ed. by T. R. Kelly, *Tetrahedron*, **40**, 4539—4793 (1984).
3) *a*) Y. Tamura, A. Wada, M. Sasho, K. Fukunaga, H. Maeda, and Y. Kita, *J. Org. Chem.*, **47**, 4376 (1982); *b*) Y. Tamura, M. Sasho, S. Akai, A. Wada, and Y. Kita, *Tetrahedron*, **40**, 4539 (1984); *c*) Y. Tamura, M. Sasho, K. Nakagawa, T. Tsugoshi, and Y. Kita, *J. Org. Chem.*, **49**, 473 (1984).
4) Y. Tamura, M. Sasho, S. Akai, H. Kishimoto, J. Sekihachi, and Y. Kita, *Tetrahedron Lett.*, **27**, 195 (1986).
5) Introduction of an α-OAc group into esters with LTA *via* ketene silyl acetals, see: G. M. Rubottom, J. M. Gruber, R. Marrero, H. D. Juve, Jr., and C. W. Kim, *J. Org. Chem.*, **48**, 4940 (1983) and references cited therein.
6) Introduction of an α-OH group into esters with *m*-CPBA *via* ketene silyl acetals, see: G. M. Rubottom and R. Marrero, *Synth. Commun.*, **11**, 505 (1981); R. Z. Andriamialisoa, N. Langlois, and Y. Langlois, *J. Org. Chem.*, **50**, 961 (1985).
7) Oxidation of dimethyl homophthalate under standard conditions using PIDA or phenyl iodosyl bis(trifluoroacetate) (PIFA)/KOH–MeOH gave a complex mixture accompanied with a small amount of **18**. Hypervalent iodine oxidation of carbonyl compounds, see: R. M. Moriarty and H. Hu, *Tetrahedron Lett.*, **22**, 2747 (1981); Y. Tamura, T. Yakura, H. Terashi, J. Haruta, and Y. Kita, *Chem. Pharm. Bull.*, **35**, 570 (1987) and references cited therein.
8) Attempts to use the benzyl ester failed.
9) This is an excellent reagent for the preparation of carboxylic anhydrides under mild conditions, see: Y. Kita, S. Akai, M. Yoshigi, Y. Nakajima, H. Yasuda, and Y. Tamura, *Tetrahedron Lett.*, **25**, 6027 (1984); Y. Kita, S.

Akai, N. Ajimura, M. Yoshigi, T. Tsugoshi, H. Yasuda, and Y. Tamura, *J. Org. Chem.*, **51**, 4150 (1986).
10) The possibility of the isomeric structure (**26'**) was readily ruled out from the characteristic non hydrogen-bonded quinone absorption band in its IR spectrum.
11) *a*) A. S. Kende, Y.-g. Tsay, and J. E. Mills, *J. Am. Chem. Soc.*, **98**, 1967 (1976); *b*) A. S. Kende, D. P. Curran, Y.-g. Tsay, and J. E. Mills, *Tetrahedron Lett.*, **1977**, 3537.
12) Y. Tamura, M. Sasho, H. Ohe, S. Akai, and Y. Kita, *Tetrahedron Lett.*, **26**, 1549 (1985).
13) While this work was in progress, a similar elaboration method for **7** was reported by Terashima.[14] The weakly basic alkylcerium(III) reagents were shown to have greater nucleophilicity than the parent organolithium reagents by Imamoto *et al.*, see: T. Imamoto, T. Kusumoto, and M. Yokoyama, *J. Chem. Soc., Chem. Commun.*, **1982**, 1042; T. Imamoto, Y. Sugiura, and N. Takiyama, *Tetrahedron Lett.*, **25**, 4233 (1984); T. Imamoto, Y. Tawarayama, T. Kusumoto, and M. Yokoyama, *Yuki Gosei Kagaku Kyokai Shi*, **42**, 143 (1984); T. Imamoto, N. Takiyama, and K. Nakamura, *Tetrahedron Lett.*, **26**, 4763 (1985).
14) *a*) M. Suzuki, Y. Kimura, and S. Terashima, *Chem. Lett.*, **1984**, 1543; *b*) *Idem, Chem. Pharm. Bull.*, **34**, 1531 (1986).
15) *a*) K. Krohn and K. Tolkiehn, *Chem. Ber.*, **112**, 3453 (1979); *b*) T. H. Smith, A. N. Fujiwara, W. W. Lee, H. Y. Wu, and D. W. Henry, *J. Org. Chem.*, **42**, 3653 (1977); *c*) R. J. Blade and P. Hodge, *J. Chem. Soc., Chem. Commun.*, **1979**, 85; *d*) K. Ravichandran, F. A. J. Kerdesky, and M. P. Cava, *J. Org. Chem.*, **51**, 2044 (1986).
16) H. Inouye, T. Okuda, Y. Hirata, N. Nagakura, and M. Yoshizaki, *Chem. Pharm. Bull.*, **15**, 786 (1967); S. Ruhemann, *J. Chem. Soc.*, **97**, 2025 (1910).
17) D. N. Gupta, P. Hodge, and N. Khan, *J. Chem. Soc., Perkin Trans. 1*, **1981**, 689.
18) T. Imamoto, T. Kusumoto, Y. Tawarayama, Y. Sugiura, T. Mita, Y. Hatanaka, and M. Yokoyama, *J. Org. Chem.*, **49**, 3904 (1984).
19) *a*) J. R. Wiseman, N. I. French, R. K. Hallmark, and K. G. Chiong, *Tetrahedron Lett.*, **1978**, 3765; *b*) M. J. Broadhurst, C. H. Hassall, and G. J. Thomas, *J. Chem. Soc., Perkin Trans. 1*, **1982**, 2239; *c*) D. Dominguez, R. J. Ardecky, and M. P. Cava, *J. Am. Chem. Soc.*, **105**, 1608 (1983); *d*) S. Terashima, K. Tamoto, and M. Sugimori, *Tetrahedron Lett.*, **23**, 4107 (1982); Y. Kimura, M. Suzuki, T. Matsumoto, R. Abe, and S. Terashima, *Chem. Lett.*, **1984**, 473; *e*) M. Suzuki, T. Matsumoto, R. Abe, Y. Kimura, and S. Terashima, *ibid.*, **1985**, 57.
20) *a*) R. D. Gleim, S. Trenbeath, R. S. D. Mittal, and C. J. Sih, *Tetrahedron Lett.*, **1976**, 3385; F. Suzuki, S. Trenbeath, R. D. Gleim, and C. J. Sih, *J. Org. Chem.*, **43**, 4159 (1978); *b*) M. J. Broadhurst and C. H. Hassall, *J. Chem. Soc., Perkin Trans. 1*, **1982**, 2227.

[Chem. Pharm. Bull. 35(4)1413—1426(1987)]

Acid-Catalyzed Regioselective Acylation of α-Silylallylic Sulfides and Its Application to a Novel Cyclopentannelation and Furan Annelation

KUNIO HIROI,* HIROYASU SATO, LIH-MING CHEN, and KUMIKO KOTSUJI

Department of Synthetic Chemistry, Tohoku College of Pharmacy, 4-4-1 Komatsushima, Sendai, Miyagi 983, Japan

(Received September 26, 1986)

Introduction of a silyl group at the α-position of allylic sulfides, followed by the aluminum chloride-catalyzed reaction of the resulting α-silylallylic sulfides with acid chlorides resulted in regioselective acylation at the γ-position of the allylic system to give γ-acylated vinylic sulfides, chemically equivalent to 1,4-dicarbonyl compounds. Heating of the products in refluxing benzene with an equimolar amount of *p*-toluenesulfonic acid produced 2-cyclopentenone derivatives. Treatment of the acylated products with an equimolar amount of concentrated sulfuric acid gave α-phenylthiofuran derivatives. These procedures provide a novel method for cyclopentannelation and furan annelation.

Keywords——α-silylallylic sulfide; acid chloride; aluminum chloride; acid-catalyzed acylation; vinylic sulfide; 2-cyclopentenone; α-phenylthiofuran; furan; cyclopentannelation; furan annelation

Recently much attention has been devoted to regioselective alkylations of the carbanions of allylic systems[1,2] with many methodologies using alkylboranes[3] and alkylaluminums,[4] or introducing functionalities at the α′-position of allylic sulfides such as thioamides,[5] and 2-pyridyl,[6] 2-thiazolinyl,[7] and 2-imidazolyl groups[1a] for stabilization of the α-carbanion by chelation.

This report deals with the regioselective acid-catalyzed γ-acylation of allylic sulfides *via* α-silyl intermediates[8] and its use in organic synthesis to develop a novel method for cyclopentannelation[9] and furan annelation.[10] This γ-acylation method is based on the idea that introduction of a silyl group at the α-position of allylic sulfides would enhance the nucleophilicity of the olefinic bond (γ-position) in the allylic system to give γ-acylated products.[11]

A regioselective α-silylation of allylic sulfides was readily accomplished in the following manner.[12] Treatment of allylic phenyl sulfides **1a**—**c** with lithium diisopropylamide (LDA) at −78 °C, followed by addition of trimethylsilyl chloride, resulted in regioselective silylation at the α-carbon of the allylic sulfides to give **2a**—**c** quantitatively with complete regioselectivity.

α-Silylallylic sulfides failed to undergo acid-catalyzed intermolecular alkylation with alkyl halides, aldehydes, and ketones using various acidic catalysts such as titanium (IV) chloride, tin (IV) chloride, boron trifluoride etherate, and trifluoroacetic acid, although intramolecular alkylation was observed previously.[13] However, the acid-catalyzed acylation of α-silylallylic sulfides with various acid halides proceeded successfully in the presence of aluminum chloride under mild conditions with extremely high regioselectivity.

Reactions of **2a** with 1.2 eq of the acid halides **3a**—**e** were carried out in dichloromethane in the presence of 1.2 eq of aluminum chloride at −78 °C for 7 h to give γ-phenylthio-β,γ-unsaturated ketones **4a**—**e**, without any formation of α-acylated allylic sulfides, in

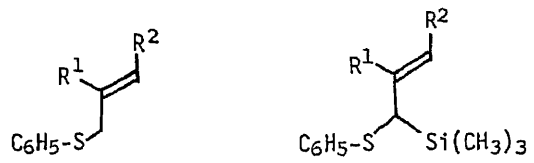

1a—c **2a—c**

a: $R^1=CH_3$, $R^2=H$
b: $R^1=H$, $R^2=CH_3$
c: $R^1=H$, $R^2=H$

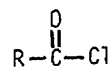

3a: $R=CH_3$
3b: $R=CH_3(CH_2)_2$
3c: $R=CH_3(CH_2)_3$
3d: $R=CH_3(CH_2)_5$
3e: $R=CH_3(CH_2)_6$
3f: $R=C_6H_5CH_2$
3g: $R=C_6H_5CH=CH$
3h: $R=C_6H_5CH_2CH_2$

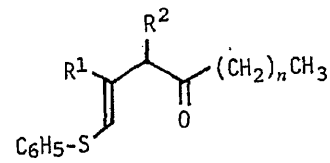

4a—i

Chart 1

TABLE I. Studies on Aluminum Chloride-Catalyzed Acylations of **2a—c** with **3a—e**[a]

4	R^1	R^2	n	Reaction time (h)	Yields of 4[b] (%)
4a	CH_3	H	0	7.0	63
4b	CH_3	H	2	7.0	84
4c	CH_3	H	3	7.0	92
4d	CH_3	H	5	7.0	84
4e	CH_3	H	6	7.0	86
4f	H	CH_3	0	8.0	21 (32)
4g	H	CH_3	2	8.0	75 (91)
4h	H	CH_3	3	8.0	67 (90)
4i	H	CH_3	5	8.0	63 (75)
4j	H	CH_3	6	8.0	56 (66)
4k	H	H	0	5.0	21 (27)
4l	H	H	2	7.5	51 (67)
4m	H	H	3	5.0	57 (75)
4n	H	H	5	6.0	44 (54)
4o	H	H	6	5.0	31 (38)

a) The α-silylallylic sulfides **2a—c** were treated with **3a—e** (1.2 eq) in the presence of aluminum chloride (1.2 eq) in dichloromethane at −78 °C. *b*) Yields corrected for recovered starting materials are given in parentheses.

the yields listed in Table I. Regioselective acylation of **2b, c** under the same conditions afforded **4f—o** in the yields shown in Table I with some recovery of the starting materials. Migration of the double bond in **4k—o** was observed during the reactions to afford the α,β-unsaturated ketones (17—25%).

The structures of the products **4a—o** were assigned on the basis of infrared (IR) and nuclear magnetic resonance (NMR) spectral analyses; the products **4a—o** exhibit carbonyl absorption at 1720 cm^{-1} and olefin absorption (enol thioether) at 1620 cm^{-1} in the IR spectra. The structure of the γ-acylated product was confirmed by conversion of 3-methyl-1-phenylthio-1-octen-4-one (**4f**) into 3-methyl-1-phenylthio-2-octen-4-one upon prolonged treatment of **4f** with silica gel.

Next, we applied this method to cyclic allylic sulfides. The cyclic allylic sulfides **8a—d** were easily obtained in the following way. Addition of the carbanion (**6**), generated by treating methyl phenyl sulfide with butyllithium at 0°C, to cycloalkanones (**5a—d**) in the presence of 1,4-diazabicyclo[2.2.2]octane,[14] followed by dehydration of the resulting hydroxy compounds **7a—d** in refluxing benzene with a catalytic amount of *p*-toluenesulfonic

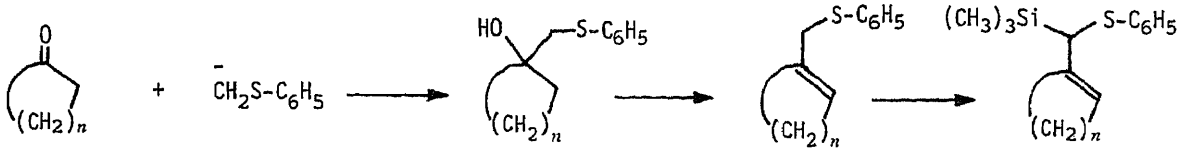

5a $n=3$
5b $n=4$
5c $n=5$
5d $n=10$

6 **7a—d** **8a—d** **9a—d**

Chart 2

TABLE II. Studies on the Aluminum Chloride-Catalyzed Acylation of **9b** with **3c**[a]

Aluminum chloride (eq)	Reaction temp. (°C)	Reaction time (h)	Yields of **10c** (%)
0.5	−78	6	18
0.8	−78	6	37
1.0	−78	6	46
1.2	−78	6	59
1.5	−78	5	65
1.5	−78	6	80
1.5	−78	8	77
1.5	−78	10	66
2.0	−78	6	71
1.5	−60	6	52
1.5	−40	6	51
1.5	−20	6	45

a) The reaction of **9b** with **3c** (1.2 eq) was carried out in dichloromethane.

TABLE III. Synthesis of **10a—g** by the Acid-Catalyzed Acylation of **9b**[a]

10	R	Lewis acids	Yields of **10** (%)
10a	CH_3	$AlCl_3$	26
10a	CH_3	$TiCl_4$	44
10a	CH_3	$SnCl_4$	36
10b	$CH_3(CH_2)_2$	$AlCl_3$	65
10c	$CH_3(CH_2)_3$	$AlCl_3$	80
10d	$CH_3(CH_2)_5$	$AlCl_3$	81
10e	$CH_3(CH_2)_6$	$AlCl_3$	74
10f	$C_6H_5CH_2$	$AlCl_3$	11
10g	$C_6H_5CH=CH$	$AlCl_3$	28

a) The reactions of **9b** with **3a—g** (1.2 eq) were carried out in the presence of Lewis acids (1.5 eq) in dichloromethane at −78 °C for 6 h.

acid produced exclusively 1-phenylthiomethylcycloalkenes (**8a—d**) in good yields. Reactions of the carbanions of the allylic sulfides **8a—d**, generated by treating **8a—d** with LDA at −78 °C, with trimethylsilyl chloride in tetrahydrofuran (THF) at −78 °C for 2 h gave exclusively α-trimethylsilylallylic sulfides **9a—d** in extremely high yields. The products showed the signals of the methine proton α to the sulfide at δ 3.00—3.20 (1H, singlet) and the olefin proton at δ 5.05—5.50 (1H, triplet or multiplet) in their NMR spectra.

The aluminum chloride-catalyzed acylations of **9b** with acid chlorides **3a—h** were carried out in dichloromethane under various conditions, and the results are summarized in Tables II

and III.

The reaction of **9b** with 1.2 eq of the acid chloride **3c** in the presence of 1.5 eq of aluminum chloride in dichloromethane at −78 °C for 6 h led to the highest yield (80%) of **10c**. The structure of the product **10c** was characterized by IR and NMR spectral analyses; the carbonyl absorption appears at 1710 cm^{-1} in the IR spectrum, while signals due to the methine proton at δ 3.00—3.27 and 3.68—3.90 (multiplets) and the olefin proton at δ 5.90 and 6.00 (singlets) were seen in the NMR spectrum. The product **10c** was calculated to be a 3 : 2 mixture of the geometrical isomers, *Z*- and *E*-**10**, from the NMR signals of the olefin protons. The stereochemistry of the olefin was determined by thermal transformation of the less stable isomer (*Z*-**10**) into the more stable one (*E*-**10**) under heating in refluxing xylene. Furthermore, the structure was unequivocally confirmed by NMR analysis; the signal of the olefin proton in *E*-**10** was shifted slightly to lower field (δ about 6.00, singlet) by the anisotropy of the carbonyl group as compared with that in *Z*-**10** (δ about 5.90, singlet).

In the aluminum chloride-catalyzed reaction of **9b** with acetyl chloride, phenyl thioloacetate was obtained in 61% yield, together with the acylated product **10a** (26% yield). The yield of **10a** was increased by using titanium (IV) chloride or tin (IV) chloride, instead of aluminum chloride, as an acidic catalyst[15] and in these cases phenyl thioloacetate was also obtained as a by-product in 37 and 32% yields, respectively. In other cases (**3b—e**), a small amount (about 10% yield) of the corresponding phenyl thioloester was obtained as a by-product. Exceptionally, a large amount (42%) of phenyl phenylthioloacetate was formed in the reaction of **9b** with phenylacetyl chloride (**3f**).

The aforementioned results indicate that the above acid-catalyzed reactions proceed partially or wholly through an intramolecular acylation *via* **11**.

The aluminum chloride-catalyzed acylations of **9a, c, d** with acid chlorides **3a—h** were carried out under the same conditions to give the γ-acylated products **12a—g**, **13a—e**, and **14a—e** with complete regioselectivity, in the yields shown in Table IV. The structures of the products were characterized by IR and NMR spectral analyses in the same way as described earlier.

These γ-acylation products would be useful as precursors to synthetically valuable 1,4-dicarbonyl compounds.[16] Therefore we attempted to construct cyclopentenone and furan ring systems by the intramolecular condensation of these 1,4-dicarbonyl equivalents.

Heating of the ketones **10a—e** in refluxing benzene with an equimolar amount of *p*-

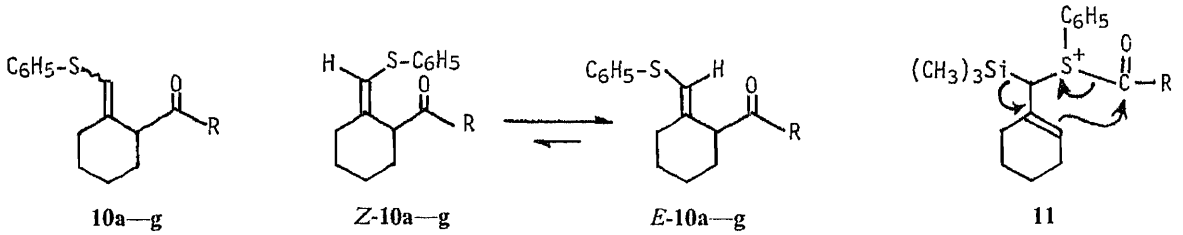

10a—g *Z*-**10a—g** *E*-**10a—g** **11**

Chart 3

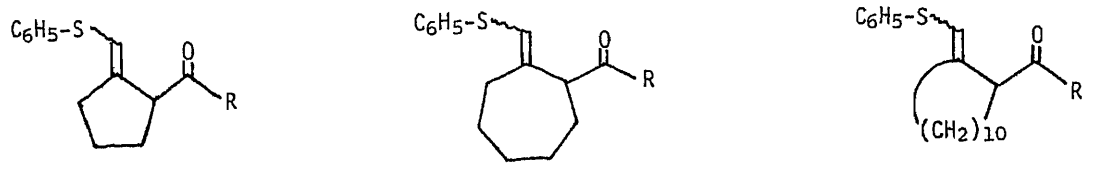

12a—g **13a—e** **14a—e**

Chart 4

toluenesulfonic acid for 2 h resulted in intramolecular condensation to give 2-cyclopentenone derivatives **15a—e** in moderate yields (51—59%). The structures of these products were confirmed by the IR, NMR, and mass spectral analyses. They exhibited carbonyl and olefin absorptions at 1700—1710 cm^{-1} and at 1640—1650 cm^{-1}, respectively, in the IR spectra, characteristic of α,β-unsaturated five-membered ketones. The stereochemistry of the fused ring systems was deduced to be the more stable *cis* configuration, on the basis of epimerization studies by treatment of the ketones with sodium hydride.

Treatment of the γ-acylated compounds with concentrated sulfuric acid afforded furan derivatives.[17] Heating of **10b—e** and **13a—d** with an equimolar amount of concentrated sulfuric acid in refluxing benzene for 15 h resulted in acid-catalyzed cyclization and subsequent air oxidation to produce the α-phenylthiofuran derivatives **16a—h**.[18] The

TABLE IV. Synthesis of **12**, **13**, and **14** by Aluminum Chloride-Catalyzed Acylation of **9a**, **9c**, and **9d**[a]

Acylated products	R	Reaction time (h)	Yields (%)
12a	$CH_3(CH_2)_2$	4	62
12b	$CH_3(CH_2)_3$	4	76
12c	$CH_3(CH_2)_5$	4	75
12d	$CH_3(CH_2)_6$	4	77
12e	$C_6H_5CH_2$	4	19[b]
12f	$C_6H_5CH_2CH_2$	4	47
12g	$C_6H_5CH=CH$	4	32
13a	$CH_3(CH_2)_2$	6	51
13b	$CH_3(CH_2)_3$	6	57
13c	$CH_3(CH_2)_5$	6	67
13d	$CH_3(CH_2)_6$	6	59
13e	$C_6H_5CH=CH$	6	48
14a	$CH_3(CH_2)_2$	6	40
14b	$CH_3(CH_2)_3$	6	41
14c	$CH_3(CH_2)_5$	6	51
14d	$CH_3(CH_2)_6$	6	47
14e	$C_6H_5CH=CH$	6	36

a) The reactions of **9a**, **9c**, and **9d** with acid chlorides **3** (1.2 eq) were carried out in the presence of aluminum chloride (1.5 eq) in dichloromethane at −78 °C. *b*) Phenyl phenylthioloacetate (32%) was obtained as a by-product.

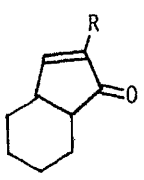

15a: R=H
15b: R=CH_3CH_2
15c: R=$CH_3(CH_2)_2$
15d: R=$CH_3(CH_2)_4$
15e: R=$CH_3(CH_2)_5$

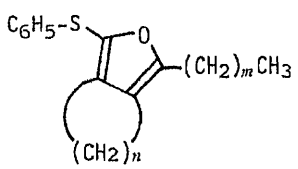

16a—h

a: $n=4$, $m=2$
b: $n=4$, $m=3$
c: $n=4$, $m=5$
d: $n=4$, $m=6$
e: $n=5$, $m=2$
f: $n=5$, $m=3$
g: $n=5$, $m=5$
h: $n=5$, $m=6$

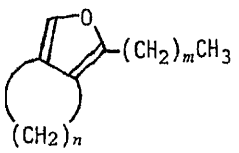

17a—h

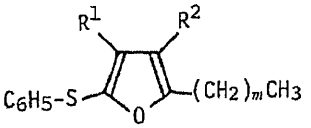

18a: $R^1=CH_3$, $R^2=H$, $m=0$
18b: $R^1=CH_3$, $R^2=H$, $m=2$
18c: $R^1=CH_3$, $R^2=H$, $m=3$
18d: $R^1=CH_3$, $R^2=H$, $m=5$
18e: $R^1=CH_3$, $R^2=H$, $m=6$
18f: $R^1=H$, $R^2=CH_3$, $m=5$
18g: $R^1=H$, $R^2=H$, $m=5$

Chart 5

hydrogenetic desulfenylation of **16a—h** with Raney Ni gave the furan derivatives **17a—h** in good yields.[19] Similar treatment of the acyclic compounds **4a—e**, **4n**, and **4i** with concentrated sulfuric acid (in refluxing benzene, 2 h) led to the formation of α-phenylthiofurans **18a—g**. The structures of **16a—h**, **17a—h**, and **18a—g** were confirmed by the IR, NMR, and mass spectral data.

In conclusion, the aluminum chloride-catalyzed γ-acylation of allylic sulfides was successfully performed *via* α-silyl intermediates with complete regioselectivity, giving γ-acylated vinylic sulfides, which are synthetically useful 1,4-dicarbonyl equivalents. The acidic treatment of these products provides a facile entry to 2-cyclopentenone and furan derivatives. Furthermore, this method is potentially very useful for cyclopentannelation[20] and furan annelation of cyclic ketones.

Experimental

Thin-layer or preparative thick layer plates were made of Merck Silica gel 60PF-254 activated by drying at 140 °C for 3.5 h. IR spectra were obtained in the indicated state with a Hitachi 215 spectrometer. NMR spectra were determined in the indicated solvent with a Hitachi R-24B high-resolution NMR spectrometer (60 MHz); chemical shifts are given in ppm from tetramethylsilane. Splitting patterns are designated as s, singlet; br s, broad singlet; d, doublet; t, triplet; q, quartet; m, multiplet. Mass spectra (MS) were taken on a Hitachi M-52G or JEOL TMS-01 SG-2 spectrometer and a JEOL JMA-DA-5000 JMS-DX-303 spectrometer.

Silylation of Acyclic Allylic Sulfides 1a—c——Phenyl 1-Trimethylsilylcrotyl Sulfide (2b): A dry 50 ml two-necked flask equipped with a septum inlet and a stirring bar was flushed with nitrogen and maintained under a positive pressure of nitrogen. A solution of 2 ml (14.6 mmol) of diisopropylamine in 15 ml of THF was added to the flask and cooled to 0 °C, then a 1.5 N hexane solution of butyllithium (9.7 ml, 14.6 mmmol) was added. After 30 min, a solution of 2.00 g (12.17 mmol) of **1b** in 5 ml of THF was added to the above solution cooled to −78 °C, and the mixture was stirred at −78 °C for 1 h, followed by dropwise addition of 1.7 ml (13.39 mmol) of trimethylsilyl chloride. The reaction mixture was stirred at −78 °C for 3.5 h, and then diluted with ether. The solution was washed with 10% aqueous HCl, saturated aqueous $NaHCO_3$, and saturated aqueous NaCl, dried over anhydrous Na_2SO_4, and concentrated *in vacuo*. The residue was purified by distillation to give 2.80 g (98% yield) of **2b**: bp 82 °C (2 mmHg) (oil bath temp.). IR ν_{max}^{film} cm^{-1}: 1605 (C=C), 1590 (phenyl). NMR (CCl_4) δ: 0.07 (9H, s, $Si(CH_3)_3$), 1.53 (3H, d, J=4 Hz, CH_3–C=C), 2.90—3.10 (1H, m, S–CH), 5.10—5.43 (2H, m, CH=CH), 6.83—7.33 (5H, m, C_6H_5). MS *m/z*: 236 (M^+). *Anal.* Calcd for $C_{13}H_{20}SSi$: C, 66.07; H, 8.53; S, 27.08. Found: C, 66.35; H, 8.81; S, 26.95.

The other acyclic α-silylallylic sulfides **2a** and **2c** were prepared in the same way as described above.

Phenyl 1-Trimethylsilylmethallyl Sulfide (**2a**): bp 80—85 °C (2 mmHg) (oil bath temp.). 87% yield. IR ν_{max}^{film} cm^{-1}: 1660 (C=C), 1588 (phenyl). NMR (CCl_4) δ: 0.15 (9H, s, $Si(CH_3)_3$), 1.73 (3H, s, CH_3-C=C), 3.17 (1H, s, S–CH–Si), 4.68 (2H, s, C=CH_2), 6.90—7.30 (5H, m, C_6H_5). MS *m/z*: 236 (M^+). *Anal.* Calcd for $C_{13}H_{20}SSi$: C, 66.07; H, 8.53; S, 27.08. Found: C, 66.25; H, 8.79; S, 26.92.

Phenyl 1-Trimethylsilylallyl Sulfide (**2c**): bp 80—85 °C (3 mmHg) (oil bath temp.). 92% yield. IR ν_{max}^{film} cm^{-1}: 1640 (C=C), 1595 (phenyl). NMR (CCl_4) δ: 0.10 (9H, s, $Si(CH_3)_3$), 3.07 (1H, d, J=9 Hz, S–CH–Si), 4.67—6.00 (3H, m, CH=CH_2), 6.87—7.43 (5H, m, C_6H_5). MS *m/z*: 222 (M^+). *Anal.* Calcd for $C_{12}H_{18}SSi$: C, 64.84; H, 8.16; S, 28.80. Found: C, 65.07; H, 8.40; S, 28.71.

Aluminum Chloride-Catalyzed Acylations of Acyclic α-Trimethylsilylallylic Sulfides 2a—c. General Procedure——A dry 25 ml two-necked flask equipped with a septum inlet and a magnetic stirring bar, and containing 338 mg (2.53 mmol) of aluminum chloride (powdered finely), was flushed with nitrogen, and maintained under a positive pressure of nitrogen. Dichloromethane (1 ml) was added to the flask. A solution of an acid chloride (**3a—e**, 2.53 mmol) in 1 ml of dichloromethane was added at −78 °C, followed by dropwise addition of a solution of an acyclic α-trimethylsilylallylic sulfide (**2a—c**, 2.11 mmol) in 1 ml of dichloromethane, and the reaction mixture was stirred at −78 °C for 8 h. The mixture was diluted with ether, washed sequentially with saturated aqueous NaCl, saturated aqueous $NaHCO_3$, and saturated aqueous NaCl, dried over anhydrous Na_2SO_4, and concentrated *in vacuo*. The residue was subjected to preparative thin layer chromatography (TLC) (ether–hexane 1 : 10) to give the γ-acylated product. In the cases of **4k—o**, the products included 17, 25, 25, 25, and 25% of α,β-unsaturated ketones formed by migration of the double bond, respectively.

4-Methyl-5-phenylthio-4-penten-2-one (**4a**): bp 120—130 °C (3 mmHg) (oil bath temp.). IR ν_{max}^{film} cm^{-1}: 1720 (C=O), 1620 (C=C), 1588 (phenyl). NMR (CCl_4) δ: 1.90 (3H, s, CH_3-C=C), 2.15 (3H, s, $\overset{O}{\overset{\|}{C}}$–$CH_3$), 3.10, 3.30 (2H, s, s, $\overset{O}{\overset{\|}{C}}$–$CH_2$–C=C), 5.96 (1H, s, CH=C), 7.00—7.40 (5H, m, C_6H_5). MS *m/z*: 206 (M^+). Exact mass determination:

206.0760 (Calcd for $C_{12}H_{14}OS$: 206.0764).

2-Methyl-1-phenylthio-1-hepten-4-one (**4b**): bp 120—130 °C (3 mmHg) (oil bath temp.). IR ν_{max}^{film} cm^{-1}: 1720 (C=O), 1620 (C=C), 1588 (phenyl). NMR (CCl_4) δ: 0.86 (3H, t, J=7 Hz, $CH_2\underline{CH_3}$), 1.20—1.70 (2H, m, $\underline{CH_2}$–CH_3), 1.86 (3H, s, CH_3–C=C), 2.06—2.50 (2H, m, $\overset{O}{\overset{\|}{C}}$–$\underline{CH_2}$–$CH_2$), 3.06, 3.27 (2H, s, s, $\overset{O}{\overset{\|}{C}}$–$CH_2$–C=C), 5.93 (1H, s, CH=C), 7.00—7.40 (5H, m, C_6H_5). MS *m/z*: 234 (M^+). *Anal.* Calcd for $C_{14}H_{18}OS$: C, 71.77; H, 7.74; S, 13.66. Found: 71.76; H, 7.79; S, 13.36.

2-Methyl-1-phenylthio-1-octen-4-one (**4c**): bp 125—135 °C (3 mmHg) (oil bath temp.). IR ν_{max}^{film} cm^{-1}: 1720 (C=O), 1620 (C=C), 1588 (phenyl). NMR (CCl_4) δ: 0.90 (3H, t, J=5 Hz, $\underline{CH_3}CH_2$), 1.15—1.70 (4H, m, $\overset{O}{\overset{\|}{C}}$–$CH_2$–$(\underline{CH_2})_2$), 1.87 (3H, s, CH_3–C=C), 2.06—2.50 (2H, m, $\overset{O}{\overset{\|}{C}}$–$\underline{CH_2}$–$CH_2$), 3.10, 3.30 (2H, s, s, $\overset{O}{\overset{\|}{C}}$–$CH_2$–C=C), 6.00 (1H, s, CH=C), 7.06—7.30 (5H, m, C_6H_5). MS *m/z*: 248 (M^+). Exact mass determination: 248.1229 (Calcd for $C_{15}H_{20}OS$: 248.1234).

2-Methyl-1-phenylthio-1-decen-4-one (**4d**): bp 130—140 °C (3 mmHg) (oil bath temp.). IR ν_{max}^{film} cm^{-1}: 1720 (C=O), 1620 (C=C), 1588 (phenyl). NMR (CCl_4) δ: 0.90 (3H, t, J=4 Hz, CH_2–$\underline{CH_3}$), 1.00—1.70 (8H, m, $\overset{O}{\overset{\|}{C}}$–$CH_2$–$(\underline{CH_2})_4$), 1.83 (3H, s, CH_3–C=C), 2.10—2.50 (2H, m, $\overset{O}{\overset{\|}{C}}$–$\underline{CH_2}$–$CH_2$), 3.06, 3.20 (2H, s, s, $\overset{O}{\overset{\|}{C}}$–$CH_2$–C=C), 5.96 (1H, m, CH=C), 7.00—7.40 (5H, m, C_6H_5). MS *m/z*: 276 (M^+). Exact mass determination: 276.1540 (Calcd for $C_{17}H_{24}OS$: 276.1546).

2-Methyl-1-phenylthio-1-undecen-4-one (**4e**): bp 150—155 °C (3 mmHg) (oil bath temp.). IR ν_{max}^{film} cm^{-1}: 1720 (C=O), 1620 (C=C), 1588 (phenyl). NMR (CCl_4) δ: 0.86 (3H, t, J=4 Hz, CH_3–CH_2), 1.00—1.70 (10H, m, $\overset{O}{\overset{\|}{C}}$–$CH_2$–$(\underline{CH_2})_5$), 1.83 (3H, s, CH_3–C=C), 2.00—2.55 (2H, m, $\overset{O}{\overset{\|}{C}}$–$\underline{CH_2}$–$CH_2$), 3.06, 3.27 (2H, s, s, $\overset{O}{\overset{\|}{C}}$–$CH_2$–C=C), 5.96 (1H, CH=C), 7.00—7.40 (5H, m, C_6H_5). MS *m/z*: 290 (M^+). *Anal.* Calcd for $C_{18}H_{26}OS$: C, 74.44; H, 9.03; S, 11.02. Found: C, 74.19; H, 9.30; S, 11.25.

3-Methyl-5-phenylthio-4-penten-2-one (**4f**): bp 120—130 °C (3 mmHg) (oil bath temp.). IR ν_{max}^{film} cm^{-1}: 1720 (C=O), 1590 (phenyl). NMR (CCl_4) δ: 1.13 (3H, d, J=8 Hz, $\underline{CH_3}$–CH), 2.08 (3H, s, CH_3–$\overset{O}{\overset{\|}{C}}$), 2.97—3.83 (1H, m, CH_3–$\underline{CH}$), 5.47 (1H, q, J=9, 18 Hz, S–CH=$\underline{CH}$), 6.22 (1H, d, J=9 Hz, S–$\underline{CH}$=CH), 6.97—7.40 (5H, m, C_6H_5). MS *m/z*: 206 (M^+). Exact mass determination: 206.0754 (Calcd for $C_{12}H_{14}OS$: 206.0764).

3-Methyl-1-phenylthio-1-hepten-4-one (**4g**): bp 120—130 °C (3 mmHg) (oil bath temp.). IR ν_{max}^{film} cm^{-1}: 1720 (C=O), 1590 (phenyl). NMR (CCl_4) δ: 0.87 (3H, t, J=6 Hz, $\underline{CH_3}$–CH_2), 1.20 (3H, d, J=6 Hz, $\underline{CH_3}$–CH)., 1.33—1.97 (2H, m, $\underline{CH_2}CH_3$), 2.17—2.83 (2H, m, $\overset{O}{\overset{\|}{C}}$–$CH_2$), 3.23—3.90 (1H, m, CH_3–$\underline{CH}$), 5.67 (1H, q, J=10, 18 Hz, S–CH=$\underline{CH}$), 6.24 (1H, d, J=10 Hz, S–CH), 7.00—7.57 (5H, m, C_6H_5). MS *m/z*: 234 (M^+). *Anal.* Calcd for $C_{14}H_{18}OS$: C, 71.77; H, 7.74; S, 13.66. Found: C, 71.78; H, 7.76; S, 13.96.

3-Methyl-1-phenylthio-1-octen-4-one (**4h**): bp 125—130 °C (3 mmHg) (oil bath temp.). IR ν_{max}^{film} cm^{-1}: 1720 (C=O), 1590 (phenyl). NMR (CCl_4) δ: 0.87 (3H, t, J=8 Hz, CH_2–$\underline{CH_3}$), 1.15 (3H, d, J=7 Hz, $\underline{CH_3}$–CH), 1.27—1.83 (4H, m, CH_3–$(\underline{CH_2})_2$), 2.20—2.60 (2H, m, $\overset{O}{\overset{\|}{C}}$–$CH_2$), 2.90—3.77 (1H, m, CH_3–$\underline{CH}$), 5.63 (1H, q, J=9, 19 Hz, S–CH=$\underline{CH}$), 6.23 (1H, d, J=9 Hz, S–$\underline{CH}$=CH), 6.97—7.47 (5H, m, C_6H_5). MS *m/z*: 248 (M^+). Exact mass determination: 248.1219 (Calcd for $C_{15}H_{20}OS$: 248.1234).

3-Methyl-1-phenylthio-1-decen-4-one (**4i**): bp 130—140 °C (3 mmHg) (oil bath temp.). IR ν_{max}^{film} cm^{-1}: 1720 (C=O), 1590 (phenyl). NMR (CCl_4) δ: 0.73 (3H, t, J=4 Hz, $\underline{CH_3}$–CH_2), 0.86—1.70 (11H, m, $\underline{CH_3}$–CH, CH_3–$(\underline{CH_2})_4$), 2.00—2.47 (2H, m, $\overset{O}{\overset{\|}{C}}$–$CH_2$), 3.13—3.70 (1H, m, CH_3–$\underline{CH}$), 5.50 (1H, q, J=10, 20 Hz, S–CH=$\underline{CH}$), 6.12 (1H, d, J=10 Hz, S–CH), 6.83—7.40 (5H, m, C_6H_5). MS *m/z*: 276 (M^+). Exact mass determination: 276.1546 (Calcd for $C_{17}H_{24}OS$: 276.1546).

3-Methyl-1-phenylthio-1-undecen-4-one (**4j**): bp 150—160 °C (3 mmHg) (oil bath temp.). IR ν_{max}^{film} cm^{-1}: 1720 (C=O), 1590 (phenyl). NMR (CCl_4) δ: 0.86 (3H, t, J=5 Hz, $\underline{CH_3}CH_2$), 1.14 (3H, d, J=7 Hz, $\underline{CH_3}$–CH), 1.23—1.90 (10H, m, $CH_3(\underline{CH_2})_5$), 3.36—3.90 (1H, m, CH_3–$\underline{CH}$), 5.63 (1H, q, J=10, 18 Hz, S–CH=$\underline{CH}$), 6.25 (1H, d, J=10 Hz, S–CH), 7.00—7.50 (5H, m, C_6H_5). *Anal.* Calcd for $C_{18}H_{26}OS$: C, 74.44; H, 9.03; S, 11.02. Found: C, 74.19; H, 9.30; S, 11.25.

5-Phenylthio-4-penten-2-one (**4k**): bp 120—130 °C (3 mmHg) (oil bath temp.). IR ν_{max}^{film} cm^{-1}: 1720 (C=O), 1590 (phenyl). NMR (CCl_4) δ: 1.97 (3H, s, CH_3–$\overset{O}{\overset{\|}{C}}$), 2.90—3.26 (2H, m, $\overset{O}{\overset{\|}{C}}$–$CH_2$), 5.50—6.47 (2H, m, CH=CH), 6.87—7.47 (5H, m, C_6H_5). MS *m/z*: 192 (M^+). Exact mass determination: 192.0650 (Calcd for $C_{11}H_{12}OS$: 192.0610).

5-Phenylthio-3-penten-2-one: bp 120—130 °C (3 mmHg) (oil bath temp.). IR ν_{max}^{film} cm^{-1}: 1675 (α,β-unsat.

ketone), 1590 (phenyl). NMR (CCl_4) δ: 1.97 (3H, s, CH_3–C(=O)), 3.26—3.57 (2H, d, J=6 Hz, S–CH_2), 5.50—6.57 (2H, m, CH=CH), 6.87—7.47 (5H, m, C_6H_5). MS *m/z*: 192 (M^+). Exact mass determination: 192.0650 (Calcd for $C_{11}H_{12}OS$: 192.0610).

1-Phenylthio-1-hepten-4-one (**4l**): bp 120—130 °C (3 mmHg) (oil bath temp.). IR ν_{max}^{film} cm^{-1}: 1720 (C=O), 1590 (phenyl). NMR (CCl_4) δ: 0.86 (3H, t, J=7 Hz, CH_3–CH_2), 1.13—2.00 (2H, m, CH_3–CH_2), 2.06—2.50 (2H, m, C(=O)–CH_2–CH_2), 2.90—3.30 (2H, m, C(=O)–CH_2–C=C), 5.57—6.50 (2H, m, CH=CH), 6.90—7.47 (5H, m, C_6H_5). MS *m/z*: 220 (M^+). Exact mass determination: 220.0873 (Calcd for $C_{13}H_{16}OS$: 220.0920).

1-Phenylthio-2-hepten-4-one: bp 120—130 °C (3 mmHg) (oil bath temp.). IR ν_{max}^{film} cm^{-1}: 1675 (α,β-unsat. ketone), 1590 (phenyl). NMR (CCl_4) δ: 0.50 (3H, t, J=6 Hz, CH_3–CH_2), 1.13—1.77 (2H, m, CH_3–CH_2), 2.30 (2H, t, J=6 Hz, C(=O)–CH_2), 3.48 (2H, t, J=6 Hz, S–CH_2), 5.83 (1H, d, J=16 Hz, C(=O)–CH=CH), 6.53 (1H, q, J=8, 16 Hz, C(=O)–CH=CH), 7.00—7.46 (5H, m, C_6H_5). MS *m/z*: 220 (M^+). Exact mass determination: 220.0873 (Calcd for $C_{13}H_{16}OS$: 220.0920).

1-Phenylthio-1-octen-4-one (**4m**): bp 130—140 °C (3 mmHg) (oil bath temp.). IR ν_{max}^{film} cm^{-1}: 1720 (C=O), 1590 (phenyl). NMR (CCl_4) δ: 0.87 (3H, t, J=7 Hz, CH_3-CH_2), 1.06—1.80 (4H, m, $(CH_2)_2CH_3$), 2.33 (2H, t, J=6 Hz, C(=O)–CH_2–CH_2), 3.10—3.37 (2H, m, C(=O)–CH_2–C=C), 5.87—6.47 (2H, m, CH=CH), 6.97—7.53 (5H, m, C_6H_5). MS *m/z*: 234 (M^+). Exact mass determination: 234.1065 (Calcd for $C_{14}H_{18}OS$: 234.1077).

1-Phenylthio-2-octen-4-one: bp 130—140 °C (3 mmHg) (oil bath temp.). IR ν_{max}^{film} cm^{-1}: 1675 (α,β-unsat. ketone), 1590 (phenyl). NMR (CCl_4) δ: 0.90 (3H, t, J=7 Hz, CH_3–CH_2), 1.13—1.77 (4H, m, CH_3–$(CH_2)_2$), 2.37 (2H, t, J=7 Hz, C(=O)–CH_2), 3.53 (2H, d, J=7 Hz, S–CH_2), 5.88 (1H, d, J=14 Hz, C(=O)–CH=CH), 6.55 (1H, q, J=8, 14 Hz, C(=O)–CH=CH), 7.00—7.60 (5H, m, C_6H_5). MS *m/z*: 234 (M^+). Exact mass determination: 234.1065 (Calcd for $C_{14}H_{18}OS$: 234.1077).

1-Phenylthio-1-decen-4-one (**4n**): bp 130—140 °C (3 mmHg) (oil bath temp.). IR ν_{max}^{film} cm^{-1}: 1720 (C=O), 1590 (phenyl). NMR (CCl_4) δ: 0.86 (3H, t, J=4 Hz, CH_3–CH_2), 1.03—1.83 (8H, m, $(CH_2)_4CH_3$), 2.33 (2H, t, J=10 Hz, C(=O)–CH_2–CH_2), 3.00—3.33 (2H, m, C(=O)–CH_2–C=C), 5.66—6.40 (2H, m, CH=CH), 6.97—7.73 (5H, m, C_6H_5). MS *m/z*: 262 (M^+). Exact mass determination: 262.1385 (Calcd for $C_{16}H_{22}OS$: 262.1390).

1-Phenylthio-2-decen-4-one: bp 130—140 °C (3 mmHg) (oil bath temp.). IR ν_{max}^{film} cm^{-1}: 1675 (α,β-unsat. ketone), 1590, (phenyl). NMR (CCl_4) δ: 0.80 (3H, t, J=5 Hz, CH_3–CH_2), 1.00—1.73 (8H, m, CH_3–$(CH_2)_4$), 2.30 (2H, t, J=6 Hz, C(=O)–CH_2), 3.47 (2H, d, J=6 Hz, S–CH_2), 5.78 (1H, d, J=14 Hz, C(=O)–CH=CH), 6.50 (1H, q, J=6, 14 Hz, C(=O)–CH=CH), 6.97—7.46 (5H, m, C_6H_5). MS *m/z*: 262 (M^+). Exact mass determination: 262.1385 (Calcd for $C_{16}H_{22}OS$: 262.1390).

1-Phenylthio-1-undecen-4-one (**4o**): bp 150—160 °C (3 mmHg) (oil bath temp.). IR ν_{max}^{film} cm^{-1}: 1720 (C=O), 1590 (phenyl). NMR (CCl_4) δ: 0.80 (3H, t, CH_3–CH_2), 0.97—1.73 (10H, m, $(CH_2)_5$–CH_3), 2.27 (2H, t, J=7 Hz, C(=O)–CH_2–CH_2), 2.90—3.30 (2H, m, C(=O)–CH_2–C=C), 5.57—6.40 (2H, m, CH=CH), 6.87—7.53 (5H, m, C_6H_5). MS *m/z*: 276 (M^+). *Anal.* Calcd for $C_{17}H_{24}OS$: C, 73.88; H, 8.75; S, 11.58. Found: C, 73.41; H, 8.95; S, 11.16.

1-Phenylthio-2-undecen-4-one: bp 150—160 °C (3 mmHg) (oil bath temp.). IR ν_{max}^{film} cm^{-1}: (α,β-unsat. ketone), 1590 (phenyl). NMR (CCl_4) δ: 0.77 (3H, t, J=5 Hz, CH_3–CH_2), 0.93—1.70 (10H, m, CH_3–$(CH_2)_5$), 2.23 (2H, t, J=7 Hz, C(=O)–CH_2–CH_2), 3.43 (2H, d, J=8 Hz, S–CH_2), 5.80 (1H, d, J=16 Hz, C(=O)–CH=CH), 6.57 (1H, q, J=12, 16 Hz, C(=O)–CH=CH), 6.97—7.33 (5H, m, C_6H_5). MS *m/z*: 276 (M^+). *Anal.* Calcd for $C_{17}H_{24}OS$: C, 73.88; H, 8.75; S, 11.58. Found: C, 73.41; H, 8.95; S, 11.16.

Migration of the Double Bond in 4h——A suspension of **4h** (20 mg) and silica gel (5 g) in ether (15 ml) was stirred at room temperature. The filtrate was concentrated *in vacuo* to give 3-methyl-1-phenylthio-2-octen-4-one (19 mg): bp 125—130 °C (3 mmHg) (oil bath temp.). IR ν_{max}^{film} cm^{-1} 1675 (C=C–C=O), 1590 (phenyl). NMR (CCl_4) δ: 0.96 (3H, t, J=6 Hz, CH_3–CH_2), 1.20—1.60 (4H, m, $CH_3(CH_2)_2$), 1.67 (3H, S, CH_3–C=C), 2.57 (2H, t, J=7 Hz, C(=O)–CH_2), 3.63 (2H, d, J=8 Hz, S–CH_2), 6.30—6.50 (1H, m, CH=C), 7.00—7.60 (5H, m, C_6H_5). MS *m/z*: 248 (M^+). Exact mass determination: 248.1219 (Calcd for $C_{15}H_{20}OS$: 248.1234).

General Synthesis of Phenyl α-Trimethylsilyl-1-cycloalkenylmethyl Sulfides (9a—d)

Addition of the Carbanion (6) of Methyl Phenyl Sulfide to Cycloalkanones 5a—d——1-Phenylthiomethylcyclohexanol (**7b**): A dry 100 ml two-necked flask equipped with a septum inlet and a magnetic stirring bar was flushed with nitrogen and maintained under a positive pressure of nitrogen. A solution of 2.39 g (21.3 mmol) of 1,4-diazabicyclo[2.2.2]octane in 25 ml of THF was added to the flask, followed by addition of a solution of 2.5 ml (21.3 mmol) of methyl phenyl sulfide in 1 ml of THF. The solution was cooled to 0 °C and a 1.5 N hexane solution of butyllithium (14.2 ml, 21.3 mmol) was added. The mixture was stirred at 0 °C for 15 min and at room temperature for 1.5 h, then 2.14 ml (20.8 mmol) of cyclohexanone was added at 0 °C, and the whole was stirred at 0 °C for 1 h and at room temperature for 1 h.

The reaction mixture was diluted with ether, washed with 10% aqueous HCl, saturated aqueous $NaHCO_3$, and saturated aqueous NaCl dried over anhydrous Na_2SO_4, and concentrated *in vacuo*. The residue was subjected to column chromatography over silica gel (ether–hexane 1 : 4) to give 4.19 g (91% yield) of **7b** as a pale yellow oil: IR ν_{max}^{film} cm^{-1}: 3470 (OH), 1580 (phenyl). NMR (CCl_4) δ: 1.20—1.80 (10H, m), 2.10 (1H, brs, OH), 2.93 (2H, s, CH_2–S), 6.90—7.40 (5H, m, C_6H_5). MS *m/z*: 222 (M^+). Exact mass determination: 222.1050 (Calcd for $C_{13}H_{18}OS$: 222.1079).

The other hydroxy compounds (**7a**, **7c**, and **7d**) were prepared in the same way as described above.

1-Phenylthiomethylcyclopentanol (**7a**): 88% yield. IR ν_{max}^{film} cm^{-1}: 3450 (OH), 1580 (phenyl). NMR (CCl_4) δ: 1.20—2.50 (8H, m), 2.33 (1H, brs, OH), 3.10 (2H, s, CH_2S), 6.90—7.50 (5H, m, C_6H_5). MS *m/z*: 208 (M^+). Exact mass determination: 208.0918 (Calcd for $C_{12}H_{16}OS$: 208.0921).

1-Phenylthiomethylcycloheptanol (**7c**): 91% yield. IR ν_{max}^{film} cm^{-1}: 3450 (OH), 1580 (phenyl). NMR (CCl_4) δ: 0.90—2.10 (12H, m), 2.18 (1H, brs, OH), 3.00 (2H, s, CH_2–S), 6.90—7.50 (5H, m, C_6H_5). MS *m/z*: 236 (M^+). Exact mass determination: 236.1223 (Calcd for $C_{14}H_{20}OS$: 236.1233).

1-Phenylthiomethylcyclododecanol (**7d**): 89% yield. IR ν_{max}^{film} cm^{-1}: 3450 (OH), 1590 (phenyl). NMR (CCl_4) δ: 1.00—1.80 (22H, m), 1.87 (1H, brs, OH), 2.93 (2H, s, CH_2–S), 7.00—7.40 (5H, m, C_6H_5). MS *m/z*: 306 (M^+). Exact mass determination: 306.2019 (Calcd for $C_{19}H_{30}OS$: 306.2017).

Synthesis of 1-Cycloalkenylmethyl Phenyl Sulfides (8a—d) by Dehydration of 1-Phenylthiomethylcycloalkanols (7a—d)——1-Cyclohexenylmethyl Phenyl Sulfide (**8b**): A solution of 4.73 g (21.3 mmol) of **7b** in 40 ml of benzene was refluxed for 7 h in the presence of a catalytic amount of *p*-toluenesulfonic acid using a Dean-Stark apparatus. After cooling, the reaction solution was diluted with ether, washed with saturated aqueous $NaHCO_3$ and saturated aqueous NaCl, dried over anhydrous Na_2SO_4, and concentrated *in vacuo*. The residue was subjected to column chromatography over silica gel (ether–hexane 1 : 4) to give 4.13 g (95% yield) of **8b** as a yellow oil: IR ν_{max}^{film} cm^{-1}: 1660 (C=C), 1580 (phenyl). NMR (CCl_4) δ: 1.40—2.20 (8H, m), 3.33 (2H, s, CH_2–S), 5.20—5.50 (1H, m, CH=C), 6.80—7.54 (5H, m, C_6H_5). MS *m/z*: 204 (M^+). Exact mass determination: 204. 0947 (Calcd for $C_{13}H_{16}S$: 204.1973).

The dehydration of the other alcohols **7a**, **7c** and **7d** was carried out in the same way as described above.

1-Cyclopentenylmethyl Phenyl Sulfide (**8a**): 95% yield. IR ν_{max}^{film} cm^{-1}: 1650 (C=C), 1580 (phenyl). NMR (CCl_4) δ: 1.50—2.60 (6H, m), 3.50 (2H, s, CH_2–S), 5.23—5.56 (1H, s, CH=C), 6.90—7.40 (5H, m, C_6H_5). MS *m/z*: 190 (M^+). Exact mass determination: 190.0816 (Calcd for $C_{12}H_{14}S$: 190.0816).

1-Cycloheptenylmethyl Phenyl Sulfide (**8c**): 96% yield. IR ν_{max}^{film} cm^{-1}: 1660 (C=C), 1595 (phenyl). NMR (CCl_4) δ: 1.10—2.50 (10H, m), 3.37 (2H, s, CH_2S), 5.50 (1H, 5, J=6 Hz, CH=C), 6.90—7.50 (5H, m, C_6H_5). MS *m/z*: 218 (M^+). Exact mass determination: 218.1135 (Calcd for $C_{14}H_{18}S$: 218.1130).

1-Cyclododecenylmethyl Phenyl Sulfide (**8d**): 91% yield. IR ν_{max}^{film} cm^{-1}: 1660 (C=C), 1590 (phenyl). NMR (CCl_4) δ: 1.00—2.60 (20H, m), 3.43, 3.47 (2H, s, s, CH_2–S), 4.97—5.57 (1H, m, CH=C), 6.90—7.50 (5H, m, C_6H_5). MS *m/z*: 288 (M^+). Exact mass determination: 288.1912 (Calcd for $C_{19}H_{28}S$: 288.1912).

Silylation of 8a—d——Phenyl α-Trimethylsilyl-1-cyclohexenylmethyl Sulfide (**9b**): A dry 100 ml two-necked flask equipped with a septum inlet and a magnetic stirring bar was flushed with nitrogen and maintained under a positive pressure of nitrogen. A solution of 2.92 ml (20.9 mmol) of diisopropylamine in 5 ml of THF was added to the flask, followed by addition of a 1.5 N hexane solution of butyllithium (13.9 ml, 20.9 mmol) at 0 °C. The mixture was stirred at 0 °C for 30 min, then to −78 °C and a solution of 2.84 g (13.9 mmol) of **8b** in 6 ml of THF was added. The whole was stirred at −78 °C for 2 h, then 2.65 ml (20.9 mmol) of trimethylsilyl chloride was added at −78 °C, and the reaction mixture was stirred at the same temperature for 4 h. The reaction mixture was diluted with ether, washed with 10% aqueous HCl, saturated aqueous $NaHCO_3$, and saturated aqueous NaCl, dried over anhydrous Na_2SO_4, and concentrated under reduced pressure. The residue was subjected to column chromatography over silica gel (ether–hexane 1 : 30) to give 3.76 g (98% yield) of **9b** as a yellow oil: IR ν_{max}^{film} cm^{-1}: 1650 (C=C), 1590 (phenyl). NMR (CCl_4) δ: 0.10 (9H, s, $Si(CH_3)_3$), 1.10—2.60 (8H, m), 3.03 (1H, s, Si–CH–S), 5.20—5.40 (1H, m, CH=C), 6.90—7.60 (5H, m, C_6H_5). MS *m/z*: 276 (M^+). Exact mass determination: 276.1313 (Calcd for $C_{16}H_{24}SSi$: 276.1348).

Silylation of **8a**, **8c**, and **8d** was carried out in the same way as described above.

Phenyl α-Trimethylsilyl-1-cyclopentenylmethyl Sulfide (**9a**): 83% yield. IR ν_{max}^{film} cm^{-1}: 1625 (C=C), 1580 (phenyl). NMR (CCl_4) δ: 0.03 (9H, s, $Si(CH_3)_3$), 1.40—2.40 (6H, m), 3.20 (1H, s, S–CH–Si), 5.05—5.25 (1H, m, CH=C), 6.70—7.20 (5H, m, C_6H_5). MS *m/z*: 262 (M^+). Exact mass determination: 262.1213 (Calcd for $C_{15}H_{22}SSi$: 262.1212).

Phenyl α-Trimethylsilyl-1-cycloheptenylmethyl Sulfide (**9c**): 95% yield. IR ν_{max}^{film} cm^{-1}: 1645 (C=C), 1585 (phenyl). NMR (CCl_4) δ: 0.67 (9H, s, $Si(CH_3)_3$), 1.00—2.30 (10H, m), 3.08 (1H, s, S–CH–Si), 5.42 (1H, t, J=6 Hz,

CH=C), 6.90—7.30 (5H, m, C_6H_5). MS *m/z*: 290 (M^+). Exact mass determination: 290.1531 (Calcd for $C_{17}H_{26}SSi$: 290.1524).

Phenyl α-Trimethylsilyl-1-cyclododecenylmethyl Sulfide (**9d**): 95% yield. IR ν_{max}^{film} cm^{-1}: 1660 (C=C), 1590 (phenyl). NMR (CCl_4) δ: 0.13 (9H, s, $Si(CH_3)_3$), 0.55—2.60 (20H, m), 3.00 (1H, s, S-CH-Si), 5.50 (1H, t, J=8 Hz, CH=C), 6.90—7.50 (5H, m, C_6H_5). MS *m/z*: 360 (M^+). Exact mass determination: 360.2271 (Calcd for $C_{22}H_{36}SSi$: 360.2236).

Aluminum Chloride-Catalyzed Acylation of 9a—d with Acid Chlorides 3a—h. General Procedure——A dry 25 ml two-necked flask equipped with a septum inlet and a magnetic stirring bar, and containing 145 mg (1.09 mmol) of aluminum chloride (powdered finely), was flushed with nitrogen and maintained under a positive pressure of nitrogen. Dichloromethane (1 ml) was added to the flask. The mixture was cooled to −78 °C. A solution of an acid chloride (**3a—h**, 0.72 mmol) in 1 ml of dichloromethane was added to the mixture at −78 °C, followed by dropwise addition of a solution of one of **9a—d** (0.72 mmol) in 1.5 ml of dichloromethane and the reaction mixture was stirred at −78 °C for the time shown in Tables II—IV. The reaction mixture was diluted with ether, washed sequentially with saturated aqueous NaCl, saturated aqueous $NaHCO_3$, and saturated aqueous NaCl, dried over anhydrous Na_2SO_4, and concentrated *in vacuo*. The residue was subjected to preparative TLC (ether–hexane 1:20) to give the γ-acylated products **10**, **12**, **13**, and **14**. The yields are listed in Tables II—IV.

1-(2-Phenylthiomethylenecyclohexyl)-1-ethanone (**10a**): IR ν_{max}^{film} cm^{-1}: 1705 (C=O), 1620 (C=C), 1580 (phenyl). NMR (CCl_4) δ: 0.90—2.50 (8H, m), 2.05 (3H, s, $\overset{O}{\overset{\|}{C}}-CH_3$), 2.90—3.20 (1H, m, $CH-\overset{O}{\overset{\|}{C}}$), 5.95 (1H, s, CH=C), 6.87—7.40 (5H, m, C_6H_5). MS *m/z*: 246 (M^+). Exact mass determination: 246.1090 (Calcd for $C_{15}H_{18}OS$: 246.1079).

1-(2-Phenylthiomethylenecyclohexyl)-1-butanone (**10b**): IR ν_{max}^{film} cm^{-1}: 1715 (C=O), 1660 (C=C), 1590 (phenyl). NMR (CCl_4) δ: 0.99 (3H, t, J=7 Hz, $CH_2\underline{CH_3}$), 1.17—2.87 (10H, m), 2.53 (2H, t, J=7 Hz, $\overset{O}{\overset{\|}{C}}-CH_2$), 2.87—3.32, 3.63—3.95 (1H, m, m, $CH-\overset{O}{\overset{\|}{C}}$), 5.92, 6.03 (1H, s, s, CH=C), 6.90—7.57 (5H, m, C_6H_5). MS *m/z*: 274 (M^+). Exact mass determination: 274.1363 (Calcd for $C_{17}H_{22}OS$: 274.1390).

Z-1-(2-Phenylthiomethylenecyclohexyl)-1-pentanone (**10c**): IR ν_{max}^{film} cm^{-1}: 1710 (C=O), 1660 (C=C), 1585 (phenyl). NMR (CCl_4) δ: 0.85 (3H, t, J=6 Hz, $CH_2\underline{CH_3}$), 1.03—2.80 (14H, m), 3.00—3.27 (1H, m, $CH-\overset{O}{\overset{\|}{C}}$), 5.90 (1H, s, CH=C), 7.00—7.40 (5H, m, C_6H_5). MS *m/z*: 288 (M^+). Exact mass determination: 288.1550 (Calcd for $C_{18}H_{24}OS$: 288.1548).

E-**10c**: IR ν_{max}^{film} cm^{-1}: 1710 (C=O), 1660 (C=C), 1585 (phenyl). NMR (CCl_4) δ: 0.90 (3H, t, J=6 Hz, $CH_2\underline{CH_3}$), 1.10—2.70 (14H, m), 3.68—3.90 (1H, m, $CH-\overset{O}{\overset{\|}{C}}$), 6.00 (1H, s, CH=C), 6.93—7.40 (5H, m, C_6H_5). MS *m/z*: 288 (M^+). Exact mass determination: 288.1547 (Calcd for $C_{18}H_{24}OS$: 288.1547).

1-(2-Phenylthiomethylenecyclohexyl)-1-heptanone (**10d**): IR ν_{max}^{film} cm^{-1}: 1705 (C=O), 1640 (C=C), 1580 (phenyl). NMR (CCl_4) δ: 0.87 (3H, t, J=5 Hz, $CH_2\underline{CH_3}$), 1.00—2.80 (18H, m), 3.00—3.28, 3.70—3.90 (1H, m, m, $CH-\overset{O}{\overset{\|}{C}}$), 5.93, 6.03 (1H, s, s, CH=C), 6.93—7.40 (5H, m, C_6H_5). MS *m/z*: 316 (M^+). Exact mass determination: 316.1881 (Calcd for $C_{20}H_{28}OS$: 316.1861).

1-(2-Phenylthiomethylenecyclohexyl)-1-octanone (**10e**): IR ν_{max}^{film} cm^{-1}: 1710 (C=O), 1650 (C=C), 1580 (phenyl). NMR (CCl_4) δ: 0.88 (3H, t, J=5 Hz, $CH_2\underline{CH_3}$), 1.03—2.90 (20H, m), 3.03—3.30, 3.70—3.93 (1H, m, m, $CH-\overset{O}{\overset{\|}{C}}$), 5.95, 6.05 (1H, s, s, CH=C), 6.90—7.47 (5H, m, C_6H_5). MS *m/z*: 330 (M^+). Exact mass determination: 330.2009 (Calcd for $C_{21}H_{30}OS$: 330.2016).

2-Phenyl-1-(2-phenylthiomethylenecyclohexyl)-1-ethanone (**10f**): IR ν_{max}^{film} cm^{-1}: 1710 (C=O), 1650 (C=C), 1580 (phenyl). NMR (CCl_4) δ: 1.00—2.50 (8H, m), 3.63 (2H, s, $\overset{O}{\overset{\|}{C}}-CH_2$), 3.87—4.07 (1H, m, $CH-\overset{O}{\overset{\|}{C}}$), 6.10 (1H, s, CH=C), 7.00—7.40 (10H, m, $2C_6H_5$). MS *m/z*: 322 (M^+). Exact mass determination: 322.1399 (Calcd for $C_{21}H_{22}OS$: 322.1392).

3-Phenyl-1-(2-phenylthiomethylenecyclohexyl)-2-propen-1-one (**10g**): IR ν_{max}^{film} cm^{-1}: 1680 (α,β-unsat. ketone), 1605 (olefin), 1580 (phenyl). NMR (CCl_4) δ: 1.10—2.70 (8H, m), 3.20—3.53 (1H, m, $CH-\overset{O}{\overset{\|}{C}}$), 5.97 (1H, s, S-CH=C), 6.37—7.73 (12H, m, C_6H_5 and $CH=CH-C_6H_5$). MS *m/z*: 334 (M^+). Exact mass determination: 334.1362 (Calcd for $C_{22}H_{22}OS$: 334.1390).

1-(2-Phenylthiomethylenecyclopentyl)-1-butanone (**12a**): IR ν_{max}^{film} cm^{-1}: 1710 (C=O), 1620 (C=C), 1585 (phenyl). NMR (CCl_4) δ: 0.88 (3H, t, J=8 Hz, $CH_2\underline{CH_3}$), 1.20—2.17 (8H, m), 2.17—2.80 (2H, m, $\overset{O}{\overset{\|}{C}}-CH_2$), 3.20—3.70 (1H, m, $CH-\overset{O}{\overset{\|}{C}}$), 5.93—6.17 (1H, m, CH=C), 7.00—7.60 (5H, m, C_6H_5). MS *m/z*: 260 (M^+). Exact mass

determination: 260.1258 (Calcd for $C_{16}H_{20}OS$: 260.1235).

1-(2-Phenylthiomethylenecyclopentyl)-1-pentanone (**12b**): IR ν_{max}^{film} cm^{-1}: 1700 (C=O), 1650 (C=C), 1580 (phenyl). NMR (CCl_4) δ: 0.90 (3H, t, J=7 Hz, CH_2CH_3), 1.03—2.17 (10H, m), 2.17—2.80 (2H, m, $\overset{O}{\overset{\|}{C}}-CH_2$), 3.20—3.70 (1H, m, $CH-\overset{O}{\overset{\|}{C}}$), 5.96—6.10 (1H, m, CH=C), 6.90—7.40 (5H, m, C_6H_5). MS *m/z*: 274 (M^+). Exact mass determination: 274.1412 (Calcd for $C_{17}H_{22}OS$: 274.1392).

1-(2-Phenylthiomethylenecyclopentyl)-1-heptanone (**12c**): IR ν_{max}^{film} cm^{-1}: 1710 (C=O), 1650 (C=C), 1580 (phenyl). NMR (CCl_4) δ: 0.87 (3H, t, J=5 Hz, CH_2CH_3), 1.07—2.17 (14H, m), 2.17—2.90 (2H, m, $\overset{O}{\overset{\|}{C}}-CH_2$), 3.20—3.70 (1H, m, $CH-\overset{O}{\overset{\|}{C}}$), 5.90—6.13 (1H, m, CH=C), 6.90—7.40 (5H, m, C_6H_5). MS *m/z*: 203 (M^+). Exact mass determination: 302.1731 (Calcd for $C_{19}H_{26}OS$: 302.1704).

1-(2-Phenylthiomethylenecyclopentyl)-1-octanone (**12d**): IR ν_{max}^{film} cm^{-1}: 1700 (C=O), 1600 (C=C), 1580 (phenyl). NMR (CCl_4) δ: 0.87 (3H, t, J=4 Hz, CH_2CH_3), 1.03—2.13 (16H, m), 2.13—2.80 (2H, m, $\overset{O}{\overset{\|}{C}}-CH_2$), 3.20—3.70 (1H, m, $CH-\overset{O}{\overset{\|}{C}}$), 5.90—6.10 (1H, m, CH=C), 6.90—7.40 (5H, m, C_6H_5). MS *m/z*: 316 (M^+). Exact mass determination: 316.1859 (Calcd for $C_{20}H_{28}OS$: 316.1859).

2-Phenyl-1-(2-phenylthiomethylenecyclopentyl)-1-ethanone (**12e**): IR ν_{max}^{film} cm^{-1}: 1705 (C=O), 1660 (C=C), 1580 (phenyl). NMR (CCl_4) δ: 1.47—2.77 (6H, m), 3.63 (2H, s, $\overset{O}{\overset{\|}{C}}-CH_2$), 3.85—4.10 (1H, m, $CH-\overset{O}{\overset{\|}{C}}$), 5.80—6.00 (1H, m, CH=C), 6.80—7.50 (10H, m, $2C_6H_5$). MS *m/z*: 308 (M^+). Exact mass determination: 308.1244 (Calcd for $C_{20}H_{20}OS$: 308.1236).

3-Phenyl-1-(2-phenylthiomethylenecyclopentyl)-1-propanone (**12f**): IR ν_{max}^{film} cm^{-1}: 1710 (C=O), 1660 (C=C), 1590 (phenyl). NMR (CCl_4) δ: 1.40—3.00 (10H, m), 3.15—3.55 (1H, m, $CH-\overset{O}{\overset{\|}{C}}$), 5.83—6.10 (1H, m, CH=C), 6.90—7.50 (10H, m, $2C_6H_5$). MS *m/z*: 322 (M^+). Exact mass determination: 322.1385 (Calcd for $C_{21}H_{22}OS$: 322.1390).

3-Phenyl-1-(2-phenylthiomethylenecyclopentyl)-2-propen-1-one (**12g**): IR ν_{max}^{film} cm^{-1}: 1660 (α,β-unsat. ketone), 1605 (C=C), 1580 (phenyl). NMR (CCl_4) δ: 1.20—2.90 (6H, m), 3.45—3.93 (1H, m, $CH-\overset{O}{\overset{\|}{C}}$), 6.90—7.87 (13H, m, $C_6H_5S-CH=C$ and $CH=CH-C_6H_5$). MS *m/z*: 320 (M^+). Exact mass determination: 320.1214 (Calcd for $C_{21}H_{20}OS$: 320.1234).

1-(2-Phenylthiomethylenecycloheptyl)-1-butanone (**13a**): IR ν_{max}^{film} cm^{-1}: 1710 (C=O), 1660 (C=C), 1580 (phenyl). NMR (CCl_4) δ: 0.95 (3H, t, J=7 Hz, CH_2CH_3), 1.03—2.85 (14H, m), 3.10—3.45, 3.70—4.03 (1H, m, m, $CH-\overset{O}{\overset{\|}{C}}$), 5.91, 6.03 (1H, s, s, CH=C), 7.00—7.50 (5H, m, C_6H_5). MS *m/z*: 288 (M^+). Exact mass determination: 288.1569 (Calcd for $C_{18}H_{24}OS$: 288.1549).

1-(2-Phenylthiomethylenecycloheptyl)-1-pentanone (**13b**): IR ν_{max}^{film} cm^{-1}: 1710 (C=O), 1665 (C=C), 1580 (phenyl). NMR (CCl_4) δ: 0.93 (3H, t, J=4 Hz, CH_2CH_3), 1.10—2.90 (16H, m), 3.27. 3.83 (1H, tt, J=8, 8 Hz, $CH-\overset{O}{\overset{\|}{C}}$), 5.95, 6.05 (1H, s, s, CH=C), 6.90—7.50 (5H, m, C_6H_5). MS *m/z*: 302 (M^+). Exact mass determination: 302.1706 (Calcd for $C_{19}H_{26}OS$: 302.1705).

1-(2-Phenylthiomethylenecycloheptyl)-1-heptanone (**13c**): IR ν_{max}^{film} cm^{-1}: 1705 (C=O), 1660 (C=C), 1580 (phenyl). NMR (CCl_4) δ: 0.90 (3H, t, J=4 Hz, CH_2CH_3), 1.07—2.80 (20H, m), 3.30, 3.87 (1H, tt, J=8, 7 Hz, $CH-\overset{O}{\overset{\|}{C}}$), 6.00, 6.10 (1H, s, s, CH=C), 7.00—7.50 (5H, m, C_6H_5). MS *m/z*: 330 (M^+). Exact mass determination: 330.2027 (Calcd for $C_{21}H_{30}OS$: 330.2017).

1-(2-Phenylthiomethylenecycloheptyl)-1-octanone (**13d**): IR ν_{max}^{film} cm^{-1}: 1710 (C=O), 1650 (C=C), 1580 (phenyl). NMR (CCl_4) δ: 0.85 (3H, t, J=4 Hz, CH_2CH_3), 1.00—2.80 (22H, m), 3.23, 3.80 (1H, tt, J=8, 7 Hz, $CH-\overset{O}{\overset{\|}{C}}$), 5.90, 6.00 (1H, s, s, CH=C), 7.00—7.40 (5H, m, C_6H_5). MS *m/z*: 344 (M^+). Exact mass determination: 344.2164 (Calcd for $C_{22}H_{32}OS$: 344.2172).

3-Phenyl-1-(2-phenylthiomethylenecycloheptyl)-2-propen-1-one (**13e**): IR ν_{max}^{film} cm^{-1}: 1670 (α,β-unsat. ketone), 1610 (olefin), 1580 (phenyl). NMR (CCl_4) δ: 1.00—2.80 (10H, m), 3.52 (1H, t, J=8 Hz, $CH-\overset{O}{\overset{\|}{C}}$), 6.00 (1H, s, $S-CH=C$), 6.43—7.80 (12H, m, $S-C_6H_5$ and $CH=CH-C_6H_5$). MS *m/z*: 348 (M^+). Exact mass determination: 348.1569 (Calcd for $C_{23}H_{24}OS$: 348.1548).

1-(2-Phenylthiomethylenecyclododecyl)-1-butanone (**14a**): IR ν_{max}^{film} cm^{-1}: 1720 (C=O), 1640 (C=C), 1595 (phenyl). NMR (CCl_4) δ: 0.97 (3H, t, J=7 Hz, CH_2CH_3), 1.12—2.80 (24H, m), 3.27—3.40, 3.87—4.03 (1H, m, m,

CH–C), 6.03, 6.13 (1H, s, s, CH=C), 6.93—7.50 (5H, m, C_6H_5). MS *m/z*: 358 (M^+). Exact mass determination: 358.2293 (Calcd for $C_{23}H_{34}OS$: 358.2329).

1-(2-Phenylthiomethylenecyclododecyl)-1-pentanone (**14b**): IR ν_{max}^{film} cm^{-1}: 1705 (C=O), 1650 (C=C), 1580 (phenyl). NMR (CCl_4) δ: 0.90 (3H, t, J=6 Hz, CH_2CH_3), 1.10—2.70 (26H, m), 3.38—3.50, 3.83—4.00 (1H, m, m, CH–C), 6.00, 6.13 (1H, s, s, CH=C), 6.97—7.45 (5H, m, C_6H_5). MS *m/z*: 372 (M^+). Exact mass determination: 372.2487 (Calcd for $C_{24}H_{36}OS$: 372.2487).

1-(2-Phenylthiomethylenecyclododecyl)-1-heptanone (**14c**): IR ν_{max}^{film} cm^{-1}: 1710 (C=O), 1660 (C=C), 1580 (phenyl). NMR (CCl_4) δ: 0.88 (3H, t, J=4 Hz, CH_2CH_3), 1.07—2.80 (30H, m), 3.40—3.58, 3.90—4.10 (1H, m, m, CH–C), 6.05, 6.13 (1H, s, s, CH=C), 7.00—7.43 (5H, m, C_6H_5). MS *m/z*: 400 (M^+). Exact mass determination: 400.2769 (Calcd for $C_{26}H_{40}OS$: 400.2799).

1-(2-Phenylmethylenecyclododecyl)-1-octanone (**14d**): IR ν_{max}^{film} cm^{-1}: 1710 (C=O), 1660 (C=C), 1580 (phenyl). NMR (CCl_4) δ: 0.88 (3H, t, J=4 Hz, CH_2CH_3), 1.03—2.73 (32H, m), 3.41—3.53, 3.90—4.08 (1H, m, m, CH–C), 6.03, 6.13 (1H, s, s, CH=C), 6.90—7.47 (5H, m, C_6H_5). MS *m/z*: 414 (M^+). Exact mass determination: 414.2947 (Calcd for $C_{27}H_{42}OS$: 414.2954).

3-Phenyl-1-(2-phenylthiomethylenecyclododecyl)-2-propen-1-one (**14e**): IR ν_{max}^{film} cm^{-1}: 1690 (α,β-unsat. ketone), 1620 (olefin), 1590 (phenyl). NMR (CCl_4) δ: 0.80—2.70 (20H, m), 4.03—4.25 (1H, m, CH–C), 6.33—7.77 (13H, m, C_6H_5S–CH=C and CH=CH–C_6H_5). MS *m/z*: 418 (M^+). Exact mass determination: 418.2325 (Calcd for $C_{28}H_{34}OS$: 418.2330).

Conversion of the Acylated Products into 2-Cyclopentenone Derivatives. General Procedure——A solution of one of **10a—e** (0.36 mmol) in 5 ml of benzene was refluxed for 2 h in the presence of 69 mg (0.36 mmol) of *p*-toluenesulfonic acid. After cooling, the solution was diluted with ether, washed with 10% NaOH and saturated aqueous NaCl, dried over anhydrous Na_2SO_4, and concentrated *in vacuo*. The residue was subjected to preparative TLC (ether–hexane 1 : 20) to give the corresponding 2-cyclopentenone derivative (**15a—e**).

3a,4,5,6,7,7a-Hexahydro-1*H*-inden-1-one (**15a**): 52% yield. IR ν_{max}^{film} cm^{-1}: 1705 (α,β-unsat. ketone), 1660 (C=C). NMR (CCl_4) δ: 0.77—2.53 (9H, m), 2.53—2.97 (1H, m, CH–C), 6.83—7.43 (2H, m, CH=CH).

3a,4,5,6,7,7a-Hexahydro-2-ethyl-1*H*-inden-1-one (**15b**): 51% yield. IR ν_{max}^{film} cm^{-1}: 1700 (α,β-unsat. ketone), 1650 (C=C). NMR (CCl_4) δ: 0.90 (3H, t, J=6 Hz, CH_2CH_3), 1.07—2.80 (12H, m), 7.07—7.20 (1H, m, CH=C). MS *m/z*: 164 (M^+). Exact mass determination: 164.1217 (Calcd for $C_{11}H_{16}O$: 164.1201).

3a,4,5,6,7,7a-Hexahydro-2-propyl-1*H*-inden-1-one (**15c**): 56% yield. IR ν_{max}^{film} cm^{-1}: 1695 (α,β-unsat. ketone), 1650 (C=C). NMR (CCl_4) δ: 0.83 (3H, t, J=6 Hz, CH_2CH_3), 1.00—2.73 (14H, m), 7.00—7.25 (1H, m, CH=C). MS *m/z*: 178 (M^+). Exact mass determination: 178.1378 (Calcd for $C_{12}H_{18}O$: 178.1358).

3a,4,5,6,7,7a-Hexahydro-2-pentyl-1*H*-inden-1-one (**15d**): 53% yield. IR ν_{max}^{film} cm^{-1}: 1700 (α,β-unsat. ketone), 1655 (C=C). NMR (CCl_4) δ: 0.90 (3H, t, J=5 Hz, CH_2CH_3), 1.03—2.75 (18H, m), 7.10—7.27 (1H, m, CH=C). MS *m/z*: 206 (M^+). Exact mass determination: 206.1669 (Calcd for $C_{14}H_{22}O$: 206.1669).

3a,4,5,6,7,7a-Hexahydro-2-hexyl-1*H*-inden-1-one (**15e**): 59% yield. IR ν_{max}^{film} cm^{-1}: 1705 (α,β-unsat. ketone), 1660 (C=C). NMR (CCl_4) δ: 0.87 (3H, t, J=5 Hz, CH_2CH_3), 1.07—2.06 (20H, m), 7.07—7.27 (1H, m, CH=C). MS *m/z*: 220 (M^+). Exact mass determination: 220.1799 (Calcd for $C_{15}H_{24}O$: 220.1827).

Conversion of the Acylated Compounds into α-Phenylthiofuran Derivatives. General Procedure——A solution of an acylated compound (**10b—e, 13a—d, 4a—e, 4n, 4i**; 0.18 mmol) in 5 ml of benzene was refluxed for 2 h in the presence of 18 mg (0.18 mmol) of concentrated sulfuric acid. After cooling, the mixture was diluted with ether, washed with 10% aqueous NaOH and saturated aqueous NaCl, dried over anhydrous Na_2SO_4, and concentrated *in vacuo*. The residue was subjected to preparative TLC (ether–hexane 1 : 20) to give the corresponding α-phenylthiofuran (**16a—h, 18a—g**).

4,5,6,7-Tetrahydro-1-phenylthio-3-propylisobenzofuran (**16a**): 61% yield. IR ν_{max}^{film} cm^{-1}: 1625 (C=C), 1585 (phenyl). NMR (CCl_4) δ: 0.92 (3H, t, J=7 Hz, CH_2CH_3), 1.17—1.97 (6H, m) 2.23—2.67 (6H, m), 6.73—7.43 (5H, m, C_6H_5). MS *m/z*: 272 (M^+). Exact mass determination: 272.1266 (Calcd for $C_{17}H_{20}OS$: 272.1232).

4,5,6,7-Tetrahydro-3-butyl-1-phenylthioisobenzofuran (**16b**): 57% yield. IR ν_{max}^{film} cm^{-1}: 1620 (C=C), 1580 (phenyl). NMR (CCl_4) δ: 0.90 (3H, t, J=5 Hz, CH_2CH_3), 1.10—1.90 (8H, m), 2.23—2.67 (6H, m), 6.70—7.57 (5H, m, C_6H_5). MS *m/z*: 286 (M^+). Exact mass determination: 286.1398 (Calcd for $C_{18}H_{22}OS$: 286.1392).

4,5,6,7-Tetrahydro-3-hexyl-1-phenylthioisobenzofuran (**16c**): 52% yield. IR ν_{max}^{film} cm^{-1}: 1625 (C=C), 1590 (phenyl). NMR (CCl_4) δ: 0.87 (3H, t, J=5 Hz, CH_2CH_3), 1.03—1.90 (12H, m), 2.10—2.63 (6H, m), 6.73—7.45 (5H, m, C_6H_5). MS *m/z*: 314 (M^+). Exact mass determination: 314.1726 (Calcd for $C_{20}H_{26}OS$: 314.1705).

4,5,6,7-Tetrahydro-3-heptyl-1-phenylthioisobenzofuran (**16d**): 59% yield. IR ν_{max}^{film} cm^{-1}: 1625 (C=C), 1590 (phenyl). NMR (CCl_4) δ: 0.85 (3H, t, J=5 Hz, CH_2CH_3), 1.00—1.95 (14H, m), 2.10—2.65 (6H, m), 6.65—7.40 (5H,

m, C_6H_5). MS *m/z*: 328 (M^+). Exact mass determination: 328.1845 (Calcd for $C_{21}H_{28}OS$: 328.1860).

5,6,7,8-Tetrahydro-1-phenylthio-3-propyl-4*H*-cyclohepta[*c*]furan (**16e**): 68% yield. IR ν_{max}^{film} cm^{-1}: 1625 (C=C), 1585 (phenyl). NMR (CCl_4) δ: 0.87 (3H, t, J=7 Hz, $CH_2C\underline{H}_3$), 1.30—1.95 (8H, m), 2.20—2.70 (6H, m), 6.67—7.67 (5H, m, C_6H_5). MS *m/z*: 286 (M^+). Exact mass determination: 286.1375 (Calcd for $C_{18}H_{22}OS$: 286.1390).

5,6,7,8-Tetrahydro-3-butyl-1-phenylthio-4*H*-cyclohepta[*c*]furan (**16f**): 56% yield. IR ν_{max}^{film} cm^{-1}: 1625 (C=C), 1585 (phenyl). NMR (CCl_4) δ: 0.87 (3H, t, J=5 Hz, $CH_2C\underline{H}_3$), 1.03—1.90 (10H, m), 2.20—2.67 (6H, m), 6.73—7.50 (5H, m, C_6H_5). MS *m/z*: 300 (M^+). Exact mass determination: 300.1552 (Calcd for $C_{19}H_{24}OS$: 300.1549).

5,6,7,8-Tetrahydro-3-hexyl-1-phenylthio-4*H*-cyclohepta[*c*]furan (**16g**): 53% yield. IR ν_{max}^{film} cm^{-1}: 1625 (C=C), 1585 (phenyl). NMR (CCl_4) δ: 0.88 (3H, t, J=5 Hz, $CH_2C\underline{H}_3$), 1.03—1.90 (14H, m), 2.23—2.70 (6H, m), 6.67—7.50 (5H, m, C_6H_5). MS *m/z*: 328 (M^+). Exact mass determination: 328.1844 (Calcd for $C_{21}H_{28}OS$: 328.1859).

5,6,7,8-Tetrahydro-3-heptyl-1-phenylthio-4*H*-cyclohepta[*c*]furan (**16h**): 71% yield. IR ν_{max}^{film} cm^{-1}: 1625 (C=C), 1585 (phenyl). NMR (CCl_4) δ: 0.85 (3H, t, J=5 Hz, $CH_2C\underline{H}_3$), 1.00—1.83 (16H, m), 2.17—2.67 (6H, m), 6.65—7.43 (5H, m, C_6H_5). MS *m/z*: 342 (M^+). Exact mass determination: 342.2030 (Calcd for $C_{22}H_{30}OS$: 342.2018).

3,5-Dimethyl-2-phenylthiofuran (**18a**): 43% yield. IR ν_{max}^{film} cm^{-1}: 1605 (C=C), 1585 (phenyl). NMR (CCl_4) δ: 2.00 (3H, s, CH_3–C=C–O), 2.23 (3H, s, C=C(O)–CH_3), 5.77 (1H, s, HC=C–O), 6.70—7.40 (5H, m, C_6H_5). MS *m/z*: 204 (M^+). Exact mass determination: 204.0598 (Calcd for $C_{12}H_{12}OS$: 204.0609).

3-Methyl-2-phenylthio-5-propylfuran (**18b**): 61% yield. IR ν_{max}^{film} cm^{-1}: 1600 (C=C), 1580 (phenyl). NMR (CCl_4) δ: 0.93 (3H, t, J=7 Hz, $CH_2C\underline{H}_3$), 1.17—2.10 (2H, m, $C\underline{H}_2CH_3$), 2.03 (3H, s, CH_3–C=C–O), 2.53 (2H, t, J=7 Hz, CH_2–C(O)=C), 5.85 (1H, s, HC=C–O), 6.83—7.50 (5H, m, C_6H_5). MS *m/z*: 232 (M^+). Exact mass determination: 232.0931 (Calcd for $C_{14}H_{16}OS$: 232.9021).

5-Butyl-3-methyl-2-phenylthiofuran (**18c**): 54% yield. IR ν_{max}^{film} cm^{-1}: 1600 (C=C), 1580 (phenyl). NMR (CCl_4) δ: 0.92 (3H, t, J=6 Hz, $CH_2C\underline{H}_3$), 1.10—1.90 (4H, m, $(C\underline{H}_2)_2CH_3$), 2.03 (3H, s, CH_3–C=C–O), 2.56 (2H, t, J=7 Hz, CH_2–C(O)=C), 5.87 (1H, s, HC=C–O), 6.90—7.43 (5H, m, C_6H_5). MS *m/z*: 246 (M^+). Exact mass determination: 246.1059 (Calcd for $C_{15}H_{18}OS$: 246.1077).

5-Hexyl-3-methyl-2-phenylthiofuran (**18d**): 51% yield. IR ν_{max}^{film} cm^{-1}: 1605 (C=C), 1585 (phenyl). NMR (CCl_4) δ: 0.84 (3H, t, J=5 Hz, $CH_2C\underline{H}_3$), 1.00—1.90 (8H, m, $(C\underline{H}_2)_4CH_3$), 2.00 (3H, s, CH_3–C=C–O), 2.50 (2H, t, J=7 Hz, CH_2–C(O)=C), 5.78 (1H, s, HC=C–O), 6.63—7.27 (5H, m, C_6H_5). MS *m/z*: 274 (M^+). Exact mass determination: 274.1374 (Calcd for $C_{17}H_{22}OS$: 274.1389).

5-Heptyl-3-methyl-2-phenylthiofuran (**18e**): 55% yield. IR ν_{max}^{film} cm^{-1}: 1605 (C=C), 1580 (phenyl). NMR (CCl_4) δ: 0.74 (3H, t, J=5 Hz, $CH_2C\underline{H}_3$), 1.07—1.87 (10H, m, $(C\underline{H}_2)_5CH_3$), 2.00 (3H, s, CH_3–C=C–O), 2.51 (2H, t, J=7 Hz, CH_2–C(O)=C), 5.80 (1H, s, HC=C–O), 6.77—7.33 (5H, m, C_6H_5). MS *m/z*: 288 (M^+). Exact mass determination: 288.1532 (Calcd for $C_{18}H_{24}OS$: 288.1547).

5-Hexyl-4-methyl-2-phenylthiofuran (**18f**): 37% yield. IR ν_{max}^{film} cm^{-1}: 1620 (C=C), 1585 (phenyl). NMR (CCl_4) δ: 0.87 (3H, t, J=5 Hz, $CH_2C\underline{H}_3$), 1.03—1.73 (8H, m, $(C\underline{H}_2)_4CH_3$), 1.93 (3H, s, CH_3–C=C–O), 2.53 (2H, t, J=7 Hz, CH_2–C(O)=C), 6.37 (1H, s, HC=C–O), 6.87—7.40 (5H, m, C_6H_5). MS *m/z*: 274 (M^+). Exact mass determination: 274.1383 (Calcd for $C_{17}H_{22}OS$: 274.1390).

5-Hexyl-2-phenylthiofuran (**18g**): 9% yield. IR ν_{max}^{film} cm^{-1}: 1585 (aromatic). NMR (CCl_4) δ: 0.83 (3H, t, J=5 Hz, $CH_2C\underline{H}_3$), 1.00—1.90 (8H, m, $(C\underline{H}_2)_4CH_3$), 2.52 (2H, t, J=7 Hz, CH_2–C=C), 5.84 (1H, d, J=3 Hz, $C\underline{H}$=C(O)–CH_2), 6.40 (1H, d, J=3 Hz, CH=C(O)–S), 6.82—7.40 (5H, m, C_6H_5). MS *m/z*: 260 (M^+). Exact mass determination: 260.1239 (Calcd for $C_{16}H_{20}OS$: 260.1234).

Hydrogenetic Desulfurization of α-Phenylthiofurans with Raney Ni. General Procedure——A mixture of an α-phenylthiofuran (**16a—h**, 0.10 mmol) and Raney Ni W_4 (deactivated by refluxing in acetone for 3 h; 0.3 ml (EtOH)) in 5 ml of ethyl alcohol was refluxed for 2 h. The mixture was filtered and the filtrate was concentrated *in vacuo*. The residue was subjected to preparative TLC (hexane) to give the corresponding furan (**17a—h**).

4,5,6,7-Tetrahydro-1-propylisobenzofuran (**17a**): 75% yield. IR ν_{max}^{film} cm^{-1}: 1640, 1610 (C=C). NMR (CCl_4) δ: 0.90 (3H, t, J=7 Hz, $CH_2C\underline{H}_3$), 1.37—2.03 (6H, m), 2.03—3.67 (6H, m), 6.83 (1H, s, C=CH–O). MS *m/z*: 164 (M^+). Exact mass determination: 164.1200 (Calcd for $C_{11}H_{16}O$: 164.1200).

4,5,6,7-Tetrahydro-1-butylisobenzofuran (**17b**): 84% yield. IR ν_{max}^{film} cm^{-1}: 1625, 1600 (C=C). NMR (CCl_4) δ: 0.85 (3H, t, J=6 Hz, $CH_2C\underline{H}_3$), 1.07—1.83 (8H, m), 2.17—2.60 (6H, m), 6.78 (1H, s, C=CH–O). MS *m/z*: 178 (M^+). Exact mass determination: 178.1360 (Calcd for $C_{12}H_{18}O$: 178.1358).

4,5,6,7-Tetrahydro-1-hexylisobenzofuran (**17c**): 94% yield. IR ν_{max}^{film} cm^{-1}: 1640, 1605 (C=C). NMR (CCl_4) δ: 0.90 (3H, t, J=5 Hz, $CH_2C\underline{H}_3$), 1.07—2.00 (12H, m), 2.10—2.63 (6H, m), 6.85 (1H, s, C=CH–O). MS *m/z*: 206

(M^+). Exact mass determination: 206.1685 (Calcd for $C_{14}H_{22}O$: 206.1670).

4,5,6,7-Tetrahydro-1-heptylisobenzofuran (**17d**): 89% yield. IR ν_{max}^{film} cm^{-1}: 1640, 1605 (C=C). NMR (CCl_4) δ: 0.90 (3H, t, J=4 Hz, $CH_2C\underline{H}_3$), 1.07—1.90 (14H, m), 2.23—2.67 (6H, m), 6.87 (1H, s, C=C$\underline{H}$–O). MS *m/z*: 220 (M^+). Exact mass determination: 220.1823 (Calcd for $C_{15}H_{24}O$: 220.1826).

5,6,7,8-Tetrahydro-1-propyl-4*H*-cyclohepta[*c*]furan (**17e**): 95% yield. IR ν_{max}^{film} cm^{-1}: 1640, 1605 (C=C). NMR (CCl_4) δ: 0.80 (3H, t, J=7 Hz, $CH_2C\underline{H}_3$), 1.25—1.90 (8H, m), 2.13—2.53 (6H, m), 6.75 (1H, s, C=C$\underline{H}$–O). MS *m/z*: 178 (M^+). Exact mass determination: 178.1386 (Calcd for $C_{12}H_{18}O$: 178.1358).

5,6,7,8-Tetrahydro-1-butyl-4*H*-cyclohepta[*c*]furan (**17f**): 77% yield. IR ν_{max}^{film} cm^{-1}: 1640, 1605 (C=C). NMR (CCl_4) δ: 0.87 (3H, t, J=5 Hz, $CH_2C\underline{H}_3$), 1.05—1.85 (10H, m), 2.17—2.83 (6H, m), 6.73 (1H, s, C=C$\underline{H}$–O). MS *m/z*: 192 (M^+). Exact mass determination: 192.1483 (Calcd for $C_{13}H_{20}O$: 192.1513).

5,6,7,8-Tetrahydro-1-hexyl-4*H*-cyclohepta[*c*]furan (**17g**): 88% yield. IR ν_{max}^{film} cm^{-1}: 1640, 1605 (C=C). NMR (CCl_4) δ: 0.87 (3H, t, J=5 Hz, $CH_2C\underline{H}_3$), 1.07—2.00 (14H, m), 2.13—2.60 (6H, m), 6.82 (1H, s, C=C$\underline{H}$–O). MS *m/z*: 220 (M^+). Exact mass determination: 220.1819 (Calcd for $C_{15}H_{24}O$: 220.1825).

5,6,7,8-Tetrahydro-1-heptyl-4*H*-cyclohepta[*c*]furan (**17h**): 76% yield. IR ν_{max}^{film} cm^{-1}: 1635, 1600 (C=C). NMR (CCl_4) δ: 0.85 (3H, t, J=5 Hz, $CH_2C\underline{H}_3$), 1.03—1.97 (16H, m), 2.15—2.70 (6H, m), 6.72 (1H, s, C=C$\underline{H}$–O). MS *m/z*: 234 (M^+). Exact mass determination: 234.1978 (Calcd for $C_{16}H_{26}O$: 234.1983).

References

1) For leading reviews see *a*) D. A. Evans and G. C. Andrews, *Acc. Chem. Res.*, **7**, 147 (1974); *b*) M. Ono, *Yuki Gosei Kagaku Kyokai Shi*, **38**, 836, 923 (1980); *c*) D. Hoppe, *Angew. Chem. Int. Ed. Engl.*, **23**, 932 (1984).
2) J. F. Biellmann and J. B. Ducep, *Tetrahedron Lett.*, **1968**, 5629; K. Oshima, H. Takahashi, H. Yamamoto, and H. Nozaki, *J. Am. Chem. Soc.*, **95**, 2693 (1973); P. L. Stotter and R. E. Hornish, *ibid.*, **95**, 4444 (1973); K. Oshima, H. Yamamoto, and H. Nozaki, *ibid.*, **95**, 4446 (1973); H. Takahashi, K. Oshima, H. Yamamoto, and H. Nozaki, *ibid.*, **95**, 5803 (1973); K. Oshima, H. Yamamoto, and H. Nozaki, *ibid.*, **95**, 7926 (1973); P. M. Atlani, J. F. Biellmann, S. Dube, and J. J. Vicens, *Tetrahedron Lett.*, **1974**, 2665; K.-H. Geiss, B. Seuring, R. Pieter, and D. Seebach, *Angew. Chem.*, **86**, 484 (1974); M. Pohmakotr, K.-H. Geiss, and D. Seebach, *Chem. Ber.*, **112**, 1420 (1979); K. Tanaka, M. Terauchi, and A. Kaji, *Chem. Lett.*, **1981**, 315.
3) Y. Yamamoto, H. Yatagai, and K. Maruyama, *Chem. Lett.*, **1979**, 385.
4) Y. Yamamoto, H. Yatagai, and K. Maruyama, *J. Org. Chem.*, **45**, 195 (1980).
5) T. Hayashi, *Tetrahedron Lett.*, **1974**, 339; T. Nakai, H. Shiono, and M. Okawara, *ibid.*, **1974**, 3625; T. Hayashi, N. Fujitaka, T. Oishi, and T. Takeshima, *ibid.*, **1980**, 303; T. Hayashi, M. Yanagida, Y. Matsuda, and T. Oishi, *ibid.*, **1983**, 2665.
6) T. Mukaiyama, K. Narasaka, K. Maekawa, and M. Furusato, *Bull. Chem. Soc. Jpn.*, **44**, 2285 (1971).
7) K. Hirai and Y. Kishida, *Tetrahedron Lett.*, **1972**, 2743.
8) K. Hiroi and L.-M. Chen, *Chem. Commun.*, **1981**, 377.
9) K. Hiroi, H. Sato, and K. Kotsuji, *Chem. Lett.*, **1986**, 743.
10) K. Hiroi and H. Sato, *Synthesis*, "in press."
11) H. Sakurai, *Pure Appl. Chem.*, **54**, 1 (1984); E. W. Colvin, "Silicon in Organic Synthesis," Butterworths, London, 1981; T. H. Chan and I. Fleming, *Synthesis*, **1979**, 761.
12) K. S. Kyler and D. S. Watt, *J. Org. Chem.*, **46**, 5182 (1981).
13) A. Itoh, K. Oshima, and H. Nozaki, *Tetrahedron Lett.*, **1979**, 1783.
14) E. J. Corey and D. Seebach, *J. Org. Chem.*, **31**, 4097 (1966).
15) K. Hiroi, H. Sato, and Y. Arinaga, *Annual Report of Tohoku College of Pharmacy*, **32**, 87 (1985).
16) K. Kojima, S. Amemiya, H. Suemune, and K. Sakai, *Chem. Pharm. Bull.*, **33**, 2750 (1985).
17) T. Takeda and T. Fujiwara, *Chem. Lett.*, **1982**, 1113.
18) D. N. Harcourt and R. D. Waigh, *J. Chem. Soc. C*, **1971**, 967; E. Felder, D. Pitre, S. Boveri, and E. B. Grabitz, *Chem. Ber.*, **100**, 555 (1967).
19) S. M. Nolan and T. Cohen, *J. Org. Chem.*, **46**, 2473 (1981).
20) For leading reviews see M. Ono, *Yuki Gosei Kagaku Kyokai Shi*, **39**, 872 (1981); M. Ramaiah, *Synthesis*, **1984**, 529.

[Chem. Pharm. Bull. 35(4)1427—1433(1987)]

Studies on the Constituents of Umbelliferae Plants. XV.[1] Constituents of *Cnidium officinale*: Occurrence of Pregnenolone, Coniferylferulate and Hydroxyphthalides

MASARU KOBAYASHI,* MIYUKI FUJITA, and HIROSHI MITSUHASHI

Faculty of Pharmaceutical Sciences, Hokkaido University, Sapporo 060, Japan

(Received October 6, 1986)

Pregnenolone (**1**), coniferylferulate (**2**) and nine mono- and dihydroxyphthalide derivatives (**5**—**13**) were isolated from the commercial *C. officinale* rhizome. Their structures were determined from the spectroscopic data and the dihydroxyphthalides senkyunolide-H (**11**) and -I (**12**) and senkyunolide-J (**13**) were synthesized from the major components ligustilide (**14**) and senkyunolide-A (**16**), respectively. These oxygenated phthalides were absent in the fresh *C. officinale* rhizome and they were shown to be derived from the major volatile phthalides during storage of the crude drug. Coniferylferulate (**2**) also decomposes partly during storage, giving ferulic acid.

Keywords——pregnenolone; coniferylferulate; senkyunolide; phthalide; hydroxyphthalide; *Cnidium officinale*; Umbelliferae

Senkyu, the dried rhizome of *Cnidium officinale* MAKINO (syn. *Ligusticum officinale* KITAGAWA, Umbelliferae) is one of the most frequently occurring drugs in the prescriptions of Chinese traditional medicine used in Japan. *C. officinale* is a variety of *L. wallichii*, the original plant of the important crude drug chuan xiong in China, and used in Japan for the same purpose as *L. wallichii*. It contains a variety of volatile non-polar alkylphthalide derivatives which have been shown to have antifungal and smooth muscle relaxing activities.[2,3] In contrast, its more polar and non-volatile components had been less well characterized. During the analysis of commercial *C. officinale* extract, we found significant amounts of unidentified components in the non-volatile fraction of the mixture. Some of them were absent or present in very minor amounts in the fresh material. Since crude drugs are generally administered after some processing and storage, analysis of these minor components possibly derived from the major original components would be of importance. The present report describes our finding that significant amounts of previously unknown components are contained in commercial *C. officinale* rhizome.

The dried rhizome of *C. officinale* was extracted with hexane, ether and methanol and the crude lipids obtained were partitioned with a mixture of hexane–methanol–water (20 : 10 : 2). This simple solvent fractionation was remarkably efficient for the removal of triglycerides, which are often the predominant components of animal and plant tissues. Double application of this fractionation made the methanol layer free from triglycerides and most of the phthalides remained in the methanol layer. The methanol layer contained unidentified polar compounds. Repetitive flash chromatography over a column of silica gel afforded compounds **1**—**13**.

Pregnenolone (1), Coniferyl Ferulate (2), and Falcarindiol (4)

Compound **1**, mp 187—188 °C, $C_{21}H_{32}O_2$, was identified as pregnenolone from its mass (MS, *m/z* 316, 298, 283, 273, 255, 231, 213), infrared (IR, 3500, 1680 cm^{-1}) and proton nuclear magnetic resonance [^{1}H-NMR, δ 0.63 (3H, s), 1.01 (3H, s), 2.13 (3H, s), 5.35 (1H, m),

3.50 (1H, m)] spectra, which were identical with those of the authentic compound. Compound **1** occurred in the *C. officinale* rhizome entirely as the free steroid. Acid treatment of the glycoside fraction of the extract only gave a small amount of phytosterol mixture but no trace of **1**. This is the first demonstration of the occurrence of C_{21} steroid in Umbelliferae plants.[4] Although C_{21} steroids have been found in a variety of plants, most of them occur as the oxygenated aglycone of the glycosides. There are a very few examples, such as in some Apocynaceae plants, in which pregnenolone was found.[5] Since **1** is the common precursor of all of the hormonal steroids and since *C. officinale* has traditionally been used in prescriptions for obstetrical and gynecological disorders, the possible significance of **1** in the crude drug is of interest. The amount of **1** found in fresh and commercial *C. officinale* was about 1 mg in 30 g of dried material. It is known that orally administered pregnenolone is mostly excreted through the enterohepatic circulation in a short period.[6] However, the average level of pregnenolone in human plasma is generally less than 10 ng/ml,[7] a minute amount compared with the total pregnenolone contained in general prescriptions of senkyu, the dried rhizome of *C. officinale*.

Compound **2**, $C_{20}H_{20}O_6$, was obtained in a fairly high yield (860 mg from 2 kg of the material). Its IR (3330, 1680, 1615, 1580, 1505 cm^{-1}) and ^{1}H-NMR [δ 3.90 (3H, s), 3.92 (3H, s), 7.66 (1H, d, J=15.6 Hz), 6.33 (1H, d, J=15.6 Hz), 6.64 (1H, d, J=15.6 Hz), 6.21 (1H, dt, J=15.6, 6.4 Hz), 4.84 (2H, br d, J=6.4 Hz] spectra were reminiscent of those of an ester of ferulic acid (**3**), which is a known component of *C. officinale*.[8] Hydrolysis of **2** in aqueous dioxane afforded **3** and coniferyl alcohol, which were identified by comparison with authentic samples. Compound **2** was thus shown to be coniferylferulate. It is labile to hydrolysis and the coniferyl alcohol formed decomposes easily. For example, treatment of **2** in 1% HCl in dioxane or in dilute dioxane at 60 °C for 10 min causes formation of **3** with a very small amount of coniferyl alcohol. Treatment under basic conditions gave a similar result. Acid treatment of **2** in methanol at room temperature resulted in formation of **3** and methylconiferyl ether because the feruloyl moiety serves as an excellent leaving group in **2**. Heating of **2** in a mixture of dioxane–H_2O (2:1) at 80 °C for 1 h gave **3** and coniferylalcohol without decomposition. Also, when the pulverized *C. officinale* was heated in boiling water for 1 h, **2** was entirely converted to **3**. Other major components such as phthalides showed little change of their contents. Since the amount of ferulic acid (**3**) in the fresh *C. officinale* is negligible, the presence of **3** in the commercial *C. officinale* rhizome is apparently due to accumulation from **2** during storage. In our opinion, determination of the ratio of **2** and **3** affords a simple method for estimation of the freshness of this crude drug. Compound **4** was identified by ^{1}H-NMR as falcarindiol, which is a common component in Umbelliferae plants.

Isolation of Hydroxyphthalides (5—13)

Compounds **5** to **13** were found to be the hydroxy derivatives of the major non-polar alkylphthalides, ligustilide (**14**),[9] butylidenephthalide (**15**),[10] and senkyunolide (**16**).[10] To simplify the nomenclature of these new compounds, senkyunolide (**16**) previously isolated by Yamagishi and Kaneshima[10] from *C. officinale* was renamed senkyunolide-A by agreement with them, and the compounds **5** to **13** were designated as senkyunolide-B to senkyunolide-J.

Senkyunolide-B (**5**), mp 150—153 °C, $C_{12}H_{12}O_3$, was a monohydroxy derivative of butylidenephthalide (**15**) as indicated by the IR (3250, 1730, 1680, 1605 cm^{-1}) and ^{1}H-NMR [butylidene side chain: δ 0.99 (3H, t, J=7.3 Hz), 1.57 (2H, sext, J=7.3 Hz), 2.47 (2H, dt, J=7.8, 7.3 Hz), 5.96 (1H, t, J=7.8 Hz)] spectra. Its MS showed the loss of ethyl (*m/z* 175) and propylene (*m/z* 162) moieties, as observed in **15**.[10] The signals due to three aromatic protons were found at δ 7.05 (d, J=7.8 Hz), 7.34 (t, J=7.8 Hz), and 7.50 (d, J=7.8 Hz). Consequently, the hydroxyl group is attached at C-4 or C-7 of the aromatic ring. The olefinic proton at C-8 (δ 5.96) was sifted 0.33 ppm to lower field than that of **15** (δ 5.63) and indicated the presence

of a deshielding effect due to a nearby hydroxyl group. It is also known that the butylidene side chain in **14** and **15** takes *Z*-form and the corresponding *E*-form is quite unstable (*vide infra*). The hydroxyl proton appeared at δ 5.97, overlapped with the C-8 proton. Simultaneous irradiation of the C-8 proton and hydroxyl proton caused nuclear Overhauser effect (NOE) at the doublet at δ 7.05, but it was not observed after deuterium exchange. These results indicate that senkyunolide-B (**5**) is 4-hydroxybutylidenephthalide. It was erroneously described as 7-hydroxybutylidenephthalide in our preliminary communication as a result of misinterpretation of the NOE.[1b]

Senkyunolide-C (**6**), mp 95—100 °C, $C_{12}H_{12}O_3$, was also a monohydroxy derivative of **15** as indicated by the IR (3250, 1730, 1680, 1605, 1590 cm^{-1}) and ^{1}H-NMR [δ 0.98 (3H, t, J=7.3 Hz), 1.54 (2H, sext, J=7.3 Hz), 2.43 (2H, dt, J=7.8, 7.3 Hz), 5.59 (1H, t, J=7.8 Hz)] spectra. Its MS showed strong ions at *m/z* 175 and 162, as in **5**. Three aromatic proton signals were found at δ 7.00 (dd, J=2.4, 8.3 Hz), 7.05 (d, J=2.4 Hz), and at 7.76 (d, J=8.3 Hz). From this coupling pattern it is evident that the hydroxyl group is attached at C-5 or C-6. The presence of NOE between the olefinic proton at δ 5.59 and the aromatic proton at δ 7.05 established the structure of **6** as 5-hydroxybutylidenephthalide. This compound was independently isolated from the Umbelliferae plant *Ligusticum wallichii*.[11]

Senkyunolide-D (**7**), $C_{12}H_{14}O_4$, was a monooxo monohydroxyderivative of **16** (IR, 3250, 1765, 1725, 1680 cm^{-1}). The presence of a cross-conjugated diene was indicated by the ultraviolet [UV, 287 nm (ε, 2600)] and ^{1}H-NMR [δ 6.09 (1H, dt, J=9.8, 4.0 Hz), 6.27 (1H, dt, J=9.8, 2.0 Hz)] spectra, which were similar to those of **16** [UV, 277 nm (ε, 3100); ^{1}H-NMR δ 5.9 (m), 6.19 (br d, J=9 Hz)].[10] Hence the carbonyl group is located at the side chain. In the ^{1}H-NMR, the signals due to protons adjacent to a hydroxyl group were absent. Two double triplet signals at δ 2.28 (J=18.1, 7.3 Hz) and 2.65 (J=18.1, 6.8 Hz) due to the protons adjacent to the carbonyl group indicated the presence of a propyl ketone side chain. This was confirmed by the MS, which showed strong peaks at *m/z* 151 and 71 due to cleavage of the ketol group. Thus, senkyunolide D (**7**) was shown to be 3-hydroxy-8-oxosenkyunolide-A.

Senkyunolide-E (**8**), $C_{12}H_{12}O_3$, was a monohydroxy derivative of butylidenephthalide (**15**) like **5** and **6**. Its IR (3400, 1780, 1685, 1610 cm^{-1}), UV [306 nm (ε, 3900), 270 nm (ε, 8600)] and ^{1}H-NMR [four aromatic protons at δ 7.52—7.76 (3H, m), 7.91 (1H, d, J=7.3 Hz)] spectra were virtually the same as those of **15**.[10] The side chain bears a hydroxyl group and the hydroxymethine proton at δ 4.87 (dt, J=8.8, 6.8 Hz) was found by a decoupling experiment to be coupled with the C-8 olefinic proton at δ 5.66 (d, J=8.8 Hz). Consequently, senkyunolide-E (**8**) was shown to be 9-hydroxybutylidenephthalide.

Senkyunolide-F (**9**), $C_{12}H_{14}O_3$, was the major component of the hydroxyphthalides found in *C. officinale*. It was a monohydroxy derivative of the major volatile alkylphthalide ligustilide (**14**). Its IR (3400, 1760, 1665 cm^{-1}) and UV [283 nm (ε, 6300), 296 nm (ε, 6100), 323 nm (ε, 7300)] spectra were virtually the same as those of **14** [IR, 1760, 1670 cm^{-1}; UV, 283 nm (ε, 8100), 296 nm (ε, 7600), 324 nm (ε, 9500)].[10] The ^{1}H-NMR chemical shifts of the C-6 and C-7 olefinic protons were observed at δ 6.06 (dt, J=9.8, 3.9 Hz) and 6.29 (dt, J=9.8, 2.0 Hz). The hydroxyl group was shown to be attached at C-9, by decoupling of the signals of the hydroxymethine proton at δ 4.74 (dt, J=8.3, 6.4 Hz) and the C-8 olefinic proton at δ 5.23 (d, J=8.3 Hz). Thus senkyunolide-F (**9**) was shown to be 9-hydroxyligustilide. It is susceptible to autoxidation and during storage in the presence of air it changed gradually into senkyunolide-E (**8**).

Senkyunolide-G (**10**), $C_{12}H_{16}O_3$, was a monohydroxy derivative of senkyunolide A (**16**). Its UV [281 nm (ε, 3200)], and ^{1}H-NMR [δ 5.97 (1H, dt, J=9.8, 3.0 Hz), 6.17 (1H, br d, J=9.8 Hz)] spectra were similar to those of senkyunolide-A (**16**), as found with **7**. Hydroxymethine signals were absent in the ^{1}H-NMR spectrum. The MS showed cleavage of the butyl group to give a base peak at *m/z* 151. Treatment of **10** with *p*-toluenesulfonic acid

afforded **14**, while on heating of **14** in dilute sulfuric acid, formation of **10** was observed. From these results senkyunolide G (**10**) was shown to be 3-hydroxysenkyunolide-A.

Senkyunolide-H and -I (**11** and **12**),[12] $C_{12}H_{16}O_4$, were an isomeric pair of dihydroxyphthalides in which **12** was the major isomer. Both of them showed the signals due to the butylidene side chain in ^{1}H-NMR spectra [δ 0.95 (3H, t, J=7.3 Hz), 1.50 (2H, sext, J=7.3 Hz), 2.36 (2H, dt, J=7.8, 7.3 Hz). They have a glycol group in the cyclohexene ring and their vicinal hydroxymethine protons appeared at δ 4.05 (ddd, J=7.8, 3.9, 2.4 Hz) and 4.62 (d, J=3.9 Hz) in **11** and at 3.95 (ddd, J=9.9, 6.4, 3.4 Hz) and 4.50 (d, J=6.4 Hz) in **12**. The MS of **11** and **12** showed the base peak at m/z 180 ($C_{10}H_{12}O_3$), due to retro-Diels–Alder cleavage at the cyclohexene ring and established the position of the glycol group at C-6 and C-7. Glycolation of ligustilide (**14**) with *m*-chloroperbenzoic acid in methylene chloride followed by hydrolysis afforded compounds **11** and **12**, of which **12** was the major product. The preferential formation of the *E*-isomer in the ordinary hydrolysis of epoxides indicates that the major product **12** is the *E*-isomer and the minor product **11** is the *Z*-isomer. The ratio of **11** and **12** obtained was about 1 : 6 which is similar to the ratio of **11** and **12** (1 : 5) isolated from *C. officinale*.

Senkyunolide-J (**13**), $C_{12}H_{18}O_4$, $[\alpha]_D$ -11° ($CHCl_3$), was also found to be a glycol derivative of senkyunolide-A (**16**). It showed the C-3 methine proton at δ 4.86 (dd, J=7.3, 2.9 Hz) and two hydroxymethine protons of the glycol group at δ 3.95 (ddd, J=8.8, 5.9, 2.9 Hz) and 4.41 (br d, J=5.9 Hz). The retro-Diels–Alder cleavage ion was observed at m/z 182 ($C_{10}H_{14}O_3$). Glycolation of **16** by the same procedure as above afforded **13**. Consequently, the structure of senkyunolide-J (**13**) was established as 6,7-*E*-dihydroxysenkyunolide-A, though the absolute configuration is unknown.

Thus, nine hydroxylated phthalides were isolated from the commercial *C. officinale* rhizome. The geometry of the butylidene side chain in compounds **5**, **6**, **8**, **9**, **11**, and **12** was shown to be *Z*. This was indicated by the chemical shifts of the C-8 olefinic protons and from the formation of trace amounts of less stable *E*-isomers on storage of the purified samples.

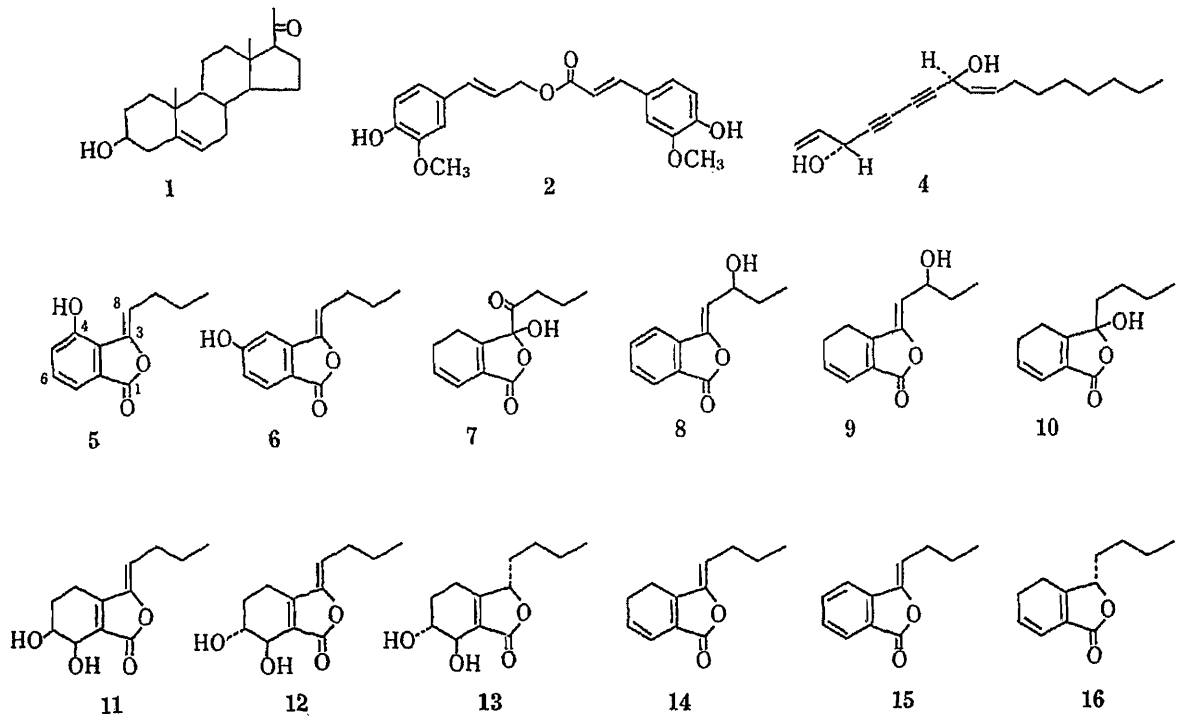

Fig. 1

Banerjee *et al.* showed that the chemical shift of the olefinic proton at C-8 of the *E*-isomer of **14** was shifted 0.51 ppm downfield from that of the stable *Z*-isomer.[13] In the present study, the downfield shifts observed in the unstable *E*-isomers were 0.44 ppm in **9**, 0.52 ppm in **11**, and **12**, and 0.25 ppm in **6** and **8**. In contrast, compound **5** was stable and no isomerization product was found.

Except for **13**, all the hydroxyphthalides isolated were optically inactive and compounds **7** to **12** were supposed to be racemic mixtures. Hydroxyphthalides obtained in the present study from the commercial material (2 kg) amounted to 1.95 g which is about one sixth of the total phthalide fraction. Of these, the major products were senkyunolide-F (**9**) and senkyunolide-I (**12**). Since the fresh *C. officinale* rhizome did not contain any of these hydroxylated phthalides (Experimental), they were supposed to be derived from the major phthalides ligustilide (**14**) or senkyunolide-A (**16**) during storage. Thus fresh and stored samples of this crude drug show marked differences in the contents of major constituent phthalides, ferulic acid and coniferylferulate. The effects of this on the quality and pharmacological evaluation are unknown, and are currently under investigation.

Experimental

Melting points were determined on a Kofler hot stage and are uncorrected. Optical rotations were determined on a JASCO DIP-4 digital polarimeter. ^{1}H-NMR spectra were determined on a JEOL FX 200 spectrometer at 200 MHz in $CDCl_3$ solution with tetramethylsilane as an internal standard. MS were determined on JEOL JMS D-300 (EI-MS) and JEOL JMS 01SG-2 (FD-MS) spectrometers. IR spectra were taken on a JASCO A-102 spectrometer. Column chromatography was carried out by the flash chromatography method.[14]

Fractionation of *C. officinale* Extract——Commercial rhizomes of *C. officinale*, cultivated in Kitami, Hokkaido, were used. The dried and pulverized material (2 kg) was extracted thoroughly with hexane and ether, then with MeOH until the extract became colorless. The MeOH extract (70 g) was partitioned with a mixture of $CHCl_3$–MeOH–H_2O (8:4:3, 2 l) and the $CHCl_3$ extract (15 g) was combined with the hexane and ether extract (72 g). It was partitioned with a mixture of hexane–MeOH–H_2O (20:10:2, 2 l) and the upper layer and lower layer were separated. The upper layer was washed with the lower layer of the same solvent mixture as above. Similarly, the lower layer of the extract was washed with the upper layer of the solvent mixture. Evaporation of the combined two upper extracts gave 41 g of non-polar extract containing mainly glycerides. Also, evaporation of the combined two lower layer extracts gave 44 g of more polar components containing phthalides and polar lipids. A portion of this (21 g) was charged on a column of silica gel (500 g) and eluted with mixtures of hexane–ethyl acetate (1:4, frs. 1—5), hexane–ethyl acetate (3.5:6.5, frs. 6—14), and 5% MeOH in hexane–ethyl acetate (3.5:6.5, frs. 15—19). The eluates (each 500 ml) were collected. Fractions 2—4 (10.5 g) were composed predominantly of volatile alkylphthalides with smaller amounts of fatty acids.

Isolation of Compounds 4—7 and 10——Fractions 5—8 were combined (500 mg) and separated into subfractions 1, 2, and 3 on a column of silica gel by eluting with 2% MeOH in $CHCl_3$. Subfraction 1 contained vanillin and compounds **5** and **7**. Chromatography of the mixture with 5% MeOH in $CHCl_3$ gave **5** (60 mg) and a mixture containing vanillin and **7**. A portion of the mixture (20 mg) was submitted to preparative thin layer chromatography (TLC) with 2% MeOH in $CHCl_3$, giving vanillin and 14.3 mg of **7**. Vanillin was identified by comparison with an authentic sample (TLC and MS). Chromatography of subfraction **2** (220 mg) with 15% MeOH in $CHCl_3$ gave compounds **6** (40 mg) and **10** (160 mg). Subfraction 3 (130 mg) contained mostly **4** and it was purified by chromatography with 15% ether in $CHCl_3$.

4: Colorless oil. $[\alpha]_D$ +180° (c=1.1, $CHCl_3$). ^{1}H-NMR (δ): 5.26 (1H, br d, J=10.3 Hz, 1-H_a), 5.47 (1H, br d, J=17.1 Hz, 1-H_b), 5.94 (1H, ddd, J=17.1, 10.3, 5.4 Hz, 2-H), 4.94 (1H, d, J=5.4 Hz, 3-H), 5.21 (1H, d, J=8.3 Hz, 8-H), 5.51 (1H, dd, J=8.3, 10.3 Hz, 9-H), 5.62 (1H, dt, J=10.3, 7.3 Hz, 10-H), 0.88 (3H, t, J=7.3 Hz, 17-H_3).

5: mp 150—153°C. $[\alpha]_D$ 0° (c=0.22, $CHCl_3$). ^{1}H-NMR (δ): 0.99 (3H, t, J=7.3 Hz, 11-H_3), 1.57 (2H, sext, J=7.3 Hz, 10-H_2), 2.47 (2H, dt, J=7.8, 7.3 Hz, 9-H_2), 5.96 (1H, t, J=7.8 Hz, 8-H), 7.05 (1H, d, J=7.8 Hz), 7.34 (1H, t, J=7.8 Hz), 7.50 (1H, d, J=7.8 Hz). UV λ_{max}^{EtOH} nm (ε): 223 (12900), 256 (6700), 330 (4200). IR ν_{max}^{Nujol} cm^{-1}: 3200, 1730, 1680, 1605, 1495. MS *m/z* (%): 204 (24, M^+), 175 (100), 162 (25), 147 (27), 134 (7), 119 (11), 91 (13), 65 (8). High-resolution MS: Found 204.0791. Calcd for $C_{12}H_{12}O_3$ (M^+)=204.0786.

6: mp 95—100°C. $[\alpha]_D$ 0° (c=0.67, $CHCl_3$). ^{1}H-NMR (δ): 0.98 (3H, t, J=7.3 Hz, 11-H_3), 1.54 (2H, sext, J=7.3 Hz, 10-H_2), 2.43 (2H, dt, J=7.8, 7.3 Hz, 9-H_2), 5.59 (1H, t, J=7.8 Hz), 7.00 (1H, dd, J=8.3, 2.4 Hz), 7.05 (1H, d, J=2.4 Hz), 7.76 (1H, d, J=8.3 Hz). UV λ_{max}^{EtOH} nm (ε): 228 (9100), 256 (19300). IR ν_{max}^{Nujol} cm^{-1}: 3250, 1730, 1680, 1605, 1590. MS *m/z* (%): 204 (24, M^+), 175 (100), 162 (73), 147 (43), 119 (21), 91 (16). High resolution MS: Found 204.0773. Calcd for $C_{12}H_{12}O_3$(M^+)=204.0785.

7: Colorless oil. $[\alpha]_D$ 0° (c=1.43, $CHCl_3$). ^{1}H-NMR (δ): 0.92 (3H, t, J=7.3 Hz, 11-H_3), 1.67 (2H, sext, J=7.3 Hz, 10-H_2), 2.28 (1H, dt, J=18.1, 7.3 Hz, 9-H_a), 2.65 (1H, dt, J=18.1, 6.8 Hz, 9-H_b), 6.09 (1H, dt, J=9.8, 4.0 Hz, 6-H), 6.27 (1H, dt, J=9.8, 2.0 Hz, 7-H). UV λ_{max}^{EtOH} nm (ε): 287 (2600), 326 (2250, shoulder). IR ν_{max}^{Nujol} cm^{-1}: 3250, 1765, 1725, 1680, 1600, 1575. MS m/z (%): 222 (1.3, M^+), 204 (1.6), 134 (100), 106 (42), 79 (38), 77 (34), 71 (73). High-resolution MS: Found 222.0872. Calcd for $C_{12}H_{14}O_4$ (M^+)=222.0890.

10: Colorless oil. $[\alpha]_D$ 0° (c=1.25, $CHCl_3$). ^{1}H-NMR (δ): 0.90 (3H, t, J=6.8 Hz, 11-H_3), 5.97 (1H, dt, J=9.8, 3.0 Hz, 6-H), 6.17 (1H, brd, J=9.8 Hz, 7-H). UV λ_{max}^{EtOH} nm (ε): 281 (3200). IR ν_{max}^{Nujol} cm^{-1}: 3350, 1760 (shoulder), 1735, 1600. MS m/z (%): 208 (3, M^+), 190 (7), 180 (11), 161 (5), 151 (100), 133 (4), 124 (26), 123 (74), 105 (14), 79 (42), 77 (33). High resolution MS: Found 208.1102. Calcd for $C_{12}H_{16}O_3$ (M^+)=208.1101.

Isolation of Compounds 1—3, 8 and 9——Fractions 9—14 (1.98 g) were combined. Chromatography of the mixture with 2% MeOH in $CHCl_3$ gave **2** (860 mg), a mixture (500 mg) containing compounds **1**, **8** and **9**, and **3** (500 mg), in order of elution. The mixture was separated on a silica gel column with 40% ethyl acetate in hexane to give **1** (19.6 mg), **8** (21.1 mg), and **9** (320 mg).

1: mp 187—188°C. ^{1}H-NMR (δ): 0.63 (3H, s, 18-H_3), 1.01 (3H, s, 19-H_3), 2.13 (3H, s, 21-H_3), 5.35 (1H, m, 6-H), 3.50 (1H, m, 3α-H). MS m/z (%): 316 (42, M^+), 298 (34), 283 (29), 273 (4), 255 (12), 231 (32), 213 (20). IR ν_{max}^{Nujol} cm^{-1}: 1680, 950, 795.

2: Colorless oil. $[\alpha]_D$ 0° (c=2.27, $CHCl_3$). ^{1}H-NMR (δ): 6.84—6.94 (4H, m), 7.03 (1H, d, J=1.5 Hz), 7.08 (1H, dd, J=8.3, 1.5 Hz), 6.64 (1H, d, J=15.6 Hz), 6.21 (1H, dt, J=15.6, 6.4 Hz), 4.84 (2H, brd, J=6.4 Hz), 3.90 (3H, s), 3.92 (3H, s), 6.33 (1H, d, J=15.6 Hz), 7.66 (1H, d, J=15.6 Hz). UV λ_{max}^{EtOH} nm (ε): 272 (11900), 298 (12800), 320 (13300). IR ν_{max}^{Nujol} cm^{-1}: 3330, 1680, 1615, 1580, 1505. MS m/z (%): 356 (14, M^+), 194 (92), 179 (25), 177 (100), 162 (30), 145 (19), 131 (67). High-resolution MS: Found 356.1284. Calcd for $C_{20}H_{20}O_6$ (M^+)=356.1261.

3: mp 169—171°C. MS m/z (%): 194 (M^+).

8: Colorless oil. $[\alpha]_D$ 0° (c=1.1, $CHCl_3$). ^{1}H-NMR (δ): 1.00 (3H, t, J=7.3 Hz, 11-H_3), 4.87 (1H, dt, J=8.8, 6.8 Hz, 9-H), 5.66 (1H, d, J=8.8 Hz, 8-H), 7.52—7.76 (3H, m), 7.91 (1H, d, J=7.3 Hz). UV λ_{max}^{EtOH} nm (ε): 216 (9500), 235 (10000), 260 (10500), 270 (8600), 306 (3900). IR ν_{max}^{Nujol} cm^{-1}: 3400, 1780, 1685, 1610. MS m/z (%): 204 (10, M^+), 186 (5), 175 (100), 147 (90), 133 (11), 129 (23), 115 (5), 105 (18), 95 (26). High-resolution MS: Found 204.0809. Calcd for $C_{12}H_{12}O_3$ (M^+)=204.0787.

9: Colorless oil. $[\alpha]_D$ 0° (c=1.89, $CHCl_3$). ^{1}H-NMR (δ): 0.97 (3H, t, J=7.3 Hz, 11-H_3), 4.74 (1H, dt, J=8.3, 6.4 Hz, 9-H), 5.23 (1H, d, J=8.3 Hz, 8-H), 6.06 (1H, dt, J=9.8, 3.9 Hz, 6-H), 6.29 (1H, dt, J=9.8, 2.0 Hz, 7-H). UV λ_{max}^{EtOH} nm (ε): 283 (6300), 296 (6100), 323 (7300). IR ν_{max}^{Nujol} cm^{-1}: 3400, 1760, 1665, 1620. MS m/z (%): 206 (18, M^+), 188 (9.6), 177 (100), 150 (62), 147 (16), 132 (28), 149 (73). High-resolution MS: Found 206.0928. Calcd for $C_{12}H_{14}O_3$ (M^+)=206.0943.

Isolation of Compounds 11—13——Fractions 15—17 (920 mg) contained a mixture of **11** and **12**. Chromatography of the mixture with 6% MeOH in $CHCl_3$ gave **11** (45.3 mg) and **12** (239 mg). Purification of fraction **18** by column chromatography with 10% MeOH in hexane–ethyl acetate (1 : 1), 10% MeOH in hexane–ether (1 : 1) and 8% MeOH in hexane–$CHCl_3$ (1 : 1) gave **13** (50 mg).

11: Colorless oil. $[\alpha]_D$ 0° (c=1.66, $CHCl_3$). ^{1}H-NMR (δ): 0.95 (3H, t, J=7.3 Hz, 11-H_3), 1.50 (2H, sext, J=7.3 Hz, 10-H_2), 2.36 (2H, dt, J=7.8, 7.3 Hz, 9-H_2), 5.31 (1H, t, J=7.8 Hz, 8-H), 4.05 (1H, ddd, J=7.8, 3.9, 2.4 Hz, 6-H), 4.62 (1H, d, J=3.9 Hz, 7-H). UV λ_{max}^{EtOH} nm (ε): 274 (12100). IR ν_{max}^{Nujol} cm^{-1}: 3400, 1755, 1675, 1635. MS m/z (%): 224 (27, M^+), 206 (4), 180 (100), 165 (17), 151 (42), 138 (14), 123 (12), 95 (18), 55 (42). High-resolution MS: Found 224.1067. Calcd for $C_{12}H_{16}O_4$ (M^+)=224.1049.

12: Colorless oil. $[\alpha]_D$ 0° (c=0.79, $CHCl_3$). ^{1}H-NMR (δ): 0.95 (3H, t, J=7.3 Hz, 11-H_3), 1.50 (2H, sext, J=7.3 Hz, 10-H_2), 2.36 (2H, dt, J=7.8, 7.3 Hz, 9-H_2), 5.29 (1H, t, J=7.8 Hz, 8-H), 3.95 (1H, ddd, J=9.9, 6.4, 3.4 Hz, 6-H), 4.50 (1H, brd, J=6.4 Hz, 7-H). UV λ_{max}^{EtOH} nm (ε): 273 (15200). IR ν_{max}^{Nujol} cm^{-1}: 3400, 1740, 1665, 1625. MS m/z (%): 224 (26, M^+), 206 (3), 180 (100), 165 (17), 151 (41), 138 (15), 123 (12), 95 (20), 55 (38). High-resolution MS: Found 224.1033. Calcd for $C_{12}H_{16}O_4$ (M^+)=224.1049.

13: Colorless oil. $[\alpha]_D$ −11° (c=1.45, $CHCl_3$). ^{1}H-NMR (δ): 0.91 (3H, t, J=6.8 Hz, 11-H_3), 4.86 (1H, dd, J=7.3, 2.9 Hz, 3-H), 3.95 (1H, ddd, J=8.8, 5.9, 2.9 Hz, 6-H), 4.41 (1H, brd, J=5.9 Hz, 7-H). UV λ_{max}^{EtOH} nm (ε): 214 (9000). IR ν_{max}^{Nujol} cm^{-1}: 3360, 1730, 1670. MS m/z (%): 226 (1, M^+), 208 (1.5), 182 (79), 139 (50), 126 (100). High-resolution MS: Found 226.1205. Calcd for $C_{12}H_{18}O_4$ (M^+)= 226.1205.

Glycolation of Ligustilide (14) and Senkyunolide-A (16)——(a) A solution of ligustilide (**14**, 200 mg) in 5 ml of methylene chloride was treated with 100 mg of *m*-chloroperbenzoic acid and the mixture was refluxed for 2 min. After cooling, the mixture was washed with saturated $NaHCO_3$ soln., H_2O, and saturated NaCl soln. The solvent was evaporated off and the residue was dissolved in a mixture of tetrahydrofuran–H_2O (6 : 1, 7 ml). Addition of a drop of 78% perchloric acid caused facile hydrolysis of the oxide and the mixture was diluted with $CHCl_3$ and washed with saturated $NaHCO_3$ soln, H_2O, and saturated NaCl soln. Evaporation of the solvent gave a mixture containing an isomeric mixture of diols. It was separated by chromatography as described for the separation of **11** and **12**. The major product (132 mg) and the less polar minor product (22 mg) were identified as **12** and **11**, respectively, by TLC (8% MeOH in $CHCl_3$ and 10% MeOH in hexane–$CHCl_3$ (1 : 1)) and MS comparisons with authentic samples.

(b) Senkyunolide-A (**16**, 40 mg) was treated in exactly the same manner as described above. The product obtained

was virtually a single diol. It was purified by the same procedure as described for **13** and identified by TLC examination as described in (a) and by IR spectral comparison with natural **13**.

General Procedure for the Small Scale Extraction and Separation of *C. officinale* Samples——Dried and pulverized rhizome *C. officinale* (30 g) was stirred for 30 min in a mixture of $CHCl_3$ (80 ml), MeOH (40 ml) ad H_2O (30 ml) and the extract was separated by suction filtration. The upper layer gave 6.3 g of H_2O-soluble compounds after evaporation of the solvent. Similarly, the lower layer gave 1.25 g of total lipids. It was stirred in a mixture of hexane (50 ml), MeOH (25 ml) and H_2O (5 ml) for 10 min. The upper layer gave triglycerides and other less polar lipids (0.79 g). The lower layer gave 0.48 g of polar lipid fraction. It was charged on a column of silica gel (Wako gel C-300, 2.2 × 13.5 cm) and eluted with ethyl acetate–hexane (1 : 9, 300 ml), ethyl acetate–hexane (1 : 3, 400 ml), MeOH–$CHCl_3$ (1 : 9, 150 ml) and MeOH (100 ml), and the fractions (16 ml each) were collected. The components eluted were as follows: non-polar alkylphthalides (frs. 2—14). **4**—**7** and **10** (frs. 22—30). **1** (frs. 31—34). **8** (frs. 36—40). **9** (frs. 40—46). **2** (frs. 48—55). **3** (frs. 52—56). **11**—**13** (frs. 56—58). This procedure was also applied to a fresh *C. officinale* sample collected in Kitami, Hokkaido. The material (100 g) was homogenized directly in the solvent mixture ($CHCl_3$–MeOH–H_2O (8 : 4 : 3, 150 ml)) and the extract was submitted to the same procedure as described above. Comparison of the column chromatographic fractions from fresh and commercial samples showed virtually the same elution pattern except that the amounts of ferulic acid (**3**) and hydroxyphthalides (**5**—**13**) obtained from the fresh material were negligible.

References and Notes

1) *a*) Part XIV, H. Mitsuhashi, U. Nagai, and T. Saito, *Rupr. Rev. Fac. Farm. Bioguim.* (S. Paulo), **6**, 237 (1968); *b*) Preliminary communication of Part XV, M. Kobayashi, M. Fujita, and H. Mitsuhashi, *Chem. Pharm. Bull.*, **32**, 3770 (1984).
2) M. Yokota and M. Nagasawa, Abstracts of Papers, 97th Annual Meeting of the Pharmaceutical Society of Japan, Tokyo, April 1977, II, p. 248.
3) H. Mitsuhashi, U. Nagai, T. Muramatsu, and H. Tashiro, *Chem. Pharm. Bull.*, **8**, 243 (1960).
4) Harker, Razdan, and Waight reported the occurrence of **1** in an Umbelliferae plant, *Angelica officinalis*, simultaneously with our preliminary communication.[1] S. Harker, T. K. Razdan, and E. S. Waight, *Phytochemistry*, **23**, 419 (1984).
5) R. Tschesche and G. Snatzke, *Justus Liebigs Ann. Chem.*, **636**, 105 (1960).
6) H. Eriksson, *Eur. J. Biochem.*, **19**, 416 (1971).
7) G. E. Abraham, J. E. Buster, F. W. Kyle, P. C. Corrales, and R. C. Teller, *J. Clin. Endocrinol. Metab.*, **37**, 158 (1973).
8) W. Ko and Y. Wang, *J. Taiwan Pharm. Assoc.*, **23**, 40 (1971).
9) H. Mitsuhashi and U. Nagai, *Tetrahedron*, **19**, 1277 (1963).
10) T. Yamagishi and H. Kaneshima, *Yakugaku Zasshi*, **97**, 237 (1977).
11) M. Puech-Baronnat, M. Kaouadji, and A. M. Mariotte, *Planta Med.*, **50**, 105 (1984).
12) Compound **12** was first reported by Yamagishi *et al.* at the 97th Annual Meeting of the Pharmaceutical Society of Japan, Tokyo, April 1977; T. Yamagishi and S. Homma, Abstracts of Papers, 97th Meeting, II, p. 238. It was renamed senkyunolide-I with their approval.
13) S. K. Banerjee, B. D. Gupta, W. S. Sheldrick, and G. Hofle, *Justus Liebigs Ann. Chem.*, 888 (1984).
14) W. C. Still, M. Kahn, and A. Mitra, *J. Org. Chem.*, **43**, 2923 (1978).

[Chem. Pharm. Bull. 35(4)1434—1442(1987)]

Synthetic Studies on *dl*-Aspterric Acid, a Carotane-Type Sesquiterpene. II. Synthesis of *dl*-Aspterric Acid

TAKASHI HARAYAMA,* KEIKO SAKURAI, KEIKO TANAKA, YUKIYA HASHIMOTO, HIDETO FUKUSHI, and YASUO INUBUSHI

Faculty of Pharmaceutical Sciences, Kyoto University, Sakyo-ku, Kyoto 606, Japan

(Received October 21, 1986)

Total synthesis of *dl*-aspterric acid (**1**) has been accomplished. Robinson annulation of the keto ester (**2**) with methyl vinyl ketone, followed by reduction with $LiAlH_4$ and oxidation with MnO_2, afforded the enone alcohol (**4**), which was converted to the hydroxy-ether (**6**) *via* three steps (I_2–Ag_2O, AgOAc, and alkaline hydrolysis). Successive treatment of **6** with *tert*-butyldimethylsilyl chloride, *tert*-BuOK–MeI, $NaBH_4$, Ac_2O–pyridine and 5% HCl afforded the hydroxy acetate (**18**). The hydroxy acetate (**18**) was converted to the hydroxy ketone (**20**) *via* catalytic hydrogenation under medium pressure, Jones oxidation, and alkaline hydrolysis. Treatment of **20** with PCl_5 gave the norketone (**21**), which is the degradation product of **1**. The dimethylacetal (**25**) of **20** was treated with Me_3SiCN–$SnCl_2$ to give the methoxy cyanides A (**26**) and B (**27**). The major methoxy cyanide B (**27**) was successively treated with KOH, Me_3SiCl–NaI, Ac_2O, and 5% HCl to give the monoacetate (**31**), which was finally converted to **1** *via* ring contraction with PCl_5 and alkaline hydrolysis.

Keywords——aspterric acid; Robinson annulation; carotane-type sesquiterpene; iodoetherification; ring contraction; C_1-unit elongation; ether cleavage

Aspterric acid was isolated as a metabolite of *Aspergillus terreus* IFO-6123 and its carotane-type sesquiterpene structure (**1**) was established by chemical means and X-ray analysis.[1] Synthesis of aspterric acid (**1**) was attempted according to the synthetic strategy shown in Chart 1. It should be noted that the formation of the isopropylidene group through the ring contraction of a six-membered ring to a five-membered ring has to be done at the later stage of the synthetic plan because of the instability of the isopropylidene moiety in **1** to acids.

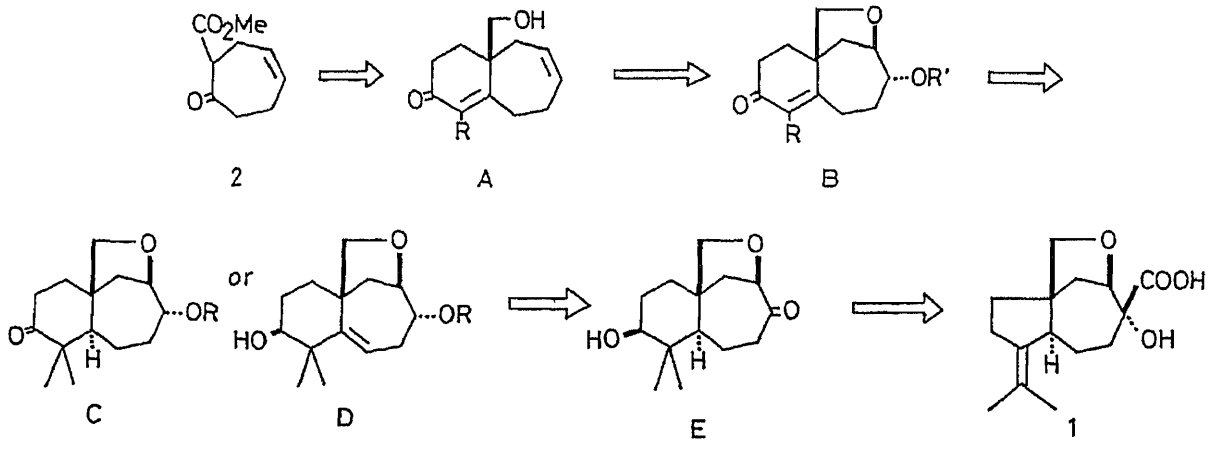

Chart 1

Moreover, for the ring contraction, the hydroxy group on the six-membered ring should be equatorial. In a preliminary communication, we have already reported the total synthesis of *dl*-aspterric acid (**1**).[2] We describe here the details of the synthesis of **1**.

In a previous paper,[3] we reported the synthesis of the key intermediate (C, R=H) *via* reductive methylation of B (R=Me). Since the yield and stereoselectivity were unsatisfactory, however, another approach to the key intermediate (C or D) starting from methyl 7-oxocyclohept-3-ene-1-carboxylate (**2**)[3] was investigated.

Robinson annulation of **2** with methyl vinyl ketone gave the enone ester (**3**) in 70.6% yield. Reduction of **3** with lithium aluminum hydride, followed by oxidation with manganese dioxide afforded the enone alcohol (**4**) in 73.4% yield, and this was treated with silver oxide–iodine in aqueous dioxane to provide the iodo-ether (**5**) and hydroxy-ether (**6**) in 73.8% and 15% yields, respectively. The stereochemical relationship of the ether and iodo groups in **5** was assumed to be *trans* from the reaction mechanism and the fact that the ether and hydroxy groups in **6** were *trans* as well, as discussed later. Treatment of **5** with silver acetate in acetic acid provided the acetoxy ether (**7**), which was converted to **6** by methanolysis in 73.5% yield from **5**. This result indicates that the substitution reaction of **5** with AgOAc proceeds with retention of the configuration of the substituent at C_4. Presumably, the reaction would proceed *via* the intermediate (**8**), where the ether oxygen participates in the retention of configuration as illustrated in Chart 2. For the purpose of dimethylation, **5** was treated with *tert*-BuOK–MeI to afford unexpectedly the three-membered ring compound (**9**), establishing the position of the ether linkage at C_3 rather than C_4 in **6**. The stereo-structure of **9** was elucidated from the reaction mechanism, which involves an *SN*2-type reaction towards the iodo group. Then, after silylation of **6** with *tert*-butyldimethylsilyl (TBDMS) chloride, dimethylation was examined. Treatment of TBDMS ether (**10**) with potassium *tert*-butoxide–methyl iodide in benzene at 70—80 °C gave the dimethyl compound (**11**) in 46.5% yield from **6**, and **11** was reduced with $NaBH_4$ to give the alcohol (**12**) in 84% yield. The stereochemistry of the newly introduced hydroxy group will be discussed later. Catalytic hydrogenation of **12** on platinum oxide under medium pressure (6.5 kg/cm^2) yielded the dihydro compound (**13**). In order to determine the stereochemistry at C_{6a} of **13**, an attempt was made to transform **13** into the alcohols A (**14**)[3] or B (**15**),[3] whose stereo-structure has already been established. Thus, **13** was successively treated with pyridinium dichromate and 5% hydrochloric acid to afford the hydroxy ketone (**14**), which was identical with the undesired alcohol A (**14**). On the other hand, desilylation of **12** with 5% hydrochloric acid, followed by catalytic hydrogenation on platinum oxide under medium pressure (10 kg/cm^2) gave the diol (**16**). The stereochemistry of **16** was determined as follows. Thus, Jones oxidation of **16** afforded the diketone (**17**), which was identical with the oxidation product of the desired alcohol B (**15**). Namely, catalytic hydrogenation of **12** possessing a bulky protective group gave the undesired *cis* compound and that of the deprotected compound gave the desired *trans* compound. The selective formation of **13** would reflect the hindrance to hydrogen attack from the α-side in **12** by an α-oriented bulky siloxy group. Therefore, the configuration of the hydroxy group at C_4 should be α, as shown in Chart 2. From these results, it was expected that the catalytic hydrogenation of the compound possessing a free hydroxy group at C_4 would afford the desired *trans* compound. Then, the hydroxy acetate (**18**) was synthesized by successive treatment of **12** with acetic anhydride in pyridine and 5% hydrochloric acid in 82% yield from **12**. Catalytic hydrogenation of **18** on platinum oxide under medium pressure (9 kg/cm^2) gave the dihydro compound (**19**) in 90% yield. The proton nuclear magnetic resonance (^{1}H-NMR) spectrum of **19** exhibited the signal due to a proton geminal to the acetoxy group at δ 4.45 (dd, J=4, 10 Hz), suggesting that the acetoxy group is equatorial. The configuration at C_{6a} was determined by conversion into the *trans* diol (**16**) by alkaline hydrolysis. Oxidation of **19** with Jones reagent, followed by alkaline hydrolysis afforded the desired key intermediate (**20**) in

72.5% yield; this product possesses a *trans* ring junction and an equatorial hydroxy group necessary for ring contraction. Then, conversion of the hydroxy ketone (**20**) into the norketone (**21**),[1] which is the degradation product of aspterric acid (**1**), was attempted.

Treatment of **20** with phosphorus pentachloride in benzene under ice-cooling yielded the isopropylidene compound (**21**) and the isopropenyl compound (**22**) in 47% and 25% yields, respectively, along with a trace of **23** and **24**. The isopropylidene compound (**21**) was identical with the norketone obtained from **1**. The structures of **22**, **23**, and **24** were elucidated on the basis of their spectral data (see Experimental). Although many approaches for the addition of C_1-unit to carbonyl group in **20** or **21** were examined, these were unfruitful because of low yields and/or instability of the products. Subsequently, the dimethylacetal (**25**) of **20** was treated with trimethylsilyl cyanide–anhydrous stannous chloride[4] to provide the methoxy cyanides A (**26**) and B (**27**) in 3 : 10 ratio and in 79% total yield from **20**. As the configurations of the cyano groups newly introduced into **26** and **27** were not determined, these products were subjected independently to conversion into aspterric acid. Thus, alkaline hydrolysis of **26** and **27**, followed by esterification with diazomethane gave the methoxy esters A (**28**) and B (**29**) in 82% and 88% yields, respectively. Successive treatments of **28** and **29** with sodium iodide–trimethylsilyl chloride,[5] acetic anhydride–*p*-toluenesulfonic acid (*p*-TsOH) (diacetylation) and 5% hydrochloric acid (partial hydrolysis) afforded the monoacetates A (**30**) and B (**31**), in 57% and 72% yields, respectively. Ring contraction of **30** with phosphorus pentachloride in benzene gave the isopropylidene compound A (**32**) in 55% yield and that of

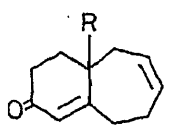

3 : R=CO_2Me
4 : R=CH_2OH

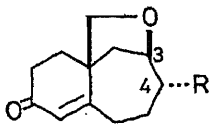

5 : R=I
6 : R=OH
7 : R=OAc
10 : R=OTBDMS

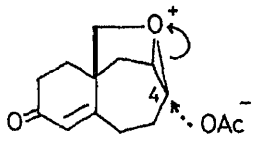

8

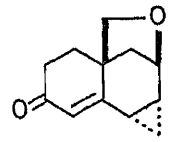

9

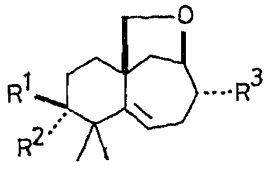

11 : $R^1=R^2=O$, R^3=OTBDMS
12 : R^1=OH, R^2=H, R^3=OTBDMS
18 : R^1=OAc, R^2=H, R^3=OH

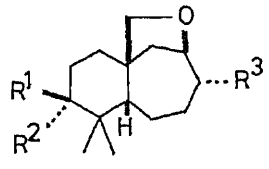

13 : R^1=OH, R^2=H, R^3=OBTDMS
14 : $R^1=R^2=O$, R^3=OH

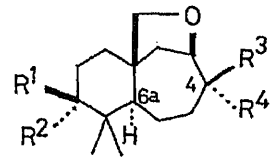

15 : $R^1=R^2=O$, R^3=H, R^4=OH
16 : R^1=OH, $R^2=R^3$=H, R^4=OH
17 : $R^1=R^2=O$, $R^3=R^4=O$
19 : R^1=OAc, $R^2=R^3$=H, R^4=OH
20 : R^1=OH, R^2=H, $R^3=R^4=O$
24 : R^1=H, R^2=Cl, $R^3=R^4=O$
25 : R^1=OH, R^2=H, $R^3=R^4$=OMe
26 : R^1=OTMS, R^2=H, R^3=OMe, R^4=CN
27 : R^1=OTMS, R^2=H, R^3=CN, R^4=OMe
28 : R^1=OH, R^2=H, R^3=OMe, $R^4=CO_2Me$
29 : R^1=OH, R^2=H, $R^3=CO_2Me$, R^4=OMe
30 : R^1=OH, R^2=H, R^3=OAc; $R^4=CO_2Me$
31 : R^1=OH, R^2=H, $R^3=CO_2Me$, R^4=OAc
35 : R^1=H, R^2=Cl, $R^3=CO_2Me$, R^4=OAc

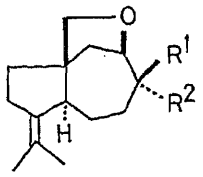

21 : $R^1=R^2=O$
32 : R^1=OAc, $R^2=CO_2Me$
33 : $R^1=CO_2Me$, R^2=OAc
36 : R^1=OH, R^2=COOH

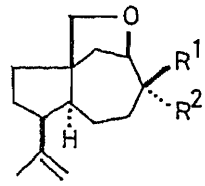

22 : $R^1=R^2=O$
34 : $R^1=CO_2Me$, R^2=OAc

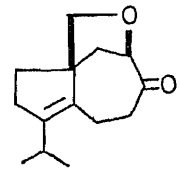

23

Chart 2

31 under the same reaction conditions gave the isopropylidene compound B (**33**), the isopropenyl compound (**34**) and the chloro compound (**35**) in 74%, 6% and 4% yields, respectively. These structures were elucidated on the basis of their spectral data. Finally, alkaline hydrolysis of **32** and **33** gave the hydroxy acids A (**36**) and B (**1**) in 61% and 76% yields, respectively. The latter, derived from the major methoxy cyanide B (**27**), was identical with an authentic sample of aspterric acid (**1**) on the basis of infrared (IR) and ^{1}H-NMR (200 MHz) comparisons.

Experimental

Melting points were determined with a Yanagimoto micro melting point apparatus, and are uncorrected. The IR spectra (ν_{max}) were determined on a Shimadzu IR-400 spectrometer in chloroform unless otherwise stated. The ^{1}H-NMR spectra were obtained in chloroform-*d* on a JNM-PMX 60 or JEOL FX 200 instrument with chemical shifts being reported in parts per million downfield from a tetramethylsilane internal standard (δ 0.0), and coupling constants in Hz. Mass spectra (MS) were taken on a JEOL JMS 01SG-2 instrument (direct inlet) at 70 eV. The extracts were washed with brine, dried over $MgSO_4$ and filtered, then the filtrates were concentrated to dryness *in vacuo*. Column chromatography was carried out on alumina (E. Merck, nach Brockmann, activity II-III) or Silica gel 60 (E. Merck, 70—230 mesh). Preparative thin layer chromatography (pTLC) was run on 20 × 20 cm plates coated with a 0.25 mm layer of Merck Silica gel PF_{254} and GF_{254}. Compounds for which no melting point is given are oily.

The Enone Ester (3)——Methyl vinyl ketone (420 mg, 6 mmol) and a solution of KOH (16.8 mg, 0.3 mmol) in MeOH (1 ml) were added to a solution of **2** (504 mg, 3 mmol) in ether (5 ml) under ice-cooling. The reaction mixture was stirred for 1 h under an argon atmosphere, diluted with water, and then extracted with CH_2Cl_2. A solution of the crude product and NaOMe (238 mg, 4.4 mmol) in dry MeOH (25 ml) was stirred at 50 °C for 1.5 h under an argon atmosphere. The reaction mixture was diluted with water and extracted with ether. The residue in hexane was chromatographed on alumina (10 g). Elution with 50% ether in hexane gave **3** (466 mg, 70.6% yield), mp 76—77 °C (colorless needles from hexane). IR ν_{max} cm^{-1}: 1727, 1670, 1622. ^{1}H-NMR (60 MHz) δ: 3.70 (3H, s, COOMe), 5.62 (2H, m, olefinic protons), 5.92 (1H, s, olefinic proton). *Anal.* Calcd for $C_{13}H_{16}O_3$: C, 70.89; H, 7.32. Found: C, 71.07; H, 7.33.

The Enone Alcohol (4)——A solution of **3** (2.1 g, 9.5 mmol) in ether (30 ml) was added dropwise to a suspension of $LiAlH_4$ (810 mg, 21.3 mmol) in ether (70 ml) at 5 °C under stirring. The reaction mixture was stirred at room temperature for 2 h. The excess reagent was decomposed with AcOEt and wet ether. The organic layer was decanted. The residue in CH_2Cl_2 was chromatographed on silica gel (80 g). Elution with 1% MeOH in CH_2Cl_2 gave the diol A (240 mg, 13% yield). IR ν_{max} cm^{-1}: 3600, 3400, 1650. ^{1}H-NMR (60 MHz) δ: 3.37 (1H, d, J=10 Hz, C$\underline{H}_A$H$_B$O), 3.62 (1H, d, J=10 Hz, CH$_A$$\underline{H}_B$O), 4.10 (1H, m, >C$\underline{H}$–OH), 5.63 (3H, m, olefinic protons). MS *m/z*: 194 (M$^+$). Elution with 2% MeOH in CH_2Cl_2 gave a mixture of the diols A and B (80 mg, 4.3% yield). Elution with 3% MeOH in CH_2Cl_2 gave the diol B (1.42 g, 77% yield). IR ν_{max} cm^{-1}: 3600, 3380, 1650. ^{1}H-NMR (60 MHz) δ: 3.42 (1H, d, J=10 Hz, C$\underline{H}_A$H$_B$O), 3.73 (1H, d, J=10 Hz, CH$_A$$\underline{H}_B$O), 4.12 (1H, m, >C$\underline{H}$–OH), 5.63 (3H, m, olefinic protons). MS *m/z*: 194 (M$^+$). A mixture of the diol (1.74 g, 9 mmol) and MnO_2 (9.93 g, 114 mmol) in CH_3CN (24 ml) and CH_2Cl_2 (103 ml) was vigorously stirred for 15 h at room temperature. The precipitates were filtered off on a celite bed and the filtrate was washed with brine. The residue in CH_2Cl_2 was chromatographed on silica gel (60 g). Elution with 2—3% MeOH in CH_2Cl_2 afforded **4** (1.35 g, 78% yield). IR ν_{max} cm^{-1}: 3390, 1655, 1615. ^{1}H-NMR (60 MHz) δ: 3.63 (2H, s, CH_2OH), 5.58 (2H, m, olefinic protons), 5.90 (1H, s, olefinic proton). MS *m/z*: 192 (M$^+$).

The Iodo-ether (5) and Hydroxy-ether (6)——I_2 (2.55 g, 10 mmol) and Ag_2O (2.33 g, 10 mmol) were added to a solution of **4** (1.29 g, 6.7 mmol) in dioxane (81 ml) and H_2O (16 ml). The reaction mixture was stirred at room temperature for 1 h in the dark and the precipitate was filtered off. The filtrate was diluted with water and extracted with $CHCl_3$. The extract was washed with 5% $Na_2S_2O_3$ solution. The residue in 50% CH_2Cl_2 in hexane was chromatographed on alumina (80 g). Elution with ether afforded **5** (1.57 g, 73.8% yield), mp 129—130 °C (colorless prisms from CH_2Cl_2–ether). IR ν_{max} cm^{-1}: 1658, 1612. ^{1}H-NMR (60 MHz) δ: 3.91 (1H, d, J=9 Hz, C$\underline{H}_A$H$_B$O), 4.08 (1H, d, J=9 Hz, CH$_A$$\underline{H}_B$O), 4.45 (1H, m, >C$\underline{H}$–O), 4.76 (1H, dd, J=4, 8 Hz, >C$\underline{H}$–I), 5.79 (1H, s, olefinic proton). *Anal.* Calcd for $C_{12}H_{15}IO_2$: C, 45.30; H, 4.75. Found: C, 45.58; H, 4.70. Elution with 5% MeOH in CH_2Cl_2 afforded **6** (208 mg, 15% yield), mp 91—92 °C (colorless plates from ether). IR ν_{max} cm^{-1}: 3420, 1662, 1610. ^{1}H-NMR (60 MHz) δ: 3.82 (1H, d, J=8 Hz, C$\underline{H}_A$H$_B$O), 3.97 (1H, d, J=8 Hz, CH$_A$$\underline{H}_B$O), 4.04 (1H, m, >C$\underline{H}$–OH), 4.43 (1H, dd, J=5, 8 Hz, >C$\underline{H}$–O), 5.78 (1H, s, olefinic proton). *Anal.* Calcd for $C_{12}H_{16}O_3$: C, 69.21; H, 7.74. Found: C, 69.16; H, 7.74.

The Acetoxy Ether (7)——AcOAg (3.48 g, 20.8 mmol) was added to a solution of **5** (3.23 g, 10.2 mmol) in AcOH (130 ml). The mixture was stirred at 80 °C for 1.5 h under an argon atmosphere in the dark. The precipitates were filtered off and the filtrate was diluted with water, and extracted with ether. The extract was washed with brine and 5% $NaHCO_3$ solution. The residue in CH_2Cl_2 was chromatographed on silica gel (60 g). Elution with the same solvent provided **7** (2.18 g, 85.5% yield), mp 102—104 °C (colorless plates from ether–hexane). IR ν_{max} cm^{-1}: 1725,

1665, 1611. ^{1}H-NMR (60 MHz) δ: 2.05 (3H, s, $COCH_3$), 3.84 (1H, d, J=8 Hz, CH_AH_BO), 4.01 (1H, d, J=8 Hz, CH_AH_BO), 4.44 (1H, dd, J=4, 8 Hz, >CH–O), 5.00 (1H, m, >CH–OAc), 5.78 (1H, s, olefinic proton). *Anal.* Calcd for $C_{14}H_{18}O_4$: C, 67.18; H, 7.25. Found: C, 67.02; H, 7.27.

Methanolysis of the Acetoxy Ether (7)——A solution of **7** (1.04 g, 41.6 mmol) in dry MeOH (20 ml) containing dissolved Na (2.2 g, 95.6 mmol) was stirred at room temperature for 1 h under an argon atmosphere. The reaction mixture was diluted with water and extracted with $CHCl_3$. The residue was recrystallized from ether–CH_2Cl_2 to provide **6** (0.75 g, 86% yield), mp 90—92 °C, which was identified by IR and ^{1}H-NMR spectral comparison with an authentic sample.

The Three-Membered Ring Compound (9)——A mixture of **5** (159 mg, 0.5 mmol), hexamethylphosphorus triamide (0.2 ml), and *tert*-BuOK (280 mg, 2.5 mmol) in *tert*-BuOH (4 ml) was stirred at room temperature for 2 h under an argon stmosphere. After adding MeI (0.6 ml, 9.5 mmol), the mixture was further stirred overnight, diluted with water, and then extracted with CH_2Cl_2. The residue was subjected to pTLC using a 0.5% MeOH in $CHCl_3$ solvent system. The upper zone gave the starting material (**5**) (38 mg, 24% yield). The lower zone gave **9** (44.8 mg, 47.2% yield). This compound was recrystallized from ether to afford colorless prisms, mp 86—87 °C. IR ν_{max} cm^{-1}: 1651, 1603. ^{1}H-NMR (60 MHz) δ: 0.70 (1H, m, CH), 1.18 (1H, m, CH), 3.78 (1H, d, J=8 Hz, CH_AH_BO), 4.07 (1H, d, J=8 Hz, CH_AH_BO), 4.70 (1H, m, >CH–O), 5.95 (1H, s, olefinic proton). *Anal.* Calcd for $C_{12}H_{14}O_2$: C, 75.76; H, 7.42. Found: C, 75.95; H, 7.34.

The TBDMS Ether (10)——A mixture of **6** (995 mg, 4.78 mmol), imidazole (1.74 g, 25.5 mmol), and TBDMS Cl (2.14 g, 14.2 mmol) in dimethylformamide (13 ml) was stirred at 80 °C for 1.5 h. The reaction mixture was diluted with water and extracted with ether. The residue in hexane was chromatographed on alumina (40 g). Elution with 30% ether in hexane gave **10** (1.28 g, 83% yield), mp 81—83 °C (colorless needles from pentane). IR ν_{max} cm^{-1}: 1660, 1606. ^{1}H-NMR δ: 0.06 (6H, s, 2 × SiMe), 0.88 (9H, s, *tert*-Bu), 3.90 (1H, m, >CH–O), 3.98 (2H, s, CH_2–O), 4.31 (1H, dd, J=4, 8 Hz, >CH–O), 5.78 (1H, s, olefinic proton). *Anal.* Calcd for $C_{18}H_{30}O_3Si$: C, 67.03; H, 9.38. Found: C, 66.79: H, 9.23.

Dimethylation of 10——A mixture of *tert*-BuOK (960 mg, 8.57 mmol) and **10** (1.27 g, 3.94 mmol) in dry benzene (33 ml) was stirred at 70—80 °C for 1 h under an argon atmosphere, and then MeI (1.87 ml, 30.0 mmol) was added dropwise. The mixture was stirred at 70—80 °C for a further 1 h. After cooling, the mixture was diluted with water and extracted with ether. The extract was washed with 5% $Na_2S_2O_3$ solution and brine. The residue in hexane was chromatographed on alumina (50 g). Elution with 20% ether in hexane gave the dimethyl compound (**11**) (773 mg, 56% yield). IR ν_{max} cm^{-1}: 1705. ^{1}H-NMR (60 MHz) δ: 0.06 (6H, s, 2 × SiMe), 0.86 (9H, s, *tert*-Bu), 1.25 (3H, s, CMe), 1.28 (3H, s, CMe), 3.66 (1H, d, J=8 Hz, CH_AH_BO), 3.88 (1H, m, >CH–O), 4.05 (1H, d, J=8 Hz, CH_AH_BO), 4.33 (1H, dd, J=4, 8 Hz, >CH–O), 5.52 (1H, dd, J=5, 6 Hz, olefinic proton). MS *m/z*: 350 (M^+).

Reduction of 11 with $NaBH_4$——A solution of $NaBH_4$ (400 mg, 12.5 mmol) in dry MeOH (10 ml) was added dropwise to a solution of **11** (359 mg, 1.0 mmol) in dry MeOH (10 ml) at −78 °C under stirring and the reaction mixture was stirred for 1 h at the same temperature. Then, the temperature was raised to room temperature over 2 h. The reaction mixture was diluted with water and extracted with CH_2Cl_2. The residue in hexane was chromatographed on alumina (20 g). The product eluted with 50% ether in hexane and ether was recrystallized from pentane to afford the alcohol (**12**) (304 mg, 84% yield), mp 113—114 °C as colorless plates. IR ν_{max} cm^{-1}: 3600, 3450. ^{1}H-NMR (60 MHz) δ: 0.07 (6H, s, 2 × SiMe), 0.87 (9H, s, *tert*-Bu), 1.05 (3H, s, Me), 1.16 (3H, s, Me), 3.20 (1H, d, J=8 Hz, CH_AH_BO), 3.66—4.20 (3H, m, CH_AH_BO and 2 × CH–O), 5.52 (1H, t, J=6 Hz, olefinic proton). *Anal.* Calcd for $C_{20}H_{36}O_3Si$: C, 68.13; H, 10.29. Found: C, 68.06; H, 10.58.

Catalytic Hydrogenation of 12 under Medium Pressure——PtO_2 (35.2 mg) was added to a solution of **12** (80.8 mg, 0.23 mmol) in MeOH (15 ml) and the mixture was stirred under hydrogen at medium pressure (6.5 kg/cm^2) for 48 h at room temperature. The catalyst was filtered off and the filtrate was evaporated to dryness *in vacuo*. The residue was purified by pTLC using a 1% MeOH in $CHCl_3$ solvent system to give the dihydro compound (**13**) (68.9 mg, 84% yield). ^{1}H-NMR (60 MHz) δ: 0.03 (6H, s, 2 × SiMe), 0.87 (9H, s, *tert*-Bu), 0.98 (3H, s, Me), 1.03 (3H, s, Me), 3.35 (1H, m, >CH–O), 3.48 (1H, d, J=9 Hz, CH_AH_BO), 3.67 (1H, m, >CH–OH), 3.73 (1H, d, J=9 Hz, CH_AH_BO), 4.08 (1H, dd, J=4, 8 Hz, >CH–O). MS *m/z*: 354 (M^+).

Conversion of 13 to 14——Pyridinium dichromate (71.9 mg, 0.19 mmol) was added to a solution of **13** (48.9 mg, 0.14 mmol) in dimethylformamide (1.5 ml). The mixture was stirred at room temperature for 23 h, and then ether was added. The precipitate was filtered off and the filtrate was washed with brine. The residue was purified by pTLC using $CHCl_3$ as a developing solvent to give the ketone (31.8 mg, 65% yield). IR ν_{max} cm^{-1}: 1700. MS *m/z*: 352 (M^+). Eight drops of 5% HCl were added to a solution of the ketone (31.8 mg, 0.09 mmol) in tetrahydrofuran (THF) (5 ml), and the reaction mixture was stirred at 60 °C for 5 h, then diluted with water and extracted with CH_2Cl_2. The residue was recrystallized from ether–hexane to afford **14**. (18 mg, 84% yield), mp 121—124 °C. This compound was identical with the alcohol A (**14**) on the basis of IR and ^{1}H-NMR spectral comparisons.

The Diol (16)——Five drops of 5% HCl were added to a solution of **12** (64 mg, 0.18 mmol) in THF (5 ml), and the reaction solution was stirred at 60 °C for 2 h, then poured into 5% $NaHCO_3$ solution and extracted with CH_2Cl_2. The residue in CH_2Cl_2 was chromatographed on silica gel (2 g). Elution with 7% MeOH in CH_2Cl_2 provided the desilyl compound (36 mg, 85% yield), mp 168—170 °C (colorless plates from acetone–ether). IR ν_{max}^{Nujol} cm^{-1}: 3340. MS Calcd

for $C_{14}H_{22}O_3$: 238.1568 (M^+). Found: 238.1572. PtO_2 (33 mg) was added to a solution of the desilyl compound (36 mg, 0.15 mmol) in MeOH (12 ml) and the mixture was stirred under a hydrogen atmosphere at medium pressure (10 kg/cm^2) for 48 h at room temperature. The catalyst was filtered off and the filtrate was evaporated to dryness. The residue was recrystallized from acetone–ether to provide **16** (25 mg, 69.4% yield), mp 188—190 °C as colorless prisms. IR ν_{max} cm^{-1}: 3600, 3400. ^{1}H-NMR (60 MHz) δ: 0.80 (3H, s, Me), 1.05 (3H, s, Me), 3.20 (1H, m, >CH–OH), 3.23 (1H, d, J=8 Hz, CH_AH_BO), 3.70 (1H, m, >CH–OH), 4.01 (1H, m, >CH–O), 4.05 (1H, d, J=8 Hz, CH_AH_BO). MS Calcd for $C_{14}H_{24}O_3$: 240.1725 (M^+). Found: 240.1724.

The Diketone (17)——i) Oxidation of the Alcohol B (15) with Jones Reagent: Five drops of Jones reagent were added to a solution of **15** (13 mg, 0.055 mmol) in acetone (3 ml) and the solution was stirred for 30 min under ice-cooling. Excess reagent was decomposed with iso-PrOH. The mixture was diluted with water extracted with ether. The residue in CH_2Cl_2 was purified on a short column of silica gel to give **17** (10 mg, 77% yield). IR ν_{max} cm^{-1}: 1705. ^{1}H-NMR (60 MHz) δ: 1.13 (3H, s, Me), 1.15 (3H, s, Me), 3.63 (1H, d, J=8 Hz, CH_AH_BO), 4.18 (1H, br d, J=9 Hz, >CH–O), 4.45 (1H, d, J=8 Hz, CH_AH_BO). MS *m/z*: 236 (M^+).

ii) Oxidation of **16** with Jones Reagent: Jones reagent (0.044 ml, 0.12 mmol) was added to a solution of **16** (21 mg, 0.088 mmol) in acetone (5 ml) and the solution was stirred for 30 min under ice-cooling. Excess reagent was decomposed with iso-PrOH. The mixture was diluted with water and extracted with ether. Purification of the residue in $CHCl_3$ on a short column of silica gel gave **17** (16.8 mg, 81% yield). This product was identical with the diketone (**17**) derived from the alcohol A on the basis of IR and ^{1}H-NMR spectral comparisons.

The Hydroxy Acetate (18)——A solution of **12** (656 mg, 1.86 mmol) in Ac_2O (6 ml) and pyridine (12 ml) was allowed to stand at room temperature for 3 h, and then evaporated to dryness *in vacuo*. The residue was diluted with water and extracted with ether. Purification of the residue in hexane on a short column of alumina gave the acetate (734 mg, 99% yield). IR ν_{max} cm^{-1}: 1723. MS *m/z*: 394 (M^+). A solution of the acetate (734 mg, 1.86 mmol) in THF (15 ml) was treated with 5% HCl (0.5 ml) and the mixture was refluxed for 1 h, then diluted with 5% $NaHCO_3$ solution and extracted with CH_2Cl_2. The residue in CH_2Cl_2 was chromatographed on silica gel (15 g). Elution with the same solvent gave **18** (428 mg, 82% yield), mp 165—167 °C (colorless prisms from ether). IR ν_{max} cm^{-1}: 3480, 1725. ^{1}H-NMR (60 MHz) δ: 1.08 (3H, s, Me), 1.12 (3H, s, Me), 1.98 (3H, s, $COCH_3$), 3.25 (1H, d, J=8 Hz, CH_AH_BO), 3.70—4.30 (2H, m, 2×CH–O), 4.00 (1H, d, J=8 Hz, CH_AH_BO), 4.50 (1H, m, >CH–OAc), 5.52 (1H, dd, J=5, 7 Hz, olefinic proton). MS Calcd for $C_{16}H_{24}O_4$: 280.1675 (M^+). Found: 280.1672.

The Dihydro Compound (19)——PtO_2 (60 mg) was added to a solution of **18** (50 mg, 0.18 mmol) in AcOEt (15 ml) containing AcOH (5 drops) and the mixture was stirred under a hydrogen atmosphere at medium pressure (9 kg/cm^2) for 24 h at room temperature. The reaction mixture was poured into 5% $NaHCO_3$ solution and extracted with CH_2Cl_2. The residue was recrystallized from ether to provide **19** (45.4 mg, 90% yield), mp 203—205 °C, as colorless plates. IR ν_{max} cm^{-1}: 3360, 1720. ^{1}H-NMR (60 MHz) δ: 0.88 (3H s, Me), 0.93 (3H, s, Me), 2.00 (3H, s, $COCH_3$), 3.25 (1H, d, J=8 Hz, CH_AH_BO), 3.76 (1H, m, >CH–OH), 4.01 (1H, m, >CH–O), 4.08 (1H, d, J=8 Hz, CH_AH_BO), 4.45 (1H, dd, J=4, 10 Hz, >CH–OAc). MS Calcd for $C_{16}H_{26}O_4$: 282.1831 (M^+). Found: 282.1833.

Hydrolysis of 19——A solution of **19** (22.7 mg, 0.08 mmol) in MeOH (2 ml) was treated with 10% NaOH solution (5 drops) and the mixture was stirred overnight at room temperature under an argon atmosphere, then diluted with water and extracted with $CHCl_3$. The residue was recrystallized from acetone–ether to give **16** (18 mg, 93% yield), mp 187—189 °C. This compound was identical with the diol (**16**) on the basis of IR and ^{1}H-NMR spectral comparisons.

The Hydroxy Ketone (20)——Jones reagent (10 drops) was added dropwise to a solution of **19** (215 mg, 0.76 mmol) in acetone (7 ml) and the solution was stirred for 10 min under ice-cooling. Excess reagent was decomposed by iso-PrOH. The mixture was diluted with water and extracted with ether. The residue in ether was chromatographed on alumina (10 g). Elution with ether afforded the acetoxy ketone (166 mg, 78% yield), mp 147—149 °C (colorless plates from hexane). IR ν_{max} cm^{-1}: 1727, 1710. ^{1}H-NMR (60 MHz) δ: 0.98 (3H, s, Me), 1.00 (3H, s, Me), 2.05 (3H, s, $COCH_3$), 3.42 (1H, dd, J=1, 8 Hz, CH_AH_BO), 4.10 (1H, dd, J=1, 8 Hz, >CH–O), 4.28 (1H, d, J=8 Hz, CH_AH_BO), 4.47 (1H, dd, J=4, 10 Hz, >CH–OAc). MS Calcd for $C_{16}H_{24}O_4$: 280.1672 (M^+). Found: 280.1655. A solution of the acetoxy ketone (166 mg, 0.59 mmol) and KOH (112 mg, 2 mmol) in MeOH (5 ml) was stirred at room temperature for 2 h under an argon atmosphere. The mixture was diluted with water and extracted with CH_2Cl_2. The residue was recrystallized from ether–hexane to give **20** (130 mg, 93% yield), mp 118—120 °C, as colorless plates. IR ν_{max} cm^{-1}: 3400, 1710. ^{1}H-NMR (60 MHz) δ: 0.87 (3H, s, Me), 1.10 (3H, s, Me), 3.23 (1H, dd, J=4, 9 Hz, >CH–OH), 3.42 (1H, dd, J=2, 8 Hz, CH_AH_BO), 4.08 (1H, dd, J=2, 9 Hz, >CH–O), 4.27 (1H, d, J=8 Hz, CH_AH_BO). *Anal.* Calcd for $C_{14}H_{22}O_3$: C, 70.55; H, 9.31. Found: C, 70.47; H, 9.60.

The Norketone (21), the Isopropenyl Compound (22), 23 and 24 from 20——PCl_5 (441 mg, 2.12 mmol) was added portionwise to a solution of **20** (300 mg, 1.26 mmol) in dry benzene (30 ml) over 1 h at 5 °C under an argon atmosphere, and the mixture was stirred for a further 1 h. The reaction mixture was poured into 5% $NaHCO_3$ solution and extracted with ether. The residue in 5% AcOEt in hexane was chromatographed on silica gel (60 g). Elution with 10—20% AcOEt in hexane gave **23** (8 mg, 2.9% yield). IR ν_{max} cm^{-1}: 1705. ^{1}H-NMR (200 MHz) δ: 0.96 (3H, d, J=6.8 Hz, >CH–Me), 0.98 (3H, d, J=6.8 Hz, >CH–Me), 3.78 (1H, d, J=8.0 Hz, CH_AH_BO), 3.93 (1H, d, J=8.0 Hz, CH_AH_BO), 4.39 (1H, d, J=9.5 Hz, >CH–O). MS *m/z*: 220 (M^+). Elution with 20% AcOEt in hexane gave

21 (131 mg, 47% yield). This product was identified by comparison of its IR and ^{1}H-NMR spectra with these of an authentic sample of the norketone (**21**). IR ν_{max} cm^{-1}: 1705. ^{1}H-NMR (200 MHz) δ: 1.64 (3H, s, Me), 1.65 (3H, s, Me), 3.54 (1H, d, J=8.3 Hz, C$\underline{H}_A$H$_B$O), 4.14 (1H, d, J=8.3 Hz, CH$_A\underline{H}_B$O), 4.42 (1H, d, J=9.2 Hz, >C$\underline{H}$–O). MS Calcd for $C_{14}H_{20}O_2$: 220.1464 (M$^+$). Found: 220.1464. Elution with 30% AcOEt in hexane gave **22** (70 mg, 25% yield). IR ν_{max} cm^{-1}: 1700, 1640, 895. ^{1}H-NMR (60 MHz) δ: 1.75 (3H, br s, Me), 3.42 (1H, d, J=8 Hz, C$\underline{H}_A$H$_B$O), 4.11 (1H, d, J=8 Hz, CH$_A\underline{H}_B$O), 4.27 (H, d, J=9 Hz, >C$\underline{H}$–O), 4.67 (1H, br s, olefinic proton), 4.83 (1H, br s, olefinic proton). MS Calcd for $C_{14}H_{20}O_2$: 220.1464 (M$^+$). Found: 220.1464. Elution with 50% AcOEt in hexane gave **24** (12 mg, 3.7% yield). This product was recrystallized from ether–hexane to afford colorless needles, mp 139—141 °C. IR ν_{max} cm^{-1}: 1710. ^{1}H-NMR (200 MHz) δ: 1.06 (3H, s, Me), 1.14 (3H, s, Me), 3.49 (1H, d, J=8.5 Hz, C$\underline{H}_A$H$_B$O), 4.07 (1H, t, J=3 Hz, >C$\underline{H}$–Cl), 4.16 (1H, d, J=9.3 Hz, >C$\underline{H}$–O), 4.33 (1H, d, J=8.5 Hz, CH$_A\underline{H}_B$O). MS Calcd for $C_{14}H_{21}ClO_2$: 256.1230 (M$^+$). Found: 256.1235.

The Dimethylacetal (25)——A mixture of **20** (60 mg, 0.25 mmol), HC(OMe)$_3$ (150 μl, 1.37 mmol), and H_2SO_4 (1 drop) in dry MeOH (4.5 ml) was stirred at room temperature for 7 h under an argon atmosphere and poured into 5% $NaHCO_3$ solution, then extracted with $CHCl_3$. The residue was recrystallized from ether–pentane to afford **25** (70 mg, 99% yield), mp 146—149 °C, as colorless flakes. IR ν_{max} cm^{-1}: 3450. ^{1}H-NMR (60 MHz) δ: 0.83 (3H, s, Me), 1.04 (3H, s, Me), 3.11 (3H, s, OMe), 3.20 (3H, s, OMe), 4.02 (1H, m, >C$\underline{H}$–O), 4.17 (1H, d, J=8 Hz, CH$_A\underline{H}_B$O). *Anal.* Calcd for $C_{16}H_{28}O_4$: C, 67.57; H, 9.93. Found: C, 67.46; H, 10.19.

The Methoxy Cyanides A (26) and B (27)——A mixture of **25** (220 mg, 0.67 mmol), Me_3SiCN (1.5 ml) and a catalytic amount of anhydrous $SnCl_2$ was stirred at room temperature for 2.5 h and poured into 5% $NaHCO_3$ solution, then extracted with ether. The residue in hexane was chromatographed on alumina (15 g). Elution with 15% ether in hexane afforded **26** (49 mg, 18.1% yield), mp 115—117 °C (colorless flakes from ether–pentane). IR ν_{max} cm^{-1}: 2240. ^{1}H-NMR (200 MHz) δ: 0.09 (9H, s, $SiMe_3$), 0.80 (3H, s, Me), 0.96 (3H, s, Me), 3.22 (1H, dd, J=3.9, 11.2 Hz, >C$\underline{H}$–O), 3.39 (1H, dd, J=1.2, 8.8 Hz, C$\underline{H}_A$H$_B$O), 3.52 (3H, s, OMe), 4.28 (1H, d, J=8.8 Hz, CH$_A\underline{H}_B$O), 4.47 (1H, br d, J=8.8 Hz, >C$\underline{H}$–O). MS Calcd for $C_{19}H_{33}NO_3Si$: 351.2230 (M$^+$). Found: 351.2227. Successive elution with the same solvent afforded **27** (165 mg, 60.9% yield), mp 118—121 °C (colorless needles from ether–pentane). IR ν_{max} cm^{-1}: 2240. ^{1}H-NMR (200 MHz) δ: 0.09 (9H, s, $SiMe_3$), 0.81 (3H, s, Me), 0.97 (3H, s, Me), 3.21 (1H, dd, J=3.6, 11.2 Hz, >C$\underline{H}$–O), 3.36 (1H, dd, J=1.2, 8.8 Hz, C$\underline{H}_A$H$_B$O), 3.45 (3H, s, OMe), 4.17 (1H, td, J=1.8, 7.3 Hz, >C$\underline{H}$–O), 4.29 (1H, d, J=8.8 Hz, CH$_A\underline{H}_B$O). MS Calcd for $C_{19}H_{33}NO_3Si$: 351.2230 (M$^+$). Found: 351.2232.

Conversion of the Methoxy Cyanide A (26) to the Monoacetate A (30) *via* the Methoxy Ester A (28)——A mixture of **26** (49 mg, 0.14 mmol) and hydrate (2 drops) in a solution of 30% KOH in ethylene glycol (1.5 ml) was refluxed for 6 h under an argon atmosphere. The reaction mixture was made acidic by adding 5% HCl solution and extracted with $CHCl_3$. The residue in MeOH was methylated with diazomethane in ether and evaporated to dryness *in vacuo*. The residue in $CHCl_3$ was chromatographed on silica gel (8 g). The product eluted with $CHCl_3$ was recrystallized from ether–hexane to give the methoxy ester A (**28**) (35 mg, 82% yield), mp 147—150 °C, as colorless prisms. IR ν_{max} cm^{-1}: 3450, 1730. ^{1}H-NMR (200 MHz) δ: 0.85 (3H, s, Me), 1.06 (3H, s, Me), 3.24 (1H, dd, J=3.5, 11.8 Hz, >C$\underline{H}$–OH), 3.34 (3H, s, OMe), 3.37 (1H, d, J=8.6 Hz, C$\underline{H}_A$H$_B$O), 3.74 (3H, s, OMe), 4.26 (1H, d, J=8.6 Hz, CH$_A\underline{H}_B$O), 4.51 (1H, d, J=9.0 Hz, >C$\underline{H}$–O). MS Calcd for $C_{17}H_{28}O_5$: 312.1937 (M$^+$). Found: 312.1943. A mixture of **28** (35 mg, 0.11 mmol), dry NaI (56 mg, 0.37 mmol), and Me_3SiCl (30 mg, 0.32 mmol) in dry CH_3CN (1.5 ml) was stirred at 80 °C for 3 h. The mixture was made acidic with 5% HCl solution and extracted with AcOEt. The residue in MeOH was methylated with diazomethane solution in ether and evaporated to dryness *in vacuo*. The residue was purified by pTLC using a 4% MeOH in $CHCl_3$ solvent system to give the dihydroxy ester A (30.5 mg, 93% yield). This product was recrystallized from ether to give colorless prisms, mp 173—175 °C. IR ν_{max} cm^{-1}: 3450, 1725. ^{1}H-NMR (200 MHz) δ: 0.85 (3H, s, Me), 1.08 (3H, s, Me), 3.26 (1H, dd, J=3.7, 11.5 Hz, >C$\underline{H}$–OH), 3.41 (1H, d, J=8.5 Hz, C$\underline{H}_A$H$_B$O), 3.75 (3H, s, OMe), 4.11 (1H, d, J=8.1 Hz, >C$\underline{H}$–O), 4.21 (1H, d, J=8.5 Hz, CH$_A\underline{H}_B$O). MS Calcd for $C_{16}H_{26}O_5$: 298.1780 (M$^+$). Found: 298.1781. A mixture of the dihydroxy ester A (30.5 mg, 0.1 mmol), a catalytic amount of *p*-TsOH, and acetic anhydride (1 ml) was stirred at room temperature for 2 h. After decomposition of excess acetic anhydride with 5% $NaHCO_3$ solution, the mixture was extracted with ether. The residue was purified by pTLC using a 1.5% MeOH in $CHCl_3$ solvent system to afford the diacetoxy ester A (32 mg, 84% yield). This compound was recrystallized from ether–hexane to afford colorless prisms, mp 137—139 °C. IR ν_{max} cm^{-1}: 1730. MS *m/z*: 382 (M$^+$). A solution of the diacetoxy ester A (32 mg, 0.084 mmol) in MeOH (2 ml) and 5% HCl solution (1 ml) was stirred at room temperature overnight, then diluted with water and extracted with $CHCl_3$. The residue was purified by pTLC using a 3% MeOH in $CHCl_3$ solvent system to afford **30** (20.8 mg, 73% yield). IR ν_{max} cm^{-1}: 3450, 1735. ^{1}H-NMR (200 MHz) δ: 0.86 (3H, s, Me), 1.08 (3H, s, Me), 2.12 (3H, s, $COCH_3$), 3.27 (1H, dd, J=4.5, 11.3 Hz, >C$\underline{H}$–OH), 3.37 (1H, dd, J=1.3, 8.5 Hz, C$\underline{H}_A$H$_B$O), 3.69 (3H, s, OMe), 4.18 (1H, d, J=8.5 Hz, CH$_A\underline{H}_B$O), 4.82 (1H, br d, J=9 Hz, >C$\underline{H}$–O). MS Calcd for $C_{18}H_{28}O_6$: 340.1886 (M$^+$). Found: 340.1885.

The Isopropylidene Compound A (32)——PCl_5 (54 mg, 0.26 mmol) was added portionwise to a solution of **30** (43 mg, 0.13 mmol) in dry benzene (3 ml) over 30 min under ice-cooling. Then the mixture was stirred for a further 20 min, poured into 5% $NaHCO_3$ solution, and extracted with ether. The residue was purified by pTLC using a 20% AcOEt in hexane solvent system to provide **32** (22 mg, 55% yield). IR ν_{max} cm^{-1}: 1735. ^{1}H-NMR (200 MHz) δ: 1.60 (3H, s, Me), 1.73 (3H, s, Me), 3.40 (1H, br d, J=8.3 Hz, C$\underline{H}_A$H$_B$O), 3.70 (3H, s, OMe), 3.76 (1H, d, J=8.3 Hz,

CH_AH_BO), 4.90 (1H, brd, J=8.8 Hz, >C$\underline{H}$–O). MS Calcd for $C_{18}H_{26}O_5$: 322.1780 (M^+). Found: 322.1785. This compound contained about 10% of the isopropenyl compound as determined by ^{1}H-NMR (200 MHz) analysis.

The Hydroxy Acid A (36)——A solution of **32** (20 mg, 0.06 mmol) in 1% NaOH in MeOH (1.5 ml) was stirred overnight at room temperature. The mixture was made acidic with 10% citric acid solution and extracted with AcOEt. The residue was recrystallized from ether–hexane to provide **36** (10 mg, 61% yield), mp 173—176 °C, as colorless flakes. IR ν_{max} cm^{-1}: 3500—3200, 1760, 1710. ^{1}H-NMR (200 MHz) δ: 1.62 (3H, s, Me), 1.74 (3H, s, Me), 3.46 (1H, d, J=8.2 Hz, CH_AH_BO), 3.79 (1H, d, J=8.2 Hz, CH_AH_BO), 4.11 (1H, brt, J=4.2 Hz, >C$\underline{H}$–O). MS Calcd for $C_{15}H_{22}O_4$: 266.1518 (M^+). Found: 266.1523.

Conversion of the Methoxy Cyanide B (27) *to* the Monoacetate B (31) *via* the Methoxy Ester B (29)——A mixture of **27** (103 mg, 0.29 mmol) and hydrazine hydrate (6 drops) in a solution of 20% KOH in ethylene glycol (8 ml) was refluxed for 5 h. The reaction mixture was worked up and methylated with diazomethane in the same way as described for the preparation of **28**. The residue in $CHCl_3$ was chromatographed on silica gel (25 g). The product eluted with $CHCl_3$ was recrystallized from ether–hexane to afford **29** (77.3 mg, 88% yield), mp 142—145 °C, as colorless prisms. IR ν_{max} cm^{-1}: 3450, 1730. ^{1}H-NMR (200 MHz) δ: 0.83 (3H, s, Me), 1.08 (3H, s, Me), 3.16 (3H, s, OMe), 3.25 (1H, dd, J=4.0, 11.4 Hz, >C$\underline{H}$–OH), 3.28 (1H, dd, J=1.4, 8.5 Hz, CH_AH_BO), 4.14 (1H, d, J=8.5 Hz, CH_AH_BO), 4.25 (1H, ddd, J=1.9, 3.9, 5.8 Hz, >C$\underline{H}$–O). MS Calcd for $C_{17}H_{28}O_5$: 312.1937 (M^+). Found: 312.1928. A mixture of **29** (77.3 mg, 0.25 mmol), dry NaI (144 mg, 0.96 mmol), Me_3SiCl (108 mg, 0.96 mmol) in dry CH_3CN (6 ml) was refluxed for 6 h. The mixture was worked up and methylated with diazomethane in the same way as described for the preparation of the dihydroxy ester A. The residue was recrystallized from ether–benzene to afford the dihydroxy ester B (65.7 mg, 29% yield), mp 89—95 °C, as colorless prisms. IR ν_{max} cm^{-1}: 3500, 1740, 1720. ^{1}H-NMR (200 MHz) δ: 0.84 (3H, s, Me), 1.08 (3H, s, Me), 3.26 (1H, dd, J=3.7, 11.5 Hz, >C$\underline{H}$–OH), 3.31 (1H, dd, J=1.2, 8.5 Hz, CH_AH_BO), 3.80 (3H, s, OMe), 4.06 (1H, dt, J=8.0, 1.7 Hz, >C$\underline{H}$–O), 4.17 (1H, d, J=8.5 Hz, CH_AH_BO). MS m/z: 298 (M^+). A mixture of the dihydroxy ester B (65.7 mg, 0.22 mmol), a catalytic amount of *p*-TsOH, and acetic anhydride (3 ml) was stirred at room temperature for 1 h. The mixture was worked up as described for the preparation of the diacetoxy ester A. The residue in ether was chromatographed on alumina (3 g). The product eluted with ether was recrystallized from ether–hexane to give the diacetoxy ester B (80 mg, 95% yield), mp 147—149 °C, as colorless needles. IR ν_{max} cm^{-1}: 1730. MS m/z: 382 (M^+). A solution of the diacetoxy ester B (80 mg, 0.21 mmol) in MeOH (5 ml) and 5% HCl solution (3 ml) was stirred at room temperature for 36 h. The mixture was worked up and purified in the same way as described for the preparation of **30** to give **31** (61 mg, 85% yield), mp 186—190 °C (colorless prisms from ether–$CHCl_3$). IR ν_{max} cm^{-1}: 3450, 1745, 1735. ^{1}H-NMR (200 MHz) δ: 0.84 (3H, s, Me), 1.07 (3H, s, Me), 2.01 (3H, s, $COCH_3$), 3.25 (1H, dd, J=3.7, 11.5 Hz, >C$\underline{H}$–OH), 3.32 (1H, dd, J=1.2, 8.6 Hz, CH_AH_BO), 3.75 (3H, s, OMe), 4.17 (1H, d, J=8.6 Hz, CH_AH_BO), 4.28 (1H, dt, J=1.5, 4.9 Hz, >C$\underline{H}$–O). MS Calcd for $C_{18}H_{28}O_6$: 340.1886 (M^+). Found: 340.1887.

The Isopropylidene Compound (33), the Isopropenyl Compound (34), and the Chloro Compound (35) from 31——PCl_5 (133 mg, 0.64 mmol) was added portionwise to a solution of **31** (108 mg, 0.32 mmol) in dry benzene (4.5 ml) over 30 min. The mixture was stirred for a further 30 min, then poured into 5% $NaHCO_3$ solution and extracted with ether. The residue was separated by pTLC using a 20% AcOEt in hexane solvent system. The upper zone gave a mixture of **33** and **34**, and the lower zone gave **35** (5 mg, 4% yield). The mixture of **33** and **34** was further separated by pTLC impregnated with $AgNO_3$ using 15% AcOEt in hexane. The less polar zone gave **33** (76 mg, 74% yield) and the more polar zone gave **34** (6 mg, 6% yield). **33**: IR ν_{max} cm^{-1}: 1750, 1735. ^{1}H-NMR (200 MHz) δ: 1.60 (3H, s, Me), 1.72 (3H, s, Me), 2.03 (3H, s, $COCH_3$), 3.37 (1H, d, J=8.3 Hz, CH_AH_BO), 3.74 (3H, s, OMe), 3.78 (1H, d, J=8.3 Hz, CH_AH_BO), 4.40 (1H, d, J=8.5 Hz, >C$\underline{H}$–O). MS Calcd for $C_{18}H_{26}O_5$: 322.1780 (M^+). Found: 322.1777. **34**: IR ν_{max} cm^{-1}: 1750, 1735, 1640. ^{1}H-NMR (200 MHz) δ: 1.77 (3H, brs, Me), 2.02 (3H, s, $COCH_3$), 3.32 (1H, dd, J=1.0, 8.1 Hz, CH_AH_BO), 3.73 (3H, s, OMe), 4.07 (1H, d, J=8.1 Hz, CH_AH_BO), 4.36 (1H, d, J=8.8 Hz, >C$\underline{H}$–O), 4.67 (1H, brs, olefinic proton), 4.88 (1H, brs, olefinic proton). MS Calcd for $C_{18}H_{26}O_5$: 322.1780 (M^+). Found: 322.1781. **35**: IR ν_{max} cm^{-1}: 1755, 1740. ^{1}H-NMR (200 MHz) δ: 0.81 (3H, s, Me), 0.88 (3H, s, Me), 2.02 (3H, s, $COCH_3$), 3.34 (1H, dd, J=1.2, 8.6 Hz, CH_AH_BO), 3.75 (3H, s, OMe), 4.03 (1H, t, J=3 Hz, >C$\underline{H}$–Cl), 4.17 (1H, d, J=8.6 H, CH_AH_BO), 4.30 (1H, dt, J=8.0, 1.7 Hz, >C$\underline{H}$–O). MS Calcd for $C_{18}H_{27}ClO_5$: 358.1546 (M^+). Found: 358.1538.

***dl*-Aspterric Acid (1)**——A solution of **33** (74 mg, 0.23 mmol) in 1% NaOH solution in MeOH (5 ml) was allowed to stand at room temperature overnight and then heated at 50 °C for 18 h. The mixture was made acidic with 10% citric acid solution and extracted with $CHCl_3$. The residue was recrystallized from ether–hexane to afford **1** (48 mg, 76% yield), mp 164—166 °C, as colorless needles. This compound was identical with natural aspterric acid (except for optical rotation) on the basis of comparisons of the IR and ^{1}H-NMR (200 MHz) spectra, and TLC behavior.

Acknowledgement The authors are indebted to Professor Y. Tsuda, Faculty of Pharmaceutical Sciences, Kanazawa University, for providing copies of the IR and ^{1}H-NMR spectra of the norketone (**21**) and an authentic sample of aspterric acid.

References

1) Y. Tsuda, M. Kaneda, A. Tada, K. Nitta, Y. Yamamoto, and Y. Iitaka, *J. Chem. Soc., Chem. Commun.*, **1978**, 160.
2) T. Harayama, Y. Shinkai, Y. Hashimoto, H. Fukushi, and Y. Inubushi, *Tetrahedron Lett.*, **24**, 5241 (1983).
3) T. Harayama, Y. Shinkai, and Y. Inubushi, *Yakugaku Zasshi*, **106**, 659 (1986).
4) K. Utimoto, Y. Wakabayashi, Y. Shishiyama, M. Inoue, and H. Nozaki, *Tetrahedron Lett.*, **22**, 4279 (1981).
5) G. A. Olah, S. C. Narang, B. G. B. Gupta, and R. Molhortra, *J. Org. Chem.*, **44**, 1247 (1979).

[Chem. Pharm. Bull. 35(4)1443—1451(1987)]

Conformational Analysis of a Diene Analog of Isocarbacyclin and Prostacyclin

SHUICHI MIYAMOTO,* MASAFUMI YOSHIMOTO and KOICHI KOJIMA

Chemical Research Laboratories, Sankyo Co., Ltd., 2-58, 1-chome, Hiromachi, Shinagawa-ku, Tokyo 140, Japan

(Received May 21, 1986)

A diene analog (**2**) of isocarbacyclin has been found to be a potent inhibitor of platelet aggregation. A molecular mechanics calculation study on model compounds of both prostacyclin (**1**) and **2** was undertaken in an attempt to elucidate the stereochemical properties and to find the active conformers. At first the ring structures were investigated, then the directions of the α-chain and finally the entire model compounds were studied. A working hypothesis that four functional groups, consisting of a carboxyl group of the α-chain, a hydroxyl group at position 11, another hydroxyl group of the ω-chain and a π-electron system at the 5, 6 and 6a positions, play an important role in binding with a receptor to elicit activities is presented. Three-dimensional arrangements of these essential functional groups in stable conformations were examined by superimposing the coordinates of the four groups of **2** on those of **1**, because these moieties in the receptor-bound conformations should be identically located in both molecules. Three candidates for the active conformers are presented as a basis for a rational approach to the design of prostacyclin agonists.

Keywords——prostacyclin; isocarbacyclin; π-electron system; conformational analysis; molecular mechanics; MMPI; MM2′; active conformation

Prostacyclin (PGI_2) (**1**) (Chart 1) is a potent, naturally occurring inhibitor of platelet aggregation and a powerful vasodilator.[1] The pharmacological properties of PGI_2 gave rise to numerous expectations as to its therapeutic potential. These ranged from more realistic prospects such as prevention of platelet loss during extracorporal circulation or hemodialysis to recanalization of occluded arteries and the vague hope of preventing stroke and myocardial infarction.[2] From a pharmacotherapeutic point of view, PGI_2 is an unfavorable candidate for drug development. Due to the presence of an enol-ether group that is susceptible to hydrolysis, PGI_2 has a very short half-life of only 3—4 min under physiological conditions.[3] Because of this instability and the extreme biological importance of PGI_2, a variety of analogs have been prepared.[4]

Synthetic studies of chemically stable derivatives with functional groups which are considered to be bioisosters of or pharmacologically similar to the enol-ether group have proceeded in our laboratories. Recently, a diene analog (**2**) (Chart 1) was shown to be a potent inhibitor of platelet aggregation with 50% inhibition concentration of 1 ng/ml.[5] Among the many factors related to the pharmacological activities of a compound, one of the most important is its conformation. Therefore, we have undertaken a conformational analysis of **1** and **2** to identify the 3-dimensional structures responsible for their activities, that is, the active conformations.

It is generally accepted that the carboxyl group of the α-chain, the 11 (*R*) hydroxyl group and the 15 (*S*) hydroxyl group of **1** and related compounds are essential for optimal activity.[6] We proposed as a working hypothesis that a π-electron system forming a vinyl ether in addition to the hydrophilic groups would serve as another essential functional group. In other

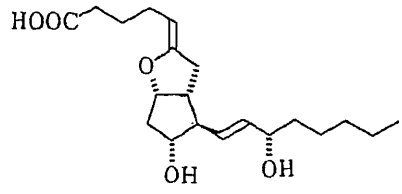

prostacyclin (PGI_2) (1)

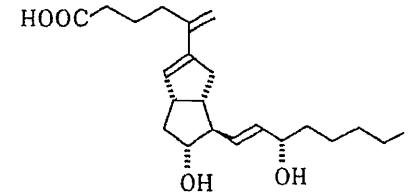

5,5-methyleneisocarbacyclin (2)

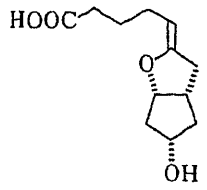

3

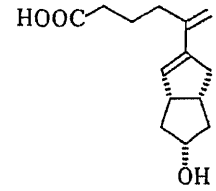

4

Chart 1

words, we postulated that these four moieties play a significant role in binding with a target receptor to elicit activities. Therefore, active conformations were evaluated in terms of the 3-dimensional arrangements of these moieties in stable conformations.

Molecules such as **1** and **2** consist of too many atoms for molecular mechanics calculations on the whole molecules to be feasible from the viewpoint of computing time. These compounds also have so many rotatable bonds that a tremendous number of initial structures would have to be taken into account. It would be reasonable, therefore, to employ model compounds of **1** and **2** instead. Since **1** and **2** have an identical ω-chain structure, we decided to ignore it. As a result, model compounds **3** and **4** having the carboxyl group of the α-chain, a hydroxyl group at position 11 and a π-electron system were to be analyzed; C12 in place of the ω-chain, including the hydroxyl group at C15, was taken as a dummy essential moiety.

Methods

Generation of Starting Structures——A model builder program named MBCS with a conformational search function was developed and used in order to generate the coordinates of a series of conformers, which were employed as the starting structures for geometry optimizations. The MBCS program uses standard bond lengths and bond angles[7] to calculate Cartesian and/or internal coordinates of conformers by varying any specified torsional angles automatically at given increments (ex. initial value = 60° and incremental value = 120° for a single bond between an sp^3 carbon atom and another sp^3 carbon atom). During the systematic scans of conformational space, structures with short contacts of atoms are excluded on the basis of van der Waals radii.[8] Here it is defined that a conformer is judged to have a short contact if the following equation is satisfied.

$$\overline{AB} < (r_A + r_B) \times R_f$$

where $\overline{AB}$ is the distance between nonbonded or nongeminal atoms A and B, r_A and r_B are the van der Waals radii of atoms A and B, respectively and R_f is a reducing factor with a general value of 0.7. As for conformers with a ring structure, any bonds can be rotated systematically (pseudorotation) and the resulting conformations are examined to exclude the structures for which ring formation is impossible. This function is convenient for obtaining a series of starting structures with various kinds of ring puckerings.

Geometry Optimization——Geometry optimizations were performed using the molecular mechanics method because of its relatively short computation time. Calculations of molecules containing a delocalized π-electron system were performed with the MMPI program[9] and those of other molecules with the MM2′ program.[10] In fact, the following approach was adopted to make the calculations more manageable: a stable conformation of a smaller structure or substructure was used as a basic skeleton for construction of starting geometries of a larger structure or parent structure, as shown in Fig. 1. In other words, first the ring structure was investigated, then the direc-

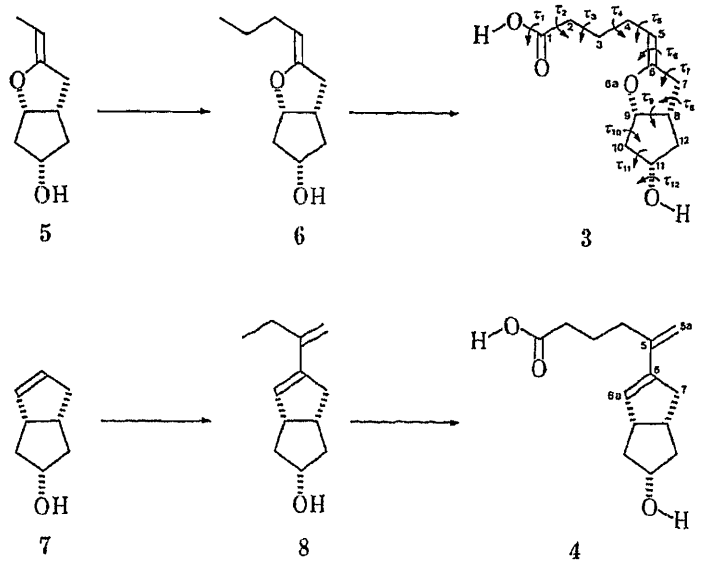

Fig. 1. Schemes to Build up the Model Compounds with Their Substructures, Showing Atom Numbering and Torsional Angles

Based on the stable conformations of 5 and 7, starting structures of 6 and 8, respectively, were obtained. Generation of initial structures of 3 and 4 was done using the preferred conformations of 6 and 8. Torsional angles used are as follows: τ_1: H–O–C1–C2, τ_2: O=C1–C2–C3, τ_3: C1–C2–C3–C4, τ_4: C2–C3–C4–C5, τ_5: C3–C4–C5–C6, τ_6: C4–C5–C6–C7, τ_7: C5–C6–C7–C8, τ_8: C6–C7–C8–C9, τ_9: C7–C8–C9–C6a, τ_{10}: C8–C9–C10–C11, τ_{11}: C9–C10–C11–O, τ_{12}: C10–C11–O–H. τ: A–B–C–D is the angle between the planes A–B–C and B–C–D, with the eclipse form being defined as 0°. Looking along A–B–C–D, a clockwise rotation of the plane B–C–D is considered positive.

tion of the α-chain and finally the entire model compound including the carboxyl group were studied.

Results and Discussion

Stable Conformations

Analysis of 5——The results of a preliminary calculation on cyclopentane with MM2′ were used in combination with the MBCS program in order to effectively generate ring structures having diverse puckerings. The bond lengths and angles shown explicity in Fig. 2 (A) were derived from the results mentioned above and were used instead of standard values. τ_{10} was changed to -25, 0 and 25° based on the same results. On the other hand, τ_8 and τ_9 were varied to -30, 0 and 30°, τ_{12} was incremented systematically by -60, 60 and 180°, and τ_5 and τ_6 were set to 0 and 180°, respectively. τ_5 was defined to be the torsional angle involving one of the three hydrogens at C4 instead of the removed C3. As the coordinates of C5 and C12 were determined spontaneously by the above assignments, τ_7 and τ_{11} did not need to be specified.

Geometry optimization with MM2′ was performed on the 46 starting conformers thus obtained to afford 18 independent stable conformers, all conformers having almost constant values for τ_5 and τ_6, *i.e.*, $-2<\tau_5<2°$ and $174<\tau_6<185°$. Among the 10 lowest energy conformers shown in Table I, the most stable two conformers 5-1 and 5-2 have almost identical 3D-structures except for τ_{12}. Features of the ring structure of these two conformers are as follows. One five-membered ring consisting of C6–C7–C8–C9–O6a has a twist conformation with C7 over the plane (when C8, C9 and O6a are placed on the plane) and C6 slightly under it. The other five-membered ring consisting of C8–C9–C10–C11–C12 also has a twist conformation with C11 over the plane (C11-up) and C12 slightly under it. As described in Table I, conformers with $\tau_{12}=60°$ are less stable than those with $\tau_{12}=-60$ and 180°, and

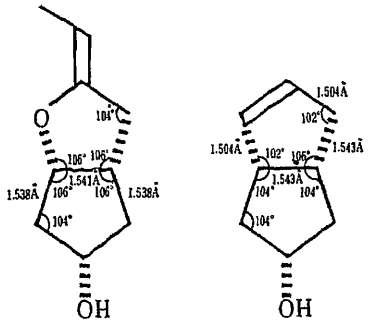

Fig. 2. Geometrical Parameters Derived from Preliminary Calculations and Used by the MBCS Program Instead of Standard Values
(A) 5; (B) 7.

TABLE I. Relative Energies and Torsional Angles of 5 with the Minimum Energies

Conformer No.	$\Delta E^{a)}$ (kcal/mol)	Torsional angles (°)					
		τ_7	τ_8	τ_9	τ_{10}	τ_{11}	τ_{12}
5-1	0	−146	−22	11	16	−156	−67
5-2	0.2	−146	−23	12	16	−156	−176
5-3	0.2	−144	−26	17	−31	−81	−58
5-4	0.3	−157	−7	−5	−17	−84	−68
5-5	0.4	180	−18	26	2	−147	−66
5-6	0.4	180	−18	26	2	−147	−176
5-7	0.5	−148	−19	8	−26	−81	−170
5-8	0.6	150	15	−3	−18	−83	−67
5-9	0.6	150	29	−25	40	−159	−66
5-10	0.6	−146	−23	13	14	−156	57

a) Difference from the lowest energy.

TABLE II. Relative Energies and Torsional Angles of 6 with the Minimum Energies

Conformer No.	$\Delta E^{a)}$ (kcal/mol)	Torsional angles (°)		
		τ_4	τ_5	τ_6
6-1	0	63	−112	175
6-2	0.5	180	−98	174
6-3	0.7	180	120	176
6-4	0.9	−63	119	176
6-5	1.0	−62	−92	174
6-6	1.5	63	93	176

a) Difference from the lowest energy.

structures with $\tau_{12} = -60°$ have slightly lower energies than those with $\tau_{12} = 180°$.

Analysis of 6——Based on the most stable conformer, 5-1, starting conformations of **6** were built using MBCS by increasing τ_5 by 30°, changing τ_4 to −60, 60 and 180°, and setting τ_3 to 60°. The resulting structures were subjected to geometry optimizations to find that the stable conformations of **6** can be divided into two major classes with respect to the value of τ_5. One class includes conformations with $\tau_5 = 80$—130° (the conformation is called C3-up because C3 comes over the plane when C4, C5 and C6 are placed on the plane) and the other class contains those with $\tau_5 = -80$——120° (C3-down). In each class τ_4 has a preference for −60, 60 and 180° as expected, as a result of which there emerge six groups of stable structures of **6**. The most stable conformations of each group are reported in Table II. The largest factor

dominating C3-up or C3-down conformations seems to be the steric repulsion between the methylene group at C3 and the lone pairs of oxygen atom (O6a) or the hydrogen atom at C5. A close inspection of Table II indicates that C3-down conformers are a little more stable than C3-up ones.

Analysis of 3——As there are two classes of conformations (C3-up and C3-down) for stable structures of **6**, conformational search was done using both conformers 6-1 and 6-3 to generate starting structures of **3**. τ_5 was changed to -112 and $120°$ and τ_4 to 63, 180 and $-63°$ ($-62°$ was used in place of $-63°$ at $\tau_5 = -112°$). Since conformational analysis of carboxylic acids by Allinger and Chang[11] showed that τ_2 has a preference for -120, 0 and $120°$ and that τ_3 has a preference for -60, 60 and $180°$, these respective values for τ_2 and τ_3 were taken into account at the time of conformational search. τ_1 was set to $180°$ (O–H being eclipsed against C=O) since conformers of this geometry were considered to have the lowest energies.

Energy calculations were carried out on the 43 starting conformers which were generated by MBCS under the above conditions. Parameters for a carboxylic acid derived by Allinger and Chang[11] were employed for computations. Table III summarizes the energies and torsional angles of the conformers with ΔE (difference from the lowest energy) less than 2.0 kcal/mol. The conformations with C3-down are slightly more stable than those with C3-up. There are three favored values for each τ_2, τ_3 and τ_4 which give the minimum energy structures. This means that the α-chain has considerable conformational flexibility.

Analysis of 7——First, a preliminary calculation on cyclopentene was done with MM2′. The resulting data on the most stable envelope conformation were then employed to generate initial structures of **7**; bond lengths and angles derived from the above calculation are explicitly shown in Fig. 2 (B) and were used with the MBCS instead of standard values. τ_8 and τ_9 had two combinations of angle values, namely, -24 and $24°$, and 24 and $-24°$. On the other hand, τ_{10} was changed to -30, 0 and $30°$ and τ_{12} to -60, 60 and $180°$.

After geometry optimizations were performed on the 14 starting conformers generated, 9

Table III. Energies and Torsional Angles of 3 with $\Delta E < 2.0$ kcal/mol

Conformation[a] class	Conformer No.	Energy (kcal/mol)	ΔE[b] (kcal/mol)	Torsional angles (°)			
				τ_2	τ_3	τ_4	τ_5
C3-up	3-1	20.1	1.1	0	180	180	118
	3-2	20.2	1.2	−1	−179	−63	121
	3-3	20.6	1.6	−15	−66	−61	114
	3-4	20.8	1.8	−8	−70	179	120
	3-5	20.9	1.9	−1	177	62	94
C3-down	3-6	19.0	0	0	178	62	−112
	3-7	19.6	0.6	−1	71	66	−109
	3-8	19.9	0.9	−118	176	62	−114
	3-9	19.9	0.9	−1	179	180	−112
	3-10	20.2	1.2	114	−179	63	−114
	3-11	20.5	1.5	10	68	178	−109
	3-12	20.6	1.6	−1	−176	−64	−108
	3-13	20.7	1.7	−119	−176	178	−111
	3-14	20.7	1.7	−10	−71	179	−112
	3-15	20.8	1.8	117	−177	−179	−111
	3-16	20.9	1.9	120	−60	179	−110

a) Conformations are divided into two major classes with respect to the τ_5 value. One class has a C3-up conformation (C3 comes over the paper when C4, C5 and C6 are placed on the paper) and the other one has a C3-down conformation. *b*) Difference from the lowest energy.

independent stable conformers were obtained (Table IV). The cyclopentene ring consisting of C6, C7, C8, C9 and C6a has some geometrical features. In all conformations, torsional angle ϕ (C7–C6–C6a–C9) falls into the range of $0\pm1°$, indicating a good planarity of the double bond. As shown in Table IV, each of the conformers 7-1, 7-2 and 7-8 has an envelope conformation with C8-down and each of 7-6 and 7-7 also has an envelope conformation with C8-up, whereas the cyclopentene ring of 7-4 is almost planar. The cyclopentane rings including C8, C9, C10, C11 and C12, on the other hand, have deformed envelope conformations as a whole. Generally speaking, conformers 7-3, 7-4 and 7-5 have C11 under the plane (C11-down) and the rest have C11 over it. More precisely, C12 of conformers 7-1, 7-2 and 7-8 is located downward while C10 of 7-6 and 7-7 is upward. The steric interaction between the hydrogen of OH at position 11 and hydrogens of positions 10 and 12 is considered to disfavor the conformation with $\tau_{12}=60°$ compared with that with $\tau_{12}=-60$ or 180°. As can be seen from the data in Tables I and IV, the cyclopentane ring (including OH) in the most stable conformer 7-1 has nearly the same 3-dimensional structure as that of 5-1, the most stable conformer of **5**.

Analysis of 8——From the nuclear magnetic resonance (NMR) data obtained for **2** by using the nuclear Overhauser effect technique, the diene (C5a–C5–C6–C6a) moiety is considered to have *s-trans* conformation,[12] although both *s-trans* and *s-cis* stable conformations are conceivable for it. Since planarity might be deformed in highly substituted dienes, τ_6 was changed to 150, 180 and 210°. τ_5 was increased by 30° and τ_4 (defined to be the torsional angle involving one of the three hydrogens at position 4 instead of C3) was set to 60° in order to create a series of starting structures of **8** based on the conformer 7-1. Only initial conformational energies were calculated on the structures thus obtained to afford a simple

TABLE IV. Relative Energies and Torsional Angles of **7** with the Minimum Energies

Conformer No.	$\Delta E^{a)}$ (kcal/mol)	Torsional angles (°)					
		$\phi^{b)}$	τ_8	τ_9	τ_{10}	τ_{11}	τ_{12}
7-1	0	−7	−11	11	18	−157	−69
7-2	0	−7	−12	11	17	−158	−177
7-3	0.1	2	3	−3	−19	−82	−71
7-4	0.2	0	0	0	−21	−81	−175
7-5	0.2	−4	−6	6	−25	−80	74
7-6	0.3	7	13	−13	36	−164	−177
7-7	0.4	9	16	−16	37	−163	−68
7-8	0.7	−7	−13	12	17	−158	58
7-9	0.8	−1	−2	2	26	−162	57

a) Difference from the lowest energy. *b*) ϕ: C6–C6a–C9–C8.

TABLE V. Relative Energies and Torsional Angles of **8** with the Minimum Energies

Conformer No.	Initial structure		Optimized structure				
	Torsional angles (°)		$\Delta E^{a)}$ (kcal/mol)	Torsional angles (°)			
	τ_5	τ_6		τ_5	τ_6	$\tau_6'^{b)}$	τ_7
8-1	90	180	0	90	172	168	−169
8-2	−90	180	0.4	−82	−179	180	−173

a) Difference from the lowest energy. *b*) τ_6': C5a–C5–C6–C6a.

TABLE VI. Energies and Torsional Angles of **4** with $\Delta E<2.0$ kcal/mol

Conformation[a] class	Conformer No.	Energy (kcal/mol)	ΔE[b] (kcal/mol)	Torsional angles (°)			
				τ_2	τ_3	τ_4	τ_5
C3-up	4-1	17.1	0.3	−116	55	−176	90
	4-2	17.5	0.7	110	−174	−176	90
	4-3	17.5	0.7	−110	174	177	91
	4-4	17.5	0.7	114	−56	178	91
	4-5	17.6	0.8	−109	173	63	84
	4-6	17.7	0.9	108	−178	63	84
	4-7	17.8	1.0	108	−177	−67	106
	4-8	17.8	1.0	−110	173	−62	105
	4-9	18.0	1.2	−125	55	66	84
	4-10	18.0	1.2	86	64	−178	90
	4-11	18.0	1.2	1	−178	180	91
	4-12	18.1	1.3	−88	−65	−178	94
	4-13	18.3	1.5	2	179	61	86
	4-14	18.4	1.6	9	71	−178	92
	4-15	18.5	1.7	17	66	64	88
	4-16	18.5	1.7	−12	−70	177	91
C3-down	4-17	16.8	0	−128	62	−61	−73
	4-18	17.5	0.7	115	−55	176	−81
	4-19	17.7	0.9	109	−174	−61	−78
	4-20	17.8	1.0	−110	175	176	−81
	4-21	17.8	1.0	110	−174	−176	−83
	4-22	17.9	1.1	−114	57	−178	−83
	4-23	18.0	1.2	−109	174	69	−97
	4-24	18.0	1.2	−108	177	−62	−78
	4-25	18.1	1.3	1	179	60	−87
	4-26	18.1	1.3	123	−55	−65	−78
	4-27	18.2	1.4	108	−175	64	−98
	4-28	18.3	1.5	0	−179	−60	−79
	4-29	18.4	1.6	−87	−64	179	−81
	4-30	18.5	1.7	88	65	178	−86
	4-31	18.5	1.7	0	−177	179	−81
	4-32	18.5	1.7	−17	−66	−63	−80

a) Conformations are divided into two major classes with respect to the τ_5 value. One class has a C3-up conformation (C3 comes over the paper when C4, C5 and C6 are placed on the paper) and the other one has a C3-down conformation. *b*) Difference from the lowest energy.

energy map for rotations τ_5 and τ_6. Four conformations with lower energies were selected and subjected to energy optimizations. Two stable conformers 8-1 and 8-2 were obtained as listed in Table V. τ_5 has a preference for $\pm 90°$, showing that C3 is positioned in the perpendicular plane to the paper plane including the diene moiety. This feature of the C3 position is similar to that of **6**.

Analysis of 4——Using the conformers 8-1 and 8-2 in Table V, starting structures were generated by varying τ_3 and τ_4 to -60, 60 and 180°, and τ_2 to -120, 0 and 120°, while τ_1 was set to 180° in the same manner as for **3**. The selected 37 initial structures were minimized with respect to energy using MMPI. The energies and torsional angles of conformers with $\Delta E<2.0$ kcal/mol are described in Table VI. As can be seen in Table VI, there seem to be no significant differences between C3-up and C3-down conformations with regard to energies. The minimum energy structures are obtained with three preferred angle values for each of τ_2, τ_3 and τ_4. This indicates that the α-chain has some conformational flexibility.

When the stable conformations of **3** and **4** were elucidated according to the scheme shown in Fig. 1, only the most stable one or two conformations of a substructure were taken into account to estimate the parent structure. The conformers listed in Tables III and IV, therefore, do not represent all of the stable 3-dimensional structures of **3** and **4**, but most of them. Although it would be more sophisticated to consider several stable conformations of a substructure, it takes too much calculation time to do so. In the current state of the energy calculation study the pragmatic strategy employed here[13,14] was considered to be reasonable for the present purpose.

Active Conformations

Because of the flexibility of the α-chain, it was difficult to predict the active 3-dimensional structures by examining the stable conformations of **3** and **4** separately. It seems to be reasonable that the four essential functional groups consisting of the carboxyl group, the hydroxyl group at C11, C12 in place of the hydroxyl group at C15 and the π-electron system over positions of 5, 6 and 6a are similarly located in the active conformations of **3** and **4**. The positions of COOH of the α-chain, OH at position 11, OH at position 15 and the π-electron system in **3** and **4** were represented by either of the two oxygen atoms, the oxygen atom, the carbon atom at position 12 and the carbon (or oxygen) atoms at positions 5, 6 and 6a, respectively. The conformers listed in Tables III and VI were compared to see if they had similar spatial arrangements of the six atoms by superimposing these atoms with a least-

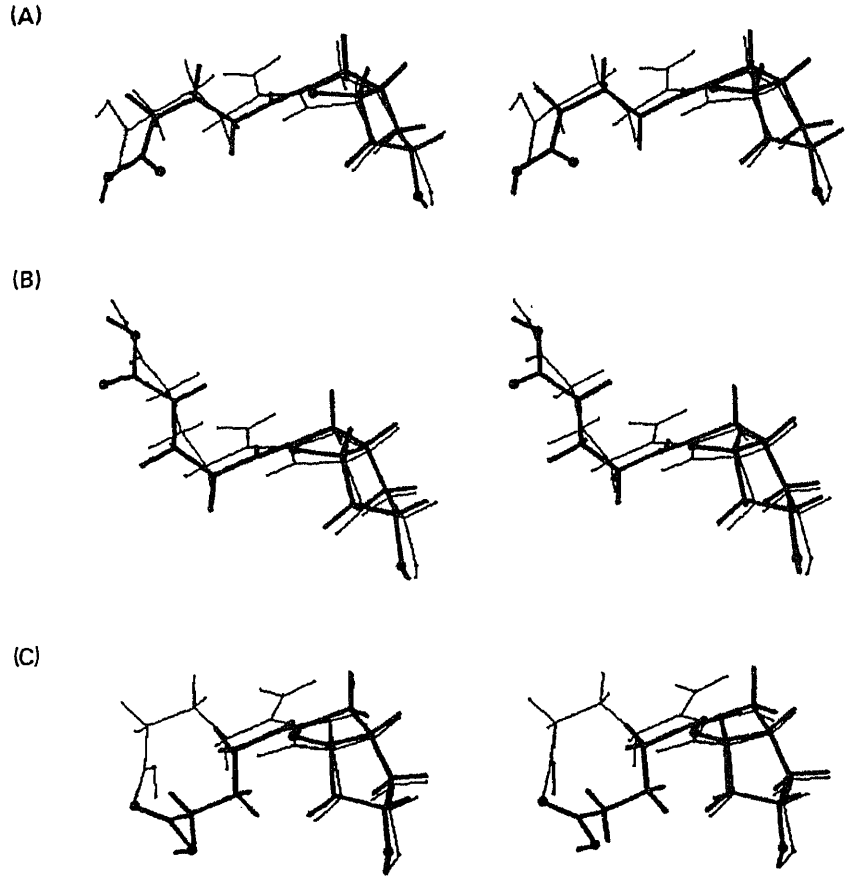

Fig. 3. Stereoscopic Views of Superposition of **3** (Thick Bonds) and **4** (Thin Bonds)

(A) Conformers 3-3 and 4-13; (B) conformers 3-4 and 4-3; (C) conformers 3-15 and 4-8. Atoms used for superimposition are one of the O atoms of the carboxylic group, C5, C6, O6a (C6a), O11 and C12. Solid circles represent oxygen atoms.

TABLE VII. Geometrical Parameters of the Superimpositions of **3** and **4**

Run	Conformer No.		Atom used for superposition of COOH[a]		Displacement (Å)						
	3	**4**	**3**	**4**	Average	O[a]	C5	C6	O6a (C6a)	O[b]	C12
1	3-3	4-13	O(-H)	O(=C)	0.36	0.50	0.47	0.25	0.47	0.42	0.09
2	3-4	4-3	O(-H)	O(-H)	0.33	0.47	0.38	0.11	0.38	0.43	0.17
3	3-7	4-18	O(=C)	O(=C)	0.36	0.35	0.50	0.21	0.39	0.47	0.22
4	3-7	4-29	O(=C)	O(-H)	0.38	0.47	0.48	0.24	0.44	0.46	0.21
5	3-15	4-8	O(=C)	O(=C)	0.24	0.08	0.46	0.09	0.28	0.37	0.14
6	3-16	4-19	O(=C)	O(-H)	0.37	0.47	0.48	0.21	0.48	0.37	0.18

a) Either of the two oxygen atoms of the carboxyl group of the α-chain. *b*) The oxygen atom of the hydroxyl group at position 11.

squares fitting.

Table VII summarizes combinations of the conformers with each displacement of the corresponding atoms less than 0.5 Å. As (6β)-PGI_1, which is formed by hydrogenation of the enol-ether double bond in PGI_2, has higher activity than (6α)-PGI_1,[15] one of the superimpositions of runs 1, 2 and 5 with C3-up conformation should represent the active conformations. Figure 3 illustrates those superimposed structures, showing that the corresponding atoms discussed above fitted well. From the present analysis the π-electron system seems to play an important role in fixing the C3 position, that is, in regulating the direction of the α-chain. Further speculation is beyond the scope of this paper. The relationship between negative charges at the π-electron system and activities is to be discussed in another paper.

Acknowledgment We wish to thank Dr. E. Osawa in Hokkaido University for helpful discussions.

References and Notes

1) S. Moncada, R. Gryglewski, S. Bunting and J. R. Vane, *Nature* (London), **263**, 663 (1976); S. Moncada and J. R. Vane, "Advances in Prostaglandin and Thromboxane Research," Vol. 6, ed. by B. Samuelsson, P. W. Ramwell and R. Paoletti, Raven Press, New York, 1980, pp. 43—60.
2) J. R. Vane and S. Bergström (eds.), "Prostacyclin," Raven Press, New York, 1979, pp. 435—444.
3) M. J. Cho and M. A. Allen, *Prostaglandins*, **15**, 943 (1978); Y. Chiang, A. J. Kresge and M. J. Cho, *J. Chem. Soc., Chem. Commun.*, **1979**, 129.
4) R. A. Johnson, F. H. Lincoln, E. G. Nidy, W. P. Schneider, J. L. Thompson and U. Axen, *J. Am. Chem. Soc.*, **100**, 7690 (1978); E. J. Corey, H. L. Pearce, I. Szekely and M. Ishiguro, *Tetrahedron Lett.*, **1978**, 1023; K. Kojima and K. Sakai, *ibid.*, **1978**, 3743; Y. Konishi, M. Kawamura, Y. Arai and M. Hayashi, *Chem. Lett.*, **1979**, 1437.
5) S. Amemiya, K. Koyama, S. Saito and K. Kojima, *Chem. Pharm. Bull.*, **34**, 4403 (1986).
6) R. C. Nickolson, M. H. Town and H. Vorbruggen, *Med. Research Rev.*, **5**, 1 (1985) and references cited therein.
7) L. E. Sutton (ed.), "Tables of Interatomic Distances and Configuration in Molecules and Ions," The Chemical Society, Burlington House, London, 1965.
8) L. Pauling, "The Nature of Chemical Bonds," 3rd ed., Cornell University Press, Ithaca, New York, 1960. A radius of 1.6 Å was employed for the carbon atom.
9) N. L. Allinger *et al.*, *QCPE*, **11**, 318 (1976).
10) C. Jaime and E. Osawa, *Tetrahedron*, **39**, 2769 (1983).
11) N. L. Allinger and S. H. M. Chang, *Tetrahedron*, **33**, 1561 (1977).
12) H. Haruyama *et al.*, to be published.
13) S. Miyamoto and M. Yoshimoto, *Chem. Pharm. Bull.*, **33**, 4856 (1985).
14) S. Miyamoto and M. Yoshimoto, *Chem. Pharm. Bull.*, **34**, 694 (1986).
15) R. A. Johnson, F. H. Lincoln, H. W. Smith, D. E. Ayer, E. G. Nidy, J. L. Thompson, U. Axen, J. W. Aiken, R. R. Gorman, E. E. Nishizawa and T. Honohan, "Prostacyclin," ed. by J. Vane and S. Bergström, Raven Press, New York, 1979, pp. 17—29.

[Chem. Pharm. Bull. 35(4)1452—1459(1987)]

Design of New Antidepressants, 4-Anilinopyrimidine Derivatives, Based on Quantitative Structure–Activity Relationships[1)]

HIDETOSHI WATANABE,[a] SHUICHI MIYAMOTO,[a] MASAFUMI YOSHIMOTO,*[,a] TOSHIHARU KAMIOKA,[b] ISAO NAKAYAMA,[b] TAKASHI KOBAYASHI[c] and TAKEO HONDA[c]

Chemical Research Laboratories[a] and Biological Research Laboratories,[b] Sankyo Co., Ltd., Hiromachi 1–2–58, Shinagawa-ku, Tokyo 140, Japan and Ube Laboratory, Corporate Research and Development, Ube Industries, Ltd.,[c] Kogushi 1978–5, Ube-shi, Yamaguchi 755, Japan

(Received September 9, 1986)

A quantitative structure–activity relationship formulated for 59 4-anilinopyrimidines inhibiting reserpine-induced ptosis was applied to the design of new, more active, antidepressant compounds. The utility of correlation equations in designing new congeners is discussed and the designed compounds synthesized show the most active group of the anilinopyrimidines.

Keywords——quantitative structure–activity relationship; 4-anilinopyrimidine; antidepressant; reserpine-induced ptosis

The study of quantitative structure–activity relationships (QSAR) has developed rapidly in recent years by feeding on the vast accumulation of results from medicinal chemical studies.[2)] There are relatively few examples in the literature where the formulation of a QSAR has been followed up by the synthesis of new derivatives to check on the predictive values of the correlation equations. Some good predictions realized *via* QSAR are discussed by Hansch with over 20 examples.[2c)]

The present paper extends our earlier correlation study of antidepressant derivatives (I), which have been discovered through random screenings, and describes the design of new, more active congeners based on the QSAR results, and the confirmation of the validity of the designs. Generally speaking, the formulation of QSAR (induction stage) should be extended to the design of more desirable compounds (deduction stage) and this should be followed by synthesis by chemists and subsequent evaluation by biologists to check on the predicted activities (proof stage). Our earlier study of 59 derivatives of I yielded Eqs. 1—4. Based on these equations we designed compounds with a strong electron-attracting group X on the 4-position in the benzene ring. These compounds were then synthesized and biologically evaluated to exhibit the very strong activities shown in Table I.

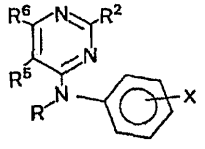

I

In Table II, A in the dependent variable $\ln A/(100-A)$[3)] refers to the percentage inhibition of reserpine (2 mg/kg) induced ptosis in mice at a 100 mg/kg dose of the tested anilinopyrimidine, where compounds with 100% inhibition activity are estimated to be $A=99$

TABLE I. A Comparison of Activities between Active Compounds Previously Examined and Designed Compounds

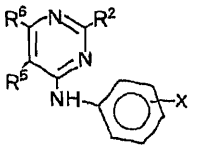

I

Previous active compounds				Designed compounds			
R^5	R^6	X	Anti-reserpine ED_{50} mg/kg *p.o.*	R^5	R^6	X	Anti-reserpine ED_{50} mg/kg *p.o.*
CH_3	CH_3	C_2H_5	36	CH_3	CH_3	CN	11
CH_3	CH_3	$CH(CH_3)_2$	27	CH_3	CH_3	SO_2CH_3	25
CH_3	CH_3	H	100	CH_3	CH_3	NO_2	100
CH_3	CH_3	Cl	35	$(CH_2)_3$		CN	6.7
CH_3	CH_3	Br	30	$(CH_2)_3$		SO_2CH_3	22
CH_3	CH_3	F	48	$(CH_2)_3$		NO_2	25
CH_3	CH_3	I	65				
CH_3	CH_3	CF_3	35				
$(CH_2)_3$		C_2H_5	27				
$(CH_2)_3$		H	39				
$(CH_2)_3$		Cl	23				
$(CH_2)_3$		Br	18				
$(CH_2)_3$		F	33				
$(CH_2)_3$		I	48				
$(CH_2)_3$		CF_3	24				
Cf. Imipramine			11				

and those with less than 0% activity are not included (compiled in Table V).

Syntheses of 4-anilinopyrimidines were carried out by heating the mixture of 4-chloropyrimidines and 1—2 equimolar anilines for 5—10 min over 100 °C to yield crystallines, which were treated with alkaline solution and recrystallized from appropriate solvent.[4]

All structural parameters examined in this work are shown in Table III, where the subsituent-constants used are from the Pomona College compilation[5] or are calculated from these values unless otherwise mentioned. Some hydrophobic constants (π) in this work are estimated from log P values of anilines or phenols shown in Table IV, since the electron-attracting groups on rings directly attached to the atoms bearing lone pair electrons afford much higher values than calculated from benzene derivatives.[5b,6]

Most of the present correlation analyses were carried out by using the Hansch 3X program.[7] However, in order to get the best results from equations with different number of variables the Biomedical Computer Program-P (BMDP) 9R[8] was used, which estimates regression equations for best subsets of predictor variables and extensive residual analysis, where best is defined in terms of the same r-squared, adjusted r-squared, or Mallows' c_p.

Results and Discussion

Equations 1—4 were derived for 59 variations of I (two compounds, No. **1** and **58** of **1**—**61** in Table II, were not used) inhibiting reserpine-induced ptosis and Eqs. 5—7 were formulated from the original 59 plus 15 new derivatives (two compounds, No. **68** and **74** of **62**—**78** in Table II, were not used) including the designed compounds.

TABLE II. Constants Used for Deriving Eqs. 1—7

No.	R^2	R^5	R^6	R	X	$\ln A/(100-A)$				π-5	σ_p	π-X	R-X	F-X	I-1	I-2	I-3	I-4	I-5	I-6	I-7	I-8
						Obsd.	Calcd.[b]	Calcd.[c]	Calcd.[d]													
1[a]	H	CH_3	CH_3	H	2-CH_3, 4-Cl	−2.75	0.35	0.34	−0.25	0.50	0.23	1.43	−0.15	0.41	0	1	0	1	0	0	0	0
2	H	CH_3	CH_3	H	3,4-$(Cl)_2$	−2.75	−1.38	−1.16	−1.93	0.50	0.00	1.42	0.00	0.00	0	0	0	0	0	0	0	1
3	H	Cl	CH_3	H	2-CH_3	−2.75	−2.73	−2.52	−2.99	0.93	0.00	0.56	0.00	0.00	0	1	0	0	0	1	0	0
4	H	C_2H_5	CH_3	H	4-OC_2H_5	−2.59	−2.43	−2.74	−1.93	1.00	−0.24	0.38	−0.51	0.26	0	0	0	0	0	0	0	0
5	H	CH_3	CH_3	H	2-F	−2.59	−1.38	−1.16	−1.16	0.50	0.00	0.31	0.00	0.00	0	1	0	0	0	0	0	0
6	H	−$(CH_2)_4$−		H	3-CH_3	−2.59	−1.93	−1.66	−2.16	0.90	0.00	0.56	0.00	0.00	0	0	0	0	0	0	0	1
7	H	Cl	CH_3	H	4-F	−2.59	−1.27	−1.69	−1.32	0.93	0.06	0.31	−0.34	0.43	0	0	0	1	0	1	0	0
8	H	Cl	CH_3	CH_3		−2.09	−2.73	−2.52	−1.95	0.93	0.00	0.00	0.00	0.00	1	0	1	0	0	1	0	0
9	H	CH_3	CH_3	H	4-CH_3	−1.99	−1.63	−1.84	−1.20	0.50	−0.17	0.56	−0.13	−0.04	0	0	0	0	0	0	0	0
10	H	CH_3	CH_3	H	3-F	−1.90	−1.38	−1.16	−1.34	0.50	0.00	0.14	0.00	0.00	0	0	0	0	0	0	0	1
11	H	CH_3	CH_3	H	2,4-$(Cl)_2$	−1.90	0.35	0.34	−0.35	0.50	0.23	1.64	−0.15	0.41	0	1	0	1	0	0	0	0
12	H	CH_3	CH_3	H	4-OC_2H_5	−1.90	−1.74	−2.12	−1.14	0.50	−0.24	0.38	−0.51	0.26	0	0	0	0	0	0	0	0
13	H	C_4H_9	CH_3	H	4-F	−1.82	−1.98	−2.21	−1.97	2.00	0.06	0.31	−0.34	0.43	0	0	0	1	0	0	0	0
14	H	CH_3	CH_3	H	2,4-$(CH_3)_2$	−1.73	−1.63	−1.84	−2.24	0.50	−0.17	1.12	−0.13	−0.04	0	1	0	0	0	0	0	0
15	H	CH_3	CH_3	H	2-CH_3, 4-OCH_3	−1.73	−1.78	−2.24	−2.00	0.50	−0.27	0.54	−0.51	0.26	0	1	0	0	0	0	0	0
16	H	CH_3	CH_3	H	3-Br	−1.59	−1.38	−1.16	−1.67	0.50	0.00	0.86	0.00	0.00	0	0	0	0	0	0	0	1
17	H	CH_3	CH_3	H	3-Cl	−1.52	−1.38	−1.16	−1.60	0.50	0.00	0.71	0.00	0.00	0	0	0	0	0	0	0	1
18	H	CH_3	CH_3	H	4-OCH_3	−1.52	−1.78	−2.24	−0.96	0.50	−0.27	−0.02	−0.51	0.26	0	0	0	0	0	0	0	0
19	H	CH_3	CH_3	H	3-OCH_3	−1.52	−1.38	−1.16	−1.26	0.50	0.00	−0.02	0.00	0.00	0	0	0	0	0	0	0	1
20	H	CH_3	CH_3	H	2-Br	−1.52	−1.38	−1.16	−1.55	0.50	0.00	1.15	0.00	0.00	0	1	0	0	0	0	0	0
21	H	C_3H_7	CH_3	H		−1.45	−1.36	−1.22	−1.81	1.50	0.00	0.00	0.00	0.00	1	0	0	0	0	0	0	0
22	H	C_3H_7	CH_3	H	4-C_2H_5	−1.45	−0.60	−0.37	−0.46	1.50	−0.15	1.02	−0.10	−0.05	0	0	0	0	1	0	0	0
23	H	CH_3	CH_3	H	4-C_4H_9	−1.39	−1.62	−1.80	−1.88	0.50	−0.16	2.00	−0.11	−0.06	0	0	0	0	0	0	0	0
24	H	CH_3	CH_3	H	2-OC_2H_5	−1.15	−1.38	−1.16	−1.19	0.50	0.00	0.38	0.00	0.00	0	1	0	0	0	0	0	0
25	H	Cl	CH_3	H		−1.15	−1.33	−1.32	−1.95	0.93	0.00	0.00	0.00	0.00	1	0	0	0	0	1	0	0
26	H	−$(CH_2)_3$−		H	4-OCH_3	−1.10	−0.50	−1.28	−0.28	0.65	−0.27	−0.02	−0.51	0.26	0	0	0	0	0	0	1	0
27	H	CH_3	CH_3	H	3-CF_3, 4-Cl	−0.99	0.35	0.34	−0.69	0.50	0.23	1.81	−0.15	0.41	0	0	0	1	0	0	0	1
28	H	Cl	CH_3	H	4-Br	−0.99	−1.01	−1.02	−0.99	0.93	0.23	1.15	−0.17	0.44	0	0	0	1	0	1	0	0
29	H	CH_3	CH_3	H	3-OC_2H_5	−0.90	−1.38	−1.16	−1.45	0.50	0.00	0.38	0.00	0.00	0	0	0	0	0	0	0	1
30	H	CH_3	Cl	H		−0.90	0.02	0.03	−0.23	0.50	0.00	0.00	0.00	0.00	1	0	0	0	0	0	0	0
31	H	−$(CH_2)_4$−		H		−0.71	−0.53	−0.47	−0.86	0.90	0.00	0.00	0.00	0.00	1	0	0	0	0	0	0	0
32	H	CH_3	CH_3	H	2,4-$(OCH_3)_2$	−0.71	−1.78	−2.24	−1.73	0.50	−0.27	−0.04	−0.51	0.26	0	1	0	0	0	0	0	0
33	H	CH_3	CH_3	CH_3	4-Cl	−0.71	0.35	0.34	0.76	0.50	0.23	0.93	−0.15	0.41	0	0	1	1	0	0	0	0
34	H	C_2H_5	CH_3	H	4-F	−0.71	−0.60	−0.96	−0.39	1.00	0.06	0.31	−0.34	0.43	0	0	0	1	0	0	0	0
35	H	CH_3	CH_3	CH_3	4-C_2H_5	−0.62	0.78	0.88	1.13	0.50	−0.15	1.00	−0.10	−0.05	0	0	1	0	1	0	0	0
36	H	CH_3	CH_3	H	4-OH	−0.58	−1.94	−2.63	−1.02	0.50	−0.37	−0.67	−0.64	0.29	0	0	0	0	0	0	0	0
37	H	−$(CH_2)_3$−		CH_3		−0.49	−0.09	−0.21	0.45	0.65	0.00	0.00	0.00	0.00	0	0	1	0	0	0	1	0

38	H	Cl	CH_3	H	4-Cl	−0.41	−1.01	−1.02	−0.96	0.93	0.23	0.93	−0.15	0.41	0	0	0	1	0	1	0	0
39	H	C_2H_5	CH_3	H	4-Br	−0.24	−0.35	−0.29	−0.06	1.00	0.23	1.15	−0.17	0.44	0	0	0	1	0	0	0	0
40	H	CH_3	CH_3	H		−0.12	0.02	0.03	−0.23	0.50	0.00	0.00	0.00	0.00	1	0	0	0	0	0	0	0
41	H	$-(CH_2)_3-$		H	4-OC_2H_5	0.00	−0.45	−1.16	−0.38	0.65	−0.24	0.38	−0.44	0.22	0	0	0	0	0	0	1	0
42	H	C_2H_5	CH_3	H		0.00	−0.67	−0.59	−1.01	1.00	0.00	0.00	0.00	0.00	1	0	0	0	0	0	0	0
43	H	Cl	H	CH_3	4-Cl	0.00	−0.25	−0.20	0.08	0.93	0.23	0.93	−0.15	0.41	0	0	1	1	0	0	0	0
44	H	F	H	H	4-C_2H_5	0.24	0.33	0.34	0.42	0.28	−0.15	1.02	−0.10	−0.05	0	0	0	0	1	1	0	0
45	H	CH_3	CH_3	H	4-I	0.62	0.27	0.14	0.32	0.50	0.18	1.44	−0.19	0.40	0	0	0	1	0	0	0	0
46	H	CH_3	CH_3	H	3,4-$(Cl)_2$	0.71	0.35	0.34	−0.61	0.50	0.23	1.64	−0.15	0.41	0	0	0	1	0	0	0	1
47	H	CH_3	CH_3	H	HCl salt	0.71	0.02	0.03	−0.23	0.50	0.00	0.00	0.00	0.00	1	0	0	0	0	0	0	0
48	H	$-(CH_2)_3-$		H	4-CF_3	0.74	0.73	1.94	2.58	0.65	0.54	1.05	0.19	0.38	0	0	0	0	0	0	1	0
49	H	CH_3	CH_3	H	4-CF_3	0.90	−0.56	0.98	1.90	0.50	0.54	1.05	0.19	0.38	0	0	0	0	0	0	0	0
50	H	$-(CH_2)_3-$		H		1.10	1.31	0.99	0.45	0.65	0.00	0.00	0.00	0.00	1	0	0	0	0	0	1	0
51	H	CH_3	CH_3	H	4-F	1.21	0.09	−0.34	0.40	0.50	0.06	0.31	−0.34	0.43	0	0	0	1	0	0	0	0
52	H	$-(CH_2)_3-$		H	4-Br	1.25	1.63	1.29	1.41	0.65	0.23	1.15	−0.17	0.44	0	0	0	1	0	0	1	0
53	H	C_2H_5	CH_3	H	4-C_2H_5	1.32	0.09	0.26	0.33	1.00	−0.15	1.02	−0.10	−0.05	0	0	0	0	1	0	0	0
54	H	CH_3	CH_3	H	4-Cl	1.52	0.35	0.34	0.76	0.50	0.23	0.93	−0.15	0.41	0	0	0	1	0	0	0	0
55	H	CH_3	CH_3	H	4-Br	1.52	0.35	0.34	0.73	0.50	0.23	1.15	−0.17	0.44	0	0	0	1	0	0	0	0
56	H	$-(CH_2)_3$		H	4-F	1.82	1.38	0.62	1.08	0.65	0.06	0.31	−0.34	0.43	0	0	0	1	0	0	1	0
57	H	CH_3	CH_3	H	4-iso-Pro	1.90	0.78	0.88	0.88	0.50	−0.15	1.53	−0.10	−0.05	0	0	0	0	1	0	0	0
58[a]	H	C_2H_5	CH_3	H	4-Cl	1.90	−0.35	−0.29	−0.03	1.00	0.23	0.93	−0.15	0.41	0	0	0	1	0	0	0	0
59	H	$-(CH_2)_3-$		H	4-Cl	1.90	1.63	1.29	1.44	0.65	0.23	0.93	−0.15	0.41	0	0	0	1	0	0	1	0
60	H	$-(CH_2)_3-$		H	4-I	1.99	1.56	1.10	1.15	0.65	0.18	1.12	−0.19	0.40	0	0	0	1	0	0	1	0
61	H	$-(CH_2)_3-$		H	4-C_2H_5	2.07	2.07	1.84	1.80	0.65	−0.15	1.02	−0.10	−0.05	0	0	0	0	1	0	1	0
62	H	CH_3	CH_3	H	3,4-OCH_2O-	−2.70	−1.62	−1.80	−2.08	0.50	−0.16	−0.05	0.00	−0.17	0	0	0	0	0	0	0	1
63	H	$-(CH_2)_3-$		H	3,4-$(CH_3)_2$	−2.70	−0.34	−0.88	−1.82	0.65	−0.17	1.12	−0.13	−0.04	0	0	0	0	0	0	1	1
64	NH_2	CH_3	H	H	2,4-$(Cl)_2$	−1.95	−1.38	−1.16	−2.82	0.50	0.00	1.64	0.00	0.00	0	1	0	0	0	0	0	1
65	H	$-(CH_2)_3-$		H	3,4-$(OCH_3)_2$	−1.46	−0.50	−1.28	−1.32	0.65	−0.27	−0.04	−0.51	0.26	0	0	0	0	0	0	1	1
66	NH_2	CH_3	H	H	3,4-$(Cl)_2$	−0.79	0.35	0.34	−0.61	0.50	0.23	1.64	−0.15	0.41	0	0	0	1	0	0	0	1
67	H	$-(CH_2)_3-$		H	3,4-$(Cl)_2$	−0.79	1.63	1.29	0.07	0.65	0.23	1.64	−0.15	0.41	0	0	0	1	0	0	1	1
68[a]	H	CH_3	CH_3	H	4-NO_2	−0.25	0.50	3.77	3.47	0.50	1.24	0.49	0.16	0.67	0	0	0	0	0	0	0	0
69	H	$-(CH_2)_3-$		H	3,4-OCH_2O-	0.00	−0.33	−0.84	−1.41	0.65	−0.16	−0.05	0.00	−0.17	0	0	0	0	0	0	1	1
70	H	CH_3	CH_3	H	3,4-$(Cl)_2$	0.12	0.35	0.34	−0.61	0.50	0.23	1.64	−0.15	0.41	0	0	0	1	0	0	0	1
71	H	$-(CH_2)_3-$		H	4-iso-Pro	1.02	2.07	1.84	1.56	0.65	−0.15	1.53	−0.10	−0.05	0	0	0	0	1	0	1	0
72	H	CH_3	C_2H_5	H	4-iso-Pro	1.39	0.78	0.88	0.88	0.50	−0.15	1.53	−0.10	−0.05	0	0	0	0	1	0	0	0
73	H	CH_3	CH_3	H	4-iso-Pro HCl salt	1.55	0.78	0.88	0.88	0.50	−0.15	1.53	−0.10	−0.05	0	0	0	0	1	0	0	0
74[a]	H	$-(CH_2)_3-$		H	4-SO_2CH_3 HCl salt	1.76	1.40	3.69	4.44	0.65	0.98	−1.02	0.22	0.54	0	0	0	0	0	0	1	0
75	H	CH_3	CH_3	H	4-SO_2CH_3	2.53	0.11	2.73	3.77	0.50	0.98	−1.02	0.22	0.54	0	0	0	0	0	0	0	0
76	H	$-(CH_2)_3-$		H	4-CN	4.60	1.24	3.29	3.64	0.65	0.88	0.14	0.19	0.51	0	0	0	0	0	0	1	0
77	H	CH_3	CH_3	H	4-CN	4.60	−0.04	2.34	2.96	0.50	0.88	0.14	0.19	0.51	0	0	0	0	0	0	0	0
78	H	$-(CH_2)_3-$		H	4-NO_2 HCl salt	4.60	1.79	4.72	4.15	0.65	1.24	0.49	0.16	0.67	0	0	0	0	0	0	1	0

a) These compounds were not used in deriving equations. *b*) Eq. 2 was used. *c*) Eq. 5 was used. *d*) Eq. 7 was used.

TABLE III. Physicochemical and Indicator Variables Studied in the Formulation of Eqs. 1—10

Variables	Substituent studied
π-5	Hydrophobic constants of R^5
π-X	Hydrophobic constants of X
π-sum	Sum of constants (R^5, R^6, R, X)
σ_m	Electronic constants of X on *meta* position
σ_p	Electronic constants of X on *para* position
σ_o [a]	Electronic constants of X on *ortho* position
MR-X	Molar refractivity constants of X on *para* position
F-X	Constants of field effects of X on *para* position
R-X	Constants of resonance effects of X on *para* position
I-1	X=H
I-2	Existence of substituent X(=H) on *ortho* position
I-3	$R=CH_3$ (R=H: *I*-3=0)
I-4	Halogen atom of X on *para* position
I-5	$X=C_2H_5$, C_3H_7, C_4H_9 on *para* position
I-6	Halogen atom of R^5
I-7	R^5, $R^6=-(CH_2)_3-$
I-8	Existence of substituent X(=H) on *meta* position

a) O. Exner, "Advances in Linear Free Energy Relationships," ed. by N. B. Chapman and J. Shorter, Plenum, New York, 1972, p. 1.

TABLE IV. Values of π-X from log *P* [a] of Anilines and Phenols

X	X–C_6H_5	4-X–$C_6H_4NH_2$	4-X–C_6H_4OH
F	0.14	0.25 [b]	0.31
Cl	0.71	0.93 [b]	0.93
Br	0.86	1.15 [b]	1.13
I	1.12	1.44 [b]	1.45
CF_3	0.88	1.05 [b]	
NO_2	−0.28	0.49 [b]	0.45
CH_3SO_2	−1.63	−1.02 [b]	
CN	−0.57		0.14 [b]

a) log *P* values refer to the data base distributed from Pomona College Medicinal Chemistry Project, Claremont, California 91711, U.S.A. b) These values were used for the correlations.

Equation 1 is the best among the 6-variable correlations of the earlier 59 compounds, whereas Eq. 2 is the best among the 7-variable correlations. The separation of the σ_p term into *R*-X and *F*-X (see Table III) results in Eq. 3 being the best. Equation 4 produces the correlation with the largest correlation coefficient (*r*) and the smallest standard deviation (*s*) among permutations of all terms in Table III. Equations 2—4 prompted us to design compounds with strong electron-attracting groups in X on the 4-position in the benzene ring. The corresponding compounds (No. **68**, **74**—**78**) were synthesized and evaluated biologically.

In the correlations of all 74 compounds, Eq. 5 has the same terms as Eq. 2, whereas Eq. 6 is the best among the 7-variable correlations and Eq. 7 produces the correlation with the largest *r* and the smallest *s* in permutations of all terms.

$$\begin{aligned}\ln A/(100-A) = &-1.441(\pm 0.77)\pi\text{-}5 + 1.501(\pm 0.70)I\text{-}1 + 1.741(\pm 0.52)I\text{-}4 \\ &+2.255(\pm 0.77)I\text{-}5 - 0.715(\pm 0.70)I\text{-}6 + 1.546(\pm 0.59)I\text{-}7 \\ &-0.753(\pm 0.57) \qquad (1)\\ &n=59,\ r=0.822,\ s=0.836\end{aligned}$$

TABLE V. Inactive Compounds

No.	X	R	R^5	R^6
1	4-CH_3	H	Br	CH_3
2	4-C_2H_5	H	C_4H_9	CH_3
3	4-Br	H	C_4H_9	CH_3
4	4-Br	H	C_3H_7	CH_3
5	4-Cl	H	C_3H_7	CH_3
6	4-F	H	C_3H_7	CH_3
7	4-OCH_3	H	C_2H_5	CH_3
8	4-CH_3	H	C_2H_5	CH_3
9	3-Br	H	C_2H_5	CH_3
10	2-Br	H	C_2H_5	CH_3
11	2-C_2H_5	H	CH_3	CH_3
12	2-CH_3	H	CH_3	CH_3
13	2-CF_3	H	CH_3	CH_3
14	2-CH_3, 4-Br	H	CH_3	CH_3
15	3-CH_3	H	CH_3	CH_3
16	3-CH_3	H	C_2H_5	Cl
17	3-C_2H_5	H	Cl	CH_3
18	H	H	Br	CH_3
19	4-CH_3	H	C_3H_7	CH_3
20	H	H	C_4H_9	CH_3
21	4-CH_3	H	C_4H_9	CH_3
22	4-CH_3	CH_3	CH_3	CH_3
23	H	H	CH_3	Br
24	4-Cl	H	C_4H_9	CH_3
25	H	C_2H_5	$-(CH_2)_4-$	
26	3-OCH_3	H	$-(CH_2)_4-$	
27	4-CH_3	H	$-(CH_2)_3-$	
28	2-CO_2CH_3	H	H	H

$$\ln A/(100-A) = -1.382(\pm 0.75)\pi\text{-}5 + 1.513(\pm 1.45)\sigma_p + 1.397(\pm 0.68)I\text{-}1 + 1.373(\pm 0.62)I\text{-}4 + 2.386(\pm 0.76)I\text{-}5 - 0.759(\pm 0.68)I\text{-}6 + 1.495(\pm 0.58)I\text{-}7 - 0.684(\pm 0.56) \quad (2)$$
$$n=59,\ r=0.837,\ s=0.810$$

$$\ln A/(100-A) = -1.393(\pm 0.78)\pi\text{-}5 - 2.756(\pm 1.71)\sigma_m + 2.624(\pm 1.38)R\text{-X} + 3.673(\pm 1.38)F\text{-X} - 1.049(\pm 0.70)I\text{-}2 - 0.786(\pm 0.80)I\text{-}3 + 1.958(\pm 0.81)I\text{-}5 - 0.779(\pm 0.70)I\text{-}6 + 1.075(\pm 0.62)I\text{-}7 + 0.175(\pm 0.72) \quad (3)$$
$$n=59,\ r=0.837,\ s=0.827$$

$$\ln A/(100-A) = -1.705(\pm 0.66)\pi\text{-}5 - 2.361(\pm 1.45)\sigma_m + 2.008(\pm 1.27)\sigma_p - 4.044(\pm 2.77)\sigma_o + 1.051(\pm 0.62)I\text{-}1 - 0.794(\pm 0.61)I\text{-}2 - 0.674(\pm 0.67)I\text{-}3 + 1.213(\pm 0.55)I\text{-}4 + 2.223(\pm 0.68)I\text{-}5 - 0.928(\pm 0.59)I\text{-}6 + 1.193(\pm 0.52)I\text{-}7 - 0.018(\pm 0.59) \quad (4)$$
$$n=59,\ r=0.895,\ s=0.689$$

$$\ln A/(100-A) = -1.248(\pm 0.87)\pi\text{-}5 + 3.957(\pm 0.83)\sigma_p + 1.194(\pm 0.78)I\text{-}1 + 0.586(\pm 0.55)I\text{-}4 + 2.639(\pm 0.74)I\text{-}5 - 0.817(\pm 0.80)I\text{-}6 + 1.143(\pm 0.55)I\text{-}7 - 0.539(\pm 0.62) \quad (5)$$
$$n=74,\ r=0.849,\ s=0.967$$

$$\ln A/(100-A) = -1.450(\pm 0.77)\pi\text{-}5 - 3.600(\pm 0.74)\sigma_p - 1.080(\pm 0.66)I\text{-}2$$

$$+1.709(\pm0.67)I\text{-}5-1.003(\pm0.71)I\text{-}6+0.905(\pm0.49)I\text{-}7$$
$$-1.339(\pm0.51)I\text{-}8+0.546(\pm0.65) \quad (6)$$
$$n=74,\ r=0.883,\ s=0.857$$

$$\ln A/(100-A)=-1.582(\pm0.77)\pi\text{-}5-0.462(\pm0.38)\pi\text{-X}+3.951(\pm1.10)R\text{-X}$$
$$+4.908(\pm1.19)F\text{-X}-0.787(\pm0.69)I\text{-}2+2.456(\pm0.85)I\text{-}5$$
$$-1.042(\pm0.71)I\text{-}6+0.914(\pm0.49)I\text{-}7-1.047(\pm0.58)I\text{-}8$$
$$+0.565(\pm0.71) \quad (7)$$
$$n=74,\ r=0.888,\ s=0.855$$

Agreement of corresponding coefficients in Eqs. 2 and 5 is realized within 95% confidence intervals (the figures in the parentheses) except for σ_p and *I*-4. The coefficient of σ_p from Eq. 5 is much larger than that from Eq. 2 and the coefficient of *I*-4 from Eq. 5 is much smaller than that from Eq. 2, which might result from a rather high collinearity of the two variables ($r^2=0.36$ computed from data of 59 compounds in Eqs. 1—4, whereas $r^2=0.08$ in Table VI) bringing about reverse deviations for compensation. The agreement of the other five pairs of coefficients is very good. Equation 5 gives a slightly better correlation with respect to correlation coefficients (r) but is slightly poorer than Eq. 2 with respect to standard deviations (s).

The hydrophobic substituents in R^5 decrease the activities in all equations, which might result from steric hindrance. The electron-attracting effects of X on the 4-position in the benzene ring are shown as the terms of σ_p, *R*-X and *F*-X which increase the activities in the 6 equations except for Eq. 1. The other electronic terms (σ_m in Eq. 3 and 4: σ_o in Eq. 4) decrease the activities, although they are not significant terms in the other equations. The indicator variables of *I*-1, *I*-4, *I*-5 and *I*-7 enhance the activities in the equations where the variables are significant. On the other hand, the indicator variables of *I*-2, *I*-3, *I*-6 and *I*-8 reduce the activities without exception in the equations where the variables are significant. High collinearity of σ_m and *I*-8 is shown ($r^2=0.63$ calculated from 59 compounds in Eqs. 1—4, whereas $r^2=0.43$ in Table VI), which would eliminate the coexistence of the two variables in the same equation as shown in Eqs. 1—7.

TABLE VI. Correlation Matrix[a] for Collinearity between Variables

	π-5	*MR*-X	σ_o	σ_m	σ_p	π-X	*R*-X	*F*-X	*I*-1	*I*-2	*I*-3	*I*-4	*I*-5	*I*-6	*I*-7	*I*-8
π-5	1.00															
MR-X	0.63	1.00														
σ_o	0.00	0.00	1.00													
σ_m	0.04	0.02	0.01	1.00												
σ_p	0.00	0.00	0.01	0.01	1.00											
π-X	0.02	0.02	0.07	0.14	0.00	1.00										
R-X	0.01	0.00	0.01	0.01	0.32	0.00	1.00									
F-X	0.00	0.00	0.00	0.00	0.42	0.01	0.06	1.00								
I-1	0.03	0.04	0.00	0.02	0.01	0.13	0.05	0.08	1.00							
I-2	0.03	0.02	0.00	0.00	0.02	0.01	0.00	0.02	0.02	1.00						
I-3	0.00	0.00	0.00	0.01	0.00	0.00	0.00	0.00	0.01	0.01	1.00					
I-4	0.03	0.01	0.01	0.02	0.08	0.15	0.07	0.48	0.05	0.03	0.00	1.00				
I-5	0.00	0.00	0.00	0.02	0.07	0.11	0.00	0.14	0.02	0.02	0.00	0.06	1.00			
I-6	0.04	0.03	0.02	0.01	0.00	0.00	0.00	0.00	0.00	0.00	0.01	0.01	0.00	1.00		
I-7	0.00	0.02	0.00	0.02	0.01	0.00	0.00	0.02	0.01	0.04	0.00	0.00	0.00	0.03	1.00	
I-8	0.04	0.01	0.02	0.43	0.00	0.03	0.02	0.03	0.04	0.01	0.02	0.00	0.04	0.03	0.00	1.00

a) Values are r^2 computed from data of 74 compounds in Table II.

There are two types of predictions which must be considered. In the first type, one can attempt to predict the activity of new derivatives whose substituents are characterized by constants within the range of substituent space span (sss) in derivatives supporting the model equation.[2d,9] Often (but not necessarily) such derivatives will have biological activities within the range already explored. After one has a reasonable distribution of data along each vector, testing of more data points in the explored substituents space is redundant. In the present case the early group of compounds (No. **1**—**61** in Table II) does not contain any with strong electron-attracting groups of X on the 4-position in I. This is one reason why the importance of designing the early set of compounds based on cluster analysis was proposed by Hansch.[10] Eleven compound (No. **62**—**67** and **69**—**73** in Table II) among the 17 new derivatives of I fall in this class and naturally the activities fall in the range of the 61 initial compounds.

On the other hand, the second type of prediction is that for derivatives possessing activity outside the range already explored (sss). In the present instance of the six designed compounds (No. **68** and **74**—**78** in Table II) with a strong electron-withdrawing X group on the 4-position outside the sss, four are much more active than any of compounds in the initial 61 compounds, although one is moderately active and one shows weak activity. Finally, RS-2232 (No. **76** in Table II), the most active congener was selected for preclinical investigations.[11,12] This result demonstrates that correlation equations can be used successfully to design highly active congeners.

References and Notes

1) Part of this study was presented in the following symposium: M. Yoshimoto, H. Watanabe, S. Miyamoto, T. Kamioka, I. Nakayama, T. Honda and T. Kobayashi, Abstracts of Papers, 11th Symposium of Structure–Activity Relationships, Kyoto, Japan, 1984, p. 7.
2) *a*) M. Yoshimoto and C. Hansch, *J. Med. Chem.*, **19**, 71 (1976); *b*) M. Yoshimoto, *Ann. Sankyo Res. Labo.*, **34**, 1 (1982); *c*) C. Hansch, *Drug Development Research*, **1**, 267 (1982); *d*) C. Hansch and M. Yoshimoto, *J. Med. Chem.*, **19**, 1089 (1976).
3) The logistic unit of *A* is employed. The transformation is used for making it easier to evaluate *A*.
4) Japan. Patent Kokai 57-203072 (EP 67, 630) [*Chem. Abstr.*, **98**, 126152*t* (1983)].
5) *a*) C. Hansch, A. Leo, S. H. Unger, K. H. Kim, D. Nikaitani and E. J. Lien, *J. Med. Chem.*, **16**, 1207 (1973); *b*) C. Hansch and A. Leo, "Substituent Constants for Correlation Analysis in Chemistry and Biology," John Wiley, New York, 1976.
6) *a*) T. Fujita, J. Iwasa and C. Hansch, *J. Am. Chem. Soc.*, **86**, 5175 (1964); *b*) C. Hansch and M. Yoshimoto, *J. Med. Chem.*, **17**, 1160 (1974).
7) Distributed from Pomona College Medicinal Chemistry Project, Claremont, California 91711, U.S.A.
8) Biomedical Computer Program-P, University of California Press, Berkeley and Los Angeles, California.
9) C. Hansch in "Pharmacochemistry Library Vol. 2, Biological Activity and Chemical Structure," J. A. Keverling Buisman, Ed., Elsevier, New York, 1977, p. 47.
10) C. Hansch, S. H. Unger and A. B. Forsythe, *J. Med. Chem.*, **16**, 1212 (1973).
11) T. Kamioka, I. Nakayama, T. Karube, T. Yokoyama, N. Iwata, T. Honda and T. Kobayashi, *Jpn. J. Pharmacol.*, **36** (Suppl.), 170 (1984).
12) N. Iwata, T. Kamioka, S. Kumakura, K. Nakamura, T. Honda and T. Kobayashi, Abstracts of Papers, 9th Intl. Cong. Pharmacol. London, 1984, p. 1466.

[Chem. Pharm. Bull. 35(4)1460—1463(1987)]

Novel Eudesmane-Type Sesquiterpenes from *Alpinia japonica* (THUNB.) MIQ.

HIDEJI ITOKAWA,* HIROSHI MORITA and KINZO WATANABE

Tokyo College of Pharmacy, 1432-1, Horinouchi, Hachioji, Tokyo 192-03, Japan

(Received August 4, 1986)

Three novel eudesmane-type sesquiterpenes, 10-*epi*-5β-hydroperoxy-β-eudesmol (I), 10-*epi*-5α-hydroperoxy-β-eudesmol (II) and 4,10-*epi*-5β-hydroxydihydroeudesmol (III), have been isolated from the rhizomes of *Alpinia japonica*. Their structures were determined by spectroscopic methods and chemical conversions.

Keywords——*Alpinia japonica*; Zingiberaceae; sesquiterpene; eudesmane; peroxide; solvent shift; biosynthesis

In our previous studies on the chemical constituents of *Alpinia japonica*, the presence of eudesmanes, agarofurans, eremophilanes, guaianes and seco-guaianes has been reported.[1,2] Our further work on the constituents of *A. japonica* has resulted in the isolation of three novel eudesmanes, 10-*epi*-5β-hydroperoxy-β-eudesmol (I), 10-*epi*-5α-hydroperoxy-β-eudesmol (II) and 4,10-*epi*-5β-hydroxydihydroeudesmol (III). In this paper, the determination of their structures is reported. The structural relationships between them and a possible biogenetic pathway of these compounds are also discussed.

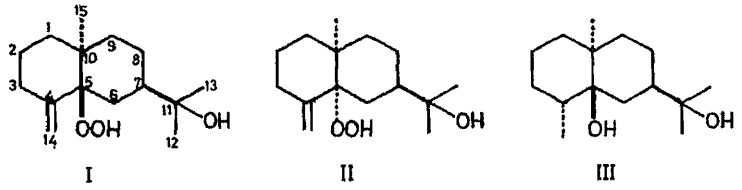

I II III

Chart 1

Compounds I and II, whose spectral data were very similar to each other as mentioned below, were each obtained as colorless needles. Both of them have the same molecular formula, $C_{15}H_{26}O_3$, and the infrared (IR) spectrum shows absorptions of a prominent hydroxyl band at 3610 cm^{-1} and exomethylene at 3090 and 900 cm^{-1}. However, no carbonyl absorption was indicated. The proton nuclear magnetic resonance (^{1}H-NMR) spectrum not only supported the presence of the exomethylene group (I: δ 4.79 and 5.03, each 1H, s; II: δ 4.91 and 5.10, each 1H, s) but also indicated the presence of a hydroxy isopropyl group (I: δ 1.32 and 1.35; II: δ 1.20 and 1.24), which was also supported by the fragment ion at *m/z* 59 in the mass spectrum (MS). The carbon 13 nuclear magnetic resonance (^{13}C-NMR) spectrum also showed the presence of two carbons bearing an oxygen function (I: δ 74.1 (s) and 87.0 (s); II: δ 72.9 (s) and 89.5 (s)) and indicated the absence of a carbonyl group. Since I and II showed a purple spot due to peroxide[3] on a silica gel thin layer plate when treated with *N,N*-dimethyl *p*-phenylenediamine dihydrochloride, the remaining two oxygen atoms were assigned to the hydroperoxy group. Based on the above spectral data and biogenetic considerations, I and II were deduced to be an isomeric pair of 10-*epi*-5-hydroperoxy-β-eudesmol, probably biosyn-

thesized from 10-*epi*-γ-eudesmol by the "ene"-type reaction of a singlet oxygen with an olefin.[4]

The dye-sensitized photooxygenation of 10-*epi*-γ-eudesmol with oxygen gave a mixture of the two isomeric hydroperoxides, I as the main product, and II as the minor product. The configurations of the hydroperoxide at C-5 were assigned on the basis of the pyridine-solvent shift[5] of the reduction products (IV and V) in the ^{1}H-NMR spectra (Table I) and the observation of internal hydrogen bonding in IV. Reduction of I and II with triphenylphosphine afforded IV and V, respectively. In the ^{1}H-NMR spectra (pyridine-d_5), both methyl groups at C-11 of IV and V showed a downfield shift (*ca.* −0.2 ppm) because of the geminal deshielding effect. However, although the methyl group at C-10 of V showed a downfield shift of −0.30 ppm due to the vicinal deshielding effect, that of IV showed a downfield shift of only −0.04 ppm. Therefore the configurations of the hydroxyl group at C-5 in V and IV were determined to be α and β, respectively. The above assignment was supported by the presence of internal hydrogen bonding in a highly diluted solution of IV, but not V, as judged from the IR spectra.

The photooxygenation of 10-*epi*-γ-eudesmol gave compound I, the more stable isomer having a β-hydroperoxy group, as the main product, and compound II, the more unstable one having an α-hydroperoxy group, as the minor product. However, the fresh rhizome of *A. japonica* was found to contain II in a larger quantity than I.

Compound III was obtained as colorless needles (mp 130.0—132.0 °C), having the molecular formula $C_{15}H_{28}O_2$, based on high-resolution MS. The presence of a hydroxy isopropyl group was indicated by the ^{1}H-NMR (δ 1.25 ppm), IR (3620 cm^{-1}) and MS (*m/z* 59) spectra. Further the NMR spectrum showed the presence of two additional methyl groups (δ 1.10 and 1.04 ppm) and two hydroxyl groups (δ 3.76 ppm, disappeared on addition of D_2O). The catalytic hydrogenation of IV gave III. Therefore, the structure of III was determined except for the configuration of the methyl group at C-4. Since a pyridine-solvent shift of

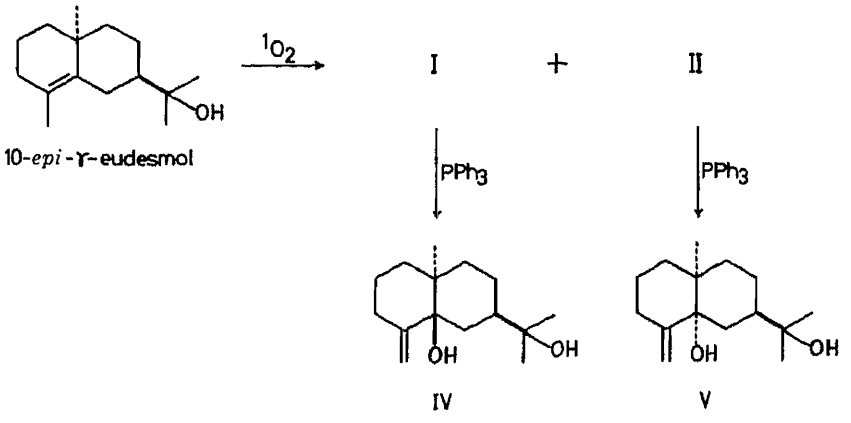

Chart 2

TABLE I. Pyridine-Solvent Shift (δ $CDCl_3$–δ Pyridine-d_5) in ^{1}H-NMR of III, IV and V

	III	IV	V
Methyl group at C-4	−0.06		
Methyl group at C-10	−0.05	−0.04	−0.30
Isopropyl methyl group at C-11	−0.18	−0.20[a]	−0.16[a]

a) The average shift value of isopropyl methyl groups at C-11.

−0.06 ppm for the methyl group at C-4 of III was observed, as shown in Table I, the configuration of the methyl group at C-4 was established to be α. Furthermore, this structure was supported by the pyridine-solvent shift of the methyl group at C-10 and the observation of internal hydrogen bonding in a highly diluted solution of CCl_4.

From the biogenetic point of view, I, II and III are considered to be biosynthesized from 10-*epi*-γ-eudesmol, which is a possible precursor of agarofuran-type sesquiterpenes obtained from *Alpinia japonica*, as discussed in our previous report.[2)]

Experimental

All melting points were recorded on a Yanagimoto micro melting point apparatus and are uncorrected. Spectral data were obtained on the following instruments; optical rotation on a JASCO DIP-4, IR on a JASCO A-302, NMR on a Brucker AM400, MS on a Hitachi M-80. High-performance liquid chromatography (HPLC) was carried out on a CIG column system (Kusano Scientific Co., Tokyo) with IATROBEADS (60 μ silica gel, IATRON CO., Tokyo) as the stationary phase.

Extraction and Isolation——The fresh rhizomes (70.0 kg) of *Alpinia japonica* were extracted twice with methanol under an argon atmosphere. The methanol extract was partitioned with *n*-hexane, and the *n*-hexane layer was concentrated to give a yellow oil (65.0 g). The *n*-hexane extract was subjected to column chromatography on silica gel with an *n*-hexane–ethyl acetate gradient system. Repeated HPLC and $AgNO_3$–HPLC of each fraction using a benzene–ethyl acetate system, a benzene–chloroform–acetonitrile system, an *n*-hexane–ethyl acetate system and an *n*-hexane–chloroform–acetonitrile system gave I (100 mg), II (500 mg) and III (200 mg). Compounds I—III were recrystallized from *n*-hexane.

Compound I (10-*epi*-5β-Hydroperoxy-β-eudesmol): Colorless needles, mp 131.0—133.0 °C, $[\alpha]_D$ −52.0° (c=0.20, $CHCl_3$). MS *m/z*(%): 254 (M^+, 12, Calcd for $C_{15}H_{26}O_3$, 254.1879; Found 254.1847), 236 (2), 221 (13), 203 (100), 162 (43), 147 (59), 133 (41), 121 (33), 109 (52), 95 (88), 81 (57), 67 (41), 59 (73), 55 (49). IR (CCl_4) cm^{-1}: 3610, 3400, 3090, 2940, 2880, 1650, 1460, 1440, 1385, 1380, 1260, 1145, 1100, 1060, 1020, 930, 900. ^{1}H-NMR ($CDCl_3$) δ ppm: 0.96 (3H, s), 1.32 (3H, s), 1.35 (3H, s), 4.79 (1H, s), 5.03 (1H, s). ^{13}C-NMR ($CDCl_3$) δ ppm: 20.1 (t), 22.7 (t), 22.8 (q), 23.4 (t), 28.7 (q), 29.9 (q), 32.4 (t), 33.5 (t), 35.2 (t), 38.1 (s), 40.7 (d), 74.1 (s), 87.0 (s), 111.1 (t), 148.7 (s).

Compound II (10-*epi*-5α-Hydroperoxy-β-eudesmol): Colorless needles, mp 146.0—147.0 °C, $[\alpha]_D$ −48.6° (c=0.21, $CHCl_3$). MS *m/z*(%): 254 (M^+, 0.5, Calcd for $C_{15}H_{26}O_3$, 254.1879; Found 254.1852), 236 (2), 219 (21), 203 (57), 161 (21), 147 (25), 135 (30), 123 (55), 121 (42), 109 (60), 95 (100), 81 (55), 69 (42), 59 (71), 54 (27). IR (CCl_4) cm^{-1}: 3610, 3400, 3090, 2940, 2870, 1640, 1465, 1445, 1380, 1325, 1185, 1130, 900. ^{1}H-NMR ($CDCl_3$) δ ppm: 0.86 (3H, s), 1.20 (3H, s), 1.24 (3H, s), 4.91 (1H, s), 5.10 (1H, s). ^{13}C-NMR ($CDCl_3$) δ ppm: 21.3 (q), 22.4 (t), 23.5 (t), 26.5 (q), 27.6 (q), 28.0 (t), 34.2 (t), 35.4 (t), 35.8 (t), 38.9 (s), 43.7 (d), 72.9 (s), 89.5 (s), 108.0 (t), 148.8 (s).

Compound III (4,10-*epi*-5β-Hydroxydihydroeudesmol): Colorless needles, mp 130.0—132.0 °C, $[\alpha]_D$ −21.8° (c=0.12, $CHCl_3$). MS *m/z*(%): 240 (M^+, 5, Calcd for $C_{15}H_{28}O_2$, 240.2087; Found 240.2097), 222 (10), 207 (30), 149 (80), 126 (100), 59 (75). IR (CCl_4) cm^{-1}: 3620, 3450, 2950, 1460, 1390, 1260, 1150, 1130, 1100, 1050, 1040, 1020, 965, 950, 930; O–H: 3460 cm^{-1} (0.004 mol/l of CCl_4, cell length: 2 mm). ^{1}H-NMR ($CDCl_3$) δ ppm: 1.04 (3H, d, J= 7.7 Hz), 1.10 (3H, s), 1.25 (6H, s). ^{13}C-NMR ($CDCl_3$) δ ppm: 17.0 (t), 17.2 (q), 20.3 (t), 21.8 (q), 28.1 (t), 29.6 (q), 30.0 (q), 31.8 (t), 34.8 (t), 36.6 (s), 36.6 (t), 40.2 (d), 41.2 (d), 72.8 (s), 75.1 (s).

Photooxygenation of 10-*epi*-γ-Eudesmol to Give I and II——A 30 mm quartz tube enclosed by a 100 W mercury lamp was charged with a solution of 90 mg of 10-*epi*-γ-eudesmol and 20 mg of hematoporphyrin in 40 ml of methanol under ice-cold water. Oxygen was admitted through a gas dispersion tube and the mixture was irradiated for 20 min. Removal of the solvent under reduced pressure afforded a crude hydroperoxide, which was immediately subjected to HPLC (*n*-hexane : ethyl acetate = 3 : 2) to give I (20 mg) and II (4 mg).

Reduction of I with Triphenylphosphine to Give IV——An ether solution (2 ml) of I (15 mg) was treated with triphenylphosphine (25 mg) for a few minutes at room temperature, and then evaporated. The residue was subjected to HPLC (*n*-hexane : ethyl acetate = 7 : 3) to give colorless needles, IV (11 mg): mp 126.0—129.0 °C. MS *m/z*(%): 238 (M^+, 5), 220 (13), 205 (40), 162 (75), 147 (100), 95 (92), 58 (60). IR (CCl_4) cm^{-1}: 3610, 3400, 3080, 2950, 1650, 1460, 1440, 1380, 1370, 1055, 1030, 1015, 900; O–H: 3440 cm^{-1} (0.003 mol/l of CCl_4, cell length: 2 mm). ^{1}H-NMR ($CDCl_3$) δ ppm: 0.91 (3H, s), 1.29 (3H, s), 1.30 (3H, s), 4.72 (1H, dd, J=1.4, 1.4 Hz), 4.82 (1H, dd, J=1.6, 1.6 Hz).

Reduction of II with Triphenylphosphine to Give V——An ether solution (2 ml) of II (17 mg) was treated with triphenylphosphine (25 mg) for a few minutes at room temperature, and then evaporated. The residue was subjected to HPLC (*n*-hexane : ethyl acetate = 3 : 2) to give a colorless oil, V (11 mg). MS *m/z* (%): 238 (M^+, 3), 220 (20), 205 (25), 162 (25), 147 (40), 124 (53), 95 (54), 58 (100). IR (CCl_4) cm^{-1}: 3620, 3480, 3080, 2950, 2880, 1640, 1450, 1370, 1120, 1060, 970, 900. ^{1}H-NMR ($CDCl_3$) δ ppm: 0.86 (3H, s), 1.18 (3H, s), 1.19 (3H, s), 4.79 (1H, br s), 4.97 (1H, br s).

Hydrogenation of IV to Give III——A solution of IV (10 mg) in $CHCl_3$ (3 ml) was stirred with PtO_2 (8 mg) for 12 h at room temperature under an H_2 atmosphere. Then the catalyst was removed by filtration and the filtrate was

evaporated. The residue was subjected to $AgNO_3$–HPLC (*n*-hexane : ethyl acetate = 7 : 3) to give III as colorless needles (3 mg).

References

1) H. Itokawa, K. Watanabe, S. Mihashi and Y. Iitaka, *Chem. Pharm. Bull.*, **28**, 681 (1980); H. Itokawa, K. Watanabe, H. Morita, S. Mihashi and Y. Iitaka, *ibid.*, **33**, 2023 (1985); H. Itokawa, H. Morita, K. Watanabe and Y. Iitaka, *Chem. Lett.*, **1984**, 451; H. Itokawa, H. Morita, K. Watanabe, A. Takase and Y. Iitaka, *ibid.*, **1984**, 1687.
2) H. Itokawa, H. Morita, K. Watanabe, S. Mihashi and Y. Iitaka, *Chem. Pharm. Bull.*, **33**, 1148 (1985).
3) E. Knappe and D. Peteri, *Z. Anal. Chem.*, **190**, 386 (1962).
4) D. R. Kearns, *Chem. Rev.*, **71**, 395 (1971).
5) P. V. Demarco, E. Farkas, D. Doddrell, B. L. Mylari and E. Wenkert, *J. Am. Chem. Soc.*, **90**, 5480 (1968).

[Chem. Pharm. Bull. 35(4)1464—1478(1987)]

Studies on Commercial Cinnamon and Allied Barks. X.[1,2] On Nikkei, *Cinnamomum sieboldii* MEISN., syn. *C. loureirii* auct. Japon non NEES

AYA NITTA

Faculty of Pharmaceutical Sciences, Kyoto University, Sakyo-ku, Kyoto 606, Japan

(Received August 25, 1986)

Japanese cinnamon on the market was investigated histologically using specimens collected in Japan. Sixteen lots of material were inspected. They were found to be diverse in internal structure with respect to the amount and combination of mechanical tissue in the bark.

In addition, the difference between the Nikkei root bark and stem bark was clarified. Neither fiber bundles nor a cutinized cell layer was observed in the root bark, which had tangentially elongated cork cells, large oil cells in the primary cortex, and less mechanical tissue than the stem bark. Marketed samples exhibiting a cutinized cell layer probably contain bark from exposed roots or are adulterated with stem bark.

Botanical specimens of the following *Cinnamomum* species were also examined histologically: Nikkei, *C. sieboldii* syn. *C. loureirii*; Yabu-nikkei, *C. insularimontanum* syn. *C. japonicum*; Kusunoki, *C. camphora*; Maruba-nikkei, *C. daphnoides*; and Shiba-nikkei, *C. daphnoides* subsp. *Doederleinii*. The root bark structures of these species were compared at five growth stages and are described in detail. At maturity, three types of structure could be distinguished. One type is shown by Nikkei and Yabu-nikkei. The second is Kusunoki, which has anatomical features not found in other species. Maruba-nikkei and Shiba-nikkei, which differ noticeably only in the amount of mechanical tissue, exhibit the third type of structure.

Keywords——histology; Nikkei; Japanese cinnamon; *C. sieboldii*; *C. loureirii*; *C. insularimontanum*; *C. camphora*; *C. daphnoides*; *C. daphnoides* subsp. *Doederleinii*; Lauraceae

Japanese cinnamon, Nikkei, was introduced from China and cultivated in various places in Japan about 260 years ago in the Edo era.[3] Both its stem and root bark were used as a substitute for cassia bark obtained from *Cinnamomum cassia* PRESL, one of the most important drug materials in Kampo. Furthermore, root bark is preferred to stem bark for medicinal use because it has the same strong odor of cinnamaldehyde as cassia bark.

Although the term "肉桂" (Róu qúi) in Chinese denotes the thick bark from the trunk of *C. cassia*, the same word in Japanese is pronounced "Nikkei", and refers to both the living plant and the drug material derived from it. The scientific name of *C. loureirii* had been assigned to Nikkei, but recently this was revised to *C. sieboldii* MEISN.[4]

The literature concerning the identity of *C. loureirii* is fraught with confusions from the outset. An old source, for instance, made the highly improbable statement that it was distributed in three isolated areas, *i.e.* Cochinchina, the Yunnan region of China, and Japan.[5] In the United States Pharmacopoeia from the 10th[6] (1925) to the 14th[7] (1950) revisions, it was described as the source plant of Saigon cinnamon imported from Cochinchina. Many pharmacists and plant taxonomists doubted the accuracy of this assignment. In particular, after comparing Saigon cinnamon with the bark of *C. loureirii* supplied by the Pharmaceutical Society of Great Britain, Redgrove[8] stated that Saigon cinnamon was probably *C. cassia*. He reported that the two specimens had a similar taste but different odors.

Notwithstanding the controversy, Youngken, who was one of the foremost American

pharmacognosists of his time, described Saigon cinnamon with a microphotograph of the bark under the name of *C. loureirii* in his 1936 textbook.[9] It seems that upon the suggestion of the well-known taxonomist K. C. Allen, Youngken had in fact compared histologically a specimen which he believed to be *C. loureirii* with both Saigon cinnamon and the bark of *C. burmanni* BL.[10] He supposedly recognized differences between these three species, though neither descriptions of the other species nor the result of the comparison was mentioned in his textbook.

Nikkei appeared in the Japanese Pharmacopoeia from the 4th[11] (1921) to the 7th[12] (1961) editions. In the 4th and 5th[13] editions both the stem and root bark were described under the name of Nikkei, but beginning with the 6th[14] edition only the root bark was listed as Nikkei and Nihon-keihi. In the first interim revision of Part II of the 7th edition in 1962,[15] it was deleted because the increasing import of cassia bark from China rendered it unnecessary as a substitute.

Although Nikkei is no longer included in the Japanese Pharmacopoeia, its cultivation was continued in Wakayama and Ehime prefectures, and its stem, root bark and small root are still available on the market. Apart from medicinal usage, root bark and small roots are used for flavoring, and stem bark in incense products such as joss sticks.

As for the internal structure of Nikkei, only the root bark was described and drawn in the Japanese Pharmacopoeia. Kimura and Ohta[16] have examined the structure of root bark in comparison with stem bark, but their description is not detailed enough and contains some mistakes.

This paper gives a more comprehensive account of the internal structure of Nikkei with a view to clarifying some of the confusions present in the literature. Nikkei found in commerce as well as root bark specimens from *C. sieboldii* are examined histologically, the latter in comparison with other Japanese *Cinnamomum* species.

Experimental

In the histological descriptions below, "U-form" sclerenchymatous cell denotes a partially lignified parenchymatous cell, while "O-form" denotes a longitudinally elongated and cylindrically lignified parenchymatous cell.

Commercial Nikkei

Marketed Material——The name, part of the plant, date and place of collection, and name of the collector or

TABLE Ia. Marketed Materials Examined

No.	Name	Part of plant	Date, place collected, and collector or contributor	
1	Nikkei	Root bark	— Drug material specimen made by Tsumura Co.	
2	Nikkei	Root bark	— Drug material specimen made by Tsumura Co.	
3	Nikkei	Root bark	— Drug material specimen made by Tsumura Co.	
4	Nikkei	Root bark	— —	
5	Chiri-chiri-keihi	Root bark	May 1939 Fujisawa Pharmaceutical Co., Ltd.	—
6	Nihon-keihi	Root bark?	— —	K. Kimura
7	Nogi/Matsuba	Root bark	Oct. 9, 1973 Wakayama, Kainan, Makino Co.	S. Yoshida
8	Jo-chiri	Root bark	Oct. 9, 1973 Wakayama, Kainan, Makino Co.	S. Yoshida
9	Tsujikawa	Root bark?	Oct. 9, 1973 Wakayama, Kainan, Makino Co.	S. Yoshida
10	Nikki/Keiboku	Root	Oct. 9, 1973 Wakayama, Kimiidera, near the temple	S. Yoshida
11	Keishin	Stem bark	Feb. 23, 1976 Wakayama, Kainan, Makino Co.	A. Nitta
12	Nikkei	Root bark	May 23, 1977 Ehime, Saijo, Sogabe Co.	S. Yoshida
13	Nikki	Root bark	May 23, 1977 Ehime, Mt. Ishizuchi, near ropeway	S. Yoshida
14	Nikki	Root	May 23, 1977 Ehime, Mt. Ishizuchi, near ropeway	S. Yoshida
15	Nikki	Root	May 23, 1977 Ehime, Mt. Ishizuchi, near ropeway	S. Yoshida
16	Nikki	Root	June 28, 1979 Ehime, Mt. Ishizuchi, near ropeway	Y. Kano

TABLE Ib. Characteristics of Marketed Materials Examined

No.	Name	Part of plant	Form	Diameter or width (mm)	Length (cm)	Thickness (mm)	Odor and taste
1	Nikkei	Root bark	Semi-cylinder to cylinder	*ca.* 10	4—11	1—2 (—3)	Weak odor of cinnamaldehyde, somewhat astringent
2	Nikkei	Root bark	Semi-cylinder to cylinder	*ca.* 10	4—11	1—2 (—3)	Weak odor of cinnamaldehyde, somewhat astringent
3	Nikkei	Root bark	Semi-cylinder to cylinder	*ca.* 10	4—11	1—2 (—3)	Weak odor of cinnamaldehyde, somewhat astringent
4	Nikkei	Root bark	Semi-cylinder to cylinder	5— 7	3— 7	*ca.* 1	Odor of cinnamaldehyde, somewhat hot
5	Chiri-chiri-keihi	Root bark	Semi-cylinder	*ca.* 1	*ca.* 2	*ca.* 1 (—2)	Strong odor of cinnamaldehyde, hot
6	Nihon-keihi	Root bark?	Small pieces	*ca.* 1	3— 5	*ca.* 1	Odor of cinnamaldehyde tinged with camphor, astringent
7	Nogi/Matsuba	Root bark	Semi-cylinder to cylinder	*ca.* 1	3— 9	*ca.* 1	Odor of cinnamaldehyde, lingering hot taste
8	Jo-chiri	Root bark	Semi-cylinder	*ca.* 10	5— 7	1—2	Odor of cinnamaldehyde, somewhat astringent
9	Tsujikawa	Root bark?	Semi-cylinder	20—30	5— 9	2—4	Weak odor of cinnamaldehyde and other unidentified compounds, astringent
10	Nikki/Keiboku	Root	Faggot	1—10	*ca.* 7	Less than 1	Odor of cinnamaldehyde, smaller root has stronger odor and hotter taste
11	Keishin	Stem bark	Semi-cylinder	10—20	*ca.* 10	1—3 (—4)	Weak odor of cinnamaldehyde tinged with camphor and other unidentified compounds, sweet taste followed by lingering hot taste
12	Nikkei	Root bark	Semi-cylinder to cylinder	*ca.* 10	3— 6	*ca.* 1	Odor of cinnamaldehyde, hot and astringent
13	Nikki	Root bark	Semi-cylinder to cylinder	*ca.* 10	3— 6	*ca.* 1	Odor of cinnamaldehyde, hot and astringent
14	Nikki	Root	Faggot	4— 8	7—10	Less than 1	Odor of cinnamaldehyde, hot and astringent
15	Nikki	Root	Special form	10— 1 2— 4	*ca.* 4 35—45	Less than 1	Odor of cinnamaldehyde, hot and astringent
16	Nikki	Root	Special form	10— 1 2— 4	*ca.* 4 35—45	Less than 1	Odor of cinnamaldehyde, hot and astringent

Fig. 1. Two Forms of Nikki on the Market

A: Collected near Kimiidera temple, Wakayama prefecture. B: Collected at the foot of Mt. Ishizuchi, Ehime prefecture.

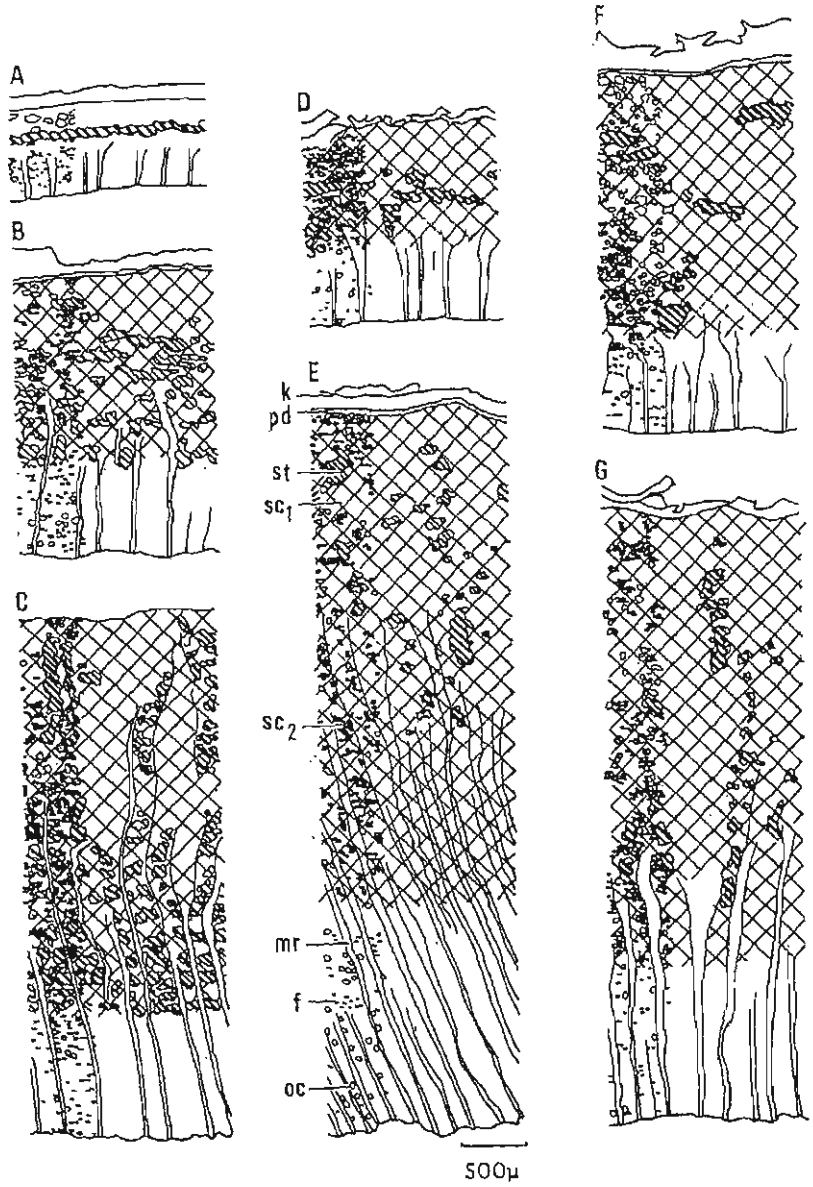

Fig. 2. Internal Structure of Japanese Cinnamon on the Market

A, Nogi 0.6 mm; B, Jo-chiri 1.6 mm; C and E, Tsujikawa 2.6 and 3.9 mm; D and G, Keishin 1.2 and 2.9 mm; F, Nihon-keihi 1.8 mm.

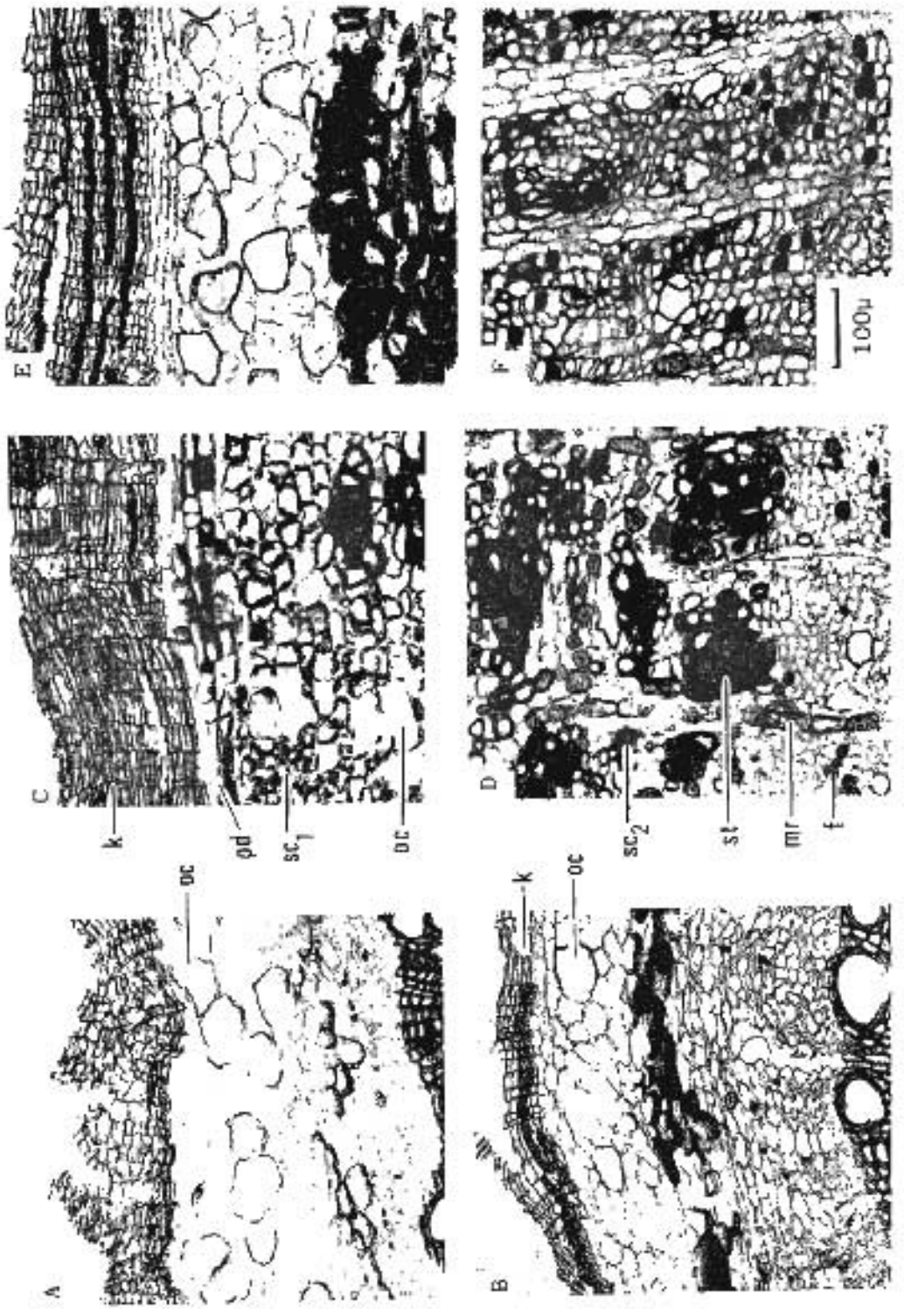

Fig. 3. Internal Structure of Japanese Cinnamon Bark on the Market
A and B, Nikki; C, D, E, F, Jo-chin.

contributor are shown in Table Ia.

Morphology——The form, size, thickness, odor and taste are described in Table Ib.

Sixteen lots of material were examined. Eleven of these were root bark specimens, which were mostly chips. Of the four lots of root specimens, two were in the form of a bunch of slender roots (Fig. 1A). The other two were supplied in a special form: as a bundle composed of a slender root or roots coiled around pieces of thicker roots (Fig 1B). The remaining lot consisted of stem bark specimens, which were straight and bigger than root bark specimens. Among the lots of root bark, No. 6 Nihon-kohi and No. 9 Tsujikawa were large and similar in shape to stem bark.

Histology——Several specimens in each lot were examined with respect to the internal structure of transverse sections. Representative sections are depicted in Fig. 2, and detailed microphotographs of selected specimens are

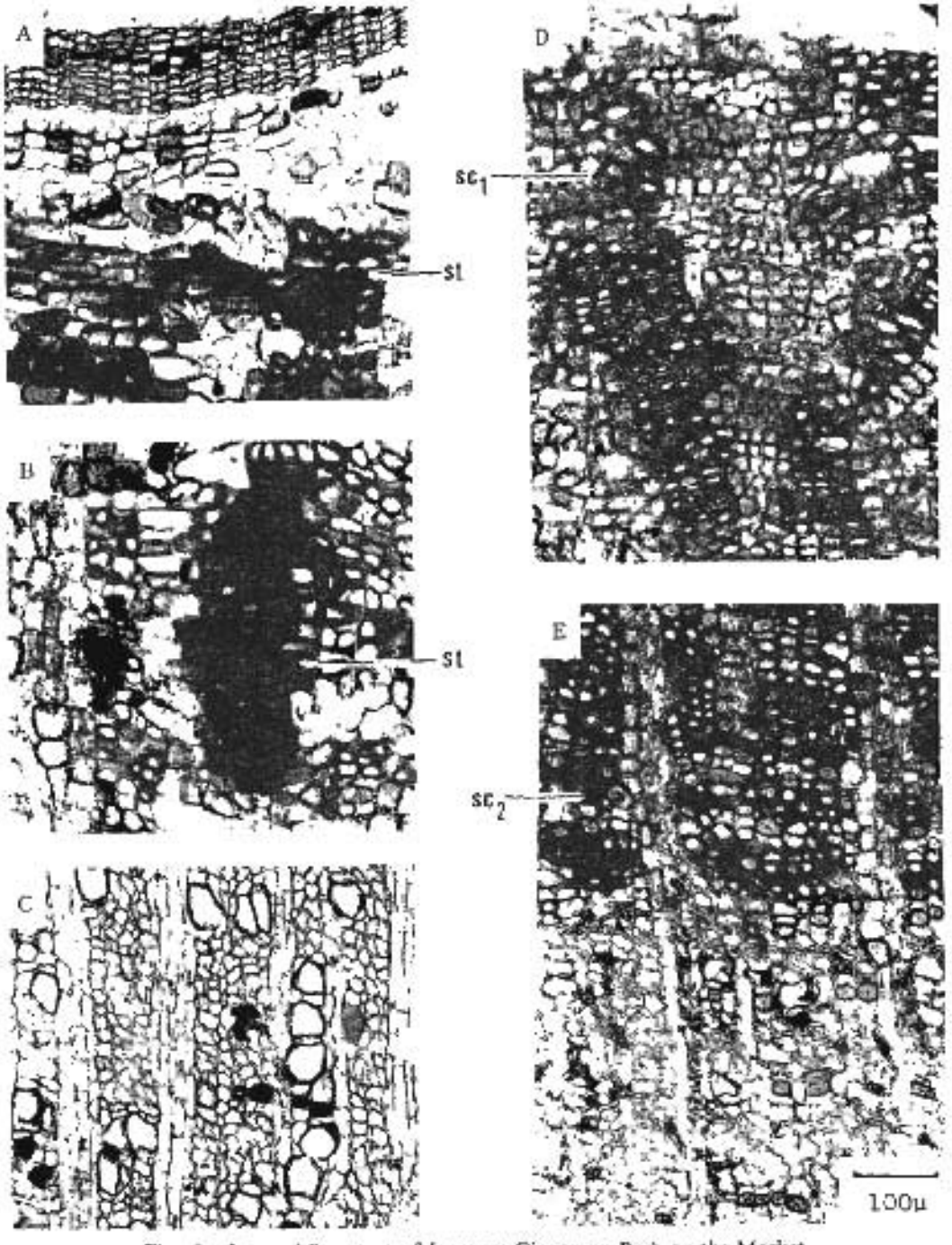

Fig. 4. Internal Structure of Japanese Cinnamon Bark on the Market

A, B, C, Tsujikawa (3.9 mm); D, E, Tsujikawa (2.6 mm).

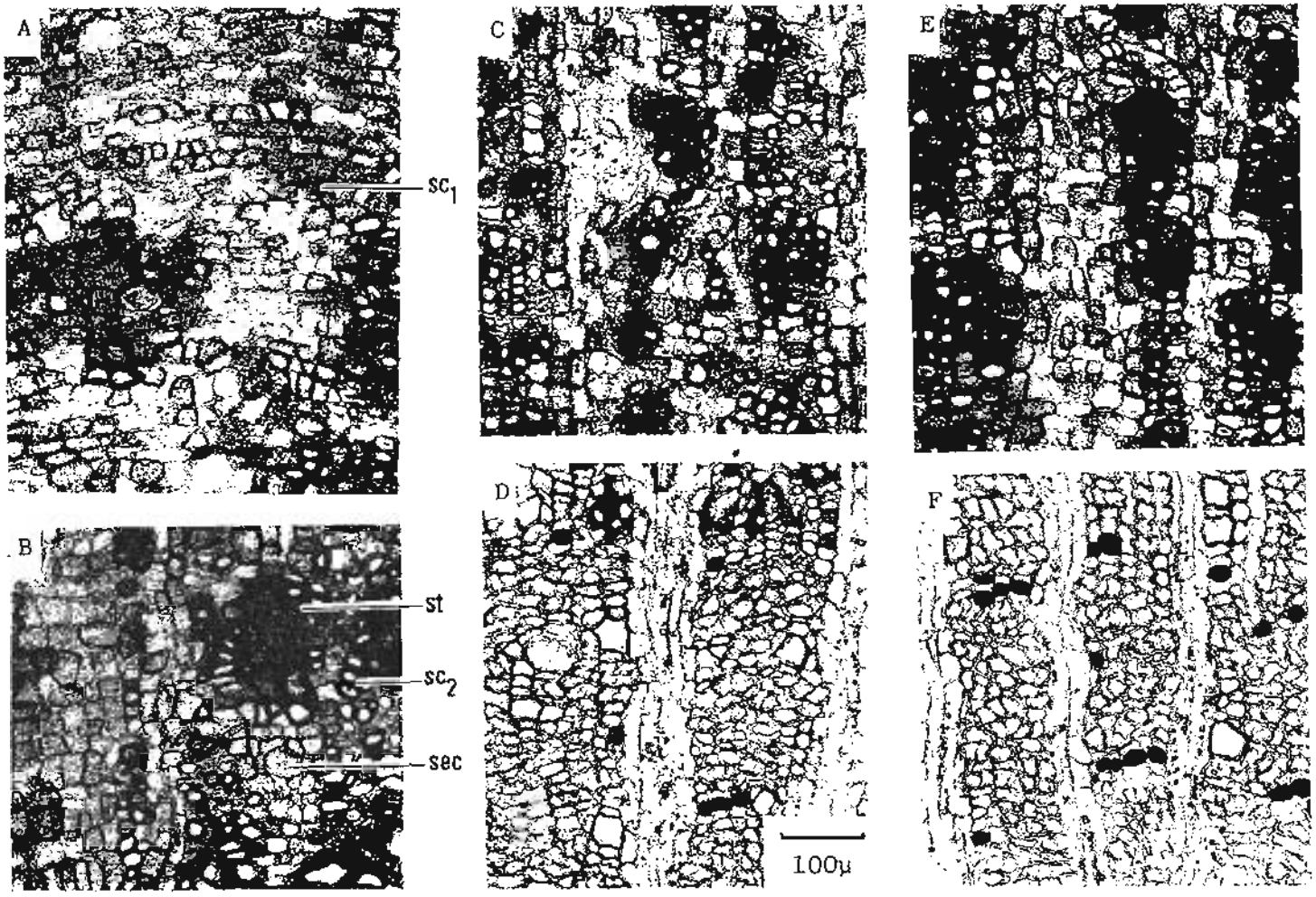

Fig. 5. Internal Structure of Japanese Cinnamon Bark on the Market

Keishin, stem bark; A, B, C, D, 5.0 mm; E, F, 2.3 mm.

shown in Fig. 3 (Nikki and Jo-chiri), Fig. 4 (Tsujikawa), and Fig. 5 (Keishin).

In Fig. 3, microphotograph A shows a specimen of Nikki root 1.3 mm in diameter. Cork tissue comprised 10 layers of cell, and one or two of the innermost layers had lignified inner and side walls. Sclerenchymatous cell groups were arranged in a circular arc. Many large secretory cells were found in the primary cortex; most of them were oil cells with sizes ranging from R=50 to 60 μ, T=70 to 100 μ. Some bigger ones (of the order of R=100 μ and T=130 μ) were also observed.

Microphotograph 3B shows a specimen of Nikki, a root 2.4 mm in diameter. Cork tissue with lignified cells was several layers thick, and some cork cells were tangentially elongated to two to three times their usual size. Phellogen and phelloderm were distinct. Sclerenchymatous cell groups formed a nearly continuous circular band, and the cells had thickened inner and side walls. Fibers were observed in the secondary cortex. Mucilage cells were fewer in number than oil cells.

Microphotographs 3C and D show a 1.6 mm thick sample of Jo-chiri root bark. Cork tissue was about 15 layers thick. Root bark with secondary thickening consisted of U-form sclerenchyma (sc_1). Stone cell groups were interspersed in both cortices, and the stone cells toward the inner region were smaller and had thinner walls than those in the outer region.

Microphotographs 3E and F are cross sectional views of a 0.9 mm thick sample of Jo-chiri. Cork tissue was lignified every two or three layers at the inner and side walls. Stone cells formed a broad band. There were many fibers, but U- and O-form (sc_2) sclerenchyma were rare. The range of sizes of smaller stone cells in the secondary cortex was R=30 to 40 μ, T=40 to 50 μ; and that of bigger ones was R=40 to 50 μ, T=60 to 70 μ.

In Fig. 4, microphotographs A, B and C show a 3.9 mm thick specimen of Tsujikawa. Cork tissue was 10 layers thick, and some of the cork cells were lignified. Phellogen and phelloderm were distinct. Large groups of tangentially elongated stone cells were few in number, and the sizes of individual stone cells ranged from R=10 to 20 μ and T=50 to 120 μ.

In addition to U- and O-form sclerenchyma, few fibers were observed. Secretory cells were found in the parenchyma at the innermost region, and prismatic and oblique-prismatic crystals were present in the medullary rays.

Transectional views of a 2.6 mm thick specimen of Tsujikawa are shown in microphotographs 4D and E. The outermost region had been peeled off. Stone cells small in size and similar to O-form sclerenchymatous cells, occurred in small groups. U- and O-form sclerenchyma occupied about 4/5 of the area of the bark cross section examined. Many fibers and a few small secretory cells were observed. The sizes of fibers were R=20 μ, T=25 μ, and L=(150—) 300 to 350 (—400) μ. Some samples of Tsujikawa had a cutinized cell layer.

TABLE II. Specimens of Nikkei, *Cinnamomum sieboldii* MEISN.

	Name	Part of plant	Date	Place collected	Collector
1	Okinawa-nikkei	Root	July 14, 1972	Okinawa, Yona Experimental Forest, Ryukyu Univ.	Shuji Yoshida
2	Nikkei	Root	Oct. 9, 1973	Wakayama, Kainan, Makino Co.	Shuji Yoshida
3	Keishin	Thick bark from trunk	Oct. 9, 1973	Wakayama, Kainan, Makino Co.	Shuji Yoshida
4	Nikkei	Root	May 23, 1977	Ehime, Komatsu, cult. by Ochi	Shuji Yoshida
5	Nikkei	Root and stem bark	May 23, 1977	Ehime, Saijo, cult. by Toki BHD 20 cm, height 7 m	Shuji Yoshida
6	Nikkei	Root	May 23, 1977	Ehime, Saijo, Hosono, Sogabe Co.	Shuji Yoshida
7	Nikkei	Stem bark of BHD level	May 23, 1977	Ehime, Saijo, Kawaguchi, cult. by Sogabe, BHD 10 cm	Shuji Yoshida
8	Nikkei	Stem bark of BHD level	May 23, 1977	Ehime, Saijo, Kawaguchi, cult. by Sogabe, BHD 10 cm	Shuji Yoshida
9	Nikkei	Stem bark of BHD level	May 23, 1977	Ehime, Saijo, Kawaguchi, cult. by Sogabe, BHD 15 cm, height 8—9 m	Shuji Yoshida
10	Nikkei	Stem bark of BHD level	May 23, 1977	Ehime, Saijo, Kawaguchi, cult. by Sogabe, BHD 15 cm, height 8 m	Shuji Yoshida
11	Nikkei	Root and stem bark	Oct. 11, 1983	Kyoto, herbal garden, Fac. of Pharm. Sci., Kyoto Univ.	Aya Nitta
12	Nikkei	Root and stem bark	Oct. 29, 1983	Kyoto, botanic garden, Fac. of Science, Kyoto Univ.	Aya Nitta
13	Nikkei	Root and stem bark	Oct. 29, 1983	Kyoto, botanic garden, Fac. of Science, Kyoto Univ.	Aya Nitta

Microphotographs of Keishin stem bark are shown in Fig. 5. Microphotographs A, B, C and D show a sample 5.0 mm thick. A few groups of small stone cells were present. U- and O-form sclerenchyma and fibers were all small in size. Microphotographs E and F show a 2.3 mm thick specimen. O-form sclerenchyma and fibers were more numerous here than in the 5.0 mm specimen.

Botanical Specimens of Japanese *Cinnamomum* Species

1. *C. sieboldii* MEISN. syn. *C. loureirii* auct. Japon, non NEES (Nikkei in Japanese). The specimens examined are listed in Table II.

2. *C. insularimontanum* HAY. syn. *C. japonicum* SIEB. ex NAKAI (Yabu-nikkei). 1) BHD 32 cm, 2) BHD 30 cm, 3) BHD 25 cm, 4) BHD 20 cm, November 1984, the botanic garden, Faculty of Science, Kyoto University.

3. *C. camphora* (L.) SIEB. (Kusunoki). 1) BHD 70 cm, 2) BHD 40 cm, 3) BHD 30 cm, November 1984, the botanic garden, Faculty of Science, Kyoto University. 4) BHD 5 cm, 5) BHD 2.5 cm, 6) BHD 1.8 cm, May 1985, the campus, Faculty of Pharmaceutical Sciences, Kyoto University.

4. *C. daphnoides* SIEB. et ZUCC. (Maruba-nikkei). 1) BHD maximum 1.8 cm, height 170 cm, 2) height 70 cm, November 1984, the herbal garden, Faculty of Pharmaceutical Sciences, Kyoto University.

5. *C. daphnoides* subsp. *Doederleinii* KITAM. (Shiba-nikkei). 1) BHD maximum 2.0 cm, height 180 cm, November 1984, the herbal garden, Faculty of Pharmaceutical Sciences, Kyoto University.

In the case of *C. daphnoides* and its subspecies, a single plant grows to form a cluster of trunks joined by lateral roots. Such a cluster yields correspondingly more specimens from the root-stem transition region.

The odor of the root specimens was camphor-like except for *C. sieboldii* and *C. insularimontanum*.

Histology——Several roots in each sample, including exposed roots, were examined from the tip to the trunk border.

Figure 6 depicts the internal bark structures at five growth stages corresponding to five cross sections taken from each specimen.

As seen in diagrams I and II, very small root of all five species have the same structure. In I, the first stage, three

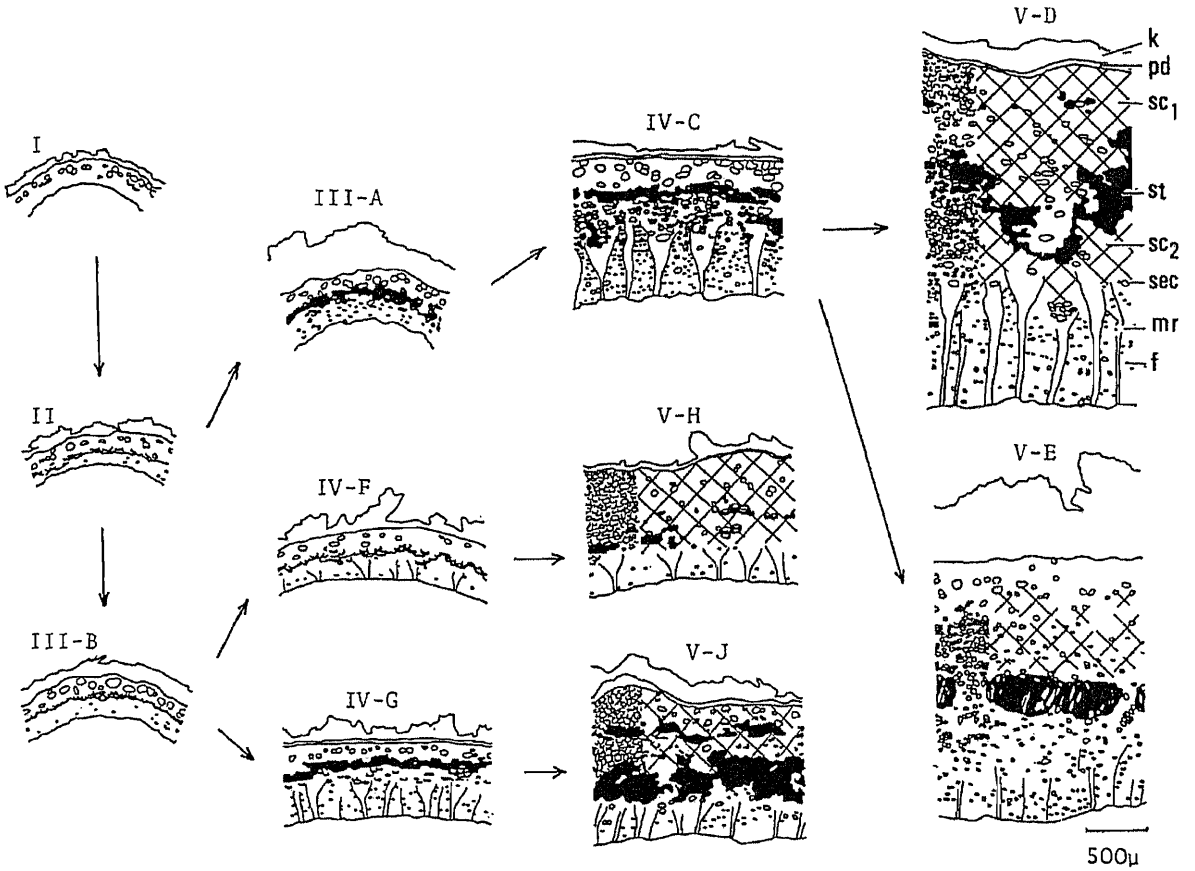

Fig. 6. Stages of Development in the Root Bark Structure of Japanese *Cinnamomum* Species

I and II, all species; III-A and IV-C, *C. sieboldii*, *C. insularimontanum* and *C. camphora*; V-D, *C. sieboldii* and *C. insularimontanum*; V-E, *C. camphora*; III-B, *C. daphnoides* and its subspecies; IV-F and V-H, *C. daphnoides*; IV-G and V-J, *C. daphnoides* subsp. *Doederleinii*.

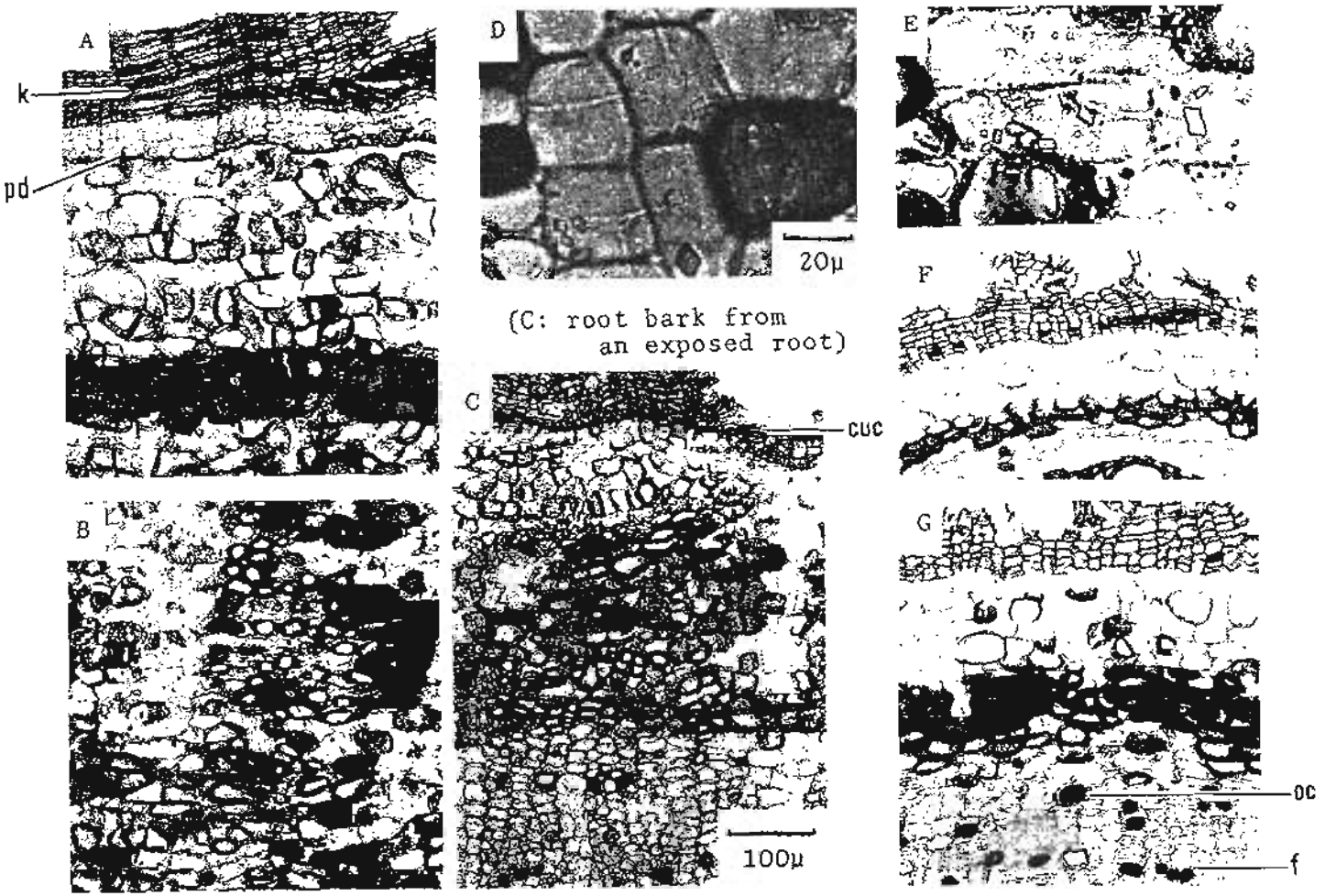

Fig. 7. Root Bark Structure of Nikkei (A—E), *C. sieboldii*, and Yabu-nikkei (F and G), *C. insularimontanum*

to four groups of single or paired U-form sclerenchymatous cells with thickened inner wall were observed. In addition, many big secretory cells, most of them oil cells, were found in the outer region of the cortex. In II, the second stage, the cork layer thickened, and fibers appeared in the secondary cortex. Sclerenchymatous cells proliferated to form an incipient ring.

Further growth and differentiation continued along two developmental pathways, as shown in III-A and III-B. In III-A, fiber cells increased, and the cell wall of the ring-formed sclerenchyma had thickened to the extent that a ring of stone cells was formed. In contrast to this, the cell wall of the sclerenchyma thickened only a little in III-B.

In the fourth stage, medullary rays had appeared and were clearly visible in all specimens. In IV-C, O-form sclerenchyma was interspersed in the secondary cortex, and fiber cells were more numerous. In IV-F, the sclerenchyma ring observed in III-B had become wavy in appearance. In IV-G, on the other hand, it had changed to a ring of stone cells, and O-form sclerenchymatous cells and fibers appeared inside the ring.

Diagrams V-D, E, H and J show the characteristic structure of each species at maturity. In V-D, which shows *C. sieboldii* and *C. insularimontanum*, the stone cell ring was fragmented, stone cell groups and O-form sclerenchyma of various sizes were found in the secondary cortex, and the outer region of stone cell groups was filled with U-form sclerenchyma.

In V-E, which depicts *C. camphora*, the cork layer had developed so much that the stone cell ring was sloughed off. Stone cells, generally radially elongated, form tangentially elongated groups which were arranged in a concentric array of fragmented rings. This phenomenon was not observed in the other species examined. A few O-form sclerenchyma were found outside the stone cell groups. Phelloderm was obscure.

C. daphnoides is shown in V-H. Here the sclerenchyma ring was fragmented and the primary cortex was filled with U-form sclerenchyma. V-J shows *C. daphnoides* subsp. *Doederleinii*. The stone cell ring was also fragmented, and stone cell groups were found in the secondary cortex.

Figures 7 to 10 depict in detail the structures of the root bark of Nikkei (*C. sieboldii*), Yabu-nikkei (*C. insularimontanum*), Kusunoki (*C. camphora*), Maruba-nikkei (*C. daphnoides*), and Shiba-nikkei (*C. daphnoides* subsp *Doederleinii*).

In Fig. 7, photographs A to E show the detailed bark structure of Nikkei, and F and G show that of Yabu-nikkei. For both species, some cork cells were tangentially elongated to three times the usual size, and phellogen and phelloderm were distinct. The stone cell ring was two to three layers thick. A few stone cell groups consisting of two to several stone cells were found in the secondary cortex. U-form sclerenchyma occurred in both the primary and secondary cortices, O-form sclerenchyma and fibers in the secondary cortex in 7A to C, and big secretory cells in

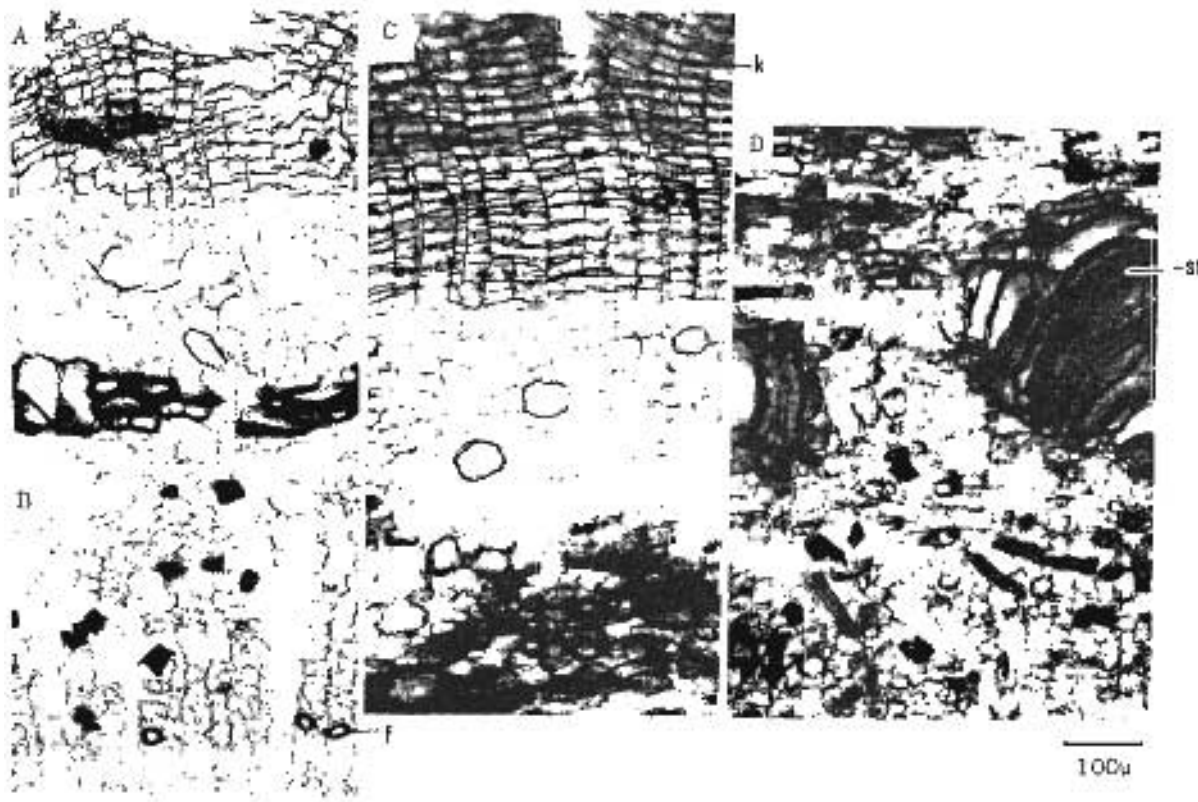

Fig. 8. Root Bark Structure of Kusunoki, *C. camphora*

the primary cortex in 7A. Prismatic and oblique-prismatic crystals were observed throughout.

In 7C, which shows a small Nikkei root that had been exposed, a cutinized layer of cells can been seen. Photograph F depicts a root of Yabu-nikkei 1.7 mm in diameter. A ring of sclerenchymatous cells had already formed, and fibers were observed. Photograph G shows a 3.2 mm root of Yabu-nikkei. Here the stone cell ring was broad and many fibers were present. Yabu-nikkei tended to have more mechanical tissue than Nikkei in the case of small roots. The sizes of fibers were R = 20 μ, T = 20 to 30 μ, and L = (200—) 300 to 350 (—450) μ.

Root bark specimens shown in Fig. 8 were obtained from a young tree of Kusunoki. Photographs A and B show a root 1.7 mm in diameter. A thick cork tissue, a narrow sclerenchyma ring, and many fibers were observed. Photographs A and D depict areas near the root-stem transition region. Here the stone cell ring was broad, and as shown in D, stone cell groups in the secondary cortex were in the process of shifting from a radial to a tangential arrangement. Stone cells were radially elongated and ranged in size from R = 150 to 300 (—330) μ, T = 30 to 70 μ.

A few O-form sclerenchyma, oil cells and rhomboid crystals were also found. The sizes of fibers were R = 20 μ, T = 25 to 30 μ, and L = (250 —) 350 to 450 (—550) μ.

The root bark structure of Maruba-nikkei is shown in Fig. 9. Photographs A and B are cross sections of roots 2.4 mm and 4.0 mm in diameter, respectively. The sclerenchyma ring was wavy in B. Photograph C shows a 1.3 mm thick bark specimen obtained at the trunk border. Cork tissue was lignified in one to two cell layers. Phellogen and phelloderm were distinct, and U-form sclerenchyma was found both in the primary cortex and near the stone cell groups. A few fibers were also observed.

Photograph 9D shows a 1.2 mm thick bark specimen taken from the trunk border of an exposed root. In contrast to C, the outermost cell layer was cutinized, phelloderm was obscure, and primary cortex was filled with U- and O-form sclerenchyma. Fibers were few in number, as in C, with dimensions R = 20 μ, T = 25 μ, and L = (100—) 250 to 300 μ.

Prismatic crystals were observed in all Maruba-nikkei specimens.

Figure 10 show in detail the structure of Shiba-nikkei. Photographs A and B are cross sections obtained from the same root, where the diameters measured 1.5 and 3.0 mm, respectively. Sclerenchymatous cells found in A proliferated to form the ring in B, and fibers, absent in A, appeared in B.

Root bark specimens obtained near the trunk border were also examined. They are depicted in C and D. In C,

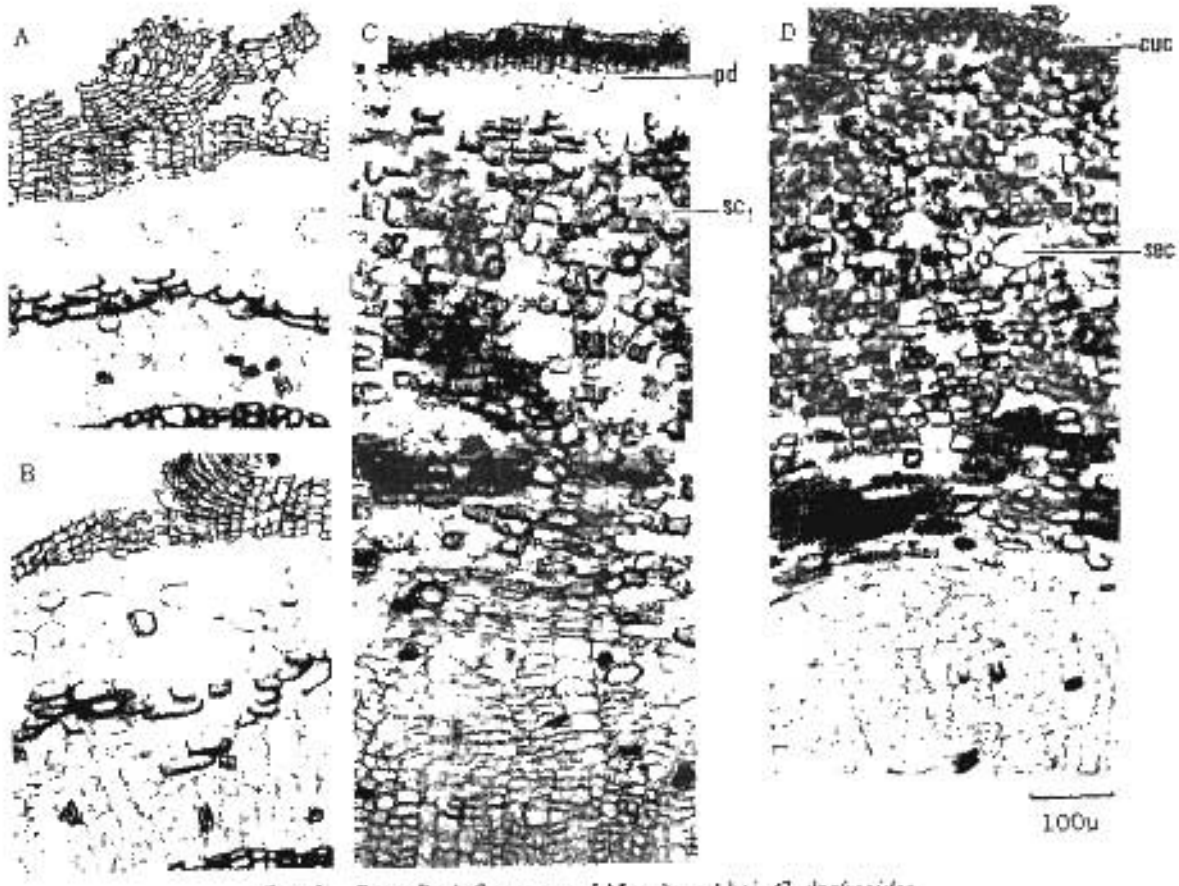

Fig. 9. Root Bark Structure of Maruba-nikkei, *C. daphnoides*

D, root bark from an exposed root.

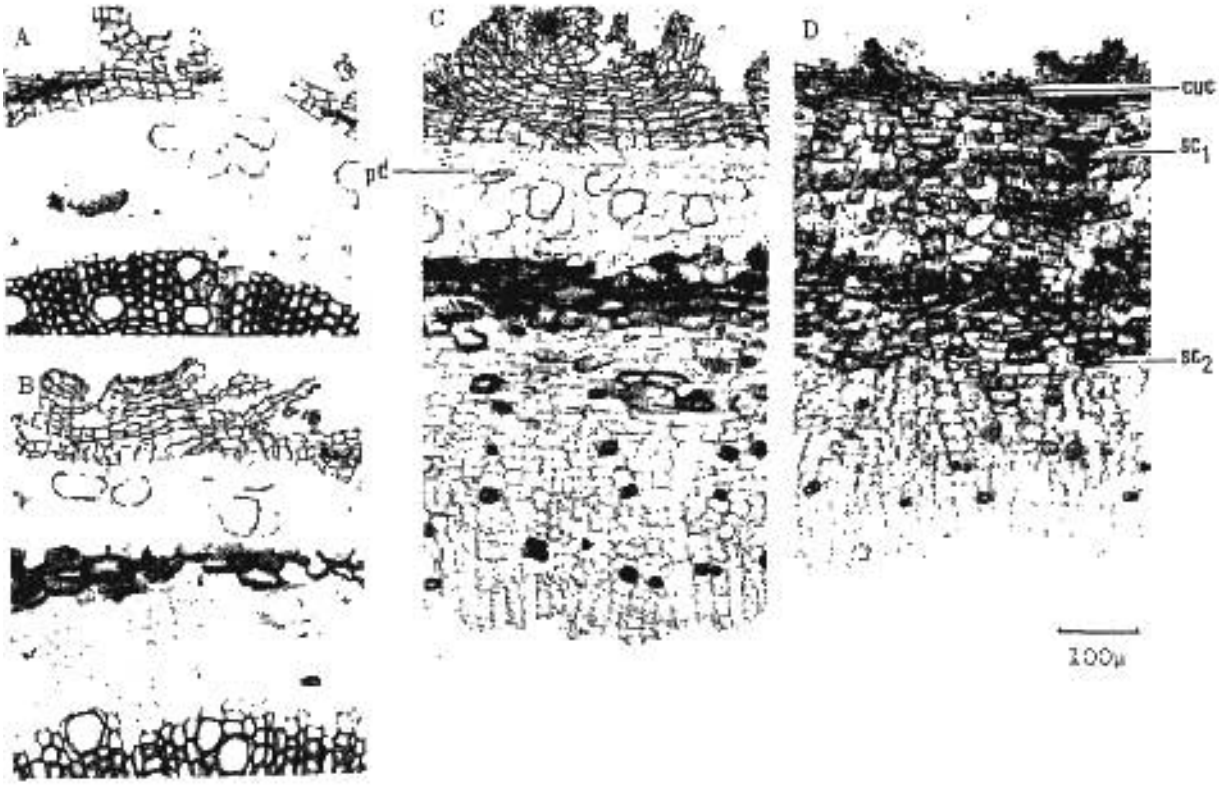

Fig. 10. Root Bark Structure of Shiba-nikkei, *C. daphnoides* subsp. *Doederleinii*
D: root bark from an exposed root.

the cross section of a 0.9 mm thick specimen, phellogen and phelloderm were distinct. A ring consisting of stone cells and other sclerenchymatous cells was present. Many fibers and a few O-form sclerenchyma were found in the secondary cortex. The size of fibers was L = 200 to 350 μ.

The same kind of contrast found in Maruba-nikkei between bark structures of normal and exposed roots is also seen in D. The 0.8 mm thick specimen shown here was taken from an exposed root. Its outermost cell layer was cutinized, phelloderm was obscure, and the primary cortex was filled with U-form sclerenchyma.

Prismatic crystals were also found in all Shiba-nikkei specimens.

Conclusion and Discussion

1) The internal structure of commercial Nikkei, root bark of *C. sieboldii* syn. *C. loureirii*, was examined in detail. It was found to vary considerably with respect to the amount and combination of mechanical tissues such as U- and O-form sclerenchyma, fibers, and stone cells of various sizes and shapes. Such structural differences arising from variations in mechanical tissues have been observed in the stem bark of *C. burmanni*. BL.[17]

The mechanical tissues of some samples were identical in structure to those observed in the stem bark of *C. pseudoloureirii* HAY., which was described in the previous report.[1]

2) The differences between the root and the stem bark of Nikkei may be characterized by the following general remarks. As reported by Kimura and Ohta,[16] root bark has neither cuticle nor fiber bundle. It contains big oil cells which are not present in stem bark. Such oil cells occur in the primary cortex and are more numerous in small roots.

Several additional differences were noted in this investigation. Root bark involved less mechanical tissue and a more distinct phelloderm than stem bark. Also, while the cork cells in stem bark are generally uniform in size and shape, some of them in the root bark are tangentially elongated to two to three times the normal size. Furthermore, with the notable

exception of bark obtained from exposed root, root bark typically lacks a cutinized cell layer. Samples that exhibit such a layer may be assumed to contain bark from exposed roots or to be adulterated with stem bark.

3) Differences between the root bark structures of Japanese *Cinnamomum* species were investigated by tracing the developmental changes which occurred over five stages of growth. Very small roots were found to be identical for all species examined. Three distinct types of structure can be observed in mature specimens.

One type is exhibited by Nikkei and Yabu-nikkei. In these two species, the sclerenchyma ring soon changed to a stone cell ring, which then became discontinuous. Various sizes and shapes of stone cell groups consisting of isodiametrically or tangentially elongated stone cells were present in the secondary cortex. U- and O-form sclerenchyma, fibers, and prismatic or oblique-prismatic crystals were also observed.

Although the two were not distinguishable, Yabu-nikkei tended to have more mechanical tissue than Nikkei in bark specimens of equal thickness.

A second type is exhibited by Kusunoki, which was quite different from the other Japanese *Cinnamomum* species examined. Its cork tissue was thick, and tangentially elongated stone cell groups consisting of radially elongated stone cells formed a concentric array of fragmented rings. U- and O-form sclerenchyma were rare, and crystals were rhombic.

Maruba-nikkei and Shiba-nikkei were nearly indistinguishable and can be considered to have a third type of structure. In Maruba-nikkei, a fluted sclerenchyma ring existed for a long time before changing to a stone cell ring. U-form sclerenchyma tended to develop from the region just under the cork layer, and crystals were prismatic. In Shiba-nikkei, the sclerenchyma ring changed to a stone cell ring before the onset of fragmentation. The form of crystals was also prismatic, but Shiba-nikkei contained more U- and O-form sclerenchyma than Maruba-nikkei.

4) Questions pertaining to the identification of *C. loureirii* with Saigon cinnamon in the United States Pharmacopoeia have been answered in part by this and earlier reports.[1,18]

References and Notes

1) Part IX: A. Nitta, *Yakugaku Zasshi*, **105**, 256 (1985).
2) The following abbreviations are used: k, cork cell; pd, phelloderm; cuc, cutinized cell; sc_1, U-form sclerenchymatous cell; sc_2, O-form sclerenchymatous cell; st, stone cell; f, fiber; mr, medullary ray; oc, oil cell; sec, secretory cell; cr, crystal; R, radial; T, tangential; L, longitudinal; BHD, breast height diameter.
3) S. Kitamura and G. Murata, "Coloured Illustrations of Woody Plants of Japan," Vol. I, Hoikusha Publishing Co., Ltd., Osaka, 1979, pp. 199—204.
4) J. Ohwi, "Flora of Japan," Shibundo, Tokyo, 1956, pp. 652—653.
5) A. D. Candolle, "Prodromus Systematis Naturalis," Regni vegetabilis, Pars XV, Sectio Prior, Victoris Masson et Filii, Parisiis, 1864, pp. 12—13, 16 (Auctore C. F. Meissner).
6) The United States Pharmacopoeial Convention Inc., "Pharmacopoeia of the United States of America, 10th Revision," Lippincott, Philadelphia, 1925, p. 111.
7) The United States Pharmacopoeial Convention Inc., "Pharmacopoeia of the United States of America, 14th Revision," Easton, Mack Printing Company, Philadelphia, 1950, pp. 142—143.
8) H. S. Redgrove, "Spices & Condiments," Sir Isaac Pitman & Sons, London, 1933, pp. 115—116.
9) H. W. Youngken, "A Textbook of Pharmacognosy," P. Blakiston's Son & Co., Inc., Philadelphia, 1936, pp. 323—325.
10) K. C. Allen, *J. Arn. Arb.*, **20**, 52 (1939).
11) H. Kondo, Y. Asahina and Y. Yasumoto (ed.), "Commentary of the Japanese Pharmacopoeia, Ed. IV," Sokyudo, Tokyo, 1921, pp. 362—363.
12) Society of Japanese Pharmacopoeia, "Commentary of the Japanese Pharmacopoeia, Ed. VII," Vol. 2, Hirokawa Book Store, Tokyo, 1961, p. 283.
13) Y. Asahina, Y. Yasumoto, N. Fujita and S. Takagi (ed.), "Commentary of the Japanese Pharmacopoeia, Ed. V," Nankodo, Tokyo, 1934, pp. 409—410.
14) Y. Asahina and S. Takagi (ed.), "Commentary of the Japanese Pharmacopoeia, Ed. VI," Nankodo, Tokyo,

1951, pp. 592—594.
15) Society of Japanese Pharmacopoeia, "Commentary of the Japanese Pharmacopoeia, Ed. VII," Part II, 1962, the preface.
16) K. Kimura and N. Ohta, *Yakugaku Zasshi*, **69**, 75 (1949).
17) S. Yoshida and A. Nitta, *Yakugaku Zasshi*, **96**, 1385 (1976).
18) A. Nitta, *Yakugaku Zasshi*, **104**, 261 (1984).

[Chem. Pharm. Bull. 35(4)1479—1485(1987)]

Sesquiterpene Lactones from *Diaspananthus uniflorus* (SCH. BIP.) KITAM.

SHIGERU ADEGAWA, TOSHIO MIYASE,* and AKIRA UENO

Shizuoka College of Pharmacy, 2-2-1, Oshika, Shizuoka 422, Japan

(Received September 12, 1986)

Five new guaiane-type sesquiterpene lactones, diaspanolides A (V) and B (VI) and diaspanosides A (VIII), B (IX) and C (X), have been isolated from *Diaspananthus uniflorus* (SCH. BIP.) KITAM. (Compositae), together with five known compounds, costunolide (I), reynosin (II), dehydrocostuslactone (III), 11,13α-dihydrozaluzanin C (IV) and glucozaluzanin C (VII). The structures were determined on the basis of spectral data and some chemical transformations.

Keywords——*Diaspananthus uniflorus*; Compositae; sesquiterpene lactone; sesquiterpene glucoside; diaspanolide A; diaspanolide B; diaspanoside A; diaspanoside B; diaspanoside C

In a previous paper, we reported that macrocliniside C, a sesquiterpene glucoside, had considerable antitumor activity in mice.[1] Thus, we have been continuing to search for sesquiterpene glycosides with antitumor activity in Compositae plants. We have investigated the constituents of *Diaspananthus uniflorus* (SCH. BIP.) KITAM., and isolated two new lactones, diaspanolide A (V) and diaspanolide B (VI), in addition to three new glycosides diaspanoside A (VIII), diaspanoside B (IX) and diaspanoside C (X), along with the known compounds costunolide (I), reynosin (II), dehydrocostuslactone (III), 11,13α-dihydrozaluzanin C (IV) and glucozaluzanin C (VII). The structures of these compounds were elucidated on the basis of spectroscopic studies and some chemical transformations.

Costunolide (I),[2] reynosin (II),[3] dehydrocostuslactone (III),[4] 11,13α-dihydrozaluzanin C (IV)[5] and glucozaluzanin C (VII)[6] were identified by direct comparison with authentic samples.

Diaspanolide A (V): $C_{20}H_{28}O_4$, $[\alpha]_D$ +373.8°. The infrared (IR) spectrum suggested the presence of a γ-lactone group (1770 cm^{-1}) and an ester group (1730 cm^{-1}). Its proton nuclear magnetic resonance (^{1}H-NMR) spectrum was quite similar to that of IV, except for the additional presence of a doublet methyl signal at δ0.99 (6H, d, J=6 Hz) characteristic of an isopropyl residue. Furthermore, the signal of H-3 was shifted downfield 1.03 ppm in comparison with that of IV.

In the carbon-13 nuclear magnetic resonance (^{13}C-NMR) spectrum, twenty signals were observed, including three methyl signals at δ22.3 ($CH_3 \times 2$) and 13.2 ppm, and two carbonyl signals at δ172.7 and 178.3 ppm, so we assumed that isovaleric acid was esterified at C-3 of IV. Thus, V was identified by direct comparison [^{1}H-NMR, ^{13}C-NMR, IR] with an authentic sample synthesized from 11,13α-dihydrozaluzanin C (IV) and isovaleric acid. These results led us to conclude that diaspanolide A has the structure V.

Diaspanolide B (VI): $C_{20}H_{26}O_4$, $[\alpha]_D$ +235.3°. The IR spectrum showed γ-lactone (1770 cm^{-1}) and ester group (1730 cm^{-1}) absorptions. The ^{1}H-NMR spectrum was similar to that of V except for the appearance of two doublet signals at δ5.52 (1H, d, J=3.3 Hz) and 6.25 (1H, d, J=3.5 Hz), characteristic of exocyclic methylene protons of the α-methylene-γ-lactone grouping (common in sesquiterpene lactones), instead of a doublet signal due to methyl protons.

A comparison of the ^{13}C-NMR spectrum of VI with that of V showed an upfield shift of 8.6 ppm at C-12 (lactone carbonyl), suggesting that the methyl group at the γ-lactone ring had been converted to an exocyclic methylene. Thus, VI was identified by direct comparison [^{1}H-NMR, ^{13}C-NMR, IR] with an authentic sample synthesized from zaluzanin C (VIIa) and isovaleric acid. These results led us to conclude that diaspanolide B has the structure VI.

Diaspanoside A (VIII): $C_{21}H_{28}O_9 \cdot 1/2\ H_2O$, $[\alpha]_D$ $-10.9°$. The IR spectrum showed hydroxyl group (3450 cm^{-1}) and γ-lactone (1765 cm^{-1}) absorptions. The ^{1}H-NMR spectrum exhibited signals due to three exomethylene groups at δ 5.50 (overlapped) and 6.28 (1H, d, J=3.3 Hz), at δ 5.42 (1H, s) and 5.83 (1H, s), and at δ 5.50 (overlapped) and 6.00 (1H, br s), suggesting that VIII has a guaianolide-type skeleton like that of glucozaluzanin C (VII).

The ^{13}C-NMR spectrum exhibited twenty-one signals including six signals due to a glucopyranosyl moiety, and also indicated the presence of three exomethylene groups. In a comparison of the ^{13}C-NMR spectrum of VIII with that of VII, various signals showed shifts: C-1 and C-7 (each γ to C-9) at δ 42.9 (Δ −1.9 ppm) and 41.4 (Δ −4.0 ppm), respectively, C-8 and C-10 (each β to C-9) at δ 40.7 (Δ +9.9 ppm) and 154.3 (Δ +5.3 ppm), respectively, and C-9 (α-position) at δ 74.6 (Δ +40.2 ppm). Thus, compound VIII was assumd to be a glucozaluzanin C analog having a hydroxyl group at C-9.

Acid hydrolysis of VIII afforded glucose as the sugar moiety, and enzymatic hydrolysis with crude hesperidinase afforded an aglycone (VIIIa). The mass spectrum (MS) of VIIIa showed a molecular ion peak at m/z 262 in agreement with the molecular formula $C_{15}H_{18}O_4$. The ^{1}H-NMR spectrum of VIIIa also exhibited three exomethylene signals at δ 5.55 (overlapped) and 6.32 (1H, d, J=3.3 Hz), at δ 5.55 (overlapped) and 5.92 (1H, s), and at δ 5.55 (overlapped) and 5.75 (1H, br s). A lactonic proton signal was observed at δ 4.26 as a triplet having a coupling constant of 9 Hz, so H-5, H-6 and H-7 are in anti-diaxial relationships.[7] Irradiation at a carbinyl proton signal at δ 4.44 affected an exomethylene proton signals at δ 5.55 and 5.92 (H-14), so we could assign the carbinyl proton to H-9. Furthermore, the carbinyl proton signal showed coupling constants of 5 and 11 Hz, so we assumed that H-9 was α-oriented (pseudo-axial), and thus the hydroxyl group at C-9 was β-oriented. In a nuclear Overhauser effect (NOE) experiment on VIIIa, irradiation of the H-2β signal increased the intensity of the H-14a signal by about 7%, so we decided that H-1 is α-oriented (H-1, H-5 *cis*) (Chart 2).

The circular dichroism (CD) spectrum of VIII showed a negative Cotton effect $[\theta]_{261}$ −1029, suggesting that the γ-lactone ring fusion is 6α,7β-*trans*.[8] A comparison of the ^{13}C-NMR spectrum of VIII with that of VIIIa revealed glycosidation shifts at C-3 (Δ +8.0 ppm), C-2 (Δ −1.5 ppm) and C-4 (Δ −4.1 ppm), so the glycosidic position was at C-3.[9] These results led us to conclude that diaspanoside A has the structure VIII. The stereochemistry of the anomeric center was deduced to be β from the $J_{H_{1'}-H_{2'}}$ coupling constant (7 Hz).

Diaspanoside B (IX): $C_{21}H_{28}O_8 \cdot 1/2\ H_2O$, $[\alpha]_D$ $-55.0°$. The IR spectrum suggested the presence of hydroxyl groups (3450 cm^{-1}), and a γ-lactone ring (1770 cm^{-1}). In the ^{1}H-NMR spectrum, three exomethylene groups were observed at δ 5.36 (overlapped) and 6.25 (1H, d, J=3.3 Hz), at δ 5.00 (1H, s) and 6.19 (1H, s), and at δ 5.05 (1H, br s) and 5.36 (overlapped).

Acid hydrolysis of IX afforded glucose as the sugar moiety, and enzymatic hydrolysis with crude hesperidinase afforded an aglycone (IXa). The MS of IXa showed a molecular ion peak at m/z 246 in agreement with the molecular formula $C_{15}H_{18}O_3$. In the ^{1}H-NMR spectrum of IXa, a lactonic proton signal was observed at δ 4.06 as a triplet having a coupling constant of 9 Hz, so H-5, H-6 and H-7 are in anti-diaxial relationships. Irradiation at a carbinyl proton signal at δ 4.39 affected exomethylene signals at δ 4.99 and 5.82 (H-14), so we could assign the carbinyl proton to H-9. The stereochemistry of the hydroxyl group at C-9 was determined as in the case of VIIIa from the fact that the carbinyl proton signal was observed as a double doublet having coupling constants of 5 and 11 Hz, so we assumed that

the H-9 proton was α-oriented (pseudo-axial), and thus the hydroxyl group was β-oriented. In the high-resolution ^{1}H-NMR difference spectrum, NOE was observed between H-14a and H-2β, so we concluded that H-1 is α-oriented (H-1, H-5 *cis*) (Chart 2).

The CD spectrum of IX showed a negative Cotton effect $[\theta]_{258}$ −1002, suggesting that the γ-lactone ring fusion is 6α,7β-*trans*. In the ^{13}C-NMR spectrum of IXa, various signals showed shifts as compared with those of VIIIa: C-1 and C-5 (each γ to C-3) at δ43.9 (Δ+1.8 ppm) and 52.2 (Δ+2.6 ppm), respectively, C-2 and C-4 (each β to C-3) at δ33.4 (Δ−6.2 ppm) and 152.7 (Δ−2.5 ppm), respectively, and C-3 (α-position) at δ30.7 (Δ−42.0 ppm). Thus, compound IXa was lacking a hydroxyl group at C-3. A comparison of the ^{13}C-NMR spectrum of IX with that of JXa revealed glycosidation shifts at C-9 (Δ+4.6 ppm), C-8 (Δ−1.5 ppm), and C-10 (Δ−5.1 ppm). Thus, we concluded that diaspanoside B has the structure IX. The stereochemistry of the anomeric center was deduced to be β from the $J_{C_1-H_1}$ coupling constant (159 Hz).[10]

Diaspanoside C (X): $C_{21}H_{30}O_9 \cdot 1/2\ H_2O$, $[\alpha]_D$ −22.1°. The IR spectrum suggested the presence of hydroxyl groups (3450 cm^{-1}), and a γ-lactone ring (1770 cm^{-1}). The ^{1}H-NMR spectrum exhibited a singlet methyl signal at δ1.66 (3H, s) and two exomethylene group signals at δ5.45 (1H, d, J=3.1 Hz); 6.28 (1H, d, J=3.3 Hz) due to exocyclic methylene protons of the α-methylene-γ-lactone group (H-13), and at δ4.95 (2H, s).

The ^{13}C-NMR spectrum was similar to that of VII, except for the appearance of a methyl carbon at δ17.9 and a quaternary carbon at δ80.7 having a hydroxyl group, instead of exomethylene carbons.

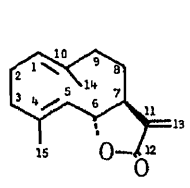

I

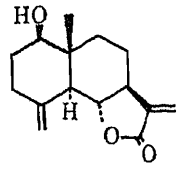

II

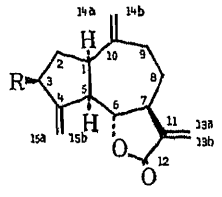

III : R=H
VI : R=O-C(=O)-CH$_2$-CH(CH$_3$)$_2$
VII : R=O-glc
VIIa : R=OH
Xb : R=O-C(=O)-CH$_3$

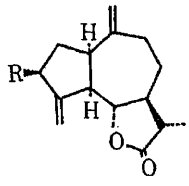

IV : R=OH
V : R=O-C(=O)-CH$_2$-CH(CH$_3$)$_2$

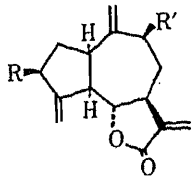

VIII : R=O-glc, R′=OH
VIIIa : R=OH, R′=OH
IX : R=H, R′=O-glc
IXa : R=H, R′=OH

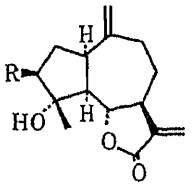

X : R=O-glc
Xa : R=OH

Chart 1

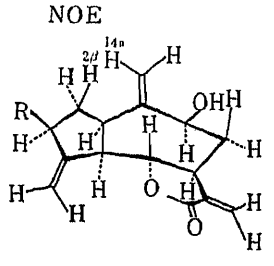

VIIIa : R=OH
IXa : R=H

Chart 2

Acid hydrolysis of X afforded glucose as the sugar moiety, and enzymatic hydrolysis with crude hesperidinase afforded an aglycone (Xa). The MS of Xa showed a molecular ion peak at *m/z* 264 in agreement with the molecular formula $C_{15}H_{20}O_4$. Treatment of Xa with pyridine and acetic anhydride gave a monoacetate and successive dehydration with phosphorus oxychloride and pyridine afforded 3-acetylzaluzanin C (Xb), which was identified by direct comparison [high-performance liquid chromatography (HPLC)] with an authentic sample synthesized from glucozaluzanin C (VII).

In a comparison of the ^{13}C-NMR spectrum of X with that of VII, C-1 and C-2 exhibited upfield shifts of 6.1 and 5.3 ppm (each γ to C-4), and C-3 and C-5 exhibited downfield shifts of

TABLE I. ^{1}H-NMR Chemical Shifts and Coupling Constants

Proton No.	IV	V	VI
Aglycone moiety			
3	4.56 (1H, brt, J=7 Hz)	5.59 (1H, dd, J=6, 8 Hz)	5.60[a]
6	4.04 (1H, t, J=9 Hz)	4.01 (1H, t, J=9 Hz)	4.08 (1H, t, J=9 Hz)
13a	1.24 (3H, d, J=7 Hz)	1.25 (3H, d, J=7 Hz)	5.52 (1H, d, J=3.3 Hz)
13b			6.25 (1H, d, J=3.5 Hz)
14	4.96 (2H, s)	4.95 (2H, s)	4.97 (2H, s)
15	5.32 (1H, brs)	5.28 (1H, brt, J=2 Hz)	5.30 (1H, brs)
	5.40 (1H, brs)	5.43 (1H, brt, J=2 Hz)	5.50 (1H, brs)
Ester moiety			
4, 5		0.99 (6H, d, J=6 Hz)	0.99 (6H, d, J=6 Hz)

Run at 89.55 MHz in $CDCl_3$ solution. *a*) Overlapped.

TABLE II. ^{1}H-NMR Chemical Shifts and Coupling Constants

Proton No.	VII	VIII	IX	X
Aglycone moiety				
13a	5.38 (1H, d, J=3.3 Hz)	5.50[a]	5.36[a]	5.45 (1H, d, J=3.1 Hz)
13b	6.22 (1H, d, J=3.3 Hz)	6.28 (1H, d, J=3.3 Hz)	6.25 (1H, d, J=3.3 Hz)	6.28 (1H, d, J=3.3 Hz)
14a	5.02 (1H, s)	5.42 (1H, s)	5.00 (1H, s)	4.95 (2H, s)
14b	4.85 (1H, s)	5.83 (1H, s)	6.19 (1H, s)	
15a	5.85 (1H, brs)	6.00 (1H, brs)	5.05 (1H, brs)	1.66 (3H, s)
15b	5.53 (1H, brs)	5.50[a]	5.36[a]	
Sugar moiety				
1	5.05[a]	5.03 (1H, d, J=7 Hz)		5.56 (1H, d, J=7 Hz)

Proton No.	VIIIa	IXa	Xa
3	4.90 (1H, brt, J=10 Hz)		4.51 (1H, brt, J=9 Hz)
6	4.26 (1H, t, J=9 Hz)	4.06 (1H, t, J=9 Hz)	4.24 (1H, dd, J=9, 11 Hz)
9	4.44 (1H, dd, J=5, 11 Hz)	4.39 (1H, dd, J=5, 11 Hz)	
13a	5.55[a]	5.53 (1H, d, J=3.1 Hz)	5.45 (1H, d, J=3.1 Hz)
13b	6.32 (1H, d, J=3.3 Hz)	6.31 (1H, d, J=3.4 Hz)	6.29 (1H, d, J=3.6 Hz)
14a	5.55[a]	4.99 (1H, s)	5.08 (1H, s)
14b	5.92 (1H, s)	5.82 (1H, s)	4.99 (1H, s)
15a	5.75 (1H, brs)	5.12 (1H, brs)	1.62 (3H, s)
15b	5.55[a]	5.43 (1H, brs)	

Run at 89.55 MHz in pyridine-d_5 solution. *a*) Overlapped.

TABLE III. ^{13}C-NMR Chemical Shifts and Coupling Constant

Carbon No.	IV[a]	V[a]	VI[a]	VII[b]	VIII[b]	VIIIa[b]	IX[b]	IXa[b]	X[b]	Xa[b]
Aglycone moiety										
1	43.5	44.0	44.6	44.8[f]	42.9	42.1	43.8	43.9	38.7	38.8
2	38.7	36.4	36.6	38.2	38.1	39.6	33.4	33.4	32.9	34.3
3	73.4	74.3	74.3	80.7	80.7	72.7	30.7	30.7	85.1	78.3
4	153.2	148.6[c]	147.7	151.1	151.1	155.2	152.5	152.7	80.7	80.5
5	50.8	50.3	50.3	50.4	49.6	49.6	52.0	52.2	53.3	53.9
6	83.7	83.7	83.8	83.8	84.4	84.8	85.8	86.1	83.4	83.7
7	49.5	50.0	45.2	45.4[f]	41.4	40.9	41.8	41.7	47.5	47.4
8	32.3	32.3	30.6	30.8	40.7	40.7	39.1	40.6	31.7	31.6
9	35.9	36.1	34.5	34.4	74.6	74.6	79.0	74.4	39.2	39.1
10	148.7	148.4[c]	147.7	149.0	154.3	155.0	150.0	155.1	148.3	148.9
11	42.0	42.0	139.6	141.1	140.3	140.1	139.8	140.1	140.3	140.4
12	178.4	178.3	169.7	170.2	169.5	170.1	170.0	170.1	170.2	170.1
13	13.1	13.2	120.1	119.6	119.1	119.7	120.0	119.8	119.6	119.4
14	114.3	113.4[d]	114.3[e]	114.1	110.5	110.4	111.1	108.5	112.6	112.5
15	113.5	113.1[d]	113.4[e]	112.4	110.7	107.3	108.7	108.5	17.9	17.7
Sugar or ester moiety										
1		172.7	172.7	104.3	104.6		101.9 (159 Hz)		104.6	
2		43.6	43.6	75.4	75.3		75.5		75.9	
3		25.7	25.7	78.7[g]	78.5[h]		78.6		78.7[i]	
4		22.3	22.3	72.0	72.2		71.9		71.8	
5		22.3	22.3	78.5[g]	77.9[h]		78.6		78.5[i]	
6				63.0	63.3		63.0		62.9	

a) Run at 22.5 MHz in $CDCl_3$ solution. *b*) Run at 22.5 MHz in pyridine-d_5 solution. *c—i*) Assignments may be interchanged in each column.

4.4 and 2.9 ppm (each β to C-4), respectively, so we concluded that X has a quaternary carbon at C-4 with a methyl group and a hydroxyl group. In an NOE experiment on Xa, irradiation of the H-15 methyl signal increased the intensity of the H-6 lactonic proton signal by about 14%, so we concluded that the methyl group at C-4 was β-oriented, and thus the hydroxyl group was α-oriented. These results led us the conclusion that diaspanoside C has the structure X. The stereochemistry of the anomeric center was deduced to be β from the $J_{H_1'-H_2'}$ coupling constant (7 Hz).

Experimental

Melting points were determined on a Yanaco MP-500 micromelting point apparatus and are uncorrected. Optical rotations were determined with a JASCO DIP-140 digital polarimeter. CD spectra were recorded with a JASCO J-20A automatic recording spectropolarimeter. IR spectra were taken on a JASCO A-202 infrared spectrophotometer. ^{1}H- and ^{13}C-NMR spectra were recorded on JEOL FX-90Q (89.55 and 22.5 MHz, respectively) and JEOL GX-400 (399.65 MHz) spectrometers. Chemical shifts are given on the δ (ppm) scale with tetramethylsilane as an internal standard (s, singlet; d, doublet; t, triplet; m, multiplet; br, broad). Gas chromatography (GC) was run on a Hitachi K 53 gas chromatograph. HPLC was run on a Kyowa Seimitsu model K880 instrument.

Isolation——Air-dried whole plant (590 g) of *D. uniflorus* collected in November 1985, in Shizuoka, Japan, was extracted three times with methanol under reflux. The extract was concentrated under reduced pressure and the residue was suspended in water. This suspension was extracted with ether to give a gum (25 g). The water layer was passed through an Amberlite XAD-2 column and the absorbed material was eluted with methanol to give an amorphous powder (17 g). The ether layer and methanol eluate were each chromatographed on a silica gel column to give compounds I—VI and VII—X, respectively.

Costunolide (I)——Amorphous powder (150 mg). IR ν_{max}^{KBr} cm^{-1}: 1765, 1670. ^{1}H-NMR ($CDCl_3$) δ: 1.43 (3H, brs, H_3-14), 1.71 (3H, d, J=1 Hz, H_3-15), 4.60 (3H, m, H-1, H-5, H-6), 5.54 (1H, d, J=3.2 Hz, H-13a), 6.28 (1H, d,

J=3.6 Hz, H-13b). ^{13}C-NMR ($CDCl_3$) δ: 16.0 (C-14), 17.2 (C-15), 26.1 (C-2), 28.0 (C-8), 39.4 (C-3), 40.9 (C-9), 50.4 (C-7), 81.8 (C-6), 119.4 (C-13), 126.9 (C-1), 127.2 (C-5), 136.8 (C-11), 140.1 (C-4), 141.3 (C-10), 170.3 (C-12).

Reynosin (II)——Amorphous powder (20 mg). IR ν_{max}^{KBr} cm^{-1}: 3460, 1760, 1655. ^{1}H-NMR ($CDCl_3$) δ: 0.81 (3H, s, H_3-14), 3.53 (1H, dd, J=5, 11 Hz, H-1), 4.04 (1H, t, J=11 Hz, H-6), 4.87 (1H, brs, H-15), 4.99 (1H, brs, H-15'), 5.42 (1H, d, J=3.1 Hz, H-13a), 6.10 (1H, d, J=3.2 Hz, H-13b).

Dehydrocostuslactone (III)——Amorphous powder (200 mg). IR ν_{max}^{KBr} cm^{-1}: 1770, 1645. ^{1}H-NMR ($CDCl_3$) δ: 3.98 (1H, t, J=9 Hz, H-6), 4.84 (1H, s, H-14), 4.91 (1H, s, H-14'), 5.09 (1H, brs, H-15), 5.29 (1H, brs, H-15'), 5.51 (1H, d, J=3.2 Hz, H-13a), 6.25 (1H, d, J=3.5 Hz, H-13b). ^{13}C-NMR ($CDCl_3$) δ: 30.2 (C-3), 30.8 (C-8), 32.5 (C-2), 36.1 (C-9), 45.1 (C-7), 47.6 (C-1), 52.0 (C-5), 85. 1 (C-6), 109.5 (C-15), 112.5 (C-14), 120.0 (C-13), 139.7 (C-11), 149.2 (C-10), 151.1 (C-4), 169.5 (C-12).

11,13α-Dihydrozaluzanin C (IV)——Amorphous powder (25 mg). IR ν_{max}^{KBr} cm^{-1}: 3450, 1770, 1460. ^{1}H- and ^{13}C-NMR: Tables I and III.

Diaspanolide A (V)——Colorless oil (60 mg). $[\alpha]_D^{27}$ +373.8° (c=0.011, chloroform). *Anal.* Calcd for $C_{20}H_{28}O_4$: C, 72.26; H, 8.49. Found: C, 72.35; H, 8.52. IR $\nu_{max}^{CHCl_3}$ cm^{-1}: 1770, 1730, 1300. MS *m/z*: 332 (M^+, trace), 248 ($M^+ - C_5H_8O$, 42), 247 ($M^+ - C_5H_9O$, 44), 85 (C_5H_9O, 100). ^{1}H- and ^{13}C-NMR: Tables I and III.

Diaspanolide B (VI)——Colorless oil (300 mg), $[\alpha]_D^{27}$ +235.3° (c=0.034, chloroform). *Anal.* Calcd for $C_{20}H_{26}O_4$: C, 72.70; H, 7.93. Found: C, 72.91; H, 8.04. IR $\nu_{max}^{CHCl_3}$ cm^{-1}: 1770, 1730, 1300, 1260. MS *m/z*: 330 (M^+, trace), 246 ($M^+ - C_5H_8O$, 35), 245 ($M^+ - C_5H_9O$, 40), 85 (C_5H_9O, 100). ^{1}H- and ^{13}C-NMR: Tables I and III.

Glucozaluzanin C (VII)——Recrystallized from water as colorless needles (2 g), mp 106—108 °C. IR ν_{max}^{KBr} cm^{-1}: 3425, 1745, 1640, 1270. ^{1}H- and ^{13}C-NMR: Tables II and III.

Diaspanoside A (VIII)——Amorphous powder (100 mg). $[\alpha]_D^{20}$ −10.9° (c=0.32, methanol). *Anal.* Calcd for $C_{21}H_{28}O_9 \cdot 1/2\ H_2O$: C, 58.19; H, 6.74. Found: C, 58.29; H, 6.63. IR ν_{max}^{KBr} cm^{-1}: 3450, 1765. CD (c=0.32, methanol) [θ] (nm): −1029 (261). ^{1}H- and ^{13}C-NMR: Tables II and III.

Diaspanoside B (IX)——Amorphous powder (300 mg). $[\alpha]_D^{20}$ −55.0° (c=0.30, methanol). *Anal.* Calcd for $C_{21}H_{28}O_8 \cdot 1/2\ H_2O$: C, 60.42; H, 7.00. Found: C, 60.23; H, 6.73. IR ν_{max}^{KBr} cm^{-1}: 3450, 1770. CD (c=0.30, methanol) [θ] (nm): −1002 (258). ^{1}H- and ^{13}C-NMR: Tables II and III.

Diaspanoside C (X)——Amorphous powder (18 mg). $[\alpha]_D^{20}$ −22.1° (c=0.34, methanol). *Anal.* Calcd for $C_{21}H_{30}O_9 \cdot 1/2\ H_2O$: C, 57.92; H, 7.18. Found: C, 58.11; H, 6.99. IR ν_{max}^{KBr} cm^{-1}: 3450, 1770, 1650. ^{1}H- and ^{13}C-NMR: Tables II and III.

Synthesis of Diaspanolide A (V)——Isovaleric acid (1 ml) was mixed with thionyl chloride (1 ml) and stirred for 4 h at room temperature. The excess thionyl chloride was evaporated off *in vacuo*, and 11,13α-dihydrozaluzanin C (IV) (124 mg) dissolved in pyridine (3 ml) was added to the residue. The mixture was stirred for 12 h at room temperature, then the reaction product was purified by silica gel column to afford a colorless oil (V) (40 mg). IR $\nu_{max}^{CHCl_3}$ cm^{-1}: 1770, 1730, 1300. ^{1}H- and ^{13}C-NMR: Tables I and III.

Synthesis of Diaspanolide B (VI)——Zaluzanin C (VIIa) (45 mg) was also esterified in the same way as V, and the isovalerate was obtained as a colorless oil (VI) (21 mg). IR $\nu_{max}^{CHCl_3}$ cm^{-1}: 1770, 1730, 1300, 1260. ^{1}H- and ^{13}C-NMR: Tables I and III.

Enzymatic Hydrolysis of Diaspanoside A (VIII)——VIII (18 mg) was dissolved in water (1 ml) and stirred with crude hesperidinase (*ca.* 10 mg) for 5 h at 37 °C. After being diluted with water, the mixture was passed through an Amberlite XAD-2 column, which was washed with water. The methanol eluate was purified on a silica gel column to give the aglycone (VIIIa) (7 mg). IR ν_{max}^{KBr} cm^{-1}: 3450, 1770. MS *m/z*: 262 (M^+, 5), 244 ($M^+ - H_2O$, 7), 226 ($M^+ - 2H_2O$, 6), 149 (26), 33 (100). ^{1}H- and ^{13}C-NMR: Tables II and III.

Enzymatic Hydrolysis of Diaspanoside B (IX)——IX (11 mg) was hydrolyzed in the same way as VIII, giving the aglycone (IXa) (4 mg). IR ν_{max}^{KBr} cm^{-1}: 3450, 1770. MS *m/z*: 246 (M^+, 2), 228 ($M^+ - H_2O$, 16), 149 (47), 42 (100). ^{1}H- and ^{13}C-NMR: Tables II and III.

Enzymatic Hydrolysis of Diaspanoside C (X)——X (13 mg) was also hydrolyzed in the same way as VIII, giving the aglycone (Xa) (3 mg). IR ν_{max}^{KBr} cm^{-1}: 3450, 1770. MS *m/z*: 264 (M^+, 2), 246 ($M^+ - H_2O$, 6), 228 ($M^+ - 2H_2O$, 3), 149 (18), 33 (100). ^{1}H- and ^{13}C-NMR: Tables II and III.

Dehydration of Diaspanoside C (X)——X was hydrolyzed in the same way as VIII, then the aglycone (Xa) (*ca.* 0.1 mg) was dissolved in acetic anhydride and pyridine (1 drop each), and the mixture was left standing for 2 h at room temperature. The reaction product was evaporated to dryness, and phosphorus oxychloride and pyridine (each 2 drops) were added successively to the residue. The mixture was left to stand for 3 h at room temperature, then excess H_2O was added in order to destroy the reagent. The aqueous solution was extracted with *n*-BuOH 3 times. The residue was evaporated to dryness. This product was examined by HPLC and shown to be identical with authentic 3-acetylzaluzanin C (Xb). HPLC conditions: column, Develosil ODS-7, 4.6 mm × 25 cm; eluent, H_2O–CH_3CN (40 : 60); UV detector 205 nm; flow rate, 1.1 ml/min; t_R, 8.5 min.

Acid Hydrolysis of Diaspanosides A (VIII), B (IX) and C (X)——A solution of a glycoside (*ca.* 0.1 mg) in 10% H_2SO_4 (2 drops) was heated in a boiling water bath for 30 min. The solution was passed through an Amberlite IR-45 column and concentrated to give a residue, which was reduced with $NaBH_4$ (*ca.* 0.1 mg) for 1 h at room temperature. The reaction mixture was passed through an Amberlite IR-120 column and concentrated to dryness. Boric acid was

removed by distillation with methanol and the residue was acetylated with acetic anhydride (1 drop) and pyridine (1 drop) at 100 °C for 1 h. The reagents were evaporated off *in vacuo*. Glucitol acetate was detected by GC. GC conditions: column, 1.5% OV-17, 3 mm × 1 m; column temperature, 200 °C; carrier gas, N_2; t_R, 4.0 min.

Acknowledgement We thank Professor S. Arihara, Institute of Pharmacognosy, Tokushima-Bunri University, for measurement of the 400 MHz NMR spectrum, Dr. M. Uchida for measurement of mass spectra and Mrs. H. Kitamura for elemental analyses.

References and Notes

1) T. Miyase, K. Yamaki, and S. Fukushima, *Chem. Pharm. Bull.*, **32**, 3912 (1984).
2) A. S. Rao, G. R. Kelkar, and S. C. Bhattacharyya, *Chem. Ind.*, **1958**, 1359; *idem*, *Tetrahedron*, **9**, 275 (1960).
3) H. Yoshioka, W. Renold, N. H. Fisher, A. Higo, and T. J. Mabry, *Phytochemistry*, **9**, 823 (1970); Z. Samek, M. Holub, H. Grabarczyk, B. Drozdz, and V. Herout, *Collect. Czech. Chem. Commun.*, **38**, 1971 (1973).
4) S. B. Mathur, S. V. Hiremath, G. H. Kulkarni, G. R. Kelkar, and S. C. Bhattacharyya, *Tetrahedron*, **21**, 3575 (1965).
5) H. Yoshioka, T. J. Mabry, and B. N. Timmerman, "Sesquiterpene Lactones," University of Tokyo Press, Tokyo, 1973, p. 334.
6) T. Miyase and S. Fukushima, *Chem. Pharm. Bull.*, **32**, 3043 (1984).
7) W. Herz, K. Aota, M. Holub, and Z. Samek, *J. Org. Chem.*, **35**, 2611 (1970).
8) W. Stocklin, T. G. Waddel, and T. A. Geissman, *Tetrahedron*, **26**, 2397 (1970).
9) O. Tanaka, *Yakugaku Zasshi*, **105**, 323 (1985).
10) K. Bock, I. Lundt, and C. Pedersen, *Tetrahedron Lett.*, **1973**, 1037.

[Chem. Pharm. Bull. 35(4)1486—1490(1987)]

Saponins from Chinese Folk Medicine, "Liang Wang Cha," Leaves and Stems of *Nothopanax delavayi*, Araliaceae

RYOJI KASAI,[a] TOSHIHIKO OINAKA,[a] CHONG-REN YANG,[b] JUN ZHOU,[b] and OSAMU TANAKA*,[a]

Institute of Pharmaceutical Sciences, Hiroshima University School of Medicine,[a] Kasumi, Minami-ku, Hiroshima 734, Japan and Kunming Institute of Botany, Academia Sinica,[b] Kunming, China

(Received October 15, 1986)

From the Chinese folk medicine "Liang Wang Cha" (leaves and leafstalks of *Nothopanax delavayi*, Araliaceae), two new oleanane type triterpene glycosides, named liangwanosides I (**1**) and II (**2**), were isolated. The structures of **1** and **2** were determined as the 28-β-D-glucopyranosyl and 28-α-L-rhamnopyranosyl(1→4)-β-D-glucopyranosyl(1→6)-β-D-glucopyranosyl esters of 3-*O*-α-L-arabinopyranosyl-3β-hydroxyolean-12-ene-28,29-dioic acid, respectively.

Keywords——*Nothopanax delavayi*; Araliaceae; liangwanoside I; liangwanoside II; Liang Wang Cha; saponin; serratagenic acid; oleanane type triterpene glycoside; Chinese folk medicine

Nothopanax delavayi (FR.) HARMS (Araliaceae) is a tall tree which grows in Yunnan province, China. Leaves and leafstalks of this plant are used as a well known folk medicine "Liang Wang Cha," as an anti-pyretic and anti-inflammatory. We now report the isolation and structural elucidation of two new saponins from this plant.

A methanolic extract of leaves and stems of the young plant was partitioned between water and *n*-hexane. The water layer was passed through a column of highly porous polymer resin (Diaion HP-20). The 80% MeOH eluate, a crude glycosides mixture was further chromatographed on silica gel, affording two new glycosides named liangwanosides I (**1**) and II (**2**) in yields of 0.6% and 1.0%, respectively.

On mineral acid hydrolysis, **1** and **2** gave a common aglycone (**3**). On treatment with diazomethane, **3** gave a dimethyl ester (**4**). The proton nuclear magnetic resonance (^{1}H-NMR) spectrum of **3** exhibited signals due to six methyls on quaternary carbons, an olefinic proton, a carbinyl proton and an allylic proton at δ 2.62, a characteristic signal due to 18β-H of olean-12-ene type triterpenes having a carboxyl group at C-17. Comparison of the carbon-13 nuclear magnetic resonance (^{13}C-NMR) spectrum of **4** with that of methyl oleanolate (**5**)[1] suggested the formulation of **3** as 3β-olean-12-ene-28,29-dioic acid, which has already been isolated as a sapogenin named serratagenic acid from *Clerodendron serratum* SPRENG (Verbenaceae).[2] The presence of an α-carbomethoxyl group at C-20 of **4** was confirmed by the difference of its carbon signals due to the *E*-ring carbons from those of phytolaccagenin (**6**),[3] which has a β-carbomethoxyl group at C-20. The identification of **3** was finally established by comparison of the physical constants and ^{1}H-NMR spectrum with reference data.[2]

Acid hydrolysis of **1** gave D-glucose and L-arabinose. Identification of the absolute configuration of these monosaccharides was carried out by the procedure reported by Oshima *et al.*[4] The electron impact mass (EI-MS) spectrum of peracetylated **3** exhibited fragment ions at *m/z* 331[(Glc)Ac$_4$, terminal glucose] and 259 [(Ara)Ac$_3$, terminal arabinose]. The ^{13}C-NMR spectrum of **1** as well as anomeric proton signals showed the presence of one β-D-glucopyranoside unit and one α-L-arabinopyranoside unit in **1**. The ^{13}C-NMR glycosylation

shifts[5,6] observed between **1** and **3** indicated that **1** is a bisdesmoside of **3** with glycosyl linkages at 3-OH and either 28- or 29-COOH. On selective cleavage of the ester glycosidic linkage with LiI and 2,6-lutidine in anhydrous methanol,[7] **1** gave a methyl glucoside and a prosapogenin (**7**) which was formulated as the 3-*O*-α-L-arabinopyranoside of **3** based on the ^{13}C-NMR spectrum. The location of a glucosyl linkage not at 29-COOH but at 28-COOH was revealed as follows. Formation of the characteristic bromolactone has been used as chemical evidence of the presence of a free carboxyl group at C-17 of olean-12-ene triterpenes.[8] On treatment with diazomethane, **1** afforded a monomethyl ester (**8**). On selective hydrolysis of the ester glycoside linkage with alkali, **8** gave a monodesmoside (**9**). Formation of a bromolactone (**10**) from **9** was observed on treatment of **9** with bromine in the presence of sodium acetate. It follows that **1** is formulated as the 28-β-D-glucopyranosyl ester of 3-*O*-α-L-arabinopyranosyl-serratagenic acid.

Acid hydrolysis of **2** gave D-glucose, L-arabinose and L-rhamnose. The EI-MS of peracetylated **2** exhibited fragment ions at *m/z* 259 [(Ara)Ac$_3$, terminal arabinose], 273[(Rha)Ac$_3$, terminal rhamnose], 849 [(Glc-Glc-Rha)Ac$_9$] and 561 [(Glc-Rha)Ac$_6$]. The ^{1}H- and ^{13}C-NMR spectra of **2** revealed the presence of four monosaccharide units. The

TABLE I. ^{13}C-NMR Chemical Shifts of Aglycone Moieties in C_5D_5N

Carbon	1	2	3	4[d]	5[d,1]	6[3]	7
1	38.9	38.9	38.9	38.5	38.5	44.8	38.7
2	26.3	26.5	28.0	27.2	27.1	71.5	26.3
3	88.9	88.8	78.1	79.0	78.7	73.0	88.7
4	39.4	39.3	39.4	38.7	38.7	42.4	39.5
5	56.1	55.9	55.8	55.2	55.2	48.1	55.8
6	18.6	18.5	18.8	18.3	18.3	18.2	18.5
7	33.3	33.1	33.2	32.7	32.6	33.0	33.1
8	40.0	39.8	39.7	39.3	39.3	39.8	39.7
9	48.1	48.0	48.0	47.6	47.6	48.5	48.0
10	37.1	36.9	37.4	37.0	37.0	37.2	37.0
11	23.8	23.6	23.8	23.2	23.1	23.9	23.8
12	123.5	123.6	122.2	123.4	122.1	123.3	123.1
13	143.5	143.4	144.3	142.8	143.4	144.4	144.4
14	42.4	42.2	42.5	41.6	41.6	42.2	42.7
15	28.3	28.2	28.3	28.3	27.7	28.4	28.2
16	23.8	23.6	23.8	23.4	23.4	23.9	23.8
17	47.0	46.9	46.6	46.4	46.6	46.1	46.6
18	40.8	40.7	41.1	40.2	41.3	43.3	41.1
19	40.8[a]	40.7[a]	41.1[a]	39.7[a]	45.8	42.7	41.1[a]
20	42.2	42.0	42.2	42.2	30.6	44.1	42.2
21	29.1[a]	29.1[a]	29.4[a]	27.6[a]	33.8	30.8	29.3[a]
22	31.7[a]	31.6[a]	32.4[a]	31.2[a]	32.3	34.5	32.5[a]
23	28.3	28.2	28.3	28.1	28.1	67.7	28.2
24	16.8[b]	16.8[b]	16.6[b]	15.5[b]	15.6[a]	14.5	17.0[b]
25	15.5[b]	15.5[b]	15.5[b]	15.3[b]	15.3[a]	17.4	15.5[b]
26	17.5[b]	17.4[b]	17.4[b]	16.8	16.8	17.2	17.4[b]
27	25.9	25.9	26.1	25.9	26.0	26.2	26.1
28	176.0[c]	176.2[c]	180.0[c]	178.0[c]	177.9	179.7	180.2[c]
29	180.9[c]	180.8[c]	181.2[c]	177.2[c]	33.1	28.4	181.5[c]
30	19.9	19.8	20.0	19.3	23.6	177.1	20.1
COOMe				51.7 51.9	51.3	51.6	

a—*c*) Assignments may be reversed in each column. *d*) In $CDCl_3$.

TABLE II. ^{13}C-NMR Chemical Shifts of Sugar Moieties in C_5D_5N

Sugar	1	2	Sugar	1	2
28-Sugar			Rha-1		102.4
Glc-1	95.5	95.5	Rha-2		72.4
Glc-2	74.0	73.6	Rha-3		72.4
Glc-3	78.4	78.6[a)]	Rha-4		73.6
Glc-4	71.4	70.7	Rha-5		70.1
Glc-5	78.4	76.7	Rha-6		18.1
Glc-6	62.5	69.2	3-Sugar		
Glc-1′		104.4	Ara-1	106.3	106.6
Glc-2′		74.9	Ara-2	72.6	72.1
Glc-3′		76.3	Ara-3	73.8	74.1
Glc-4′		78.3[a)]	Ara-4	68.6	68.0
Glc-5′		77.5	Ara-5	65.7	65.9
Glc-6′		61.4			

a) Assignments may be interchanged.

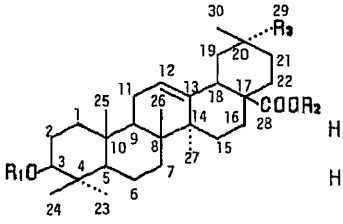

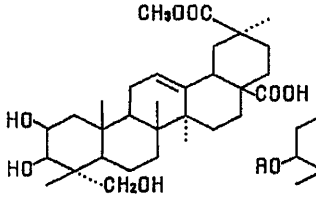

6

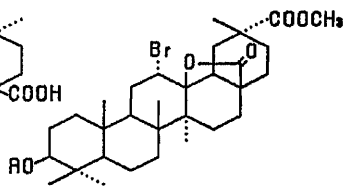

10: α-L-Ara

1: R_1=α-L-Ara, R_2=β-D-Glc, R_3=COOH
2: R_1=α-L-Ara, R_2=β-D-Glc^6—β-D-Glc^4—α-L-Rha, R_3=COOH
3: R_1=H, R_2=H, R_3=COOH
4: R_1=H, R_2=CH_3, R_3=$COOCH_3$
5: R_1=H, R_2=CH_3, R_3=CH_3
7: R_1=α-L-Ara, R_2=H, R_3=COOH
8: R_1=α-L-Ara, R_2=β-D-Glc, R_3=$COOCH_3$
9: R_1=α-L-Ara, R_2=H, R_3=$COOCH_3$

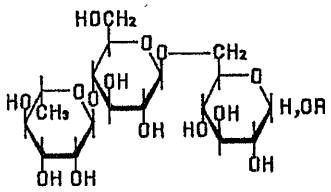

11: R=CH_3
12: R=H

Chart 1

selective cleavage of the ester glycosidic linkage of **2** with LiI and 2,6-lutidine in anhydrous methanol afforded the same prosapogenin **7** as that of **1**, together with a methyl glycoside (**11**) of the trisaccharide (**12**). This methyl glycoside (**11**) was identified as methyl α-L-rhamnopyranosyl(1→4)-β-D-glucopyranosyl(1→6)-β-D-glucoside by comparison of the ^{13}C-NMR spectrum with that of an authentic sample which has already been obtained from huzhangoside B.[9] A carbon signal at δ 95.5 indicated that the terminal glucose moiety of **12** is linked with one of the carboxyl groups of **2** in β-anomeric configuration. Location of this ester-glycosyl linkage at 28-COOH was established by the formation of the bromolactone (**10**), as in the case of **1**. Based on these results, the structure of **2** was established as illustrated in Chart 1.

Experimental

General Procedure——Melting points were determined on a Yanaco micro hot stage and are uncorrected. Optical rotations were measured with a Union PM-101 automatic digital polarimeter. Infrared (IR) spectra were

taken on a Shimadzu IR-408 spectrometer. NMR spectra were recorded on a JEOL FX-100 instrument using tetramethylsilane (TMS) as an internal standard. For gas liquid chromatography (GLC), a Shimadzu GC-8A apparatus was used. Mass spectra (MS) were taken on a JEOL JMS-01-SG-2 spectrometer by the direct inlet method; ionization voltage 75 eV. For column chromatography, Kieselgel 60 (70—230 mesh, Merck) and Diaion HP-20 (Mitsubishi Chem. Ind. Co., Ltd.) were used. All solvent systems for chromatography were homogeneous.

Plant Material——The plant was collected at Mt. Xi San, Kunming, Yunnan and identified by Kunming Institute of Botany. A specimen has been deposited in the Herbarium of this Institute.

Extraction and Separation of 1 and 2——Dried leaves and stems of the young plant (186 g) were extracted with MeOH. The MeOH extract was evaporated to dryness. The residue (25.4 g) was partitioned between H_2O and *n*-C_6H_{14}. The aqueous layer was chromatographed on a Diaion HP-20 column and eluted with H_2O, 10% MeOH, 50% MeOH, 80% MeOH, MeOH and then $CHCl_3$, successively. The 80% MeOH eluate was purified by column chromatography on silica gel (EtOAc–EtOH–H_2O, 7 : 2 : 1) to give **1** and **2** in yields of 0.6% and 1.0%, respectively.

Compound **1**: A white powder, $[\alpha]_D^{19}$ +19.1° (*c*=1.89, MeOH). *Anal.* Calcd for $C_{41}H_{64}O_{14}\cdot 5/2H_2O$: C, 59.61; H, 8.13. Found: C, 59.34; H, 8.13. IR (Nujol): 3400 (OH), 1720 (COOH), 1700 (COOH) cm^{-1}. ^{1}H-NMR (C_5D_5N) δ: 4.75 (1H, d, *J*=7 Hz, anomeric proton of α-Ara), 6.30 (1H, d, *J*=6 Hz, anomeric proton of β-Glc). The ^{13}C-NMR data are given in Tables I and II.

Compound **2**: A white powder, $[\alpha]_D^{20}$ −11.9° (*c*=1.59, MeOH). *Anal.* Calcd for $C_{53}H_{84}O_{23}\cdot 9/2H_2O$: C, 54.39; H, 8.01. Found: C, 54.48; H, 7.84. IR (Nujol): 3400 (OH), 1720 (COOR), 1690 (COOH) cm^{-1}. ^{1}H-NMR (C_5D_5N) δ: 4.66 (1H, d, *J*=6 Hz, anomeric proton of α-Ara), 4.80 (1H, d, *J*=7.5 Hz, anomeric proton of β-Glc), 5.50 (1H, s, anomeric proton of Rha), 6.01 (1H, d, *J*=6.5 Hz, anomeric proton of β-Glc'). The ^{13}C-NMR data are given in Tables I and II.

Acid Hydrolysis of 1 and 2——A solution of **1** (29.6 mg) in 7% HCl–dioxane (1 : 1, 5 ml) was refluxed for 4 h. The reaction mixture was diluted with H_2O and then extracted with Et_2O. The Et_2O layer was dried over anhydrous Na_2SO_4 and evaporated to dryness. The residue was crystallized from MeOH to give **3** (7.6 mg): colorless needles, mp 300 °C, $[\alpha]_D^{25}$ +22.9° (*c*=0.85, C_5H_5N). IR (Nujol): 3450, 1710 cm^{-1}. ^{1}H-NMR (C_5D_5N) δ: 0.91, 1.03, 1.04, 1.24, 1.29, 1.60 (each 3H, s), 2.62 (1H, *J*=6.2, 6 Hz, H-18), 5.57 (1H, m, H-12). The ^{13}C-NMR data are given in Table I. **2** (33.4 mg) afforded **3** (16.7 mg). The H_2O layer was neutralized with Amberlite MB-3 ion exchange resin and evaporated to dryness. Identification of the resulting monosaccharides, including the absolute configuration, was carried out according to the method reported by Oshima *et al.*[4]

Methylation of 3——Compound **3** was methylated with CH_2N_2 in MeOH as usual to give **4**: colorless needles, mp 202—204 °C (from MeOH), $[\alpha]_D^{25}$ +31.5° (*c*=0.91, $CHCl_3$). IR ($CHCl_3$): 1710 ($COOCH_3$) cm^{-1}. ^{1}H-NMR ($CDCl_3$) δ: 0.72, 0.78, 0.91, 0.99, 1.14, 1.25, 3.46, 3.67 (each 3H, s), 2.85 (1H, dd, *J*=6.2, 6 Hz, H-18), 5.30 (1H, m, H-12). The ^{13}C-NMR data are given in Table I.

Selective Cleavage of the Ester Glycosyl Linkage[7] of 1 and 2——A solution of **1** (25 mg), anhydrous LiI (20 mg) and 2,6-lutidine (3 ml) in anhydrous MeOH was refluxed for 15 h under an N_2 stream. After cooling, the reaction mixture was diluted with 50% MeOH (5 ml), neutralized with Amberlite MB-3 resin and evaporated to dryness. The residue was chromatographed on a column of silica gel ($CHCl_3$–MeOH–H_2O, 80 : 10 : 1—6 : 4 : 1) to give **7** (7 mg) and an anomeric mixture of methyl glucoside (3 mg); the latter was trimethylsilylated with trimethylsilylimidazole and identified by GLC comparison with an authentic sample.

By the same method, **2** (106 mg) afforded **7** (16 mg) and **11** (34 mg); the latter was identified as methyl α-L-rhamnopyranosyl (1→4)-β-D-glucopyranosyl(1→6)-D-glucopyranoside by comparison of the ^{13}C-NMR spectrum with that of an authentic sample obtained from huzangoside B[9] under the same conditions. Compound **7**: A white powder, $[\alpha]_D^{20}$ −8.9° (*c*=1.23, C_5H_5N). *Anal.* Calcd for $C_{35}H_{54}O_9\cdot 2H_2O$: C, 64.19; H, 8.93. Found: C, 64.37; H, 8.68. IR (Nujol): 3400 (OH), 1690 (COOH) cm^{-1}. ^{1}H-NMR (C_5D_5N) δ: 0.86, 0.95, 1.00, 1.27, 1.30, 1.58 (each, 3H, s), 4.78 (1H, d, *J*=6.6 Hz, anomeric proton of α-Ara), 5.54 (1H, m, H-12). The ^{13}C-NMR data are given in Table I.

Formation of the Bromolactone (10)[8]——**1** (7 mg) was methylated with CH_2N_2 in MeOH, and the product (**8**) was dissolved in 1 N NaOH (3 ml) and heated at 80 °C for 2 h. After cooling, the reaction mixture was neutralized with 2 N H_2SO_4 and passed through a SEP-PAK (C-18, Waters Assoc.) to remove the resulting sugar component. The solution was evaporated to dryness to give **9**. A solution of AcOH (2 ml) containing Br_2 (0.1 ml) was added to a solution of **9** and AcONa (10 mg) in 90% AcOH (1 ml) and the mixture was stirred at room temperature for 15 h under an N_2 stream. The reaction mixture was poured into an aqueous solution saturated with $NaHSO_3$ and extracted with $CHCl_3$. The $CHCl_3$ layer was evaporated to dryness and the residue was purified by silica gel column chromatography ($CHCl_3$–MeOH–H_2O, 80 : 10 : 1 and AcOEt–EtOH–H_2O, 8 : 2 : 1) to give **10** (4.1 mg) as a white powder, IR ($CHCl_3$): 3500 (OH), 1765 (five-membered ring lactone), 1720 ($COOCH_3$) cm^{-1}, ^{1}H-NMR (C_5D_5N) δ: 0.86, 0.90, 1.23, 1.46 (each 3H, s), 3.72 (3H, s, H-29), 4.12 (1H, br s, H-12), 4.34 (1H, m, H-3). When subjected to the same procedure, **2** (7 mg) also afforded **10** (2.2 mg).

Acknowledgement We are grateful to the Japan China Medical Association for a Grant-in-Aid.

References

1) K. Tori, S. Seo, A. Shimaoka, and Y. Tomita, *Tetrahedron Lett.*, **1974**, 4227.
2) S. Rangaswami and S. Saragan, *Tetrahedron*, **25**, 3701 (1969).
3) W.-S. Woo, S.-S. Kang, K. Yamasaki, and O. Tanaka, *Arch. Pharm. Res.*, 1, 21 (1978).
4) R. Oshima, J. Kumanotani, and C. Watanabe, *J. Chromatogr.*, **259**, 159 (1983).
5) R. Kasai, M. Okihara, J. Asakawa, K. Mizutani, and O. Tanaka, *Tetrahedron*, **35**, 1427 (1979).
6) H. Ishii, I. Kitagawa, M. Matsushita, K. Shirakawa, K. Tori, T. Tozyo, M. Yoshikawa, and Y. Yoshimura, *Tetrahedron Lett.*, **22**, 1592 (1981).
7) K. Ohtani, K. Mizutani, R. Kasai, and O. Tanaka, *Tetrahedron Lett.*, **25**, 4537 (1984).
8) Y. Oshima, T. Ohsawa, and H. Hikino, *Planta Medica*, **51**, 254 (1984).
9) K. Mizutani, K. Ohtani, J.-X. Wei, R. Kasai, and O. Tanaka, *Planta Medica*, **51**, 327 (1984).

[Chem. Pharm. Bull. 35(4)1491—1496(1987)]

Benzoylthiocholine Derivatives as Substrates for Pseudocholinesterase: Synthesis and Application

MAGOHEI YAMADA,[a] YOJI MARUI,[b] CHOZO HAYASHI,[b] and SHOJI TAKEMURA*,[c]

International Reagents Co., Ltd.,[a] Takatsukadai 4-3-2, Nishi-ku, Kobe 673-02, Japan, The Central Laboratory for Clinical Investigation, Osaka University Hospital,[b] 1-1-50, Fukushima-ku, Osaka 535, Japan, Faculty of Pharmaceutical Sciences, Kinki University,[c] Kowakae 3-4-1, Higashi-Osaka 577, Japan

(Received September 4, 1986)

Substituted benzoylthiocholines were synthesized and their application as reagents for clinical measurement of pseudocholinesterase was investigated. Among 21 compounds, 2,3-dimethoxybenzoylthiocholine (**19b**) was found to be an excellent substrate for the measurement of the enzyme. The procedure was simple and self-hydrolysis of the substrate at the optimum pH of the enzyme was minimal.

Keywords——substituted benzoylthiocholine; synthetic substrate; pseudo-cholinesterase; clinical test reagent; colorimetry

The clinical measurement of serum cholinesterase, pseudocholinesterase, EC 3.1.1.8, is important for the diagnosis of liver diseases,[1] hyperlipemia,[2] fatty liver,[3] and intoxication with organophosphorous compounds.[4] A variety of methods for measurement of the enzyme in the clinical setting have been proposed, and colorimetry of the hydrolysate formed by the action of the enzyme on an appropriate synthetic substrate is widely applied.

Esters of aromatic carboxylic acid[5] and thioesters of aliphatic carboxylic acids[6] are generally used as such substrates. The former compounds, however, need carefully controlled conditions and require a conjugated enzyme system and dissolved oxygen, whereas thiocholine esters are extremely simple to use, and give accurate results. Thiocholine esters of acetic, propionic, or butyric acids have been used for this purpose. The common procedure

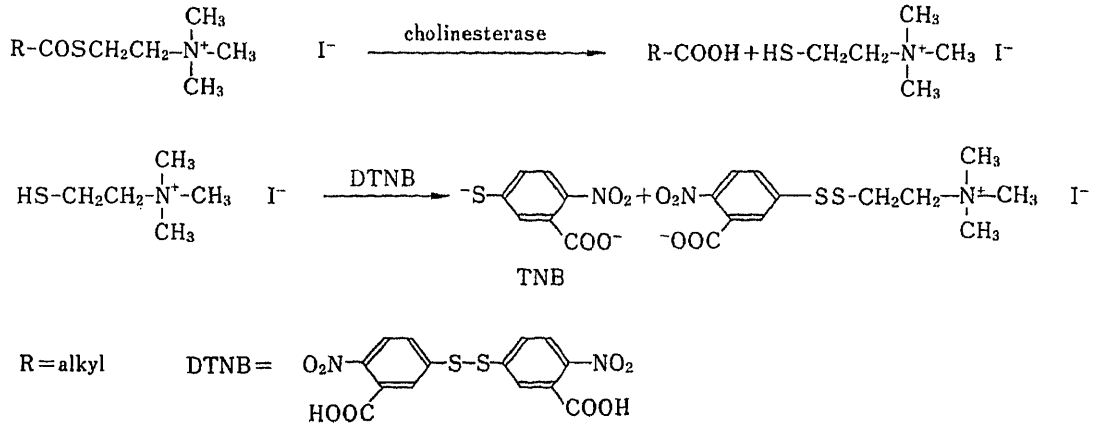

Fig. 1. Reactions Involved in Cholinesterase Assay Using Thiocholine Esters and DTNB

TABLE I. Dimethylaminoethanthiol Benzoate Hydroiodides (**a**) and Thiocholine Benzoate Iodides (**b**)

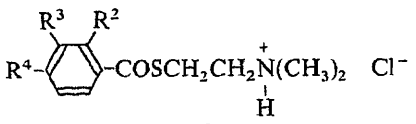

a

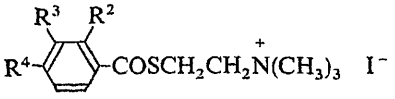

b

No.	Substituents			mp (°C)		Overall yield (%) of **b**[a]	Formula of **b**	Analysis of **b** (%) Calcd (Found)		
	R^4	R^3	R^2	of **a**	of **b**			C	H	N
1	H	H	H[7]		257	61.1	$C_{12}H_{18}INOS$	41.03 (—)	5.17 (—)	3.99 (—)
2	Me	H	H	152—153	224—225	52.3	$C_{13}H_{20}INOS$	42.74 (42.65)	5.52 5.40)	3.83 3.86)
3	H	Me	H	135—136	234—236	41.2	$C_{13}H_{20}INOS$	42.74 (42.76)	5.52 5.48)	3.83 3.88)
4	H	H	Me	161—163	188—190	51.2	$C_{13}H_{20}INOS$	42.74 (42.78)	5.52 5.55)	3.83 3.91)
5	*tert*-Bu	H	H	172—173	181—183	40.3	$C_{16}H_{26}INOS$	47.17 (46.98)	6.43 6.33)	3.44 3.55)
6	NO_2	H	H[7]	179—181	204—205	54.3	$C_{12}H_{17}IN_2O_3S$	36.37 (36.43)	4.32 4.25)	7.07 7.24)
7	H	NO_2	H	184—186	210—213	56.8	$C_{12}H_{17}IN_2O_3S$	36.37 (36.26)	4.32 4.47)	7.07 7.13)
8	Cl	H	H	192—193	227—228	25.2	$C_{12}H_{17}ClINOS$	37.37 (37.32)	4.44 4.51)	3.63 3.57)
9	H	Cl	H	151—152	206—207	26.2	$C_{12}H_{17}ClINOS$	37.37 (37.48)	4.44 4.33)	3.63 3.65)
10	H	H	Cl	141—142	178—180	65.2	$C_{12}H_{17}ClINOS$	37.37 (37.50)	4.44 4.43)	3.63 3.66)
11	MeO	H	H	171—172	198—200	42.4	$C_{13}H_{20}INO_2S$	40.95 (41.02)	5.19 5.09)	3.67 3.78)
12	H	H	MeO	179—180	191—192	40.3	$C_{13}H_{20}INO_2S$	40.95 (40.78)	5.19 5.21)	3.67 3.67)
13	HO	H	H	138—140[b]	232—234	42.0	$C_{12}H_{18}INO_2S$	39.24 (39.32)	4.94 4.88)	3.81 3.92)
14	Me_2N	H	H	180—183[c]	205—208	72.6	$C_{14}H_{23}IN_2OS$	42.64 (42.42)	5.88 5.90)	7.10 7.05)
15	AcNH	H	H	171—173	220—222	28.0	$C_{14}H_{21}IN_2O_2S$	41.18 (41.22)	5.18 5.21)	6.86 7.01)
16	H	AcNH	H	182—184	232—234	49.2	$C_{14}H_{21}IN_2O_2S$	41.18 (41.31)	5.18 5.08)	6.86 6.96)
17	H	H	AcNH	165—166	251—253	42.4	$C_{14}H_{21}IN_2O_2S$	41.18 (41.11)	5.18 5.16)	6.86 6.98)
18	MeO	H	MeO	178—180	191—192	77.8	$C_{14}H_{23}INO_3S$	40.78 (40.88)	5.62 5.54)	3.40 3.23)
19	H	MeO	MeO	166—167	188—190	78.2	$C_{14}H_{23}INO_3S$	40.78 (40.65)	5.62 5.38)	3.40 3.58)
20	MeO	MeO	H	178—180	180—181	69.0	$C_{14}H_{23}INO_3S$	40.78 (40.66)	5.62 5.60)	3.40 3.51)
21	$-OCH_2O-$		H	197—199	239—241	76.0	$C_{13}H_{18}INO_3S$	39.50 (39.62)	4.59 4.58)	3.54 3.62)

a) Overall yield based on benzoyl chlorides. *b*) The melting point after hydrazinolysis of *p*-acetoxybenzoylthiocholine to give **13b**.[8] *c*) The intermediate **14a** was prepared by the reaction of the corresponding acid chloride with aminothiol in the presence of excess pyridine.

for measurement with thiocholine esters is based on a reaction of thiocholine produced by enzymic hydrolysis with 5,5′-dithio-bis-2-nitrobenzoic acid (DTNB) to give 5-thio-2-nitrobenzoate anion (TNB) which is colorimetrically measured at 405 nm (Fig. 1). Despite the simplicity of the procedure, disadvantages of these methods are (1) the concentration of sample must be too low for convenient measurement because of the high sensitivity of these substrates, (2) an increase of self-hydrolysis of the reagents over pH 7.9 makes measurement at pH 8.0—8.5 impossible, though this is the optimum pH range for the enzyme action.

The authors attempted to find a new substrate to overcome these disadvantages by changing the aliphatic acid moieties of thioesters to aromatic ones. Twenty one compounds were synthesized and evaluated as substrates of this reaction (Table I).

Materials and Methods

Materials——Pseudo-cholinesterase from human serum was supplied by Sigma Chemical Co., Ltd. (Osaka, Japan) and the analytical reagents and the starting materials to synthesize acylthiocholines were purchased from Aldrich Chemical Co. (Milwaukee, Wisconsin, U.S.A.).

Synthesis——Substituted benzoylthiocholines were synthesized by a modification of the method of Renshaw *et al.*[7]

An ether solution of dimethylaminoethanethiol, prepared from its hydrochloride by treatment with aqueous sodium carbonate, was added dropwise to the corresponding acid chloride in ether to give dimethylaminoethanethiol ester hydrochloride (**a**). An aqueous solution of the ester hydrochloride (**a**) was alkalized with sodium carbonate and extracted with ether. The ether extract was dried over $MgSO_4$ and stirred with excess methyl iodide until no more solid (**b**) precipitated. The separated crude product was recrystallized from hot water.

Data for the 21 benzoylthiocholines obtained are listed in Table I.

$$\underset{}{HSCH_2CH_2\overset{+}{N}H(CH_3)_2Cl^-} \xrightarrow{OH^-} \underset{}{HSCH_2CH_2N(CH_3)_2} \xrightarrow[2)\ OH^-]{1)\ ArCOCl} \underset{}{ArCOSCH_2CH_2N(CH_3)_2} \xrightarrow{CH_3I} \underset{}{ArCOSCH_2CH_2\overset{+}{N}(CH_3)_3\ \ I^-}$$

a b

Fig. 2. Synthetic Route to Substituted Benzoylthiocholines

Methods——The conditions for measurement of pseudo-cholinesterase activity were investigated by the standard method of Ellman.[9] Each synthesized benzoylthiocholine was incubated with the esterase in Tris buffer at pH 8 in the presence of DTNB.

The compositions of the reagents and the procedure were as follows: reagent 1 (DTNB), 0.3 mmol/l; reagent 2 (substituted benzoylthiocholine), 6.0 mmol/l; sample (in the case of human serum), 0.10 ml; buffer (Tris; pH 8.2), 240 mmol/l.

Procedure: A mixture of reagent 1 and sample in Tris buffer was preincubated for 5 min at 30 °C and reagent 2 was added to the mixture. After incubation for 1 min, the absorption (ΔE) of the solution at 405 nm was continuously measured for 2 min.

Results and Discussion

The reaction rate of the benzoylthiocholines with pseudo-cholinesterase was presumed to be correlated with the electronic effect of the substituents in the aromatic moiety of the substrate. Therefore the correlation was examined on five compounds. Figure 3 shows the relationship between the enzyme reaction rate, V_{max}/K_m, and the Hammett constant, σ. The linearity of the plot was satisfactory. It was shown that an electron-attracting group on the aromatic ring accelerated the reaction, while an electron-releasing one lowered the rate. However at the same time, the accelerating groups increase the rate of self-hydrolysis (blank reaction) the rate-decreasing groups (such as hydroxy or methoxy group) also lower the blank reaction rate, as shown in Table II and Fig. 4. Thus we concluded that a convenient substrate might be found among the compounds bearing an electron releasing group on the aromatic

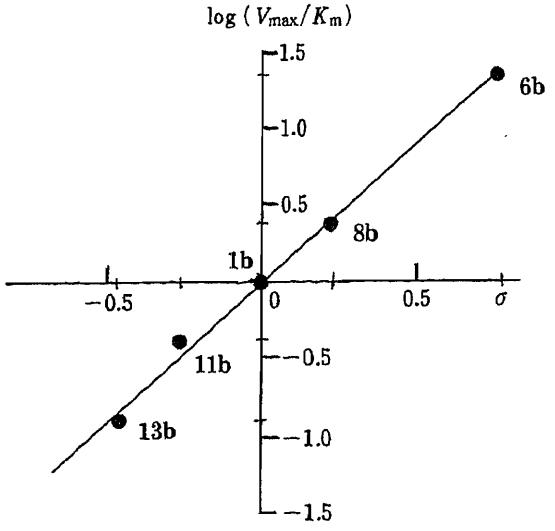

Fig. 3. Relationship between Enzyme Reaction Rate of Benzoylthiocholines and Hammett Constant of the Substituents

1b, benzoylthiocholine; **6b**, *p*-nitrobenzoylthiocholine; **8b**, *p*-chlorobenzoylthiocholine; **11b**, methoxybenzoylthiocholine; **13b**, *p*-hydroxybenzoylthiocholine.

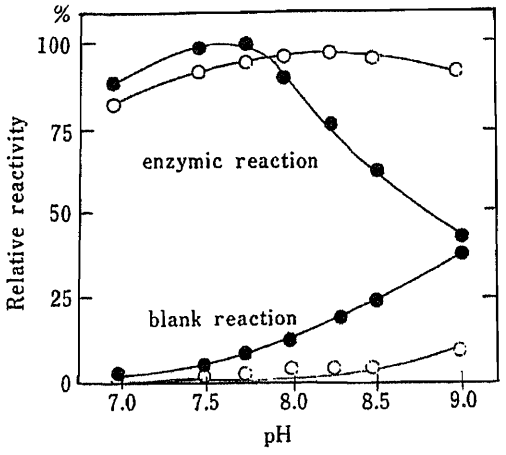

Fig. 4. Relationship between Enzymic and Blank Reaction Activities at Various pH Values

○, 2,3-dimethoxybenzoylthiocholine (**19b**); ●, benzoylthiocholine (**1b**).

TABLE II. Properties of Substituted Benzoylthiocholines as Pseudo-cholinesterase Substrates

No.	Substituents			Solubility for		Self-hydrolysis E/min	Activity E/min
	R^4	R^3	R^2	H_2O	dil. EtOH[a]		
1	H	H	H	Sol.	Sol.	<0.005	>0.05
6	NO_2	H	H	Sol.	Sol.	>0.01	>0.03[b]
7	H	NO_2	H	Insol.	Sol.	>0.06	>0.04
8	Cl	H	H	Insol.	Sol.	>0.02	>0.25
9	H	Cl	H	Insol.	Sol.	>0.04	>0.07
10	H	H	Cl	Sol.	Sol.	>0.03	>0.01
11	MeO	H	H	Insol.	Sol.	<0.005	>0.01
13	HO	H	H	Sol.	Sol.	<0.003	<0.01
14	Me_2N	H	H	Insol.	Sol.	<0.003	<0.02
15	AcNH	H	H	Sol.	Sol.	>0.01	>0.12
18	MeO	H	MeO	Insol.	Sol.	<0.003	>0.03
19	H	MeO	MeO	Sol.	Sol.	<0.003	>0.07
20	MeO	MeO	H	Sol.	Sol.	<0.003	>0.03
Butyroylthiocholine methiodide				Sol.		<0.003	>4.40[c]

a) Water-insoluble reagents were dissolved in a minimum volume of EtOH and diluted with H_2O. *b*) The solution of reagent was diluted 10 times. *c*) The solution of reagent was diluted 100 times.

ring.

Detailed examination of the solubility, enzymic reaction rate, and the blank reaction value of the 21 synthetic substrates also indicated that an effective reagent might be found in the expected group of compounds (Table II). Among the compounds examined, the best one was found to be 2,3-dimethoxybenzoylthiocholine (**19b**) in terms of water solubility, rate of

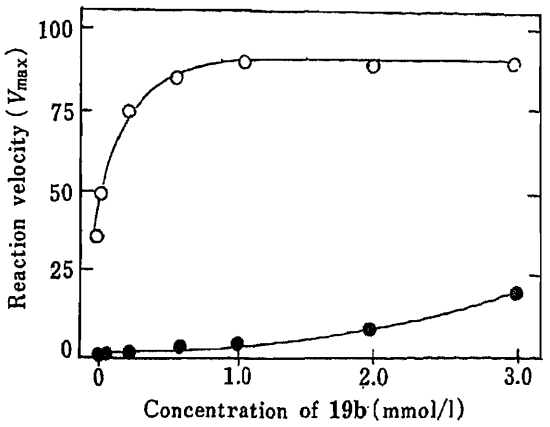

Fig. 5. Influence of Substrate Concentration on the Enzymic and Blank Reaction Velocities

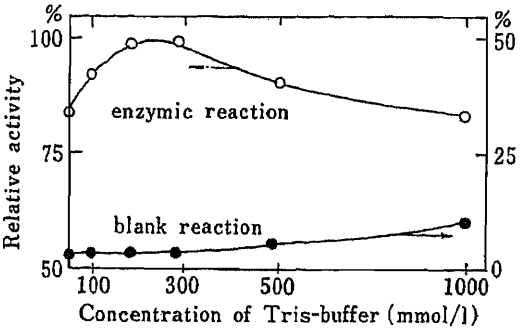

Fig. 6. Influence of the Concentration of Tris-Buffer on the Enzymic and Blank Reactions

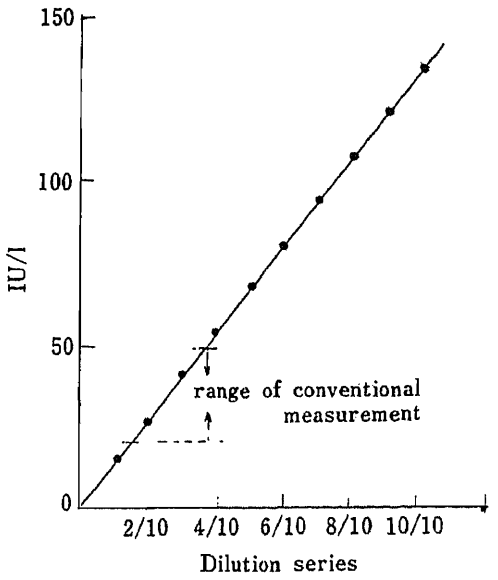

Fig. 7. Calibration Curve for Pseudo-cholinesterase Obtained by Measurement Using **19b** in Tris-Buffer (300 mmol/l)

Reproducibility: C.V. 2% at 12, 48, and 121 IU/l.

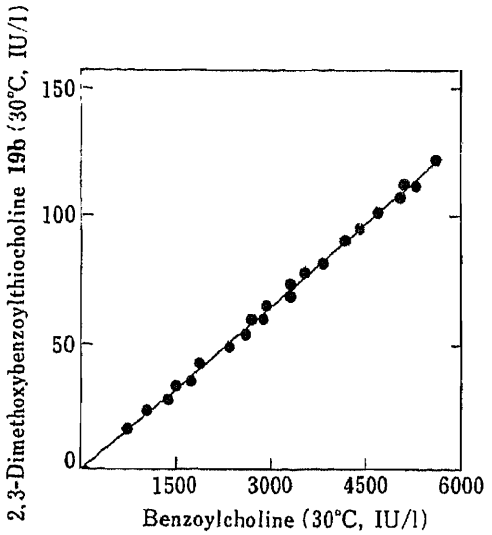

Fig. 8. Correlation of the Results Obtained by the Benzoylcholine Method and the New Method Using 2,3-Dimethoxybenzoylthiocholine

enzymic reaction, and low self-hydrolysis rate (Table II).

The relations between pH and the relative rates of enzymic and self hydrolyses were compared between benzoylthiocholine (**1b**) and compound **19b**. Figure 4 shows that the enzymic reaction rate of **1b** (relative to the maximum rate for **1b**) falls over at above pH 7.5, while the optimum pH for **19b** is 8.25. The self-hydrolysis (blank reaction) of **1b** increased significantly in the higher pH region but that of **19b** was still not more than 10% at pH 9. A disadvantage of conventional thioesters for clinical use is the discrepancy of optimum pH for enzyme action and that for avoiding undesirable side reactions, *e.g.*, self-hydrolysis. This can be overcome by the use of compound **19b**.

In order to determine practical conditions for measurement the effects of the concentrations of the substrate **19b** and Tris on the reaction rate were examined. The results are illustrated in Figs. 5 and 6.

The relation between the reaction velocity of enzymic hydrolysis (V_{max}) and the blank reaction (percentage of hydrolized **19b**) indicates that a suitable concentration of the substrate is 1.0 mmol/l (Fig. 5). The optimum concentration of Tris is 300 mmol/l (Fig. 6).

The linearity of the measurement was then examined under the above conditions and a calibration curve (Fig. 7) was obtained. It shows excellent linearity over a very wide range up to about three times that of the conventional method, and the reproducibility is good (coefficients of variation (C.V.) within 2%).

The relation between our method and the method using benzoylcholine was then checked, and the results were satisfactory as can be seen in Fig. 8.

In view of the above examination and results, 2,3-dimethoxybenzoylthiocholine (**19b**) is concluded to be an excellent reagent for assay of pseudo-cholinesterase in clinical use.[10]

References and Notes

1) H. G. Kunkel, E. H. Ahrens, Jr., *J. Exper. Med.*, **67**, 325 (1947).
2) K. M. Kutty, G. Rowden, and A. R. Cox, *Can. J. Biochem.*, **51**, 883 (1972); M. Cucuianu, A. Opincaru, and D. Tapalag, *Clin. Chim. Acta*, **85**, 73 (1978); M. Cucuianu, D. Zdenghea, M. Pop, and A. Opincaru, *ibid.*, **71**, 49 (1976).
3) H. Shibata, *Liver*, **17**, 755 (1976).
4) K. Uono, *Nippon Rinsho*, **38**, 833 (1980).
5) W. Kalow and K. Genest, *Canad. J. Biochem. Physiol.*, **35**, 316 (1957); E. M. Gal and E. Roth, *Clin. Chim. Acta*, **2**, 316 (1957); R. L. Smith, H. Loewenthal, H. Lehmann, and E. Ryan, *ibid.*, **4**, 384 (1959); K. Gomi and M. Kashiyama, *Rinsho Byori*, **24**, 759 (1976); M. Asai, K. Nakane, Y. Morishita, N. Kageyama, S. Sonoda, T. Aoki, Y. Kato, and I. Takahashi, *Eisei Kensa*, **29**, 1392 (1980).
6) P. J. Garry and J. L. Routh, *Clin. Chim.*, **11**, 91 (1965); G. Sza's, *Clin. Chim. Acta*, **19**, 191 (1968); A. M. Karahasaog'lu and P. T. Oezand, *J. Lab. & Clin. Med.*, **70**, 343 (1967); M. Kenedel and R. Boettger, *Klin. Washr.*, **45**, 325 (1967); A. A. Dietz, H. M. Rubinstein, and T. Lubrano, *Clin. Chim.*, **19**, 1309 (1973).
7) R. R. Renshaw, P. F. Dresbach, M. Ziffand, and D. Green, *J. Am. Chem. Soc.*, **60**, 1765 (1938).
8) Y. Midorikawa, H. Motonaga, and M. Naito, Japan. Patent 57-21352 (1982); Kokai Tokkyo Koho **1982**, 301.
9) G. P. Ellman, *Arch. Biochem. Biophys.*, **82**, 70 (1959).
10) Y. Marui, M. Yamada, N. Kaneda, S. Takemura, and C. Hayashi, Japan. Patent 143689 (1985).

[Chem. Pharm. Bull. 35(4)1497—1502(1987)]

An Enzyme Immunoassay System with a Monoclonal Antibody for the Determination of 11-Deoxycortisol[1)]

HIROSHI HOSODA,[a] SAKIKO TAMURA,[a] REIKO TSUKAMOTO,[a] NORIHIRO KOBAYASHI,[a] JUN-ICHI SAWADA,[b] TADAO TERAO,[b] and TOSHIO NAMBARA*,[a]

Pharmaceutical Institute, Tohoku University,[a] Aobayama, Sendai 980, Japan and National Institute of Hygienic Sciences,[b] 1-18-1, Kamiyoga, Setagaya-ku, Tokyo 158, Japan

(Received September 27, 1986)

An enzyme immunoassay method using a monoclonal antibody for the determination of 11-deoxycortisol is described. The anti-11-deoxycortisol antibody was produced in ascites by inoculating antibody-secreting hybridoma cells into BALB/c mice. The enzyme labeling of 11-deoxycortisol was carried out by the *N*-succinimidyl ester method. The activated esters of three carboxylated steroids were treated with β-galactosidase to give enzyme-labeled antigens. A protein A–double antibody method was employed for separation of the bound and free fractions in the immunoassay. It was found that the monoclonal antibody had a high affinity for a homologous enzyme-labeled antigen prepared from 4-(2-carboxyethylthio)-11-deoxycortisol and the binding was inhibited by the analyte, 11-deoxycortisol. In the heterologous systems using labels prepared from 11-deoxycortisol 3-(*O*-carboxymethyl)oxime and 11-deoxycortisol 21-hemisuccinate, a lower and no significant immunoreactivities were observed, respectively. These results indicate that the antigen-binding site of the monoclonal antibody is complementary to and covers the 11-deoxycortisol portion remote from the position used for attachment to the carrier in the preparation of the immunogen. The homologous assay system showed high sensitivity and specificity comparable to those of the radioimmunoassay using tritium as a tracer. These findings should be helpful in the development of various immunoassay systems with the monoclonal antibody.

Keywords——11-deoxycortisol; monoclonal anti-11-deoxycortisol antibody; enzyme immunoassay; β-galactosidase-labeled 11-deoxycortisol; protein A

The hybridoma technique developed by Köhler and Milstein[2)] has been shown to be useful for the preparation of monoclonal antibodies to steroid hormones.[3)] An important advantage of monoclonal antibodies in clinical-chemical analysis is their availability in unlimited supply as reagents with constant binding properties.

Immunoassays of 11-deoxycortisol in human plasma are useful in the metyrapone test,[4)] an assessment of pituitary-adrenal reserve. We have recently produced a hybridoma clone (S.CET.M8.1.1) secreting an anti-11-deoxycortisol antibody by the fusion of mouse spleen cells with myeloma cells.[5)] The monoclonal antibody (CET-M8) has been shown to be highly specific for 11-deoxycortisol and applicable to the metyrapone test by radioimmunoassay, using tritium as a tracer. It is desirable to develop non-radioisotopic 11-deoxycortisol immunoassay systems having high specificity and sensitivity with the monoclonal antibody. For this purpose, the antibody must first be capable of binding an appropriate labeled antigen, and then the reaction between the antigen and antibody molecules should be efficiently responsive to a minimum amount of the analyte, 11-deoxycortisol. These specifications depend on the specificity or antigen-binding site structure of the antibody and its relative binding affinities to the analyte and labeled antigen. We report here successful results

on enzyme immunoassay procedures with the monoclonal antibody for the determination of 11-deoxycortisol.

Materials and Methods

Materials——β-Galactosidase (EC 3.2.1.23) from *E. coli* (grade VI, 500 units per mg protein) was purchased from Sigma Chemical Co. (U.S.A.); *o*-nitrophenyl β-D-galactopyranoside, from Nakarai Chemicals, Ltd. (Kyoto). Rabbit anti-mouse immunoglobulin G (IgG) antiserum and IgGsorb (a suspension of *Staphylococcus aureus*) were obtained from MBL Co. (Nagoya) and the Enzyme Center Inc. (U.S.A.), respectively. The assay buffer used in the immunoassay was 0.05 M phosphate buffer (pH 7.3) (PB) containing 0.1% gelatin, 0.9% NaCl and 0.1% NaN_3.

Production of Monoclonal Anti-11-deoxycortisol Antibody——A hybridoma clone (S.CET.M8.1.1) secreting an antibody to 11-deoxycortisol was derived from fusion of P3-NS1/1-Ag4-1 myeloma cells with spleen cells of BALB/c mice immunized with 4-(2-carboxyethylthio)-11-deoxycortisol (CET) linked to bovine serum albumin.[5] The cultured hybridoma cells (1.6×10^6/mouse) were injected intraperitoneally into 19 female BALB/c mice that had received pristane (2,6,10,14-tetramethylpentadecane) (0.5 ml) 7 d prior to cell inoculation. The ascites fluid was isolated 10—14 d later. After a check of titer and cross-reactivities with cortisol and related steroids by the radioimmunoassay method,[5] the antibody solutions obtained from 18 mice were combined and stored at −20 °C until use.

Synthesis of Steroid *N*-Succinimidyl Esters——The *N*-succinimidyl esters of CET, 11-deoxycortisol 3-(*O*-carboxymethyl)oxime (CMO),[6] and 11-deoxycortisol 21-hemisuccinate (HS) were prepared by the method described previously.[7] In short; a solution of 1-ethyl-3-(3-dimethylaminopropyl)carbodiimide·HCl (0.14 mmol), *N*-hydroxysuccinimide (0.14 mmol), and CET, CMO or HS (0.1 mmol) in 95% dioxane (0.5 ml) was stirred at room temperature for 2 h. The resulting solution was diluted with AcOEt, washed with H_2O, dried over anhydrous Na_2SO_4, and passed through an Al_2O_3 layer. The filtrate was evaporated down, yielding the activated ester as colorless crystals.

Preparation of β-Galactosidase-Labeled Antigen——Dioxane solutions (0.1 ml) containing calculated amounts of the 11-deoxycortisol *N*-succinimidyl ester corresponding to steroid/enzyme molar ratios of 5, 10, 15, 20, 30 and 60 (M_r of β-galactosidase, 540000)[8] were each added to a solution of β-galactosidase (1 mg) in PB (0.2 ml) at 0 °C, and the mixture was gently stirred at 4 °C for 4 h. After dialysis against cold PB (2 l) for 2 d, the resulting solutions were stored at 4 °C at a concentration of 500 μg/ml, adjusted with the assay buffer.

Immunoreactivity——The enzyme immunoassay procedure was carried out in duplicate or triplicate in glass test tubes (10 ml) as follows: β-galactosidase-labeled 11-deoxycortisol (100 ng) in the assay buffer (0.2 ml) was added to the monoclonal antibody CET-M8 (0.1 ml) diluted 1 : 5000 or more, and the mixture was incubated at 4 °C for 16 h. Rabbit anti-mouse IgG antiserum (0.1 ml) diluted 1 : 500 or more and 5% IgGsorb (0.1 ml) in the assay buffer were added to the incubation mixture, and the suspension was vortex-mixed, then allowed to stand at 4 °C for 2 h. After addition of the assay buffer (1.5 ml), the resulting solution was centrifuged at 3000 rpm for 20 min, and the supernatant was removed by aspiration. The precipitate was washed once with the assay buffer (1.5 ml) and used for measurement of the enzymic activity. At the same time, the procedure without addition of the first antibody CET-M8 was carried out to provide a blank value. An experiment using only the enzyme-labeled steroid was also carried out to obtain 100% enzymic activity.

Dose–Response Curve for 11-Deoxycortisol Enzyme Immunoassay——The β-galactosidase-labeled CET prepared at a molar ratio of 10 was used. The antibody CET-M8 (0.1 ml) diluted 1 : 100000 and label CET (100 ng) in the assay buffer (0.1 ml) were added to a series of standard solutions (0, 10, 20, 50, 100, 200 and 500 pg of 11-deoxycortisol) in the assay buffer (0.1 ml), and the mixture was incubated at 4 °C for 16 h. Separation of bound and free fractions was carried out just as described above, using a 1 : 500 dilution of the second antibody. Cross-reaction studies were also done by a method similar to that described previously.[5]

Measurement of β-Galactosidase Activity——The precipitate obtained above was diluted with the assay buffer (1 ml) containing 0.2% $MgCl_2$ and 0.7% 2-mercaptoethanol, vortex-mixed, and preincubated at 37 °C for 3 min. *o*-Nitrophenyl β-D-galactopyranoside (0.06%, 1 ml) in the assay buffer was added to the resulting solution, and the mixture was incubated for 40—60 min. The reaction was terminated by addition of 1 M Na_2CO_3 (2 ml), and the

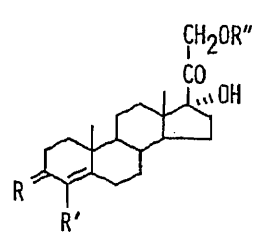

11-deoxycortisol: R=O, R′=R″=H
CET: R=O, R′=S(CH$_2$)$_2$COOH, R″=H
CMO: R=NOCH$_2$COOH, R′=R″=H
HS: R=O, R′=H, R″=CO(CH$_2$)$_2$COOH

Chart 1

resulting mixture was centrifuged at 3000 rpm for 30 min. The absorbance of *o*-nitrophenol released in the supernatant was measured at 420 nm. For the determination of 100% enzymic activity as described above, the same procedure was applied to the enzyme solution, and the reaction was terminated after a 20-min incubation; the absorbance obtained was corrected for the incubation time.

Results and Discussion

The monoclonal hybridoma, S.CET.M8.1.1, secreting an IgG_1 with kappa light chains used in this work was that derived from fusion of P3-NS1/1-Ag4-1 myeloma cells with spleen cells of BALB/c mice immunized with CET linked to bovine serum albumin.[5] The monoclonal antibody CET-M8 was produced in ascites by inoculating the hybrid cells i.p. into pristane-treated BALB/c mice. Three steroid derivatives were employed for enzyme labeling: the homologous CET and typical heterologous haptenic compounds, CMO and HS. The *N*-succinimidyl esters prepared from these carboxylated steroids by condensation with *N*-hydroxysuccinimide in the presence of a water-soluble carbodiimide were each reacted with *β*-galactosidase to give enzyme-labeled antigens (labels CET, CMO, and HS). The enzyme labeling was carried out by mixing the activated ester with the enzyme in phosphate buffer (pH 7.3)–dioxane.[9] The activated ester should react readily with free amino groups of this enzyme. Various molar ratios of the steroid to enzyme, ranging from 5 to 60, were used, since the molar ratio influences the immunoreactivity of the resulting labels and the enzyme immunoassay sensitivity.[9,10] The reaction mixtures were dialyzed against the buffer to remove the unreacted steroid. No significant loss of enzymic activity occurred under the coupling conditions used. *β*-Galactosidase activity was measured colorimetrically with *o*-nitrophenyl *β*-D-galactopyranoside as a substrate.

In enzyme immunoassay, a protein A–double antibody method was investigated for separation of bound and free enzyme-labeled antigens, using the label CET prepared at a molar ratio of 10. Protein A, a bacterial cell wall protein, has recently been used as a tool for binding and detection of antibodies. Its binding ability depends on immunoglobulin classes

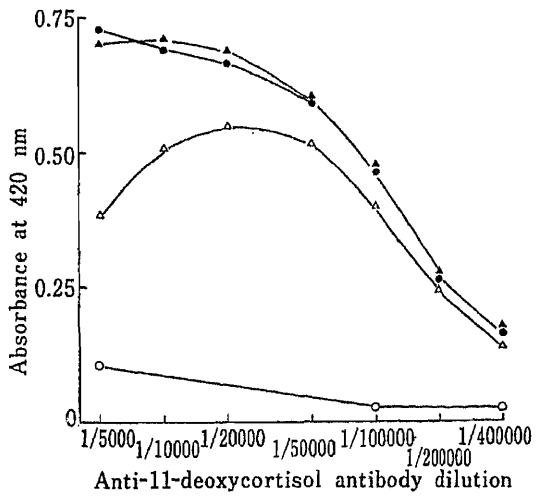

Fig. 1. Enzyme Activities of Bound Fraction in the Protein A Method with and without (○) Rabbit Anti-mouse IgG Antiserum

The *β*-galactosidase-labeled CET prepared at a molar ratio of 10 was used; dilutions of the second antibody were 1:500 (●), 1:1000 (▲), and 1:5000 (△). The absorbance values were obtained after a 1 h enzyme reaction.

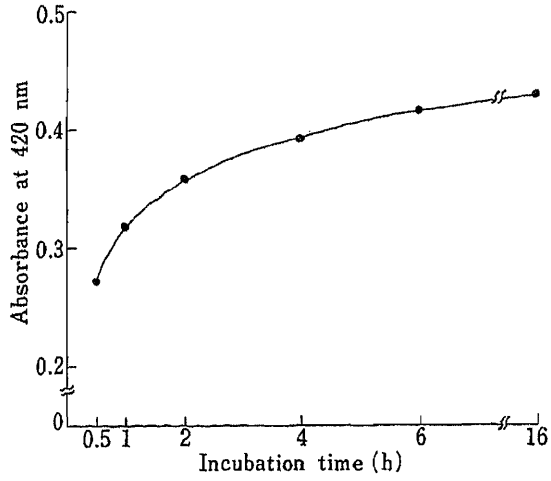

Fig. 2. Time Course of Reaction between the Labeled Antigen CET and the Antibody CET-M8 in the Protein A–Double Antibody Method

The dilutions of the antibody CET-M8 and the second antibody used were 1:100000 and 1:1000, respectively.

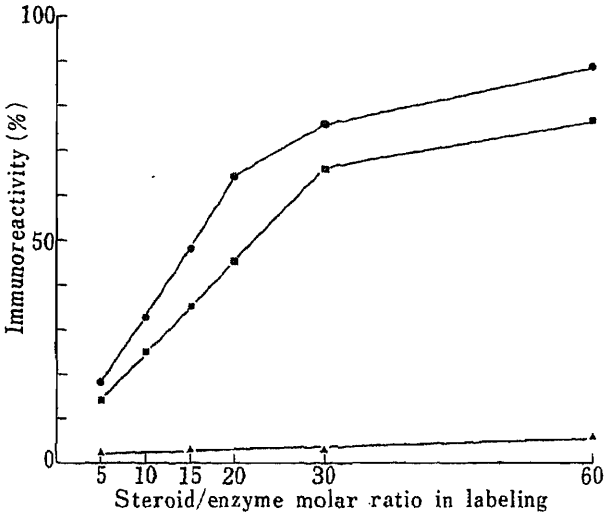

Fig. 3. Reactivities of Labels CET (●), CMO (■), and HS (▲) with the Antibody CET-M8

The dilutions of the antibody CET-M8 and the second antibody used were 1 : 10000 and 1 : 500, respectively.

and a low reactivity with mouse IgG_1 has been reported.[11] This was also the case in the present monoclonal antibody, and hence, we employed rabbit anti-mouse IgG antibody as a binding agent in combination with the protein A reagent, IgGsorb. Enzyme activities of bound fraction in the presence and absence of the second antibody are shown in Fig. 1. A typical zone phenomenon can be seen with a 1 : 5000 dilution of the rabbit antibody. Satisfactory reactivities were obtained at 1 : 500 and 1 : 1000 dilutions of the second antibody, showing that the appropriate dilution of the first antibody CET-M8 for use in 11-deoxycortisol assay is *ca.* 1 : 100000. A time course of reaction of the labeled antigen with the antibody CET-M8 is shown in Fig. 2. The results demonstrated that the reaction was relatively rapid and reaction times of over 4 h gave satisfactory absorbances under the conditions used.

The reactivities of a fixed amount of labels CET, CMO, and HS with the antibody CET-M8 were then compared, and the results are shown in Fig. 3. In the homologous assay system using label CET, the immunoreactivity increased with increasing molar ratio and satisfactory binding abilities were obtained with molar ratios higher than 10. A lower reactivity was observed in the case of label CMO. On the other hand, the monoclonal antibody did not significantly bind label HS even when the label prepared at a molar ratio of 60 (the degree of hapten substitution was *ca.* 12) was used; a similar result was also obtained with an assay system using horseradish peroxidase as a label (M_r of this enzyme is *ca.* one-fourteenth of that of β-galactosidase). These results, together with the previous radioimmunoassay cross-reaction studies,[5] indicate that the monoclonal antibody CET-M8 recognizes the functional groups at C-11 and C-21 in 11-deoxycortisol and, to a lesser extent, the functional groups near the C-4 position. In other words, the antigen-binding site of the antibody is complementary to and covers the steroid portion remote from the position used for attachment to the carrier in the preparation of the immunogen. Similar features of specificity have mostly been obtained, in radioimmunoassay methods, with the monoclonal anti-steroid antibodies prepared hitherto. This seems to be rather reasonable, since the binding of the hapten portion of a haptenized immunogen with steroid-specific surface receptors of B lymphocytes, which must be influenced by the steric interaction between the receptor and the carrier portion of the immunogen, is essential in the antibody production according to the clonal selection theory.[12] However, it should be mentioned that an exception has been reported in the specificity of monoclonal antibodies to progesterone.[13]

A typical dose–response curve obtained with the homologous assay system employing a 1 : 100000 dilution of the antibody CET-M8 and the label CET prepared at a molar ratio of 10

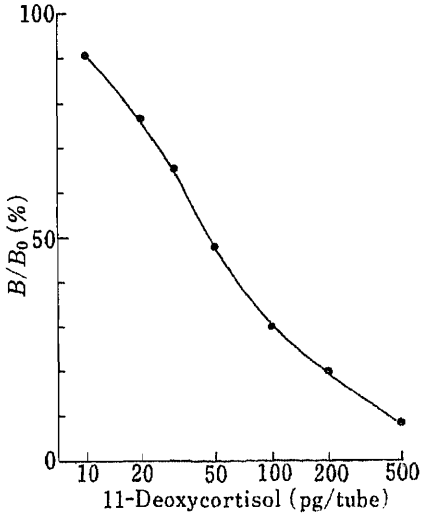

Fig. 4. A Dose-Response Curve for 11-Deoxycortisol Enzyme Immunoassay Using Label CET

TABLE I. Cross-Reactivity of the CET-M8 Antibody with Various Related Steroids in the Enzyme Immunoassay

Steroid	% cross-reaction (50%)
11-Deoxycortisol	100
Cortisol	0.3
Cortisone	0.4
Corticosterone	0.03
11-Deoxycorticosterone	7
17α-Hydroxyprogesterone	8
Progesterone	0.3
21-Deoxycortisol	0.01

is shown in Fig. 4: the amount of 11-deoxycortisol needed to displace 50% of the bound label was 47 pg. The sensitivity of the assay is comparable to that of the radioimmunoassay,[5] showing that this antibody has weak, if any, binding affinity for the bridge portion between the enzyme and steroid in the homologous label CET. The specificity of the assay system was satisfactory, when examined by cross-reaction studies with related steroids, including cortisol and cortisone (Table I).

Thus, the present findings suggest that the monoclonal antibody may be useful in the development of practical enzyme immunoassays for plasma 11-deoxycortisol. Little information has been available concerning methods for separating free and bound fractions in steroid enzyme immunoassay procedures with monoclonal antibodies. In this work, a protein A–double antibody method was employed. When applied to the assay system using horseradish peroxidase-labeled antigens, however, the separation method did not give satisfactory results owing to loss of enzyme activity (data not shown). Development of other immunoassay systems using ^{125}I-radioligands or fluorescent and chemiluminescent labels should be possible, if the C-4 position of the steroid molecule is employed as a labeling site; the use of the C-3 position also seems to be worthy of examination. X-Ray crystallographic studies of the antibody molecule or its Fab fragment may lead to further insights into the antigen-binding site and specificity. Application of the present assay system to the metyrapone test on patients with Cushing's syndrome are being conducted.

Acknowledgement This work was supported in part by grants from the Ministry of Education, Science and Culture, and from the Science and Technology Agency of Japan.

References and Notes

1) A part of this work was reported as a communication: H. Hosoda, S. Tamura, N. Kobayashi, T. Nambara, J. Sawada, and T. Terao, *Chem. Pharm. Bull.*, **33**, 448 (1985).
2) G. Köhler and C. Milstein, *Nature* (London), **256**, 495 (1975).
3) V. E. Fantl, D. Y. Wang, and A. S. Whitehead, *J. Steroid Biochem.*, **14**, 405 (1981); Z. Eshhar, J. B. Kim, G. Barnard, W. P. Collins, S. Gilad, H. R. Lindner, and F. Kohen, *Steroids*, **38**, 89 (1981).
4) G. W. Liddle, H. L. Estep, J. W. Kendall, Jr., W. C. Williams, Jr., and A. W. Townes, *J. Clin. Endocrinol. Metab.*, **19**, 875 (1959).

5) H. Hosoda, N. Kobayashi, S. Tamura, M. Mitsuma, J. Sawada, T. Terao, and T. Nambara, *Chem. Pharm. Bull.*, **34**, 2914 (1986).
6) A. Tsuji, M. Smulowtiz, J. S. C. Liang, and D. K. Fukushima, *Steroids*, **24**, 739 (1974).
7) H. Hosoda, Y. Sakai, H. Yoshida, S. Miyairi, K. Ishii, and T. Nambara, *Chem. Pharm. Bull.*, **27**, 742 (1979).
8) G. R. Craven, E. Steers, Jr., and C. B. Anfinsen, *J. Biol. Chem.*, **240**, 2468 (1965).
9) H. Hosoda, Y. Sakai, H. Yoshida, and T. Nambara, *Chem. Pharm. Bull.*, **27**, 2147 (1979).
10) H. Hosoda, T. Karube, N. Kobayashi, and T. Nambara, *Chem. Pharm. Bull.*, **33**, 249 (1985).
11) G. Kronvall, H. M. Grey, and R. C. Williams, *J. Immunol.*, **105**, 1116 (1970); J. J. Langone, *J. Immunol. Methods*, **24**, 269 (1978).
12) L. E. Hood, I. L. Weissman, W. B. Wood, and J. H. Wilson, "Immunology," the Benjamin/Cummings Publishing Company, California, 1984, p. 9.
13) V. E. Fantl, D. Y. Wang, and R. E. Knyba, *J. Steroid Biochem.*, **17**, 125 (1982).

[Chem. Pharm. Bull. 35(4)1503—1508(1987)]

Separation of Unsaturated Chondroitin Sulfate Disaccharides in Thin-Layer Chromatography on Silica Gel and Their Quantitative Determination by Densitometry

EIJI SHIMADA,* NAOKO KUDOH, MITSUGU TOMIOKA, and GO MATSUMURA

School of Pharmaceutical Sciences, Showa University, Hatanodai 1-5-8, Shinagawa-ku, Tokyo 142, Japan

(Received October 20, 1986)

A simple and rapid method has been developed to determine the relative amounts of 4- and 6-sulfate in chondroitin sulfate or proteoglycan preparations. Unsaturated disaccharide products derived from the samples by chondroitinase ABC digestion in 0.01 M Tris–HCl buffer (pH 8.0) were applied to a silica gel-coated thin-layer chromatographic plate and separated in a solvent system of *n*-propanol–isopropanol–*n*-butanol–water (55:20:5:20, v/v) containing 0.04 M NaCl and 0.01 M ammonia without a desalting step, which was necessary in paper chromatography or thin-layer chromatography on cellulose. The developing time was as short as 2—2.5 h at room temperature. After staining of the separated products with a carbazole reagent followed by immersing the plate in liquid paraffin, the ratio of monosulfated disaccharides, generally found as major components in chondroitin sulfate chains, was estimated by densitometry.

Keywords——unsaturated chondroitin sulfate disaccharide; chondroitin sulfate; proteoglycan; TLC; densitometry

For the separation of disaccharides with a 4,5-unsaturated uronosyl residue at their nonreducing ends (2-acetamido-2-deoxy-3-*O*-(β-D-gluco-4-enepyranosyluronic acid)-D-galactose (ΔDi-0S), 2-acetamido-2-deoxy-3-*O*-(β-D-gluco-4-enepyranosyluronic acid)-4-*O*-sulfo-D-galactose (ΔDi-4S), and 2-acetamido-2-deoxy-3-*O*-(β-D-gluco-4-enepyranosyluronic acid)-6-*O*-sulfo-D-galactose (ΔDi-6S)) in the digests of chondroitin sulfates by chondroitinase ABC or AC, thin-layer chromatography (TLC) on cellulose plates has been adapted by many workers[1-3] with the same solvents as those used in paper chromatography.[4] These chromatographic techniques require a prior developing step for desalting before separation. Wasserman *et al.*[1] found that the total developing time, about 36 h, in the above paper chromatography could be shortened to 12 h in TLC on cellulose. As reported previously,[5] we separated hyaluronate oligosaccharides by TLC on a silica gel plate of Kieselgel 60 (Merck & Co.). We attempted to use this plate for the resolution of unsaturated disaccharides derived from chondroitin sulfates and found a suitable solvent system after a series of trials. For the chondroitinase digest of glycosaminoglycans obtained in enriched Tris–HCl buffer,[4] a desalting step was desirable for satisfactory resolution even on silica gel plates. No suitable solvent system for one-step development was found. However, the digestion in a low concentration of Tris–HCl buffer alone instead of the enriched buffer permitted a satisfactory separation of disaccharide products without a desalting process. This finding resulted in a considerable reduction of the developing time necessary to characterize these products. The separated disaccharides were visualized as blue spots by carbazole staining and their relative amounts were estimated by densitometric scanning.

In this paper, we report the application of TLC on silica gel for the separation of unsaturated chondroitin sulfate disaccharides and discuss their quantitative analysis by

densitometry.

Experimental

Materials——Standard unsaturated disaccharides (⊿Di-0S, ⊿Di-4S, and ⊿Di-6S), chondroitin, chondroitin 4-sulfate (ChS-A), chondroitin 6-sulfate (ChS-C), and chondroitinase ABC (EC 4.2.2.5) were obtained from Seikagaku Kogyo Co. (Tokyo, Japan). Samples of proteoglycan (D1 fraction) were prepared from osteoarthritic human femoral head cartilage by the known method.[6] The femoral heads obtained by clinical surgery were kindly supplied by Prof. Y. Kuroki (Fujigaoka Hospital, Showa University). Another unsaturated disaccharide, 2-acetamido-2-deoxy-3-*O*-(β-D-gluco-4-enepyranosyluronic acid)-D-glucose (⊿Di-HA) was prepared by chondroitinase ABC digestion of hyaluronate tetrasaccharide having unsaturated glucuronic acid at the nonreducing end.[5]

Digestion of Glycosaminoglycans and Proteoglycans with Chondroitinase ABC——A mixture of chondroitin, ChS-A, and ChS-C (100 μg of each glycosaminoglycan) was digested with 0.2 unit of chondroitinase ABC in 50 μl of enriched Tris buffer (0.05 M Tris, 0.06 M sodium acetate, 0.05 M sodium chloride, and 0.1 mg of bovine serum albumin per ml), pH 8.0,[4] for 16 h at 37 °C. This digest is herein called ET-100. Alternatively, the glycosaminoglycan mixture (20 μg each) was treated in the same manner, except that the digestion was done in 0.01 M Tris-HCl buffer, pH 8.0. This digest is herein called T-20. Judging from the absorbance at 549 nm after application of the periodate-thiobarbituric acid method for unsaturated disaccharides,[7] each glycosaminoglycan was quantitatively degraded in 0.01 M Tris alone at the enzyme level mentioned above.

Proteoglycan samples (a-, b-, and c-D1), each about 30 μg as uronic acid, from three femoral head cartilages were separately digested with chondroitinase ABC in 0.01 M Tris-HCl buffer under the same conditions as described for T-20. Uronic acid was measured by the method of Bitter and Muir,[8] using glucuronolactone as a standard.

TLC——Aqueous solutions containing standard disaccharides (⊿Di-0S, -4S, and -6S) and each digestion mixture (T-20, ET-100, *etc.*) were applied to a plate (5 × 12 cm) of Kieselgel 60 (plastic plate, 0.2 mm thickness, Merck & Co.) with a microsyringe or glass capillary tubes. Although chromatoplates were usually employed without prior activation, it should be noted that, in the rainy season in Japan, these plates after sample application had to be kept in a desiccator over P_2O_5 at least overnight to achieve a reproducible separation. After saturation of a closed cylindrical chamber (9 cm diameter) with 25 ml of solvent for 1 h, the plate was placed in the chamber and allowed to develop until the solvent front reached about 10 cm above the origin, then it was air-dried.

Standard disaccharides and degradation products were detected by spraying the plate with 10% H_2SO_4 in ethanol containing 0.125% carbazole and heating it for a few minutes at 100 °C; these oligosaccharides appeared as purple spots during the heating at 100 °C against a pink background and, on cooling to room temperature, they rapidly became dark blue against a pale-blue background. The staining reagent containing carbazole, with which about 0.2 μg (as disaccharide) was detectable, was more sensitive than 10% H_2SO_4 in ethanol. When silica gel plates are employed in TLC, the carbazole reagent is useful to visualize uronic acid itself or oligosaccharides having it as a major component.

Determination of Unsaturated Disaccharides by Densitometry——A silica gel plate, on which migrating disaccharides had been visualized by carbazole staining, was immersed in liquid paraffin for about 30 min. After removal of excess paraffin on the gel surface, the plate was scanned on a Fuji-Riken FD-AIV densitometer at a chart speed of 12.5 mm/min using a 600 nm filter and a 0.2 × 3 mm slit. Peak areas corresponding to disaccharide products were measured by weighing. The composition of different disaccharides in a sample determined by densitometry was compared with that found by high-performance liquid chromatography (HPLC).

A UVIDEC-100-II HPLC system (Japan Spectroscopic Co.) equipped with a UV spectrophotometer was employed. Separation was achieved by use of a 250 × 4.6 mm Fine SIL NH_2 column (Japan Spectroscopic Co.), which was eluted with 0.01 M Na_2SO_4 containing 0.005 M sodium acetate, pH 5.0. Peak areas of absorbance at 232 nm were measured by weighing the chart peaks.

Results and Discussion

Developing Solvents

Using standard disaccharides (⊿Di-0S, -4S, and -6S) as samples, two solvent systems, isopropanol–water (80 : 20, v/v) and *n*-propanol–water (80 : 20, v/v) each containing NaCl at a final concentration of 0.05 M, were examined. In both systems, the mobilities of ⊿Di-0S, -6S, and -4S increased in this order. The isopropanol system was effective to separate ⊿Di-4S and -6S, while the *n*-propanol system showed good separation of ⊿Di-0S from ⊿Di-6S. Therefore, the standard mixture was developed with ternary solvent systems in which the total concentration of alcohols was fixed at 80% by volume. The results are shown in Fig. 1. A small amount of NaCl (0.05 M final concentration) in the solvents was essential to resolve

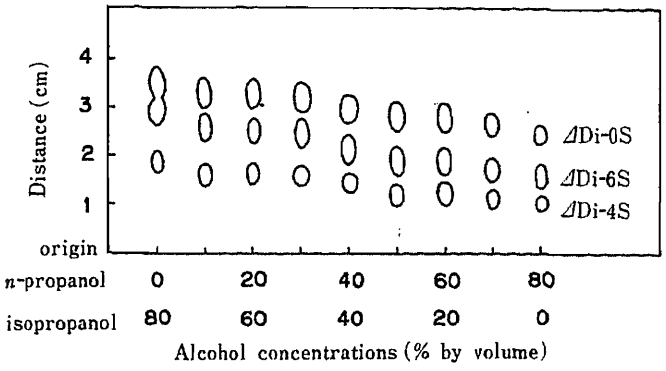

Fig. 1. Tracing of Thin-Layer Chromatograms of Standard Disaccharides Obtained with Various Proportions of *n*-Propanol and Isopropanol

A mixture of ΔDi-0S, -4S, and -6S was developed with propanols–water (80:20, v/v) containing 0.05 M NaCl, until the solvent front reached 9.8—10.2 cm above the origin at 20—22 °C.

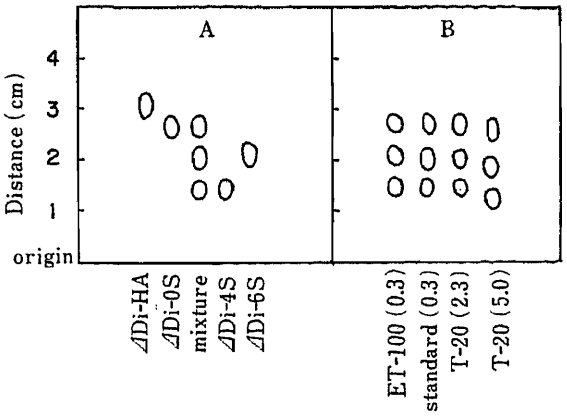

Fig. 2. Tracing of Thin-Layer Chromatograms of ΔDi-HA and Standard Disaccharides (A), and Digestion Products of a Glycosaminoglycan Mixture (Chondroitin, ChS-A, and ChS-C) with Chondroitinase ABC in 0.01 M or Enriched Tris Buffer (B)

Samples in the figure were developed for about 2 h at 24 °C. In Fig. 2B, volumes (μl) applied on the plate are given in parentheses. Standard, an aqueous solution containing standard disaccharides (2 mg each/ml); ET-100 and T-20, see Experimental.

these acidic oligosaccharides, as discussed in a previous paper.[5] Appropriate proportions of the alcohols seemed to be in the range of 1:3 to 3:1 by volume. Addition of small amounts of *n*-butanol and ammonia was effective to give round spots, though they slightly changed the mobilities of samples. Thus we established a suitable solvent system consisting of *n*-propanol–isopropanol–*n*-butanol–water (55:20:5:20, v/v) containing 0.04 M NaCl and 0.01 M ammonia as final concentrations. Figure 2A shows thin-layer chromatograms of individual disaccharides and a mixture of standard disaccharides. *Rf* values for ΔDi-0S, -6S, and -4S were 0.27, 0.20, and 0.13, respectively. ΔDi-HA (*Rf*=0.31) moved faster than ΔDi-0S, but they were not separated satisfactorily in this solvent system.

Separation of Digestion Products

Figure 2B illustrates thin-layer chromatograms of the digestion products from a mixture of chondroitin and chondroitin sulfates in two buffer systems (T-20 and ET-100). As can be seen in the figure, 2.3 μl of T-20 permitted the identification of these products but an excess volume (5 μl) of the solution depressed their mobilities. An experiment with ET-100 (Fig. 2B) showed that *Rf* values of products agreed well with those of the standards only when a very small amount (<0.5 μl) of the digestion mixture was applied to the plate. *Rf* values gradually decreased with increasing volume above 0.5 μl.

TLC of a mixture of chondroitinase ABC and standard disaccharides indicated that as much as 3 μl of the enzyme solution (0.2 units/50 μl H_2O) applied had no influence on the mobilities of standards; the enzyme was found to remain at the origin by staining with Ponceau 3R (0.8% in 6% trichloroacetic acid) followed by washing with 3% acetic acid (data not shown).

These observations suggest that the retardation of products (T-20(5.0) in Fig. 2B) is caused by large amounts of tris(hydroxymethyl)aminomethane applied to the plate.

Quantitative Determination of Unsaturated Disaccharides by Densitometry

Figure 3 illustrates a plot of the quantity of a standard disaccharide applied to a TLC plate against its peak area obtained by densitometry. These areas (expressed as their relative weights to that of 2.0 μg of ΔDi-0S) were proportional to the concentration of each disaccharide type in the range (0.4—2.0 μg) examined, though overlapping between ΔDi-6S and -0S was observed above 1.2 μg. At the same content of each standard, the peak areas (mean$\pm$S.D.) of ΔDi-4S and -6S based on the area of ΔDi-0S were 77$\pm$2% and 85$\pm$3%, respectively. These ratios (0.77 for ΔDi-4S, 0.85 for ΔDi-6S, and 1.00 for ΔDi-0S) were used to calculate the proportions of different components in chondroitin sulfate chains; peak areas of disaccharide products to be analyzed were divided by the corresponding ratios and expressed as relative values to the sum of them.

To quantify the disaccharide types in glycosaminoglycans (chondroitin, ChS-A, and ChS-C) and proteoglycans (a-, b-, and c-D1), aliquots (2 or 3 μl) of chondroitinase ABC digests of these samples were applied to TLC plates and developed in the solvent system described before. Thin-layer chromatograms (2 μl application) of degradation products derived from commercial glycosaminoglycans are shown in Fig. 4. Their densitograms (not

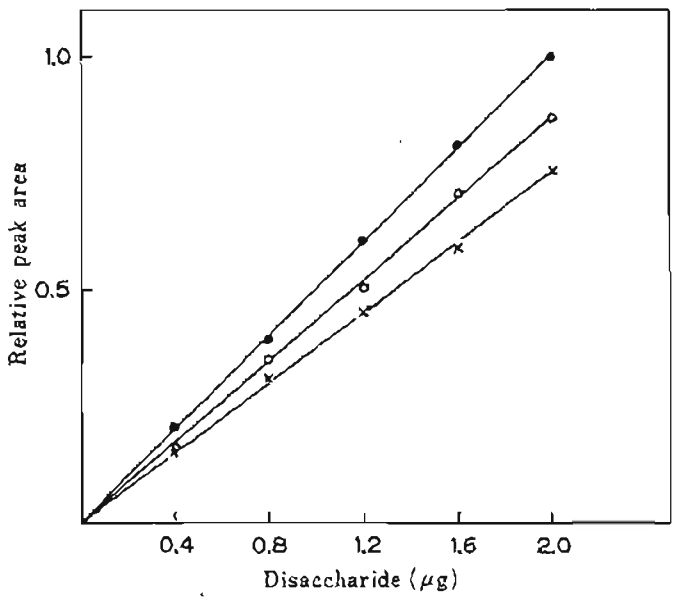

Fig. 3. Relations between Amounts of Standard Unsaturated Disaccharides and Their Peak Areas Obtained by Densitometry

Various amounts of a mixture of standard ΔDi-0S, -4S, and -6S (2 mg each/ml) were spotted on a silica gel plate.

After separation followed by carbazole staining and then immersing the plate in liquid paraffin, the absorbance of disaccharide spots at 600 nm was measured by densitometric scanning. The weights of peak areas were expressed on the basis of that of ΔDi-0S corresponding to a 2.0 μg application.

●—●, ΔDi-0S; ○—○, ΔDi-6S; × —×, ΔDi-4S.

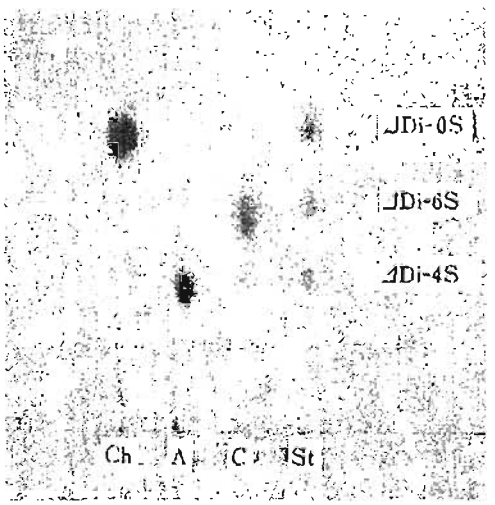

Fig. 4. Thin-Layer Chromatograms of Digestion Products of Each Commercial Glycosaminoglycan

Ch, A, and C mean chondroitin, ChS-A, and ChS-C, respectively. Each polysaccharide (100 μg) was digested in 0.01 M Tris–HCl, pH 8.0 (50 μl) with chondroitinase ABC (0.2 units) for 16 h at 37 °C and an aliquot (2 μl) of the reaction mixture was applied to the plate. St means an aqueous solution containing standards (2 mg each/ml); an aliquot of 0.6 μl was applied. Development time was 2.5 h at 24 °C. This photograph was taken after immersing the plate in liquid paraffin for 30 min.

shown) did not show the presence of ⊿Di-0S in the chondroitin sulfates. Three D1 preparations behaved like ChS-C. A densitogram of a-D1 (2 μl application) as a representative pattern among proteoglycan samples is given in Fig. 5C. As can be seen in the figure, ⊿Di-0S was not detected. Since the nonsulfated disaccharide was always found by HPLC, the volume to be applied to the TLC plate was increased to 3 μl. The resulting densitograms of disaccharide products of ChS-A and a-D1 are shown in Figs. 5A and B, respectively. A small and broad peak (or shoulder) of ⊿Di-0S was revealed in both samples. This minor component was also found in ChS-C, b-D1, and c-D1. In the application of 3 μl, the products were not

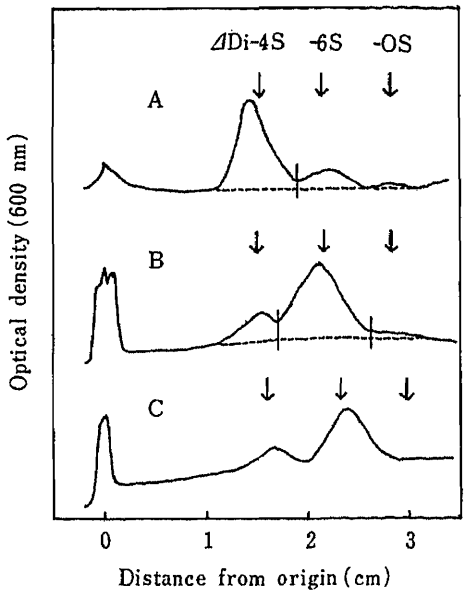

Fig. 5. Densitograms of Unsaturated Disaccharides Liberated from ChS-A and a Proteoglycan Preparation (a-D1) by Chondroitinase ABC Digestion

The optical density adjustment of a densitometer was set at 3. Arrows indicate the locations of markers in separate experiments. Scans of plate sites with no sample application are indicated as blank absorbances in A and B by dotted curves, respectively. A, 3 μl application of the digestion mixture of ChS-A; B and C, 3 and 2 μl applications of the digestion mixture of a-D1, respectively.

TABLE I. Disaccharide Composition of Glycosaminoglycan and Proteoglycan Samples

Samples	Aliquot applied (μl)	Proportion (%)			4S/6S or 6S/4S	
		⊿Di-4S	⊿Di-6S	⊿Di-0S		
Chondroitin	2	12	4	83		
	3	10	5	85		
		(12)	(4)	(84)		
ChS-A	2	82	18	n.d.		0.22
	3	82	15	3		0.18
		(81)	(17)	(2)		(0.21)
ChS-C	2	20	81	n.d.	0.25	
	3	19	78	3	0.24	
		(18)	(79)	(3)	(0.23)	
a-D1	2	19	81	n.d.	0.23	
	3	18	77	5	0.23	
		(18)	(75)	(7)	(0.24)	
b-D1	2	14	86	n.d.	0.16	
	3	15	81	4	0.19	
		(12)	(83)	(5)	(0.14)	
c-D1	2	16	84	n.d.	0.19	
	3	17	79	3	0.22	
		(16)	(80)	(4)	(0.20)	

HPLC data are shown in parentheses. n.d.: not detected.

well resolved, as can be seen in Figs. 5A and B, and so a scan of a plate site with no sample application was necessary for the correction of peak areas. In the application of 2 μl (Fig. 5C), the ΔDi-4S and -6S peaks appeared to be separated to the baseline at the sacrifice of a minor component, ΔDi-0S. In this case, peak areas were determined on the assumption that the baseline was straight in the region of the peaks. Relatively large peaks at the origins of a-D1 (Figs. 5B and C) would be due to chondroitinase ABC itself and materials not degraded by the enzyme.

Table I summarizes the proportion of disaccharide types in glycosaminoglycan and proteoglycan samples. The values obtained by TLC with 3 μl application were comparable with those by HPLC. An applied volume of 2 μl was insufficient to detect a minor component such as ΔDi-0S, whose content was less than about 5%, but sufficient to estimate the ratios of ΔDi-4S and -6S in the chondroitin sulfate isomers examined.

TLC on silica gel for the separation of disaccharide components of chondroitin sulfates is faster than TLC on cellulose and the quantitative analysis by densitometry was convenient to estimate the proportions of ΔDi-4S and -6S. Although the present method is not as sensitive as the recent HPLC methods,[9,10] it provides a simple means for preliminary examination of uncharacterized chondroitin sulfates.

References

1) L. Wasserman, A. Ber, and D. Allalouf, *J. Chromatogr.*, **136**, 342 (1977).
2) Y. Mikuni-Takagaki and B. P. Toole, *J. Biol. Chem.*, **254**, 8409 (1979).
3) A-M. Säämänen and M. Tammi, *Anal. Biochem.*, **140**, 354 (1984).
4) H. Saito, T. Yamagata, and S. Suzuki, *J. Biol. Chem.*, **243**, 1536 (1968).
5) E. Shimada and G. Matsumura, *J. Biochem.* (Tokyo), **96**, 721 (1984).
6) V. C. Hascall and S. W. Sajdera, *J. Biol. Chem.*, **244**, 2384 (1969).
7) M. Koseki, A. Kimura, and K. Tsurumi, *J. Biochem.* (Tokyo), **83**, 553 (1978).
8) T. Bitter and H. Muir, *Anal. Biochem.*, **4**, 330 (1962).
9) A. Hjerpe, C. A. Antonopoulas, and B. Engfeldt, *J. Chromatogr.*, **171**, 339 (1979).
10) D. P. Norby, V. M. Goldberg, R. V. Moscovitz, and C. J. Malemud, *Anal. Biochem.*, **131**, 324 (1983).

[Chem. Pharm. Bull. 35(4)1509—1514(1987)]

The Mechanisms of Delayed Insecticidal Action of Streptothricin Antibiotics. III. The Mode of Delayed Insecticidal Action of Racemomycin-A

YOSHIHIKO INAMORI,* MAYURI KUBO and HIROSHI TSUJIBO

Osaka University of Pharmaceutical Sciences, Kawai, Matsubara-shi, Osaka 580, Japan

(Received July 23, 1986)

Racemomycin-A (RM-A) showed delayed insecticidal activity against female adults (3 d after adult emergence) of *Musca domestica* and *Blattella germanica* treated by the topical application method; the LD_{50} values were 3.76 μg/insect (3 d) and 32.5 μg/insect (7 d), respectively. RM-A also showed delayed insecticidal activity against the 3rd instar larva of *Culex pipiens pallens* and *M. domestica* treated by the immersion method; the LC_{50} value for the former was 2.46 ppm (3 d), but the insecticidal effect against the latter was weak. RM-A applied by the immersion method also inhibited the adult emergence of *C. pipiens pallens* and *M. domestica*, with IC_{50} values of 1.41 and 199.5 ppm, respectively. Furthermore, RM-A exhibited insecticidal activity against female adults of *B. germanica* and larvae of *Periplaneta fuliginosa* treated by the bait method. The insecticidal activity of RM-A on adults of *B. germanica* was almost equal to that of boric acid bait agent (15%) at the concentration of 2.0%.

Keywords——racemomycin-A; delayed insecticidal effect; bait method; topical application method; immersion method; *Culex pipiens pallens*; *Blattella germanica*; *Musca domestica*; *Periplaneta fuliginosa*

It was already reported by the authors that racemomycin-D (RM-D, Fig. 1),[1] a streptothricin antibiotic containing four β-lysine residues in the molecule, shows phytogrowth-inhibitory,[2,5] insecticidal[2-4] and ichthyotoxic activities.[2] As regards the insecticidal activity of RM-D, it was found that the symptoms caused by RM-D developed slowly; namely, RM-D is a delayed toxicant. This conclusion was supported by the finding that the action of RM-D on the 5th instar larvae of silkworm, *Bombyx mori*, involved severe damage to the Malpighian tubule.[4] We also reported that racemomycin-A (RM-A)[6] (Fig. 1), containing one β-lysine residue in the molecule, had delayed insecticidal activity, although its activity was weaker than that of RM-D. However, no detailed work has been done on the mechanism of delayed insecticidal activity of RM-A.

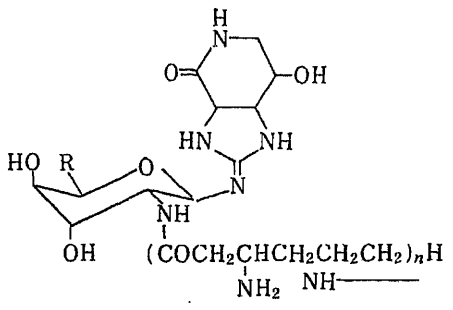

$n=1$, racemomycin-A
$n=4$, racemomycin-D

$R=CH_2OCONH_2$

Fig. 1. Chemical Structures of Racemomycin-A and -D

In the present study, as a preliminary step to investigate the mechanism of the delayed insecticidal action of RM-A, the mode of the insecticidal effect of this antibiotic on various insects was examined by using three assay methods.

Materials and Methods

Chemicals——RM-A was isolated from the culture broth of *Streptomyces lavendulae* OP-2[7] according to the method of Inamori *et al.*[1] Arutandondon (Fumakilla Limited, bait agent containing 15% boric acid, 2.5 g/tablet) was used as a standard for the bait method.

Insects——Female adults of *Musca domestica* (3 d after adult emergence) (body weight: 2.5 mg/insect) and *Blattella germanica* (body weight: 60 mg/insect), and the 3rd instar larvae of *Culex pipiens pallens* (body weight: 0.3 mg/insect), *Musca domestica* (body weight: 25 mg/insect) and *Periplaneta fuliginosa* (fifth molting) (body weight: 711 mg/insect) were used.

Insecticidal Activity Tests——1) Topical Application Method: A solution of detergent (EP-4c, 0.04%) containing RM-A was applied to the ventral surface of the abdomen of female adults of *Musca domestica* (0.77 μl) and *Blattella germanica* (1.54 μl) under ether anesthesia. Both bait (Oriental Yeast Co., Ltd.) and water were available to the insects. The number of deaths was observed at intervals of 24 h for 3 d in *M. domestica* and for 7 d in *B. germanica*. The LD_{50} value was calculated from the dose–mortality relationship.

2) Immersion Method: The 3rd instar larvae of *Culex pipiens pallens* and *Musca domestica* were released into water containing RM-A and left for 1 and 3 d. The numbers of deaths and adult emergences were observed at intervals of 24 h. The LC_{50} and IC_{50} values were calculated from the concentration–mortality relationship.

3) Bait Method: A 2 g tablet of RM-A was prepared at various concentrations in a mixture of equal quantities of sugar and peanut powder. Female adults of *Blattella germanica* and larvae of *Periplaneta fuliginosa* were allowed to feed on the tablet with water in an acrylic box (30 × 30 × 6 cm). The number of deaths was observed for 15 d.

Temperature——Every experiment was carried out at 25±2°C.

Illumination Time——All experiments were carried out for 12 h/d (8.00 a.m.—8.00 p.m.) under illumination.

Results

Insecticidal Activities of RM-A by the Topical Application Method

The insecticidal effect of RM-A against female adults (3 d after adult emergence) of *Musca domestica* and *Blattella germanica* was examined by the topical application method. The results are summarized in Tables I and II. RM-A showed delayed insecticidal activities against both insects. The insecticidal effect increased with the passage of time and LD_{50} values were 3.76 μg/insect in *M. domestica* (3 d) and 32.5 μg/insect in *B. germanica* (7 d).

TABLE I. Insecticidal Effect of Racemomycin-A against Female Adults (3 d after Adult Emergence) of *Musca domestica* by the Topical Application Method

Concentration of sample (%)	Dose (μg/insect)	Mortality (%)		
		1 d	2 d	3 d
2.0	15.4	0.0	25.0	68.3
1.0	7.7	0.0	11.7	56.7
0.5	3.85	0.0	20.0	51.7
0.25	1.93	0.0	1.7	21.7
0.125	0.96	0.0	11.7	20.0
0.063	0.48	0.0	0.0	23.3
0.031	0.24	0.0	0.0	18.3
0.016	0.12	0.0	0.0	3.3
Control	—	0.0	5.0	8.3
LD_{50} value (μg/insect)		—	—	3.76

Assay method: topical application method. Experimental size: 60 insects/group, 2 groups. Temperature: 25±2°C.

After the RM-A treatment, spontaneous movement in the insect was little different from that of control insects until 24 h after RM-A treatment. However, at 48 h all insects of the treated groups were paralyzed and most of them were becoming immobilized. Immobilization increased with the passage of time.

Insecticidal Activities of RM-A by the Immersion Method

The insecticidal effect of RM-A against the 3rd instar larvae of *Culex pipiens pallens* and *Musca domestica* was examined by the immersion method. As shown in Table III, this antibiotic showed delayed insecticidal activity against larvae of *C. pipiens pallens*. The LC_{50} value of RM-A was 2.46 ppm (3 d). This antibiotic also inhibited the adult emergence of *C. pipiens pallens* and the IC_{50} value was 1.41 ppm.

On the other hand, the insecticidal effect of RM-A against the 3rd instar larva of *Musca domestica* was weak, as shown in Table IV. That is, the 24 h mortality (%) was 24.1 at a

TABLE II. Insecticidal Effect of Racemomycin-A against Female Adults of *Blattella germanica* by the Topical Application Method

Concentration of sample (%)	Dose (μg/insect)	Mortality (%)			
		1 d	3 d	5 d	7 d
8.0	123.2	3.3	5.0	53.3	93.3
4.0	61.6	0.0	0.0	27.1	78.0
2.0	30.8	0.0	5.1	11.9	42.4
1.0	15.4	0.0	3.3	5.0	21.7
0.5	7.7	0.0	0.0	1.7	6.7
0.25	3.85	0.0	1.7	1.7	3.3
0.125	1.93	3.3	3.3	5.0	3.3
Control	—	0.0	1.7	5.0	5.0
LD_{50} (μg/insect)		—	—	114.7	32.5

Assay method: topical application method. Experimental size: 60 insects/group, 2 groups. Temperature: 25±2°C.

TABLE III. Insecticidal Effect of Racemomycin-A against 3rd Instar Larva of *Culex pipiens pallens* by the Immersion Method

Concentration of sample (ppm)	Mortality (%)		Adult emergence (%)
	1 d	3 d	
50.0	18.0	98.7	1.3
25.0	8.7	92.7	7.3
12.5	4.0	88.0	12.0
6.25	6.0	88.0	12.0
3.13	3.4	56.4	22.0
1.56	0.0	35.4	48.3
0.78	0.7	25.0	68.2
0.39	0.7	4.0	89.9
0.19	0.0	2.0	88.0
Control	2.0	6.6	90.7
LC_{50} and IC_{50} values (ppm)	—	2.46	1.41

Assay method: immersion method. Experimental size: 50 insects/group, 2 groups. Temperature: 25±2°C.

TABLE IV. Insecticidal Effect of Racemomycin-A against 3rd Instar Larva of *Musca domestica* by the Immersion Method

Concentration of sample (%)	24-hour mortality (%)	Pupation (%)	Adult emergence (%)
4000	23.3	63.3	0
2000	24.1	73.3	7.8
1000	8.9	82.2	7.8
500	7.8	86.7	28.9
250	8.9	90.0	44.4
125	8.9	87.8	64.4
62.5	11.1	88.9	65.6
31.3	8.9	90.0	66.6
15.1	2.2	87.8	68.9
Control	5.6	93.3	70.0
IC_{50} value (ppm)	—	—	199.5

Assay method: immersion method. Experimental size: 30 insects/group, 2 groups. Temperature: 25±2°C.

TABLE V. Insecticidal Effects of Racemomycin-A against Female Adults of *Blattella germanica* and Larva of *Periplaneta fuliginosa* by the Bait Method

Insect	Concentration of sample (%)	Number of deaths (out of 20 insects) at the indicated time (d) after baiting				
		1d	3d	6d	11d	15d
Blattella germanica	2.0	0	0	4	18	20
	1.0	0	1	1	12	13
	0.5	0	1	1	8	8
	0.25	0	0	1	2	3
	Arutandondon (15%)	0	6	16	19	19
	Control	0	1	1	1	1
Periplaneta fuliginosa	2.0	0	1	2	4	7
	1.0	0	0	3	3	6
	0.5	1	1	1	3	3
	0.25	0	0	1	2	4
	Arutandondon (15%)	3	5	8	12	19
	Control	0	0	0	2	2

Assay method: bait method. Experimental size: 20 insects/group, 2 groups. Temperature: 25±2°C.

concentration of 2000 ppm. This antibiotic also inhibited the adult emergence of *M. domestica* and the IC_{50} value was 199.5 ppm. However, the activity against *M. domestica* was weaker than that against *C. pipiens pallens*.

Insecticidal Activities of RM-A by the Bait Method

The insecticidal effect of RM-A against female adults of *Blattella germanica* and larva of *Periplaneta fuliginosa* was examined by the bait method. As shown in Table V, RM-A showed delayed insecticidal activity against female adults of *B. germanica*. At 4d after RM-A treatment, the spontaneous movement decreased gradually. The insecticidal effect of RM-A was almost equal to that of the conventional insecticide, Arutandondon (boric acid-bait

agent, Fumakilla Limited).

On the other hand, as shown in Table V, the insecticidal effect of RM-A against larva of *Periplaneta fuliginosa* was weak.

Discussion

The mode of delayed insecticidal action of RM-A (Fig. 1) on four kinds of insects was clarified.

Topical Application Method——The toxicity to housefly adults has not previously been studied. Thus, the mode of insecticidal effect of RM-A against female adults (3 d after adult emergence) of *Musca domestica* was examined, and RM-A was found to show delayed insecticidal activity (Table I). The insecticidal effect of RM-A was one-sixth of that of allethrin (LD_{50}: 0.64 μg/insect). Further, RM-A showed delayed insecticidal activity against female adults of *Blattella germanica* (Table II). The insecticidal effect of RM-A was one-sixth of that of allethrin (LD_{50}: 5.30 μg/insect). This is first report of examination of RM-A action on cockroach adults by the topical application method.

Immersion Method——The toxicity to mosquito larvae has not yet been investigated. The mode of insecticidal effect of RM-A against the 3rd instar larvae of *Culex pipiens pallens* was examined, and RM-A was found to show delayed insecticidal activity (Table III). A rather strong insecticidal effect of RM-D (Fig. 1) on *C. pipiens molestus* was already reported, with a mortality of 90% at 10 ppm.[2] In this respect, the insecticidal activity of streptothricin antibiotics on mosquito larva is of considerable interest. RM-A also inhibited the adult emergence of *C. pipiens pallens* and *Musca domestica* (Tables III and IV), but the activity against *M. domestica* was far weaker than against *C. pipiens pallens*. However, the inhibitory effect of RM-A on the adult emergence of both insects is reported for the first time in this paper.

Bait Method——The insecticidal effect of RM-A on female adults of *Blattella germanica* and larvae of *Periplaneta fuliginosa* was examined in comparison with that of a conventional insecticide, Arutandondon (Fumakilla Limited). RM-A showed delayed insecticidal activity against adults of *B. germanica* (Table V). RM-A also exhibited delayed insecticidal activity against larvae of *P. fuliginosa* (Table V), but the activity against *P. fuliginosa* was far lower than that against *B. germanica*. However, RM-A seems to be potentially useful as a bait agent from the following three points of view. 1) The strength of insecticidal activity of RM-A (2.0%) is almost equal to that of the conventional insecticide, Arutandondon (15% boric acid, Fumakilla Limited) (Table V), 2) RM-A did not show any repellent action against adults of *Blattella germanica* even at the high concentration of 2.0% (data not shown), and 3) RM-A exhibited the lowest toxicity to mice (LD_{50}: 300 mg/kg, i.v.)[8] among the streptothricin group, and its toxicity was lower than that of streptomycin (LD_{50}: 200 mg/kg, i.v. in mice).

As regards the mechanisms of delayed insecticidal activity of streptothricin,[3,4] a histopathological investigation and an analysis of the distribution into tissues of 5th instar larvae of the silkworm, *Bombyx mori*, showed that RM-D caused delayed damage to the Malpighian tubules. However, the mechanisms on delayed insecticidal action of these antibiotics have not yet been clarified. Further studies on the mechanisms of delayed insecticidal action of streptothricins seem desirable.

Acknowledgement The authors wish to thank Mr. Yasuharu Kodama of Fumakilla Limited for his support during this project.

References and Notes

1) Y. Inamori, S. Sunagawa, M. Tsuruga, Y. Sawada and H. Taniyama, *J. Ferment. Technol.*, **56**, 15 (1978).

2) T. Takemoto, Y. Inamori, Y. Kato, M. Kubo, K. Morimoto, K. Morisaka, M. Sakai, Y. Sawada and H. Taniyama, *Chem. Pharm. Bull.*, **28**, 2884 (1980).
3) M. Kubo, Y. Kato, K. Morisaka, K. Nomoto and Y. Inamori, *Chem. Pharm. Bull.*, **31**, 325 (1983).
4) Y. Kato, M. Kubo, K. Morisaka, Y. Waku, K. Hayashiya and Y. Inamori, *Chem. Pharm. Bull.*, **31**, 305 (1983).
5) M. Kubo, Y. Kato, N. Ōta, T. Takemoto, K. Nomoto, H. Tsujibo and Y. Inamori, *Chem. Pharm. Bull.*, **33**, 2910 (1985).
6) M. Kubo, Y. Kato, K. Morisaka, Y. Inamori, K. Nomoto, T. Takemoto, M. Sakai, Y. Sawada and H. Taniyama, *Chem. Pharm. Bull.*, **29**, 3727 (1981).
7) Y. Inamori, S. Sunagawa, Y. Sawada and H. Taniyama, *Hakko Kogaku Kaishi*, **54**, 795 (1976).
8) H. Taniyama, Y. Sawada and T. Kitagawa, *J. Antibiot.*, **24**, 662 (1971).

[Chem. Pharm. Bull. 35(4)1515—1522(1987)]

Serum Pepsinogen Levels in Normal and Experimental Peptic Ulcer Rats Measured by Radioimmunoassay

SATORU TANI,* AKIRA ISHIKAWA, HIROSHI YAMAZAKI and YUHKOH KUDO

Faculty of Pharmaceutical Sciences, Josai University, 1-1, Keyaki-dai, Sakado-shi, Saitama 350-02, Japan

(Received August 22, 1986)

Antiserum to the rat pepsinogen (PG) purified by us was raised in the rabbit. We established a radioimmunoassay system for PG and measured the content of it in the digestive and urinary organs. Immunoreactive PG in serum was confirmed to be PG by high-performance liquid chromatography using an ion exchange column. Serum PG levels in pregnant or lactating rats were higher than normal. The maximum level during lactation was 6 or 7 times the normal value, and began to decrease from about the 16th day after delivery. Serum PG in infant rats was elevated along with the content of mucosal PG. In the measurement of serum PG levels in experimental peptic ulcer rats, no significant change was observed in Shay and cysteamine ulcers produced in the forestomach or/and the duodenum. However, serum PG levels rose significantly in rats with indomethacin, stress and ethanol ulcers, which represent injuries on the glandular portion.

Keywords——radioimmunoassay; serum pepsinogen level; experimental gastric ulcer; pepsinogen; rat; pregnancy; lactation; stomach

We have already reported that there are two kinds of acid proteinase in the rat gastric mucosa; pepsinogens (PGs) and cathepsins, and only PGs are secreted in gastric juice.[1-5] Human PGs are classified into A, B and C type zymogens, whereas rat PGs are C type zymogens. Secreted PGs change into pepsins which hydrolyze nutritional proteins under acidic conditions. Usually, pepsins do not digest healthy gastric mucosa, but they are able to digest it in peptic ulcer. Samloff and Liebman showed that serum PG levels were decreased in patients with pernicious anemia[6] and increased in those with peptic ulcer.[7] Thus, measurement of serum PG levels may provide important information for the diagnosis of gastrointestinal diseases. However, in order to utilize serum PG level for diagnosis of gastric disease, we must know what factors affect the serum PG level. Since several kinds of experimental gastric ulcers are available in the rat, we measured the serum PG levels of normal rats and rats with experimental gastric ulcers. The results are presented here.

Materials and Methods

Chemicals——Sheep anti-rabbit immunoglobulin G (IgG) antiserum, ^{125}I- and complete Freund's adjuvant were obtained from UCB Bioproducts (Belgium), New England Nuclear (Boston, Mass) and DIFCO Lab. (Detroit, Mich), respectively. Pentagastrin from Sumitomo Chem. (Osaka, Japan), histamine from Wako Pure Chem. (Osaka, Japan) and carbamylcholine, cysteamine (2-mercaptoethylamine), indomethacin and porcine pepsin from Sigma Chem. (St. Louis, Mo) were used.

Radioimmunoassay of Rat Pepsinogen——Purification of rat PG was described previously.[1] Briefly, ammonium sulfate was added to the supernatant of 10% rat stomach homogenate in 50 mM phosphate buffer (pH 7.3), and the precipitate at 25 to 80% saturation of ammonium sulfate was collected. The precipitate was purified by diethylaminoethyl (DEAE)-cellulose and DEAE-Sepharose column chromatography. Anti-rat PG antiserum was raised in New Zealand white rabbits immunized with the purified PG dissolved in saline and emulsified with an equal

volume of complete Freund's adjuvant. Radioimmunoassay (RIA) was carried out according to Samloff,[8] by the double antibody technique with sheep anti-rabbit IgG antiserum as the second antibody. Radioiodination of PG was performed by the chloramine T method; 7.3 μg of PG was iodinated with 1 mCi of ^{125}I and 2.7 μg of chloramine T for 1 min. Iodinated PG was purified by passage through a Sephadex G-50 column. For this RIA, the final incubation mixture (280 μl) contained 50 μl of antiserum at a final dilution of 1 : 560000.

Assay of Peptic Activity——Peptic activity was measured by Anson's hemoglobin method[9]; an enzyme solution (0.1 ml) was incubated at 37 °C for 10 min with 2% hemoglobin solution (pH 1.8) (1 ml), and the reaction was stopped by addition of 5% trichloroacetic acid (5 ml). The absorption at 280 nm of the supernatant of the reaction mixture was measured.

High-Performance Liquid Chromatography (HPLC) of Serum Pepsinogen——Serum (1 ml) was loaded on a TSKgel DEAE-5PW column (Toyo Soda, Tokyo, Japan) and eluted with a linear gradient of 0 to 0.8 M NaCl in 20 mM phosphate buffer (pH 7.3) using an LC-3A liquid chromatograph (Shimadzu, Kyoto, Japan). The content of PG in each fraction was measured by RIA.

Perfused Rat Stomach Preparation——Male Wistar rats weighing over 300 g were starved for a day and the perfused rat stomach preparation was obtained according to Ghosh and Schild.[10] The gastric effluent was collected at 10-min intervals, and acidity and peptic activity of each fraction were estimated as described previously.[11] An aliquot of blood was collected from the tail vein every 30 min, and the content of PG in serum was measured by RIA.

Preparation of Rat Experimental Ulcers——Male Wistar rats weighing about 200 g were used for these experiments. For Shay ulcer, the pyloric ligature was performed under ether anesthesia in rats starved for 48 h according to Shay *et al.*,[12] and sham operation was done as the control. For stress ulcer, rats were immobilized in stress cages and immersed in a water bath at 23 °C to the height of the xiphoid process according to the method of Takagi and Okabe.[13] For indomethacin ulcer, indomethacin (30 mg/kg) suspended in 0.5% carboxymethyl cellulose sodium (CMC) was injected subcutaneously into rats starved for 48 h, and 0.5% CMC was injected as the control. For ethanol ulcer, absolute ethanol (1 ml) was directly given to rats starved for 24 h and water-restricted for 19 h, through a stomach tube, according to Robert *et al.*,[14] and water (1 ml) was given as the control. For cysteamine ulcer, cysteamine (400 mg/kg) was injected subcutaneously into rats starved for 24 h, and saline was injected as the control. After a certain time, blood was collected from the inferior vena cava of each experimental ulcer rat under ether anesthesia, and serum was separated. The ulcer index was expressed as total length (mm) of injuries after fixation by instillation of 2% formalin (10 ml) into the isolated stomach for indomethacin, stress and ethanol ulcers, or as a score (0, no change; 1, erosion; 2, 1 to 4 small injuries of diameter less than 3 mm; 3, more than 5 small injuries or 1 large injury of diameter more than 3 mm; 4, more than 2 large injuries; 5, perforation) for Shay and cysteamine ulcers. The ulcer index of duodenal ulcer was expressed as an area (mm^2). The statistical significance of differences was determined by using Student's *t*-test.

Results

Calibration Curve of Rat Pepsinogen

Dose–response curves of rat PG and its analogs, measured by RIA of PG, are shown in Fig. 1. Rat pepsin competed with the binding of ^{125}I-rat PG to its antibody in a similar

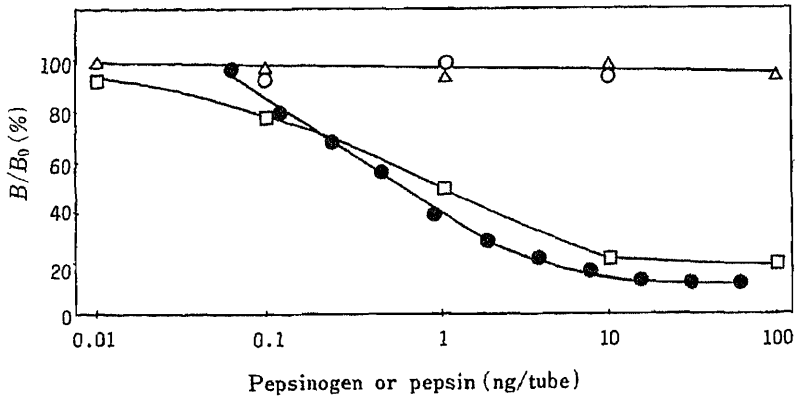

Fig. 1. Dose–Response Curves of Pepsinogen and Pepsins in Radioimmunoassay by Using ^{125}I-Rat Pepsinogen as a Label

○, heat-treated rat pepsin; △, porcine pepsin; □, rat pepsin; ●, rat pepsinogen. Rat pepsin was prepared by acid activation from rat PG on a Sephadex G-75 column.[1]

TABLE I. Contents of Pepsinogen in Various Organs, Serum and Urine

Organ	Pepsinogen immunoreactivity[a)]
Esophagus	0.15±0.03
Forestomach	4.67±.3.20
Glandular portion	5016.67±1149.03
Duodenum	2.86±1.94
Pancreas	0.17±0.01
Jejunum	0.19
Ileum	0.23
Cecum	0.53±0.38
Colon	0.05
Rectum	0.05
Kidney	0.09
Urinary bladder	0.03
Seminal vesicle	0.07
Prostate	0.00
Serum	10±1
Urine	118±91

Each organ was homogenized with 50 mM phosphate buffer (pH 7.3), and a suitable amount of supernatant was used for RIA. Values are means±S.E. of 3 male rats. The values which lack S.E. include one or more cases under the limit of detection. *a*) μg/g wet weight tissue, or ng/ml for serum and urine.

TABLE II. Serum Pepsinogen Levels in Rats in Various States

	Serum PG (ng/ml)
Male adult	17±2 (6)
(starvation for) 24 h	44±4 (8)
48 h	69±14 (9)
72 h	36±5 (5)
Female adult	11±2 (8)
Pregnant (15—20 d)	16±3 (5)
Lactating (after delivery)	
12 d	73±3 (5)
14 d	74±3 (5)
16 d	67±4 (5)
20 d	50±4 (5)
25 d	34±2 (4)
30 d	36±3 (4)

The numbers of rats are given in parentheses. The values are mean±S.E.

manner to rat PG, but heat-treated rat pepsin (100 °C, 10 min) and porcine pepsin did not.

Contents of Pepsinogen in Various Organs

The contents of PG in serum, urine and the digestive and the urinary organs were measured (Table I). A large amount of PG was found in the glandular portion of the stomach, but only small amounts in the forestomach and the duodenum. Other organs contained negligible amounts of PG. Although the content of PG in urine varied widely, it was about 10 times that in serum.

The content of PG in the glandular portion determined by measuring peptic activities was 5.3±0.8, and that by RIA was 5.0±1.1 mg/g wet weight.

Identification of Immunoreactive Pepsinogen in Serum

We also examined immunoreactive PG in serum by HPLC. The elution profiles of PG and acid-activated PG are shown in Fig. 2a. Pepsinogen and pepsin were separately eluted at different NaCl concentrations. Elution profiles of PG in 1 ml of serum, obtained from a normal rat or ethanol (1 h after instillation) or indomethacin (25 h after administration) ulcer rat are shown in Fig. 2b, c and d, respectively. We estimated that immunoreactive PG in serum showed the same retention time as PG and no contamination by pepsin was detected.

Serum Pepsinogen Levels

Serum PG levels in fed and starved male rats, as well as normal, pregnant and lactating female rats were measured (Table II). Serum PG levels in male rats during starvation gradually rose, then decreased on the 3rd day. Those in rats on the 2nd day of starvation were 4 times as high as in fed rats.

Serum PG levels in pregnant rats were about 1.5 times those of ordinary female rats. Interestingly, serum PG levels in lactating rats were 6 or 7 times higher than that of normal rats, and they began to fall gradually from about the 16th day after delivery. However, the

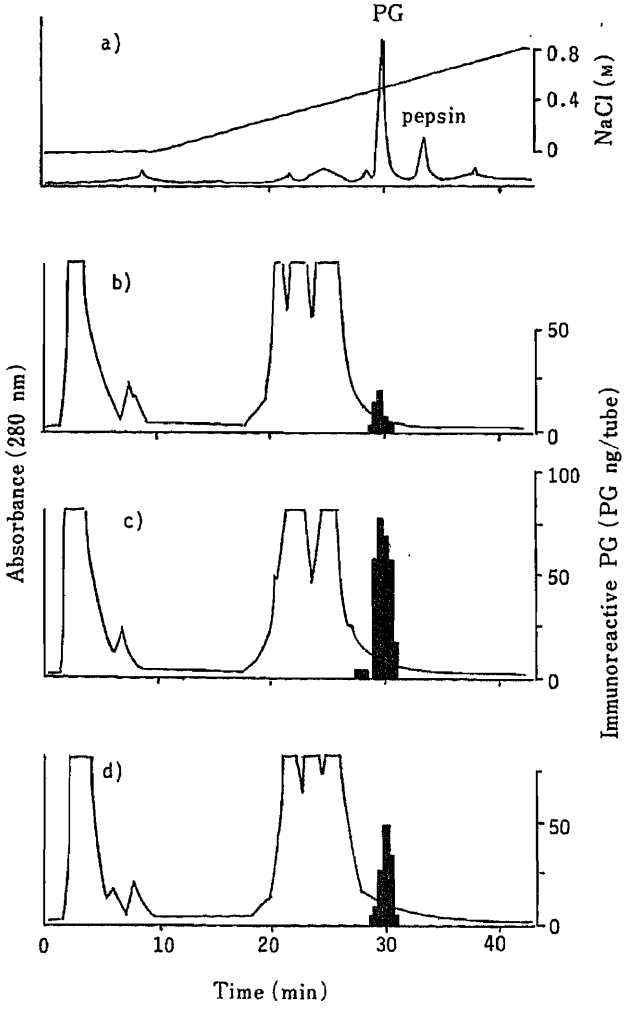

Fig. 2. Typical HPLC Elution Profiles of Pepsinogen in Sera from Normal Rats and Rats with Experimental Gastric Ulcer Induced by Ethanol or Indomethacin

The samples were eluted with a linear gradient of 0 to 0.8 M NaCl in 20 mM phosphate buffer (pH 7.3) at 0.94 ml/min on a TSKgel DEAE-5PW (7.5 × 75 mm) column; fractions were collected every 30 s. The samples were (a) a mixture of PG and acid-activated PG, (b) normal serum (1 ml), (c) serum from ethanol ulcer rat, (d) serum from indomethacin ulcer rat. Each serum (1 ml) was eluted under the same conditions as in (a), and immunoreactive PG is indicated by closed columns. Each elution profile was obtained in one of three experiments.

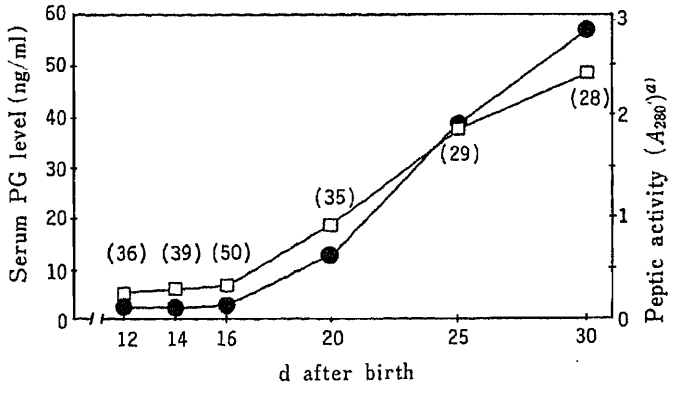

Fig. 3. Changes of Serum Pepsinogen Levels and Mucosal Peptic Activities in Rats after Birth

□, mucosal peptic activity; ●, serum PG level. The numbers of rats are given in parentheses. *a*) Absorbance (280 nm) of the reaction mixture obtained as described in Materials and Methods.

content at the 30th day after delivery remained 3 times higher.

In regard to changes of PG content during development, the peptic activities of gastric mucosa and serum PG levels in immature rats of both sexes from the 12th to the 30th day after birth are shown in Fig. 3. No significant difference in serum PG levels between male and female immature rats was observed. The contents of mucosal and serum PGs similarly increased on about the 20th day after birth. Serum PG levels at the 30th day after birth were about 4 times those of adult male rats, but mucosal PG content was about half.

Effects of Pentagastrin, Histamine and Carbamylcholine on Serum Pepsinogen Levels in Perfused Rat Stomach Preparation *in Vivo*

The correlation between PG secretion and serum PG levels was examined. Submaximal doses of three secretagogues, pentagastrin, histamine and carbamylcholine, were injected

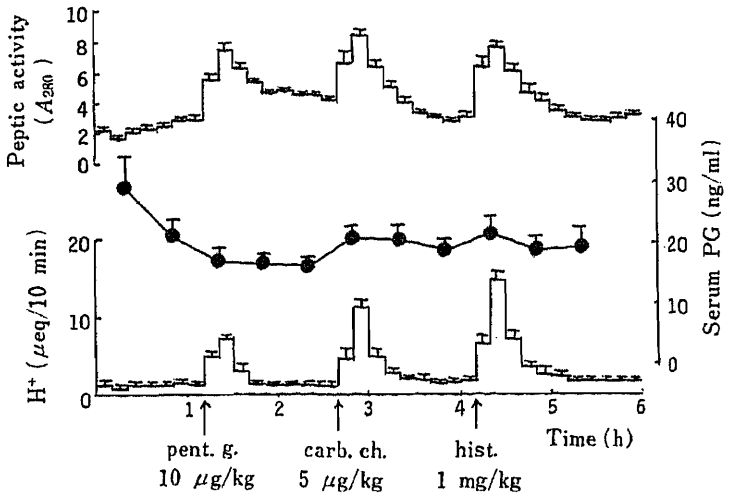

Fig. 4. Effects of Pentagastrin, Carbamylcholine and Histamine on Serum Pepsinogen Levels and Acid and Pepsin Secretions in Perfused Rat Stomach *in Vivo*

Pentagastrin (pent.g.), carbamylcholine (carb.ch.) and histamine (hist.) were intravenously injected at the indicated times and doses. Acid secretion and peptic activity in gastric effluent and serum PG level (●) are mean values ± S.E. from 5 rats.

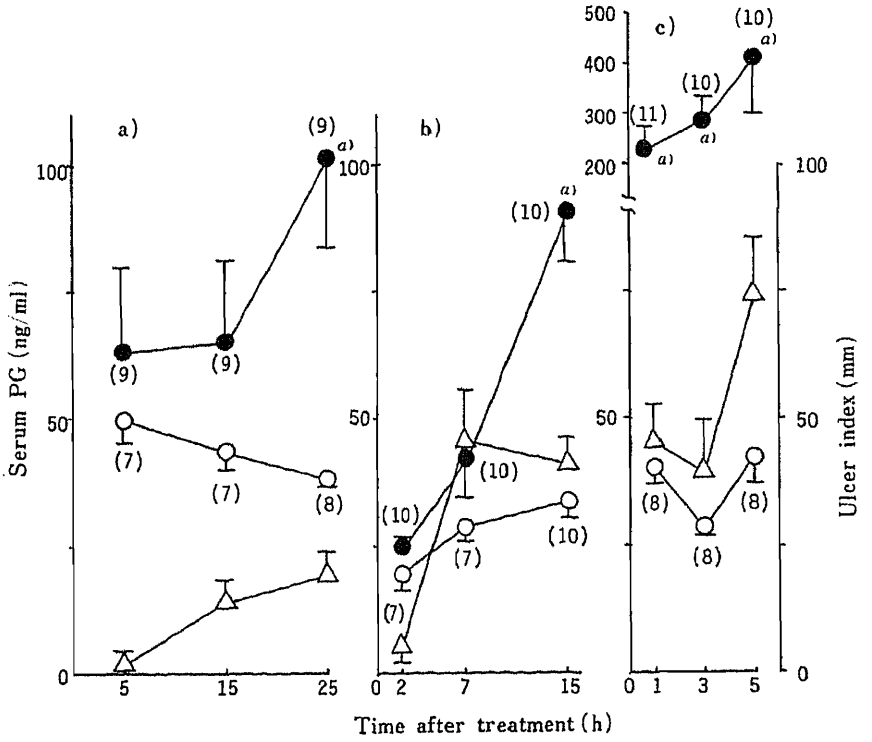

Fig. 5. Changes of Serum Pepsinogen Levels and Ulcer Indexes in Indomethacin (a), Stress (b), and Ethanol (c) Ulcer Rats

Serum PG levels in rats with experimental gastric ulcer (●) and corresponding control rats (○) are mean values ± S.E. from the numbers of rats indicated in parentheses. Ulcer indexes (△) in experimental gastric ulcer were obtained from the same rats. *a*) $p<0.01$.

TABLE III. Changes of Serum Pepsinogen Levels and Ulcer Indexes in Shay and Cysteamine Ulcer Rats

	Shay ulcer		
Time (h)[a]	2	5	10
Serum PG (ng/ml)		Sham operation	
	26±2 (6)	26±2 (7)	39±3 (7)
		Shay ulcer	
	38±5 (10)	37±4 (10)	52±9 (9)
Ulcer index[b]	0	0.3±0.2	3.0±0.2

	Cysteamine ulcer		
	Control	Duodenal	Duodenal and gastric
Serum PG (ng/ml)	34±3 (8)	25±8 (4)	53±16 (10)
Ulcer index			
Duodenal[c]	—	9±4	11±3
Gastric[b]	—	—	2.3±0.2

The values are means±S.E. from the numbers of rats given in parentheses. *a*) Time after ligation. *b*) Scores. *c*) mm^2.

intravenously at 90 min intervals (Fig. 4). Acid and pepsin secretion were stimulated by these secretagogues, whereas serum PG levels were only slightly elevated by histamine and carbamylcholine.

Serum Pepsinogen Levels in Experimental Gastric or/and Duodenal Ulcer Rats

The experimental gastric or/and duodenal ulcers were divided into two groups, one consisting of glandular injury induced by indomethacin, ethanol or stress, and the other of forestomach or/and duodenal injury induced by cysteamine or pyloric ligature. Serum PG levels in these experimental ulcer rats are summarized in Fig. 5 and Table III.

Serum PG levels of starved rats at 25 h after injection of indomethacin were about 2.5 times the control. Clear injuries were seen at 15 and 25 h judging from the ulcer indexes. Serum PG levels of rats under restraint and immersion stress at 15 h were about 4 times the control and significant changes in ulcer indexes were observed, even at 2 h after the stress. After instillation of ethanol through a stomach tube into starved rats, great increases in serum PG levels were seen; within 1 h, the level increased about 5 times, and at 5 h, about 10 times. However, the ulcer indexes determined at 5 h were only twice those at 1 h.

On the other hand, ulcer indexes in rats with experimental forestomach ulcer caused by pyloric ligature were large at 5 and 10 h, but serum PG levels showed no significant difference from those of the sham operation. In cysteamine ulcer, serum PG levels and ulcer indexes were measured at 18 h after cysteamine administration. Cysteamine ulcer was divided into two groups, one in which the duodenum is injured and the other affecting both the duodenum and the forestomach. Serum PG levels in cysteamine ulcer rats with injuries of both the duodenum and the forestomach were higher than those of the duodenum only. However, neither group showed a significant difference from the control.

Discussion

We have shown that anti-rat PG antiserum raised in the rabbit gave a positive Ouchterlony test with mouse and hamster PG, but a negative one with porcine PG.[2] The antiserum also reacted to rat pepsins. Using this antiserum, we quantified the contents of PG in the digestive and urinary organs, serum and urine by RIA. A very large amount of PG was found in the glandular portion of the stomach. Immunoreactive PG was not detected in the prostate gland, which is known to produce gastricsin.[15,16] Therefore it seems probable that immunoreactive PG in serum and urine comes from the glandular portion of the stomach, and anti-rat PG antiserum does not react with intrinsic proteins other than rat PGs and pepsins. The content of PG in urine varied so widely that we concluded that the measurement of PG in serum would be more useful.

Proceeding to the measurement of serum PG levels, we examined whether or not immunoreactive PG in serum is PG itself. If serum PG diffuses back from the gastric lumen, immunoreactive PG in serum should be pepsin. However, the elution profile of immunoreactive PG in serum on HPLC with a TSKgel DEAE-5PW column showed that the serum PG obtained from normal or ulcer rat had the same retention time as PG derived from the gastric mucosa. The following experiments were done on the premise that immunoreactive PG in serum is PG itself.

First of all, serum PG levels in normal rats of different age, sex and condition were measured. We found that serum PG levels changed during starvation; they increased first and fell later. These results suggest that serum PG levels in man depend upon the time after eating. Waldum *et al.* reported that there was no significant difference of mean human serum PG I levels at different stages during pregnancy.[17] However, slightly higher levels during pregnancy were obtained in the rat. Furthermore, serum PG levels during lactation were much higher than those during pregnancy. Needless to say, the content of mucosal PG and the size of the stomach during pregnancy or lactation are almost normal, so that higher serum PG levels might be due to enhancement of the stomach function. It was confirmed that the high serum PG levels during lactation began to decline from the 16th day, that is around the weaning period.

On the other hand, in immature rats mucosal PG began to be synthesized from around the weaning period and serum PG levels paralleled the increase. Much PG was found in the circulation at the 30th day after birth, even in healthy immature rats. These results also suggest that serum PG levels reflect stomach function. It is not clear why an exocrine enzyme should be released into the circulation as a result of an enhancement of stomach function in normal conditions.

We examined whether or not serum PG levels were elevated in perfused rat stomach *in vivo* by the stimulation of PG secretion. Serum PG levels were slightly elevated by carbamylcholine and histamine, whereas peptic activities in gastric effluent were about twice the basal ones. Similar results in man were observed by Waldum,[18] *i.e.*, vagal and hormonal stimulation increased serum PG levels.

There are many reports about the relationship between serum PG levels and gastric diseases in man, and high serum PG levels were described in gastric and duodenal ulcer patients. We were uncertain why high serum PG levels were observed in duodenal ulcer patients, though only a very small amount of PG existed in the duodenal mucosa. We separately examined serum PG levels in two kinds of experimental peptic ulcer in the rat, in relation to the amount of PG in the injured part, *i.e.*, the glandular portion of the stomach and the forestomach or/and the duodenum. High serum PG levels were observed in the experimental injury at the glandular portion, but not at the forestomach or/and the duodenum in rats. High serum PG levels were found in rats with experimental ulcers in the

glandular portion. However, there is a big discrepancy in serum PG levels between duodenal ulcer patients and experimental duodenal ulcer in the rat. It is known that hereditary factors are similar in each type of experimental rat, whereas this would not be the case in patients. As we have suggested that serum PG levels might reflect stomach function, it seems likely that enhanced stomach function causes duodenal ulcer in most cases in man. Serum PG levels and ulcer indexes in the same ulcer model were not correlated, and this may suggest that serum PG does not originate from the injured mucosa but from the repairing mucosa. Moreover, among the experimental ulcers of the glandular portion of the stomach, there were marked differences in serum PG levels between stress and ethanol ulcers, even if they showed similar ulcer indexes (which represent the degree of injury). Different types of mucosal injuries may occur in stress and ethanol ulcers.

References

1) N. Muto and S. Tani, *J. Biochem.* (Tokyo), **85**, 1143 (1979).
2) N. Muto, K. Murayama, K. Akahane and S. Tani, *J. Biochem.* (Tokyo), **87**, 717 (1980).
3) N. Muto, K. M. Arai and S. Tani, *Biochim. Biophys. Acta*, **745**, 61 (1983).
4) K. M. Arai, N. Muto, S. Tani and K. Akahane, *Biochim. Biophys. Acta*, **788**, 256 (1984).
5) N. Muto and S. Tani, *Biochim. Biophys. Acta*, **843**, 114 (1985).
6) I. M. Samloff and W. M. Liebman, *Gastroenterology*, **66**, 494 (1974).
7) I. M. Samloff, W. M. Liebman and N. M. Penitch, *Gastroenterology*, **69**, 83 (1975).
8) I. M. Samloff, *Gastroenterology*, **82**, 26 (1982).
9) M. L. Anson, *J. Gen. Physiol.*, **22**, 79 (1938).
10) M. N. Ghosh and H. O. Schild, *Br. J. Pharmacol.*, **13**, 54 (1958).
11) S. Tani and N. Mutoh, *Biochem. Pharmacol.*, **28**, 678 (1979).
12) H. Shay, S. A. Komarov, S. S. Fels, D. Meranze, M. Gruenstein and H. Siplet, *Gastroenterology*, **5**, 43 (1945).
13) K. Takagi and S. Okabe, *Jpn. J. Pharmacol.*, **18**, 9 (1968).
14) A. Robert, J. E. Nezamis, C. Lancaster and A. J. Hanchar, *Gastroenterology*, **77**, 433 (1979).
15) L. Chiang, L. Contreras, J. Chiang and P. H. Ward, *Arch. Biochem. Biophys.*, **210**, 14 (1981).
16) L. Chiang, M. Maldonado, E. E. Vivaldi and P. H. Ward, *Biochem. Int.*, **4**, 161 (1982).
17) H. L. Waldum, B. K. Straume and R. Lundgren, *Scand. J. Gastroent.*, **15**, 61 (1980).
18) H. L. Waldum, "Pepsinogens in Man: Clinical and Genetic Advances," ed. by J. Kreuning, I. M. Samloff, J. I. Rotter and A. W. Eriksson, Alan R. Liss, New York, 1985, pp. 115—127.

[Chem. Pharm. Bull. 35(4)1523—1530(1987)]

Potentiation of Host-Mediated Antitumor Activity by a β-Glucan Derived from Mycelia of *Cochliobolus miyabeanus*

HIROAKI NANBA* and HISATORA KURODA

Department of Microbiology, Kobe Women's College of Pharmacy, Motoyama, Higashinada, Kobe 658, Japan

(Received August 27, 1986)

A polysaccharide (6-branched β-1,3-glucan, As-I) extracted from mycelia of *Cochliobolus miyabeanus* (*Ascomycetes*) inhibited the growth of against mouse syngeneic tumors (80% inhibition of MM-46 carcinoma and 30% inhibition of IMC carcinoma) when injected i.p. (0.1 mg/kg/d). As-I enhanced the phagocytosis of syngeneic tumor cells by macrophages about 1.5 times, and the production of superoxide anion about 1.2 times. As-I also activated natural killer cells and increased the activity of killer T cells about 1.3 times.

Keywords——antitumor glucan; macrophage; natural killer cell; T cell; *Cochliobolus miyabeanus*

As described in a previous paper,[1] a β-glucan having 1,6 branches, isolated from mycelia of *Cochliobolus miyabeanus* (*Ascomycetes*), caused about 50% growth inhibition of allogeneic tumors when injected at the dose of 0.5 mg/kg for 9 consecutive days. When intraperitoneal macrophages of mice were treated with this glucan either *in vitro* or *in vivo*, the spreading rate and phagocytic activity were increased.[2] Activated macrophages, cytotoxic cells, natural killer (NK) cells, and killer cells have important roles in tumor immunity. As found for lentinan[1,2] antitumor glucans activate multiple sites in the cellular immune systems. In this paper, the antitumor action of As-I (6-branched β-1,3-glucan) on syngeneic tumors was investigated, and the mechanisms of action on macrophage, cytotoxic cells, and NK cells were also examined.

Materials and Methods

Preparation of Polysaccharide (As-I)——The polysaccharide As-I was prepared from mycelia of *Cochliobolus miyabeanus* (ATCC 38724, *Ascomycetes*) as described previously.[1]

Animals——Male ICR (4 weeks), C3H (6 weeks), CDF_1 (6 weeks) and BALB/C (5 weeks) mice were purchased from Japan Charles River Ltd. After acclimation for one week, mice were used for tests.

Tumor Growth Inhibitory Effect——MM-46 tumor cells (2×10^6) were transplanted s.c. into male C3H mice (7 weeks), IMC-carcinoma cells (2×10^6) into male CDF_1 mice (7 weeks), and Meth-A fibrosarcoma cells (1×10^6) into male BALB/C mice (6 weeks) in the axilla. After 24 h, 1 mg/kg/d of As-I was injected i.p. daily for 10 d. On the 25th day after tumor transplantation, the solid tumor was extirpated and weighed to obtain the tumor growth inhibition ratio (TIR) according to the method described in the previous paper.[2]

Collection of Macrophages in Peritoneal Cavity——Peritoneal cells were obtained by washing with Hanks' solution from the peritoneal cavity of mice killed by vertebral dislocation. After centrifugation at 1200 rpm for 10 min, the precipitated cells were collected and adjusted with RPMI-1640 medium to 1×10^6 cells/ml. These cells were pipetted (1.5 ml) onto a plate and cultured at 37 °C for 2 h in a 5% CO_2 atmosphere in air; Mφ were adsorbed selectively on the plate wall. The non-adherent cells were eliminated by washing 3 times with Hanks' solution.

Measurement of Superoxide Anion (SOA)——As-I (50 μg) was injected i.p. into male ICR (5 weeks), C3H (7 weeks) and BALB/C (6 weeks) mice daily for 5 d. On the 5th day after completion of administration, Mφ were collected and SOA was measured according to the method of Ito *et al.*[3] Then 1.5 ml of phosphate buffered saline (PBS) containing 10 mM glucose, 80 mM ferricytochrome c and 0.2 mg/ml of opsonized zymosan was added to

adherent Mϕ on the plate. After centrifugation at 3000 rpm for 5 min, the supernatant was collected in an ice-chilled test tube and the absorbance at 550 nm was measured. On the other hand, 1 ml of 0.5% sodium dodecyl sulfate (SDS) was added to the precipitated cells, and after standing for 5 min, the cells were well dispersed. The amount of ferricytochrome c was obtained from the absorbance at 550 nm, based on $\Delta E\ 550 = 2.1 \times 10^4\ M^{-1}$, and released SOA per unit protein was calculated.

Opsonization of Zymosan[4]——Zymosan A was adjusted with PBS to 10 mg/ml, boiled for 1 h, washed 3 times, and readjusted with PBS to 50 mg/ml. Human serum (4 volumes) was added to 1 volume of zymosan (50 mg/ml), and the mixture was incubated at 37 °C for 30 min. Zymosan was collected by centrifugation, and 10 mg/ml of opsonized zymosan was obtained by dilution with PBS.

Preparation of Spleen Cell Suspension[5]——A male mouse of C3H strain (7—8 weeks) was killed by vertebral dislocation. The femoral vein was cut, and the spleen was extirpated after exsanguination. After being washed with Eagle's minimum essential medium (MEM), the spleen was sufficiently untangled and passed through an 80 mesh stainless steel sieve. Cells were collected by centrifugation at 1200 rpm for 10 min, then 2 ml of 10-fold dilution of Eagle's MEM was added. Immediately after hypotonic elimination of erythrocytes mixed therein for 10 s, 2 ml of Eagle's MEM at 2-fold concentration was added and mixed. The cells were collected by centrifugation at 1200 rpm for 10 min, and diluted with RPMI-1640 medium to 1×10^7 cells/ml. This was used as the whole spleen cell suspension. An aliquot was incubated for 60 min in a Petri dish of 5 cm in diameter. Non-adherent cells were collected and adjusted to 1×10^7 cells/ml with RPMI-1640 medium. This was used as non-adherent spleen cell suspension.

Elimination of T Cells[6]——Non-adherent spleen cell suspension (1 ml) obtained from male C3H mice (9 weeks) was mixed with 20 μl of 5% Thy-1.2 F7D5 monoclonal immunoglobulin M (IgM) cytotoxic antibody (Serotec Ltd., England), incubated for 30 min, and washed once with RPMI-1640 medium. Then, 1 ml of RPMI-1640 medium with fetal bovine serum containing 5% guinea-pig complement was added and the whole was further incubated for 30 min. The cells that reacted with antibody were selectively destroyed. The remaining cells were centrifuged at 1200 rpm for 10 min and adjusted to 1×10^7 cells/ml.

Labeling of Target Cells[7]——After being washed with RPMI-1640 medium, P-815 tumor cells were adjusted to 1×10^6 cells/ml. Then 25 μl of ^{3}H-uridine solution (40 μCi/ml) was added to 1 ml of the cell suspension, and the mixture was incubated for 54 min, then centrifuged at 1200 rpm for 10 min. The cells were washed with RPMI-1640 medium and adjusted to 2×10^5 cells/ml (1.0×10^5—2.1×10^5 dpm/1×10^6 cells).

Cytotoxicity[7]——The labeled target cell suspension (1 ml; 2×10^5 cells/ml) was mixed with 1 ml of the lymphocyte suspension (1×10^7 cells/ml) prepared as described previously.[8] Portions of 0.5 ml each were incubated for 4 h, then 0.4 ml was dropped on a Millipore filter (0.45 nm in pore size) and suction-filtered. The filter was washed with 15 ml of ice-cold 5% trichloroacetic acid (TCA) solution, dried and mixed with 10 ml of lipophilic scintillator (5 g of 2,5-diphenyloxazole (PPO), 0.3 g of 1,4-bis[2-(4-methyl-5-phenyloxazolyl)]benzene (DMPOPOP), and 1000 ml of toluene). Radioactivity was measured with an Aloka LSC-700 scintillation counter. The cytotoxicity (P) was calculated according to the following formula:

$$P\ (\%) = \left(1 - \frac{\text{dpm with immunolymphocytes} - \text{background dpm}}{\text{dpm when target cells only were incubated} - \text{background dpm}}\right) \times 100$$

Preparation of Medium Containing Interleukin-1 (IL-1)[9]——Male mice of C3H strain (7 weeks) were given 50 μg/d of As-I i.p. for 5 d. On the 5th day, after the final dose, Mϕ were collected and adjusted to 1×10^6 cells/ml. Aliquots of 0.4 ml were placed on 24-well plates, and incubated for 60 min. The plates were washed with RPMI-1640 medium, 0.4 ml of RPMI-1640 medium without fetal bovine serum was added, and the plates were incubated for 72 h. The supernatant was passed through a 0.45 μm Millipore filter for sterilization, and preserved at −80 °C.

Measurement of Lymphocyte Growth Reaction[9]——Male C3H mice (7 weeks) were killed by vertebral dislocation and bled from the femoral vein, then the thymus was extirpated. It was untangled in the Eagle's MEM, then passed through an 80-mesh stainless steel sieve, and a cell suspension was prepared. After adjustment to 1.5×10^7 cells/ml with RPMI-1640 medium containing 25 μM 2-mercaptoethanol, it divided into 0.1 ml aliquots on a 96-well plate (Corning Glass Works). Then, 0.05 ml of Mϕ supernatant (see preceding section) and 0.05 ml of RPMI-1640 medium or 0.05 ml of PHA-P at 10 μg/ml were added, and the total volume of 0.2 ml was incubated for 72 h. At 6 h before the end of incubation, 0.5 μCi of [methyl-^{3}H]thymidine was added, and mixed gently by shaking the plate. The reaction fluid was filtered through a glass-fiber filter, which was dried after being washed with 5% TCA solution. The radioactivity was measured with a liquid scintillation counter.

Preparation of Lymphokines[10]——The spleen of a mouse was untangled and the cells were suspended in 10 ml of RPMI-1640 medium, to which 0.5 ml of 100 μg/ml Concanavarin-A was added. The mixture was incubated at 37 °C for 48 h. After centrifugation the obtained supernatant was preserved at −80 °C. It was used as the supernatant containing lymphokines.

Statistical Processing of the Experimental Data——Student's t-test was used to evaluate the significance of differences between the control and As-I administration groups.

Results and Discussion

As described in the previous paper,[1] the administration of As-I (0.5 mg/kg/d) caused 50% inhibition of Sarcoma-180 tumor growth. This inhibitory effect, however, might in part have derived from allograft rejection because of the difference of major histocompatibility antigen (MHA) between the tumor cells and host cells. Thus, in the present study, IMC carcinoma tumors in CDF_1 mice and MM-46 carcinoma tumors in C3H mice were used as syngeneic tumor systems with the same MHA. As-I was injected i.p. at the daily dose of 0.1 or 0.5 mg/kg for 10 d and the inhibition of tumor growth was determined. As shown in Table I, As-I inhibited the growth of IMC carcinoma and MM-46 carcinoma by about 30.1—32.0% and 79.8—82.7%, respectively. These results indicate that As-I potentiated the host immune

Table I. Antitumor Activities of As-I on Syngeneic or Allogeneic Tumor

Mouse and tumor	Dose (mg/kg/d)	Weight (g)	Inhibition ratio (%)
ICR-Sarcoma-180	Saline	8.21±0.75	0.0
	0.5	4.12±1.13[a]	49.8
	0.1	6.58±0.83[b]	20.2
CDF_1-IMC carcinoma	Saline	6.12±0.77	0.0
	0.5	4.13±0.96[b]	32.0
	0.1	4.21±1.22[a]	30.1
C3H-MM-46 carcinoma	Saline	7.32±0.65	0.0
	0.5	1.46±1.35[a]	79.8
	0.1	1.26±1.52[a]	82.7

t-Test: *a*) $p<0.05$, *b*) $p<0.01$.

Table II. Effect of As-I on Phagocytic Activity of ^{3}H-Uridine-Labeled IMC Carcinoma Cells by Macrophages from CDF_1 Mice

Mouse and tumor	Agent	Incorporation (dpm/10^5 Mϕ)		Ratio	
		In vivo (a)	*In vitro* (b)	(a)	(b)
Normal CDF_1	Saline	560.0±63.6	237.5±97.3	1.00	1.00
	As-I	351.2±75.4[a]	219.3±74.7[a]	0.62	0.92
IMC-bearing CDF_1	Saline	141.0±26.3	83.7±13.1	1.00	1.00
	As-I	172.1±11.8[b]	106.4±29.8[a]	1.22	1.27

t-Test: *a*) $p<0.05$, *b*) $p<0.01$.

Table III. Effect of As-I on Phagocytic Activity of ^{3}H-Uridine-Labeled MM-46 Carcinoma Cells by Macrophages from C3H Mice

Mouse and tumor	Agent	Incorporation (dpm/10^5 Mϕ)		Ratio	
		In vivo (a)	*In vitro* (b)	(a)	(b)
Normal C3H	Saline	143.7±24.2	42.5±9.7	1.00	1.00
	As-I	185.5±21.5[b]	71.8±7.3[b]	1.29	1.69
MM-46-bearing C3H	Saline	570.0±76.8	160.9±25.1	1.00	1.00
	As-I	861.1±33.6[b]	183.2±19.6[a]	1.51	1.14

t-Test: *a*) $p<0.05$, *b*) $p<0.01$.

response regardless of allograft rejection.

Thus, to clarify the mechanism of tumor growth inhibition by As-I, its influence on the activation of Mϕ, natural killer cells and cytotoxic T cells (effectors of host-mediated tumor growth inhibition) was assessed.

In the previous paper,[2] the phagocytic activity of latex particles and spreading rate of Mϕ were increased by the administration of As-1. However, phagocytosis of latex particle by Mϕ is nonspecific phagocytic activity. Therefore, the effects of As-I on phagocytosis of syngeneic tumor cells were tested *in vivo* and *in vitro*. As shown in Table II, in the case of IMC tumor-bearing CDF_1 mice, in which As-I administration gave only about 30% inhibition of tumor growth, the phagocytic activity of Mϕ was increased about 1.2—1.3 times by injection of As-I at 30 μg/kg/d for 5 d, compared with that of the tumor-bearing control group receiving saline. On the other hand, in syngeneic MM-46 tumor-bearing C3H mice, in which As-I gave about 80% growth inhibition, phagocytic activity was increased about 1.5 times by As-I *in vivo*, compared with the control group. The results are given in Table III.

The effect of As-I on cytolytic activity against phagocytosed cells by Mϕ was examined in syngeneic tumor–host systems. As shown in Table IV, in the IMC carcinoma tumor cell–CDF_1 mouse system, which responded poorly to As-I, the activity was not increased by As-I administration *in vivo* or *in vitro*. As shown in Table V, however, in the MM-46 carcinoma tumor cell–C3H mouse system, the cytolytic activity against MM-46 cell was increased about 1.3 times by As-I when Mϕ obtained from tumor-bearing mice were used. This increase was about 1.5—1.6 times when the Mϕ obtained from normal mice were used.

These results indicate that As-I potentiates the phagocytolytic and cytolytic activity of Mϕ against syngeneic tumor cells, and this suggests that the extent of inhibition of tumor growth by As-I may vary depending on the extent of potentiation. Since it was already clarified that Mϕ were potentiated by As-I, we examined SOA release by Mϕ in phagocytosis,

TABLE IV. Cytolytic Activity against IMC Carcinoma Cells by Macrophages from CDF_1 Mice

Mouse and tumor	Agent	Degradation (dpm/10^5 Mϕ)		Ratio	
		In vivo (a)	*In vitro* (b)	(a)	(b)
Normal CDF_1	Saline	164.8±11.8	—	1.00	—
	As-I	181.2±34.1	—	1.10	—
IMC-bearing CDF_1	Saline	207.9±21.4	81.5±18.2	1.00	1.00
	As-I	241.2±21.1[a)]	93.3±6.8[a)]	1.14	1.18

t-Test: *a*) $p<0.05$.

TABLE V. Cytolytic Activity against MM-64 Carcinoma Cells by Macrophages from C3H Mice

Mouse and tumor	Agent	Degradation (dpm/10^5 Mϕ)		Ratio	
		In vivo (a)	*In vitro* (b)	(a)	(b)
Normal	Saline	257.3±21.3	74.7±11.5	1.00	1.00
	As-I	419.4±12.1[c)]	109.1±10.1[b)]	1.63	1.46
MM-46-bearing C3H	Saline	186.2±9.7	65.7±7.3	1.00	1.00
	As-I	247.6±18.4[b)]	83.2±11.6[a)]	1.33	1.28

t-Test: *a*) $p<0.05$, *b*) $p<0.01$, *c*) $p<0.001$.

as a parameter of cytotoxicity of activated Mϕ.[3] Table VI shows the SOA release by Mϕ obtained from C3H mice injected i.p. with As-I (30 μg/d) for 5 d after MM-46 carcinoma tumor transplantation. SOA was released rapidly only during the first 90 min of phagocytosis in both the As-I group and the control group. Table VI shows the SOA released during the first 90 min after As-I administration, SOA production was increased about 1.2 times in Mϕ obtained from normal mice. In general, immunity is lowered in tumor-bearing hosts. SOA production by Mϕ obtained from MM-46 tumor-bearing mice decreased when saline was injected in place of As-I, but As-I restored the normal level, 1.2 times higher than that for Mϕ from control mice. Next, 30 μg/d of As-I was injected for 5 d after grafting MM-46 carcinoma into C3H mice, and SOA release from Mϕ collected on the 7th, 12th and 18th days after tumor implantation was measured. The results are given in Table VII.

While the SOA volume rapidly decreased in the control group, the decrease was comparatively less in the As-I group and tended to approach the level of normal mouse as time passed. Thus, the tumor growth inhibition may arise because As-I prevents deterioration of immune functions caused by the tumor-bearing state, or activates the cytotoxicity of Mϕ. Next, the effects of As-I on NK cells nonspecifically injuring tumor cells and Tc specifically

TABLE VI. Amount of SOA Released by Macrophages from C3H Mice

Mouse and tumor	Agent	SOA release (nmol/mg protein)	Ratio
Normal C3H	Saline	10.64±2.11	1.00
	As-I	12.91±1.37	1.20[a]
MM-46-bearing C3H	Saline	9.15±1.18	0.86 (1.00)
	As-I	13.08±2.14	1.23[a] (1.43)

t-Test: *a*) $p<0.05$.

TABLE VII. Time Course of SOA Release by Macrophages from MM-46-Bearing C3H Mice (*in Vivo* System)

Days after tumor inoculation	Agent	SOA release (A) (nmol/mg protein)	Ratio (A/B°)
7	Saline	60.09±3.14	0.83
	As-I	84.82±4.30	1.17[a]
12	Saline	51.41±0.93	0.71
	As-I	71.68±1.17	0.99
18	Saline	38.38±2.83	0.53
	As-I	68.06±3.37	0.96[a]

B°: normal C3H mice 72.41±2.83 (*t*-test: *a*) $p<0.05$).

TABLE VIII. Effect of As-I on NK Activity of Non-adherent Spleen Lymphocytes against YAC-1 Tumor Cells

Agent	NK activity (%) (Relative cytotoxicity)	Ratio
Saline	4.71±1.09	1.00
As-I	8.10±0.87[a]	1.72

t-Test: *a*) $p<0.05$.

injuring only the antigen-presenting cells were studied. The effects of As-I on NK cells indicated by interferon from pre-NK cells were assessed by measuring the activity in spleen cell using, as target cells, YAC-1 and P-815 tumor cells labelled with ^{3}H-uridine.

As-I (30 μg/d) was given for 3 d to C3H mice, and the non-adherent extirpated spleen. The cytotoxic activity against YAC-1 tumor cells (believed to be most susceptible to NK cells) was measured. As shown in Table VIII, the cytotoxicity was potentiated about 1.7 times by As-I administration.

After transplantation of MM-46 tumor cells into C3H mice, 30 μg/d of As-I was administered for 3 d and the spleen was extirpated after the periods indicated. Cytotoxic activity of the non-adherent spleen cell suspension against P-815 tumor cells was measured. As shown in Table IX, the activity was potentiated about 1.7 times on the 7th day after completion of the treatment, but the increase was only 1.15 times on the 9th day.

The cytotoxicity in tumor-bearing mice dosed with As-I may be due in part to lymphokine-activated killer cells (LAK), but the whole cytotoxic activity including both NK and LAK was taken as activity of NK cells in this experiment.

Next, the effect of As-I *in vitro* was examined, and the results are shown in Table X. After a 48 h incubation with 5 μg/ml of As-I, cytotoxic activity against P-815 tumor cells was measured. The cell suspension prepared from the spleen of MM-46 tumor-bearing mice on the 6th day of saline administration showed 0.9 times the cytotoxic activity of the control, but when As-I was injected, the activity was increased to 1.3 times the control. The potentiation was nullified 9 d after tumor implantation. These results suggest that As-I may potentiate the cytotoxicity of NK cells directly or may accelerate the differentiation of inactive pre-NK cells to active NK cells. Such activity has been reported in a muramic acid derivative (N-CWS)

TABLE IX. Effect of As-I on NK Activity of Non-adherent Spleen Lymphocytes in Relation to the Timing of Administration (*in Vivo*) to Tumor-Bearing Mice

Days after As-I administration	Agent	NK activity (%) (Relative cytotoxicity)	Ratio
3	Saline	8.08 ± 3.57	1.00
	As-I	9.59 ± 0.84[a)]	1.19
5	Saline	9.13 ± 1.18	1.00
	As-I	11.29 ± 0.34[b)]	1.24
7	Saline	7.47 ± 2.14	1.00
	As-I	12.81 ± 0.65[b)]	1.71
9	Saline	8.83 ± 0.97	1.00
	As-I	10.18 ± 1.36	1.15

t-Test: *a*) $p<0.05$, *b*) $p<0.01$.

TABLE X. Effect of As-I on NK Activity of Non-adherent Spleen Lymphocytes (*in Vivo*) from C3H Mice

Mouse and tumor	Agent	NK activity (ratio) (Relative cytotoxicity)	
		6 d	9 d
Normal mice	Saline	1.00	1.00
	As-I	1.06	0.95
MM-46-bearing mice	Saline	0.89	1.03
	As-I	1.33	1.11

TABLE XI. Effect of As-I on the Development of Alloreactive Cytotoxic T-Lymphocytes

Agent	Treatment (*in vivo*)	Cytolysis (%)	Ratio	
Saline	Non	21.07±1.83	1.00	1.00
	Anti-Thy 1.2+C′	8.39±0.91	0.40	
As-I	Non	27.07±0.74[a)]	1.00	1.28
	Anti-Thy 1.2+C′	14.31±1.14[a)]	0.53	

t-Test: *a*) $p<0.05$.

isolated from the cell walls of actinomyces by Saijo *et al.*,[5] and in lentinan obtained from shiitake by Herberman *et al.*[11]

Some structurally related β-glucans extracted from Basidiomycetes spp. (including lentinan) potentiate the induction of T cells (Tc).[12] Accordingly, the effect of As-I was examined, and the results are given in Table XI. After sensitization by i.p. inoculation of P-815 tumor cells as antigen cells into C3H mice, 30 μg/d of As-I was injected for 3 d. On the 9th day, whole spleen cell suspension was obtained from the spleen. The cytotoxic activity of this cell fraction was about 1.3 times that of mice given saline in place of As-I. When T cells were excluded from this cell suspension by treatment with anti-Thy 1.2 F7D5 monoclonal IgM cytotoxic antibody and complement, the cytotoxic activity was almost halved. This suggests that the cytotoxicity potentiated by As-I administration is derived from T cells. That is, As-I accelerated the induction of Tc. For such induction of Tc, in addition to antigen cells and precursors of T cells, IL-1 produced by activated Mϕ and IL-2 produced by helper T cells stimulated by IL-1 are required.

Rosenberg *et al.*[13] succeeded in inducing Tc injuring NK-resistant tumor cells by processing mouse spleen cells with IL-2. As-I is able to activate Mϕ *in vivo* and *in vitro*. Therefore, it is considered that As-I activates the production of IL-1 by Mϕ and subsequently the production of IL-2 from helper Tc, thus accelerating the induction of Tc.

In brief, As-I, a β-1,3-glucan isolated from mycelia of *Cochliobolus miyabeanus* (*Ascomycetes*), inhibited the growth of syngeneic tumors in mice. It not only caused direct activation of various effector cells to attack tumor cells, but also inhibited the secondary deterioration of immune function in the tumor-bearing hosts. Similar actions have been reported by β-glucans extracted from fruit bodies of *Basidiomycetes*, but this is the first report concerning a glucan from *Ascomycetes*. The action of As-I on lymphokines and IL-1 remains to be elucidated.

References

1) H. Nanba and H. Kuroda, *Chem. Pharm. Bull.*, **35**, 1285 (1987).
2) H. Nanba and H. Kuroda, *Chem. Pharm. Bull.*, **35**, 1289 (1987).
3) M. Ito, H. Suzuki, N. Nakano, N. Yamashita, E. Sugiyama, M. Maruyama, K. Hoshino and S. Yana, *Jpn. J. Cancer Res.* (*Gann*), **74**, 128 (1983).
4) R. B. Johnston, B. B. Keele, H. P. Misra, J. E. Lehmeyer, L. S. Webb, R. L. Baehner and K. V. Rajagopalan, *J. Clin. Invest.*, **55**, 1357 (1975).
5) N. Saijo, A. Ozaki, Y. Beppu, N. Irimajiri, N. Shibuya, E. Shimizu, T. Takizawa, T. Taniguchi and A. Hoshi, *Jpn. J. Cancer Res.* (*Gann*), **74**, 137 (1983).
6) H. Nakajima, S. Abe, Y. Masuko, J. Tsubouchi, M. Yamazaki and D. Mizuno, *Jpn. J. Cancer Res.* (*Gann*), **72**, 723 (1981).
7) K. Hashimoto and T. Kitagawa, *Cell Antigen*, **4**, 352 (1972).
8) K. Adachi, H. Nanba and H. Kuroda, *Chem. Pharm. Bull.*, **35**, 262 (1987).
9) H. Nakajima, Y. Kita, T. Takashi, M. Akasaki, F. Yamaguchi, S. Ozawa, W. Tsukada, S. Abe and D. Mizuno, *Jpn. J. Cancer Res.* (*Gann*), **75**, 260 (1984).

10) M. S. Meltzer and J. J. Oppenheim, *J. Immunol.*, **8**, 77 (1977).
11) R. B. Herberman, J. Y. Djeu, H. D. Kay, J. R. Ortaldo, C. Riccardi, G. D. Bonnard, H. T. Holden, R. Fargnani, A. Santoni and P. Pucetti, *Immunol. Rev.*, **44**, 43 (1979).
12) J. Hamuro, H. Wagner and M. Rollinghoff, *Cell Immunol.*, **38**, 328 (1978).
13) M. Rosenstein, I. Yron, Y. Kaufmann and S. A. Rosenberg, *Cancer Res.*, **44**, 1946 (1978).

[Chem. Pharm. Bull. 35(4)1531—1537(1987)]

Indispensability of Ubiquinone in the Aerobic Respiratory Chain of *Photobacterium phosphoreum*

KIYOSHI KONISHI,*,[a] HIROKAZU ADACHI,[b] and ISAMU HORIKOSHI[b]

Department of Biochemistry, Faculty of Medicine,[a] and Department of Hospital Pharmacy,[b] Toyama Medical and Pharmaceutical University, Sugitani, Toyama 930-01, Japan

(Received October 15, 1986)

Quinones contained in the membrane of *Photobacterium phosphoreum* grown aerobically were studied. Ubiquinone-8 (Q-8), menaquinone-8 (MK-8), and demethylmenaquinone-8 (DMK-8) were identified by mass spectroscopy. To establish the function of the quinones in the aerobic respiratory chain, depletion and reincorporation experiments were performed. Quinones were removed efficiently by *n*-pentane–acetone (9 : 1, v/v) extraction. The depleted membrane showed no reduced nicotinamide adenine dinucleotide (NADH) oxidase activity and yet retained NADH dehydrogenase activity and ubiquinol-1 (Q_1H_2) oxidase activity.

When Q-8 was reincorporated into quinone-depleted membrane vesicles by a freeze-thaw-sonication method, the NADH oxidase activity was restored completely. However, the other quinones contained in *P. phosphoreum* (MK-8 and DMK-8) did not have the ability to restore the activity of NADH oxidase. The Q_1H_2 oxidase or NADH dehydrogenase activity did not alter with the addition of the three kinds of quinones. These results suggest that Q-8 is a component of the aerobic respiratory chain of *P. phosphoreum*.

Keywords——ubiquinone-8; menaquinone-8; demethylmenaquinone-8; *Photobacterium phosphoreum*; respiratory chain

Introduction

Although ubiquinone, a small molecule, was discovered as early as 1957, the role of this component in the respiratory chain continues to be investigated. The indispensability of ubiquinone has been proved in many electron-transporting systems, such as those of mitochondria,[1,2] chloroplasts,[1,2] and bacteria.[1-5] We have purified and characterized the terminal oxidase of the respiratory chain of *Photobacterium phosphoreum* grown aerobically,[6] but the function and structure of other components of the respiratory chain have not been clarified in this organism. It is speculated that ubiquinone is an obligatory component of the native respiratory chain, because the purified enzyme has ubiquinol-1 (Q_1H_2) oxidase activity.

In order to clarify the role of ubiquinone in electron transport activity, the direct removal of quinone by extraction with an organic solvent from mitochondria,[7-9] submitochondrial particles,[7,10] or bacteria[11,12] and examination of the activity before and after reincorporation of quinone have been carried out in many laboratories.

In this paper, we identify the quinones of the respiratory chain of *P. phosphoreum*, report the results of experiments on quinone-depletion and reincorporation, and discuss the function of ubiquinone in the electron-transport system of *P. phosphoreum*.

Materials and Methods

Organism——Strain IAM12085 was from the Institute of Applied Microbiology, University of Tokyo, and was

grown in the medium described by Watanabe *et al.*[13] Inocula of 10 ml of seed culture were incubated in 2 l of medium in 5-liter glass containers at 25 °C for 20 h with vigorous aeration, and cells were harvested in the middle of the exponential phase of growth. The yield was 5 g wet weight of cells/l. The cells were stored at −20 °C before use.

Preparation of Membrane Vesicles——The frozen cell pellet was thawed and suspended in buffer A (10 mM Tris–HCl (pH 7.0) containing 10 mM $MgCl_2$). The suspension was sonicated with a Tomy Seiko UR-200p ultrasonic disruptor with cooling in an ice bath. The sonicated lysate was centrifuged at $20000 \times g$ for 30 min, and the supernatant obtained was centrifuged at $100000 \times g$ for 1 h. The precipitate was washed with buffer A by centrifugation, and suspended in buffer A.

Determination of Quinones——The extraction of quinones from sonicated membrane was carried out according to the method of Kröger[14] with some modifications. A suspension of membrane vesicles (100 mg of protein, 9 ml) was extracted with 27 ml of methanol–light petroleum (60 : 40, v/v) and the phases were separated by centrifugation. The upper phase was retained and the lower phase was extracted a further three times with light petroleum (14 ml). The extracts were combined, 18 ml of an ethanolic solution of ferric chloride (5 mg $FeCl_3 \cdot 6H_2O$/ml) was added, and the mixture was allowed to stand for 10 min at room temperature in the dark. The addition of $FeCl_3$ oxidized any reduced quinones present. The mixture was then extracted with water (12 ml) to remove $FeCl_3$, and the upper light petroleum layer was concentrated on a steam bath, and applied to Merck precoated silica gel plates (F_{254}). Each plate was then developed in a chloroform–light petroleum (70 : 30, v/v) solvent system. Ubiquinone was detected by its yellow color ($Rf = 0.5$) and naphthoquinones ran with Rf of approximately 0.7 (orange color). Each compound was eluted with ether, and the eluate was applied to a reversed-phase silica gel plate (F_{254}) as described by Dunphy and Brodie.[15] Ubiquinone ran as almost a single peak ($Rf = 0.6$), and naphthoquinones were determined as two spots ($Rfs = 0.34, 0.27$). These three quinone compounds were extracted with ether, and the eluate was taken to dryness by evaporation under reduced pressure. These samples were assayed by mass spectroscopy. The contents of quinones were calculated by the method of Wallace and Young.[16]

Mass Spectroscopy——Mass spectra (MS) were obtained with a Nippon Denshi JMS D-200 mass spectrometer.

Depletion of Quinones——To prepare the lyophilized and quinone-depleted particles, an improved version of the method described by Ernster *et al.*[17] was used. Lyophilization was performed with the membrane particles suspended in buffer A (about 20 mg of protein per ml) for 20—25 h to achieve complete dehydration. To deplete the quinones, 10 mg of the lyophilized particles was suspended in *n*-pentane (analytical grade, dried over anhydrous sodium sulfate) by gentle homogenization, and the suspension was shaken in a glass-stoppered tube for 5 min at 0 °C. The extraction was repeated 4 times, and the quinone-depleted membrane was dried in a rotary vacuum evaporator at room temperature to remove residual *n*-pentane.

Assay of Flavin and Cytochrome of Membrane Vesicles——The contents of protoheme and heme c were measured as pyridine hemochromogen ($\varepsilon = 34400$ and 29100 for protoheme and heme c, respectively) after separating protoheme from heme c by acid acetone treatment. The content of cytochrome d was calculated from the reduced minus oxidized difference spectrum using $\varepsilon = 10700$ ($E_{627} - E_{650}$).[6] The flavin content was also determined from the difference spectrum by the method of Cox *et al.*, ($E_{465} - E_{510}$, $\varepsilon = 11000$).[18]

Assay of Oxidase Activity—— Ubiquinol-1 oxidase activity was assayed spectrophotometrically as described previously.[19] The activity for oxidation of reduced nicotinamide adenine dinucleotide (NADH) was measured according to the method of Kasahara and Anraku,[20] using a Clark-type oxygen electrode (Rank Brothers, Rank oxygen electrode).

Assay of NADH Dehydrogenase Activity——NADH-ferricyanide and NADH-ubiquinone-1 dehydrogenase activities were assayed according to the methods of Dancey *et al.*[21] and Hatefi,[22] respectively.

Reconstitution with Quinone——The reconstitution was carried out by a freeze-thaw-sonication method.[23] Aliquots (500 μl) containing 6 mg of protein of membrane vesicles/ml, 50 mM Tris–HCl (pH 7.5), and 5 mM $MgCl_2$ were ultrasonicated for 1 min in a bath-type sonifier. An ethanol solution containing quinone (5 μl) was added, and sonication was repeated for 1 min. Each sample was frozen at −70 °C with cooled acetone solution. The frozen aliquot was thawed slowly at room temperature, and sonicated for 1 min. If the freeze-thaw was omitted, the restoration of NADH oxidase activity failed. On the other hand, if the third sonication step was omitted, the restoration was about 90% but the reproducibility of the extent of restoration was less good.

Other Method——Protein was determined by the method of Lowry *et al.*[24] with bovine serum albumin as a standard.

Chemicals——Ubiquinone-1 was a generous gift from Eisai Co., Ltd. 2-*n*-Heptyl-4-hydroxyquinoline-*N*-oxide (HQNO) was purchased from Sigma. Other chemical reagents used were of the highest purity commercially available.

Results

Identification of Quinones of *P. phosphoreum*

Extraction of quinones from sonicated membrane of *P. phosphoreum* was carried out as described under Materials and Methods. Thin layer chromatography (TLC) revealed a

benzoquinone fraction and a naphthoquinone fraction. Reversed-phase TLC indicated that the benzoquinone and naphthoquinone fractions contained one and two compounds, respectively.

The identification of these compounds was performed by mass spectroscopy. The MS of benzoquinone extracted from the reversed-phase TLC plate showed the expected molecular

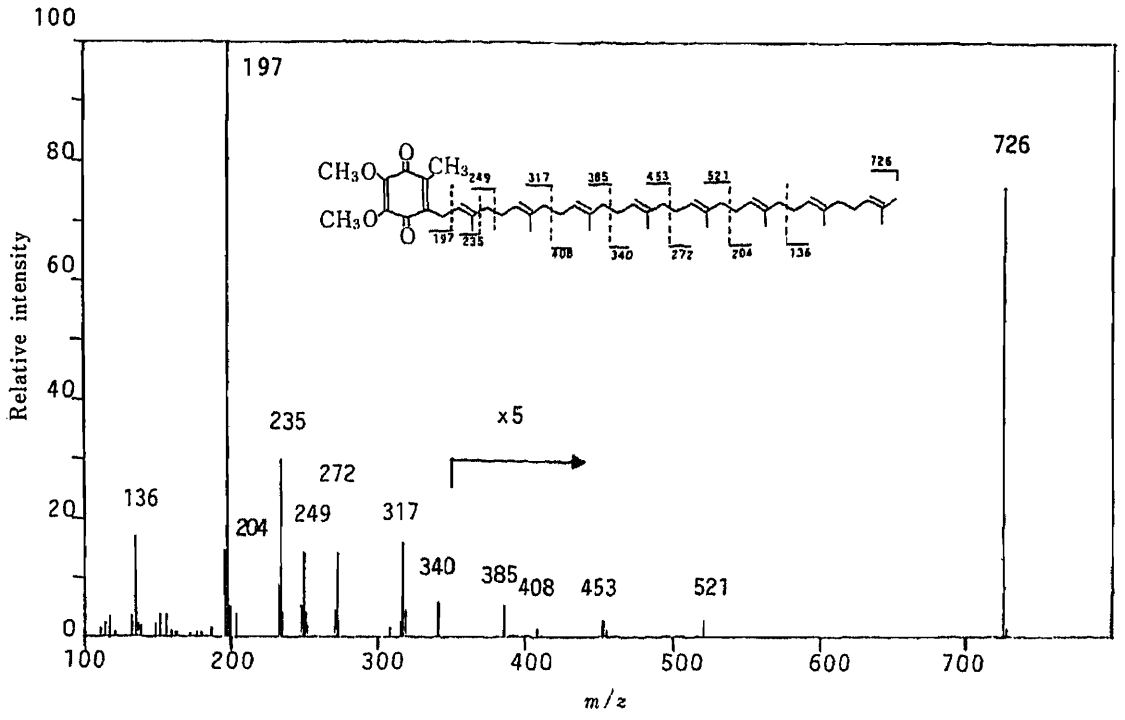

Fig. 1. Mass Spectrum of Q-8

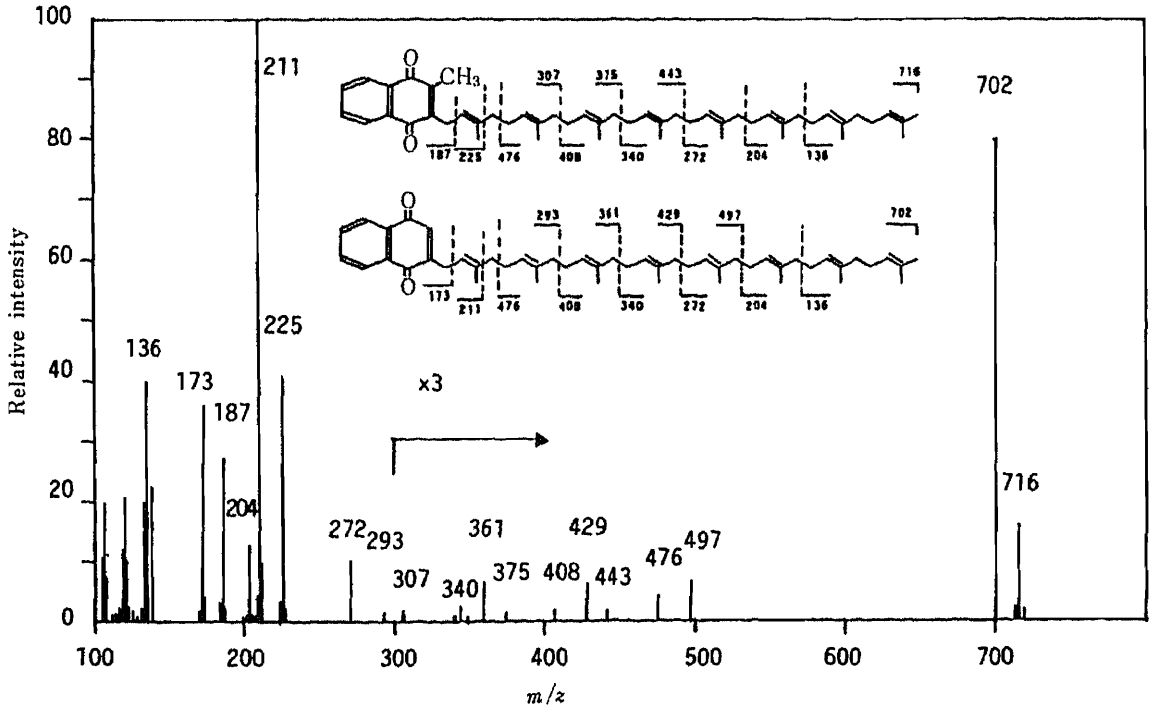

Fig. 2. Mass Spectrum of DMK-8 and MK-8

TABLE I. Contents of Some Membrane Components in Sonicated and Lyophilized Membrane Vesicles

	Content of component (nmol/mg of protein)[a]						
	Flavin	Q-8	DMK-8	MK-8	Cyt d[b]	Heme c	Protoheme
Sonicated membrane	3.02	1.20	0.38	0.08	0.309	0.336	0.220
Lyophilized membrane	3.15	1.39	0.39	0.08	0.295	0.314	0.201

a) Flavin and cytochrome d were determined by direct spectrophotometric examination of suspensions of the membrane. Heme c and protoheme were measured as pyridine hemochromogen after separation by acid acetone treatment. Quinones were extracted and purified before spectrophotometric determination. Details of methods are given in the Materials and Methods section. *b*) Cytochrome d.

ion at *m/z* 726 and this value indicated that the material was ubiquinone-8 (Q-8) (Fig. 1). The base peaks in the spectrum at *m/z* 235 and 197 can be attributed to the formation of a stable ion in which all but four and one of the carbon atoms of the isoprenoid side chain have been lost, respectively. In Fig. 2, the MS of the naphthoquinone fraction, containing two compounds, is shown; characteristic fragmentation patterns of menaquinone-8 (MK-8) and demethylmenaquinone-8 (DMK-8) are apparent. The strong peaks at *m/z* 702 and 716 correspond to molecular ions of DMK-8 and MK-8, respectively. The base peaks were also observed at *m/z* 211 and 225, and are derived from the naphthoquinone nucleus. The sequential degradation of the isoprene side chain can be seen (Figs. 1 and 2). Moreover, when each naphthoquinone separated by reversed-phase TLC was examined by mass spectroscopy, peaks at 702 and 211 were assigned to the larger *Rf* fraction (*Rf*=0.34), and peaks at 716 and 225 to the smaller *Rf* fraction (*Rf*=0.27) (data not shown). It was concluded that the smaller *Rf* compound was MK-8, and the other compound was DMK-8.

The contents of cytochromes and quinones of sonicated membrane vesicles prepared from *P. phosphoreum* are indicated in Table I. The content of ubiquinone was about 4 times that of cytochrome d (molar ratio). The contents of DMK-8 and MK-8 were only 32% and 7%, respectively, of that of Q-8.

Depletion of Quinones

We tried to remove quinones from the lyophilized particles of *P. phosphoreum* with various organic solvents. Neither *n*-pentane (Table II), *n*-hexane, nor isooctane could extract the quinones completely (not shown), and thus 20%—30% of the activity of NADH oxidase was always retained after the solvent treatment. About 90% of ubiquinone, menaquinone, and demethylmenaquinone were extracted with acetone, and the activity of NADH oxidase decreased to below 10%. However, the NADH oxidase activity of the membrane extracted with acetone was restored by the addition of Q-8 to only a half of the activity of the original membrane vesicles (data not shown). Since the NADH dehydrogenase activity was reduced by extraction of acetone (Table II), it is suggested that the activity of NADH oxidase could not be restored completely because of the impairment of the dehydrogenase.

Furthermore, *n*-pentane containing various concentrations of acetone could deplete quinones more efficiently than *n*-pentane alone, and NADH oxidase activity disappeared almost completely on extraction with *n*-pentane containing acetone. The extraction with pentane–acetone (9 : 1) was more efficient than that with pentane–acetone (19 : 1), but the efficiency of extraction decreased on increasing the concentration of acetone in the *n*-pentane (pentane–acetone (4 : 1)). On the other hand, cytochrome oxidase activity (Q_1H_2 oxidase) was retained almost completely after extraction with *n*-pentane containing acetone (Table II). Therefore, in our experiment, pentane–acetone (9 : 1) was used for extraction of quinones

TABLE II. Dehydrogenase Activities, Oxidase Activities, and Contents of Quinones in Quinone-Depleted Membranes

Treatment	Quinone content[a]			NADH[b] oxidase	Q_1H_2[c] oxidase	Dehydrogenase	
	Q-8	DMK-8	MK-8			NADH-Q_1[d]	NADH-ferri[e]
Lyophilized membrane	1.39	0.39	0.08	48.8	1.03	0.401	0.580
Pentane	0.31	0.07	0.02	14.9	1.09	0.320	0.544
Acetone	0.14	0.04	0.01	4.26	1.14	0.212	0.343
Pentane–acetone							
(19:1, v/v)	0.16	0.03	0.03	1.81	1.05	0.479	0.890
(9:1)	0.02	0.01	0.01	1.08	1.08	0.385	0.738
(4:1)	0.19	0.04	0.01	1.60	1.04	0.412	0.750

a) nmol/mg of protein. *b*) nmol O_2/min/mg of protein. *c*) μmol Q_1H_2/min/mg of protein. *d*) NADH-Q_1 oxidoreductase (μmol Q_1/min/mg of protein). *e*) NADH-ferricyanide oxidoreductase (μmol ferricyanide/min/mg of protein).

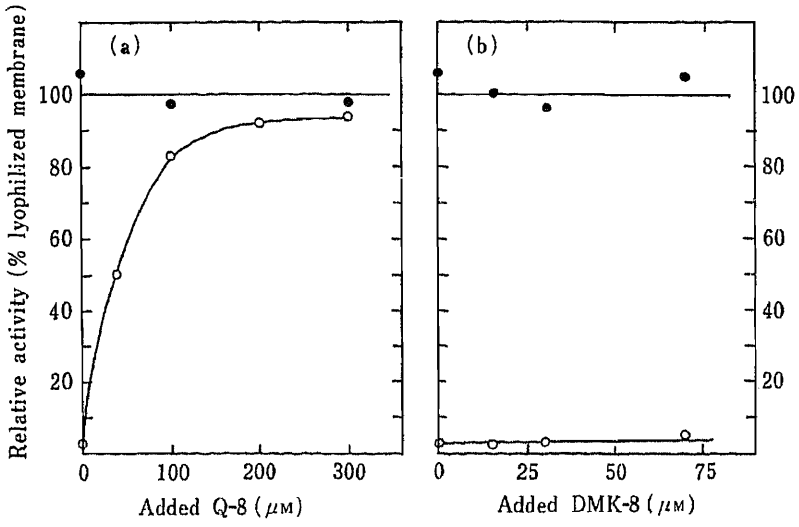

Fig. 3. Effect of Increasing Concentrations of Quinones on NADH Oxidation and Q_1H_2 Oxidation in Membrane Vesicles

Quinone depleted membrane vesicles were suspended in buffer containing 33 mM Tris-HCl (pH 7.5) and 5 mM $MgCl_2$, and were subjected to freeze-thaw-sonication as described under Materials and Methods. The final concentrations of quinones in the mixture at the freeze-thaw-sonication step are indicated. The activity of lyophilized membrane was taken as 100%. (○), NADH oxidase; (●), Q_1H_2 oxidase. a, reconstitution of Q-8; b, DMK-8.

from the membrane. The NADH-Q_1 oxidoreductase activity of the quinone-depleted membrane was the same as that of control membrane vesicles. NADH-ferricyanide dehydrogenase activity was not altered by the extraction. These results indicate that the intrinsic quinone is not required for these activities, except the NADH oxidase activity.

Reincorporation of Quinones

First we tried to use the method of Stroobant and Kaback.[25] The procedure is carried out by the addition of ubiquinone dissolved in the aprotic solvent dimethyl sulfoxide. This method, used on *Escherichia coli* membrane vesicles, was not suitable for our experiments, because NADH oxidase activity was restored to no more than 30% as compared with that of the control membrane.

In order to reincorporate quinone successfully, a freeze-thaw-sonication method[23] was used. This method can be carried out quickly, since complete removal of the organic solvent is

TABLE III. Effect of Inhibitors on NADH Oxidase Activities of Sonicated and Reconstituted Membrane Vesicles

Membrane	Inhibitor (concentration for 50% inhibition)		
	KCN	HQNO	$ZnCl_2$
Sonicated membrane	1.9 mM	1.7 μM	34 μM
Reconstituted membrane	2.4 mM	1.8 μM	27 μM

not required (ethanol is contained at below 1% in the reconstituted membrane fraction, but the activity is not inhibited by this concentration of alcohol). The composition of phospholipids of vesicles was not changed, because the addition of lipid, which is required in the method of Bergsma *et al.*,[26] was not done. The contents of flavin, protoheme, heme c, and cytochrome d were scarcely altered in the lyophilized (Table I), depleted, and reincorporated particles (data not shown).

Figure 3 shows the effect of concentration of additional Q-8 on the restoration of the oxidase activity. The oxidase activity was saturated in the concentration range of 200 to 300 μM Q-8, and was restored completely by the addition of Q-8. However, the addition of DMK-8 (Fig. 3) or MK-8 (not shown) did not restore the activity of NADH oxidase of depleted membrane vesicles, indicating that the MK-8 and DMK-8 do not have an important role in the aerobic respiratory chain of *P. phosphoreum*. The Q_1H_2 oxidase activity did not alter with the addition of ubiquinone. The addition of DMK-8 (Fig. 3) or MK-8 (not shown) did not affect Q_1H_2 oxidase either. The concentration of Q-8 binding to the membrane is 1.4 nmol/mg of protein on freeze-thaw-sonication treatment with 300 μM Q-8. The concentrations of DMK-8 and MK-8 were 0.4 and 0.3 nmol/mg of protein, respectively (at 100 μM DMK-8 and MK-8). These results exclude the possibility that DMK or MK does not bind to the membrane on freeze-thaw-sonication. The data obtained in this paper indicate that Q-8 is a constituent of NADH oxidase.

The effect of respiratory inhibitors was studied using membrane restored with 200 μM Q-8 and original sonicated membrane vesicles or lyophilized particles. $ZnCl_2$, KCN, and HQNO inhibited the NADH oxidase activity of the reconstituted particles to the same degree as that of the intact membrane (Table III) or lyophilized membrane (data not shown).

Discussion

We have purified the terminal oxidase (cytochrome bd complex) of the aerobic respiratory chain of *P. phosphoreum* to near homogeneity and characterized it.[6] The purified cytochrome bd complex showed Q_1H_2 oxidase activity, and the kinetic study indicated that the K_m and V_{max} values for the Q_1H_2 oxidase activity of the purified enzyme were the same as those of the sonicated membrane vesicles. These findings suggest that the physiological electron mediator is ubiquinone.

We first examined the quinones contained in *P. phosphoreum*. Q-8, DMK-8, and MK-8 were identified. Facultative aerobes, such as *E. coli*, often have three kinds of quinones (Q, MK, and DMK), and ubiquinone is essential to the function of electron transport of the aerobic respiratory chain. MK and DMK are involved in the anaerobic respiratory chain and the synthesis of uracil, as it was reported.[3,16]

Depletion and reincorporation of quinones were performed to establish their function in aerobic electron transport. This has also been done in the case of *Azotobacter vinerandii*[11] by the method described by Szarkowska.[9] Although *P. phosphoreum* is also a gram-negative

bacterium, we could not achieve the complete extraction of quinones from the organism by the method of Szarkowska. A similar observation was reported for *Pseudomonas aeruginosa*.[27] From our results, it is necessary to use *n*-pentane containing acetone as the extracting solvent for complete extraction of quinones.

Although the procedure of Stroobant and Kaback[25] was used for the reconstitution, complete restoration of activity was not obtained. Thus, we tried a freeze-thaw-sonication method.[23] With this procedure, activity about equal to that of the control membrane was obtained. Three kinds of quinones were contained in *P. phosphoreum*, but the restoration of NADH oxidase activity was achieved only by the addition of Q-8. These results imply that Q-8 is a component of the aerobic respiratory chain, and the other quinones are not.

References

1) F. L. Crane, *Ann. Rev. Biochem.*, **46**, 439 (1977).
2) Y.-P. Wan and K. Folkers, "Methods in Enzymology," Vol. 53, ed. by S. Fleischer and L. Packer, Academic Press, New York, 1978, pp. 591—599.
3) B. A. Haddock and C. W. Jones, *Bacteriol. Rev.*, **41**, 47 (1977).
4) M. D. Collins and D. Jones, *Microbiol. Rev.*, **45**, 316 (1981).
5) F. Gibson, *Biochem. Soc. Trans.*, **1**, 317 (1973).
6) K. Konishi, M. Ouchi, K. Kita, and I. Horikoshi, *J. Biochem.* (Tokyo), **99**, 1227 (1986).
7) F. L. Crane, C. Widmer, R. L. Lester, and Y. Hatefi, *Biochim. Biophys. Acta*, **31**, 476 (1959).
8) R. L. Lester and S. Fleischer, *Biochim. Biophys. Acta*, **47**, 358 (1961).
9) L. Szarkowska, *Arch. Biochem. Biophys.*, **113**, 519 (1966).
10) L. Ernster, I.-Y. Lee, B. Norling, and B. Persson, *FEBS Lett.*, **3**, 21 (1969).
11) R. T. Swank and R. H. Burris, *J. Bacteriol.*, **98**, 311 (1969).
12) A. Kröger, V. Dadak, M. Klingenberg, and F. Diemar, *Eur. J. Biochem.*, **21**, 322 (1971).
13) H. Watanabe, N. Miura, A. Takimoto, and T. Nakamura, *J. Biochem.* (Tokyo), **77**, 1147 (1975).
14) A. Kröger, "Methods in Enzymology," Vol. 53, ed. by S. Fleischer and L. Packer, Academic Press, New York, 1978, pp. 579—591.
15) P. J. Dunphy and A. F. Brodie, "Methods in Enzymology," Vol. 18C, ed. by R. W. Estabrook and M. E. Pullman, Academic Press, New York, 1967, pp. 407—461.
16) B. J. Wallace and I. G. Young, *Biochim. Biophys. Acta*, **461**, 84 (1977).
17) L. Ernster, E. Glaser, and B. Norling, "Methods in Enzymology," Vol. 53, ed. by S. Fleischer and L. Packer, Academic Press, New York, 1978, pp. 573—579.
18) G. B. Cox, N. A. Newton, F. Gibson, A. M. Snoswell, and J. A. Hamilton, *Biochem. J.*, **117**, 551 (1970).
19) K. Kita, K. Konishi, and Y. Anraku, *J. Biol. Chem.*, **259**, 3368 (1984).
20) M. Kasahara and Y. Anraku, *J. Biochem.* (Tokyo), **72**, 777 (1972).
21) G. F. Dancey, A. E. Levine, and B. M. Shapiro, *J. Biol. Chem.*, **251**, 5911 (1976).
22) Y. Hatefi, "Methods in Enzymology," Vol. 53, ed. by S. Fleischer and L. Packer, Academic Press, New York, 1978, pp. 11—14.
23) K. Konishi, K. Kita, and Y. Anraku, Abstracts of Papers, 52nd Annual Meeting of the Japanese Biochemical Society, Tokyo, August 1979, p. 628.
24) O. H. Lowry, N. J. Rosebrough, A. L. Farr, and R. J. Randall, *J. Biol. Chem.*, **193**, 265 (1951).
25) P. Stroobant and H. R. Kaback, *Biochemistry*, **18**, 226 (1979).
26) J. Bergsma, K. E. Meihuizen, W. V. Oeveren, and W. N. Konings, *Eur. J. Biochem.*, **125**, 651 (1982).
27) K. Matsushita, M. Yamada, E. Shinagawa, O. Adachi, and M. Ameyama, *J. Biochem.* (Tokyo), **88**, 757 (1980).

[Chem. Pharm. Bull. 35(4)1538—1545(1987)]

Studies on Dissolution Mechanism of Drugs from Ethylcellulose Microcapsules[1)]

YOSHIYUKI KOIDA,* HIDEO TAKAHATA, MASAO KOBAYASHI and MASAYOSHI SAMEJIMA

Products Formulation Research Laboratory, Tanabe Seiyaku Co., Ltd., 16-89 Kashima-3-chome, Yodogawa-ku, Osaka 532, Japan

(Received August 28, 1986)

The dissolution behavior of 4 drugs from ethylcellulose (EC) microcapsules (MC) was examined at various temperatures. From the early dissolution curves, the apparent dissolution rate constants and permeability constants (P_m) were estimated. The permeation across a Millipore filter and an EC cast membrane were also examined for comparison. The values of activation energy of P_m of MC ranged from 4.0 to 7.6 kcal/mol, independently of the drug solubility, and were close to those obtained for permeation through the Millipore filter and EC cast membrane. P_m values of the EC cast membrane (thickness: 10 μm) were small and decreased greatly with increase in the thickness. These results suggested that the drugs were not transported through the polymer phase but through the water channels existing in the MC membrane. Superposition analysis was applied to the dissolution curves measured at various temperatures and it was found that the extent of the superposition was better for less water-soluble drugs. The dependency of drug permeation through MC on wall thickness (from 5 to 20 μm) was examined using isoniazid. P_m values decreased linearly up to about 12 μm and were constant for a thicker wall at all dissolution temperatures. The activation energy of the dissolution rate constants increased with increasing wall thickness. The water-channels were classified into two types, one with fairly large pores or cracks and which was predominant in thinner films, and another with fine and uniformly distributed channels and which was predominant in thicker films.

Keywords——microcapsule; dissolution mechanism; ethylcellulose; dissolution rate; permeability; dissolution curve; activation energy; superposition

To develop microcapsules (MC) for sustained release dosage forms, the mechanism of drug transport from MC must be understood. So far, for the release from MC, the following three pathways[2)] have been considered; 1) through the continuous polymer phase, 2) through inter-connecting channels such as fine pores or minute cracks and 3) through parallel pathways of continuous polymer phase and channels.

In the case of 1), the flux is expressed by Eq. 1:

$$dQ/dt = P_c P_m A(C_i - C_o)/l_m \quad (1)$$

where Q is the amount of drug permeated at time t, P_c is the partition coefficient of the drug between bulk solution and membrane, P_m is the permeability constant, A is the surface area of the membrane, l_m is the wall thickness, and C_i and C_o are the concentrations of the drug in donor and receiver solutions, respectively. In the case where the sink condition is satisfied, Eq. 1 can be rewritten as Eq. 2 at the early stage of dissolution.

$$dQ/dt = P_c P_m A C_s/l_m \quad (2)$$

where C_s is the solubility of the drug.

On the other hand, if drugs are transported through water channels existing in the film, the flux is expressed by Eq. 3:

$$dQ/dt=(\varepsilon/\tau)DAC_s/l_m \quad (3)$$

where ε is the fractional area, τ is the tortuosity and D is the diffusion constant of a drug in the aqueous phase.

Whichever mechanism, 1) or 2), is predominant, the dissolution curve from MC seems to be zero order, as is clear from Eqs. 2 and 3, if the nature of the film does not change throughout the dissolution test. Therefore, it is difficult to distinguish between the dissolution mechanisms 1) and 2) only from an analysis of the dissolution pattern. However, since the energy barrier to drug transport through the polymer phase should be larger than that through the liquid phase, we studied the dependency of the dissolution rate on temperature and estimated the activation energy. Four drugs were used in this study to examine the influence of solubility on the transport mechanism.

Experimental

Preparation of Core Materials——Isoniazid, vitamin B_6, trimebutine maleate and theophylline, whose solubilities at 25 °C in the 1st fluid of disintegration test in JP XI were 18.2, 14.2, 2.0 and 0.74 g in 100 ml, respectively, were used as model drugs. To eliminate the geometrical factor due to the difference in crystal shapes, spherical core materials were prepared by the following methods.

Method 1[1]: Powdered drugs (400g) were mixed with microcrystalline cellulose (90 g) and kneaded with a polyvinyl alcohol (10 g) solution. The kneaded materials were extruded through a 0.5 mm screen by use of a blade-type extruder and were spheronized by treatment with a marumerizer. Unless otherwise noted, all granules were prepared by this method.

Method 2: A mixture of isoniazid (800 g), microcrystalline cellulose (180 g) and polyvinyl alcohol (20 g) solution was treated in a high-speed mixer (Fukae Kogyo Co., Ltd.) with an impeller speed of 400 rpm and a chopper speed of 3000 rpm and the mixture was granulated into spherical particles.

After drying, the particles which passed through a 28 mesh (590 μm) screen and remained on a 36 mesh (420 μm) screen were used as spherical core materials. The values of the index of sphericity, the ratio of the length of the longest diameter to that of the perpendicular diameter to the longest one passing through the middle point of the core materials, were 1.1—1.3 in all cases.

Preparation of MC——Ethylcellulose (EC) MC were prepared by the coacervation method from cyclohexane using polyisobutylene (PIB) as the coacervation inducing agent as described in the previous paper.[1]

Evaluation of MC Properties——The release measurement was carried out in the 1st fluid of the disintegration test of JP XI as described in the previous paper[1] using spherical MC having diameters ranging from 420 to 710 μm. From the dissolution curve, P_m was calculated by using Eq. 4.

$$P_m=k_{app}Vl_m/(AC_s) \quad (4)$$

where k_{app} is the dissolution rate constant calculated from the early stage of the dissolution curve and V is the volume of the dissolution medium. The average wall thickness (l_m) was calculated by means of Lafont's equation as previously reported.[3]

Preparation of Plane Cast Membrane of EC[4]——Chloroform solution containing 10% EC (Dow Chemical Company, standard type, viscosity in toluene–ethanol mixture: 100 cP) was spread on a glass plate by means of an applicator and dried at room temperature for more than a day. The glass plates were immersed into water and the cast film was peeled off carefully. The film thickness was determined after drying by the use of a dial gauge (Ozaki Mfg. Co.) at 9 points and the mean thickness was estimated.

Determination of the Permeability Constant of EC Cast Membrane and Millipore Filter——The dissolution measurement apparatus developed by Muranishi *et al.*[5] was used. A Millipore filter (VC, pore size 0.1 μm, diameter 4.5 cm) or EC cast membrane was fixed at the end of the donor cell. In the case of the Millipore filter, the donor cell containing 55 ml of the 1st fluid was immersed into the receiver cell containing 600 ml of the 1st fluid. At that time, the fluid level in the donor cell was kept at the same height as the receiver solution. The solution was degassed under vacuum. Then this dissolution apparatus was put into a thermostated water bath. After the temperature of the solution had become constant, 5 ml of a 0.5% drug solution in the 1st fluid at the same temperature was added to the donor cell and the surface height was adjusted again. At suitable intervals, about 5 ml of the bulk solution was taken from the receiver solution and the concentration of the released drugs was spectrophotometrically determined. Then the solution was immediately returned to the bulk solution to maintain the original volume.

For the EC cast membrane, the concentration of the drug in the donor cell was increased to above 0.8% because the transported amounts were small. In the case of potassium chloride, permeation experiments were performed in water and not in the 1st fluid, and the amount of potassium chloride transported to water was determined by means

of a conductivity meter.

P_m values were calculated by means of Eq. 5.[6]

$$P_m t = \frac{l_m/A}{(1/V_i + 1/V_o)} \ln\left(\frac{1+(C_o/C_i)(V_o/V_i)}{1-(C_o/C_i)}\right) \quad (5)$$

where t is the permeation time, and V_i and V_o are the volumes of the donor cell and receiver cell, respectively. The plot of the value of the right-hand side in Eq. 5 against t showed good linearity. Thus the P_m values were calculated from the slope.

Adsorption of Drugs on EC——EC (5 g) was dispersed in 100 ml of the 1st fluid which contained 10 mg of drug and the mixture was maintained at 25 °C under agitation for more than 24 h. The amount of adsorbed drug was calculated from the decrease of drug concentration in the solution.

Calculation of Activation Energy and Heat of Solubilization——Activation energies of dissolution rate constant (k_{app}), permeability constant (P_m) and heat of solubilization (H_s) were calculated as (K·gas constant) from the slopes (K) obtained by plotting the logarithm of k_{app}, P_m and C_s against the reciprocal temperature ($1/T$).

Results and Discussion

Dissolution Behavior from MC Containing Various Drugs

In Fig. 1, the dissolution curves of vitamin B_6, trimebutine maleate, and theophylline at various temperatures are shown as examples. These drugs were released linearly at the early stage of dissolution, and thus the zero order dissolution constant, k_{app}, was estimated from the early dissolution data, and P_m values were calculated as reported previously. The logarithms of these values at different temperatures were plotted against $1/T$ and the activation energy was determined. In Fig. 2, plots of k_{app} and C_s are shown as examples. As shown in Fig. 2, linear relationships were observed for both $\ln k_{app}$ and $\ln C_s$, and the drugs of higher solubility gave higher k_{app} values.

The activation energy of the dissolution rate constant of MC, $(Ek_{app})_{MC}$, that of the permeation constant of MC, $(EP_m)_{MC}$, and the heat of solubilization, H_s, are shown in Table I. On the other hand, the P_m values of the drugs through the Millipore filter, which was used as a model of a porous membrane, and those of isoniazid through the EC cast membrane were determined at various temperatures by means of Eq. 5. The activation energies were calculated by the same method and are also shown in Table I as $(EP_m)_{Mf}$ and $(EP_m)_{EC}$, respectively.

As shown in Table I, the values of $(EP_m)_{MC}$, $(EP_m)_{Mf}$ and $(EP_m)_{EC}$ were 4.0—7.6, 3.6—5.7 and 4.6 kcal/mol, respectively, and can be regarded as similar. The values of $(Ek_{app})_{MC}$ were

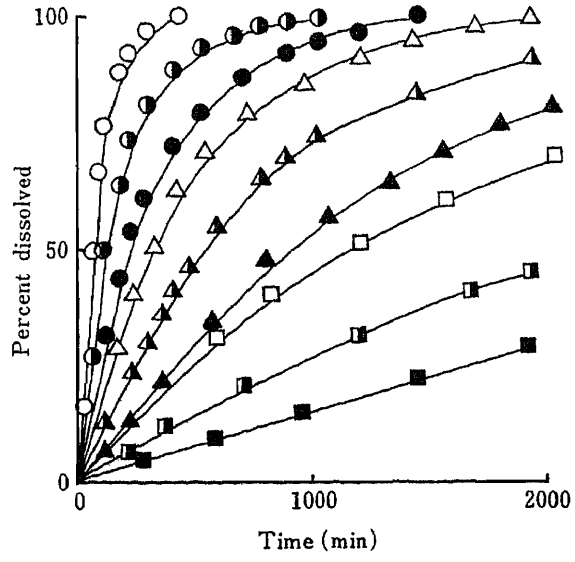

Fig. 1. Dissolution Curves of Drugs from MC at Various Temperatures

The drugs in core material: vitamin B_6 (○, ◑, ●), trimebutine maleate (△, ▲, ▲) and theophylline (□, ◨, ■). Dissolution temperature: 25 °C (●, ▲, ■), 37 °C (◑, ▲, ◨) and 50 °C (○, △, □).

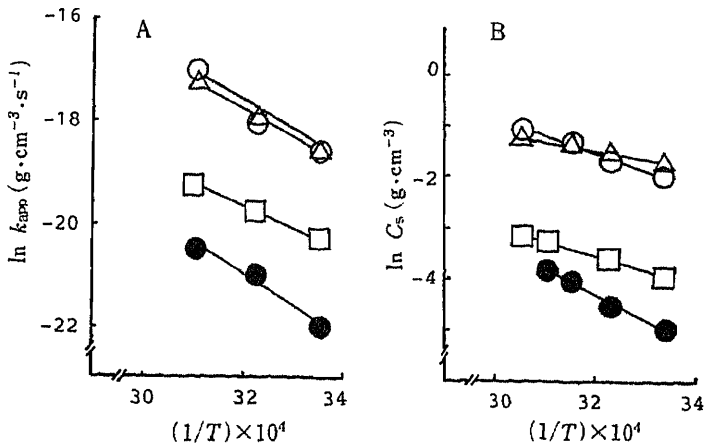

Fig. 2. Dependency of Dissolution Rate Constants and the Solubilities of Drugs on Temperature

A, dissolution rate constants from MC; B, solubilities of drugs in the 1st fluid. Isoniazid (○), vitamin B_6 (△), trimebutine maleate (□) and theophylline (●).

TABLE I. Comparison of Activation Energies[a] of k_{app} and P_m

	Isoniazid	Vitamin B_6	Trimebutine maleate	Theophylline
$(Ek_{app})_{MC}$	10.7	10.7	9.1	12.7
$(EP_m)_{MC}$	4.9	7.6	4.1	4.0
$(EP_m)_{Mf}$	4.7	5.7	3.7	3.6
$(EP_m)_{EC}$	4.6	—	—	—
H_s	5.9	3.1	6.5	8.8

a) kcal/mol.

between 9.1 and 12.7 kcal/mol and were nearly equal to $(EP_m)_{Mf}+H_s$. Diffusion of the molecule as it proceeds exchanges the space between two molecules, and the activation energy corresponds to the energy barrier for this exchange. Thus the energy barrier of diffusion through the polymer phase should be much higher than that through the aqueous phase because the movement of the polymer segment is more restricted than that of the water molecules. Barrie[2c] suggested that the diffusion activation energy of low-molecular-weight and nonelectrolyte materials in the fluid is about 5 kcal/mol, whereas the activation energy is 15—20 kcal/mol for permeation through solid materials. Table I shows that $(EP_m)_{MC}$, $(EP_m)_{Mf}$ and $(EP_m)_{EC}$ were similar to each other and quantitatively close to 5 kcal/mol. Therefore, drugs are presumed to be transported mainly through water channels existing in the wall materials.

Vidmar *et al.*[7] reported that such plots of apparent diffusion constant values for EC MC of sodium barbital showed two phases and they explained the phenomena in terms of a parallel pathway. However, our drugs did not show such a discontinuity. The reason for this difference is not clear at present. However, the difference in drugs used, in the dissolution medium or in the shape of the core material might be the cause.

To examine our hypothesis in more detail, drug transport experiments through an EC cast membrane were done. First, P_m values of potassium chloride in 0.1 N solution were determined using EC cast membranes with various thicknesses. As shown in Table II, the P_m values decreased significantly from the order of 10^{-10} to nearly zero with increasing wall

thickness from 7.5 to 40 μm. The membrane constant, f, defined by Eq. 6 was calculated and is also shown in Table II:

$$f = P_m/D \tag{6}$$

where 1.887×10^{-5} cm$^2 \cdot$s^{-1} was used as the diffusion constant (D) of the 0.1 N potassium chloride solution.[8] The f value corresponds to ε/τ in Eq. 3 and changed from the order of 10^{-5} to 10^{-10} with increase of the wall thickness from 7.5 to 15 μm and became almost zero at 40 μm. This phenomenon also supports the water channel pathway release mechanism theory, because if the drugs are transported through the polymer phase, the P_m and f values of the cast membrane should be constant (independent of the film thickness), as can be anticipated from Eq. 2. The great decrease of P_m and f values with increase in the film thickness could be caused by the closure of the channels by the increase in film thickness.

The same Millipore filter and apparatus were used to obtain the diffusion constants of drugs by applying Eq. 7.

$$D = (\alpha/\alpha_s)D_s \tag{7}$$

where α and α_s are the slope of a drug and a standard material (potassium chloride) obtained in Eq. 5, respectively, and D_s is the diffusion constant of potassium chloride.[8] Thus, the f values of MC and those of the EC cast membrane obtained using the same membrane were calculated for the drugs (Table II). The f values of MC were of the order of 10^{-4} whereas those of the cast membrane were of the order of 10^{-5}, being independent of the solubility of the four drugs. The large difference in the f values between the cast membrane and MC suggests that there were more water channels in the MC wall than in the EC cast membrane.

Donbrow and Friedman[4] found that the P_m values of salicylic acid and caffeine through a cast plane membrane of EC differed greatly (0.27×10^{-8} cm$^2 \cdot$s^{-1} and 0.44×10^{-10} cm$^2 \cdot$s^{-1}, respectively). They considered that the difference is based on the difference in the affinity of the drugs to EC. Therefore, we also determined the adsorption of the four drugs on EC in the 1st fluid. The adsorbed amounts of vitamin B_6, isoniazid, trimebutine maleate were undetectably small. That of theophylline was detectable, but only 0.13 mg of theophylline was adsorbed per 1 g of EC. Thus dissolution of these drugs in the polymer phase seems to be negligibly small. This supports the model of the water-channel process.

In the development of pharmaceutical dosage forms, overall dissolution patterns are

TABLE II. Comparison of P_m and f Values between Cast Membrane and MC (at 25 °C)

	Cast membrane			MC		
	Wall thickness (μm)	P_m ($\times 10^{10}$) (cm$^2 \cdot$s^{-1})	f ($\times 10^5$)	Wall thickness (μm)	P_m ($\times 10^{10}$) (cm$^2 \cdot$s^{-1})	f ($\times 10^5$)
Potassium chloride	7.5	5.1	2.7	—	—	—
	10.0	4.2	2.2	—	—	—
	15.0	0.0012	0.00064	—	—	—
	40.0	0[a]	—	—	—	—
Isoniazid	10.0	2.3	4.3	11.9	28	54
Vitamin B_6	10.0	1.1	2.4	13.7	27	58
Trimebutine maleate	10.0	1.9	3.8	15.1	42	83
Theophylline	10.0	1.1	1.9	18.1	25	44

a) Not detected.

important as well as the drug dissolution rate. The applicability of Higuchi, zero order, 1st order and other equations for drug release has been examined by many researchers.[9] However, no equation can fit the whole range of dissolution patterns. Donbrow *et al.*[10] recently noted that the release of the drugs from an individual MC obeyed zero order kinetics, though the release curve of total MC reflected the variance of dissolution curves of individual MC. From Fick's diffusion law, zero-order release would be expected under the sink condition, as shown in Eqs. 2 and 3. However in practice, the dissolution patterns do not always show zero order release. Thus in a case where the kinetic mechanism is not clear, superposition analysis of the dissolution curve by the use of reduced time, T_r, defined by Eq. 8, is useful to compare the whole dissolution pattern.[1]

$$T_r = t/T_s \tag{8}$$

where T_s is the time necessary for a definite amount of drug to be released from MC. Here, the quarter-release time t_{25} was chosen for T_s because all MC showed linear release at an early stage. The release proceeds by the same mechanism and only the dissolution rate differs, if the

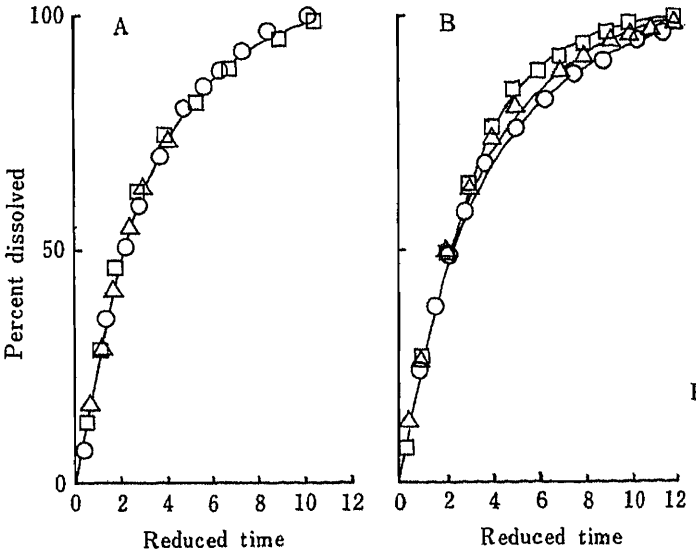

Fig. 3. Superposition of Dissolution Curves from MC at Various Temperatures

Dissolution tests were carried out at 25 °C (○), 37 °C (△) and 50 °C (□).
A, trimebutine maleate; B, vitamin B_6.

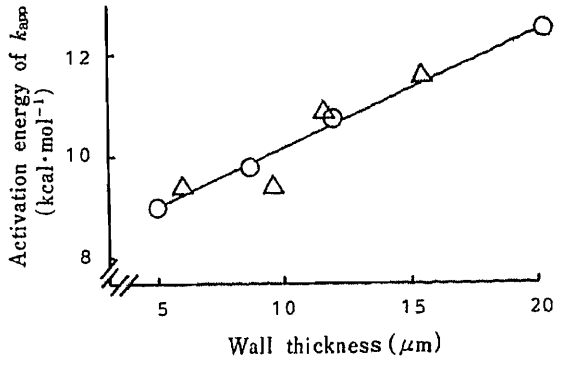

Fig. 4. Influence of the Wall Thickness on the Activation Energy of Dissolution from Isoniazid MC

Core spherical materials were prepared using an extruder-marumerizer (○) and a high-speed mixer (△).

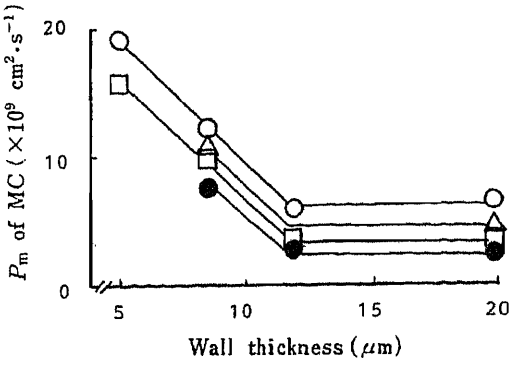

Fig. 5. P_m Values Calculated at Various Temperatures for Isoniazid MC Having Various Wall Thicknesses

The dissolution temperatures were 25 °C (●), 37 °C (□), 50 °C (△) and 55 °C (○).

dissolution patterns at various temperatures are superposed perfectly.

The dissolution curves of trimebutine maleate were superposed well as shown in Fig. 3A. Those of theophylline were also superposed well. These results indicate that the mechanism of dissolution was basically the same, being independent of the dissolution temperature. However those of vitamin B_6 (Fig. 3B) and isoniazid showed slight discrepancies and the degree of delay from zero-order dissolution was more at lower temperature. Such a discrepancy was more obvious for the drugs with higher solubility. The reason for this discrepancy is not clear, but it may be due to the osmotic pressure, because the increase in the osmotic pressure with increase in the temperature is greater in the MC containing drugs with higher solubility such as vitamin B_6 and isoniazid; consequently MC might be expanded more, resulting in faster drug release at higher temperature.

Dissolution of Isoniazid from MC with Different Values of Wall Thickness

Using MC of isoniazid having various wall thicknesses, k_{app} values were determined at

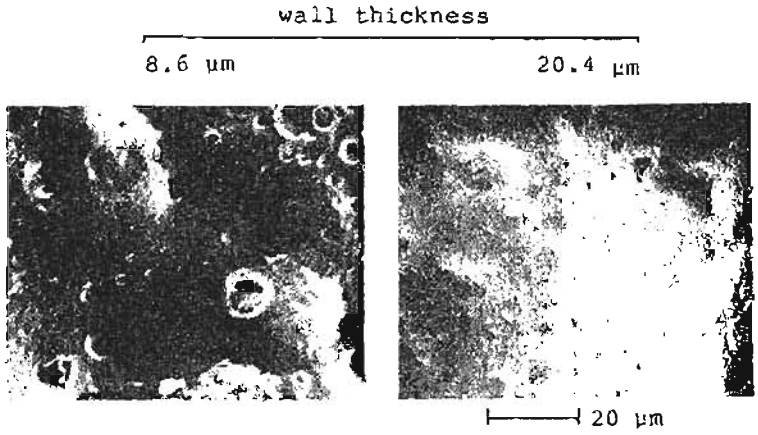

Fig. 6. The Surface of MCs Having Different Wall Thicknesses

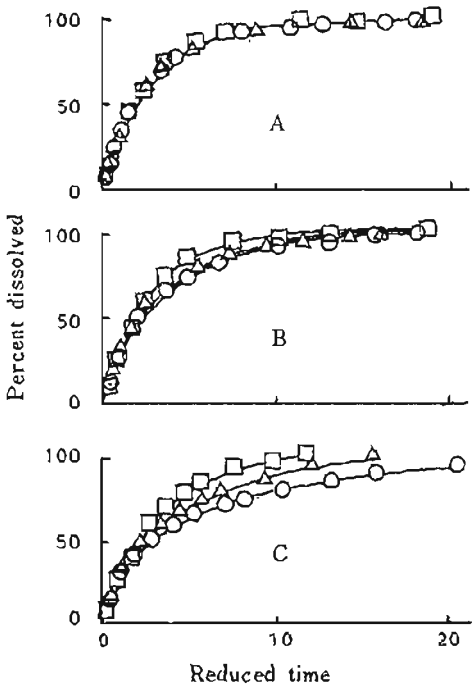

Fig. 7. Superposition of Dissolution Curves Obtained from Isoniazid MCs Having Various Wall Thicknesses

The wall thicknesses of MC were 8.6 μm (A), 11.9 μm (B) and 20.4 μm (C).
Dissolution tests were carried out at 25 °C (○), 37 °C (△) and 55 °C (□).

various temperatures. The values of activation energy of dissolution of isoniazid from MC $(EK_{app})_{MC}$ were estimated and plotted against the wall thickness (Fig. 4). $(EK_{app})_{MC}$ values increased with increasing wall thickness. This tendency was also observed in the case where core materials were prepared by use of the high-speed mixer.

As shown in Fig. 5, the P_m values decreased with increase of the wall thickness up to 12 μm at every temperature, and took a constant value over 12 μm. Many pores of about 3 μm were observed on the surface of the MC with a thickness of 8 μm by the use of a scanning electron microscope. However, these pores were rarely observed in the MC with a wall thickness of 20 μm (Fig. 6). The appearance of the wall surface was essentially the same before and after the dissolution test.

The superposition method was also applied for MC with various wall thicknesses (Fig. 7). The dissolution curves of the MC with a wall thickness of 5.0 and 8.6 μm were well superposed. However, the dissolution curves for the MC with a wall thickness of 11.9 μm were less well superposed, and the discrepancy increased at 20.4 μm. The delay from zero order increased with decrease in temperature.

From the above results, the water channels of MC could be classified into two types, one with fairly large pores or cracks and which is predominant at wall thickness less than 12 μm, and another type with very fine and uniformly distributed channels and which is predominant in walls thicker than 12 μm (Figs. 5 and 6). The difference of transport with film thickness might be explained as follows. When the film thickness is less than 12 μm, the dissolved drug would predominantly be transported through the fairly large pores and the resistance to transport would be small, so that the activation energy is lower, and the $(Ek_{app})_{MC}$ value was nearly equal to $(EP_m)_{Mf}+H_s$ (Fig. 4). As the wall became thicker, the percentage of the drug transported through the fine pores would increase. The increase of $(Ek_{app})_{MC}$ with the wall thickness suggests that some changes occur in the pore structure of a thicker film with increase in the temperature. The swelling of the EC membrane is a possible reason for the change, but no swelling was observed after 3 d of immersion of the EC film in the 1st fluid, and this is in agreement with the findings of Senjkovic and Jalsenjak.[11] Another reason may be the higher osmotic pressure produced by an elevated temperature. Slackness of the polymer network, expansion of pores, and increase of the fine pore number might be produced by the higher osmotic pressure, and might account for the poorer superposition in the thicker films (Fig. 7).

References and Notes

1) Y. Koida, M. Kobayashi and M. Samejima, *Chem. Pharm. Bull.*, **34**, 3354 (1986).
2) *a*) G. L. Flynn, S. H. Yalkowsky and T. J. Roseman, *J. Pharm. Sci.*, **63**, 479 (1974); *b*) P. B. Deasy, "Microencapsulation and Related Drug Processes," Marcel Dekker, Inc., New York and Basel, 1984, pp. 289—319; *c*) J. A. Barrie, "Diffusion in Polymers," ed. by J. Crank and G. S. Park, Academic Press, New York, 1968, pp. 280—283.
3) Y. Koida, G. Hirata and M. Samejima, *Chem. Pharm. Bull.*, **31**, 4476 (1983).
4) M. Donbrow and M. Friedman, *J. Pharm. Pharmacol.*, **27**, 633 (1975).
5) M. Muranishi, Y. Okubo and H. Sezaki, *Yakuzaigaku*, **39**, 1 (1979).
6) M. Nakagaki and N. Koga, "Yakuhin Buturikagaku," Nankodo, Japan, 1975, p. 144.
7) V. Vidmar, I. Jalsenjak and T. Kondo, *J. Pharm. Pharmacol.*, **34**, 411 (1982).
8) Nihon Kagakukai (ed.), "Kagaku Binran," Maruzen Co., Ltd., Tokyo, 1960, p. 465.
9) *a*) H. S. Yolabik-Kas, *Drug Dev. Ind. Pharm.*, **9**, 1047 (1983); *b*) H. W. Jun and J. W. Lai, *Int. J. Pharmaceut.*, **16**, 65 (1983); *c*) J. R. Nixon and S. E. Walker, *J. Pharm. Pharmacol.*, **23**, 147 suppl. (1971); *d*) S. Benita and M. Donbrow, *ibid.*, **34**, 77 (1982).
10) *a*) A. Hoffman, M. Donbrow, S. T. Gross, S. Benita and R. Bahat, *Int. J. Pharmaceut.*, **29**, 195 (1986).
11) R. Senjkovic and I. Jalsenjak, *J. Pharm. Pharmacol.*, **33**, 279 (1981).

[Chem. Pharm. Bull. 35(4)1546—1554(1987)]

Gastric-Acidity-Controlled Rabbits: Control of Gastric pH of Rabbits by the Use of Antacids

TERUTAKA TAKAHASHI,* YUKO UEZONO, and YUTAKA NAKANISHI

Pharmaceutical Research Laboratories, Dainippon Pharmaceutical Co., Ltd., Enoki 33–94, Suita, Osaka 564, Japan

(Received September 1, 1986)

A method for controlling the gastric pH of rabbits to low acidity (pH>4) by using different antacids was investigated, and the physiological state of rabbits during gastric-acidity control and repeated bioavailability tests was also examined in terms of hemocytological and clinico-biochemical parameters. Neither dried aluminum hydroxide gel (DAH) nor synthetic aluminum silicate (SAS) could elevate the gastric pH to more than 4. In the case of sodium bicarbonate (SBB), the gastric pH increased transiently to around 6 immediately after ingestion of the diet containing SBB and then decreased rapidly to the region of high acidity (pH<3). On the other hand, magnesium aluminosilicate (MAS) could maintain the gastric pH in the range from 4 to 6 over a period of 3 h after ingestion of the diet containing MAS. Thus, we conclude that MAS is the preferred antacid for maintaining the gastric pH at low acidity over a long period. Analysis of hemocytological and clinico-biochemical data suggested that the physiological state of rabbits is hardly affected by gastric-acidity control and repeated bioavailability tests.

Keywords——gastric pH; antacid; low acidity; gastric-acidity-controlled rabbit; physiological state

Introduction

Since the gastric pH or the gastric acidity in humans varies between subjects,[1,2] the bioavailability of drug preparations whose dissolution and stability will be influenced by the gastric pH commonly varies between subjects.[3–6] Therefore, the gastric acidity of humans and experimental animals should be taken into consideration when bioavailability tests and bioequivalent tests with regard to such preparations are carried out. The gastric pH in fasting humans varies between subjects and can be divided into two groups: above and below pH.[1,2] Ogata *et al.*[3] divided the gastric fluid acidity of humans into two groups before bioavailability studies by using Gastrotest tablets (Chugai Pharmaceuticals, Tokyo), which contain a protein-bound dye[7] that is released in the stomach by acid at pH 3 or less. The groups evaluated as hypo- or anacidic and as normal or hyperacidic by means of the Gastrotest[8] were designated as low and high acidity subjects, respectively. Thus, we designated rabbits having gastric pHs of less than 3 and more than 4 as high and low acidity rabbits, respectively. In our previous paper,[9] a method for controlling the gastric pH of rabbits to pH>4 (low acidity) by using magnesium aluminosilicate (MAS) as an antacid and to pH<3 (high acidity) by using hydrochloric acid was partly presented. In addition, the usefulness of rabbits having gastric pHs of low and high acidities (gastric-acidity-controlled rabbits: GAC-rabbits) has been demonstrated in bioavailability studies.[9–11] However, when the gastric contents of GAC-rabbits were observed after bioavailability tests, the gastric contents of some rabbits sometimes contained hair, which may retard the gastric emptying of food or controlled-release preparations that do not disintegrate in the stomach. Thus, we considered that gastric lavage should be incorporated in the method for gastric-acidity control to remove hair

completely. Further, it has not yet been elucidated whether the physiological state of rabbits changes during gastric-acidity control and bioavailability tests.

This paper describes in detail a slightly modified method for controlling the gastric pH of rabbits to low acidity by using different antacids and also describes the physiological state of rabbits during gastric-acidity control and repeated bioavailability tests.

Experimental

Materials——Commercial solid diet (CR-1, Nihon Clea Co.) and special solid diet (CR-S, Nihon Clea Co.), which is prepared by removing alfalfa from CR-1, were employed for pre-feeding and controlling the gastric emptying, respectively. Magnesium aluminosilicate (Neusilin, Fuji Chemical Industry Co.; MAS), sodium bicarbonate (JPX grade; SBB), dried aluminum hydroxide gel (Kyowa Chemical Industry Co.; DAH) and synthetic aluminum silicate (Kyowa Chemical Industry Co.; SAS) were employed as antacids.

Preparation of Special Soft Diet——Special soft diet (soft CR-S) was prepared by adding 60 parts of water to 40 parts of CR-S according to the method reported by Maeda *et al.*[12] This mixture was allowed to stand overnight in a cool place to swell and was divided into prescribed amounts and made into balls. Special soft diet with antacids (soft CR-A) was prepared by adding 30 g of water to a mixture consisting of 20 g of pulverized CR-S and 1, 2 or 3 g of antacid.

***In Vitro* Tests of Antacid Potency**——The use of 25 ml of 0.1 N hydrochloric acid was selected as an initial condition because it seemed likely to simulate the condition in the empty stomach of rabbits, as shown in Fig. 1. First, 50 g of soft CR-S or CR-A and 20 ml of water were added to 25 ml of 0.1 N hydrochloric acid. This mixture was then vigorously shaken for 10 min at 37 °C and was allowed to stand for 5 min to sediment the solid materials in the mixture. The pH of the upper liquid layer was measured with a pH-meter. This pH was taken as that immediately after ingestion of the soft diet. Subsequently, 20 ml of 0.1 N hydrochloric acid was added. The mixture was shaken for 20 min and then the pH was measured as described above. These procedures were repeated after every addition of hydrochloric acid.

Procedures for Gastric-Acidity Control——Gastric acidity of rabbits was controlled by a slight modification of the previous method.[9] White male rabbits fed with CR-1, weighing about 3 kg, were used for this experiment. After fasting for 24 h (stage I), the rabbit was lightly anesthetized by intravenous injection of pentobarbital sodium (15 mg/kg), and the stomach was washed with about 200 ml of warm saline (37 °C) using a rubber stomach tube. After gastric lavage (stage II), the rabbit was given 100 g of CR-S per day for 5 d. After fasting again for 24 h (stage III), the rabbit was given 100 g of soft CR-S per day for 2 d. On the next day (stage IV), the rabbit was given 50 g of soft CR-A. During gastric-acidity control, the rabbit was allowed water freely, and a cangue was fixed to the neck to prevent coprophagy.

Measurement of pH and Amount of Gastric Contents——After the rabbits at stage IV had been fed soft CR-S or soft CR-A with antacids other than MAS, 50 ml of water was orally administered through a rubber stomach tube to aid in collecting the gastric contents. About 5 ml of the gastric contents was withdrawn by suction with a syringe at predetermined times and centrifuged, and the pH of the supernatant was measured. On the other hand, in the cases of the rabbits fed soft CR-A with MAS and the rabbits at stages II—IV, a rabbit was sacrificed at predetermined times and the stomach was immediately isolated. The wet weight of the gastric contents was measured, the contents were centrifuged to obtain a solid layer and a liquid layer, and the pH of the liquid layer and the dry weight of the solid layer were measured. The difference between wet weight and dry weight was taken as representing the amount of the gastric juice.

Measurement of Physiological Parameters——Hemocytological and clinico-biochemical parameters were measured at stages I—IV of gastric-acidity control and at each stage of a sham bioavailability test. The sham bioavailability test was carried out as follows. About 2 ml of arterial blood of a rabbit in which the gastric pH was controlled by MAS was drawn by cardiac puncture six times at intervals of 2 h after oral administration of one capsule with no drug. After washout for 2 weeks, the gastric acidity of the rabbit was again controlled and the sham bioavailability test was repeated three times. The physiological parameters were measured at the following stages: immediately after the 1st administration (stage A), 12 d after the 1st administration (stage B) and 12 d after the 2nd administration (stage C).

Arterial blood (5 ml) was collected by cardiac puncture when the physiological parameters were measured. With regard to the hemocytological and clinico-biochemical parameters, the range of assay values obtained with 12 untreated rabbits was taken as the normal clinical range. It was estimated by comparing the range for treated rabbits with the normal range whether rabbits are normal or not.

Hemocytological Analysis——The blood specimen was immediately mixed with ethylenediaminetetraacetic acid tripotassium salt (EDTA-3K) and hemocytological parameters were analyzed by using a Microcellcounter CC-150 (Sysmex, Toa Medical Electronics Co.). Parameters measured were packed cell volume (PCV), hemoglobin

concentration, white blood cell count (WBC) and red blood cell count (RBC).

Clinico-biochemical Analysis——The blood specimen was centrifuged and the plasma was subjected to clinico-biochemical analysis using a Technicon SMA 12/60 and a Technicon AA BASIC (Technicon Inst. Co.). Parameters measured were as follows: sodium, potassium, calcium, inorganic phosphorus, chloride, creatinine, bilirubin, total protein, albumin, glucose, urea nitrogen, total cholesterol, alkaline phosphatase, glutamic-pyruvic transaminase and glutamic-oxaloacetic transaminase.

Results and Discussion

pH and Amount of Gastric Contents during Gastric-Acidity Control

Figure 1 shows the pH and amount of the gastric contents at each stage of gastric-acidity control. On the morning after gastric lavage (stage II), no injury to the stomach wall was observed and no solid material was detected in the gastric contents. This indicates that gastric lavage was effectively performed. The amount of the gastric contents, consisting of only the gastric juice, was 29.3 ± 6.4 g and the pH was 1.15 ± 0.02 (mean $\pm$ S.E., $n=3$). Thus, it was found that the rabbit has a basal secretion of acid. When rabbits were fasted for 24 h after feeding with CR-S for 5 d (stage III), the amount of the gastric contents was 44.3 ± 2.3 g, more than 90% of which was gastric juice with the pH of 2.06 ± 0.08 ($n=3$). On the morning after rabbits had been given 100 g of soft CR-S (stage IV), the amount of the gastric contents was 24.9 ± 2.3 g, about 95% of which was gastric juice with the pH of 1.08 ± 0.02 ($n=3$). This gastric condition was approximately the same as that after gastric lavage; the amount of solid materials remained negligibly small. Although gastric lavage transiently produced loss of appetite, the rabbit's appetite was restored by stage IV. Thus, we could make the stomach of rabbits almost empty by these procedures.

After rabbits at stage IV had freely ingested CR-S for 1 h, the amount of the gastric contents increased remarkably and in particular, the amount of the gastric juice (123.3 ± 6.6 g; $n=3$) increased about four times as compared with stage IV. This appears to be due to secretion of acid, promoted by ingestion of the diet. The amount of acid secretion by 1 h after diet ingestion was roughly estimated at 100 ml or more. However, the pH of the gastric contents (3.81 ± 0.12, $n=3$) did not become as low as expected. This is considered to be due to the buffering capacity of the diet used in this experiment.

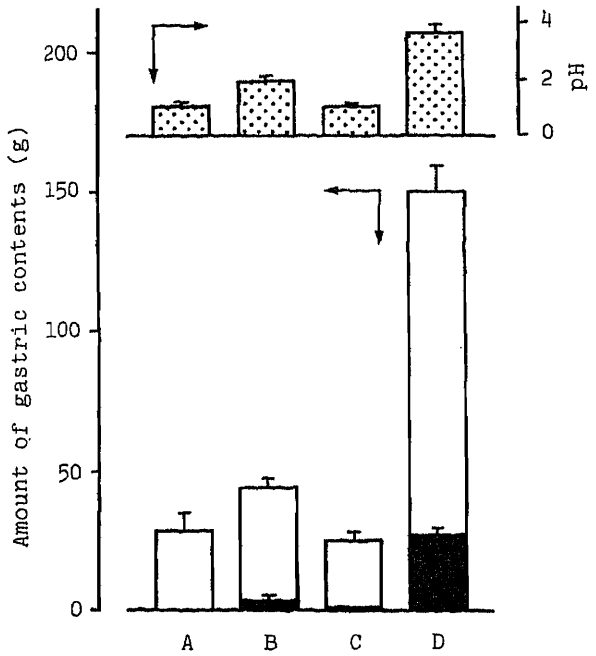

Fig. 1. Amount and pH of Gastric Contents during Gastric-Acidity Control

Each column is the mean $\pm$ S.E. for three animals. □, wet weight (total weight); ▥, dry weight in total weight; ▨, gastric pH. A, stage II; B, stage III; C, stage IV; D, 1 h after receiving CR-S at stage IV.

Gastric pH after Ingestion of Soft CR-S

Each line in Fig. 2 shows the individual gastric pH–time profile after a rabbit at stage IV ingested 50 g of soft CR-S. Although the gastric pH was about 1 before ingestion of soft CR-S, the gastric pH in each rabbit, except for one (solid line), increased and was maintained in the range of 3—4 during the first 1 h after ingestion because of the buffering capacity of soft CR-S. Thereafter, one of 4 rabbits (dotted line) showed a slow decrease of the gastric pH while the other three showed relatively rapid decreases of the gastric pH, and the pH at 3 h after ingestion became 3 or less. On the other hand, the gastric pH of the rabbit which is represented by the solid line increased initially, then decreased rapidly from 0.5 h and again increased gradually from 1.5 h. The reason for this is not clear. Thus, the changes of gastric pH after ingestion of soft CR-S showed moderate inter-subject variation. This seems to be ascribable to inter-subject variation in the extent of acid secretion and in the rate of gastric emptying of soft CR-S having the buffering capacity. The gastric pH values at all times in this experiment were about one unit or more lower than that in our previous paper.[9] This may be ascribable to the differences between the groups in acid secretion and gastric emptying.

Thus, the pH change of the gastric contents after ingestion of soft CR-S showed inter-subject and inter-group variations, and the gastric pH changed from near low acidity (pH > 4) to high acidity (pH < 3). Therefore, although the gastric emptying can be controlled by CR-S,[9] the rabbit in which the gastric pH is not controlled is not a suitable animal to test the bioavailability of drug preparations that show gastric pH-dependent bioavailability in humans. Thus, we attempted to maintain the gastric pH at low acidity over a long period by using different antacids.

***In Vitro* Antacid Potency**

Figure 3 shows the relationship between the amount of 0.1 N hydrochloric acid added to soft CR-S and the *in vitro* pH, together with the *in vivo* results described above. The *in vitro* pH change with every 20 ml addition after 40 ml of 0.1 N hydrochloric acid was initially added corresponded better with the gastric pH change every 0.5 h from 0.5 h after ingestion of soft CR-S. This indicates that this *in vitro* method may permit the prediction of antacid activity *in vivo* after ingestion of soft diet containing antacid (soft CR-A). The antacid activity of each antacid was evaluated under *in vitro* conditions corresponding to the half life (about 2 h) of gastric emptying with regard to soft CR-S.[9] Figure 4 shows the *in vitro* pH when 100 ml of 0.1 N hydrochloric acid was added to soft CR-S (50 g) containing 1, 2 or 3 g of each antacid. When no antacid was added, the pH was 2.5. In the cases of DAH and SAS, the pH did not exceed 2.5 even when 3 g of each antacid was added. In the cases of MAS and SBB, the pH increased with increasing added amount of antacid and when 1 g of antacid was added, the pHs with MAS and SBB were 4.3 and 5.8, respectively. SBB had the strongest antacid

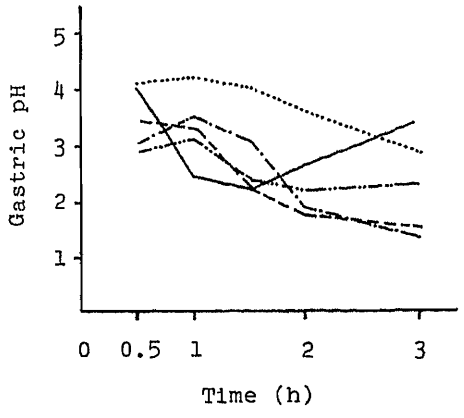

Fig. 2. Individual Gastric pH–Time Profiles after Ingestion

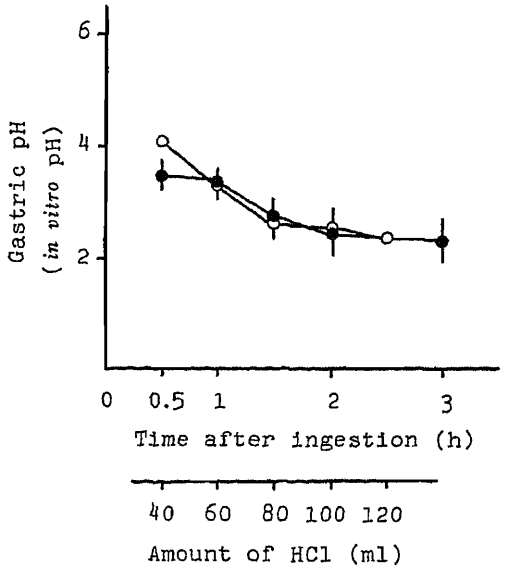

Fig. 3. Relationship between *in Vivo* and *in Vitro* Buffering Capacity of Diet

○, *in vitro* pH after addition of 0.1 N HCl (mean of three determinations); ●, *in vivo* pH after ingestion of soft CR-S (mean ± S.E. of five animals).

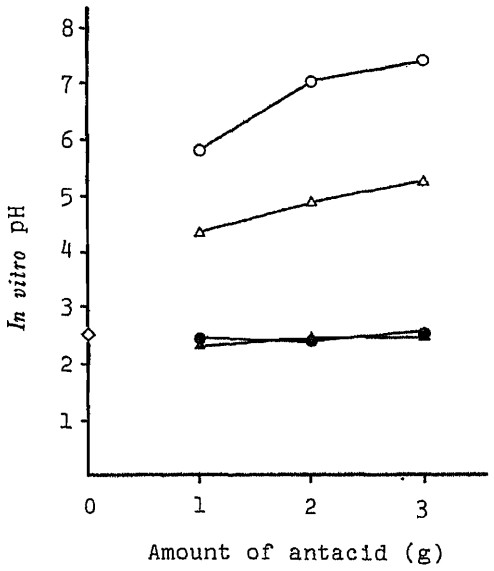

Fig. 4. Relationship between Added Amount of Antacids and *in Vitro* pH

Antacid: ○, SBB; △, MAS; ●, SAS; ▲, DAH; ◇, no antacid. Each point is the mean of three determinations.

potency, although it reacts with hydrochloric acid to produce carbonic acid gas. When soft CR-A with 1 g or more of MAS or SBB is ingested, it is predicted that the gastric pH will be maintained in the region of low acidity (pH > 4) for 2 h or more.

Thus, MAS and SBB were considered to be promising candidates as antacids for controlling the gastric pH to low acidity. In this experiment, 2 g of antacid was used for control of the gastric pH to make sure that the gastric pH is maintained at low acidity.

Gastric-Acidity Control by the Use of Different Antacids

Figure 5 shows the individual time courses of gastric pH after rabbits at stage IV ingested 50 g of soft CR-A with 2 g of antacid. With regard to MAS, each point represents the gastric pH of an individual rabbit because the gastric pH was measured by using the isolated gastric contents at each time. Neither DAH nor SAS showed antacid activity as effectively as had been expected from the *in vitro* results. In the case of SBB, the gastric pH increased rapidly to low acidity and then decreased rapidly to high acidity within 3 h after ingestion. The reasons why SBB could not maintain the gastric pH at low acidity (pH > 4) over a long period are considered to be as follows. SBB was rapidly emptied from the stomach because it is readily water-soluble, and/or physicochemical stimulating actions on the stomach wall, such as pressure of carbonic acid gas or acute pH elevation, might promote acid secretion. Another serious disadvantage of SBB is that most of the rabbits refused to ingest soft CR-A containing SBB, possible because the rabbits dislike the taste of the diet. Consequently, we did not adopt SBB as an antacid for controlling the gastric pH to low acidity.

On the other hand, although the gastric pH at each time varied widely between subjects, MAS could maintain the gastric pH in the region of low acidity (pH 4—6) over a period of 3 h after ingestion. MAS, which is poorly soluble in water, reacts with the acid to dissolve in the gastric juice. In generally, the liquid layer in the gastric contents is emptied from the stomach faster than the solid layer.[13-15] Most of the MAS is presumably in the solid state in the stomach because enough MAS to neutralize the acid is added to soft CR-A. Accordingly, MAS seems to remain for a long period in the stomach as compared with water-soluble SBB

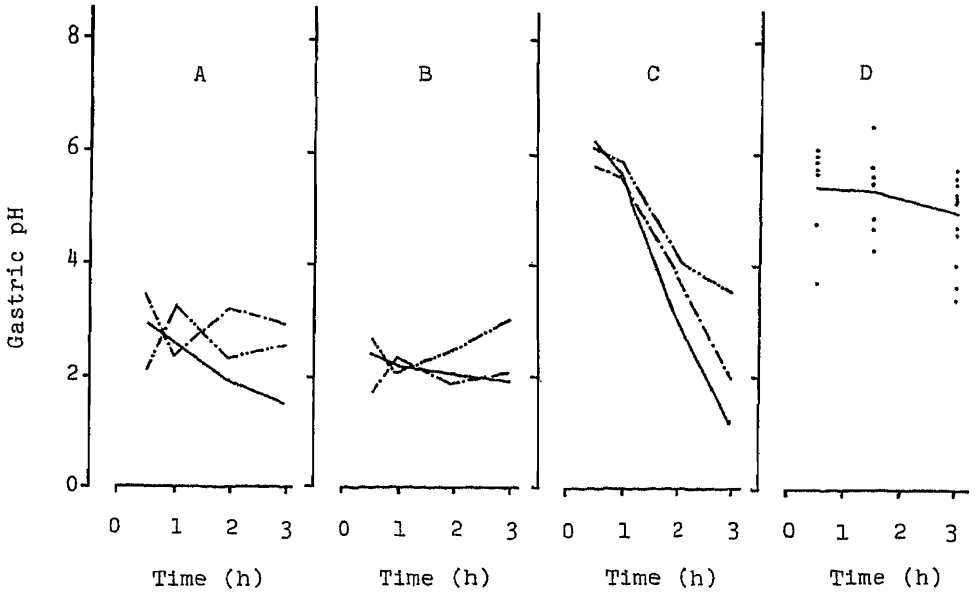

Fig. 5. Individual Gastric pH–Time Profiles after Ingestion of Soft Diet with Different Antacids

In the case of D, the solid line is constructed with the mean value at each time. Antacid: A, DAH; B, SAS; C, SBB; D, MAS.

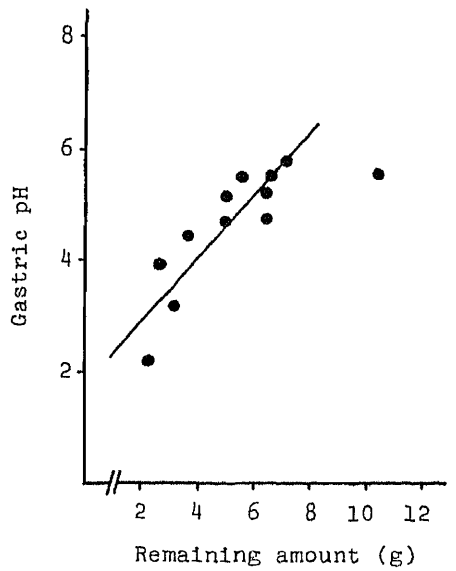

Fig. 6. Correlation between Remaining Amount of Gastric Contents and Gastric pH

Remaining amount is dry weight. The solid line is the regression line; $r=0.844$, $p<0.01$.

and to exert a prolonged antacid action. However, the gastric pH at each time varied in the range of 4—6, although it was within the low-acidity region, and one of 7 rabbits at 0.5 h and 3 of 12 rabbits at 3 h after ingestion showed gastric pH below the low-acidity region (pH <4). As a good correlation between the amount and the pH of the remaining contents in the stomach at 3 h after ingestion of soft CR-A with MAS was observed, as shown in Fig. 6, the variation and noncontrol of the gastric pH seem to be ascribable to inter-subject variation in the gastric emptying rate, besides the acid secretion.

Thus, although it is difficult to control the gastric pH of all rabbits in the low-acidity region because some rabbits always have high acid secretion and/or rapid gastric emptying, we could control the gastric pH of most rabbits in the low-acidity region by using MAS as an

antacid.

Physiological State of Rabbits during Gastric-Acidity Control

The influence of each procedure of gastric-acidity control on the physiological state of rabbits was examined in terms of blood parameters. The range of each parameter at each stage is shown in Tables I and II. All parameters in these tablets were approximately within the normal range. Accordingly, it was found that the physiological state of rabbits was not affected by the gastric-acidity control procedures, including ingestion of special diet, fasting and gastric lavage, although the body weight of the rabbits was reduced by about 6% (200 g) by fasting and gastric lavage.

Physiological State in Bioavailability Tests

In considering the practical use of GAC-rabbits, it is very important to know whether the rabbit can endure repeated bioavailability test (crossover test), including repeated blood sampling and repeated gastric-acidity control. In order to examine this, sham bioavailability tests were carried out in GAC-rabbits. Tables III and IV show the ranges of hemocytological

TABLE I. Hemocytological Parameters in Rabbits during Gastric-Acidity Control

Stage[a]	PCV (%)	WBC (10^2/mm^3)	Hemoglobin (g/dl)	RBC (10^2/mm^3)
Untreated	36—42	63—114	11.3—13.5	533—676
I	40—44	63—96	12.3—14.0	564—658
II	32—43	76—117	9.7—13.7	424—626
III	34—41	62—118	10.4—12.8	540—592
IV	37—46	96—130	11.5—14.4	546—683

a) Each stage is described in Experimental. Data represent the ranges for three (stages I—IV) or twelve (untreated) animals.

TABLE II. Clinico-biochemical Parameters in the Plasma of Rabbits during Gastric-Acidity Control

Stage[a]	Na^+ (meq/l)	K^+ (meq/l)	Cl^- (meq/l)	Ca^{2+} (mg/dl)	P[b] (mg/dl)	Glu[c] (mg/dl)	UN[d] (mg/dl)	Cr[e] (mg/dl)
Untreated	135—143	2.7—6.1	98—109	10.0—13.3	3.4—6.7	138—200	13—25	0.6—1.2
I	135—139	3.6—3.8	102—106	11.4—11.7	3.4—4.8	151—160	20—39	1.0—1.2
II	136—139	5.8—5.9	95—103	12.6—13.7	5.4—6.0	162—173	15—22	1.1
III	142—146	4.2—4.8	102—103	12.2—13.7	4.9—5.7	151—165	12—19	1.0—1.5
IV	135—139	7.7—8.0	99—102	11.0—12.5	8.1—9.7	69—175	13—19	1.0—1.1

Stage[a]	TC[f] (mg/dl)	TP[g] (g/dl)	Alb[h] (g/dl)	Bil[i] (mg/dl)	Al-P[j] (u/l)	GPT[k] (u/l)	GOT[m] (u/l)
Untreated	47—179	5.4—6.9	3.3—4.3	0.05—0.15	55—154	27—105	16—105
I	88—114	5.5—6.3	3.6—3.8	0.10	74—77	59—74	61—146
II	59—76	5.1—5.9	3.3—3.7	0.05—0.10	74—103	29—89	45—78
III	45—69	5.0—5.9	3.4—3.8	0.10	62—120	31—59	40—71
IV	76—185	5.4—7.5	3.1—4.6	0.10—0.20	75—96	36—59	21—54

a) Each stage is described in Experimental. *b*) Inorganic phosphorus. *c*) Glucose. *d*) Urea nitrogen. *e*) Creatinine. *f*) Total cholesterol. *g*) Total protein. *h*) Albumin. *i*) Bilirubin. *j*) Alkaline phosphatase. *k*) Glutamic-pyruvic transaminase. *m*) Glutamic-oxaloacetic transaminase. Data represent the ranges for three (stages I—IV) or twelve (untreated) animals.

TABLE III. Hemocytological Parameters in GAC-Rabbits during Sham Bioavailability Tests

Stage[a]	PCV (%)	WBC (10^2/mm^3)	Hemoglobin (g/dl)	RBC (10^2/mm^3)
Untreated	36—42	63—114	11.3—13.5	533—676
A	34—43	86—163	11.7—14.4	564—705
B	31—42	84—147	9.5—14.9	490—647
C	31—42	65—101	9.9—13.1	474—624

a) Each stage is described in Experimental. Data represent the ranges for five (stage C), six (stages A, B) or twelve (untreated) animals.

TABLE IV. Clinico-biochemical Parameters in the Plasma of GAC-Rabbits during Sham Bioavailability Tests

Stage[a]	Na^+ (meq/l)	K^+ (meq/l)	Cl^- (meq/l)	Ca^{2+} (mg/dl)	P[b] (mg/dl)	Glu[c] (mg/dl)	UN[d] (mg/dl)	Cr[e] (mg/dl)
Untreated	135—143	2.7—6.1	98—109	10.0—13.3	3.4—6.7	138—200	13—25	0.6—1.2
A	134—140	3.8—4.7	95—100	11.3—12.7	3.6—4.1	156—184	28—41	1.1—1.4
B	135—139	3.8—4.4	98—104	12.8—13.3	4.8—5.4	145—174	12—18	1.0—1.4
C	123—134	4.2—4.9	93—99	12.1—13.8	4.1—6.2	119—159	22—35	1.0—1.7

Stage[a]	TC[f] (mg/dl)	TP[g] (g/dl)	Alb[h] (g/dl)	Bil[i] (mg/dl)	Al-P[j] (u/l)	GPT[k] (u/l)	GOT[m] (u/l)
Untreated	47—179	5.4—6.9	3.3—4.3	0.05—0.15	55—154	27—105	16—105
A	78—225	5.9—6.9	3.9—4.4	0.10—0.15	36—64	30—76	25—115
B	51—89	6.0—6.8	4.0—4.8	0.10—0.15	44—117	29—64	31—91
C	71—143	6.1—6.9	3.4—3.8	0.10—0.15	26—67	20—100	11—96

a) Each stage is described in Experimental. *b*) Inorganic phosphorus. *c*) Glucose. *d*) Urea nitrogen. *e*) Creatinine. *f*) Total cholesterol. *g*) Total protein. *h*) Albumin. *i*) Bilirubin. *j*) Alkaline phosphatase. *k*) Glutamic-pyruvic transaminase. *m*) Glutamic-oxaloacetic transaminase. Data represent the ranges for five (stage C), six (stages A, B) or twelve (untreated) animals.

and clinicobiochemical parameters at each stage, respectively. All parameters at each stage were approximately within the normal range, although urea nitrogen at stage A showed a somewhat high value. With regard to the reduction of the body weight caused by fasting and gastric lavage, the body weight recovered very smoothly during the period of washout and rabbits apparently recovered well before the next bioavailability test. Consequently, it was found that the physiological state of GAC-rabbits is hardly affected by repeated bioavailability tests.

From the results obtained in this study, we conclude that MAS is the preferred antacid for controlling the gastric pH of rabbits in the low-acidity region and that it is possible to use GAC-rabbits for crossover bioavailability studies from a physiological point of view.

Acknowledgement We are grateful to Drs. M. Shimizu and M. Kono, Dainippon Pharmaceutical Co., Ltd., for advice and helpful discussions. Thanks are also due to Mr. N. Matsuoka for assistance in the experimental work.

References

1) P. Finholt and S. Solvang, *J. Pharm. Sci.*, **57**, 1322 (1968).

2) R. Iinuma and T. Toyama, *Yakuzaigaku*, **21**, 48 (1961).
3) H. Ogata, N. Aoyagi, N. Kaniwa, M. Koibuchi, T. Shibazaki, and A. Ejima, *Int. J. Clin. Pharmacol. Ther. Toxicol.*, **20**, 166 (1982).
4) H. Ogata, N. Aoyagi, N. Kaniwa, T. Shibazaki, A. Ejima, Y. Takagishi, T. Ogura, K. Tomita, S. Inoue, and M. Zaizen, *Int. J. Pharm.*, **23**, 277 (1985).
5) N. Aoyagi, H. Ogata, N. Kaniwa, M. Koibuchi, T. Shibazaki, A. Ejima, M. Mizobe, K. Kohno, and M. Samejima, *Chem. Pharm. Bull.*, **34**, 281 (1986).
6) H. Ogata, N. Aoyagi, N. Kaniwa, A. Ejima, N. Sekine, M. Kitamura, and Y. Inoue, *Int. J. Pharm.*, **29**, 113 (1986).
7) E. Bianchetti and Th. Gerber, *Schweiz. Med. Wschr.*, **88**, 736 (1958).
8) T. Kiyama, H. Kinoshita, and Y. Ishii, *Rinsho Shokakigaku*, **12**, 857 (1960).
9) T. Takahashi, Y. Uezono, and H. Fujioka, *Yakuzaigaku*, **43**, 61 (1983).
10) T. Takahashi, M. Mori, Y. Uezono, H. Fujioka, and Y. Imasato, *Yakuzaigaku*, **43**, 187 (1983).
11) T. Takahashi, Y. Uezono, and Y. Nakanishi, *Chem. Pharm. Bull.*, **34**, 3370 (1986).
12) T. Maeda, H. Takenaka, Y. Yamahira, and T. Noguchi, *J. Pharm. Sci.*, **66**, 69 (1977).
13) R. R. Dozois, K. A. Kelly, and C. F. Code, *Gastroenterology*, **61**, 675 (1971).
14) D. S. Grimes and J. Goddard, *Gut*, **18**, 725 (1977).
15) P. E. Christian, J. G. Moore, J. A. Sorenson, R. E. Coleman, and D. M. Welch, *J. Nucl. Med.*, **21**, 883 (1980).

[Chem. Pharm. Bull. 35(4)1555—1563(1987)]

Calcium-Induced Gelation of Alginic Acid and pH-Sensitive Reswelling of Dried Gels

TOSHIHISA YOTSUYANAGI,* TSUNEO OHKUBO, TAKAFUMI OHHASHI and KEN IKEDA

Faculty of Pharmaceutical Sciences, Nagoya City University, Mizuho-ku, Nagoya 467, Japan

(Received September 4, 1986)

Calcium-induced alginate gelation was examined in terms of water content changes. The gelation was accompanied with considerable water loss, which reached about 50—60% (w/w) reduction in the fully-cured state. The calcium association with the polymer was strong enough to maintain the shape of fully-cured beads in distilled water and the amount of the ions associated with the alginate used in the present study was 1.6×10^{-3} mol/g of polymer. The diffusion coefficients of several model compounds having molecular weights ranging from 122 to 1050 were estimated as a function of the polymer concentration in the fully-cured beads.

The swelling property of dried gel particles prepared from fully-cured hydrogels was of interest: the particles remained unchanged in distilled water or acidic medium (pH 1.5 KCl–HCl) but swelled rather rapidly in pH 7.0 phosphate buffer to a size greater than their original size before being dried. Such a pH-sensitive swelling property could be advantageous for orally-administered drug vehicles, especially when an acid-sensitive drug is incorporated in the gel.

Keywords——alginic acid; calcium-induced alginate gel; dry gel swelling; pH-sensitive swelling; gel matrix; gel water content; controlled delivery

Although the definition of "gel" is controversial,[1] from a pharmaceutical point of view, gels can be regarded as semi-solid systems consisting of a lyophilic gel component which forms a three-dimensional network structure in which a liquid phase is constrained. Gel components used to prepare pharmaceutical vehicles include such synthetic and semi-synthetic polymers as carboxy vinyl polymer, hydroxyethylcellulose and hydroxypropylcellulose, in addition to the natural substances, pectin, tragacanth and alginic acid. These materials have generally been used as lyogels for topical application.

Alginic acid/Na-alginate, which is a polysaccharide found in brown algae, has a broad range of applications ranging from pharmaceutical and food adjuvant to an immobilization matrix for cells and enzymes due to its cation-induced gelation.[2-5] The polysaccharide can spontaneously form a translucent gel in association with calcium ions, and the mechanism of gelation, for which guluronic acid blocks are mainly responsible, has been intensively investigated by circular dichroism (CD) and nuclear magnetic resonance (NMR) studies.[6-10]

The purpose of this paper is to explore the possible applicability of alginate gel beads as orally-administered drug delivery vehicles. Because of the reswelling properties of alginate xerogels which are susceptible to surrounding pH, the following advantages may be envisaged: (1) acid-sensitive drugs are protected from gastric juice, (2) the reswelling process of xerogels in the intestine offers controlled-release drug delivery, (3) appropriately-sized particles of xerogels avoid local build-up of released drugs, (4) alginate is known to be nontoxic when taken orally.

We describe here the characteristics of the gelation process of alginate followed in terms of water content changes, calcium content in the fully-cured gel beads, diffusion properties of

several substances and reswelling behavior of dried gel particles.

Experimental

Materials——Na-alginate (lot no. AR01, Tokyo Kasei Kogyo, Tokyo) was used after dialysis against distilled water using Visking cellulose tubing (36/32) for 2 d (4 water replacements/d) followed by lyophilization. Calcium chloride, dihydrate (special grade, Wako Chemicals, Osaka) was used. Benzoic acid and indigo carmine were purchased from Wako Chemicals. Bromocresol green was from Katayama Chemicals, Osaka, and rose bengal from Yoneyama Pharmaceuticals, Osaka. All other chemicals were of reagent grade.

Determination of Uronic Acid Residues——The following methods were used. (1) The Haug and Larsen method.[11] Briefly, alginate (50 mg) was mixed with 0.5 ml of 80% sulfuric acid and completely hydrolyzed for 18 h at 20 °C. After being neutralized by adding a slight excess of calcium carbonate, the hydrolysate was applied to an anion exchange column (Amberlite CG-400 Type 2, 20 cm × 2 cm i.d., Tokyo Yukikagaku Kogyo, Tokyo) to separate guluronic acid (G) and mannuronic acid (M). The fractions of each acid group were combined and the amount of each acid was determined by the orcinol method.[12] (2) The proportion of the homopolymeric fraction (GG plus MM) to the alternating (MG) fraction of alginate was determined by the phenol–sulfuric acid reaction method after partial acid hydrolysis with diluted hydrochloric acid.[13] (3) The proportions of GG and MM blocks were determined by NMR after partial hydrolysis.[14] (4) CD spectra of alginate were analyzed to assess the uronic acid composition (G to M) according to the peak/trough ratio method of Morris *et al.*[15] CD spectra of alginate dissolved in distilled water (0.8 mg/ml) were recorded on a CD spectropolarimeter (J-40A, JASCO, Tokyo) using a time constant of 4 s and a 10 mm pathlength. The proportions of GG, MM and MG blocks in Na-alginate used are shown in Table I.

Preparation of Alginate Gel Beads——Gel beads were prepared by dropping Na-alginate solution (1, 2, 3 and 4% (w/v) in distilled water) into $CaCl_2$ solution (0.02—0.1 M), using a peristaltic pump (MP-3, Tokyo Rikakikai Co., Tokyo) with a polyethylene-tubing nozzle (0.85 mm i.d. and 1.67 mm o.d.). The pumping rate was 0.11 ml/min. The falling distance was 3.5 cm. The weights of one droplet of the various alginate solutions were almost equal to each other, being 35.2±0.2 (S.D.) mg. The gel beads which were allowed to stand in the $CaCl_2$ solution for more than 300 h were assumed to be fully cured.

Weight Changes of Curing Gel Beads——Curing beads (10 beads) were taken out from the salt solution at appropriate intervals and weighted after the removal of surface moisture on filter paper. The weight of 10 droplets was assumed to be the initial weight at $t=0$. Instant curing at the immediate surface of the droplets made it possible to form almost spherical beads.

Determination of Calcium Contents in Fully-Cured Beads——Fully-cured gel beads formed in 0.1 M $CaCl_2$ were repeatedly washed for 24 h with fresh distilled water to remove excess calcium which was not associated with the gelation of alginate. A sample of gel beads was ashed after disintegration with ammonia water (0.001 M) as follows: the solution (0.5 ml) was placed in a 15 × 100 mm glass test tube to which 1 ml of sulfuric acid (6 N) was added, and heated on a heating block at 180 °C for 2 h. After cooling, 4—5 drops of hydrogen peroxide (30%) were added and the mixture was heated again at 180 °C for 1 h for final ashing. After cooling, the volume was appropriately adjusted by adding distilled water. The amount of calcium was then measured by using an atomic absorption analyzer (AA-630-12, Shimadzu, Kyoto) with reference to a calibration curve constructed with known amounts of $CaCl_2$.

Determination of Water Content in Fully-Cured Beads——Fully-cured beads were dried by various methods, heating in an oven at 110 °C overnight, drying in a silica gel desiccator for a week and natural drying at room temperature (R.H. 65%) for a week. The weight difference before and after drying was assumed to be the water content.

Determination of Diffusion Coefficients——The diffusion coefficients of benzoic acid (mol wt. 122.1), indigo carmine (466.4), bromocresol green (698.1) and rose bengal (1049.8) in various fully-cured beads formed in 0.1 M

Table I. The Composition of Alginate Used

Method[a]	Proportion (%)				
	M	G	MM	GG	MG
1	56.3	43.7			
2			50.2		49.8
3			72.5	27.5	
4	56.7	43.3			
Calc.[b]			36.3	13.9	49.8

a) See Experimental. *b*) Proportions calculated from the values obtained above.

$CaCl_2$ were estimated from the penetration rate of the substances into the beads, which were suspended in a well-stirred solution, based on the mathematical treatments of Crank applicable to diffusion in a sphere (see Appendix).[16] One hundred beads were introduced into a solution of each substance (1×10^{-4}—10^{-5} M, 10 ml of distilled water), and the concentration changes were followed with a perfusion cell system connected to a spectrophotometer (Hitachi 124, Tokyo). The temperature was 25 °C.

Swelling Rate of Dried Gel Particles——Fully-cured beads prepared with initial alginate concentrations of 2, 3 and 4% were dried at 110 °C overnight. The resulting dried particles were gently incubated in distilled water, pH 1.6 KCl–HCl (0.2 M) and pH 7.0 phosphate buffer (0.067 M) at 25 °C, and the diameter of each swelling particle, taken out of the solution, was measured with a micrometer. Because the shape of a swelling particle was not always perfectly spherical, the diameter was measured at three different positions of each particle and the average of five particles was calculated. The magnitude of swelling was represented by the ratio of the diameter of a swelling particle to the corresponding diameter of the fully-cured bead before drying.

Results and Discussion

Gelation Rate of Beads Measured in Terms of Weight Changes

When a droplet of the alginate solution contacted the $CaCl_2$ solution, gelation seemed to occur instantly on the surface of the droplet, which formed an almost spherical bead without splashing on contact. Soon the process could be visually detected as the appearance of a translucent spherical figure, followed by contraction of the figure. Although the intrinsic rate of curing is likely to be extremely fast, the apparent rate of spherical gel formation is primarily controlled by the penetration of calcium ions into the interior of droplets and therefore is dependent on the droplet size of alginate solution. Also water has to be squeezed out of the interior, traversing the already cured outer part to the bulk solution. It is therefore reasonable to consider that the overall rate of bead formation can be represented by the weight changes of the beads with time.

Figure 1 shows the weight changes of beads formed with various initial alginate concentrations in 0.1 M $CaCl_2$. The results indicate a rapid initial decrease and a subsequent slow stage: 60—70% weight loss out of the final weight loss occurred in the first several hours and it took about 70 h to reach constant weight. According to the CD study reported by Thom *et al.*,[6] spectral changes of alginate gelation by metal ions continued for 15—20 d. It seems that the apparent gelation is finished rather quickly on the basis of gel weight but fine rearrangement of the gel structure continues for a long time.

The weight of curing beads should be the sum of the weights of the calcium-associated polymer and water, but the contribution of the metal ions was negligible even for fully-cured beads, as described later. The total weight loss is assumed to be solely due to the amount of

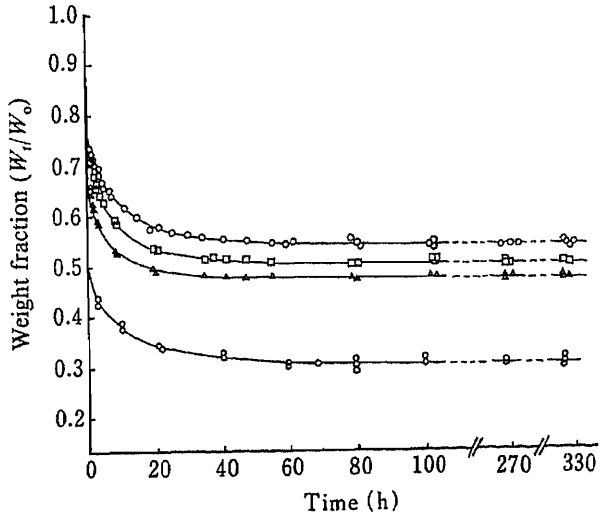

Fig. 1. Weight Fraction Changes of Curing Beads in 0.1 M $CaCl_2$

W_0, weight of 10 droplets of alginate solution ($t=0$); W_t, weight of 10 beads at time t. Initial alginate concentrations: ○, 4% (w/v); □, 3; △, 2; ○, 1. Temp., 25 °C.

water squeezed out of the beads. If the process of curing proceeds concentrically from the surface of a droplet to the center, squeezing out interior water, the amount of water leached out would be related to the third power of the radius as the contraction proceeds, *i.e.* the further out a hypothetical concentric segment in the sphere, the greater the volume of water squeezed out, resulting in a more rapid weight loss in the early stages. It was furthermore noted that the rate of the subsequent slow stages was similar irrespective of the initial alginate concentration. This result indicates that the cured structures of the hydrogels are loose enough for water to traverse to the outside bulk solution. As the consequence of water loss, the initial alginate concentration should be increased in the beads. Accordingly, the alginate concentration in the fully-cured beads may have to be corrected.

The Magnitude of Contraction to Form Fully-Cured Gel Beads

Table II summarizes the effect of $CaCl_2$ concentration on the weight fraction of fully-cured gel beads formed with various initial alginate concentrations. The amount of water squeezed out reached about 50%. The weight of beads decreased with increasing $CaCl_2$ concentration and appeared to become constant at salt concentrations above 0.08 M, suggesting that the fully-cured state depends on the bulk $CaCl_2$ concentration and a threshold bulk $CaCl_2$ concentration is required for the ultimately-cured condition, *i.e.* in this case

Table II. Weight Fractions of Fully-Cured Gel Beads Formed with Various Combinations of Initial Alginate Concentration and $CaCl_2$ Concentration

Initial alginate conen. (%, w/v)	Weight fraction (W_e/W_0)			
	$CaCl_2$ conen. (M) 0.02	0.05	0.08	0.1
1	—[a]	—[a]	—[a]	0.306[b]
2	0.545	0.501	0.467	0.472
3	0.590	0.571	0.502	0.493
4	0.712	0.633	0.539	0.536

W_0, weight of droplets (assumed at $t=0$); W_e, weight of fully-cured beads ($t=270-330$ h).
a) Incomplete gelation. *b*) Incomplete beads.

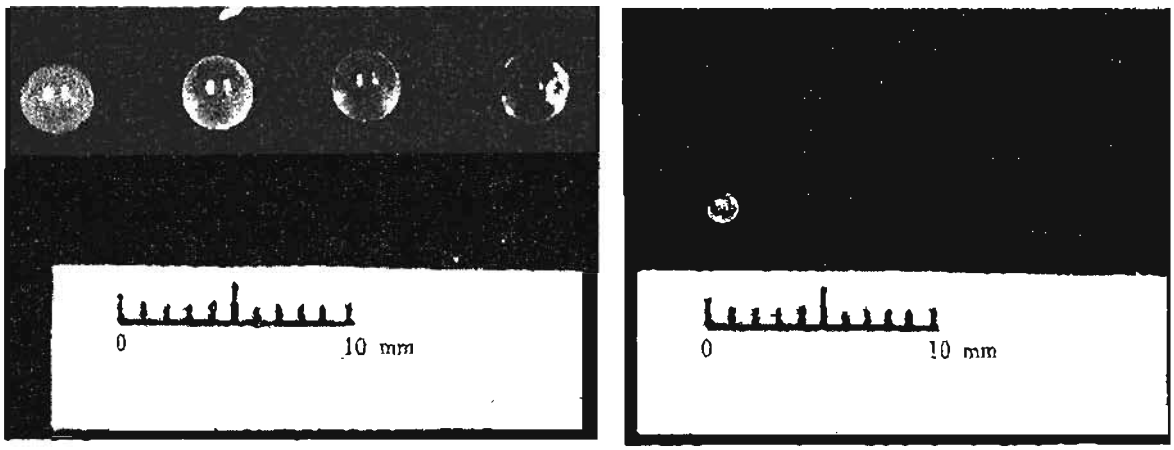

A B

Fig. 2. Photographs of Fully-Cured Beads in 0.1 M $CaCl_2$ (A) and a Dried Gel Particle (110 °C) (B)

A. initial alginate concentrations from the left, 4% (w/v), 3, 2, and 1; B. 4% (w/v).

TABLE III. Physical Dimensions of Fully-Cured Gel Beads Formed in 0.1 M Calcium Chloride

Initial alginate concn. (%, w/v)	Radius[a] (mm)	Weight[a] (mg/bead)	Volume (mm^3/bead)	Density
1	—	15.6	—	—
2	1.55	16.7	15.6	1.07
3	1.59	17.7	16.8	1.05
4	1.60	18.7	17.2	1.09

a) Average of 10 beads.

0.08 M. If the amount of $CaCl_2$ were in excess of the amount of alginate, as was the case in this study even for 0.02 M $CaCl_2$, the weight changes should converge to the values of 0.1 M $CaCl_2$ provided that the initial alginate concentration was kept constant. It was assumed that the greater contraction of the beads with increasing $CaCl_2$ concentration is mainly due to the increase of dehydration from alginate molecules.

As the initial alginate concentration was increased, a weight increase was generally observed, probably due to increasing density of the beads. Figure 2 shows typical fully-cured beads (in 0.1 M $CaCl_2$) with almost completely spherical shape, from which the physical dimensions were obtained as shown in Table III. The radius of the beads, and hence the volume, was little affected by the initial alginate concentration, but a higher initial concentration resulted in more translucent beads. This means that the greater the initial concentration, the denser the fully-cured state of the gel structure.

As shown in Table II, a considerable amount of water was squeezed out during the curing process. Thus, the final alginate concentration in fully-cured beads should be much higher than the initial polymer concentration. The final concentration was calculated from the weight fraction changes of fully-cured beads: 2% initial concentration increased to 4.2% (w/w), 3% to 6.1% and 4% to 7.5%. Alternatively, the w/v expression calculated from the final volume and the density gave 4.5% (w/v), 6.4% and 8.2%, respectively.

Calcium Content in Fully-Cured Beads

Before assaying Ca^{2+} involved in the gelation, the beads were subjected to repeated washing with distilled water to remove unassociated Ca^{2+}, during which their physical appearance remained unchanged. This indicates that the association of Ca^{2+} with the polymer is strong, being barely affected in distilled water but completely destroyed by ethylenediaminetetraacetic acid (EDTA).

Figure 3 shows a plot of the Ca^{2+} content in fully-cured beads (in 0.1 M $CaCl_2$), *i.e.* ultimately-cured beads, against the final alginate concentration (w/w). The amount of Ca^{2+} involved in the gelation was proportional to the alginate concentration and there was no interference by coexisting sodium ions, indicating that Ca^{2+} is quantitatively and specifically associated with the polymer molecules. From the slope of the linear plot, the amount of Ca^{2+} associated with the polymer molecules was found to be 1.6×10^{-3} mol/g of polymer. As mentioned earlier, the contribution of the calcium association to the weight changes in the curing process of beads was negligible.

Water Content in Fully-Cured Beads

The water content held in fully-cured beads was estimated from the weight difference between hydrogel and xerogel dried under various conditions. Figure 4 shows the relation between the water content and the calculated polymer concentration (w/v). The water content was inversely proportional to the polymer concentration but was dependent on the drying

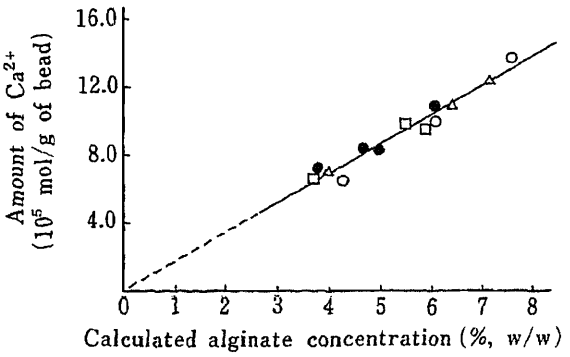

Fig. 3. The Amount of Ca^{2+} Associated with Fully-Cured Beads

○, formed in 0.1 M $CaCl_2$; △, 0.1 M $CaCl_2$ and 0.1 M NaCl; □, 0.1 M $CaCl_2$ and 0.15 M NaCl; ●, 0.1 M $CaCl_2$ and 0.2 M NaCl. The abscissa indicates the alginate concentration (w/w) calculated from the data of Fig. 1.

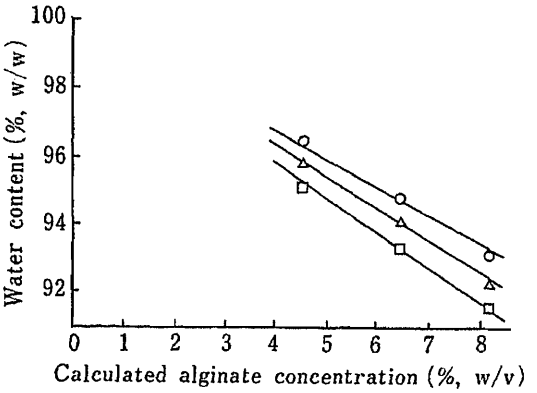

Fig. 4. Water Contents in Fully-Cured Beads in 0.1 M $CaCl_2$

Drying methods: ○, dried at 110 °C; △, silica gel in a desiccator; □, natural drying. The abscissa indicates the alginate concentration (w/v) calculated from the data of Fig. 1 and Table III.

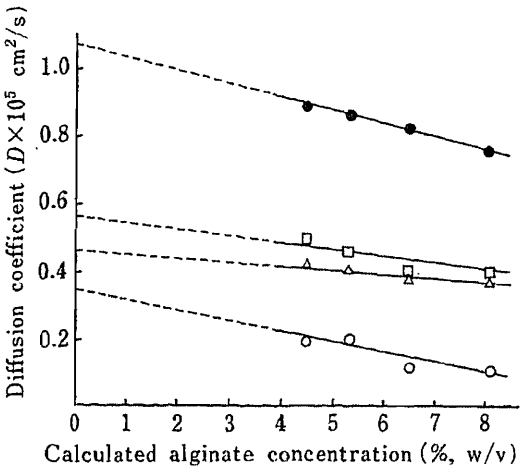

Fig. 5. Diffusion Coefficients of Various Substances in Fully-Cured Beads

●, benzoic acid; □, indigo carmine; △, bromocresol green; ○, rose bengal. Temp., 25 °C. The abscissa indicates the alginate concentration (w/v) calculated from the data of Fig. 1 and Table III.

method. Drying at 110 °C seemed to remove all of the water entrapped in the hydrogels because the weight of dried gel corresponded to the amount of polymer in the initial droplet. Drying over silica gel in a desiccator gave slightly lower values, *i.e.*, it was less effective. The resulting gel particles had a relatively round shape with a smooth surface (Fig. 2), and were extremely hard; it was difficult to crush them in an agate mortar.

Diffusion Characteristics of Substances in Fully-Cured Beads

The diffusion behavior of substances in gels is one of the important aspects to be considered when the gel beads are to be used as a drug delivery system. Several substances of various molecular weights such as benzoic acid (mol wt. 122), indigo carmine (466), bromocresol green (698) and rose bengal (1050) were selected as model compounds. Based on the mathematical treatment for diffusion in a sphere,[16] the diffusion coefficient was calculated from the penetration rate into the beads in well-stirred solution.

Figure 5 shows a plot of the diffusion coefficient obtained against the alginate concentration (w/v) calculated in the fully-cured beads (in 0.1 M $CaCl_2$). The diffusion coefficient became smaller as the polymer concentration increased, though the dependency on the polymer concentration was apparently similar irrespective of the molecular weights of

TABLE IV. Estimated Diffusion Coefficient in Water and the Concentration Ratio between Bulk Solution and Gel Beads (25 °C)

Drug	D_w (10^5 cm^2/s)	$R^{a)}$
Benzoic acid	1.07	1.02
Indigo carmine	0.555	1.03
Bromocresol green	0.448	1.03
Rose bengal	0.328	2.33

a) R=concentration in gel beads/concentration in bulk solution at equilibrium. The beads were prepared at an initial alginate concentration of 2% with 0.1 M $CaCl_2$.

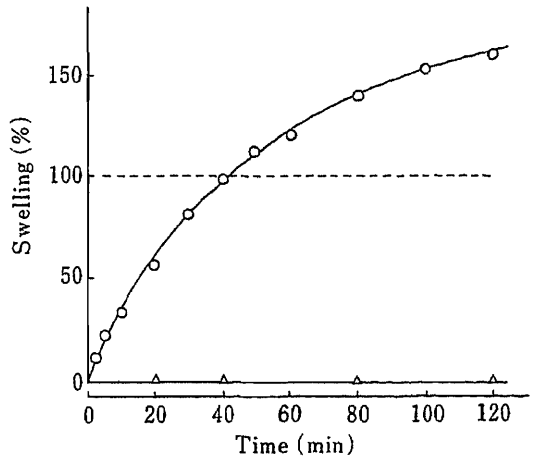

Fig. 6. The Swelling Rate of Dried Gel Particles in Aqueous Solutions

○, pH 7.0 phosphate buffer; △, pH 1.5 KCl–HCl buffer. Temp., 25 °C. The dotted line (100%) indicates the size of the original hydrated bead (diameter). The sample particles were prepared with an initial alginate concentration of 4% and 0.1 M $CaCl_2$, and were dried at 110 °C.

these substances. The diffusion coefficients in water were estimated by extrapolation to the ordinate (Table IV). The value of benzoic acid thus estimated agrees well with the literature value of 1.03×10^{-5} cm^2/s.[17]

In the beads prepared with the initial concentration of 4%, *i.e.* 8.2% in the fully-cured state, the diffusion coefficients of benzoic acid, indigo carmine and bromocresol green were reduced to about 70—80% of the respective aqueous diffusion coefficients, while that of rose bengal was reduced to about 30%. As shown by the concentration ratio of the bulk aqueous phase and the gel beads determined at equilibrium (Table IV), these substances other than rose bengal were little associated with the polymer molecules. The interaction of rose bengal with the polymer molecules would have apparently given a higher value of D_w than the actual value, since the calculation was made under the assumption that no interaction occurs.

Swelling of Dried Gel Particles

The swelling behavior of dried gel particles in aqueous solution was followed by measuring the diameter of the swelling particles with time. Figure 6 shows the magnitude of swelling in various aqueous environments where the magnitude is represented by the ratio of the diameter of swelling particles to that of the fully-cured hydrated beads. The value of 100% indicates that a swelling particle reached the original size of the hydrated bead before being dried. It should be noted here that no swelling was observed in distilled water and in pH 1.6 KCl–HCl buffer, while in pH 7.0 phosphate buffer the dried particle swelled to its original size in about 1 h, followed by further swelling beyond its original size, and then it gradually disintegrated and dispersed over several hours. These results suggest that the dried gel particles keep their intact form in the stomach and when subsequently transferred to the intestine, the particles are likely to swell and function as matrices for controlled-release of

incorporated drugs.

There was little difference in the rate of swelling among the gel particles prepared at various initial alginate concentrations, 2—4%. This result, however, may be confined to the size range of dried particle examined in the present study. Because the swelling rate should be related to the penetration rate of water into the porous gel structure, particles much smaller in size would swell at faster rates.

Such a pH-sensitive swelling property of the alginate gel particles means that an acid-sensitive drug incorporated may be effectively shielded from the attack of gastric juice and be released at desirable rates from the particles in the intestine. However, further studies are needed for the rational design of controlled-release alginate matrices.

Appendix

When a spherical bead having a diameter a, which is free from solute, is suspended in a well-stirred solution with an initial solute concentration of C_0 and a volume V, the amount of solute, M_t, in the sphere after time t can be represented as a fraction of the corresponding quantity after infinite time, M_∞, by the following equation[16]:

$$\frac{M_t}{M_\infty}=1-\sum_{n=1}^{\infty}\frac{6\alpha(1+\alpha)\exp(-Dq_n^2t/a^2)}{9+9\alpha+q_n^2\alpha^2} \tag{1}$$

where the q_n's are the non-zero roots of

$$\tan q_n=\frac{3q_n}{3+\alpha q_n^2} \tag{2}$$

α is the ratio of the volumes of solution and bead, $3V/4\pi a^3$, and D is the diffusion coefficient. The parameter α can be expressed in terms of the final fractional uptake of solute by the bead, as follows:

$$\frac{M_\infty}{VC_0}=\frac{1}{1+\alpha} \tag{3}$$

The solute concentration in the bulk solution may be expressed as follows:

$$C_b=\frac{\alpha C_0}{1+\alpha}\left[1+\sum_{n=1}^{\infty}\frac{6(1+\alpha)\exp(-Dq_n^2t/a^2)}{9+9\alpha+q_n^2\alpha^2}\right] \tag{4}$$

where C_b is the solute concentration in the bulk phase.

Acknowledgement The authors are grateful to Misses M. Tasaka, M. Horiba and T. Kikuchi for technical assistance and computer programming.

References

1) P. J. Flory, *Faraday Disc. Chem. Soc.*, **57**, 7 (1974).
2) B. Svensson and M. Ottesen, *Carlsberg Res. Commun.*, **46**, 13 (1981).
3) M. Kierstan, G. Darcy and J. Reilly, *Biotechnol. Bioeng.*, **24**, 1507 (1982).
4) A. Awad and O. Awad, *J. Chem. Tech. Biotechnol.*, **30**, 583 (1980).
5) A. A. Badwan, A. Abumalooh, E. Sallam, A. Abuhalaf and O. Jawan, *Drug. Dev. Ind. Pharm.*, **11**, 239 (1985).
6) T. A. Bryce, A. A. McKinnon, E. R. Morris, D. A. Rees and D. Thom, *Faraday Disc. Chem. Soc.*, **57**, 221 (1974).
7) A. Penman and G. R. Sanderson, *Carbohydr. Res.*, **25**, 273 (1972).
8) E. R. Morris, D. A. Rees and D. Thom, *Carbohydr. Res.*, **66**, 145 (1978).
9) E. R. Morris, D. A. Rees and D. Thom, *Carbohydr. Res.*, **81**, 305 (1980).
10) D. Thom, G. T. Grant, E. R. Morris and D. A. Rees, *Carbohydr. Res.*, **100**, 29 (1982).
11) A. Haug and B. Larsen, *Acta Chem. Scand.*, **16**, 1919 (1962).
12) H. H. Brown, *Arch. Biochem.*, **11**, 269 (1946).

13) M. Dubois, K. A. Gills, J. K. Hamilton, P. A. Rebers and F. Smith, *Anal. Chem.*, **28**, 350 (1956).
14) A. Penman and G. R. Sanderson, *Carbohydr. Res.*, **25**, 273 (1972).
15) E. R. Morris, D. A. Rees and D. Thom, *Carbohydr. Res.*, **81**, 305 (1980).
16) J. Crank, "The Mathematics of Diffusion," Oxford University Press, London, 1970, pp. 84—98.
17) H. Nogami, T. Nagai and K. Itoh, *Chem. Pharm. Bull.*, **14**, 35 (1966).

[Chem. Pharm. Bull. 35(4)1564—1570(1987)]

Evaluation of Crystallite Orientation in Tablets by X-Ray Diffraction Methods[1)]

EIHEI FUKUOKA,* MIDORI MAKITA and SHIGEO YAMAMURA

Faculty of Pharmaceutical Sciences, Toho University, 2-2-1 Miyama, Funabashi, Chiba 274, Japan

(Received September 18, 1986)

The crystallite orientation in intact tablets was investigated by X-ray diffraction methods. X-Ray diffraction patterns were obtained by the symmetrical-reflection method and the symmetrical-transmission method. Crystallite orientation was evaluated by comparing the diffraction intensities obtained experimentally with those calculated theoretically from the structure factors for the respective planes of the crystal. The (100) planes of aspirin crystallites and the (110) and the (120); (210) planes of salicylic acid crystallites were found to align parallel to the upper surface of the tablet during compression. The crystallite orientation varied with applied pressure for salicylic acid tablet. The flat film technique (pinhole technique) was also used and the results obtained agreed well with those obtained by the diffractometric methods.

Keywords——crystallite orientation; tablet; X-ray diffraction; diffractometry; flat film photograph; aspirin; salicylic acid

It is considered that crystals and crystallites in a tablet are oriented preferentially because of the anisotropic force applied to the crystalline powder in the die during compression, and the preferred orientation of crystallites may affect various pharmaceutical properties such as compressibility, strength and so on of a tablet. Many studies have been reported on the rearrangements of particles and the deformation of crystals during compression.[2)] However, most of them did not employ X-ray diffraction analysis, but evaluated the arrangements of particles and crystals from scanning electron microscope photographs or by analysis of the compression behavior. A method has been reported in which selected faces in a tablet were exposed to the X-ray beam and diffraction intensities were measured in order to evaluate the preferred orientation in a tablet.[3)] However, it is preferable, if possible, to evaluate the crystallite orientation in a tablet by using an intact tablet.

In the present paper, a method for the evaluation of the crystallite orientation in intact tablets was developed. The method is based on the fact that when the specimen has random orientation the X-ray diffraction intensities from particular planes can be calculated theoretically from the structure factors of the crystal.

Experimental

Materials——Aspirin and salicylic acid were of JP XI grade (Iwaki Pharm. Co., Ltd.). The fraction of 200—250 mesh was used as a sample powder. The tablets used for diffractometric and photographic methods were prepared by direct compression of the sample powder using a KBr disc press (1.3 cm in diameter) and a KBr micro-disc press (2.5 mm in diameter) for infrared spectroscopy. The tablet weighted 200 and 20 mg, respectively. The thickness of each tablet was about 1.2 mm.

X-Ray Diffraction (Powder Method)——A Geigerflex RAD-type diffractometer (Rigaku Denki Co., Ltd.) was used. The X-ray source was Ni-filtered Cu-K_α radiation, and a scintillation counter was used as the detector.

1) Diffractometric Technique: X-ray diffraction patterns were obtained by the symmetrical-reflection method

and by the symmetrical-transmission method. The measurement conditions were as follows: voltage, 35 kV; current, 10 mA; time constant, 2 s; scan speed, 1 °/min; scan range, 5—35° (2θ); divergence and scattering slit, 1/2°; receiving slit, 0.15 mm.

The tablet was mounted in a circular hole with a diameter of 1.4 cm in an aluminum plate, with the upper surface in line with the front of the plate. The intensities of diffraction lines were determined as integrated intensity by the weight method after subtracting the background scattering.

2) Photographic Technique: The precession camera (Rigaku Denki Co., Ltd.) was used as a flat film camera (pinhole camera). The measurement conditions were as follows: voltage, 35 kV; current, 10 mA; distance between sample and film, 75 mm; time of exposure, 60 min.

When the photograph was taken by irradiating the upper surface of a tablet, the sample was mounted on the goniometer head so that the cylindrical axis of the tablet was coincident with the incident X-ray beam. When the photograph was taken by irradiating the die-wall surface of a tablet, the sample was mounted on the goniometer head so that diametral direction of the tablet was coincident with the incident X-ray beam and the cylindrical axis of the tablet was parallel to the meridian of the film.

Results and Discussion

Evaluation of the Crystallite Orientation by Diffractometry

Geometrical Arrangements of Sample, X-Ray Source and Counter for the Symmetrical-Reflection Method and Symmetrical-Transmission Method——Two principal geometrical arrangements of the sample with respect to the X-ray source and counter were used, as shown in Fig. 1.[4] Figure 1a shows the method for the symmetrical-reflection analysis, which is widely used for powder diffractometry, and Fig. 1b shows the method for the symmetrical-transmission analysis. In the symmetrical-reflection method, the diffraction lines are observed only from the crystal planes having the reciprocal lattice vectors normal to the upper surface, that is, the diffraction lines are obtained only from crystal planes parallel to the upper surface.

On the other hand, in the symmetrical-transmission method, the diffraction lines are observed only from the crystal planes normal to the upper surface of the tablet. Thus, the two methods can be used to observe two crystal planes normal to each other.

Calculation of Theoretical Diffraction Intensities——It is well known that when the specimen has random orientation, the intensities of the X-ray diffraction lines are expressed as Eq. 1.[5]

$$I(hkl)=|F(hkl)|^2 P\frac{1+\cos^2 2\theta}{\sin^2\theta\cos\theta}T(\theta) \qquad (1)$$

where $I(hkl)$ is the integrated intensity of (hkl) planes, $F(hkl)$ is the crystal structure factor of (hkl) planes, P is the multiplicity factor, θ is the Bragg angle and $T(\theta)$ is the temperature factor. The theoretical integrated intensities of the diffraction lines for aspirin and salicylic

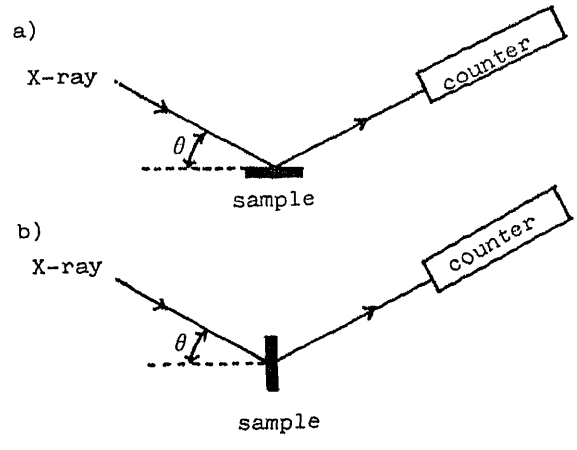

Fig. 1. Geometrical Arrangements of the Specimen with Respect to the X-Ray Source and Counter for Diffractometry

a), symmetrical-reflection geometry; b), symmetrical-transmission geometry.

acid were calculated according to Eq. 1. The crystal structures were determined by Wheatley[6] and Sundaralingam and Jensen,[7] respectively. The crystal data are as follows: aspirin is monoclinic, space group $P2_1/c$, $a=11.445\pm0.0013$, $b=6.596\pm0.006$, $c=11.388\pm0.009$ Å and $\beta=95°33'\pm2'$; salicylic acid is monoclinic, space group $P2_1/a$, $a=11.52\pm0.012$, $b=11.21\pm0.011$, $c=4.92\pm0.005$ Å and $\beta=90°50'\pm2'$.

The structure factors used have already been corrected for thermal vibration. Thus, the theoretical integrated intensities were calculated using above parameters except for the temperature factor. The results are shown in Tables I and II (plane indices, structure factors and multiplicity factors). The intensities were expressed as relative values (percent of maximum intensity).

Crystallite Orientation in Tablets of Aspirin and Salicylic Acid——Figure 2 shows the calculated X-ray diffraction patterns and the observed X-ray diffraction patterns (symmetrical-reflection method) of aspirin and salicylic acid powders. Diffraction intensities were expressed as relative integrated intensity, determined from the area of the coherent scattering curve after subtracting the background scattering from the total intensity curve.

Table I. Relative Integrated Intensities of the Diffraction Lines on an X-Ray Diffraction Pattern of Aspirin

2θ	$(hkl)^{a)}$	$F^{b)}$	$P^{c)}$	Relative integrated intensity (%)
7.8	(100)	3828	2	19
15.6	(002)	10804	2	100
	(011)	−3119	4	
	(110)	−2664	4	
	(200)	−4609	2	
20.6	(012)	4977	4	22
	(210)	2841	4	
22.6	(112)	−7613	4	63
	(211)	7653	4	
23.1	(202)	−6850	2	12
26.8	(212)	−9211	4	32

a) The reflecting plane indices. *b*) The structure factor. *c*) The multiplicity factor.

Table II. Relative Integrated Intensities of the Diffraction Lines on an X-Ray Diffraction Pattern of Salicylic Acid

2θ	$(hkl)^{a)}$	$F^{b)}$	$P^{c)}$	Relative integrated intensity (%)
11.0	(110)	398	4	61
15.5	(020)	−206	2	10
	(200)	256	2	
17.5	(120)	−179	4	58
	(210)	−591	4	
19.7	(011)	−328	4	12
25.3	(121)	1058	4	100
	(211)	584	4	
28.8	(221)	730	4	28
30.6	(311)	618	4	20
	(31$\bar{1}$)	−246	4	

a) The reflecting plane indices. *b*) The structure factor. *c*) The multiplicity factor.

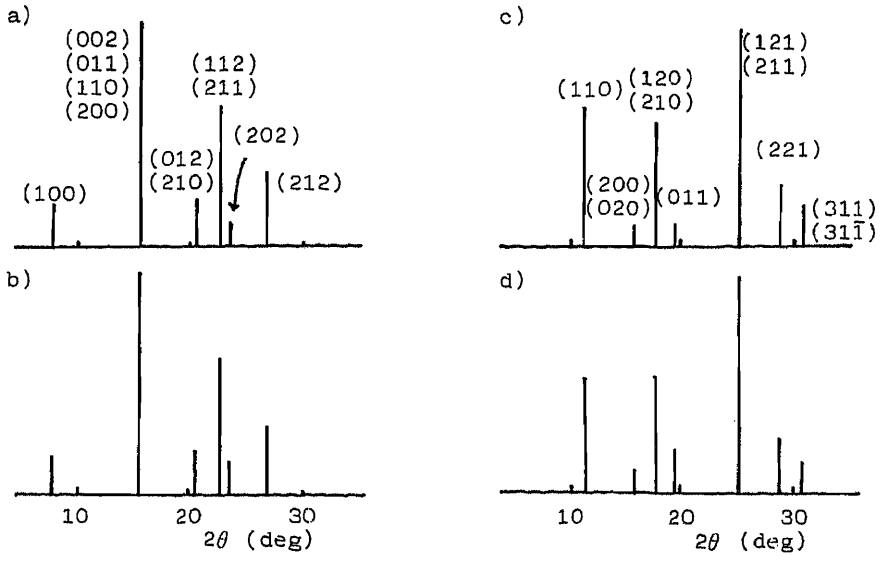

Fig. 2. Calculated and Observed (Symmetrical-Reflection Method) X-Ray Diffraction Patterns of Aspirin and Salicylic Acid Powder

a), calculated pattern of aspirin; b), observed pattern of aspirin; c), calculated pattern of salicylic acid; d), observed pattern of salicylic acid.

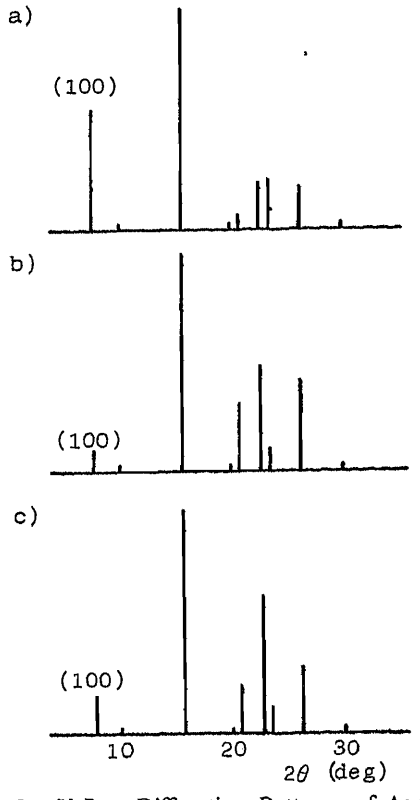

Fig. 3. X-Ray Diffraction Patterns of Aspirin Tablet

a), symmetrical-reflection method; b), symmetrical-transmission method; c), calculated pattern.

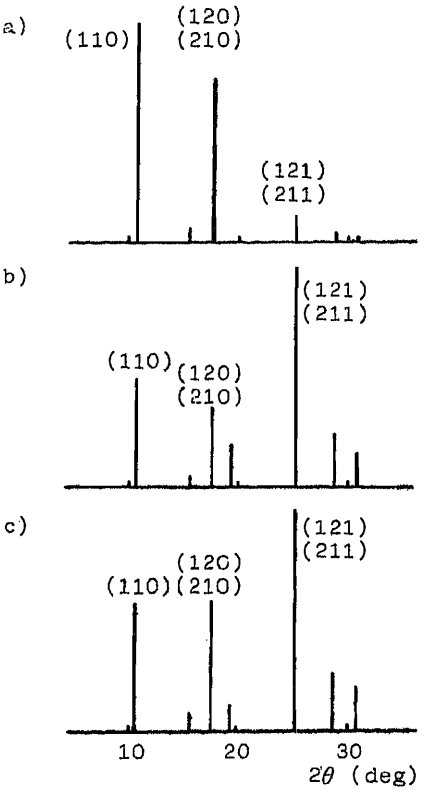

Fig. 4. X-Ray Diffraction Patterns of Salicylic Acid Tablet

a), symmetrical-reflection method; b), symmetrical-transmission method; c), calculated pattern.

The experimentally observed diffraction patterns agreed well with the calculated diffraction patterns, and this indicates that a random orientation of drug crystallites was maintained in the sample powders.

Figures 3 and 4 show the X-ray diffraction patterns obtained by the symmetrical-reflection method and by the symmetrical-transmission method for aspirin and salicylic acid tablets compressed under the pressure of 750 kg/cm^2, respectively. For the symmetrical-transmission method, the correction for absorption was done according to Eq. 2.[4)]

$$\frac{I_{0^\circ}}{I_{2\theta}} = \frac{\exp(-\mu t(1-\sec\theta))}{\sec\theta} \tag{2}$$

where μ is the linear absorption coefficient, t is the thickness of the specimen and θ is the Bragg angle. The value of μt was determined experimentally.

On comparing the diffraction patterns of aspirin tablet with that calculated according to Eq. 1, an increase in the relative intensity from the (100) planes was observed by the symmetrical-reflection method. On the other hand, a slight decrease in the intensity from these planes was observed by the symmetrical-transmission method, as shown in Fig. 3. Similarly, for salicylic acid tablet, an increase in the integrated intensities from the (110) and (120); (210) planes and a decrease in the intensity from the (121); (211) planes were observed by the symmetrical-reflection method, while a decrease in the intensity from the (120); (210) planes were observed by the symmetrical-transmission method, as shown in Fig. 4. These results indicate that the (100) planes of aspirin crystallites and the (110) and the (120); (210) planes of

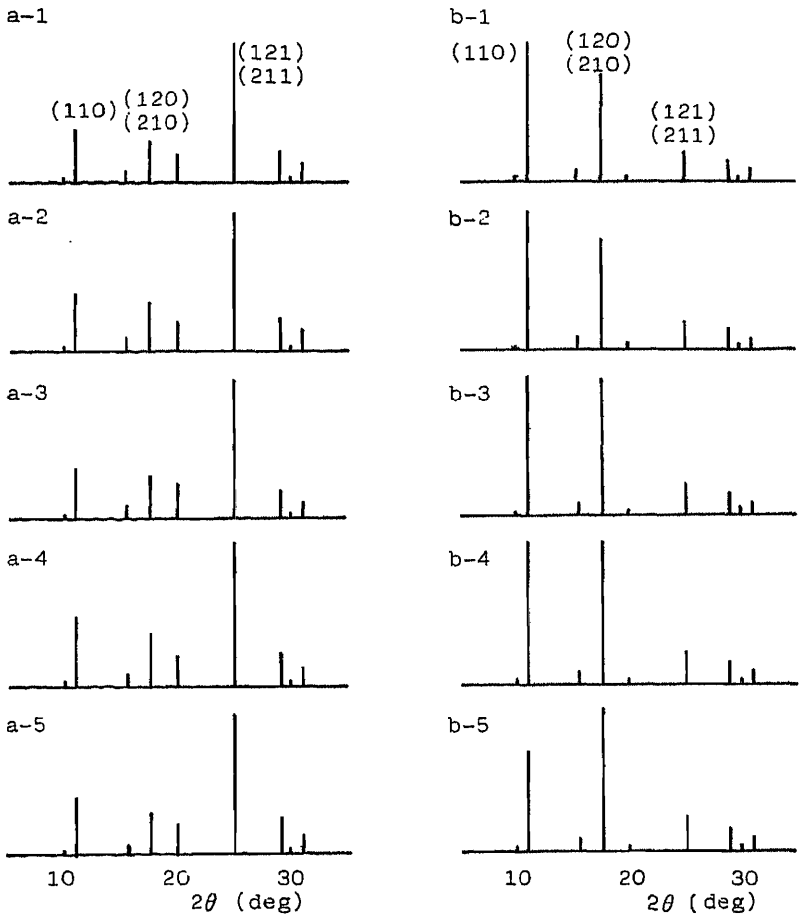

Fig. 5. X-Ray Diffraction Patterns of Salicylic Acid Tablets Compressed under Various Pressures Obtained by the Symmetrical-Transmission Method (a) and Symmetrical-Reflection Method (b)

Compaction pressure: a-1 and b-1; 750 kg/cm^2, a-2 and b-2; 1500 kg/cm^2, a-3 and b-3; 2250 kg/cm^2, a-4 and b-4; 3000 kg/cm^2, a-5 and b-5; 3750 kg/cm^2.

salicylic acid crystallites have a tendency to align in parallel with the upper surface of a tablet. The results agree well with those reported by Nakai *et al.*[3]

It was found that the intensities of characteristic lines were significantly different in the two methods, that is, although random orientation of crystallites was maintained in the powder, the crystallites were oriented preferentially in the tablet.

Thus, by using the present methods, the crystallite orientation in powders and in tablets can be easily evaluated by comparing the observed intensities with the theoretical intensities calculated according to Eq. 1.

Effect of Compaction Pressure on the Crystallite Orientation

X-ray diffraction patterns of salicylic acid tablets compressed under various pressures are shown in Fig. 5. The diffraction patterns obtained by the symmetrical-transmission method did not vary with the compaction pressure. However, the ratio of the intensity from the (110) planes and the (120); (210) planes ($\text{ratio}_{(110)(120)(210)}$) obtained by the symmetrical-reflection method did vary with the compaction pressure, that is, the $\text{ratio}_{(110)(120)(210)}$ decreased gradually with increase in the compaction pressure. This indicates that the crystallite orientation occurred preferentially at the upper surface of the tablet at relatively low compaction pressure and then varied with increase in the compaction pressure, presumably because destruction and movement of crystallites occurred at high compaction pressures.

Crystallite Orientation by the Photographic Method

The analysis of crystallite orientation has usually been carried out by the X-ray photographic method in the field of polymer science. This method was applied for the evaluation of the crystallite orientation in a tablet. X-ray photographs were taken by irradiating the upper and die-wall surfaces of a tablet with a monochromatic X-ray beam. Figures 6 and 7 show the photographs for aspirin and salicylic acid tablets, respectively.

All the Debye-Scherrer rings were continuous and uniform when the upper surface was irradiated perpendicularly to the X-ray beam, so the planes of the crystallites observed are found to be oriented randomly (Figs. 6a and 7a). On the other hand, in the photograph taken by irradiating the die-wall surface of aspirin tablet, the Debye-Scherrer rings from the (100) planes (innermost ring) and from the (202) and the (212) planes (the outer two) were

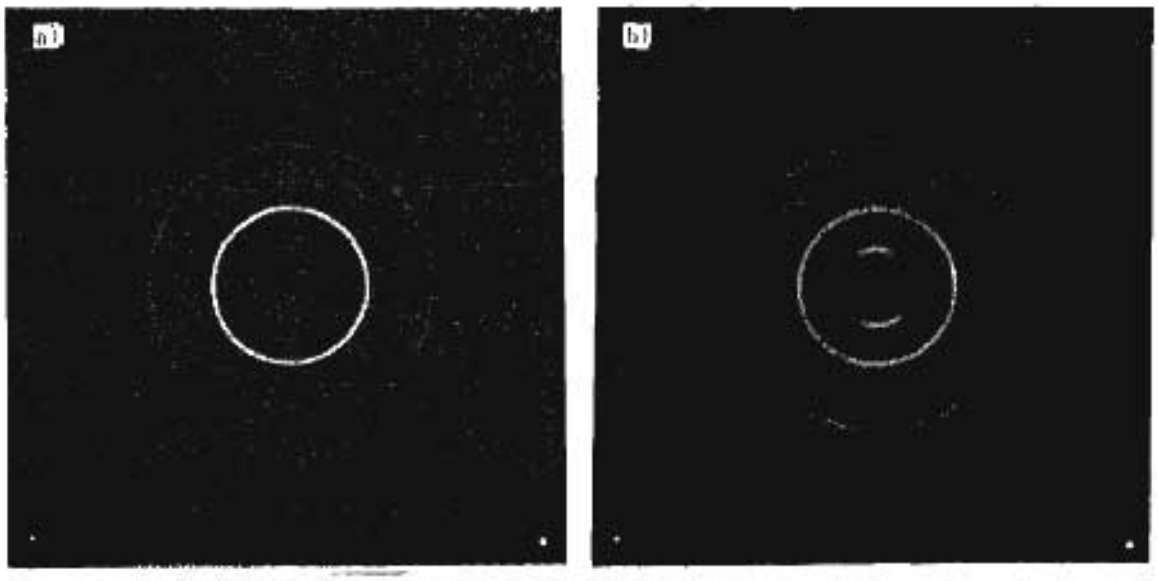

Fig. 6. X-Ray Flat Film Photographs for Aspirin Tablet

a), X-ray beam was normal to the upper surface; b), X-ray beam was normal to the die-wall surface. The mericion of the film was parallel to the cylindrical axis of the tablet.

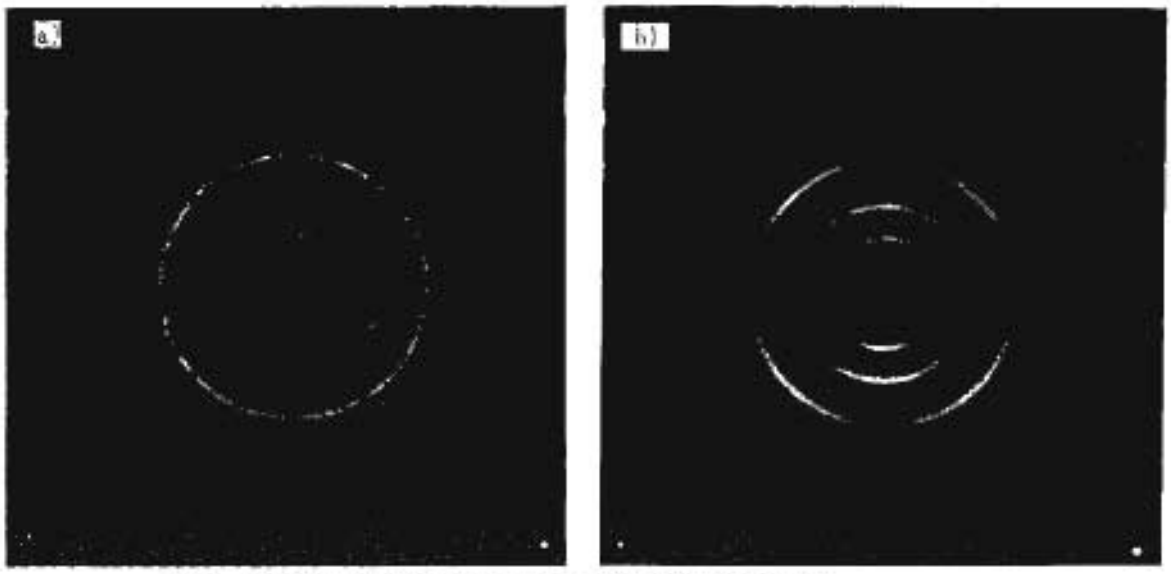

Fig. 7 X-Ray Flat Film Photographs for Salicylic Acid Tablet

a). X-ray beam was normal to the upper surface; b). X-ray beam was normal to the die-wall surface. The meridian of the film was parallel to the cylindrical axis of the tablet.

discontinuous and incomplete, as shown in Fig. 6b. Similarly, in the photograph from the die-wall surface of salicylic acid tablet, the rings from the (110) and (120); (210) planes (the inner two) were discontinuous and arc-like, as shown in Fig. 7b.

These results agree well with those obtained by the diffractometric method for the preferred orientations of aspirin and salicylic acid crystallites in the tablets, that is, 1) the Debye–Scherrer rings at low diffraction angle obtained by irradiating the upper surface of a tablet consist of the diffraction lines from the crystal planes arranged almost normal to the upper surface of the tablet. Thus, these crystal planes are almost the same as those observed by the symmetrical-transmission method. 2) Meridional reflections at low diffraction angle in the photograph taken by irradiating the die-wall surface of a tablet consist of the diffraction lines from the crystal planes arranged almost parallel to the upper surface of the tablet and so these crystal planes are almost the same as those observed by the symmetrical-reflection method.

Although the flat film photographic method is effective to evaluate the crystallite orientation in a tablet qualitatively, it is not applicable for the quantitative investigation of crystallite orientation, because the direction of the reciprocal lattice vector of the crystal contributing to the intensity changes with the diffraction angle and it is impossible to obtain the diffraction lines only from the planes arranged in the specified direction.

References and Notes

1) This work was presented at the 104th Annual Meeting of the Pharmaceutical Society of Japan, Sendai, March 1984.
2) J. T. Fell and J. M. Newton, *J. Pharm. Sci.*, **60**, 1866 (1971); P. York, *J. Pharm. Pharmacol.*, **30**, 6 (1978); H. Hess, *Pharm. Technol.*, **2**, 38 (1978).
3) Y. Nakai, E. Fukuoka and H. Nakagawa, *Yakugaku Zasshi*, **98**, 23 (1978); *idem*, *ibid.*, **98**, 184 (1978); H. Nakagawa, E. Fukuoka and Y. Nakai, *ibid.*, **99**, 936 (1979); H. Nakagawa, *Chem. Pharm. Bull.*, **30**, 1401 (1982).
4) L. E. Alexander, "X-Ray Diffraction Methods in Polymer Science," John Wiley and Sons, New York, 1969; H. Klug and L. E. Alexander, "X-Ray Diffraction Procedures for Polycrystalline and Amorphous Materials," 2nd Ed., John Wiley and Sons, New York, 1974.
5) B. D. Cullity, "Elements of X-Ray Diffraction," 2nd Ed., Addison Wesley, Reading, Massachusetts, 1978.
6) P. J. Wheatley, *J. Chem. Soc.*, **1964**, 6036.
7) M. Sundaralingam and L. H. Jensen, *Acta Cryst.*, **18**, 1053 (1965).

[Chem. Pharm. Bull. 35(4)1571—1578(1987)]

Augmentation of Antibody-Dependent Cellular Cytotoxicity of Polymorphonuclear Leukocytes by Interferon-Gamma: Mechanism Dependent on Enhancement of Fc Receptor Expression and Increased Release of Activated Oxygens

SHUU MATSUMOTO,* MAKIKO TAKEI, MASAMI MORIYAMA and HIDEYO IMANISHI

Basic Research Laboratories, Toray Industries Inc., Tebiro 1111, Kamakura 248, Japan

(Received September 19, 1986)

The effect of recombinant human interferon (IFN)-gamma(Met–Gln form), having the same amino acid sequence as that of natural human IFN-gamma except for the N-terminal Met residue, on antibody-dependent cellular cytotoxic (ADCC) activity of human peripheral polymorphonuclear leukocytes (PMNs) against anti-chicken red blood cell (CRBC) immunoglobulin G (IgG)-coated CRBC was investigated comparatively with those of natural human IFN-alpha and -beta *in vitro*. IFN-gamma dramatically induced the ADCC activity at all doses tested when examined at a $1/10^4$ dilution rate of the IgG, while no significant induction was observed with IFN-alpha or -beta. The Fc receptor (FcR) analysis by flow cytometry using fluorescein isothiocyanate-labelled (FITC)-anti-CRBC IgG revealed that IFN-gamma but not IFN-alpha or -beta remarkably increased the number of PMNs bearing FcR. By applying an *in vitro* measurement system for activated oxygen species using luminol solution, it was demonstrated that activated oxygen species were actually released from PMNs in the ADCC reaction. Further, inhibition experiments using three oxygen scavengers (superoxide dismutase, catalase and dimethyl sulfoxide) demonstrated the involvement of superoxide anion and hydroxy radical as cytolytic mediators in the PMN-ADCC activity induced by IFN-gamma.

These results indicate a much more potent PMN-activating ability of IFN-gamma than IFN-alpha or -beta and involvement of a mechanism dependent on the enhancement of FcR expression on the PMN surface and the increased release of superoxide anions and hydroxy radicals in the PMN-ADCC augmentation by IFN-gamma.

Keywords——interferon; polymorphonuclear leukocyte; antibody-dependent cellular cytotoxicity; Fc receptor; activated oxygen

Introduction

It is well known that polymorphonuclear leukocytes (PMNs) in human peripheral blood have Fc receptors (FcRs) on their surface and have antibody-dependent cellular cytotoxic (ADCC) activity against target cell sensitized with specific antibody.[1] Many reports have described the interferon (IFN)-induced augmentation of various immunomodulating activities, including ADCC activities of human peripheral lymphocytes and monocytes.[2] However, there are few reports dealing with the effects of IFNs on ADCC activity of PMNs.[3] Hokland and Berg reported that human leukocyte IFN enhanced the ADCC activity of human PMNs,[3a] but Farr *et al.* found that human PMN functions including ADCC activity were unaffected by recombinant human IFN-alpha2.[3b] Recently, Basham *et al.* have demonstrated that recombinant human IFN-gamma (Cys–Tyr–Cys–Gln form) having Cys–Tyr–Cys–Gln at the N-terminal[4] augmented the PMN-ADCC activity more effectively than

recombinant human IFN-alpha and -beta at a low dose.[3c] Shalaby *et al.*[3d] have also reported the augmentation of PMN-ADCC activity induced by recombinant human IFN-gamma (Met–Gln form) which has the same amino acid sequence as that of natural human IFN-gamma as elucidated by Rinderknecht *et al.*[5] except for the N-terminal Met residue.[3d] In spite of these studies, the mechanism of the IFN-gamma-induced augmentation is still unclear.

In the present study, we first attempted to compare the PMN-ADCC activity-augmenting ability of recombinant human IFN-gamma (Met–Gln form) with those of natural human IFN-alpha and -beta. IFN-gamma had a much stronger ability to induce PMN-ADCC activity than IFN-alpha or -beta at a low concentration of antibody. Further, to clarify the mechanism of the IFN-gamma-induced augmentation, we investigated the effects of these IFNs on the expression of FcR on human PMNs, because our previous studies had revealed that IFN-gamma augments the ADCC activity of human monocytes by increasing the number of monocytes bearing FcR.[6] As expected, IFN-gamma but not IFN-alpha or -beta actually increased the number of PMNs bearing FcR.

Next, we attempted to identify cytolytic mediators participating in the PMN-ADCC reaction. Since it was reported that one of the cytolytic mediators involved in the PMN-ADCC reaction was superoxide anion (O_2^-),[7] enhancement of the production and release of O_2^- by IFN-gamma is one possibility. To test this hypothesis, we tried to measure the amount of activated oxygen species released from PMNs during the PMN-ADCC reaction. The data indicate actual release of activated oxygen species in the ADCC reaction. Further, to elucidate the species of activated oxygen, we performed inhibition experiments using three scavengers of activated oxygen species. It was indicated that the cytolytic mediators involved were O_2^- and hydroxy radical (·OH), and that IFN-gamma possibly augmented the PMN-ADCC activity by enhancing the production and release of these two species of activated oxygen.

Experimental

Interferons——Recombinant human IFN-gamma (specific activity: 2.72×10^7 unit/mg protein, % purity (sodium dodecyl sulfate-polyacrylamide gel electrophoresis): 99.9%, lymulus amoebocyte lysate: 0.03 ng/mg protein) was supplied by Genentech, Inc. (South San Francisco, U.S.A.). Natural human IFN-beta (1.0×10^7 unit/mg protein) was prepared by the super induction method using human diploid fibroblasts in our laboratories as previously described.[8] Natural human IFN-alpha (3.72×10^6 unit/mg protein) was kindly provided by Dr. K. Cantell (Central Public Health Laboratory, Helsinki, Finland). The titer of each IFN represents the antiviral activity determined by the 50% cytopathic effect reduction method using FL cells and VSV or Sindbis virus.

Preparation of PMNs——Heparinized human peripheral blood (50 ml) obtained from a normal volunteer was mixed with 15 ml of saline containing 6% dextran, and the mixture was left for 60 min. The upper layer was removed and layered over Lymphoprep (Nyegaad, Oslo, Norway). After centrifugation for 30 min at $400 \times g$, a pellet containing PMNs was obtained. The pellet was washed with Dulbecco's phosphate-buffered saline not containing Mg^{2+} and Ca^{2+} (Dulbecco PBS(−)). Contaminating red blood cells in the pellet were destroyed by adding Tris-buffer containing 0.83% NH_4Cl, and PMNs were resuspended in RPMI 1640 medium (Nissui Seiyaku, Tokyo, Japan) containing heat-inactivated 10% fetal calf serum (FCS; Commonwealth Serum Laboratories, Melbourne, Australia). The purity of PMNs in the suspension was 93% as judged by Giemsa staining. The percentage of the PMNs which were able to phagocytose Immunobeads (BIO-RAD, Cal., U.S.A.) was 89% in the suspension.

Treatment of PMNs with IFNs——For ADCC assay, 100 μl of PMN suspension containing from 2×10^4 to 2×10^5 cells in RPMI 1640 medium containing 10% FCS and 100 μl of IFN solution or control solution were mixed in each well of Nunc plastic tissue culture plates (U-bottomed, 96 wells; Inter Med, Denmark) prior to incubation at 37 °C for 20 h in humidified atmosphere of 95% air–5% CO_2. After the incubation, PMNs in wells were washed three times with RPMI 1640 medium containing 10% FCS and 100 μl of the same medium was added to each well.

For flow cytometry, 1×10^6 PMNs in 1 ml of RPMI 1640 medium containing 10% FCS were treated with 1 ml of IFN solution or control solution in Falcon 60 × 15 mm plastic dishes (Becton Dickinson, Oxnard, U.S.A.). These dishes were incubated for 20 h under the same conditions as described above. At the end of this incubation period, PMNs were gently exfoliated by using a rubber policeman, and then washed with RPMI 1640 medium containing 10% FCS and suspended in the same medium.

For measurement of activated oxygens, 5×10^5 PMNs in 250 μl of RPMI-1640 medium containing 10% FCS and

250 μl of IFN solution or control solution were added to flat-bottomed glass tubes (1 cm i.d. × 4.5 cm). These tubes were incubated for 20 h under the same conditions as described above. After the incubation, the supernatants were removed and 100 μl of Dulbecco PBS(−) was added to each tube.

The viability of the IFN-treated PMNs was >99% as evaluated by the trypan-blue exclusion test.

ADCC Assay——ADCC activity was measured by ^{51}Cr-release assay using chicken red blood cells (CRBCs) as target cells. CRBCs were separated from heparinized fresh whole blood of White Leghorn chickens (female). After washing, 5×10^7 CRBCs were incubated in 600 μl of RPMI 1640 medium containing 300 μCi of $Na_2{}^{51}CrO_4$ (New England Nuclear, Boston, U.S.A.) and 5% FCS for 3 h at 37 °C in humidified atmosphere of 95% air–5% CO_2. These ^{51}Cr-labelled CRBCs were subsequently washed three times and adjusted to the desired density with RPMI 1640 medium containing 10% FCS. Then 50 μl of ^{51}Cr-labelled CRBC suspension (1×10^4 cells) and 50 μl of antibody solution of 1/250 or 1/2500 diluted rabbit anti-CRBC IgG (Fujizoki Pharmaceutical, Tokyo, Japan) were added to the wells containing PMNs treated with IFNs or control solution. In the inhibition experiments on the ADCC reaction by activated oxygen scavengers, 10 μl of a solution containing 63 units of superoxide dismutase (SOD, Sigma, St. Louis, U.S.A.), 210 units of catalase (Sigma, St. Louis, U.S.A.), or 21 μmol of dimethyl sulfoxide (DMSO, Kishida Chemical, Osaka, Japan) was added to each well. These plates were incubated at 37 °C for 6 h under the same conditions as described above prior to separation of the supernatants by automated equipment (Titertek Supernatant Collection System; Flow Laboratories, Virginia, U.S.A.). Their radioactivities were measured by using a well-type gamma counter (Packard AUTO-GAMMA 5780, Packard Instrument, Downers Grove, Ill., U.S.A.). The following formula was used to calculated the percent specific lysis;

$$\% \text{ specific lysis} = \frac{\text{experimental cpm} - \text{SR cpm}}{\text{MR cpm} - \text{SR cpm}} \times 100$$

In this formula, MR cpm was determined as cpm in the supernatant obtained after the lysis of ^{51}Cr-labelled CRBCs with distilled water. SR cpm was determined as cpm released from ^{51}Cr-labelled CRBCs incubated with RPMI 1640 medium containing 10% FCS alone in the absence of PMNs.

FcR Analysis by Flow Cytometry——FcR analyses were performed by the same method as described previously.[6] In brief, 1×10^6 PMNs which had been treated with IFN or control solution were labelled with rabbit FITC-anti-CRBC IgG (Cappel Laboratories, Cochranville, U.S.A.). These labelled PMNs were analyzed by using a Cytofluorograf system 50H (Ortho Diagnostic Systems, Raritan, U.S.A.) or Spectrum III (Ortho Diagnostic Systems, Raritan, U.S.A.).

Measurement of Activated Oxygen Species in ADCC Reaction——Flat-bottomed glass tubes containing 5×10^5 PMNs treated with IFN or control solution were preincubated at 37 °C for 2 min, and then 100 μl of luminol solution (0.56 mM in Dulbecco PBS(−)), 50 μl of 1/250 or 1/2500 diluted solution of rabbit anti-CRBC IgG and 50 μl of fresh CRBC suspension (1×10^7 cells) were added to each tube. Chemiluminescence was measured by a luminescence analyzer (Picolite 6100; Packard Instrument, Downers Grove, Ill., U.S.A.) for 10 s every 1 min up to 15 min after the addition of these solutions.

Results

Effects of Anti-CRBC IgG and *E/T* Ratio on ADCC Activity

Figure 1A shows the effects of anti-CRBC IgG on the ADCC activity of PMNs treated with IFN-gamma and control solution. PMNs treated with control solution had a weak ADCC activity at the $1/10^3$ and $1/10^2$ dilution rates of the IgG but no ADCC activity was found at the $1/10^5$ and $1/10^4$ dilution rates. On the other hand, PMNs treated with IFN-gamma had strong ADCC activities at all dilution rates except the higher one, at which a very weak ADCC activity was noted.

Figure 1B shows the effects of *E/T* ratio on the ADCC activity of PMNs treated with IFN-gamma and control solution at the $1/10^4$ dilution rate. ADCC activities of PMNs treated with IFN-gamma were increased in proportion to the increase of *E/T* ratio, but not with control solution.

Comparison of ADCC-Augmenting Abilities among IFNs

Figure 2 shows the dose-dependent effects of IFN-gamma on the ADCC activity of PMNs compared with those of IFN-alpha and -beta. Both IFN-gamma and -beta but not IFN-alpha induced an ADCC activity, and the induction by IFN-gamma was more marked than that by IFN-beta regardless of the IFN dose. In particular, at 10 unit/ml, the ADCC

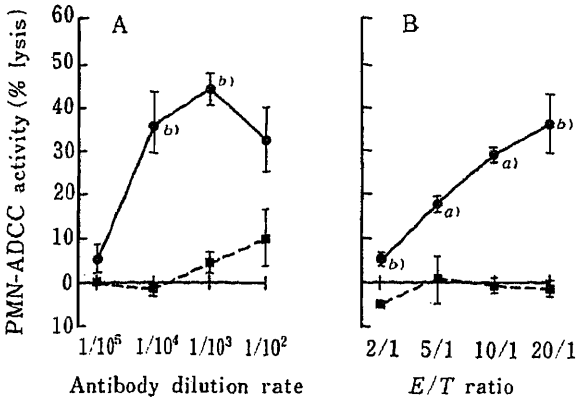

Fig. 1. Effects of Antibody Dilution Rate and *E/T* Ratio on PMN-ADCC Augmentation by IFN-Gamma

A, *E/T*=20/1; B, antibody dilution rate=1/10⁴. ■---■, control; ●—●, IFN-gamma.
Each point represents the mean±S.E. of three donors. *a*) Significant difference from control, $p<0.05$. *b*) Significant difference from control, $p<0.01$.

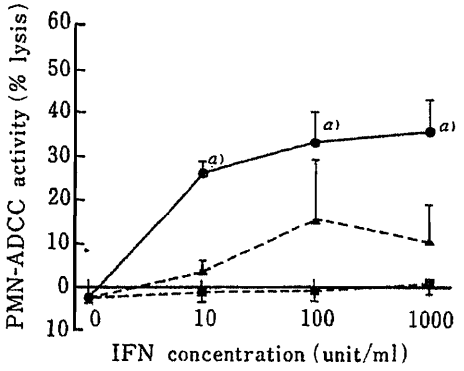

Fig. 2. Effects of IFNs on PMN-ADCC Activity

Antibody dilution rate=1/10⁴. ■---■, IFN-alpha; ▲---▲, IFN-beta; ●—●, IFN-gamma.
Each point represents the mean±S.E. of three donors. *a*) Significant difference from control, $p<0.05$.

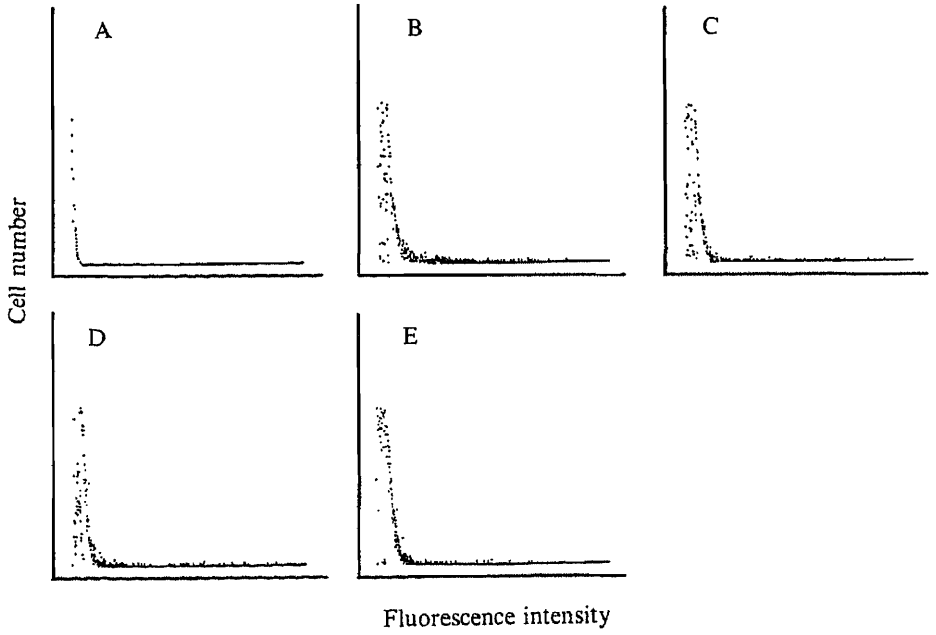

Fig. 3. Effects of IFNs on FcR Expression in PMNs

A, fresh control; B, overnight control; C, IFN-alpha; D, IFN-beta; E, IFN-gamma.
These data were obtained from a single donor. Similar results were also obtained from two other donors (data not shown).

activity of PMNs induced by IFN-gamma was about 8-fold higher than that by IFN-beta.

Effects of IFNs on FcR Expression in PMNs

Figure 3 shows the histograms of PMNs treated with IFN and control solution and fresh PMNs obtained by flow cytometry using FITC-anti-CRBC IgG. As shown in the figure the patterns of these histograms are very similar to each other, indicating that the overnight incubation of PMNs with the three IFNs and control solution induced no significant effect on the FcR expression on the PMN surface. On the other hand, the number of PMNs bearing

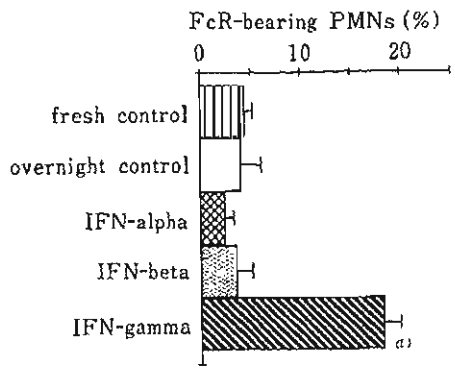

Fig. 4. Effects of IFNs on FcR Expression in PMNs

Percentage of PMNs bearing FcR binding to anti-CRBC IgG in PMN preparation.
The results represent the mean±S.E. of three donors. *a*) Significant difference from control, $p<0.01$.

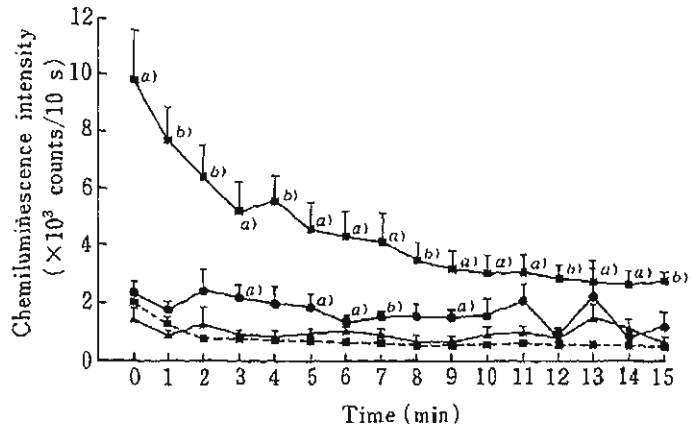

Fig. 5. Effects of IFNs on Activated Oxygen Production by PMNs in PMN-ADCC Reaction

■---■, control; ▲—▲, IFN-alpha; ●—●, IFN-beta; ■—■, IFN-gamma.
Each point represents the mean±S.E. of three donors. *a*) Significant difference from control, $p<0.05$. *b*) Significant difference from control, $p<0.01$.

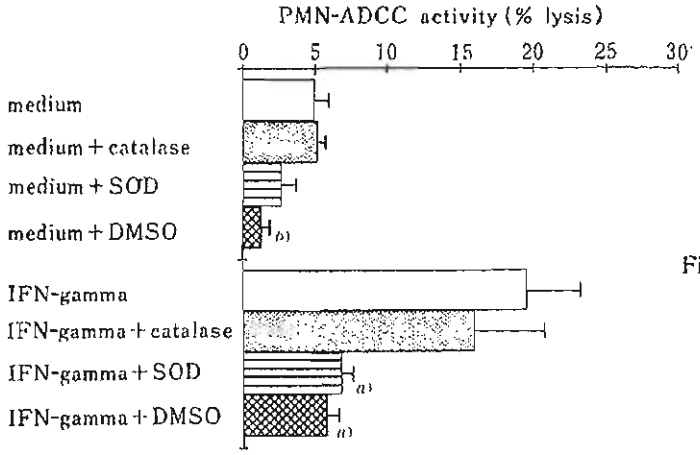

Fig. 6. Effects of Activated Oxygen Scavengers on PMN-ADCC Augmentation by IFN-Gamma

The results represent the mean±S.E. of three donors. *a*) Significant difference from control, $p<0.05$. *b*) Significant difference from control, $p<0.01$.

FcR was significantly increased by treatment with IFN-gamma but not IFN-alpha or -beta when compared with fresh and overnight controls, as shown in Fig. 4. The overnight incubation in control solution had no effect on the percentage of PMNs bearing FcR in total PMNs (Fig. 4).

Effects of IFNs on Activated Oxygen Production in the ADCC Reaction

The effects of IFNs on the production of activated oxygen species for 15 min after the initiation of the ADCC reaction are shown in Fig. 5. IFN-gamma significantly augmented the production more effectively than IFN-beta and -alpha. The significant augmentation induced by IFN-gamma persisted for 30 min (data not shown).

Effects of Oxygen Scavengers on ADCC Augmentation by IFN-gamma

Figure 6 shows the effects of three oxygen scavengers, *i.e.* SOD, catalase and DMSO, on the ADCC augmentation induced by IFN-gamma at a 1/10000 dilution rate of anti-CRBC IgG. The figure indicates significant inhibitory effects of SOD and DMSO on the augmentation, while catalase had no effect. DMSO but not SOD or catalase inhibited the ADCC

activity of control PMNs. Similar results were obtained at the 1/1000 dilution rate of the IgG (data not shown).

Discussion

The present study confirms that recombinant human IFN-gamma (Met–Gln form) augmented ADCC activity against anti-CRBC IgG-coated CRBC of human peripheral PMNs, as reported by Shalaby *et al.*[3d] Although Basham *et al.* have repoted that recombinant human IFN-gamma (Cys–Tyr–Cys–Gln form) augmented the PMN-ADCC activity more effectively than IFN-alpha and -beta at low doses (1 and 100 unit/ml) but not at 500 unit/ml in the presence of a suboptimal concentration of the IgG,[3c] the present study showed that only IFN-gamma (Met–Gln form) significantly induced strong ADCC activity at high doses ranging from 10 to 1000 unit/ml, while IFN-alpha and -beta did not, when the dilution rate of the IgG was $1/10^4$ (Fig. 2). It is considered that this discrepancy may be caused by the difference of the concentration of the IgG used, not the difference in the form of recombinant IFN-gamma. Namely, it is likely that the amount of the IgG at the $1/10^4$ dilution rate in our system is smaller than that in their system, because the ADCC activity of control PMNs in their system was very high (50% lysis) whereas that in our system was very low (almost 0% lysis) as shown in Fig. 2. Therefore, we speculate that the suboptimal concentration of the IgG in their study may correspond to a lower dilution rate than the $1/10^4$ dilution rate used in our study. This speculation may be supported by the finding that IFN-gamma augmented the PMN-ADCC activity more effectively than IFN-alpha and -beta at low dose (10 unit/ml) when the dilution rate of the IgG was $1/10^3$ (data not shown). Taking into account these findings, it is conceivable that IFN-gamma is able to show a stronger inducing ability of PMN-ADCC activity against CRBC than IFN-alpha and -beta when examined at a very low concentration of anti-CRBC IgG which induces no PMN-ADCC activity in control PMNs.

The present study also demonstrates that IFN-gamma remarkably increased the number of PMNs bearing FcR binding to anti-CRBC IgG (Fig. 4), indicating that IFN-gamma induced or augmented the PMN-ADCC activity by increasing the number of PMNs bearing the FcR. Namely, the increase in FcR-bearing PMNs may in turn imply a substantial increase of the *E/T* ratio. The FcR-bearing PMNs were about 5% of control PMNs as shown in Fig. 4, which is in conflict with the results reported by Zighelboim *et al.*, who gave a value of 56%.[9] However, they also reported that the PMNs binding to non-aggregated rabbit IgG amounted to 8%,[9] which is consistent with our results. We believe that the increasing effect of IFN-gamma on the number of FcR-bearing PMNs observed in this study is reliable because $F(ab')_2$ of FITC-anti-CRBC IgG did not bind to PMNs (data not shown).

On the other hand, the PMN-ADCC augmenting abilities of IFN-alpha and -beta as mentioned above cannot be explained simply in terms of the number of FcR-bearing PMNs, because of the lack of increase of the number (Fig. 4). Since a recent report indicated that there are different IFN-receptors for IFN-gamma and for IFN-alpha and -beta on human cells,[10] there may be different IFN receptors on human PMNs, and IFN-alpha and -beta may have different effects from IFN-gamma on PMNs. Recently, Philip and Epstein have reported that tumor necrosis factor mediated human monocyte cytotoxicity against human tumor cells induced by IFN-gamma but not IFN-alpha.[11] Therefore, it is possible that different molecules may mediate the PMN-ADCC augmentation induced by IFN-alpha and -beta. In addition, the involvement of other mechanisms in the PMN-ADCC augmentation by IFNs, such as an enhancement of lytic ability of PMNs after binding to target cells or of recruitment of PMNs participating in the ADCC reaction, cannot be excluded.

The inhibition experiments using three oxygen scavengers indicated that O_2^- and hydroxy radical ($\cdot OH$) play a role as cytolytic mediators in the expression of the ADCC activity of

PMNs treated with IFN-gamma (Fig. 6). Since SOD as well as dimethyl sulfoxide (DMSO) completely inhibited the ADCC augmentation induced by IFN-gamma (Fig. 6), it is unlikely that O_2^- damaged CRBC independently of ·OH. Although it is generally known that ·OH is produced from O_2^- and H_2O_2,[12] catalase had no effect on the ADCC augmentation (Fig. 6), which is consistent with the finding reported by Capsoni *et al.* that catalase did not inhibit PMN-ADCC activity against anti-CRBC IgG-coated CRBC.[7] Therefore, we speculate that only O_2^- but not H_2O_2 may have been converted into ·OH, which acted cytotoxically on CRBC. However, the conversion mechanism is unclear. On the contrary, our experiments indicated that only ·OH but not O_2^- was the cytolytic mediator in the ADCC reaction of control PMNs (Fig. 6). In this case, ·OH may be generated from the prostaglandin-biosynthesis system[13] because SOD and catalase had no effect on the control PMN-ADCC reaction (Fig. 6). However, the results are in conflict with the finding reported by Capsoni *et al.* that the cytolytic mediator was O_2^- in the control PMN-ADCC reaction.[7] The reason for the discrepancy is unknown, but the possibility that the cytolytic mediators may be different depending on the level of the ADCC activity cannot be excluded because the ADCC activity in their system was high (60% lysis) while that in our system was low (from 5% to 15% lysis) (Fig. 2).

There are several reports demonstrating that the mechanism of the PMN-ADCC reaction is oxygen-independent. For instance, Cordier and Revillard reported that phospholipase A_2 was a cytolytic mediator in the PMN-ADCC reaction using CRBC as target cells.[14] Recently, Dallegri *et al.* have shown that PMNs released both activated oxygen species and phospholipase A_2 in the PMN-ADCC reaction using Raji cells as target cells, and pointed out the possibility that either of the two cytolytic mediators may become dominant depending on the experimental conditions.[15] Therefore, the participation of phospholipase A_2 in the PMN-ADCC reaction in our study is also possible, but the contribution of the enzyme to the augmentation by IFN-gamma may be slight because SOD and DMSO completely inhibited the augmentation (Fig. 6).

In conclusion, we have found in the present study (1) strong inducing ability of IFN-gamma for PMN-ADCC activity, (2) the mechanism of IFN-gamma-induced augmentation is dependent on enhancement of FcR expression and increased release of O_2^- and ·OH and (3) weak or no effects of IFN-alpha and -beta on the PMN functions. Since the pharmacological significance of these PMN-modulating activities of IFN-gamma is unclear, further investigations in animals using animal IFN-gamma seem to be necessary.

Acknowledgments The authors thank Miss M. Kondoh and Mrs. K. Yamanaka for their skillful technical assistance. We are grateful to Dr. A. Kitai and Mr. N. Naruse for their encouragement and support of this study.

References

1) *a*) R. P. Gale and J. Zighelboim, *J. Immunol.*, **114**, 1047 (1975); *b*) R. A. Clark and S. J. Klebanoff, *ibid.*, **119**, 1413 (1977); *c*) J. M. Oleske, R. B. Ashman, S. Kohl, S. L. Shore, S. E. Starr, P. Wood and A. J. Nahmias, *Clin. Exp. Immunol.*, **27**, 446 (1977); *d*) D. G. Hafeman and Z. J. Lucas, *J. Immunol.*, **123**, 55 (1979).
2) *a*) E. De Maeyer, "Interferon vol 1. General and Applied Aspects," ed. by A. Billiau, Elsevier Science Publishers B. V., Amsterdam, 1984, pp. 167—185; *b*) R. B. Herberman, "Interferon vol. 2. Interferons and the Immune System," ed. by J. Vilček and E. De Maeyer, Elsevier Science Publishers B. V., Amsterdam, 1984, pp. 61—84.
3) *a*) P. Hokland and K. Berg, *J. Immunol.*, **127**, 1585 (1981); *b*) B. Farr, J. M. Gwaltney, F. G. Hayden and G. L. Mandell, *Infect. Immun.*, **42**, 1195 (1983); *c*) T. Y. Basham, K. S. Wendelin and T. C. Merigan, *Cell. Immunol.*, **88**, 393 (1984); *d*) M. R. Shalaby, B. B. Aggarwal, E. Rinderknecht, L. P. Svedersky, B. S. Finkle and M. A. Palladino, *J. Immunol.*, **135**, 2069 (1985).
4) P. W. Gray, D. W. Leung, D. Pennica, E. Yelverton, R. Najarian, C. C. Simonsen, R. Derynck, P. J. Sherwood, D. M. Wallace, S. L. Berger, A. D. Levinson and D. V. Goeddel, *Nature* (London), **295**, 503 (1982).
5) E. Rinderknecht, B. H. O'Connor and H. Rodriguez, *J. Biol. Chem.*, **259**, 6790 (1984).
6) S. Matsumoto, M. Moriyama and H. Imanishi, *Chem. Pharm. Bull.*, **35**, 335 (1987).

7) F. Capsoni, P. L. Meroni, G. F. Ciboddo and G. Colombo, *N. Engl. J. Med.*, **300**, 44 (1979).
8) S. Kobayashi, M. Iizuka, M. Hara, H. Ozawa, T. Nagashima and J. Suzuki, "The Clinical Potential of Interferons," ed. by R. Kono and J. Vilček, University of Tokyo Press, Tokyo, 1982, pp. 57—68.
9) J. Zighelboim, R. P. Gale and E. Kedar, *Transplantation*, **21**, 524 (1976).
10) S. J. Littman, C. R. Faltynek and C. Baglioni, *J. Biol. Chem.*, **260**, 1191 (1985).
11) R. Philip and L. B. Epstein, *Nature* (London), **323**, 86 (1986).
12) J. A. Badwey and M. L. Karnovsky, *Ann. Rev. Biochem.*, **49**, 695 (1980).
13) F. A. Kuehl, E. A. Ham, R. W. Egan, H. W. Dougherty, R. J. Bonney and J. L. Humes, "Pathology of Oxygen," ed. by A. P. Autor, Academic Press, New York, 1982, pp. 175—190.
14) G. Cordier and J. P. Revillard, *Experientia*, **36**, 603 (1980).
15) F. Dallegri, F. Patrone, G. Frumento and C. Sacchetti, *J. Natl. Cancer Inst.*, **73**, 331 (1984).

[Chem. Pharm. Bull. 35(4)1579—1586(1987)]

Metabolism of 2,4-Dinitrotoluene, 2,4-Dinitrobenzyl Alcohol and 2,4-Dinitrobenzaldehyde by Rat Liver Microsomal and Cytosol Fractions

Miki Shoji,*,[a] Masa-aki Mori,[b] Tadashi Kawajiri,[b] Michio Sayama,[b] Yoshihiro Mori,[b] Tatsuro Miyahara,[b] Takashi Honda[c] and Hiroshi Kozuka[b]

Radioisotope Laboratory,[a] Faculty of Pharmaceutical Sciences,[b] and School of Medicine,[c] Toyama Medical and Pharmaceutical University, 2630 Sugitani, Toyama 930-01, Japan

(Received August 28, 1986)

The metabolism of 2,4-dinitrotoluene (2,4-DNT), 2,4-dinitrobenzyl alcohol (2,4-DNB) and 2,4-dinitrobenzaldehyde (2,4-DNAl) in rat liver microsomal and cytosol fractions was investigated. The objectives of these studies were to determine whether 2,4-DNAl, a potent mutagen, is produced in the oxidation of 2,4-DNB to 2,4-DNBA and to clarify the nature of the enzymes responsible for the oxidation of 2,4-DNT to 2,4-DNB, 2,4-DNAl and 2,4-dinitrobenzoic acid (2,4-DNBA). Data obtained from high-performance liquid chromatography indicated that the major products of 2,4-DNT, 2,4-DNB and 2,4-DNAl in the microsomal and cytosol preparations were 2,4-DNB, 2,4-DNAl, and 2,4-DNBA and 2,4-DNB, respectively. The results indicate that 2,4-DNAl is an intermediate in the oxidation of 2,4-DNB to 2,4-DNBA. In addition, data obtained by incubating 2,4-DNT, 2,4-DNB or 2,4-DNAl with microsomal or cytosol fraction under air, nitrogen and various concentrations of CO in oxygen, using cofactors nicotinamide adenine dinucleotide phosphate and reduced nicotinamide adenine dinucleotide phosphate [NAD(P) and NAD(P)H] and inhibitors (SKF-525A, dimethyl sulfoxide, chloral hydrate, allopurinol, pyrazole and *o*-phenanthroline) suggest that: (a) oxidation of 2,4-DNT to 2,4-DNB is mediated by microsomal P-450; (b) oxidation of 2,4-DNB to 2,4-DNAl is mediated mainly by cytochrome P-450 and NAD-dependent alcohol dehydrogenase; (c) oxidation of 2,4-DNAl to 2,4-DNBA and reduction of 2,4-DNAl to 2,4-DNB may be mediated by NAD(P)-dependent aldehyde dehydrogenases and NAD(P)H-dependent aldehyde reductases, respectively. These results indicate that 2,4-DNT is metabolized stepwise to 2,4-DNB, 2,4-DNAl and 2,4-DNBA in the rat liver and suggest that the oxidation of 2,4-DNB to 2,4-DNAl is a metabolic activation of 2,4-DNT and that the microsomal cytochrome P-450 and alcohol dehydrogenase may play an important role in the metabolic activation of 2,4-DNT.

Keywords——2,4-dinitrotoluene; 2,4-dinitrobenzyl alcohol; 2,4-dinitrobenzaldehyde; 2,4-dinitrobenzoic acid; metabolism; microsomal cytochrome P-450; cytosol; alcohol dehydrogenase; aldehyde dehydrogenase; aldehyde reductase

2,4-Dinitrotoluene (2,4-DNT) is a major constituent of technical grade DNT (75% 2,4-DNT, 20% 2,6-DNT, 5% other isomers) which is a precursor of toluenediisocyanate, used in the manufacture of polyurethane foams and elastomers.[1] Although technical grade DNT,[2] 2,4-DNT[3] and 2,6-DNT[4] have been shown to produce hepatocellular carcinomas when administered in the diet of rats, unequivocal mutagenic activity of DNT isomers has not been detected in the Ames assay using histidine-requiring *Salmonella typhimurium* strains with or without S9 mix.[5] These findings suggest that the metabolic activation of DNT is very complicated. Rickert *et al.* proposed a hypothesis for the metabolism and toxicity of DNT isomers: the activation of DNT requires biotransformation to dinitrobenzyl alcohol glucuronide, excretion in the bile, deconjugation, further metabolism by intestinal microorganisms

and reabsorption, and the reabsorbed metabolites are presumably converted to toxic metabolites.[1]

We have reported that the urinary major metabolites of 2,4-DNT in rats are 2,4-dinitrobenzyl alcohol (2,4-DNB) and 2,4-dinitrobenzoic acid (2,4-DNBA),[6] and that 2,4-dinitrobenzaldehyde (2,4-DNAl), which is not detected as a urinary metabolite of 2,4-DNT, is a direct potent mutagen (about 10000 his^+ revertants/μmol) in the Ames assay using *Salmonella typhimurium* strains TA 98 and TA 100.[7] As 2,4-DNAl is considered to be a possible intermediate in the oxidation of 2,4-DNB to 2,4-DNBA, it is worth investigating the oxidative metabolism of 2,4-DNT in rat liver in order to understand the metabolic activation of the agent. In the present study, we have examined the metabolism of 2,4-DNT, 2,4-DNB and 2,4-DNAl by using hepatic microsomal and cytosol fractions prepared from rats pretreated with phenobarbital (PB) and 5,6-benzoflavone (BF). Experiments were performed with various inhibitors under air, nitrogen and various concentrations of CO in oxygen to assess the nature of the enzymes responsible for the consecutive oxidations of 2,4-DNT.

Experimental

Chemicals——2,4-DNT and 2,4-DNBA (>99% chromatographically pure after recrystallization from methanol) were obtained from Wako Pure Chemical Industries Ltd. 2,4-DNAl (>98% pure) was obtained from Aldrich Chemical Co. 2,4-DNB was prepared as previously described.[8] β-Diethylaminoethyl diphenyl-*n*-propylacetate hydrochloride (SKF-525A) was a gift from Prof. H. Yoshimura, Kyushu University (Japan). Other chemicals were obtained from the following sources: dimethyl sulfoxide (DMSO, ultra grade), PB, BF, chloral hydrate, allopurinol, pyrazole and *o*-phenanthroline from Wako Pure Chemical Industries Ltd.; reduced nicotinamide adenine dinucleotide phosphate (NADPH), reduced nicotinamide adenine dinucleotide (NADH), NADP, NAD and alcohol dehydrogenase (345 IU/mg protein, from yeast) from Oriental Yeast Co., Ltd.; tetra-*n*-butylammonium chloride (TBACl) from Nakarai Chemicals Ltd. Solvents used were of the highest grade commercially available.

Preparation of Liver Fractions——Male Sprague-Dawley rats (160—180 g) obtained from Sankyo Laboratories Co. were pretreated with PB (80 mg/kg in 0.9% NaCl, i.p., 96, 72, 48 and 24 h before death) and BF (80 mg/kg in corn oil, i.p., 48 h before death) in a similar manner to that used for pretreatment in the case of hepatic preparations used for the assay of mutagenicity.[7] Animals were killed by decapitation. The livers were removed, minced and homogenized in three volumes of ice-cold 1.15% KCl. The microsomal and cytosol fractions were prepared by differential centrifugation as previously described.[9] Protein was determined by the method of Lowry *et al.*[10] with bovine serum albumin as a standard.

Incubation of Enzyme Preparations with 2,4-DNT, 2,4-DNB and 2,4-DNAl——Standard incubation mixtures (2 ml) contained 65 mM phosphate buffer (pH 7.4), 4 mM cofactors (NADPH, NADH, NADP or NAD in H_2O), 1 mM substrates (2,4-DNT, 2,4-DNB or 2,4-DNAl in DMSO or acetone) and 2.2 or 2.7 mg of microsomal or cytosol proteins. In some experiments, 0.1 to 5 mM inhibitor (SKF-525A, DMSO, chloral hydrate, pyrazole, allopurinol or *o*-phenanthroline) was added. The incubations were carried out at 37 °C for 5 to 60 min under air, nitrogen or various concentrations of CO in oxygen. The CO–O_2 mixtures were prepared in gas burettes and passed into Thunberg vessels containing the reaction mixtures. The incubations were terminated by addition of 0.2 ml of 0.5 N HCl followed by the addition of 10 ml of ether.

Analysis of Metabolites Produced in 2,4-DNT, 2,4-DNB or 2,4-DNAl Metabolism by High-Performance Liquid Chromatography (HPLC)——Incubation mixtures from triplicate reaction tubes were extracted three times with 10 ml of ether. The ether layer was dried over anhydrous Na_2SO_4, and the solvent was evaporated off under an N_2 stream and reconstituted in 5 ml of 40% methanol solution. Then 10 μl of this solution was injected into a high-performance liquid chromatograph equipped with a multi-wavelength ultraviolet (UV) monitor (Hitachi model 655). The reversed-phase column used was TSK gel ODS-80TM (150 × 4.6 mm i.d., particle size 5 μm, Toyo Soda Kogyo Co.). The mobile phase used was 40% methanol in 0.18 mM TBACl. HPLC operating conditions were as follows: flow rate, 1.0 ml/min; UV monitor, 250 nm; column temperature, ambient. Under these conditions, 2,4-DNT, 2,4-DNB, 2,4-DNAl and 2,4-DNBA gave retention times of 20.2, 8.6, 11.3 and 4.7 min, respectively. Quantities of metabolites were determined from standard curves plotted as peak area *vs.* amount of standard injected. The range of concentrations used in determination of the standard curves was 0.15—2.8 ng/μl. Standard curves generated were linear over the concentration range measured ($r=0.999$) with no more than 5% variability between replicate samples. The amounts of metabolites were expressed as nanomoles produced per milligram of protein or gram of liver.

Results

The detection of metabolites was carried out by comparing the chromatograms of incubated samples with those of blanks, and by the co-chromatography of incubated samples with authentic samples. Table I shows the products detected chromatographically in the

TABLE I. Metabolites Detected by HPLC in the Hepatic Metabolism of 2,4-DNT, 2,4-DNB and 2,4-DNAl

Substrate	Incubation system		Metabolite	Retention time (min)	Activity
	Enzyme source	Cofactor			nmol/g liver/min
2,4-DNT	MS	NADH	2,4-DNB	8.6	8.60±0.49
		NADPH	2,4-DNB	8.6	64.48±1.62
		NADH+NADPH	2,4-DNB	8.6	74.68±1.19
		NAD or NADP	n.d.	—	—
2,4-DNB	MS	NADH	2,4-DNAl	11.3	4.10±0.78
		NADPH	2,4-DNAl	11.3	7.45±0.86
		NAD	2,4-DNAl	11.3	2.95±0.44
		NADP	2,4-DNAl	11.3	3.73±0.68
	CS	NADH	2,4-DNAl	11.3	8.54±0.76
		NADPH	2,4-DNAl	11.3	7.48±1.23
		NAD	2,4-DNAl	11.3	17.63±2.86
		NADP	2,4-DNAl	11.3	18.87±3.21
	MS	NAD	2,4-DNBA	4.7	60.30±1.52
			2,4-DNB	8.6	4.12±0.78
			Unknown	3.1	—
		NADP	2,4-DNBA	4.7	60.59±4.23
			2,4-DNB	8.6	1.29±0.32
			Unknown	3.1	—
		NADH	2,4-DNBA	4.7	6.89±0.91
			2,4-DNB	8.6	24.57±1.25
			Unknown	5.3	—
		NADPH	2,4-DNBA	4.7	1.58±0.10
			2,4-DNB	8.6	5.01±0.19
			Unknown	5.3	—
2,4-DNAl	CS	NAD	2,4-DNBA	4.7	64.53±4.60
			2,4-DNB	8.6	7.76±0.09
		NADP	2,4-DNBA	4.7	13.98±0.43
			2,4-DNB	8.6	1.00±0.02
		NADH	2,4-DNBA	4.7	52.19±7.03
			2,4-DNB	8.6	109.02±0.88
			Unknown	3.1	—
		NADPH	2,4-DNBA	4.7	15.18±2.46
			2,4-DNB	8.6	320.29±7.89
			Unknown	3.1	—

Incubation mixtures (2 ml) contained 65 mM phosphate buffer (pH 7.4), 4 mM cofactor, 1 mM substrate and 2.2 or 2.7 mg of microsomal or cytosol proteins. Incubations were carried out at 37°C for 15 min under air. HPLC operating conditions were as follows: column, TSK gel ODS-80TM; mobile phase, 40% MeOH in 0.18 mM TBACl; flow rate, 1.0 ml/min; UV monitor, 250 nm; column temperature, ambient. Values are means±S.D. for three samples. n.d., not detected; MS, microsomes; CS, cytosol; 2,4-DNT, 2,4-dinitrotoluene; 2,4-DNB, 2,4-dinitrobenzyl alcohol; 2,4-DNAl, 2,4-dinitrobenzaldehyde; 2,4-DNBA, 2,4-dinitrobenzoic acid.

metabolism of 2,4-DNT, 2,4-DNB or 2,4-DNAl by hepatic microsomal or cytosol preparations. The detection limit of each compound in this experiment was 1.0 ng. No peaks corresponding to metabolites were detected after incubating substrates with heat-in-activated (90 °C, 10 min) microsomes or cytosol, or without microsomes or cytosol (chromatograms not shown).

The metabolite produced by incubation of 2,4-DNT with microsomal preparations was 2,4-DNB (Table I). This enzyme reaction required reduced forms of pyridine nucleotides, of which NADPH was much more effective than NADH as a cofactor. Synergism of the two cofactors was seen under these experimental conditions. No metabolites were produced by incubating 2,4-DNT with cytosol instead of microsomes as an enzyme source (data not shown). The rate of 2,4-DNT oxidation to 2,4-DNB was nearly linear with respect to microsomal protein concentration (0 to 1 mg/ml), NADPH concentration (0 to 4 mM), incubation time (0 to 30 min) and substrate concentration (0 to 0.4 mM). The rate reached a plateau at 5 mg/ml protein concentration, 6 mM NADPH concentration, 60 min incubation time and 0.6 mM substrate concentration. The oxidation of 2,4-DNT to 2,4-DNB by NADPH-dependent microsomal enzyme was almost completely inhibited in an atmosphere of

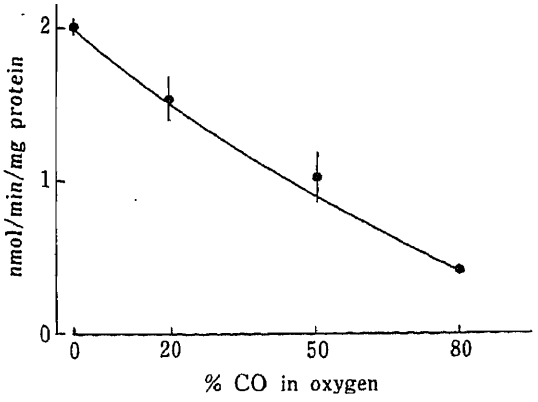

Fig. 1. Effect of CO on Microsomal NADPH-Dependent Oxidation of 2,4-DNT to 2,4-DNB

Incubation mixtures (2 ml) contained 65 mM phosphate buffer (pH 7.4), 4 mM NADPH, 1 mM 2,4-DNT and 2.2 mg of microsomal protein. Incubations were carried out at 37 °C for 15 min under various CO concentrations. Each point represents the mean ± S.D. of three samples.

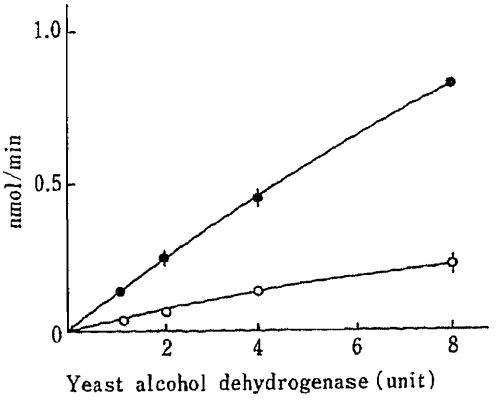

Fig. 2. Oxidation of 2,4-DNB to 2,4-DNAl by Yeast Alcohol Dehydrogenase Requiring NAD

Incubation mixtures (2 ml) contained 65 mM phosphate buffer (pH 7.4), 4 mM NAD or NADP, 1 mM 2,4-DNAl, and 1 to 8 units of yeast alcohol dehydrogenase. Incubations were carried out at 37 °C for 20 min under air. Each point represents the mean ± S.D. of three samples.
—●—, NAD; —○—, NADP.

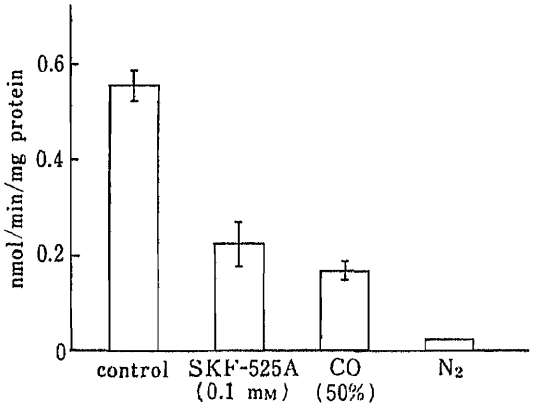

Fig. 3. Effects of SKF-525A, CO and N_2 on Microsomal NADPH-Dependent Oxidation of 2,4-DNB to 2,4-DNAl

Incubation mixtures (2 ml) contained 65 mM phosphate buffer (pH 7.4), 4 mM NADPH, 1 mM 2,4-DNB, 2.2 mg of microsomal protein and 0 or 0.1 mM SKF-525A. Incubations were carried out at 37 °C for 20 min under air, 50% CO in oxygen or N_2. Each bar represents the mean ± S.D. of three samples.

nitrogen (data not shown). In addition, this oxidation was inhibited by about 25, 50 and 80%, respectively, in atmospheres of 20, 50 and 80% of CO in oxygen (Fig. 1) and inhibited by about 85% by a low concentration (0.1 mM) of SKF-525A, an inhibitor of cytochrome P-450 dependent monooxygenase.[11] These findings indicate that the oxidation of 2,4-DNT to 2,4-DNB is mediated by hepatic microsomal cytochrome P-450.

The production of 2,4-DNAl from 2,4-DNB was mainly dependent on the cytosol preparations containing NAD(P) and microsomal preparation containing NADPH as a cofactor (Table I). The 2,4-DNB oxidation to 2,4-DNAl by cytosol preparation containing NAD was inhibited by about 50 and 40% by addition of 1 mM DMSO[12] and 5 mM *o*-phenanthroline,[13] inhibitors of NAD-dependent alcohol dehydrogenase, but this oxidation was not inhibited by addition of 1 mM pyrazole,[13] an inhibitor of alcohol dehydrogenase (data not shown). In addition, this oxidation was mediated by yeast alcohol dehydrogenase, requiring NAD as a cofactor (Fig. 2). The 2,4-DNB oxidation to 2,4-DNAl by cytosolic preparation containing NADP was not inhibited by DMSO, *o*-phenanthroline or pyrazole (data not shown). Therefore, it seems that the NADP-dependent activity may differ from the NAD-dependent activity. Further characterization of the NAD(P)-dependent activities was not attempted. The 2,4-DNB oxidation to 2,4-DNAl by microsomal preparation containing NADPH was inhibited by about 60, 70 and 95% by addition of 0.1 mM SKF-525A and in the

Table II. Effect of Chloral Hydrate on Microsomal and Cytosol NAD(P)-Dependent Oxidations of 2,4-DNAl to 2,4-DNBA

Inhibitor (mM)		Incubation system		Percent inhibition
		Enzyme source	Cofactor	
Chloral hydrate	(0.5)	CS	NAD	5.3±2.8
			NADP	42.8±6.8
		MS	NAD	28.5±4.6
			NADP	42.5±6.7
	(1.0)	CS	NAD	8.6±1.9
			NADP	63.2±5.9
		MS	NAD	50.2±4.8
			NADP	78.5±7.2

Incubation mixtures (2.0 ml) contained 65 mM phosphate buffer (pH 7.4), 4 mM NAD or NADP, 1 mM 2,4-DNAl, 0.5 or 1.0 mM chloral hydrate and 2.2 or 2.7 mg of microsomal or cytosol proteins. Incubations were carried out at 37 °C for 20 min under room air. Results are expressed as percent inhibition of 2,4-DNBA production. Values are means±S.D. for three samples.

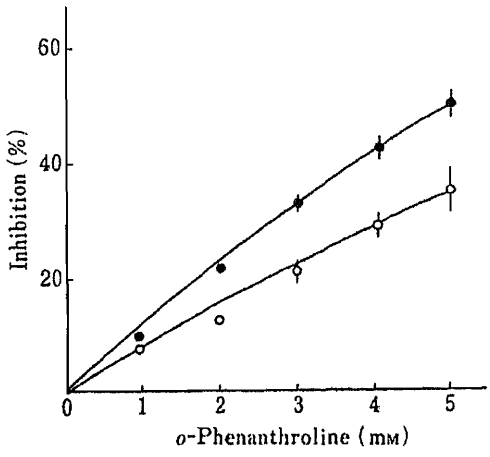

Fig. 4. Effect of *o*-Phenanthroline on Microsomal and Cytosol NADH-Dependent Reductions of 2,4-DNAl to 2,4-DNB

Incubation mixtures (2 ml) contained 65 mM phosphate buffer (pH 7.4), 4 mM NADH, 1 mM 2,4-DNAl, 2.2 or 2.7 mg of microsomal or cytosol proteins and 0 or 1 to 5 mM *o*-phenanthroline. Incubations were carried out at 37 °C for 20 min under air. Each point represents the mean±S.D. of three samples. —○—, microsomes; —●—, cytosol.

atmospheres of 50% CO in oxygen or nitrogen (Fig. 3). These findings strongly suggest that a large proportion of 2,4-DNB oxidation to 2,4-DNAl is mediated by both NAD-dependent alcohol dehydrogenase and microsomal cytochrome P-450 but a part of that may be due to NADP-dependent cytosolic dehydrogenase.

When 2,4-DNAl was incubated with cytosol or microsomal preparations containing oxidized and reduced forms of pyridine nucleotides, it was found to be metabolized to 2,4-DNBA and 2,4-DNB, and two unknown metabolites with retention times of 3.1 or 5.3 min (Table I, chromatograms not shown). Characterization of the unknown compounds was not attempted. The oxidation of 2,4-DNAl to 2,4-DNBA was mainly dependent on the cytosol and microsomal preparations containing oxidized forms of pyridine nucleotides. The 2,4-DNAl oxidation to 2,4-DNBA was inhibited partially by chloral hydrate, an inhibitor of NAD(P)-dependent aldehyde dehydrogenases[14] (Table II). However, allopurinol, an inhibitor of xanthine oxidase, which is a dehydrogenase requiring NAD as a cofactor,[15] did not inhibit the 2,4-DNAl oxidation to 2,4-DNBA (data not shown). These findings suggest the participation of NAD(P)-dependent aldehyde dehydrogenases in the 2,4-DNAl oxidation to 2,4-DNBA. The reduction of 2,4-DNAl to 2,4-DNB was dependent on the cytosol and microsomal preparations containing reduced forms of pyridine nucleotides (Table I). The 2,4-DNAl reduction to 2,4-DNB by cytosol and microsomal preparations containing NADH was inhibited by about 50 and 35%, respectively, by 5 mM *o*-phenanthroline (Fig. 4).

Discussion

The present investigations have demonstrated that: (a) the metabolites of 2,4-DNT, 2,4-DNB and 2,4-DNAl produced by hepatic preparations are 2,4-DNB, 2,4-DNAl and 2,4-DNBA; (b) 2,4-DNT oxidation to 2,4-DNB can be accomplished by microsomal cytochrome P-450 dependent monooxygenase; (c) 2,4-DNB oxidation to 2,4-DNAl is mediated by either alcohol dehydrogenase or cytochrome P-450; (d) 2,4-DNAl oxidation to 2,4-DNBA is mediated by aldehyde dehydrogenases and aldehyde oxidases; (e) 2,4-DNAl reduction to 2,4-DNB is mediated by aldehyde reductases. Based on these results, the probable hepatic metabolism of 2,4-DNT in the rat can be summarized as follows (Chart 1).

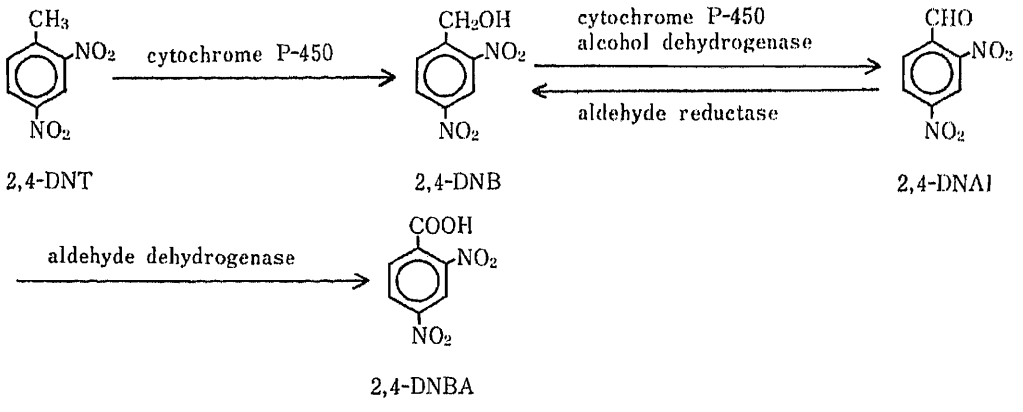

Chart 1. Hepatic Metabolism of 2,4-DNT in the Rat

The finding that the oxidation of 2,4-DNT to 2,4-DNB is mediated by the microsomal cytochrome P-450 of Sprague-Dawley rats is in accord with the result of Decad *et al.*,[16] who have shown the participation of microsomal cytochrome P-450 of Fischer-344 rat liver in the 2,4-DNT oxidation to 2,4-DNB. It seems to be a novel finding that the production of 2,4-DNAl from 2,4-DNB is mediated not only by alcohol dehydrogenases but also by cytochrome P-450, since oxidation of alcohol to aldehyde, in general, is mediated by

dehydrogenases such as alcohol dehydrogenases. In this connection, Watanabe *et al.* also reported that the microsomal oxidation of 11-hydroxy-Δ^8-tetrahydrocannabinol to 11-oxo-Δ^8-tetrahydrocannabinol is mediated by a mixed function oxidase involving cytochrome P-450.[17]

Erwin *et al.*[13] showed that an NADH-linked aldehyde reductase mediating the reduction of aliphatic and aromatic aldehydes such as hepataldehyde and *m*-nitrobenzaldehyde was inhibited about 60% by 5 mM *o*-phenanthroline, but this reductase was not inhibited by pyrazole. In addition, Tabakoff and Erwin[18] and Takahashi *et al.*[19] reported that a non specific aldehyde reductase requiring NADPH was located in cytosol and microsomal fractions. Therefore, it seems that NAD(P)H-dependent microsomal and cytosolic aldehyde reductases may be responsible for the 2,4-DNAl reduction to 2,4-DNB. Moreover, the NADH-dependent cytosolic aldehyde reductase activity may be attributed to the reverse action of NAD-dependent cytosolic alcohol dehydrogenase, because both NAD- and NADH-dependent activities are inhibited by *o*-phenanthroline.

2,4-DNB and 2,4-DNBA were major urinary metabolites of 2,4-DNT in the rat, but 2,4-DNAl was not detected in the urine.[6] However, the finding that 2,4-DNAl can be produced by incubating 2,4-DNB with microsomal and cytosol preparations (Table I and Fig. 3) indicates that 2,4-DNAl is an intermediate in the oxidation of 2,4-DNB to 2,4-DNBA. The discrepancy between *in vivo* and *in vitro* metabolism may be due to the high activities in the oxidation and reduction of 2,4-DNAl to 2,4-DNBA and 2,4-DNB compared with those in the oxidation of 2,4-DNB to 2,4-DNAl (Table I) and an interaction between 2,4-DNAl and hepatic macromolecules, because compounds containing an aldehyde group damage bacterial deoxyribonucleic acid.[5c] In fact, we have shown that 2,4-DNAl is a potent direct-acting mutagen that does not require metabolic activation in the Ames assay using *Salmonella typhimurium*.[7] Thus it seems that the oxidation of 2,4-DNB to 2,4-DNAl, which is mediated by microsomal cytochrome P-450 and alcohol dehydrogenases, may be a metabolic activation of 2,4-DNT in the rat. In addition, the data presented here indicate that the microsomal cytochrome P-450 and cytosolic alcohol dehydrogenase may play an important role in the metabolic activation of 2,4-DNT.

Acknowledgments We are grateful to Professor H. Yoshimura of Kyushu University for supplying SKF-525A.

References and Notes

1) D. E. Rickert, B. E. Butterworth and J. A. Popp, *CRC Critical Rev. Toxicol.*, 13, 217 (1984).
2) Anon., Interim Report, CIIT Docket no. 327N8, Chemical Industry Institute of Toxicology, Research Triangle Park, 1979.
3) H. V. Ellis, J. H. Hagensen, J. R. Hodgson, J. L. Minor, C. B. Hong, E. R. Ellis, J. D. Girvin, D. O. Helton, B. L. Herndon and C. C. Lee, Final Report no. 7, Project 3900-B, Midwest Research Institute, Kansas City, Mo., 1979.
4) J. A. Popp and T. B. Leonard, *Proc. Am. Assoc. Cancer Res.*, 24, 361 (1983).
5) *a*) D. B. Couch, P. Flowe and D. Ragan, *Environ. Mutagenesis*, 1, 168 (1978); *b*) H. Tokiwa, R. Nakagawa and Y. Ohnishi, *Mutat. Res.*, 91, 321 (1981); *c*) C. W. Chiu, L. H. Lee, C. Y. Wang and T. Bryan, *ibid.*, 58, 11 (1978).
6) M. Shoji, M. Mori, K. Moto-o, H. Kozuka and T. Honda, *Chem. Pharm. Bull.*, 34, 1687 (1985).
7) M. Mori, T. Miyahara, K. Taniguchi, K. Hasegawa, H. Kozuka, M. Miyagoshi and T. Nagayama, *Toxicol. Lett.*, 13, 1 (1982); M. Mori, T. Miyahara, K. Moto-o, M. Fukukawa, H. Kozuka, M. Miyagoshi and T. Nagayama, *Chem. Pharm. Bull.*, 33, 4556 (1985).
8) M. Mori, Y. Naruse and H. Kozuka, *Chem. Pharm. Bull.*, 29, 1147 (1981).
9) M. Mori, T. Matsuhashi, T. Miyahara, S. Shibata, C. Izima and H. Kozuka, *Toxicol. Appl. Pharmacol.*, 76, 105 (1984).
10) O. H. Lowry, N. J. Rosebrough, A. L. Farr and R. J. Randall, *J. Biol. Chem.*, 193, 265 (1951).
11) P. L. Gigon, T. E. Gram and J. R. Gillette, *Mol. Pharmacol.*, 5, 109 (1969).
12) M. Sharkawi and B. Elfassy, *Toxicol. Lett.*, 25, 185 (1985).

13) V. G. Erwin, W. D. W. Heston and B. Tabakoff, *J. Neurochem.*, **19**, 2269 (1972).
14) R. Lindahl and S. Evces, *J. Biol. Chem.*, **259**, 11986 (1984).
15) H. H. H. Oei, H. C. Zoganas, J. M. McCord and S. W. Schaffer, *Res. Commun. Chem. Pathol. Pharmacol.*, **51**, 195 (1986).
16) G. M. Decad, M. E. Graichen and J. G. Dent, *Toxicol. Appl. Pharmacol.*, **62**, 325 (1982).
17) K. Watanabe, I. Yamamoto, K. Oguri and H. Yoshimura, *Biochem. Biophys. Res. Commun.*, **88**, 178 (1979).
18) B. Tabakoff and V. G. Erwin, *J. Biol. Chem.*, **245**, 3263 (1970).
19) N. Takahashi, T. Saito, Y. Goda and T. Tomita, *J. Biochem.* (Tokyo), **99**, 513 (1986).

[Chem. Pharm. Bull. 35(4)1587—1595(1987)]

Studies of the Influence of Chloro-Substituent Sites in Tetrachlorobiphenyls on the Uncoupling of Oxidative Phosphorylation in Isolated Rat Liver Mitochondria

YOSHIMASA NISHIHARA,*[,a] LARRY W. ROBERTSON[b] and KOZO UTSUMI[a]

Department of Medical Biology, Kochi Medical School,[a] Kohasu, Okocho, Nangokushi, Kochi 781-51, Japan and Graduate Center for Toxicology, University of Kentucky,[b] 204 Funkhouser Building, Lexington, KY, 40506-0054, U.S.A.

(Received September 5, 1986)

Treatment of isolated rat liver mitochondria with certain tetrachlorobiphenyls (TCBs) resulted in uncoupling of oxidative phosphorylation. In the present study, we examined the effects of chloro-substituent sites in TCB on the uncoupling action. Furthermore, the mechanism by which effective TCBs induce uncoupling action was explored. 2,3,2',3'- (23-), 2,4,2',4'- (24-), 2,5,2',5'- (25-), and 2,6,2',6'- (26-)TCBs caused uncoupling of oxidative phosphorylation, whereas 3,4,3',4'- (34-)TCB did not. TCBs which were effective in causing uncoupling action contained chlorine atoms at the 2,2'-positions in the biphenyl ring. 2,2'-Chloro substitutions give the molecule a highly angular (non-planar) conformation. On the other hand, 34-TCB, which was ineffective, possesses chlorine atoms at lateral adjacent positions in the biphenyl ring. This substitution pattern allows a coplanar conformation of the molecule. Thus, the conformation of effective TCBs was non-planar, whereas that of ineffective isomers was coplanar. The permeability of mitochondrial membranes to ions was increased by the effective TCBs (23-, 24-, 25-, and 26-TCBs) as evidenced by K^+-, and Ca^{2+}-release from mitochondria, which was followed by the dissipation of membrane potential. However, the ineffective TCB (34-TCB) neither increased the ion-permeability nor dissipated the membrane potential. These facts led us to propose to the following uncoupling mechanism; the effective TCBs, when intercalated into the mitochondrial membranes, produce non-specific increases in membrane permeability to ions, which leads to the dissipation of membrane potential. These effects of non-planar TCBs appear to be different from the mechanism of protonophoric uncouplers in which the dissipation of membrane potential is performed by only H^+ transfer across the mitochondrial membranes.

Keywords——tetrachlorobiphenyl; uncoupling action; oxidative phosphorylation; membrane potential; membrane permeability; rat liver mitochondria

An uncoupled state can be produced in mitochondria by a rather wide range of chemicals. Although chemically diverse, the uncoupling agents can be classified into two types. A large number of agents, classified as the first type, resemble 2,4-dinitrophenol (DNP) in their action. The unique property is that they specifically induce cyclical transport of protons across the mitochondrial inner membranes through an acid-dissociable group on the molecule. They are thus called classical or protonophoric uncouplers.[1] The second type of uncoupling agents are non-protonophoric uncouplers. Among the most commonly used are valinomycin (active in the presence of K^+), and nigericin (active in combination with valinomycin and K^+).[2] Most recently, cyanine dye, a hydrophobic cation, has been reported to act as an uncoupler in the presence of inorganic phosphate or arsenate.[3] These agents are often called nonclassical or pseudo-uncouplers.[4] The actions of classical and nonclassical uncouplers show similarity in that the membrane potential is collapsed in the former case by the protonophoric activity of the molecule, and in the latter case by specific ion transport.

Polychlorinated biphenyls (PCBs) are persistent organochlorine compounds ubiquitously distributed as environmental pollutants. Because of their lipophilicity, PCBs tend to accumulate in lipid-rich parts of cells, such as biomembranes; intercalation of these compounds into biomembranes causes alterations of membrane-associated functions.[5] PCBs consist of 209 possible congeners and isomers whose position and degree of chlorination are different, and evaluation of their effect on human health is dependent on a knowledge of the properties of the individual compounds.

While investigating the toxic effects of tetrachlorobiphenyls (TCBs) on energy-transducing functions of mitochondria, we have found that some TCBs uncouple oxidative phosphorylation in rat liver mitochondria.[6] The uncoupling action of a compound is interesting in evaluating its toxicity.[7] Since TCBs do not possess an acid-dissociable group within the molecule (essential for protonophoric activity), they are not expected to be protonophores. Therefore, they may uncouple by a different mechanism from that of protonophoric uncouplers. This paper examines the structural requirements for TCB to show uncoupling action. Furthermore, the possible mechanism by which effective TCBs uncouple oxidative phosphorylation is explored in relation to the structural alteration in the lipid bilayer of mitochondrial inner membranes brought about by the incorporation of these TCBs.

Materials and Methods

Chemicals——2,3,2′,3′-(23-), 2,4,2′,4′- (24-), and 2,6,2′,6′- (26-) TCBs were synthesized by the Ullman condensation of the corresponding dichloroiodobenzenes.[8] 2,5,2′,5′-TCB (25-TCB) was synthesized by the reductive deamination of 2,5,2′,5′-tetrachlorobenzidine using excess hypophosphorous acid.[9] 3,4,3′,4′-TCB (34-TCB) was synthesized from 3,3′-dichlorobenzidine *via* the Sandmeyer reaction as modified by van Roosmalen.[10] The purities of these isomers were found to be more than 99% by gas liquid chromatography. The stock solutions of these isomers except 34-TCB were prepared in ethanol, and that of 34-TCB was prepared in dimethylformamide. The following compound were obtained from Sigma Chemical Co. (St Louis, MO, U.S.A.): adenosine triphosphate (ATP), 2,4-dinitrophenol (DNP), and ruthenium red. Tetraphenylphosphonium chloride (TPP^+) was from Wako Pure Chemical Industries Ltd. (Osaka, Japan). Antipyrylazo III was purchased from Nakarai Chemicals (Kyoto, Japan). Other reagents were commercial products of the highest purity.

Isolation of Mitochondria——Liver mitochondria were isolated from adult male Wistar rats (body weight, 200—300 g) in 0.25 M sucrose, and 5 mM Tris-HCl (pH 7.4) containing 0.1 mM ethylenediaminetetraacetic acid (EDTA) by the method of Hogeboom.[11] EDTA was omitted in the final wash and resuspension. The stock suspension of mitochondria containing about 50 mg of protein/ml was stored on ice until used. The protein content of mitochondria was determined by the biuret analysis using bovine serum albumin as a standard.[12] In all experiments, mitochondrial protein concentration in an assay medium was 1 mg/ml.

Measurements of Respiration Rate——Respiration rates of mitochondria were monitored polarographically with a Clark-type oxygen electrode in a 2 ml glass reaction vessel at 25 °C. The composition of the incubation medium was 0.2 M sucrose, 20 mM KCl, 3 mM $MgCl_2$, and 5 mM potassium phosphate buffer (pH 7.4). 5 mM α-Ketoglutarate/5 mM malate was used as a respiratory substrate.

Measurement of Membrane Potential——Membrane potential across the mitochondrial membranes was monitored at 25 °C with a TPP^+ electrode constructed according to Kamo *et al.*[13] The incubation medium was the same one as used for the respiration rates plus 5 μM TPP^+ in a final volume of 2.5 ml. The calibration of the electrode was performed by multiple additions of a known amount of TPP^+ after each experiment.

Measurement of K^+ Release——The measurements of efflux of endogenous K^+ were carried out with a K^+ electrode connected to a pH meter at 25 °C in a volume of 2.5 ml. The incubation medium consisted of 0.15 M choline chloride, and 5 mM Tris-HCl (pH 7.4). In some experiments, the temperature was changed from 5 to 35 °C. The electrode was calibrated by multiple additions of a known amount of KCl after each experiment.

Measurement of Ca^{2+} Release——Ca^{2+} movement was measured with the metallochromic indicator, antipyrylazo III,[14] with a Shimadzu UV-300 dual-wavelength spectrophotometer, equipped with magnetic stirring and thermostatic control (volume, 2.5 ml; temperature, 25 °C). The wavelength pair was 720—790 nm. Calibration was performed by adding a known amount of $CaCl_2$ in the presence of uncoupler (25 μM DNP) at the end of each experiment. Firstly, mitochondria were loaded with 75 μM Ca^{2+} with 3 mM ATP as the source of energy in 0.2 M sucrose, 20 mM KCl, 3 mM $MgCl_2$, 10 mM potassium acetate, 5 mM Tris-HCl (pH 7.4), and 75 μM antipyrylazo III. After Ca^{2+} loading was complete, 1 μM ruthenium red was added to block re-uptake of Ca^{2+}. Ca^{2+} release from mitochondria was monitored by measuring the absorbance changes of antipyrylazo III; net Ca^{2+} uptake by

mitochondria is accompanied by a decrease in absorbance, and net release is reflected by an increase in absorbance.

In all experiments, the control contained the same volume of solvent (ethanol or dimethylformamide), and the final concentration of the solvent was less than 1% (v/v). This concentration of solvent did not affect the activities assayed.

Results

Effects on State 4 Respiration

Figure 1 shows the effects of TCBs on the oxygen consumption during state 4 respiration of rat liver mitochondria with α-ketoglutarate/malate as the substrate. The addition of 23-, 24-, 25-, and 26-TCBs to a suspension of rat liver mitochondria caused a marked stimulation of the respiration. These TCBs showed a similar stimulation pattern. Namely, these TCBs began to stimulate state 4 respiration at 40 μM. As the concentration was increased, oxygen consumption was accelerated, reaching a peak rate at 80 μM, after which further increases in concentration repressed the respiration. The repression of the respiration was due to the inhibition of the electron transport chain.[15] In contrast, 34-TCB did not stimulate state 4 respiration. In addition to the stimulation of state 4 respiration, 23-, 24-, 25-, and 26-TCBs released the oligomycin-inhibited respiration completely (data not shown). Furthermore,

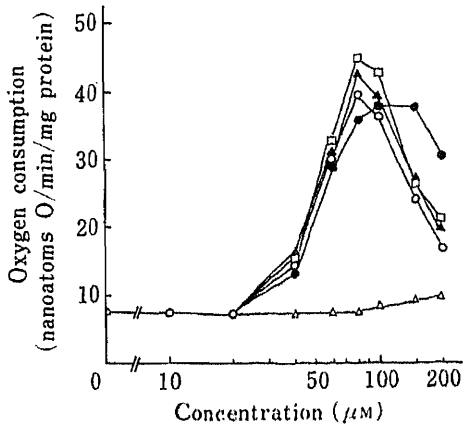

Fig. 1. Effects of TCBs on State 4 Respiration of Rat Liver Mitochondria

Oxygen consumption was measured polarographically with a Clark-type oxygen electrode at 25 °C in a volume of 2 ml. The reaction buffer consisted of 0.2 M sucrose, 20 mM KCl, 3 mM $MgCl_2$, 5 mM potassium phosphate (pH 7.4); 5 mM α-ketoglutarate/5 mM malate was used as the substrate, and the mitochondrial protein concentration was 1 mg/ml. Data are the rates of oxygen consumption 3 to 4 min after addition of TCBs during state 4 respiration. Each point is a mean of 3 separate experiments. Symbols are as follows: 23-TCB, ○; 24-TCB, ▲; 25-TCB, □; 26-TCB, ●; 34-TCB, △. At 10, and 20 μM, the symbol for 23-TCB (○) also represents other TCBs.

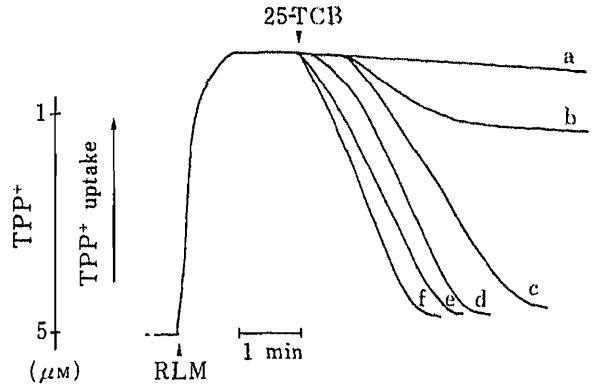

Fig. 2. Effects of 25-TCB on the Movement of TPP^+ Across the Mitochondrial Membranes

Rat liver mitochondria (RLM, 1 mg/ml) were incubated with various concentrations of 25-TCB in the respiration buffer containing 5 mM α-ketoglutarate/5 mM malate, and 5 μM TPP^+. a, none; b, 40; c, 60; d, 80; e, 100; f, 200 μM. Temperature, 25 °C; volume, 2.5 ml.

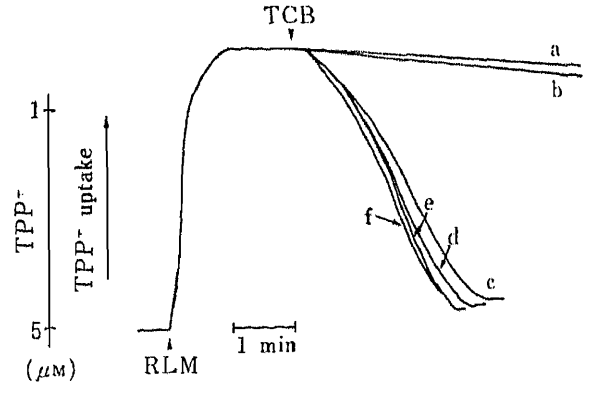

Fig. 3. Comparison of the Effects of Various TCBs on the Movement of TPP^+ Across the Mitochondrial Membranes

Rat liver mitochondria (RLM, 1 mg/ml) were incubated with a fixed concentration (80 μM) of various TCBs in the respiration buffer containing 5 mM α-ketoglutarate/5 mM malate, and 5 μM TPP^+. a, none; b, 34-TCB; c, 26-TCB; d, 25-TCB; e, 24-TCB; f, 23-TCB. Temperature, 25 °C; volume, 2.5 ml.

adenosine triphosphatase (ATPase) was also activated by these TCBs except for 26-TCB.[6] On the other hand, 34-TCB neither released the oligomycin-inhibited respiration nor activated the ATPase (data not shown). These results indicate that 23-, 24-, 25-, and 26-TCBs act as uncouplers of oxidative phosphorylation in mitochondria, and that 34-TCB does not act as an uncoupler. 26-TCB has an interesting characteristic in that this agent showed an uncoupling action without the activation of mitochondrial ATPase. This is similar to fatty acids such as oleic acid, which also uncouple without significantly affecting ATPase.[16] In contrast to a protonophoric uncoupler such as DNP, which showed an instantaneous stimulation of state 4 respiration, the stimulation induced by either 23-, 24-, 25-, and 26-TCB was preceded by a lag period (1—2 min), the length of which was shortened as the TCB concentration was increased. However, the extent of stimulation by these TCBs was as great as that observed with DNP.

Effects on Membrane Potential

In order to confirm further that 23-, 24-, 25-, and 26-TCBs are uncouplers, membrane potential across the mitochondrial membranes was monitored (Figs. 2 and 3). Uncouplers, in general, dissipate the memebrane potential, which is the direct driving force for ATP synthesis.[17] Figure 2 shows the concentration dependence of the effects of 25-TCB on the membrane potential. Addition of mitochondria to an incubation medium containing the substrate (α-ketoglutarate/malate) caused an uptake of TPP^+ from the incubation medium into the mitochondria (upward deflection in the figure, formation of membrane potential). When the uptake of TPP^+ by mitochondria was complete, various concentrations of 25-TCB were added, and each TPP^+ movement was monitored. 25-TCB began to release the incorporated TPP^+ into the incubation medium at 40 μM (downward deflection in the figure, trace b, dissipation of membrane potential). As the 25-TCB concentration was increased, the rate of TPP^+ release was increased (traces, c—f). As is clear from the figure, the release induced by 25-TCB was preceded by a lag period, the length of which decreased with increasing 25-TCB concentration. This was in contrast to the weakly acidic uncoupler, DNP, which showed an instantaneous release (data not shown).

Figure 3 compares the release of TPP^+ induced by a fixed concentration (80 μM) of various TCBs. 23-, 24-, 25-, and 26-TCBs caused similar rates of release, while 34-TCB did not cause any release. 23-, 24-, and 26-TCBs also exhibited concentration-dependent TPP^+-release similar to that of 25-TCB. On the other hand, 34-TCB did not release TPP^+ up to a concentration of 200 μM (data not shown). Thus, 23-, 24-, 25-, and 26-TCBs dissipated the membrane potential after certain lag periods, and the potencies of these TCBs to dissipate it were almost the same. However, 34-TCB did not dissipate the membrane potential.

Effects on K^+ and Ca^{2+} Release

To correlate the dissipation of membrane potential induced by effective TCBs with the increases in ion-permeability across the mitochondrial inner membranes, the effects of TCBs

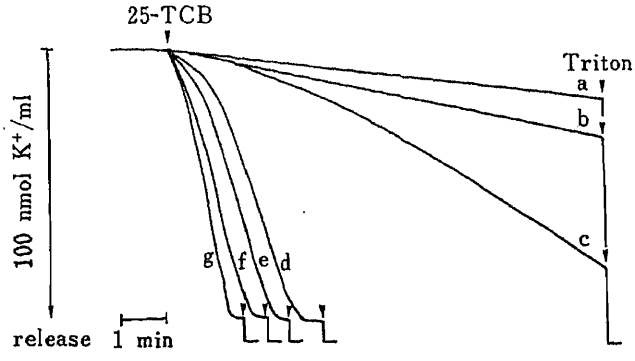

Fig. 4. Release of Endogenous K^+ from Mitochondria Treated with 25-TCB

Rat liver mitochondria (1 mg/ml) were incubated at 25 °C with various concentrations of 25-TCB in a 2.5 ml of medium composed of 0.15 M choline chloride, and 5 mM Tris-HCl (pH 7.4). a, none; b, 20; c, 40; d, 60; e, 80; f, 100; g, 200 μM. At the end of each run, Triton X-100 at a final concentration of 0.1% was added to obtain the complete release of K^+.

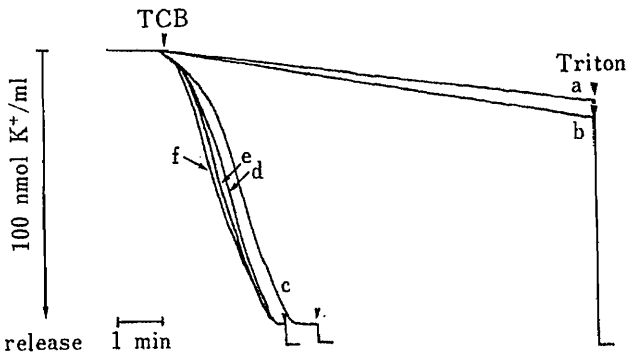

Fig. 5. Comparison of the K^+ Release from Mitochondria Induced by Various TCBs

Rat liver mitochondria (1 mg/ml) were incubated at 25 °C with a fixed concentration (80 μM) of various TCBs in 2.5 ml of medium composed of 0.15 M choline chloride, and 5 mM Tris-HCl (pH 7.4). a, none; b, 34-TCB; c, 26-TCB; d, 25-TCB; e, 24-TCB; f, 23-TCB. At the end of each run, Triton X-100 at a final concentration of 0.1% was added to obtain the complete release of K^+.

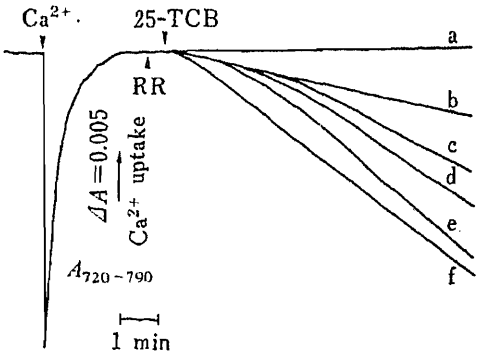

Fig. 6. Release of Ca^{2+} from Mitochondria Induced by 25-TCB

The incubation medium consisted of 0.2 M sucrose, 20 mM KCl, 3 mM $MgCl_2$, 10 mM potassium acetate, 5 mM Tris-HCl (pH 7.4), and 75 μM antipyrylazo III. Rat liver mitochondria (1 mg/ml) were loaded with 75 μM Ca^{2+} with 3 mM ATP as the source of energy. After Ca^{2+} loading was complete, 1 μM ruthenium red (RR) was added. After that, various concentrations of 25-TCB were added, and each Ca^{2+} movement was monitored with antipyrylazo III (wavelength pair, 720—790 nm). Net Ca^{2+} uptake by mitochondria is accompanied by a decrease in absorbance (upward deflection in the figure), and net release is reflected by an increase in absorbance (downward deflection in the figure). a, −RR, −25-TCB; b, +RR, −25-TCB; c, +RR, 40 μM 25-TCB; d, +RR, 60 μM 25-TCB; e, +RR, 80 μM 25-TCB; f, +RR, 100 μM 25-TCB. Temperature, 25 °C; volume, 2.5 ml.

on K^+ and Ca^{2+} movements were examined. Figure 4 shows the release of endogenous K^+ from mitochondria treated with various concentrations of 25-TCB. 25-TCB did not release K^+ up to a concentration of 40 μM (traces a and b). Above this concentration, the rate of K^+ release increased progressively with increasing 25-TCB concentration (traces c—g). The release of K^+ induced by 25-TCB was preceded by a lag period, the length of which was shortened with increasing 25-TCB concentration. This suggests that a critical amount of 25-TCB must intercalate into the lipid bilayer of the inner membranes of mitochondria before the membranes are rendered permeable to K^+.

Figure 5 compares the capacity of various TCBs to release endogenous K^+. 23-, 24-, 25-, and 26-TCBs at a concentration of 80 μM exhibited similar releasing capacities, while 34-TCB did not release K^+ even at a concentration of 200 μM.

In order to determine whether the increase in ion-permeability induced by the effective TCBs is specific to a particular ion or nonspecific, the effects of 25-TCB on the permeability for another ion (Ca^{2+}) were studied. Figure 6 shows the release of Ca^{2+} induced by 25-TCB from mitochondria that had accumulated Ca^{2+}. Firstly, mitochondria were allowed to accumulate 75 nmol of Ca^{2+}/mg protein from the incubation medium with ATP as the source of energy, since isolated mitochondria usually contain very little Ca^{2+} (5 nmol/mg protein) compared to K^+ (120 nmol/mg protein).[18] Once accumulation was complete, ruthenium red (a potent inhibitor of Ca^{2+} uniporter[19]) was added to block the re-uptake of Ca^{2+}. After ruthenium red addition, various concentrations of 25-TCB were added, and Ca^{2+} movements were monitored. Trace b shows a experiment illustrating the control release of Ca^{2+} which became apparent on blocking re-uptake ("basal Ca^{2+} release"). The release of Ca^{2+} is in contrast to the retention observed in the absence of ruthenium red (trace a). At concentrations below 20 μM 25-TCB, the efflux rate of Ca^{2+} was very similar to that of basal Ca^{2+} release. 25-TCB

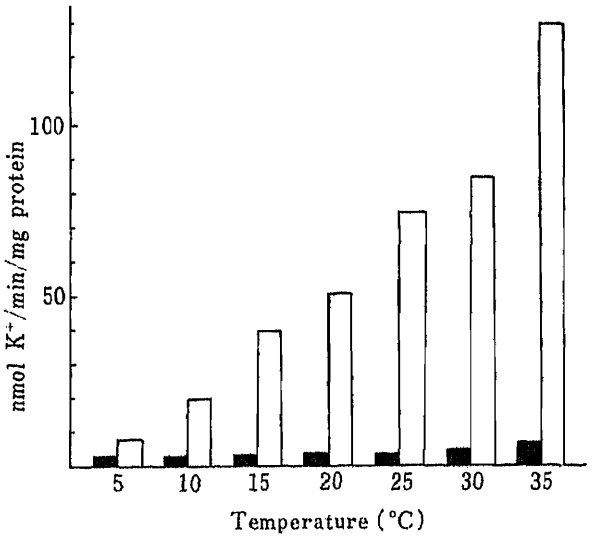

Fig. 7. Effects of Temperature on the Spontaneous and 25-TCB-Induced K^+ Release

Rat liver mitochondria (1 mg/ml) were incubated at the indicated temperature with 80 μM 25-TCB in 2.5 ml of reaction medium (see legend to Fig. 4). Filled bars, spontaneous release; unfilled bars, 25-TCB-induced release.

began to accelerate Ca^{2+} release at 40 μM (trace c). The rate of Ca^{2+} release was proportional to 25-TCB concentration (traces d—f). As was observed in the case of K^+ release, there was a 1—2 min lag period before the Ca^{2+} release by 25-TCB became obvious. Similar results were obtained with 23-, 24-, and 26-TCBs, while 34-TCB did not release Ca^{2+} (data not shown). Thus, 23-, 24-, 25-, and 26-TCBs induced the release of not only K^+ but also Ca^{2+}, indicating that these TCBs increase ion-permeability in a nonspecific manner.

Temperature Effects on the Release of K^+ Induced by 25-TCB

Figure 7 shows the effects of temperature on the spontaneous and 25-TCB-induced release of K^+. The experiment was conducted to obtain data concerning the mode of interaction of 25-TCB with the lipid bilayer of mitochondrial membranes. Below 10 °C, 25-TCB (80 μM)-induced K^+ release was not apparent. Above this temperature, however, the 25-TCB-induced K^+ release was strongly enhanced with raising temperature. On the other hand, the spontaneous release of K^+ showed a negligible increase with temperature. The above data indicate that the elevated temperature is required to let the membranes be rendered permeable to K^+ by the incorporation of 25-TCB. Similar results were obtained with 23-, 24-, and 26-TCBs (data not shown).

Discussion

The present study has shown that TCBs except for 34-TCB uncouple oxidative phosphorylation in rat liver mitochondria. The results demonstrate several important structural characteristics of TCB isomers with respect to their ability to induce uncoupling of oxidative phosphorylation. Namely, certain substituent sites for chlorine atoms in TCB play a key role in evoking uncoupling action. The uncoupling TCBs (23-, 24-, 25-, and 26-TCBs) are those in which chlorine occupies the 2,2′ positions of the biphenyl ring. The information obtained by molecular orbital calculations on TCB molecule indicated that the molecule becomes highly angular and rigid as a result of the 2,2′-chloro substitutions.[20] Therefore, non-planar structure is required for TCB to induce uncoupling action. Because of their non-planar character, these agents, when intercalated into the lipid bilayer of inner membranes of mitochondria, increase nonspecific ion-permeability across the inner membranes (Figs. 4—6), thereby causing dissipation of membrane potential (Figs. 2 and 3). On the other hand, 34-TCB did not induce uncoupling action. The 3,4-chloro substitution gives a highly coplanar character to the molecule.[20] 34-TCB, when intercalated into the lipid bilayer of the inner

membranes of mitochondria, does not increase the ion-permeability which is essential for the dissipation of membrane potential. Because of its coplanarity, perturbation of the lipid bilayer of the inner membranes by the intercalation of 34-TCB may be relatively small compared to that produced by non-planar-type TCBs.

Although both the uncoupling TCBs and protonophoric uncouplers uncouple oxidative phosphorylation due to the dissipation of membrane potential, there is a great difference in the mechanism by which they dissipate it. Namely, protonophoric uncouplers shuttle protons across the inner membranes in a neutral acid form, which is membran-permeable, donating protons to the matrix side. The anionic conjugate base thus formed moves back electrophoretically to the positively charged outside from the negatively charged inside of the inner membranes. In the complete cycle, the protonophoric uncoupler dissipates the proton gradient and membrane potential. On the other hand, it is clear that the uncoupling TCBs do not dissipate the membrane potential by the proton shuttling mechanism since these compounds do not possess an acid-dissociable group (proton carrier) within the molecule. As is evident from the experiments on the releases of K^+ and Ca^{2+} (Figs. 4—6), the uncoupling TCBs increased the ion-permeability properties of the inner membranes of mitochondria nonspecifically (*i.e.*, by damaging mitochondrial membranes), leading to the dissipation of membrane potential.

In the present study, H^+ movement across the inner membranes was not tested. However, it is possible that the inner membranes are made permeable to H^+ by the uncoupling TCBs. This is inferred from the fact that the inner membranes of intact mitochondria are impermeable to reduced nicotinamide adenine dinucleotide (NADH),[21] while those of mitochondria treated with the uncoupling TCBs are permeable to NADH (data not shown). Namely, this indicates that the uncoupling TCBs alter the permeability properties of the membranes to a relatively large molecule, suggesting that small ions such as H^+ also may permeate across the inner membranes of mitochondria. Regarding the Ca^{2+} release induced by the uncoupling TCBs, there is a possibility that the release of this ion is caused by a secondary effect due to the dissipation of membrane potential, as well as nonspecific increases in mitochondrial ion-permeability, since Ca^{2+} is released from mitochondria when the membrane potential is dissipated by an uncoupling agent.[14] The following idea is less probable: the uncoupling TCBs liberate fatty acids; the uncoupling action observed is primarily due to the fatty acid thus produced. The reason why this is unlikely is that the lag time seen in the stimulation of state 4 respiration by the uncoupling TCBs coincided with that of both K^+ release and the dissipation of membrane potential. This indicates that the uncoupling phenomena observed are caused by the uncoupling TCBs themselves (not by fatty acids liberated) through the dissipation of membrane potential produced by nonspecific increases in mitochondrial ion-permeability. Furthermore, it should be emphasized that the dissipation of membrane potential by fatty acid is partial.[22,23] Therefore, if the uncoupling action is due to fatty acids liberated, the dissipation of membrane potential observed should be partial. However, the observed dissipation was complete, as seen in the case of DNP.

The K^+ release induced by 25-TCB, a non-planar TCB, became obvious at 10 °C. Starting at this temperature, the K^+ release by this agent was strongly enhanced by raising the temperature (Fig. 7). It was repoted that the phase transition of mitochondrial lipids occurs at 8 °C; mitochondrial membranes are in a gel phase below this temperature, and above this temperature they are in a liquid-crystalline phase.[24,25] It is clear therefore, that 25-TCB can not induce K^+ release from mitochondria when the membranes are in a gel phase, and that 25-TCB causes the K^+ release with increasing temperature when the membrane state is changed to the liquid-crystalline phase. One of the possible explanations for this phenomenon is that partition of 25-TCB molecules into the lipid phase is insufficient to induce the membrane perturbation when the mitochondrial membranes are in a gel phase. However,

using lindane, a chlorinated hydrocarbon insecticide, Madeira and Madeira demonstrated that a significant partition of the compound into the gel phase of mitochondrial membranes occurs, and the dependence of the partition on temperature changes at about 24 °C.[26] Thus, the above explanation of the temperature effect in the case of 25-TCB seems improbable. An alternative speculation is that 25-TCB forms clusters in the lipid bilayer when the membranes are in a liquid-crystalline phase. When the temperature is low, and the membranes are in a gel phase, 25-TCB molecules intercalated into the lipid bilayer may exist rather randomly, and lateral diffusion of the molecules does not occur. When the temperature is raised, and the membranes enter a liquid-crystalline phase, the lateral diffusion of 25-TCB molecules occurs and 25-TCB forms clusters in the lipid bilayer as a result of increased fluidity of the lipid bilayer. If this happens, phase separation might occur and gaps might appear at the boundary between the more fluid lipid phase and the less fluid 25-TCB clusters; K^+ could leak out through these gaps. On the other hand, 34-TCB did not induce K^+ release even at high temperature. Because of the coplanarity, 34-TCB may mix well with lipids within the membranes and not form clusters, similar to cholesterol, which is also coplanar.

Finally, the relation between the uncoupling action of 23-, 24-, 25-, and 26-TCBs and the mechanism of toxicity of these TCBs should be discussed. Stotz and Greichus reported alterations in the shape of liver mitochondria from the white pelican as a result of *in vivo* treatment with PCB.[27] That is, mitochondria from the PCB-treated white pelican were rounded and swollen instead of long and slender as in the untreated animal; this change is similar to that produced by DNP,[7] suggesting uncoupling of oxidative phosphorylation. The uncoupling interferes with the energy production by mitochondria (ATP synthesis) which is essential for cellular activities such as active transport of ions. In addition, it has been proposed that alteration in intracellular Ca^{2+} homeostasis is a common pathway to cell death.[28] The uncoupling action of TCBs could be important in relation to this theory. Lin *et al.* reported that the administration of an acute lethal dose of 25-TCB (1.7 g/kg body weight) to rats caused a marked inhibition of $(Ca^{2+}+Mg^{2+})$-ATPase located in plasma membranes of the hepatocytes.[5] The decreased activity of this enzyme leads to an accumulation of Ca^{2+} in the cytosol. In the situation where the cytosol of hepatocyte is flooded with Ca^{2+}, the major fraction of Ca^{2+} is sequestered in mitochondria by an energy-dependent pathway.[29,30] However, the ability of mitochondria to sequester Ca^{2+} is totally abolished in the presence of an uncoupling agent.[14] This keeps the cytosolic free Ca^{2+} at high levels, an event which converts initially non-lethal damage into irreversible cell injury.[31] Therefore, the uncoupling action of 23-, 24-, 25-, and 26-TCBs may play a role in the toxicity of these TCBs.

There are several examples in the literature of mitochondrial impairment as a mechanism for the toxicitiy of organochlorine insecticides. Dichlorodiphenyltrichloroethane (DDT) was shown to impair mitochondrial energy production mainly by inhibition of the electron transport chain.[32,33] End *et al.* reported that chlordecone, an organochlorine insecticide, inhibits both succinate- and ATP-supported Ca^{2+} uptake in rat brain mitochondria, and suggested that mitochondrial impairment with the accompanying changes in cellular Ca^{2+} homeostasis is an attractive mechanism which would account for several aspects of chlordecone toxicity.[34] These authors also demonstrated that impairment of rat brain mitochondria by chlordecone leads to major alterations in neuronal Ca^{2+} transport and neurotransmitter release.[35] Chlordecone was also shown to impair functions in rat liver mitochondria by producing nonspecific increases in ion-permeability, as seen with the uncoupling TCBs.[36]

References

1) H. Terada, *Biochim. Biophys. Acta*, **639**, 225 (1981).
2) R. J. Kessler, H. V. Zande, C. A. Tyson, G. A. Blondin, J. Fairfield, P. Glasser and D. E. Green, *Proc. Natl.*

Acad. Sci. U.S.A., 74, 2241 (1977).
3) H. Terada, H. Nagamune, N. Morikawa and M. Ikuno, *Biochim. Biophys. Acta*, **807**, 168 (1985).
4) P. G. Heytler, *Methods Enzymol.*, **55**, 462 (1979).
5) F. S. Lin, M. T. Hsia and J. R. Allen, *Arch. Environ. Contam. Toxicol.*, **8**, 321 (1979).
6) Y. Nishihara, L. W. Robertson, F. Oesch and K. Utsumi, *J. Pharmacobio-Dyn.*, **8**, 726 (1985).
7) M. George, R. J. Chenery and G. Krishna, *Toxicol. Appl. Pharmacol.*, **66**, 349 (1982).
8) O. Hutzinger, S. Safe and U. Zitko, *Bull. Environ. Contam. Toxicol.*, **6**, 209 (1971).
9) N. Kornblum, "Organic Reactions II," ed. by R. Adams, John Wiley and Sons Inc., London, 1944, pp. 262—340.
10) F. L. W. van Roosmalen, *Recl. Trav. Chim. Pays-Bas*, **53**, 359 (1934).
11) G. H. Hogeboom, *Methods Enzymol.*, **1**, 16 (1955).
12) A. G. Gornall, C. J. Bardawill and M. M. David, *J. Biol. Chem.*, **177**, 751 (1949).
13) N. Kamo, M. Muratsugu, R. Hongoh and Y. Kobatake, *J. Membrane Biol.*, **49**, 105 (1979).
14) A. Scarpa, F. J. Jr. Brinley and G. Dubyak, *Biochemistry*, **17**, 1378 (1978).
15) Y. Nishihara, L. W. Robertson, F. Oesch and K. Utsumi, *Life Sci.*, **38**, 627 (1986).
16) J. Matsuoka and T. Nakamura, *J. Biochem.* (Tokyo), **86**, 675 (1979).
17) P. Mitchell, "Chemiosmotic Coupling in Oxidative and Photosynthetic Phosphorylation," Glynn Research Ltd., Bodmin, U.K., 1966, pp. 135—156.
18) A. D. Beavis, R. D. Brannan and K. D. Garlid, *J. Biol. Chem.*, **260**, 13424 (1985).
19) F. D. Vasington, P. Gazzotti, R. Tiozzo and E. Carafoli, *Biochim. Biophys. Acta*, **256**, 43 (1972).
20) S. Sassa, O. Sugita, N. Ohnuma, S. Imajo, T. Okumura, T. Noguchi and A. Kappas, *Biochem. J.*, **235**, 291 (1986).
21) L. Ernster and B. Kuylenstierna, "Membranes of Mitochondria and Chloroplast," ed. by E. Racker, Van Nostrand Reinhold, New York, 1970, pp. 172—212.
22) P. Arslan, A. N. Corps, T. R. Hesketh, J. C. Metcalfe and T. Pozzan, *Biochem. J.*, **217**, 419 (1984).
23) H. Rottenberg and S. S. Mordoch, *FEBS Lett.*, **202**, 314 (1986).
24) J. K. Raison and E. J. McMurchie, *Biochim. Biophys. Acta*, **363**, 135 (1974).
25) D. Bach, I. Bursuker and I. R. Miller, *Experientia*, **15**, 717 (1978).
26) M. C. A. Madeira and M. C. Madeira, *Biochim. Biophys. Acta*, **820**, 165 (1985).
27) I. J. Stotz and T. A. Greichus, *Bull. Environ. Contam. Toxicol.*, **19**, 319 (1978).
28) F. A. X. Schanne, A. B. Kane, E. E. Young and J. L. Farber, *Science*, **206**, 700 (1979).
29) S. Foden and P. J. Randle, *Biochem. J.*, **170**, 615 (1978).
30) S. K. Joseph, K. E. Coll, R. H. Cooper, J. S. Marks and J. R. Williamson, *J. Biol. Chem.*, **258**, 731 (1983).
31) J. L. Farber, *Life Sci.*, **29**, 1289 (1981).
32) T. Ohyama, T. Takahashi and H. Ogawa, *Biochem. Pharmacol.*, **31**, 397 (1982).
33) Y. Nishihara and K. Utsumi, *Food Chem. Toxicol.*, **23**, 599 (1985).
34) D. W. End, R. A. Carchman, R. Ameen and W. L. Dewey, *Toxicol. Appl. Pharmacol.*, **51**, 189 (1979).
35) D. W. End, R. A. Carchman and W. L. Dewey, *Fed. Proc.*, **38**, 845 (1979).
36) J. A. Manring and D. E. Moreland, *Toxicol. Appl. Pharmacol.*, **59**, 483 (1981).

Notes

[Chem. Pharm. Bull. 35(4)1596—1598(1987)]

Evidence for Ambivalent Azomethine Ylide Intermediate in the 1,3-Cycloaddition of Trimethylsilylmethylamine Derivatives

YOSHIYASU TERAO, NOBUYUKI IMAI, and KAZUO ACHIWA*

Shizuoka College of Pharmacy, 2-2-1 Oshika, Shizuoka 422, Japan

(Received September 17, 1986)

Evidence for an ambivalent azomethine ylide intermediate was provided by the 1,3-cycloaddition of deuterated *N*-benzyl-*N*-(methoxymethyl)trimethylsilylmethylamine to dimethyl benzylidene malonate and related reactions.

Keywords——azomethine ylide; 1,3-cycloaddition; ambivalence; *N*-benzyl-*N*-(methoxymethyl)trimethylsilylmethylamine; tetrabutylammonium fluoride

Since the concept of 1,3-dipolar cycloaddition was introduced more than 25 years ago by Huisgen,[1] 1,3-dipole species have been known to have an ambivalent property; this is one of the lines of evidence in support of the 1,3-dipole intermediate itself.[1,2] However, this fundamental property has not been clearly reflected in experimental findings. In this paper, we wish to describe in detail our work[3] aimed at obtaining chemical evidence for an ambivalent azomethine ylide derived from trimethylsilylmethylamine derivatives.

Because the electronic or steric interaction between substituents of a dipole and those of a dipolarophile is considered to affect the regioselectivity, non-substituted azomethine ylide was required in order to reveal the net ambivalence. One of the simplest azomethine ylides has been provided by Hosomi *et al.*[4] and by us.[5] We designed a deuterated azomethine ylide (**3**) which was produced *in situ* by the acid- or fluoride anion-catalyzed reaction of deuterated *N*-benzyl-*N*-(methoxymethyl)trimethylsilylmethylamine (**1**). The starting material **1** was pre-

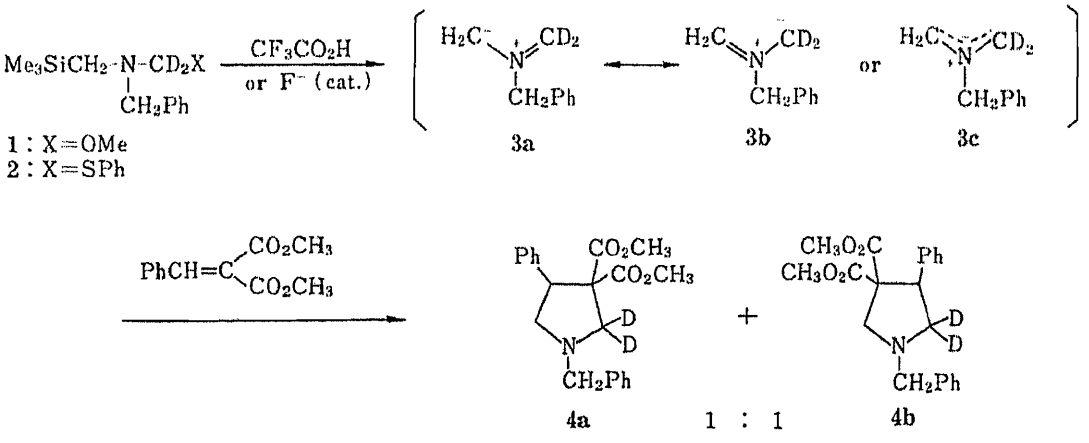

Chart 1

pared from *N*-(benzyl)trimethylsilylmethylamine, methanol, and deuterated formaldehyde by a usual Mannich reaction. Treatment of **1** with dimethyl benzylidenmalonate as an unsymmetrical dipolarophile in the presence of a catalytic amount of trifluoroacetic acid in dichloromethane afforded a 1 : 1 mixture of the pyrrolidines **4a** and **4b** in 65% yield. The ratio of the regioisomers was determined on the basis of the proton and carbon-13 nuclear magnetic resonance (^{1}H-NMR and ^{13}C-NMR) spectra of the product by reference to the non-deuterated cycloadduct (**4c**) prepared in a similar manner. The apparent ^{1}H-NMR signal due to the methine proton of **4a** and **4b** appears as a triplet having relative intensities of 1 : 6 : 1 at 4.34 ppm, while the corresponding signal of **4c** was also observed as a triplet at the same chemical shift but with relative intensities of 1 : 2 : 1. These results suggest that the methine protons of **4a** and **4b** appear as a singlet and a triplet, respectively, which are overlapped. In the ^{13}C-NMR spectrum of **4c**, two peaks due to methylene carbon appear at 59.59 and 60.68 ppm with the same intensities. On the other hand, the corresponding two peaks of the mixture of **4a** and **4b** were observed at 59.92 and 60.62 ppm, and the intensities were decreased in the same ratios in comparison with those of **4c**. These observations also indicate that the quantity of non-deuterated methylene carbon of **4a** is equal to that of **4b**. The experimental results suggest that the negative charge formed by desilylation is delocalized between the two carbons adjacent to the nitrogen atom. Thus, the terminus of the azomethine ylide is an ambivalent nucleophile and electrophile.

Next, we carried out the reaction in the presence of tetrabutylammonium fluoride (TBAF) in the expectation of an increase of **4a** owing to two-step cyclization. However, the two regioisomers (**4a** and **4b**) were obtained in the same ratios. Furthermore, we examined the 1,3-cycloaddition of deuterated *N*-benzyl-*N*-(phenylthiomethyl)trimethylsilylmethylamine (**2**), which is more stable than **1**, under similar conditions. The reaction furnished the same result as that with **1**, though in slightly lower yield.

These reactions are initiated by the formation of the iminium cation (**5**) as recognized in a series of 1,3-cycloaddition reactions[6] of silylmethylamine derivatives (Chart 2). The silicon-

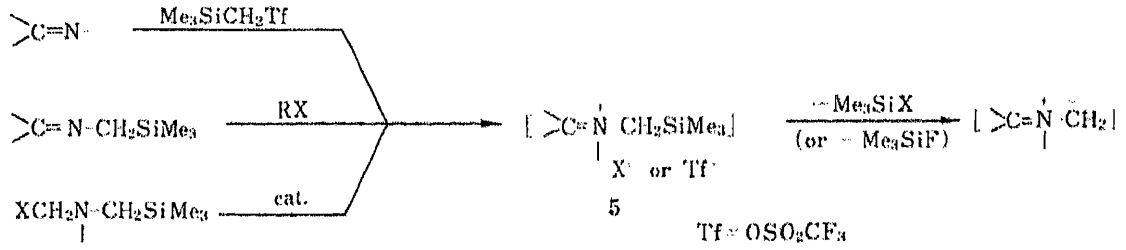

Chart 2

carbon bond adjacent to such an iminium cation is liable to be cleaved even by the attack of a nucleophile (except fluoride anion) because the resulting carbanion is apparently stabilized owing to the formation of the azomethine ylide. In the case of the TBAF-catalyzed reaction, such Mannich bases are known[7] to be in equilibrium with the iminium cation under various conditions. Therefore, a fluoride anion seems to promote the cleavage of the silicon–carbon bond after the formation of the iminium cation. The concerted mechanism of this reaction is supported by the experimental results described in the previous paper[5]: In the 1,3-cycloaddition of **1′** (non-deuterated) to dimethyl maleate and dimethyl fumarate, the stereochemistry at the 3- and 4-positions of the products was concluded to retain that of the dipolarophiles.

In conclusion, we have obtained evidence that the 1,3-cycloaddition of trimethylsilylmethylamine derivatives proceeds *via* azomethine ylide, the ambivalent property of which is reflected in the experimental outcome.

Experimental

All boiling points are uncorrected. Infrared (IR) spectra and mass spectra (MS) were recorded on a JASCO IRA-2 spectrophotometer and a JEOL JMS-D 100 mass spectrometer, respectively. ^{1}H-NMR and ^{13}C-NMR spectra were measured on a JEOL FX90Q spectrometer and chemical shifts are expressed in ppm downfield from tetramethylsilane. Abbreviations are as follows: s=singlet, d=doublet, t=triplet, q=quartet, m=multiplet.

Deuterated *N*-Benzyl-*N*-(methoxymethyl)trimethylsilylmethylamine (1)——*N*-Benzyltrimethylsilylamine (1.9 g, 10 mmol) was added dropwise to a solution of 30% formaldehyde-d_2 in deuterium oxide (1.1 g, 12 mmol) and methanol (0.4 g, 12 mmol) in an ice-bath and the mixture was stirred at room temperature for 3 h. After the addition of potassium carbonate, the separated oil was extracted with ether. The ethereal solution was dried over $MgSO_4$ and concentrated to give an oily product, 1.9 g (85%). ^{1}H-NMR δ ($CDCl_3$): 0.07 (9H, s, Si $(CH_3)_3$), 2.18 (2H, s, NCH_2Si), 3.20 (3H, s, OCH_3), 3.71 (2H, s, NCH_2Ph), 7.71 (5H, s, C_6H_5). No singlet signal was observed at 3.95 due to OCH_2N of non-deuterated **1'**.

Deuterated *N*-Benzyl-*N*-(phenylthiomethyl)trimethylsilylmethylamine (2)——*N*-Benzyltrimethylsilylmethylamine (1.9 g, 10 mmol), 30% formaldehyde-d_2 in deuterium oxide (1.1 g, 1.2 mmol), and benzyl mercaptan (1.1 g, 10 mmol) were treated by a method similar to that described above to give an oily product, 2.8 g (90%). ^{1}H-NMR δ ($CDCl_3$): 0.31 (9H, s, $Si(CH_3)_3$), 2.21 (2H, s, NCH_2Si), 3.65 (2H, s, NCH_2Ph), 7.13—7.45 (10H, m, $2\times C_6H_5$). No singlet was observed at 4.41 due to NCH_2SPh of the non-deuterated compound.

1,3-Cycloaddition of 1 to Dimethyl Benzylidenemalonate——A 1 M solution of trifluoroacetic acid (0.5 ml) in CH_2Cl_2 was added to a cold solution of **1** (1.4 g, 6 mmol) and dimethyl benzylidenemalonate (1.1 g, 5 mmol) in CH_2Cl_2 (10 ml). After being stirred for 3 h at room temperature, the solution was washed with saturated sodium bicarbonate and with brine, and then dried over $MgSO_4$. After removal of the CH_2Cl_2, the residual oil was subjected to column chromatography on silica gel with benzene–tetrahydrofuran (9:1) to afford the cycloadduct (**4a**+**4b**) (1.15 g, 65%). IR ν_{max}^{neat} cm^{-1}: 1720 (CO). MS *m/z*: 355 (M^+). ^{1}H-NMR δ ($CDCl_3$): 2.75—3.20 (m, CH_2NCH_A), 3.05 (s, OCH_3), 3.53 (d, J=10.0 Hz, NCH_B), 3.66 (s, NCH_2Ph), 3.72 (s, OCH_3), 4.34 (t, J=7.1 Hz, the relative intensities = 1:6:1), 7.10—7.23 (m, C_6H_5). ^{13}C-NMR δ ($CDCl_3$): 49.41 (d), 49.60 (d), 51.74 (q), 52.83 (q), 59.54 (t), 59.92 (t), 60.62 (t), 65.45 (s), 65.61 (s), 127.05 (d), 127.91 (d), 128.30 (d), 128.56 (d), 129.05 (d), 138.57 (s), 139.75 (s), 169.47 (s), 171.86 (s).

Non-deuterated cycloadduct **4c** was synthesized by a method similar to that described above. Its ^{1}H-NMR spectrum showed the same pattern as that of the mixture of **4a** and **4b**, except that the relative intensities of the triplet at 4.34 ppm were 1:2:1. ^{13}C-NMR δ ($CDCl_3$): 49.57 (d), 51.74 (q), 52.84 (q), 59.59 (t), 59.97 (t), 60.68 (t), 65.55 (s), 127.05 (d), 127.91 (d), 128.30 (d), 128.56 (d), 129.00 (d), 138.70 (s), 139.89 (s), 169.47 (s), 171. 80 (s). *Anal.* Calcd for $C_{21}H_{23}NO_4$: C, 71.37; H, 6.56; N, 3.96. Found: C, 71.61; H, 6.56; N, 4.06.

The reaction of **1** (1.4 g, 6 mmol) with dimethyl benzylidenemalonate (1.1 g, 5 mmol) in the presence of TBAF (0.5 mmol eq) in dimethylformamide (10 ml) was carried out by a method similar to that described above. A 1:1 mixture of **4a** and **4b** was obtained in 30% yield.

1,3-Cycloaddition of 2 to Dimethyl Benzylidenemalonate——The reaction of **2** (1.9 g, 0.6 mmol) with dimethyl benzylidenemalonate (1.1 g, 5 mmol) in the presence of trichloroacetic acid (0.5 mmol eq) was carried out by a method similar to that used in the case of **1**. A 1:1 mixture of **4a** and **4b** was obtained in 52% yield.

In the presence of TBAF, the same mixture was obtained in 25% yield. The structure and the ratio of regioisomers of these products were determined by direct comparison of the spectral data with those of the product obtained by the reaction of **1**.

References

1) R. Huisgen, *Angew. Chem., Int. Ed. Engl.*, **2**, 567 (1963); *idem, ibid.*, **2**, 633 (1963).
2) A. Padwa ed., "1,3-Dipolar Cycloaddition Chemistry," John Wiley & Sons, New York, 1984.
3) Y. Terao, H. Kotaki, N. Imai, and K. Achiwa, *Chem. Pharm. Bull.*, **33**, 896 (1985).
4) A. Hosomi, Y. Sakata, and H. Sakurai, *Chem. Lett.*, **1984**, 1117.
5) Y. Terao, H. Kotaki, N. Imai, and K. Achiwa, *Chem. Pharm. Bull.*, **33**, 2762 (1985).
6) E. Vedejs and G. R. Martinez, *J. Am. Chem. Soc.*, **101**, 6452 (1979); K. Achiwa and M. Sekiya, *Chem. Lett.*, **1981**, 1213; for a review, see N. Imai, Y. Terao, and K. Achiwa, *Yuki Gosei Kagaku Kyokai Shi*, **43**, 862 (1985).
7) G. M. Robinson and R. Robinson, *J. Chem. Soc.*, **1923**, 532; H. Hellmann and G. Opitz, *Angew. Chem.*, **68**, 265 (1956).

[Chem. Pharm. Bull. 35(4)1599—1603(1987)]

Synthetic Approach to Diterpene Alkaloids. II. Unusual Reaction of Angular Nitromethyl Group with Diazomethane to Give Aldoxime

YOSHIHISA SHIBANUMA*,[a] and TOSHIHIKO OKAMOTO[b]

Meiji College of Pharmacy,[a] Nozawa, Setagaya-ku, Tokyo 154, Japan and Sato Pharmaceutical Co., Ltd.,[b] Higashiooi, Shinagawa-ku, Tokyo 140, Japan

(Received September 27, 1986)

The 7-methoxyhydrophenanthrone (**8**) was synthesized from the 4a-nitromethylhydrophenanthrone (**3**) *via* nitration, reduction, and conversion of the resulting amino group to a methoxy group. On methylation of the intermediary phenol (**7**) with diazomethane, two products (**9** and **10**) were obtained along with the desired **8**. The structures of these compounds having an aldoxime moiety were determined by physico-chemical methods. The mechanism of this unusual aldoxime formation from a nitromethyl group is discussed.

Keywords——aconite alkaloid; aromatic nitration; diazotization; diazomethane; nitromethane derivative; aldoxime; selective reduction

In the course of our synthetic studies of an aconite alkaloid, kobusine (**1**), we previously reported[1] the synthesis of (±)-6,15,16-iminopodocarpane-8,11,13-triene (**2**), a model compound having a bridged azabicyclic structure on the A/B rings, *via* (±)-4a-nitromethylhydrophenanthrone (**3**) using a Hofmann-Löffler type photocyclization in the final step.

Functionalization of the aromatic C-ring of **2**, which is required for pursuing the synthesis further, was then examined. Thus, nitration of **3** was carried out using fum. HNO_3 (d=1.52)-conc. H_2SO_4 (10:1),[2] giving the 7-nitro compound (**4**)[3] (79% yield) along with a small amount of the 8-nitro isomer (**5**)[3] (2.7% yield). The aromatic nitro group in **4** could be reduced selectively to the amino group with 10% Pd-C in EtOH in the presence of the aliphatic nitromethyl group to give **6** (74% yield), which was converted to the phenol (**7**) by diazotization followed by hydrolysis in 73.8% yield.

On the subsequent step, we encountered a rather unexpected reaction. Namely, when **7** was treated with diazomethane in ether at room temperature, an isomeric mixture of aldoximes (**9** and **10**) was obtained (24.5% and 18.7% yields, respectively), along with the desired methoxy derivative (**8**) (16.0% yield). Methylation of **7** with a small excess of trimethyloxonium tetrafluoroborate afforded the *O*-methylated product (**8**) exclusively in 59% yield. The structures of **9** and **10** were rigorously established as follows. 1) The molecular formulas of both compounds were determined to be $C_{18}H_{23}NO_3$ from the elemental analytical and mass spectral (MS) data. 2) In the proton nuclear magnetic resonance (^{1}H-NMR) spectra, two singlets appearing at δ 7.67 and 6.88 can be assigned reasonably to the olefinic protons of aldoxime isomers **9** and **10** (HO–N=C<u>H</u>–) and two singlets appearing at δ 7.81 and 8.42 (disappeared on D_2O treatment), to hydroxyl groups of the same isomers (<u>H</u>O–N=CH–). Signals due to a nitromethyl group should appear at δ 4.0—5.0. 3) The presence of an aldoxime carbon (HO–N=<u>C</u>H–) was supported by the observation that in the carbon-13 nuclear magnetic resonance (^{13}C-NMR) spectra, the nitromethyl carbon signal appearing at δ 78.5—79.5 in **4**—**8** was shifted to much lower field in **9** and **10** (δ 152.9 and 148.7, respectively). 4) The aminomethyl derivative (**11**) obtained from both **9** and **10** by

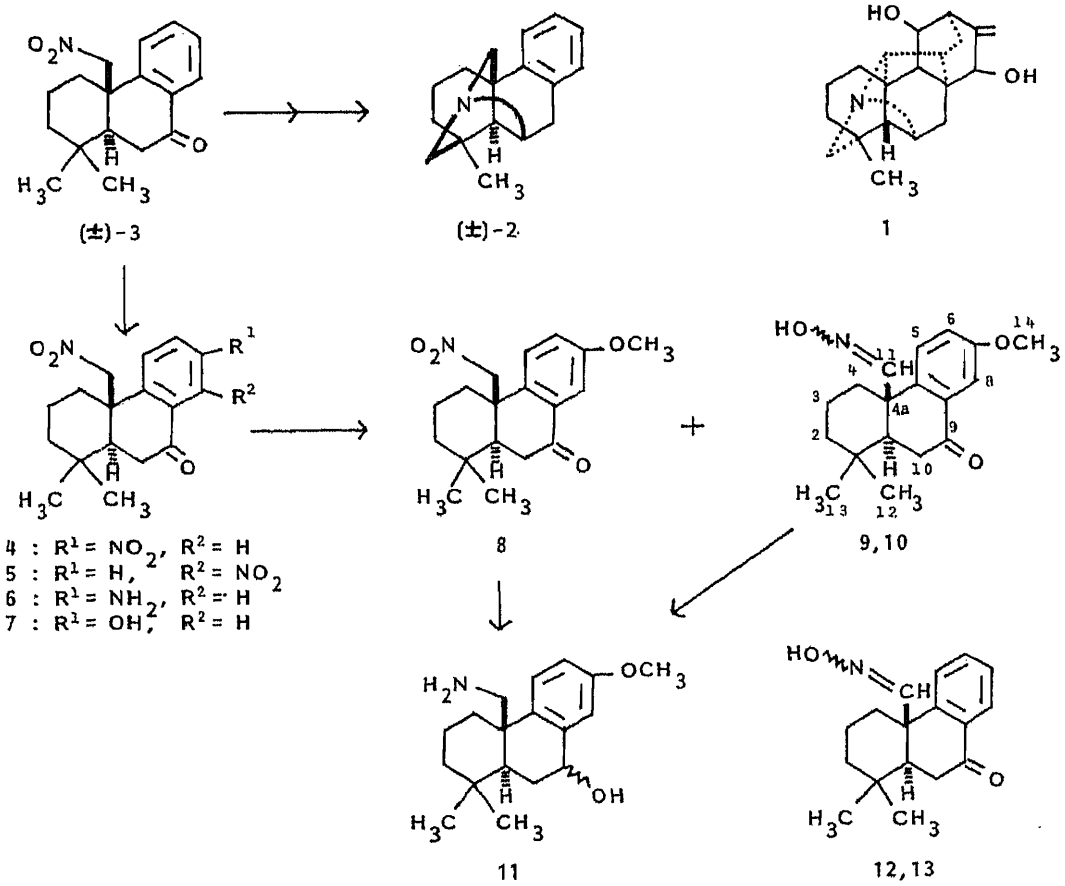

Chart 1

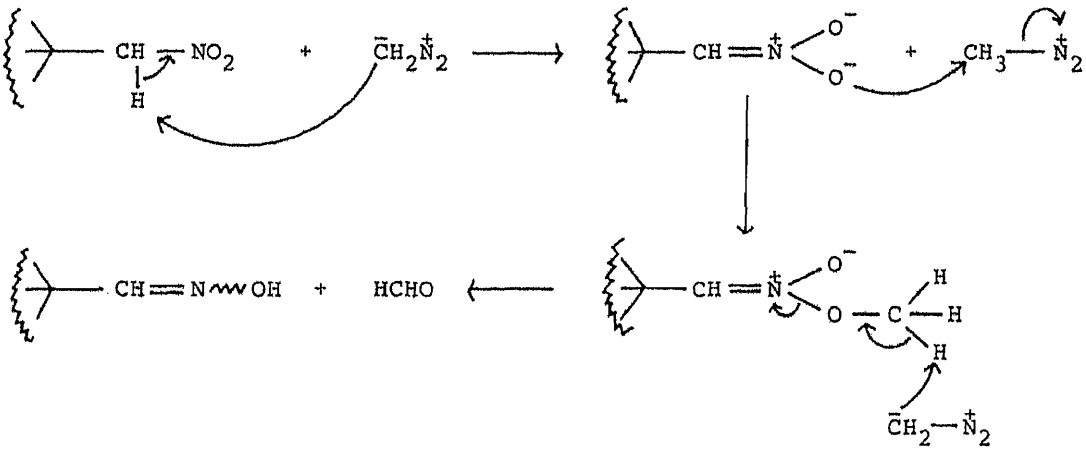

Chart 2

catalytic hydrogenation with Raney Ni was found to be identical with the product obtained from **8** under the same conditions.

Compound **3** having the same carbon skeleton as **7** also produced aldoximes (**12** and **13**) in 13.1% and 15.9% yields, respectively, which suggests that the present diazomethane-promoted reductive conversion of a nitromethyl group to an aldoxime group should take place in general, at least in compounds of this type.

It has been shown that aliphatic nitro compounds react with diazomethane to produce

TABLE I. MS and IR Spectral and Analytical Data for the Products

Compd. No.	Formula	Analysis (%) Calcd (Found) C	H	N	MS *m/z*	IR ν_{max}^{KBr} cm^{-1}
4	$C_{17}H_{20}N_2O_5$	61.43 (61.14	6.07 6.02	8.43 8.25)	332 (M^+), 302, 286, 272	1690 (C=O), 1545, 1380 (NO_2)
5	$C_{17}H_{20}N_2O_5$	61.43 (61.42	6.07 6.10	8.43 8.33)	332 (M^+), 302, 286, 272	1700 (C=O), 1546, 1364 (NO_2)
6	$C_{17}H_{22}N_2O_3$	67.52 (67.69	7.33 7.48	9.27 9.13)	302 (M^+), 256, 242	3472, 3376 (NH_2), 1680 (C=O), 1632, 1330 (NH_2), 1548, 1380 (NO_2)
7	$C_{17}H_{21}NO_4$	67.31 (67.13	6.98 7.07	4.62 4.61)	303 (M^+), 243	3492 (OH), 1690 (C=O), 1540, 1382 (NO_2)
8	$C_{18}H_{23}NO_4$	68.12 (67.84	7.31 7.40	4.41 4.36)	317 (M^+), 271, 257	1680 (C=O), 1546, 1370 (NO_2)
9	$C_{18}H_{23}NO_3$	71.73 (71.63	7.69 7.82	4.65 4.56)	301 (M^+), 283	3260 (OH), 1680 (C=O), 1608 (C=N)
10	$C_{18}H_{23}NO_3$	71.73 (71.55	7.69 7.88	4.65 4.48)	301 (M^+), 286, 283	3264 (OH), 1688 (C=O), 1610 (C=N)
11	$C_{18}H_{27}NO_2$	74.70 (74.57	9.84 9.67	4.84 4.77)	289 (M^+), 271, 259, 241	3360, 3276 (NH_2), 3176 (OH)
12	$C_{17}H_{21}NO_2$	271.1572[a] (271.1556)			271 (M^+), 254, 253, 238	3268 (OH), 1680 (C=O), 1596 (C=N)
13	$C_{17}H_{21}NO_2$	271.1572[a] (271.1554)			271 (M^+), 254, 253, 238	3262 (OH), 1689 (C=O), 1596 (C=N)

a) High-resolution mass.

TABLE II. ^{1}H-NMR Spectral Data for the Products

Compd. No.	δ ppm (J in Hz) ($CDCl_3$)
4	1.01 (6H, d, J=4.9), 4.54 (1H, dd, J=1.5, 10.4), 5.09 (1H, d, J=10.4), 7.47 (1H, d, J=8.9), 8.31 (1H, dd, J=2.4, 8.9), 8.85 (1H, d, J=2.4)
5	1.00 (6H, d, J=8.9), 4.37 (1H, dd, J=1.2, 10.7), 5.02 (1H, d, J=10.7), 7.44 (1H, dd, J=0.9, 7.9), 7.52 (1H, dd, J=1.2, 7.9), 7.59 (1H, t, J=7.9)
6	0.95 (6H, d, J=12.8), 3.70—3.72 (2H, m), 4.48 (1H, dd, J=0.9, 10.1), 4.97 (1H, d, J=10.1)
7[a]	0.96 (6H, d, J=9.2), 4.57 (1H, d, J=10.3), 4.99 (1H, d, J=10.3)
8	0.97 (6H, d, J=10.4), 3.84 (3H, s), 4.50 (1H, dd, J=1.2, 10.1), 5.00 (1H, d, J=10.1)
9	0.92 (3H, s), 0.96 (3H, s), 3.82 (3H, s), 7.67 (1H, s), 7.81 (1H, s)
10	0.95 (3H, s), 1.01 (3H, s), 3.81 (3H, s), 6.88 (1H, s), 8.42 (1H, br)
11	0.92 (3H, s), 0.94 (3H, s), 1.30—1.60 (6H, br), 2.48 (1H, d, J=13.1), 3.00 (1H, d, J=13.1), 3.78 (3H, s)
12	0.93 (3H, s), 0.97 (3H, s), 7.69 (1H, s)
13	0.96 (3H, s), 1.02 (3H, s), 6.89 (1H, s)

a) In DMSO-d_6.

nitronic esters, which readily break down into aldoximes. However, the reaction is reported to take place only when the substrates are negatively substituted nitroalkanes.[4] In the present experiments, we have found a case where even a nitromethyl group not activated by an additional functional group affords the aldoxime. The pathway for diazomethane-promoted aldoxime formation from nitroalkanes may be illustrated as shown in Chart 2.[5] The crucial step would be α-hydrogen abstraction by diazomethane, but the reason why this reaction took place in 7 or 3 is not known.

TABLE III. ^{13}C-NMR Spectral Data for the Products[a,b]

Carbon No.	Compound									
	4	5	6	7[c]	8	9	10	11	12	13
1	33.52	33.43	33.10	31.02	33.37	33.39	33.65	33.00	33.53	33.74
2	40.42	40.46	40.76	39.60	40.70	41.01	41.26	41.62	40.99	41.17
3	18.09	18.05	18.21	17.03	18.19	18.85	19.89	18.74	18.88	19.84
4	34.92	35.61	35.17	34.02	35.11	35.39	35.24	28.69[d]	34.30	35.16
4a	42.52	42.46	41.64	40.54	41.74	42.92	44.93	41.91	43.47	45.40
4b	147.66	148.61	137.11	136.86	139.40	140.68	139.70	139.30	148.18	146.93
5	127.46[d]	128.52	126.47	125.66	126.81	126.90	128.32	127.04	125.46	126.81
6	127.46[d]	133.16	120.66	120.28	121.19	122.32	121.44	114.07	134.31	130.52
7	152.98	122.93	145.74	155.81	159.01	158.51	158.45	157.98	127.33[d]	127.03[d]
8	122.91	149.54	113.01	112.10	110.46	109.29	109.15	113.00	127.22[d]	127.02[d]
8a	132.66	125.16	132.14	131.47	132.49	132.74	132.94	136.37	131.78	131.97
9	195.00	194.03	197.43	196.20	196.95	197.54	198.44	67.34	198.04	198.66
10	33.28	33.38	33.31	32.30	33.37	34.27	35.75	32.62[d]	35.48	35.78
10a	49.96	49.30	50.67	49.48	50.68	50.90	51.60	45.83	50.70	51.40
11	79.18	79.75	79.48	78.54	79.43	152.92	148.70	43.14	152.95	148.55
12	32.31	32.06	32.31	31.17	32.31	31.36	31.70	33.24	31.42	31.67
13	21.60	21.45	21.46	21.34	21.48	20.83	21.01	22.35	20.95	21.04
14					55.43	55.48	55.46	55.18		

a) These assignments were based on data from reference 6. *b*) δ (ppm) in $CDCl_3$ from TMS. *c*) In DMSO-d_6. *d*) Assignments in each column may be reversed.

Experimental

All melting points were measured under a microscope (Yanaco MP-S2) and are uncorrected. Infrared (IR) spectra were recorded on a Hitachi 270-30 spectrophotometer. Nuclear magnetic resonance (NMR) spectra were taken on a JEOL GX-400 machine with tetramethylsilane (TMS) as an internal standard. The abbreviations used are as follows: s=singlet, d=doublet, dd=double doublet, t=triplet, q=quartet, m=multiplet, br=broad. MS were determined with a JEOL 01SG-2 instrument.

1,1-Dimethyl-7-nitro-4a-nitromethyl-9-oxo-1,2,3,4,4a,9,10,10a-octahydrophenanthrene (4)——Finely powdered 9-oxodihydro compound (3, 2.9 g, 7.3 mmol) was added to a solution of fum. HNO_3 (d=1.52, 20 ml)-conc. H_2SO_4 (2.0 ml) under ice-salt cooling. The reaction mixture was stirred for 2 h, then poured into ice-water and the whole was extracted with CH_2Cl_2 (50 ml). The extract was washed with H_2O, 10% Na_2CO_3 and H_2O, then dried over Na_2SO_4. The solvent was evaporated off *in vacuo* to give 2.08 g (61.9%) of **4**, mp 143—145 °C (white crystals from MeOH). Chromatography of the mother liquor on SiO_2 (50 g) with benzene–AcOEt (49 : 1) gave 0.6 g (17.4%) of **4** and 0.1 g (2.7%) of an isomer (**5**), mp 183—187 °C (colorless crystals from MeOH–acetone).

7-Amino-1,1-dimethyl-4a-nitromethyl-9-oxo-1,2,3,4,4a,9,10,10a-octahydrophenanthrene (6)——A solution of **4** (678.5 mg, 2.0 mmol) in EtOH (100 ml) was hydrogenated over 10% Pd-C at room temperature. The catalyst was filtered off and the filtrate was evaporated *in vacuo* to give 413 mg (66.9%) of **6**, mp 196—198 °C (pale green needles from EtOH).

7-Hydroxy-1,1-dimethyl-4a-nitromethyl-9-oxo-1,2,3,4,4a,9,10,10a-octahydrophenanthrene (7)——A solution of **6** (1.5 g, 4.9 mmol) in 30% H_2SO_4 (50 ml) was treated with 5% $NaNO_2$ (12 ml) under ice cooling (0—5 °C) and stirred for a further 1.5 h. The mixture was poured into a solution of cupric sulfate (prepared from conc. H_2SO_4 15 g, $CuSO_4 \cdot 5H_2O$ 63 g, urea 4 g and H_2O 100 ml) at 100—120 °C (bath temperature) with stirring. The colored mixture was heated for a further 1.5 h, diluted with H_2O (150 ml) after cooling to room temperature, and extracted twice with CH_2Cl_2 (70 ml). The extract was dried over Na_2SO_4 and evaporated *in vacuo* to give a brown oil, which was chromatographed on SiO_2 (200 g) with AcOEt–n-C_6H_{12} (1 : 5) to give 1.1 g (73.8%) of **7**, mp 178—180 °C (colorless crystals from CH_2Cl_2–n-C_6H_{12}).

7-Methoxy-1,1-dimethyl-4a-nitromethyl-9-oxo-1,2,3,4,4a,9,10,10a-octahydrophenanthrene (8)——1) With Diazomethane: **7** (1.06 g, 3.5 mmol) was added to an ether solution of diazomethane [prepared from p-toluenesulfonyl-N-methyl-N-nitrosoamide (10.8 g)] and the mixture was stirred for 4 d at room temperature. After removal of the solvent *in vacuo*, the residue was treated with CH_2Cl_2 (50 ml) and H_2O (50 ml). The CH_2Cl_2 layer was dried over Na_2SO_4 and evaporated *in vacuo*. The residue was chromatographed on SiO_2 (150 g) with AcOEt–n-C_6H_{12}

(1:5) to give 177.1 mg (16.0%) of **8**, 258.5 mg (24.5%) of methoxyloxime-1 (**9**) and 196.7 mg (18.7%) of methoxyloxime-2 (**10**), successively. **8**: mp 140—141 °C (colorless prisms from CH_2Cl_2-*n*-C_6H_{12}). **9**: mp 162—163 °C (colorless prisms from MeOH). **10**: mp 155—157 °C (colorless needles from MeOH).

2) With Meerwein Reagent: A mixture of **7** (606 mg, 2 mmol), Meerwein reagent (352 mg, 2.5 mmol) and diisopropylethylamine (268 mg, 2 mmol) in CH_2Cl_2 (40 ml) was stirred for 24 h at room temperature. The mixture was washed with 10% HCl (20 ml), 10% Na_2CO_3 (20 ml) and brine (20 ml), and dried over Na_2SO_4. Evaporation of the solvent gave the crude product, which was chromatographed on SiO_2 (60 g) with AcOEt–*n*-C_6H_{12} (1:5) to give 374.1 mg (59%) of **8** and 225.6 mg of recovered **7**. The product was identical with the above sample (IR spectral comparison).

Reaction of 3 with Diazomethane——A mixture of **3** (289 mg, 1 mmol) and diazomethane in ether (50 ml) [prepared from *p*-toluenesulfonyl-*N*-methyl-*N*-nitrosoamide (5.4 g)] was stirred for 4 d at room temperature. The mixture was worked up as described in the case of **8** to give 169 mg of recovered **3**, 35.6 mg (13.1%) of oxime-1 (**12**) and 43.2 mg (15.9%) of oxime-2 (**13**). **12**: mp 160—161 °C (colorless crystals from CH_2Cl_2-*n*-C_6H_{12}). **13**: mp 157—158 °C (colorless crystals from CH_2Cl_2-*n*-C_6H_{12}).

7-Amino-4a-aminomethyl-9-hydroxy-1,1-dimethyl-1,2,3,4,4a,9,10,10a-octahydrophenanthrene (11)——1) From **8**: A solution of **8** (237.8 mg, 0.75 mmol) in EtOH (40 ml) was hydrogenated over Raney Ni at room temperature. The catalyst was filtered off and the filtrate was evaporated *in vacuo*. The residue was dissolved in CH_2Cl_2 (30 ml), the solution was filtered to remove the insoluble matter, and the filtrate was evaporated *in vacuo* to give 80.3 mg (37.3%) of **11**, mp 178—180 °C (colorless needles from AcOEt).

2) From **9** and **10**: As described above, hydrogenation of **9** (301 mg, 1 mmol) and **10** (180 mg, 0.6 mmol) gave the same product in 42.1% (120.7 mg) and 30.7% (52.7 mg) yields, respectively. This product was identical with the above sample (IR spectral comparison).

Acknowledgment We are grateful to Dr. T. Oishi, the Institute of Physical and Chemical Research, for his advice, to Miss Y. Hatori for her assistance and to the staff of the analytical center of this college for spectral measurement and elemental analysis.

References and Notes

1) Y. Shibanuma and T. Okamoto, *Chem. Pharm. Bull.*, **33**, 3187 (1985).
2) *a*) A. Tahara, H. Akita and Y. Ohtsuka, *Chem. Pharm. Bull.*, **22**, 1547 (1974); *idem, ibid.*, **22**, 1555 (1974); *b*) H. Akita and T. Oishi, *Chem. Pharm. Bull.*, **29**, 1567 (1981).
3) The structure of **4** was determined based on a comparison of its NMR data with those of 13-amino- or 13-methoxy-7-oxo-13-deisopropyldehydroabietane.[2a] The pattern of aromatic peaks of **4** is typical of a 1,3,4-trisubstituted benzene system. See Table II. The structure of **5** was also determined from ^1H- and ^{13}C-NMR data. See Tables II and III.
4) A. T. Nielsen, "The Chemistry of the Nitro and Nitroso Groups," Part 1, ed. by H. Feuer, Interscience Publisher, 1969, p. 423 and references cited therein.
5) One of the referees has proposed the following alternative pathway in which carbene liberated from diazomethane plays an important role. The authors are grateful for this suggestion.

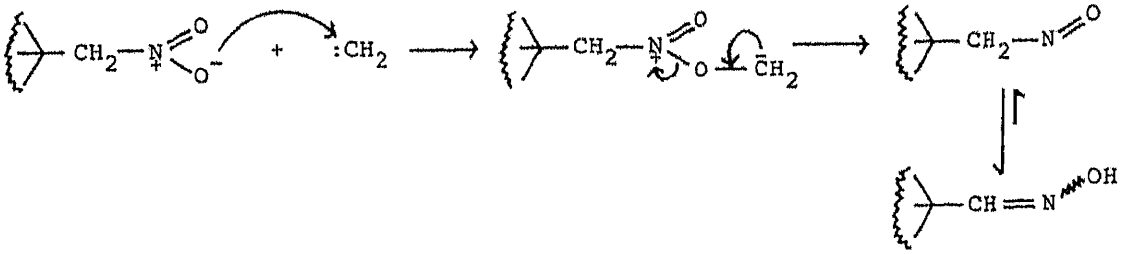

Chart 3

6) E. Wenkert, "Topics in ^{13}C-NMR Spectroscopy," Vol. 2, ed. by G. C. Levy, John Wiley and Sons, Inc., New York, 1976, p. 97.

[Chem. Pharm. Bull. 35(4)1604—1607(1987)]

Enantioselective Carbon–Carbon Bond Formation by Chiral Organotitanium Compounds; Methyltitanium (*S*)-*N*-Acylpyrrolidinylmethoxide Diisopropoxides

HIROSHI TAKAHASHI,* AKIHIRO KAWABATA, and KIMIO HIGASHIYAMA

Institute of Medicinal Chemistry, Hoshi University, 2-4-41, Ebara, Shinagawa, Tokyo 142, Japan

(Received October 2, 1986)

New chiral compounds, (*S*)-*N*-acylpyrrolidinylmethanols (**1b**—**f** and **1h**), were synthesized and chiral methyltitanium diisopropoxides (**2a**—**h**) were prepared from **1a**—**h**. Enantioselective carbon–carbon bond formation between aromatic carbaldehydes and **2a**—**h** was achieved in yields of 90—97% and 10.5—54.1% ee. The chiral auxiliaries (**1a**—**h**) were recovered in almost quantitative yields without any loss of optical purity.

Keywords——(*S*)-*N*-acylpyrrolidinylmethanol; carbon–carbon bond formation; enantioselective reaction; methyltitanium diisopropoxide; (*R*)-1-(1-naphthyl)ethanol; (*R*)-1-phenylethanol; (*S*)-prolinol

Enantioselective carbon–carbon bond formation by the use of chiral organotitanium reagents has recently received much interest. We wish to describe herein an enantioselective reaction of aromatic carbaldehydes with new chiral methyltitanium reagents whose ligands are (*S*)-*N*-acylpyrrolidinylmethanols.

The (*S*)-*N*-acylpyrrolidinylmethanols (**1a**—**h**) were synthesized from commercially available ethyl (*S*)-prolinate, (*S*)-prolinol, and (*S*)-*N*-benzyloxycarbonylproline in good yields. These compounds (**1a**—**h**) contain a hydroxymethyl, 1,1-dimethylhydroxymethyl, or 1,1-diphenylhydroxymethyl group at the 2-position of the pyrrolidine ring, and a formyl, acetyl, or benzyloxycarbonyl group at the 1-position of the ring, as shown in Chart 1. (*S*)-*N*-Formylpyrrolidinylmethanol (**1a**)[1] and (*S*)-*N*-benzyloxycarbonylpyrrolidinyl-1,1-dimethylmethanol (**1g**)[2] have already been reported. The structures of **1b**—**f** and **1h** were confirmed by infrared (IR), mass, and proton nuclear magnetic resonance (^{1}H-NMR) spectral analyses.

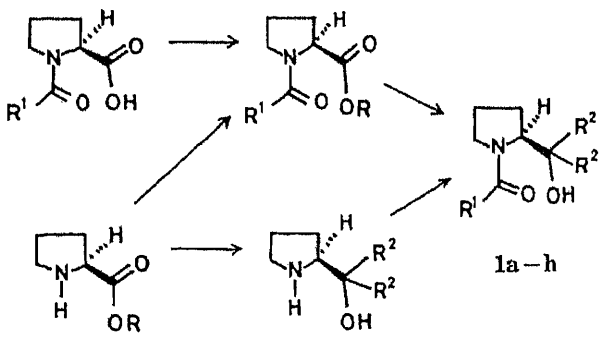

1a: $R^1=R^2=H$ **1b**: $R^1=H$, $R^2=Ph$ **1c**: $R^1=Me$, $R^2=H$ **1d**: $R^1=R^2=Me$
1e: $R^1=Me$, $R^2=Ph$ **1f**: $R^1=Ph$, $R^2=H$ **1g**: $R^1=C_6H_5CH_2O$, $R^2=Me$
1h: $R^1=C_6H_5CH_2O$, $R^2=Ph$

Chart 1

Methyltitanium (*S*)-*N*-acylpyrrolidinylmethoxide diisopropoxides (**2a—h**) were synthesized by the reaction of dimethyltitanium diisopropoxide with **1a—h**. The chiral methyltitanium compounds (**2a—h**) were allowed to react with benzaldehyde and 1-naphthalenecarbaldehyde at −20—10 °C for 10—20 h to give enantiomeric mixtures of (*R*)- and (*S*)-1-phenylethanol (**3a**) and 1-(1-naphthyl)ethanol (**3b**), respectively, in yields of 90—98% as shown in Chart 2.

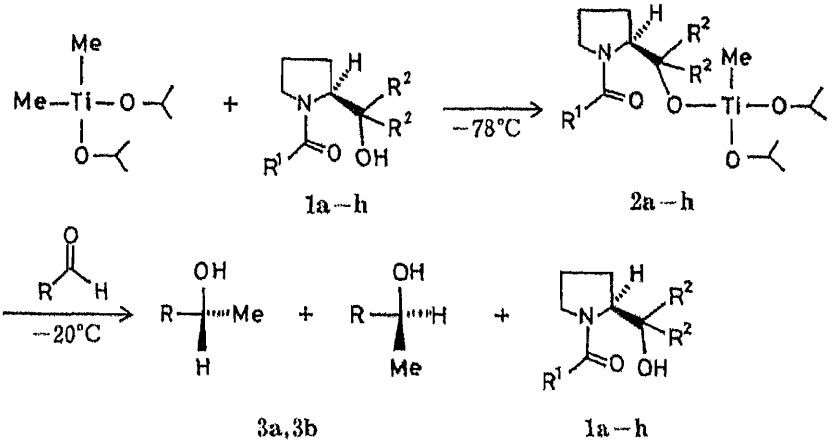

1a,2a: $R^1=R^2=H$ **1b,2b**: $R^1=H$, $R^2=Ph$ **1c,2c**: $R^1=Me$, $R^2=H$ **1d,2d**: $R^1=R^2=Me$
1e,2e: $R^1=Me$, $R^2=Ph$ **1f,2f**: $R^1=Ph$, $R^2=H$ **1g,2g**: $R^1=C_6H_5CH_2O$, $R^2=Me$
1h,2h: $R^1=C_6H_5CH_2O$, $R^2=Ph$ **3a**: R=Ph **3b**: R=1-naphthyl

Chart 2

TABLE I. Enantioselective Reaction between Aromatic Carbaldehydes and Methyltitanium (*S*)-*N*-Acylpyrrolidinylmethoxide Diisopropoxides (**2a—h**)

Compd. No.	Reagent		Product			
	R^1	R^2		$[\alpha]_D$ (c)[a]	ee (%)	Configuration
2a	H	H	**3a**	−14.2° (0.89)	33.0	*S*
2b	H	Ph	**3a**	−7.6° (0.52)	17.6	*S*
2c	Me	H	**3a**	+10.3° (0.56)	23.9	*R*
2c	Me	H	**3b**	+21.1° (0.33)	27.6	*R*
2d	Me	Me	**3a**	+8.0° (0.56)	18.6	*R*
2e	Me	Ph	**3a**	+16.8° (0.42)	39.0	*R*
2e	Me	Ph	**3b**	+8.1° (0.29)	10.5	*R*
2f	Ph	H	**3a**	+6.0° (0.53)	13.9	*R*
2g	$C_6H_5CH_2O$	Me	**3a**	−9.9° (0.55)	23.0	*S*
2g	$C_6H_5CH_2O$	Me	**3b**	−20.6° (0.53)	27.0	*S*
2h	$C_6H_5CH_2O$	Ph	**3a**	+23.3° (0.30)	54.1	*R*
2h	$C_6H_5CH_2O$	Ph	**3b**	+22.8° (0.18)	29.8	*R*

a) The optical rotations were measured at 20—23 °C in cyclopentane (for **3a**) and ethanol (for **3b**).

The values of enantiomeric excess (ee) of **3a** and **3b** were estimated by comparison of the specific rotations with those of optically pure (*R*)-1-phenylethanol[3] and (*R*)-1-(1-naphthyl)ethanol,[4] respectively, and it was found that these reactions proceeded in 10.5—54.1% ee. These experimental results are summarized in Table I. The chiral auxiliaries, (*S*)-*N*-acylpyrrolidinylmethanols (**1a—h**) were recovered in almost quantitative yields, and the optical purities of these compounds were unaltered.

[Chem. Pharm. Bull. 35(4)1608—1609(1987)]

A Novel Electrochemical Method of Acetylation of Alcohols by Methyl Acetate

TATSUYA MASUMIZU,[1] KOOHEI NOZAWA, KEN-ICHI KAWAI and SHOICHI NAKAJIMA*

Faculty of Pharmaceutical Sciences, Hoshi University, Ebara 2-4-41, Shinagawa-ku, Tokyo 142, Japan

(Received October 8, 1986)

A new electrochemical method of acetylation, using methyl acetate at room temperature, was developed. The current efficiency in all the reactions with primary alcohols exceeded 100%, ranging from 126 to 166%, indicating that this method of acetylation is advantageous for the preparation of acetates from the viewpoint of energy economy.

Keywords——acetic acid methyl ester; acetylation; alcoholysis; electrochemical reduction; transesterification; alcoholate anion

In many cases, acetylation of alcohols by the use of alkyl acetate does not proceed without another reagent such as sulfuric acid,[2] *p*-toluenesulfonic acid,[3] alkali alcoholates[4] and potassium cyanide.[5] In addition, some of these procedures[2-4] require heating. In this paper, we report a new, simple method of acetylation, at room temperature, by using methyl acetate without any other reagent.

As we reported recently,[6] alcoholysis of esters takes place electrochemically in the cathodic compartment, in an acetonitrile solution of the substrate ester, alcohol, and tetraethylammonium perchlorate (TEAP) or lithium perchlorate as a supporting electrolyte. It is clear that the acetylation of alcohol by the use of methyl acetate is a modification of this transesterification reaction. The reaction conditions, in terms of electrodes, solvent, electrolyte, and potential, were the same as those established in the previous paper,[6] except for the amount of methyl acetate *vs.* that of alcohol: the acetylating agent, methyl acetate, was used in 20-fold molar excess over the alcohol in this procedure.

TABLE I. Electrochemical Acetylation with Methyl Acetate

Alcohol	Product	Yield[a] (%)	Recovered[a] (%)
Benzyl alcohol	Benzyl acetate	83	6
p-Methylbenzyl alcohol	*p*-Methylbenzyl acetate	63	24
β-Phenethyl alcohol	*β*-Phenethyl acetate	77	15
Methyl mandelate	Methyl 2-acetoxyphenacetate	12	56
Benzhydrol	Benzhydryl acetate	25	68
1,2:5,6-Di-*O*-isopropylidene-D-glucofuranose	1,2:5,6-Di-*O*-isopropylidene-*O*-acetyl-D-glucofuranose	27	64

a) Isolated yield.

The results are summarized in the table. Since the amount of electricity passed was only 0.5 F/mol of substrate alcohol, the percentage current efficiency is twice the percentage

(*S*)-*N*-Benzyloxycarbonylpyrrolidinyl-1,1-diphenylmethanol (1h)——The method used to synthesize (*S*)-*N*-benzyloxycarbonylpyrrolidinyl-1,1-dimethylmethanol (**1g**)[2] was modified. A solution of 2 molar equivalents of CH_2N_2 in ether (100 ml) was added to (*S*)-*N*-benzyloxycarbonylproline (10 g, 40 mmol) in ether (140 ml). The reaction mixture was stirred at room temperature for 3 h, and removal of the solvent gave methyl (*S*)-*N*-benzyloxycarbonylprolinate.

PhMgBr (88 mmol in 44 ml of ether) was added dropwise to a solution of methyl (*S*)-*N*-benzyloxycarbonylprolinate in ether (44 ml) under a nitrogen atmosphere. After being stirred at room temperature for 1 h, the reaction mixture was worked up as described above for **1e** to give a colorless solid (9.83 g, 64%). Recrystallization from *n*-hexane gave colorless prisms of mp 88—89 °C. *Anal.* Calcd for $C_{25}H_{25}NO_3$: C, 77.49; H, 6.50; N, 3.62. Found: C, 77.64; H, 6.53; N, 3.53. $[\alpha]_D$ +9.0° (*c*=0.33, ethanol). IR ($CHCl_3$): 3350 (OH), 1660 (C=O) cm^{-1}. MS *m/z*: 388 (MH^+), 91 (base peak). ^{1}H-NMR ($CDCl_3$) δ: 5.14 (2H, s, $PhCH_2O$).

Preparation of Methyltitanium (*S*)-*N*-Acylpyrrolidinylmethoxide Diisopropoxides (2a—h)——MeMgBr (14 mmol in 4.7 ml of ether) was added dropwise over 30 min to a stirred solution of $Cl_2Ti(OPr^i)_2$ (7 mmol in 7 ml of THF) in THF (12 ml) at −20 °C under a nitrogen atmosphere and the stirring was continued at −20 °C for 1.5 h. A solution of (*S*)-*N*-acylpyrrolidinylmethanol (**1a—h**, 7 mmol) in CH_2Cl_2 (29 ml) was added dropwise over a period of 2.5 h to the above prepared dimethyltitanium reagent at −78 °C, and the stirring was continued at −78 °C for 2 h.

Reaction of Aromatic Carbaldehydes with 2a—h——A solution of an aromatic carbaldehyde (2 mmol) in CH_2Cl_2 (10 ml) was added dropwise over 30 min to a stirred solution of **2a—h** (6 mmol in 60 ml of the solvent) under a nitrogen atmosphere. After being stirred at −20 °C for 10—20 h, the reaction mixture was treated with a 20% aqueous KF solution (*ca.* 4 ml), the resulting white precipitate was filtered off, and the filtrate was extracted with ether. The organic layer was dried over anhydrous Na_2SO_4 and concentrated under reduced pressure. The oily residue was chromatographed on silica gel with CH_2Cl_2–benzene (3:1). The first fraction gave **3a** and **3b**, and the second fraction gave **1a—h**, in almost quantitative yields. These products were identical with authentic samples by ^{1}H-NMR spectral comparison. The specific rotations of the products (**3a**, **3b**, and **1a—h**) thus obtained in each reaction were measured. The ee and configurations of **3a** and **3b** were estimated by comparison with the values of $[\alpha]_D^{20}$ +43.1° (*c*=7.19, cyclopropane) of (*R*)-1-phenylethanol[3] and $[\alpha]_D^{20}$ +76.4° (*c*=4.81, ethanol) of (*R*)-1-(1-naphthyl)ethanol.[4] The experimental results are summarized in Table I. The optical purities of **1a—h** were unaltered.

Acknowledgment We are grateful to Mrs. M. Yuyama, Miss T. Tanaka, and Mrs. T. Ogata of Hoshi University for ^{1}H-NMR spectra, MS, and elemental analysis.

References

1) D. Seebach, H-O. Kalinowski, B. Bastani, G. Crass, H. Daum, H. Dörr, N. P. DuPreez, V. Ehrig, W. Langer, C. Nüssler, H-A. Oei, and M. Schmidt, *Helv. Chim. Acta*, **60**, 301 (1977).
2) L. E. Overman, K. L. Bell, and F. Ito, *J. Am. Chem. Soc.*, **106**, 4192 (1984).
3) S. Yamaguchi and H. S. Mosher, *J. Org. Chem.*, **38**, 1870 (1973).
4) M. P. Balfe, E. A. W. Downer, A. A. Evans, J. Kenyon, R. Poplett, C. E. Searle, and A. L. Tarnoky, *J. Chem. Soc.*, **1946**, 797.
5) M. T. Reetz, R. Steinbach, B. Wenderoth, and J. Westermann, *Chem. Ind.* (London), **1981**, 541.
6) A. G. Olivero, B. Weidmann, and D. Seebach, *Helv. Chim. Acta*, **64**, 2485 (1981).
7) D. Seebach, B. Weidmann, and L. Widler, "Modern Synthetic Methods," Vol. 3, ed. by R. Scheffold, Otto Salle Verlag, Frankfurt am Main, 1983, pp. 217—353.
8) T. Mashiko, S. Terashima, and S. Yamada, *Yakugaku Zasshi*, **100**, 319 (1980).

[Chem. Pharm. Bull. 35(4)1608—1609(1987)]

A Novel Electrochemical Method of Acetylation of Alcohols by Methyl Acetate

TATSUYA MASUMIZU,[1] KOOHEI NOZAWA, KEN-ICHI KAWAI and SHOICHI NAKAJIMA*

Faculty of Pharmaceutical Sciences, Hoshi University, Ebara 2-4-41, Shinagawa-ku, Tokyo 142, Japan

(Received October 8, 1986)

A new electrochemical method of acetylation, using methyl acetate at room temperature, was developed. The current efficiency in all the reactions with primary alcohols exceeded 100%, ranging from 126 to 166%, indicating that this method of acetylation is advantageous for the preparation of acetates from the viewpoint of energy economy.

Keywords——acetic acid methyl ester; acetylation; alcoholysis; electrochemical reduction; transesterification; alcoholate anion

In many cases, acetylation of alcohols by the use of alkyl acetate does not proceed without another reagent such as sulfuric acid,[2] *p*-toluenesulfonic acid,[3] alkali alcoholates[4] and potassium cyanide.[5] In addition, some of these procedures[2-4] require heating. In this paper, we report a new, simple method of acetylation, at room temperature, by using methyl acetate without any other reagent.

As we reported recently,[6] alcoholysis of esters takes place electrochemically in the cathodic compartment, in an acetonitrile solution of the substrate ester, alcohol, and tetraethylammonium perchlorate (TEAP) or lithium perchlorate as a supporting electrolyte. It is clear that the acetylation of alcohol by the use of methyl acetate is a modification of this transesterification reaction. The reaction conditions, in terms of electrodes, solvent, electrolyte, and potential, were the same as those established in the previous paper,[6] except for the amount of methyl acetate *vs.* that of alcohol: the acetylating agent, methyl acetate, was used in 20-fold molar excess over the alcohol in this procedure.

TABLE I. Electrochemical Acetylation with Methyl Acetate

Alcohol	Product	Yield[a] (%)	Recovered[a] (%)
Benzyl alcohol	Benzyl acetate	83	6
p-Methylbenzyl alcohol	*p*-Methylbenzyl acetate	63	24
β-Phenethyl alcohol	*β*-Phenethyl acetate	77	15
Methyl mandelate	Methyl 2-acetoxyphenacetate	12	56
Benzhydrol	Benzhydryl acetate	25	68
1,2:5,6-Di-*O*-isopropylidene-D-glucofuranose	1,2:5,6-Di-*O*-isopropylidene-*O*-acetyl-D-glucofuranose	27	64

a) Isolated yield.

The results are summarized in the table. Since the amount of electricity passed was only 0.5 F/mol of substrate alcohol, the percentage current efficiency is twice the percentage

product yield. In all three cases of primary alcohols, the current efficiency exceeded 100%, ranging from 126 to 166%. This suggests that a catalytic process is involved in this reaction, so that this method of acetylation is advantageous from the viewpoint of energy economy. Mechanistically it can be postulated that the alcoholate anion, RO^-, was formed by electrolysis as the active species, and it reacted with the ester to cause transesterification. The low yields with secondary alcohols are possibly caused by the instability of their alcoholate anions. The mechanistic pathway for this acetylation reaction is actually the same as that of other transesterification reactions. Further work is in progress.

Experimental

Melting points are uncorrected. Infrared (IR) spectra were measured on a Hitachi model 215 spectrometer. Mass spectra (MS) were taken on a JEOL JMS-D 300 instrument.

Electrolysis Apparatus——Electrolyses were performed by using a Hokuto Denko HA-105 potentio-galvanostat connected with a Hokuto Denko HF-201 coulometer in an ordinary glass cylinder (50 mm dia.) containing a smaller glass cylinder (10 mm dia.) with a G-3 glass filter diaphragm as the anodic compartment. Glassy carbon (6 mm dia., 100 mm length, Tokai Carbon, RA-6) was used as the cathode and the anode was a platinum plate (20 mm × 8 mm). The catholyte solution was kept at 26 °C by external cooling with circulating water and stirred with a magnetic stirrer. A saturated calomel electrode and saturated KCl agar salt bridge were used for the control of the reaction potential at −1.7 V *vs.* SCE.

Materials——Acetonitrile used as a solvent was of guranteed reagent grade, and was distilled after being dried by refluxing with calcium hydride for 3 h. Standard acetates of *p*-methylbenzyl alcohol, methyl mandelate, benzhydrol and 1,2:5,6-di-*O*-isopropylidene-3-*O*-acetyl-D-glucofuranose were prepared by acetylation of the corresponding alcohol with acetic anhydride and pyridine, and purified by column chromatography on silica gel using methyl acetate–hexane (1:8 for 1,2:5,6-di-*O*-isopropylidene-3-*O*-acetyl-D-glucofuranose, and 1:50 for other acetates) as the eluent. *p*-Methylbenzyl acetate: IR ν_{max}^{film} cm^{-1}: 1722 (C=O). MS *m/z*: 164 (M^+). Methyl 2-acetoxy-2-phenylacetate: IR ν_{max}^{film} cm^{-1}: 1738, 1750. MS *m/z*: 208 (M^+). Benzhydryl acetate: IR ν_{max}^{film} cm^{-1}: 1728. MS *m/z*: 226 (M^+). 1,2:5,6-Di-*O*-isopropylidene-3-*O*-acetyl-D-glucose: mp 62 °C (lit.[7] 62–63 °C). IR ν_{max}^{KBr} cm^{-1}: 1750 (C=O). MS *m/z*: 302 (M^+).

Other acetates and chemicals were obtained from commercial sources.

General Procedure for Electrochemical Acetylation and Isolation of Products——Acetonitrile (40 ml) containing TEAP (4 mmol), methyl acetate (80 mmol), and each substrate alcohol (4 mmol) was placed in the cathodic compartment, and an acetonitrile solution (5 ml) of TEAP (0.5 mmol) was placed in the anodic compartment. Electrolyses were conducted by passing electricity at 0.5 F/mol of substrate alcohol. After electrolysis, the anolyte and catholyte were combined and the solvent was removed *in vacuo*. The residue was extracted with ether (100 ml), and the ether extract was washed with saturated aq. NaCl (50 ml × 3), and dried over anhydrous Na_2SO_4. The ether was evaporated off and the residue was purified by column chromatography on silica gel using ethyl acetate–hexane (1:8 for 1,2:5,6-di-*O*-isopropylidene-3-*O*-acetyl-D-glucofuranose, and 1:50 for other acetates) as the eluent. Products were identified by comparison with standard samples by thin layer chromatography, IR spectroscopy, and/or mixed fusion. Yields of the products and starting materials recovered are shown in the Table I.

Acknowledgement We thank Mrs. M. Yuyama of this university for measurement of MS.

References and Notes

1) Present address: *Hokko Chemical Industry Co., Ltd., Toda 2165, Atsugi-shi, Kanagawa 243, Japan.*
2) J. C. Sauer, B. E. Hain and P. W. Boutwell, "Organic Syntheses," Coll. Vol. III, ed. by E. C. Horning, John Wiley and Sons, Inc., New York, 1955, p. 605.
3) C. E. Rehberg, "Organic Syntheses," Coll. Vol. III, ed. by E. C. Horning, John Wiley and Sons, Inc., New York, 1955, p. 146.
4) D. D. Roelofsen, A. J. Hagendoorn and H. van Bekkum, *Chem. Ind.* (London), **1966**, 1622.
5) K. Mori, M. Tominaga and M. Matsui, *Synthesis*, **1973**, 790.
6) T. Masumizu, K. Nozawa, K. Kawai and S. Nakajima, *Tetrahedron Lett.*, **27**, 55 (1986).
7) E. Fisher and H. Noth, *Ber.*, **51**, 335 (1918).

[Chem. Pharm. Bull. 35(4)1610—1614(1987)]

Studies on the Constituents of Goat's Rue (*Galega officinalis* L.)

TAKEHIKO FUKUNAGA,*[,a] KOICHI NISHIYA,[a] KOICHI TAKEYA,[b] and HIDEJI ITOKAWA[b]

Nippon Hoechst Co., Ltd.,[a] 1-3-2, Minami-dai, Kawagoe, Saitama 350, Japan and Tokyo College of Pharmacy,[b] 1432-1, Horinouchi, Hachioji, Tokyo 192-03, Japan

(Received September 11, 1986)

A new saponin, 3-*O*-[*β*-D-glucopyranosyl(1→2)-*β*-D-glucuronopyranosyl]soyasapogenol B (XII) has been isolated from the herb of goat's rue (*Galega officinalis* L.), together with phytosterol (I), medicagol methyl ether (IV), medicagol (VI), phytosterol-*β*-D-glucoside (VIII), and allantoin (XI). The structures of the compounds were derermined on the basis of chemical and spectral evidence. This is the first time that I, IV, VI, VIII and XI have been isolated from this plant.

Keywords——goat's rue; *Galega officinalis*; Leguminosae; saponin; soyasapogenol B; medicagol; allantoin; ^{13}C-NMR

Goat's rue (*Galega officinalis* L.) (Leguminosae) was once much prescribed as an antidiabetic and a diuretic agent. An active principle, galegin, was isolated from this plant by Tanret[1] and recognized as a guanidine derivative, (3-methylbut-2-en-1-yl)guanidine, by Späth and Prokop.[2] Several other constituents were also obtained, namely 4-hydroxygalegin, the alkaloid peganine, flavones, tannins, saponin, bitter principle, sucrose, and a fatty oil.[3] The present paper described the isolation and the structural elucidation of further constituents of this herb.

The methanolic extract of goat's rue was partitioned between chloroform and water. The chloroform extract was subjected to silica gel column chromatography and Sephadex LH-20 column chromatography. We isolated a new saponin (XII), together with phytosterol (I), medicagol methyl ether (IV),[4] medicagol (VI),[5] phytosterol-*β*-D-glucoside (VIII), and allantoin (XI)[6] from the chloroform extract.

Compound XII was obtained as colorless needles, mp 285—287 °C. The infrared (IR) spectrum of XII showed hydroxyl (3385, 1073—1034 cm^{-1}) and carboxylate (1600 cm^{-1} br) absorption bands. The proton nuclear magnetic resonance (^{1}H-NMR) spectrum of XII showed seven tertiary methyl signals. Compound XII was hydrolyzed with EtOH–5% HCl to give an aglycone (XIIa), glucose, and glucuronic acid. The electron impact-mass spectrum (EI-MS) of XIIa showed peaks at *m/z* 458 (M$^+$), 224 (A/B ring) and 234 (D/E ring) due to the retro-Diels–Alder-type fragmentation of 3*β*-hydroxyolean-12-ene derivatives on ring C.

The triacetate (XIIb), prepared by acetylation of XIIa, showed peaks at *m/z* 584 (M$^+$), 276, and 216 (D/E ring) in the EI-MS. The ^{1}H-NMR spectrum of XIIb showed signals due to three acetoxyl groups and the 24-methyleneoxy function (as an AB quartet). On the basis of a comparison of the carbon nuclear magnetic resonance (^{13}C-NMR) data for XIIa with those of *β*-amyrin,[7] XIIa was suggested to have the hydroxy group at C-22. Therefore, XIIa was deduced to be 3*β*,22*β*,24-trihydroxyolean-12-ene and this was confirmed by direct comparison with an authentic sample of soyasapogenol B (Table I).[8]

A comparison of the ^{13}C-NMR data of XII with those of XIIa showed that the C-2 and

C-3 signals of XII undergo an upfield shift of 2.0 ppm, and a downfield shift of 10.7 ppm, respectively, on going from XIIa to XII. These can be considered as glycosylation shifts[9] and therefore the sugar moiety in XII was determined to be linked at the C-3 hydroxyl group.

The ^{13}C-NMR spectrum of XII exhibited two anomeric carbon signals at 104.2 and 104.9 ppm, and the acetylated derivative (XIIc) of XII showed a peak at m/z 331 (glc(Ac)$_4^+$) in the EI-MS,[10] suggesting the attachment of a glucuronopyranoside moiety to 3β-OH of the aglycone. In addition, on the basis of a comparison of the ^{13}C-NMR data for sugar moieties of saponins, glycosylation shifts at C-1 and C-2 of glucuronic acid were considered to be

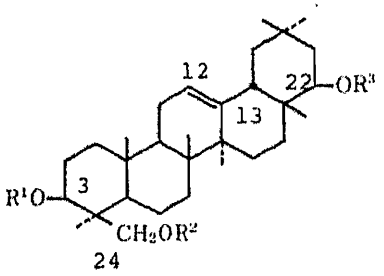

XII: R^1 = glcA-(1→2)-glc, $R^2 = R^3 = H$
XIIa: $R^1 = R^2 = R^3 = H$ (soyasapogenol B)
XIIb: $R^1 = R^2 = R^3$ = Ac
X: R^1 = glcA-6-Me ester-(1→2)-glc, $R^2 = R^3 = H$

Chart 1

TABLE I. ^{13}C-NMR Spectral Data for XII and Related Compounds

	β-Am.[a]	XII[b]	XIIa[b]	XIIb[c]	X[b]	Soya.[d]
C-1	38.6	38.6	39.0	38.4	38.6	39.0
C-2	27.2	26.5	28.5	23.7	26.7	28.4
C-3	78.9	90.9	80.2	80.2	90.9	80.1
C-4	38.7	43.7	43.2	41.7	43.8	43.2
C-5	55.1	56.3	56.4	56.0	56.2	56.4
C-6	18.4	18.7	19.2	19.3	18.6	19.1
C-7	32.6	33.3	33.6	33.0	33.3	33.6
C-8	39.7	40.0	40.1	39.9	40.0	40.1
C-9	47.6	47.7	48.2	47.7	47.8	48.1
C-10	36.9	36.5	37.1	36.3	36.5	37.1
C-11	23.5	24.1	24.1	23.6	24.1	24.1
C-12	121.7	122.5	122.5	122.3	122.4	122.4
C-13	145.1	144.9	144.9	143.9	144.9	144.8
C-14	41.6	42.4	42.4	41.1	42.4	42.4
C-15	26.1	26.5	26.5	26.0	26.5	26.5
C-16	26.9	28.7	28.7	26.9	28.7	28.7
C-17	32.4	38.0	38.1	36.8	38.0	38.0
C-18	47.1	45.4	45.4	44.5	45.3	45.4
C-19	46.8	46.9	46.9	46.0	46.8	46.8
C-20	31.0	30.9	30.9	30.4	30.9	30.9
C-21	34.7	42.4	42.4	38.5	42.4	42.3
C-22	37.1	75.6	75.6	78.4	75.6	75.5
C-23	28.0	22.8	23.6	22.5	22.6	23.6
C-24	15.6	63.4	64.6	65.4	63.4	64.6
C-25	15.6	15.8	16.3	15.5	15.7	16.3
C-26	16.7	17.1	17.1	16.7	17.0	17.1
C-27	26.1	25.8	25.8	26.1	25.8	25.7
C-28	28.4	28.7	28.7	27.0	28.7	28.7
C-29	33.3	33.4	33.3	33.6	33.3	33.3
C-30	23.6	21.2	21.2	20.8	21.2	21.1

a) β-Am.: β-amyrin in $CDCl_3$. *b*) In pyridine-d_5. *c*) In $CDCl_3$. *d*) Soya.: soyasapogenol B in pyridine-d_5.[8c]

TABLE II. ^{13}C-NMR Spectral Data for Sugar Moieties (Pyridine-d_5)

		XII	X	G-Ro[a]	C-IVa[b]
3-GlcA	C-1′	104.9[c]	105.2[c]	105.5	107.4
	C-2′	81.7	81.7	82.5	75.7
	C-3′	75.7[d]	75.8[d]	77.1	78.3
	C-4′	73.2	72.6	73.2	73.6
	C-5′	78.2[d]	78.3[d]	77.8	78.3
	C-6′	177.2	170.3	175.0	175.0
	COOMe		52.2		
2′-Glc	C-1″	104.2[c]	104.8[c]	105.5	
	C-2″	76.3[d]	77.1[d]	77.8	
	C-3″	78.4[d]	78.6[d]	78.1	
	C-4″	70.0	69.9	71.7	
	C-5″	78.2[d]	78.1[d]	77.8	
	C-6″	61.7	61.6	62.7	

a) G-Ro: ginsenoside Ro.[10] *b*) C-IVa: chikusetsusaponin IVa.[11] *c*, *d*) Assignments may be interchanged in each column.

indicative of a 1→2 linkage between glucuronic acid and glucose (Table II).[11]

Compound X was obtained as colorless needles, mp 202—205 °C. The IR spectrum of X showed hydroxyl (3410, 1070—1029 cm^{-1}) and ester carbonyl (1730 cm^{-1}) absorption bands. The ^{1}H-NMR spectrum of X showed seven tertiary methyl signals, a methoxyl signal at δ 3.67, and two sets of anomeric proton signals due to glucuronic acid and glucose were observed at δ 4.95 (d, J=7.7 Hz) and δ 5.61 (d, J=7.7 Hz), showing that these sugars have β-configuration. On the basis of a comparison of the ^{13}C-NMR data of X with those of XII, X was deduced to be the methyl ester of XII. Since X was also isolated from the mother liquor of XII, X is considered to be an artifact derived from XII.

Based on the above-mentioned evidence, the structure of XII has been determined as 3-*O*-[β-D-glucopyranosyl(1→2)-β-D-glucuronopyranosyl]soyasapogenol B.

Experimental

All melting points were determined on a Yanagimoto micro melting point apparatus and are uncorrected. IR spectra were obtained with a Hitachi IR285 spectrometer. Ultraviolet (UV) spectra were recorded on a Hitachi 220A spectrophotometer. Gas liquid chromatography (GLC) was run on a Hewlett Packard 5730 with a flame ionization detector, using a glass column (6 ft×4 mm i.d.) packed with 2% SE-30 on Uniport HP (60—80 mesh); column temperature 260 °C. MS were recorded on a Hitachi M-80 or JEOL DX300 mass spectrometer. ^{1}H-NMR and ^{13}C-NMR spectra were taken at 400 and 100 MHz with a Bruker AM400 spectrometer, and chemical shifts are given as δ (ppm) with tetramethylsilane (TMS) as an internal standard (s, singlet; d, doublet; dd, doublet of doublets; t, triplet; q, quartet). Thin layer chromatography (TLC) was carried out on precoated Kieselgel 60F_{254} plates (Merck). Spots were detected by spraying 10% H_2SO_4 followed by heating. Column chromatography was carried out with Wakogel C-200 (Wako Pure Chemical Ind. Ltd.) and Sephadex LH-20 (Pharmacia Fine Chemicals). High performance liquid chromatography (HPLC) was carried out on the CIG column system (22 mm i.d.×300 mm, 50 μ silica gel, Kusano Scientific Co., Tokyo).

Isolation of Constituents——The herb (9.5 kg) of goat's rue (*Galega officinalis* L.) was extracted three times with MeOH. The methanolic extract was evaporated to dryness (1.5 kg) and then partitioned between $CHCl_3$ and water to give the chloroform extract (420 g). The aqueous layer was further extracted with *n*-BuOH to give the butanol extract (352 g). The chloroform extract was mixed with silica gel (300 g) with the aid of $CHCl_3$–MeOH, dried, and placed on a column of silica gel (1.7 kg). The column was eluted with *n*-hexane–EtOAc (4:1, 7:3, 1:1), EtOAc, and EtOAc–MeOH (1:1) successively. Phytosterol (I), medicagol methyl ether (IV), and medicagol (VI) were isolated from the *n*-hexane–EtOAc fractions. Phytosterol-β-D-glucoside (VIII), compound X, allantoin (XI), and compound XII were also isolated from the EtOAc–MeOH fractions.

I (Phytosterol)——Colorless needles from EtOAc (1.58 g), mp 138—144 °C. IR ν_{max}^{KBr} cm^{-1}: 3420, 2940, 1640 br,

1463, 1387, 1061. ^{1}H-NMR ($CDCl_3$) δ: 3.52 (m), 5.02 (dd, J=15.3, 8.6 Hz), 5.19 (dd, J=15.3, 8.6 Hz), 5.35 (d, J=5.2 Hz). This was analyzed by GLC (2% SE-30, column temp. 260 °C, He 60 ml/min) and identified as a mixture of β-sitosterol, stigmasterol, and campesterol (5 : 4 : 1). The composition was determined from the GLC peak areas.

IV (Medicagol Methyl Ether)——Colorless needles from $CHCl_3$–MeOH (1.2 mg), mp 270—273 °C. UV λ_{max}^{EtOH} nm: 345, 308, 243. IR ν_{max}^{KBr} cm^{-1}: 1745, 1632, 1603, 1290, 1277, 1035, 938. EI-MS m/z (%): 310 (M^+, 31). ^{1}H-NMR ($CDCl_3$) δ: 3.91 (3H, s, –OMe), 6.08 (2H, s, $-OCH_2O-$), 6.97 (1H, dd, J=8.3, 2.3 Hz), 6.99 (1H, br s), 7.12 (1H, s), 7.48 (1H, s), 7.86 (1H, dd, J=8.3, 0.8 Hz).

VI (Medicagol)——Cream-colored powder (23 mg), mp 326—327 °C (dec.). UV λ_{max}^{EtOH} nm (log ε): 347 (4.44), 309 (3.99), 243 (4.24). UV $\lambda_{max}^{EtOH-NaOAc}$ nm (log ε): 365 (4.45), 320 (4.03), 244 (4.21). IR ν_{max}^{KBr} cm^{-1}: 1713, 1634, 1612, 1277, 1037, 943. EI-MS m/z (%): 296 (M^+, 100). ^{1}H-NMR (DMSO-d_6) δ: 6.15 (2H, s, $-OCH_2O-$), 6.69 (1H, d, J=2.2 Hz), 6.93 (1H, dd, J=8.6, 2.2 Hz), 7.26 (1H, s), 7.53 (1H, s), 7.82 (1H, d, J=8.6 Hz).

VIII (Phytosterol-β-D-glucoside)——Colorless needles from $CHCl_3$–MeOH (2.47 g), mp 285—290 °C (dec.). IR ν_{max}^{KBr} cm^{-1}: 3385, 2930, 1625 br, 1460, 1378, 1071, 1023. A solution of VIII (2 mg) in 20 ml of EtOH–5% HCl (1 : 1) was heated under reflux for 1.5 h. After removal of the EtOH under reduced pressure, the reaction mixture was extracted with benzene. The benzene extract was analyzed by GLC (2% SE-30, column temp. 260 °C, He 60 ml/min) and identified as a mixture of β-sitosterol, stigmasterol, and campesterol (5 : 2 : 1). The composition was determined from the GLC peak areas. The aqueous layer was evaporated to dryness and analyzed by TLC (*n*-BuOH–AcOH–H_2O=6 : 3 : 1, anisaldehyde reagent), which indicated the presence of glucose. VIII was identical with an authentic sample on the basis of TLC comparisons.

XI (Allantoin)——Colorless needles from $CHCl_3$–MeOH (35 mg), mp 230—233 °C (dec.). UV $\lambda_{max}^{H_2O}$ nm: does not display any maximum. IR ν_{max}^{KBr} cm^{-1}: 3440, 3345, 3210, 3055, 2760, 1779, 1715, 1655, 1602, 1526, 1182. ^{1}H-NMR (DMSO-d_6) δ: 5.25 (1H, d, J=8.2 Hz), 5.77 (2H, s), 6.89 (1H, d, J=8.2 Hz), 8.04 (1H, s), 10.52 (1H, s). XI was identical with an authentic sample on the basis of mp, IR, NMR and TLC ($CHCl_3$–MeOH=7 : 3, 0.5% ninhydrin) comparisons.

X——Colorless needles from EtOAc (82 mg), mp 202—205 °C. IR ν_{max}^{KBr} cm^{-1}: 3410, 2950, 1730, 1638, 1170, 1079, 1052, 1029. EI-MS m/z (%): 313 (96), 239 (100). ^{1}H-NMR (pyridine-d_5) δ: 0.74, 0.96, 1.00, 1.22, 1.25, 1.30, 1.39 (each 3H, each s, *tert*-Me×7), 3.78 (3H, s, –OMe), 4.95 (d, J=7.7 Hz), 5.61 (d, J=7.7 Hz).

XII——Colorless needles from $CHCl_3$–MeOH (1.07 g), mp 285—287 °C. IR ν_{max}^{KBr} cm^{-1}: 3385, 2945, 1600 br, 1163, 1073, 1034. FD-MS m/z: 835 $(M+K)^+$. EI-MS m/z (%): 440 (1), 234 (100). CI-MS m/z (%): 441 (23), 234 (65), 113 (100). ^{1}H-NMR (pyridine-d_5) δ: 0.74, 0.97, 1.05, 1.23, 1.30, 1.33, 1.37 (each 3H, each s, *tert*-Me×7).

Hydrolysis of XII——A solution of XII (1 mg) in 2 ml of EtOH–5% HCl (1 : 1) was heated under reflux for 30 min on a water bath and then neutralized with Ag_2CO_3. The precipitate was filtered off and the filtrate was concentrated and analyzed by TLC (*n*-BuOH–AcOH–H_2O=6 : 3 : 1, anisaldehyde reagent), which indicated the presence of glucose and glucuronic acid.

XIIa——XII (53 mg) in EtOH–5% HCl (1 : 1) 40 ml was heated under reflux for 4 h on a water bath and concentrated to a small volume. The precipitate was filtered, washed with water, dried, and subjected to column chromatography on silica gel with $CHCl_3$–MeOH=20 : 1 to give XIIa (7.9 mg) as colorless needles (from MeOH), mp 253—255 °C. EI-MS m/z (%): 458 (M^+, 2), 440 (M^+-H_2O, 2), 234 (100), 224 (9), 219 (33). ^{1}H-NMR (pyridine-d_5) δ: 0.97, 1.00, 1.04, 1.24, 1.26, 1.31, 1.58 (each 3H, each s, *tert*-Me×7).

XIIb——XII (203 mg) in EtOH–5% HCl (1 : 1) 100 ml was heated under reflux for 4 h on a water bath, then concentrated, dried, and subjected to column chromatography on silica gel with $CHCl_3$–MeOH=20 : 1 to give XIIa. A solution of XIIa in pyridine (10 ml) was treated with Ac_2O (10 ml) at room temperature for 10 h. The reaction mixture was poured into ice-water and the precipitate was filtered, washed with water, dried, and subjected to silica gel HPLC (*n*-hexane–EtOAc=4 : 1) to give XIIb (73.5 mg) as a colorless oil. EI-MS m/z (%): 584 (M^+, 3), 524 (M^+–AcOH, 1), 465 (<1), 405 (<1), 276 (2), 216 (100). ^{1}H-NMR ($CDCl_3$) δ: 0.82, 0.90, 0.97, 0.98, 1.00, 1.03, 1.15 (each 3H, each s, *tert*-Me×7), 2.03, 2.04, 2.06 (each 3H, each s, acetoxyl Me×3), 4.14, 4.37 (2H, ABq, J=11.7 Hz, 24-H_2), 4.59 (1H, dd, J=10.8, 5.3 Hz, 3αH), 4.64 (1H, t, J=3.6 Hz, 22αH), 5.26 (1H, t, J=3.4 Hz, 12-H).

XIIc——XII (33 mg) in pyridine (6 ml) was treated with Ac_2O (6 ml) at room temperature for 10 h. The reaction mixture was poured into ice-water and the precipitate was filtered, washed with water, dried, and subjected to silica gel HPLC ($CHCl_3$–MeOH=9 : 1) to give XIIc (6.7 mg) as a colorless oil. EI-MS m/z: 331.

Acknowledgement The authors are grateful to Prof. Isao Kitagawa, Faculty of Pharmaceutical Sciences, Osaka University, for supplying soyasapogenol B.

References and Notes

1) G. Tanret, *Compt. Rend.*, **158**, 1182 (1914).
2) E. Späth and S. Prokop, *Ber.*, **57**, 474 (1924).
3) F. H. List and L. Hörhammer (eds.), "Hager's Handbuch der Pharmazeutischen Praxis," völlstandige(vierte) Neuausgabe, 1973, p. 1082; J. B. Harborne, *Phytochemistry*, **6**, 1569 (1967); J. Petricić and Z. Kalodera, *Acta*

Pharm. Jugosl., **32**, 219 (1982).
4) L. Jurd, *J. Pharm. Sci.*, **54**, 1221 (1965).
5) A. L. Livingston, S. C. Witt, R. E. Lundin, and E. M. Bickoff, *J. Org. Chem.*, **30**, 2353 (1965).
6) *Aldrich* IR 358 B, and *Aldrich* NMR **3**, 138 C.
7) H. Beierbeck, J. K. Saunders, and J. W. ApSimon, *Can. J. Chem.*, **55**, 2813 (1977).
8) *a*) I. Kitagawa, M. Yoshikawa, and I. Yosioka, *Chem. Pharm. Bull.*, **24**, 121 (1976); *b*) I. Kitagawa, M. Yoshikawa, H. K. Wang, M. Saito, V. Tosirisuk, T. Fujiwara, and K. Tomita, *ibid.*, **30**, 2294 (1982); *c*) J. Kinjo, I. Miyamoto, K. Murakami, K. Kida, T. Tomimatsu, M. Yamasaki, and T. Nohara, *ibid.*, **33**, 1293 (1985).
9) O. Tanaka, *Yakugaku Zasshi*, **105**, 323 (1985).
10) Y. Takemoto, S. Arihara, K. Yoshikawa, K. Hino, T. Nakajima, and M. Okuhira, *Yakugaku Zasshi*, **104**, 1155 (1984).
11) T. R. Yang, Z. D. Jiang, M. Z. Wu, J. Zhou, and O. Tanaka, *Acta Pharm. Sinica.*, **19**, 232 (1984).

[Chem. Pharm. Bull. 35(4)1615—1618(1987)]

Technique of Measuring Rapid Water Penetration Rate into Tablets

LUCY SAI CHEONG WAN* and PAUL WAN SIA HENG

Department of Pharmacy, National University of Singapore
Lower Kent Ridge Road, Singapore-0511

(Received September 19, 1986)

An accurate method for measuring the fast uptake of water into tablets was established. The method involved the use of a video camera to monitor the flow of liquid in the capillary tube of the water penetration apparatus. Measurements of water uptake could be made in as short an interval as 0.04 s from 0 s. The liquid penetration profiles show that there are three linear portions of the double logarithmic plot of volume penetrated *vs.* time, with a different slope for each linear portion.

Keywords——water penetration; measurement technique; rapid water uptake; water penetration profile

The penetration of liquid into tablets has been studied extensively.[1-8] The kinetics of liquid capillary penetration and the limitations of the Washburn equation have also been examined.[9,10] Hitherto water uptake and penetration rate were derived from data obtained from measurements made after a lapse of several seconds following tablet contact with the liquid. This was because accurate measurement of fast water uptake was difficult. This report shows that rapid penetration of water into tablets can be determined accurately with the aid of a video camera.

Experimental

Materials——Sulfanilamide of B.P. grade (A/S Synthetic, Denmark) was used as a model drug with microcrystalline cellulose (Avicel PH 101, Asahi Chemistry Industry, Japan) as a disintegrant. The surfactant employed was Polysorbate 80 (Tween 80, Honeywill-Atlas Division of ICI, England).

Preparation of Granules——The drug and microcrystalline cellulose (10%) were mixed thoroughly in a mortar for 5 min. As the amount of powder involved did not exceed 30 g, a mixing mill was not used. The powder mixture was moistened with water, 1 ml/10 g, and granulated through a 1.0 mm sieve; the granules were dried in an oven at 60°C for 4 h and regranulated through the same sieve. Those granules retained on a 0.75 mm sieve were used for

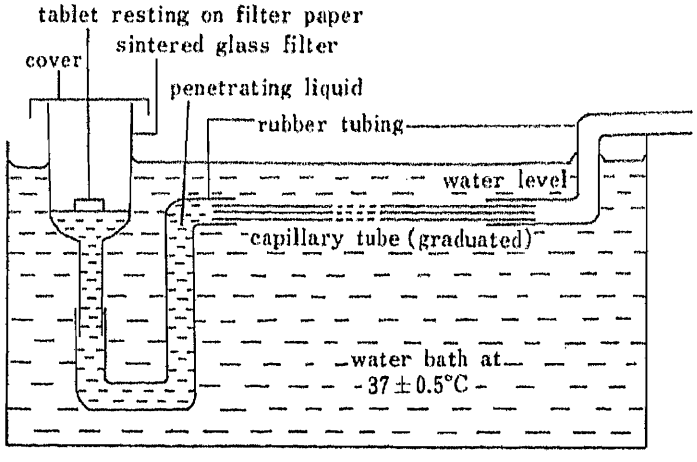

Fig. 1. Apparatus for Measuring Penetration of Liquid into Tablets

compression. In the case where Polysorbate 80 was used, this was incorporated with the moistening liquid.

Preparation of Tablets——The granules were compressed manually using a single-punch tabletting machine (Manesty, model E2, England) with flat-surface punches of diameter 9.53 mm. Tablets were compressed to contain 250 mg of sulfanilamide by calculation and to a specified thickness calculated so as to give an average porosity of 0.14 ± 0.01. Only those tablets that were within ± 10 mg of the target weight were used.

Measurements of Liquid Penetration——The measurement of penetration rate of liquid into the tablet was carried out using the apparatus shown in Fig. 1. It consists of a sintered glass filter connected with tubing to a horizontally positioned graduated capillary tube with external diameter of 6.0 mm and internal diameter of 1.017 mm. The entire assembly was immersed in a water-bath thermostatically controlled at 37 ± 0.5 °C. To prevent water from entering the capillary tube, the open end of the capillary was attached to tubing which was led out of the water-bath. The base of the sintered glass filter was lined with a piece of filter paper of exact size and on this paper was placed a rubber disc with a central hole on which to seat the tablet. To prevent loss of water due to evaporation, the glass filter was covered during the entire course of measurement. The change in the length of liquid column in the capillary tube with time was measured. This was done through the use of a video camera (Sony, model BVP 150 PAL) filming at 25 frames per second with a lens with macro facilities (Canon 12 × Zoom). The recording and slow motion playback were done on a High-band U'matic recorder (Sony, model BVP 820). The volume of liquid penetrated with time was calculated. Five replicates of each tablet formulation were taken.

Results and Discussion

Figure 2 shows the liquid penetration profile of tablets containing sulfanilamide and microcrystalline cellulose with and without Polysorbate 80. The rate of liquid uptake into the tablets containing the surfactant is much greater than that into tablets without Polysorbate. This is probably due to the surface tension-lowering effect of the surfactant, which enhances wetting and thereby allows easier entry of water into the tablet.

The classical Washburn equation is

$$L^2 = \frac{R\gamma \cos\theta}{2\eta} \cdot t$$

where L=length of penetration, R=capillary radius, γ=surface tension of the liquid, θ=solid/liquid contact angle, η=liquid viscosity and t=time. As the volume of penetrated liquid (v) is directly proportional to penetration length, as was first shown by Washburn,[11] the above equation can be written as

$$v^2 = K'L^2 = Kt$$

with K' and K as constants, or

$$v = K^{1/2}t^{1/2}$$

In logarithmic form this equation can be written as

$$\log v = \frac{1}{2}\log K + \frac{1}{2}\log t$$

There are three linear portions along the liquid penetration curve (Fig. 2). The first linear portion is observed for liquid uptake within 1 s of the start of the liquid penetration process, followed by the second linear portion between 1—30 s and the third linear portion from 30 s onwards. The slopes of the linear portions are different. The values obtained for the first, second and third linear portions for the tablets are shown in Table I. It is seen that these slopes are not equal to 0.5, as was assumed in the Washburn equation. It has also been found that the value of the slope depends on the pore size distribution of the porous structure being penetrated.[12]

At the start of the penetration process, the rate of water uptake is fast; this depends on the filling of the space between the tablet and the filter paper with water, thereby establishing contact between the tablet surface and the liquid front. This process is dependent on the

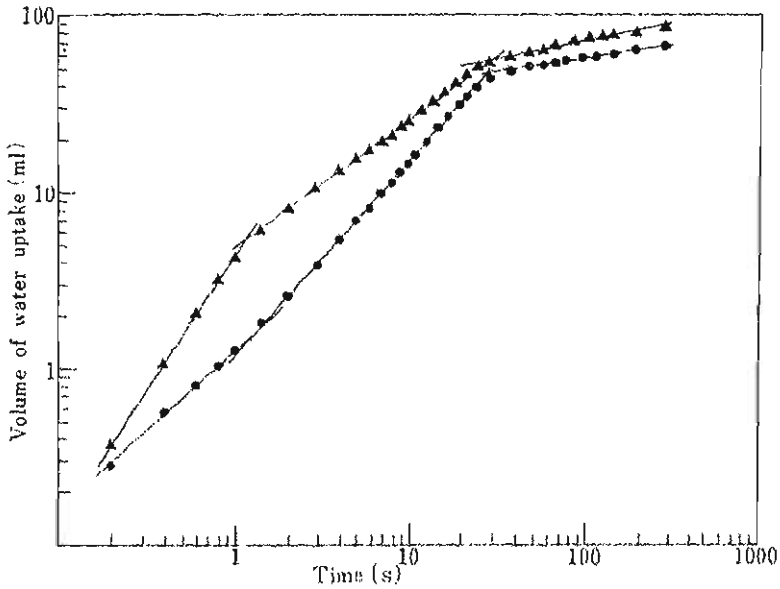

Fig. 2. Water Penetration into Sulfanilamide Tablets without Polysorbate 80 (●) and with 0.2% Polysorbate 80 (▲) at 37 °C

Table I. Regression Parameters[a] of $\log r$ *vs.* $\log t$ Curves for Liquid Penetration into Tablets without Polysorbate 80 (A) and with Polysorbate 80 (B)

Parameters	Linear portions of curves					
	A			B		
	1st	2nd	3rd	1st	2nd	3rd
Intercept	0.1110	0.0808	1.4069	0.6511	0.6681	1.4519
Slope	0.9274	1.0923	0.1786	1.5470	0.7475	0.2005
Correlation coefficient	0.9992	0.9997	0.9842	0.9996	0.9995	0.9963

a) Least-mean-squares regression analysis.

surface-wetting properties of the tablet. In the case of tablets containing surfactant, the penetration rate was very high at the initial stage with a subsequent decrease in rate followed by a further reduction in rate as the liquid penetration process reached saturation. In these tablets, the presence of the surfactant enabled a very rapid filling of the space between the tablet and the filter paper, as reflected by the high rate of liquid penetration during the first second. The second linear phase in the water uptake curve probably represents the filling of the capillary system within the tablet.

The video camera recording technique for determining penetration rate of liquid into tablets can provide information on the rate of water uptake during the first few seconds of the penetration process, which hitherto may have been missed by the methods of measurement reported in the literature.

Acknowledgement The authors wish to thank the Centre for Educational Technology, National University of Singapore for their invaluable technical assistance.

References

1) H. Nogami, H. Fukuzawa and Y. Nakai, *Chem. Pharm. Bull.*, **11**, 1389 (1963).

2) D. Ganderton, *J. Pharm. Pharmacol.*, **21**, Suppl. 9S (1969).
3) D. Ganderton and A. B. Selkirk, *J. Pharm. Pharmacol.*, **22**, 345 (1970).
4) A. B. Selkirk and D. Ganderton, *J. Pharm. Pharmacol.*, **22**, Suppl. 86S (1970).
5) D. Ganderton and D. R. Fraser, *J. Pharm. Pharmacol.*, **22**, Suppl. 95S (1970).
6) D. R. Fraser and D. Ganderton, *J. Pharm. Pharmacol.*, **23**, Suppl. 18S (1971).
7) H. V. van Kamp, G. K. Bolhuis, A. H. de Boer, C. F. Lerk and L. Lie-A-Huen, *Pharm. Acta Helv.*, **61**, 22 (1986).
8) L. S. C. Wan and P. W. S. Heng, *Chem. Pharm. Bull.*, **33**, 2569 (1985).
9) F. Carli and L. Simioni, *Pharm. Acta Helv.*, **53**, 320 (1978).
10) G. Rowley and J. M. Newton, *J. Pharm. Pharmacol.*, **22**, 966 (1970).
11) E. W. Washburn, *Phys. Revs.*, **17**, 273 (1921).
12) F. Carli and L. Simioni, *J. Pharm. Pharmacol.*, **31**, 128 (1979).

[Chem. Pharm. Bull. 35(4)1619—1623(1987)]

Effect of Diethyl Maleate and Sodium Salicylate on Cefmetazole Transport in the *in Vitro* Rat Everted Intestinal Sac: Influence of Ca^{2+} and Vanadate in the Media

TAKUMI SUZUKA, ATSUSHI FURUYA, AKIRA KAMADA, MASARU YAMAZAKI, and TOSHIAKI NISHIHATA*

Faculty of Pharmaceutical Sciences, Osaka University, 1–6 Yamadaoka, Suita, Osaka 565, Japan

(Received October 1, 1986)

In Ca^{2+}-containing media, 1 mM diethyl maleate (DEM) increased the *in vitro* cefmetazole transport in rat everted colonic sac rapidly after a significant nonprotein thiol loss, but the increase in the ileal sac occurred only slowly after a significant nonprotein thiol loss. However, Ca^{2+}-free media promoted the adjuvant effect of DEM rapidly even in the ileal sac. Since vanadate in the Ca^{2+}-containing media also promoted the adjuvant effect of DEM, it is suggested that a perturbation of Ca^{2+} homeostasis as a secondary effect after nonprotein thiol loss is related to the increase of the intestinal mucosal permeability and that the ileal mucosa has stronger resistance to the secondary effect than the colonic mucosa does. The adjuvant effect of 300 mM salicylate (SA) was also promoted in Ca^{2+}-free media. Since the effect of SA was stronger than that of DEM even though SA caused less nonprotein thiol loss, it is considered that the effect of SA involves at least two mechanisms.

Keywords——cefmetazole; transport; everted intestinal sac; calcium ion; vanadate; diethyl maleate; salicylate; nonprotein thiol

Since it has been reported that salicylate and its derivatives enhance rectal absorption of hydrophilic compounds,[1~3] various absorption-promoting adjuvants[1,4] have been investigated.[5~12] However, salicylate has a greater adjuvant effect at the rectum (including colon) than at small intestine.[1,3] Although it has recently been reported that nonprotein thiol loss caused by diethyl maleate might be related to the increase of intestinal mucosal permeability to cefmetazole,[14,15] cefmetazole transport in the presence of diethyl maleate also occurred at the colon more effectively than at small intestine, in spite of no difference of nonprotein thiol loss between the tissues.[14] Further, it has been reported that nonprotein thiol loss in hepatocyte induced the liberation of Ca^{2+} from cells in Ca^{2+}-free medium.[16]

In the present report, we examined the effect of Ca^{2+} in the media on the actions of diethyl maleate and salicylate in increasing the intestinal mucosal permeability to passive transport of cefmetazole, using the *in vitro* everted intestinal sac method.

Experimental

Materials——Sodium salicylate (SA) was obtained from Nakarai Chemicals Co., Ltd. (Kyoto, Japan). Diethyl maleate (DEM) and vanadium pentoxide were obtained from Sigma Inc. (St. Louis, U.S.A.) and vanadate was prepared by dissolution of vanadium pentoxide in sodium hydroxide solution. Sodium cefmetazole was supplied by Sankyo Co., Ltd (Tokyo, Japan). Other reagents used were of analytical grade.

Preparation of an Everted Intestinal Sac——Wistar male rats, weighing 200 to 300 g, were fasted for 16 h prior to experiments. After midline incision of the abdomen of rats anesthetized with sodium pentobarbital (30 mg/kg, i.p.), 20 ml of saline was injected from the aorta to rinse blood out of the intestine, and then both the ileum (as a small

intestinal region) and colon (including the upper rectum) were removed. Each segment was everted. All procedures after excising the intestine were carried out in ice-cold saline saturated with $O_2:CO_2$ gases (95%: 5%).

Transport Study——The *in vitro* rat intestinal transport of cefmetazole was studied by the method of Barr and Riegelman.[17] Krebs-Ringer III buffer (pH 7.0) (designated as Ca^{2+}-containing medium) was used as the medium, and Ca^{2+}-free buffer (Ca^{2+}-free medium) was prepared by addition of equivalent concentrations of sodium chloride instead of calcium chloride in the Krebs-Ringer III buffer. During experiments, the mucosal medium was saturated with $O_2:CO_2$ gases (95%: 5%). Each everted intestinal sac containing 0.5 ml of medium was immersed in 20 ml of medium containing cefmetazole (800 μg/ml) at 37 °C, and was taken from the medium at designated times. After gentle rinsing of the sac surface 3 times with 50 ml of ice-cold saline, the serosal fluid was collected to measure the amount of cefmetazole in the medium. An intestinal segment was homogenized for assay of nonprotein thiol. Transport of cefmetazole was represented in terms of the clearance rate (CL_{cmz}), which was calculated with the following equation.

$$CL_{cmz}\,(\text{ml/h/g-tissue}) = (S)/([M] \times (\text{incubation period}) \times (\text{wet weight of intestinal sac}))$$

where (S) represents the cumulative amount of cefmetazole in the serosal medium and [M] represents the initial concentration of cefmetazole in the mucosal medium.

Assay——Assay of cefmetazole was carried out by the high-pressure liquid chromatographic method described previously.[18] Nonprotein thiol in the homogenate was measured by the method of Ellman[19] and glutathione was used as a standard compound for nonprotein thiol assay.[20]

Statistical Analyses——Statistical analyses were performed by using Student's *t*-test.

Results

Figures 1 and 2 show the effect of Ca^{2+} in the media on cefmetazole transport (CL_{cmz})

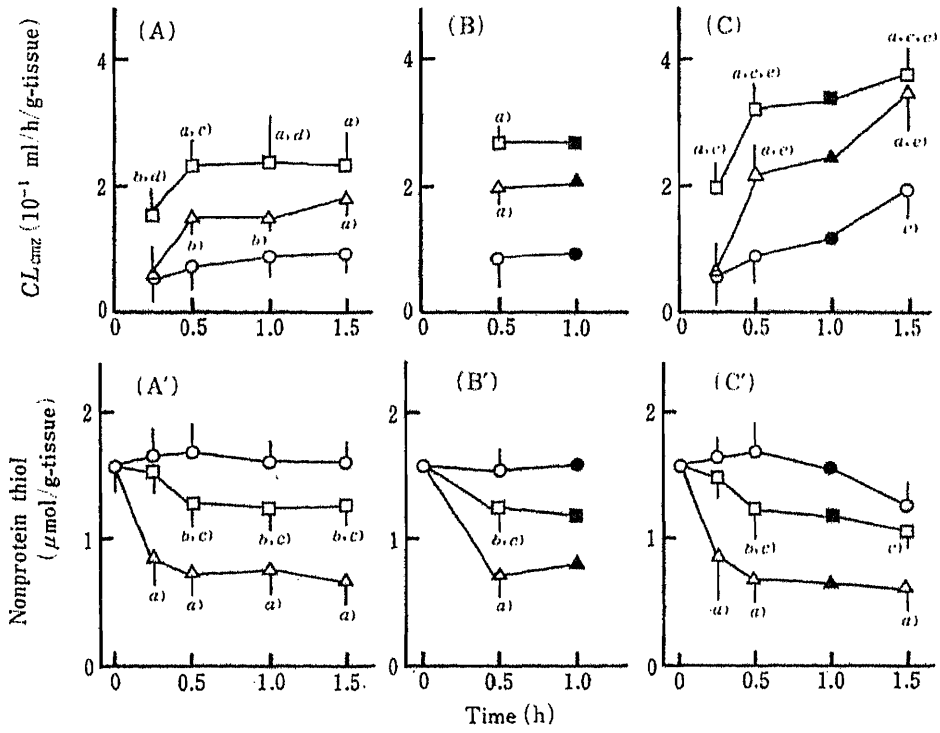

Fig. 1. Effect of DEM (Triangles, 1 mM) and SA (Squares, 300 mM) on Cefmetazole Transport (CL_{cmz}; A, B and C) as a Function of Incubation Time from the Mucosal Side to the Serosal Side through Rat Everted Colonic Sac, and on Nonprotein Thiol Concentrations in the Tissue (A', B' and C')

Circles represent the control (without DEM or SA). A and A', Ca^{2+}-containing media; B and B', Ca^{2+}-containing media with 2 mM vanadate; C and C', Ca^{2+}-free media. Experimental numbers were more than four for open symbols and one for closed symbols.

Each value represents the mean ± S.D. *a*) $p<0.01$ *versus* control (no additive); *b*) $p<0.05$ *versus* control; *c*) $p<0.01$ *versus* addition of DEM; *d*) $p<0.05$ *versus* addition of DEM; *e*) $p<0.01$ *versus* Ca^{2+}-containing media.

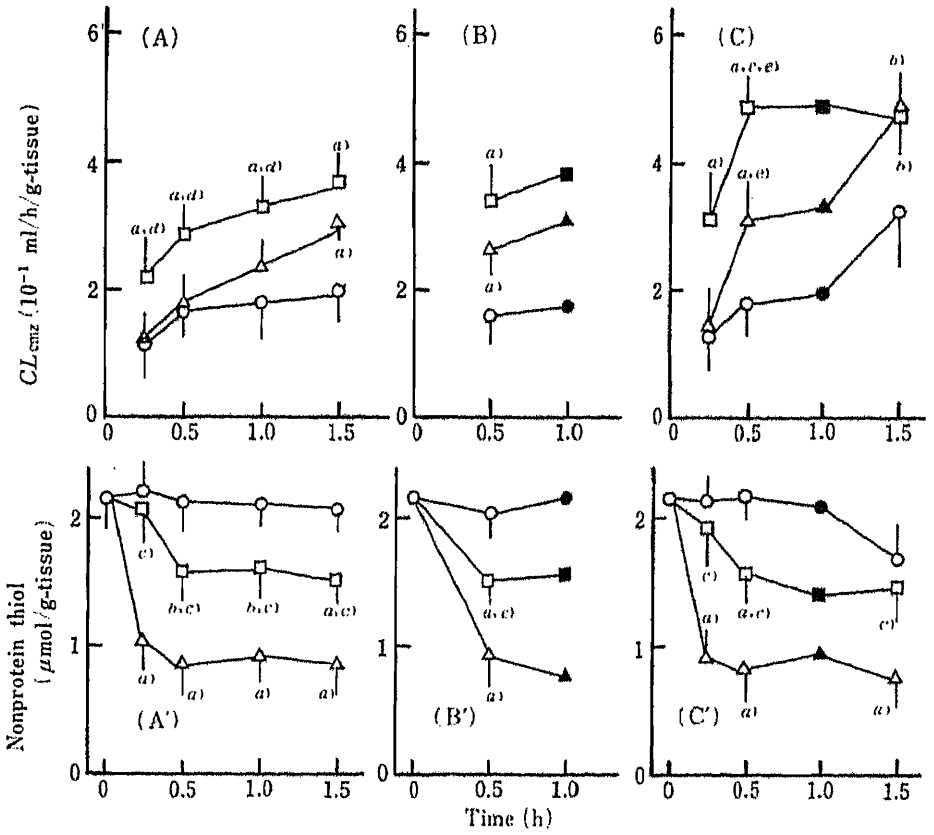

Fig. 2. Effect of DEM (Triangles, 1 mM) and SA (Squares, 300 mM) on Cefmetazole Transport (CL_{cmz}; A, B and C) as a Function of Incubation Time from the Mucosal Side to the Serosal Side through Rat Everted Ileal Sac, and on Nonprotein Thiol Concentration in the Tissue (A', B' and C')

Circles represent the control (without DEM and SA). The media used were as described in Fig. 1. Symbols are the same as in Fig. 1.

Each value represents the mean ± S.D. *a*) $p < 0.01$ *versus* control (no additive); *b*) $p < 0.05$ *versus* control; *c*) $p < 0.01$ *versus* addition of DEM; *d*) $p < 0.05$ *versus* addition of DEM; *e*) $p < 0.01$ *versus* Ca^{2+}-containing media.

from the mucosal side to the serosal side through the rat everted intestinal sac (Fig. 1 for colonic sac and Fig. 2 for ileal sac). CL_{cmz} was not influenced by Ca^{2+} in the media, though a tendency for CL_{cmz} to increase in the later stage (at 1.5 h) was observed in Ca^{2+}-free media.

The addition of DEM (final concentration; 1 mM) to the mucosal medium caused a significant nonprotein thiol loss, which was not influenced by Ca^{2+} and vanadate in the media (Fig. 1A' to C' and 2A' to C'). In Ca^{2+}-free media, CL_{cmz} in the sac of both intestines increased significantly after 0.5 h of incubation with DEM (Fig. 1C and 2C). The addition of DEM to the Ca^{2+}-containing media resulted in an increase of CL_{cmz} of the colonic sac after 0.5 h of incubation (Fig. 1A), but did not increase CL_{cmz} of the ileal sac until 1 h after the start of incubation (Fig. 2A). However, the addition of vanadate to the Ca^{2+}-containing media promoted the effect of DEM in increasing CL_{cmz} of the ileal sac even at 0.5 h after the start of incubation (Fig. 2B)

The addition of SA (final concentration; 300 mM) to the mucosal medium also caused nonprotein thiol loss, which was also not influenced by Ca^{2+} and vanadate in the media (Fig. 1A' to C' and 2A' to C'). Although the degree of nonprotein thiol loss caused by SA was less than that caused by DEM, the increase of CL_{cmz} by SA in both Ca^{2+}-containing media and Ca^{2+}-free media was greater than that by DEM. It should be noted here that the increase of CL_{cmz} by SA was observed as early as 0.25 h after the start of incubation, before nonprotein

thiol loss was observed. The Ca^{2+}-free media also promoted the effect of SA in increasing CL_{cmz}, but vanadate in Ca^{2+}-containing media did not.

Discussion

Among absorption-promoting adjuvants that enhance intestinal absorption of hydrophilic drugs, ethylenediamine tetraacetic acid (EDTA) increased cefmetazole absorption to similar extents at the colon and small intestine.[14] However, it has been reported that the effect of DEM and SA was weak at the small intestine,[13,14] as mentioned earlier. EDTA modifies the permeability of the tight junction of intestinal epithelium by removing Ca^{2+} from the junctional region,[21] indicating that agents such as EDTA which directly modify the structural components of epithelium may act to similar extents at all intestinal regions. Thus, it may be considered that the adjuvant effect of DEM occurs indirectly.

Although it has been reported that the action of 1 mM DEM might be related to its effect in causing nonprotein thiol loss,[13,15] the effect of DEM in Ca^{2+}-containing media appeared with a long lag time after nonprotein thiol loss, especially in the ileal sac (Fig. 1A, 1A′, 2A and 2A′). However, the effect of DEM in increasing CL_{cmz} in Ca^{2+}-free media appeared rapidly, even in the ileal sac. Thus, the adjuvant effect of DEM seems to be a secondary effect occurring after nonprotein thiol loss, and may be related to Ca^{2+} homeostasis in the intestinal epithelium. It has been reported that nonprotein thiol loss in hepatocytes caused a significant Ca^{2+} release from cells along with bleb formation in Ca^{2+}-free medium.[16] The results, which show that vanadate (an inhibitor of Ca^{2+} transport through cells[21]) promoted the effect of DEM, seem to support the idea that a perturbation of Ca^{2+} homeostasis after nonprotein thiol loss increases the permeability to cefmetazole. The weak effect of DEM on CL_{cmz} of the ileum in Ca^{2+}-containing media may be due to greater resistance of the ileum to the hypothetical perturbation of Ca^{2+} homeostasis, in comparison with that of the colon.

The adjuvant effect of 300 mM SA in increasing CL_{cmz} was greater in the colonic sac than in the ileal sac. Since the adjuvant effect of SA in Ca^{2+}-free media was also stronger than that in Ca^{2+}-containing media, the mechanism of SA action in increasing CL_{cmz} may also involve the perturbation of Ca^{2+} homeostasis after nonprotein thiol loss. It has been reported that SA uncouples oxidative phosphorylation to produce adenosine triphosphate (ATP) in mitochondria[22] and it is known that synthesis of glutathione requires ATP. Thus, the decrease of nonprotein thiol loss may be due to partial impairment of glutathione synthesis. However, it was observed that the effect of 300 mM SA in increasing CL_{cmz} in both intestinal sacs appeared before nonprotein thiol loss by SA and was greater than that of 1 mM DEM in spite of the lesser effect of SA on nonprotein thiol loss. This observation seems to indicate that another mechanism is involved in the effect of SA in increasing CL_{cmz}; it has been suggested that SA increases the membrane permeability by binding to membrane component(s).[23,24] Therefore, at least two mechanisms may be involved in the effect of SA in increasing cefmetazole transport.

References

1) T. Nishihata, J. H. Rytting, and T. Higuchi, *J. Pharm. Sci.*, 69, 744 (1980).
2) T. Nishihata, J. H. Rytting, T. Higuchi, and L. Caldwell, *J. Pharm. Pharmacol.*, 33, 334 (1981).
3) S. Yoshioka, L. Caldwell, and T. Higuchi, *J. Pharm. Sci.*, 71, 593 (1982).
4) L. Caldwell, T. Nishihata, J. Fix, S. Selk, R. Cargil, C. R. Gardner, and T. Higuchi, *Meth. and Find. Exptl. Clin. Pharmacol.*, 6, 503 (1984).
5) A. Kamada, Y. Kohno, H. Yaginuma, M. Saeki, M. Yamazaki, and T. Nishihata, *Yakuzaigaku*, 45, 188 (1985).
6) A. Kamada, T. Nishihata, S. Kim, M. Yamamoto, and N. Yata, *Chem. Pharm. Bull.*, 29, 2012 (1981).
7) K. Morimoto, T. Takeeda, Y. Nakamoto, and K. Morisaka, *Int. J. Pharm.*, 14, 149 (1982).

8) K. Morimoto, E. Kajima, T. Takeeda, Y. Nakamoto, and K. Morisaka, *Int. J. Pharm.*, **14**, 149 (1983).
9) K. Nishimura, Z. Nozaki, A. Yoshimi, N. Kakeya, and K. Kitao, *Jpn. J. Antibiot.*, **36**, 1692 (1983).
10) H. Okada, I. Yamazaki, T. Yashiki, and H. Mima, *J. Pharm. Sci.*, **72**, 75 (1983).
11) H. Yaginuma, T. Nakata, H. Toya, T. Murakami, M. Yamazaki, and A. Kamada, *Chem. Pharm. Bull.*, **29**, 2974 (1981).
12) T. Nishihata, H. Yoshitomi, and T. Higuchi, *J. Pharm. Pharmacol.*, **38**, 69 (1986).
13) T. Suzuka, T. Nishihata, M. Yamazaki, and A. Kamada, *Chem. Pharm. Bull.*, **33**, 4600 (1985).
14) T. Nishihata, H. Takahata, and A. Kamada, *Pharm. Res.*, **6**, 307 (1985).
15) T. Nishihata, M. Miyake, H. Takahata, and A. Kamada, *Int. J. Pharm.*, **33**, 89 (1986).
16) S. A. Jewell, G. Bellomore, H. Thor, S. Orrenius, and M. T. Smith, *Science*, **210**, 1257 (1982).
17) W. Barr and S. Riegelman, *J. Pharm. Sci.*, **59**, 154 (1970).
18) T. Nishihata, H. Takahagi, M. Yamamoto, H. Tomida, J. H. Rytting, and T. Higuchi, *J. Pharm. Sci.*, **73**, 109 (1984).
19) G. L. Ellman, *Arch. Biochem. Biophys.*, **82**, 70 (1959).
20) S. Szabo, J. S. Trier, and P. W. Frankel, *Science*, **214**, 200 (1981).
21) A. L. Palmora, I. Meza, G. Beaty, and M. Cereyide, *J. Cell. Biol.*, **81**, 736 (1980).
22) T. M. Brody, *J. Pharmacol. Exp. Ther.*, **117**, 39 (1956).
23) T. Nishihata and T. Higuchi, *Biochim. Biophys. Acta*, **775**, 269 (1984).
24) H. Kaji, T. Horie, M. Hayashi, and S. Awazu, *Life Sci.*, **37**, 523 (1985).

[Chem. Pharm. Bull. 35(4)1624—1628(1987)]

Effect of Binders on the Formation of Pellets.[1] II. Polyvinylpyrrolidone

LUCY SAI CHEONG WAN* and THANGARAJAH JEYABALAN

Department of Pharmacy, National University of Singapore 10 Kent Ridge Crescent, Singapore 0511, Republic of Singapore

(Received November 12, 1986)

The effect of polyvinylpyrrolidone (PVP) powder on the formation of pellets of lactose, paracetamol and phenacetin was studied. The high water-solubility and affinity of lactose for water affect pellet growth and properties. Lactose pelletised with PVP powder resulted in some non-wetting of the PVP powder and hence pellet growth was restricted. In the case of phenacetin, a hydrophobic material, pellet growth increased markedly with PVP concentration. This is also attributed to the large viscosity build-up in some regions of the feed material in the pelletiser dish, giving rise to large pellets being formed. Balling of the feed material occurs resulting in an increase in pellet growth. Pelletisation of mixtures of varying proportions of the feed materials showed that the properties of pellets assumed those of the major component.

Keywords——pelletisation; polyvinylpyrrolidone; lactose; paracetamol; phenacetin; lactose–paracetamol; lactose–phenacetin

In an earlier paper,[1] water, alcohol and water–alcohol mixtures were used to pelletise lactose, paracetamol and phenacetin. It was found that the high water-solubility of lactose and the greater wetting of lactose particles by alcohol in water–alcohol mixtures affected pellet growth and properties. Paracetamol pellets formed with water were smaller and of lower strength than those formed with alcohol or water–alcohol mixtures. Phenacetin, pelletised with these binding liquids were fragile. In the present study, polyvinylpyrrolidone (PVP) was employed as a binder, the aim being to determine the effect of a binder with adhesive properties on the pelletisation of feed materials. Such a binder can contribute significantly to agglomerate strength and impart cohesive qualities to powdered material through particle–particle bonding.

Experimental

Materials——Lactose, paracetamol and phenacetin used for the formation of pellets were of B.P. grade. The mean particle size and bulk density of these powders have been determined previously.[1] Polyvinylpyrrolidone (Plasdone K25, GAF Chemicals U.S.A.) of average particle size $46.3 \pm 27.2\,\mu m$ were used to pelletise the powders.

Formation of Pellets——Pellets were prepared using an inclined dish pelletiser (Erweka, Germany) as described previously.[2] It consists essentially of a shallow cylindrical dish rotating about an inclined axis. The operating conditions were: feed load, 200 g; residence time in the pelletiser, 15 min; angle of inclination of the pelletiser, 45° and agitation speed, 31.66 rpm. The PVP powder was added directly to the feed material, mixed thoroughly and then a fixed amount of water was sprayed onto this mixture to form pellets. The pellets were dried at 60 °C for 4 h.

The size analysis, bulk density, angle of repose, crushing strength and friability of pellets as well as the viscosity of PVP solutions were determined as described earlier.[2] Size fraction of pellets studied was 2.0—2.8 mm.

Results and Discussion

Lactose

The concentrations of PVP powder used to pelletise lactose were 1.5, 3.0 and 4.0%.

TABLE I. Effect of Varying Concentrations of PVP on Average Diameter of Lactose, Paracetamol and Phenacetin Pellets

PVP conc. (%)	Average pellet diameter (mm) 1.5	3.0	4.0
Lactose	2.08	1.75	2.13
Paracetamol	0.55	0.75	1.88
Phenacetin	2.78	3.40	3.83

TABLE II. Viscosity of PVP Solutions at 30°C

PVP conc. (%)	Viscosity relative to water
0	1.0
3.75	1.9
6.66	2.8
7.50	2.9
8.57	3.3
11.25	4.8

TABLE III. Properties of Lactose Pellets Formed with Different Amounts of PVP

PVP conc. (%)	Bulk density (g/ml)	Mean angle of repose (°)	Crushing strength (g)	Friability index
1.5	0.603 ± 0.01	38.38	125.81 ± 3.66	15.81 ± 1.07
3.0	0.627 ± 0.004	37.39	130.62 ± 2.91	9.93 ± 1.54
4.0	0.636 ± 0.001	37.42	143.05 ± 5.01	7.18 ± 0.85

Pellet size fraction 2.0 2.8 mm.

TABLE IV. Properties of Paracetamol Pellets Formed with Different Amounts of PVP

PVP conc. (%)	Bulk density (g/ml)	Mean angle of repose (°)	Crushing strength (g)	Friability index
1.5	0.392 ± 0.06	39.51	137.17 ± 2.45	30.14 ± 1.47
3.0	0.425 ± 0.004	38.62	144.33 ± 2.11	25.10 ± 1.16
4.0	0.456 ± 0.004	38.64	173.70 ± 6.24	23.95 ± 4.99

Pellet size fraction 2.0 – 2.8 mm.

Moistening of the lactose–PVP powder was achieved with water and the amount incorporated was maintained at 20% for all lactose pellets. The mean pellet diameter of lactose pellets decreased and then increased with PVP concentration (Table I). Pellets formed with 1.5% PVP were observed to tumble with ease in the pelletiser, without the pellets sticking to the dish pelletiser. However, with 3% PVP, balling of the pellets occurred. In the regions where water was sprayed directly, it was observed that these regions became overwetted, whilst there was limited distribution of the water to the other regions of the lactose–PVP mixture. This is due to the high viscosity that is developed when PVP comes in contact with water. The viscosity of PVP solutions increases with concentration (Table II). Coalescence of the pellets was slow and small pellets were produced. In addition, lactose being very water-soluble (22.22 g/100 ml)[1] may be preferentially dissolved in the water and thus not all the PVP present will go into solution.

With a higher PVP concentration, 4%, the incidence of overwetting regions increased. Although this slowed down the spread of water further, the greater viscosity achieved as a consequence of more PVP being present promotes the formation of large pellets. The viscous nature of PVP in contact with water allows greater rate of coalescence and thus the mean pellet size increases (Table I).

The crushing strength of lactose pellets increased whilst friability values decreased with PVP concentration (Table III). The bulk density was also greater with higher PVP

TABLE V. Properties of Phenacetin Pellets Formed with Different Amounts of PVP

PVP conc. (%)	Bulk density (g/ml)	Mean angle of repose (°)	Crushing strength (g)	Friability index
1.5	0.478 ± 0.004	35.73	24.27 ± 1.86	15.14 ± 1.87
3.0	0.499 ± 0.006	33.54	43.51 ± 3.25	6.00 ± 1.70
4.0	0.470 ± 0.005	35.87	42.66 ± 4.87	5.40 ± 0.74

Pellet size fraction 2.0—2.8 mm.

concentration. Generally, there was a reduction in the angle of repose of lactose pellets, indicating a tendency towards improved flow properties.

Paracetamol

Similar amounts of PVP were used for the pelletisation of paracetamol. Preliminary experiments showed that the amount of water required to form pellets of paracetamol with PVP was 30%, but after tumbling in the pelletiser for 10 min, the pellets became very wet and large clusters were formed, resulting eventually in lump formation. This constitutes over-wetting of the feed material. With 27.5% of water, the feed material appeared dry within the first 5 min of tumbling in the pelletiser, after which time the pellets produced were satisfactory *i.e.* neither too dry nor too wet. It was found that when the PVP concentration was increased from 1.5 to 3.0% there was only a relatively small increase in mean pellet size (Table I) but at 4% PVP there was a marked change in the mean pellet size. This corresponds with the formation of large pellets when balling occurs.

Paracetamol is hydrophilic but less soluble in water (1.42 g/100 ml)[1] than lactose. The wetting of this feed material by water is not hindered. However, PVP is more soluble in water than paracetamol (4.1 g/100 ml) and therefore has a greater affinity for water. This brings about an increase in the mean pellet size with increasing PVP concentration (Table I). This is attributed to the build-up in viscosity of PVP at locations in the feed material where water was sprayed. Consequently, this leads to the formation of large pellets, balling is also more evident resulting in layering of feed material on to the pellets. Higher PVP content gives rise to greater adhesiveness between feed material particles.

The crushing strength and bulk density of paracetamol pellets increased with PVP concentration (Table IV).

Phenacetin is hydrophobic with a very low solubility in water (0.096 g/100 ml).[1] Phenacetin pellets are "plastic" in nature and resist fragmentation on tumbling in the pelletiser as indicated by their low friability values (Table V). The pellets appeared to deform and flatten when subjected to a high load in the measurement of the crushing strength of pellets. The pellets are not brittle and do not break into smaller particles under increasing loads. It is noted that with 1.5 and 3% of PVP there was an increase in the crushing strength of the pellets (Table V) followed by a slight decrease at 4% PVP. This is believed to be due to the formation of fragmented and irregular pellets as a result of balling of pellets at high PVP concentration. PVP helps to increase the binding capacity of the pellets. This enhances pellet growth and also produces less friable pellets.

Lactose–Paracetamol Mixtures

The amount of water required to pelletise lactose–paracetamol mixtures containing 3% of PVP powder was 17.5% for mixtures with ratios of 90 : 10, 75 : 25 and 50 : 50 for lactose and paracetamol respectively. From Table VI, it is seen that the mean pellet size for 90 : 10, 75 : 25 and 50 : 50 lactose–paracetamol mixture was intermediate between those formed when either

TABLE VI. Effect of Varying the Proportion of Lactose on the Average Pellet Diameter of Lactose–Paracetamol and Lactose–Phenacetin Pellets Containing 3% PVP

Lactose : paracetamol	Average pellet diam. (mm)	Lactose : phenacetin	Average pellet diam. (mm)
100: 0	1.75	100: 0	1.75
90: 10	1.60	90: 10	2.60
75: 25	1.37	75: 25	2.43
50: 50	1.30	50: 50	2.10
0:100	0.75	0:100	3.40

TABLE VII. Properties of Lactose–Paracetamol Pellets Formed with Different Proportions of Lactose and Paracetamol Containing 3% PVP

Lactose : paracetamol	Bulk density (g/ml)	Mean angle of repose (°)	Crushing strength (g)	Friability index
100: 0	0.627 ± 0.004	37.39	130.62 ± 2.23	9.93 ± 1.54
90: 10	0.632 ± 0.05	38.69	197.81 ± 11.25	9.60 ± 2.45
75: 25	0.628 ± 0.004	37.23	249.30 ± 5.63	5.68 ± 0.43
50: 50	0.511 ± 0.016	39.16	185.65 ± 4.95	11.53 ± 0.71
0:100	0.456 ± 0.004	38.62	173.70 ± 6.24	25.10 ± 1.14

Pellet size fraction 2.0 – 2.8 mm.

TABLE VIII. Properties of Lactose–Phenacetin Pellets Formed with Different Proportion of Lactose and Phenacetin Containing 3% PVP

Lactose : paracetamol	Bulk density (g/ml)	Mean angle of repose (°)	Crushing strength (g)	Friability index
100: 0	0.627 ± 0.004	37.39	130.62 ± 2.23	9.93 ± 1.54
90: 10	0.631 ± 0.007	36.46	146.73 ± 1.72	7.22 ± 1.54
75: 25	0.629 ± 0.011	37.23	119.97 ± 2.12	7.78 ± 2.83
50: 50	0.586 ± 0.017	37.20	86.99 ± 3.26	12.73 ± 1.05
0:100	0.499 ± 0.006	33.54	43.51 ± 3.25	5.08 ± 0.68

Pellet size fraction 2.0 – 2.8 mm.

component was pelletised separately. Increasing the paracetamol content caused a reduction in pellet size (Table VI), which approached that of pellets formed with paracetamol alone.

The maximum crushing strength was obtained for pellets of 75:25 lactose–paracetamol mixture (Table VII). The reason is that with decreasing lactose content, more water could be utilised by both PVP and paracetamol, resulting in a greater amount of liquid bridges or pendular bonds. It is noted that with a higher paracetamol content, friability of the pellets increased and bulk density values decreased. Paracetamol particles are relatively large rod-like crystals which tend to form less round pellets. This is further evident by the larger angle of repose (Table VII) as the proportion of paracetamol is increased.

Lactose–Phenacetin Mixtures

Pellets were prepared using similar ratios as those of lactose–paracetamol with the same amount of PVP, 3% being incorporated. For each mixture, 20% of water sprayed on to the

feed materials.

The mean pellet size for these pellets was also intermediate between those formed when each of the components was pelletised separately. Similarly there was a reduction in pellet size with an increase in the phenacetin content of the mixture, but the mean pellet size of phenacetin alone was much larger than that of the mixture studied (Table VI).

It was found that the 90 : 10 and 75 : 25 lactose–phenacetin pellets had bulk density values higher than that of either lactose or phenacetin when pelletised separately (Table VIII). This is because of the part dissolution of lactose in water. The crushing strength of the pellets generally decreased with increase in the amount of phenacetin present in the mixture. This indicates that with more phenacetin, this hydrophobic component of the mixture exerts a dominant influence on the properties of the pellets.

Conclusions

Affinity or hydrophilicity of the feed material for water is an important factor affecting pellet growth and its properties. In the case of lactose pelletised with PVP powder, the affinity of lactose for water resulted in some non-wetting of the PVP powder. With phenacetin, a hydrophobic material, pellet growth increased markedly with increasing concentration of PVP.

The mean pellet size of pellets studied increased with PVP concentration, due to the large viscosity build-up at certain regions of feed material in the pelletiser, giving rise to large pellets being produced.

Pelletisation of mixtures of feed materials of different water-solubility and hydrophilicity produces pellets with mean pellet size that is between those of the individual components of the mixture. With lactose–paracetamol and lactose–phenacetin mixtures, increasing the proportion of one component greater than 50%, the properties of the pellets assumed that of the major component.

References

1) L. S. C. Wan and T. Jeyabalan, *Chem. Pharm. Bull.*, **34**, 4744 (1986).
2) L. S. C. Wan and T. Jeyabalan, *Chem. Pharm. Bull.*, **33**, 5449 (1985).

[Chem. Pharm. Bull. 35(4)1629—1632(1987)]

Adrenergic and Serotonergic Receptor-Blocking Potencies of Terazosin, a New Antihypertensive Agent, as Assessed by Radioligand Binding Assay

TAKAFUMI NAGATOMO,* AKIRA TAJIRI, TAKASHI NAKAMURA, REI HOKIBARA, YUKO TANAKA, JUNICHIRO AONO and HIROSHI TSUCHIHASHI

Department of Pharmacology, Niigata College of Pharmacy, Niigata 950-21, Japan

(Received November 19, 1986)

To assess the antihypertensive effect of terazosin, 2-[4-(tetrahydro-2-furanyl)carbonyl-1-piperazinyl]-6,7-dimethoxy-4-quinazolinamine hydrochloride dihydrate, the inhibitory potency of terazosin on ^{3}H-prazosin, ^{3}H-*p*-aminoclonidine, ^{3}H-dihydroalprenolol (^{3}H-DHA), ^{3}H-serotonin and ^{3}H-ketanserin bindings to α_1-, α_2- and β-adrenergic receptors and $5HT_1$ and $5HT_2$ (serotonergic) receptors was examined by using the radioligand binding method. The results were compared with those for prazosin and bunazosin. Dog brain and aorta were used in the present study. A high inhibition of ^{3}H-prazosin binding to α_1-adrenoceptors in dog aorta by terazosin was observed, but the inhibitions of ^{3}H-DHA, ^{3}H-*p*-aminoclonidine, ^{3}H-serotonin and ^{3}H-ketanserin bindings by this drug were very weak. *l*-Terazosin showed the greatest inhibitory effect on ^{3}H-prazosin binding to α_1-adrenoceptors in dog aorta and brain. These results suggest that an inhibitory effect of terazosin at α_1-adrenoceptor binding sites may contribute to the hypotensive effect; the α_2- and β-adrenoceptors and the serotonergic binding sites do not appear to be involved.

Keywords——alpha-adrenoceptor; serotonergic receptor; radioligand binding assay; brain; aorta; dog; antagonist, terazosin

Terazosin has been shown to possess antihypertensive efficacy and to be highly selective for α_1-adrenoceptor binding sites.[1] Thus, it was of interest to test whether this drug can be proved to have α_1-blocking action by using the radioligand binding assay method. The present study was designed to assess the effect of terazosin on ^{3}H-prazosin and ^{3}H-*p*-aminoclonidine bindings to α_1- and α_2-adrenoceptors in dog brain and aorta. In addition, as serotonin is also an important factor regulating blood pressure in the body, the effects of this drug on ^{3}H-serotonin and ^{3}H-ketanserin bindings to $5HT_1$ and $5HT_2$ receptors in the brain was examined.

Experimental

Radioligands——^{3}H-Prazosin (80.9 Ci/mmol), ^{3}H-*p*-aminoclonidine (42.2 Ci/mmol), ^{3}H-dihydroalprenolol (^{3}H-DHA) (90 Ci/mmol), ^{3}H-hydroxytryptamine creatinine sulfate (^{3}H-serotonin) (24.3 Ci/mmol) and ^{3}H-ketanserin (95 Ci/mmol) were purchased from New England Nuclear Corporation, Ltd. and stored at −20 °C until use.

Isolation of Membrane Fraction——Dog brain and aorta were used in the present study. The brain and descending aorta were removed, immediately frozen in liquid nitrogen and stored in a freezer (−80 °C) until use. The isolation of membrane fraction from dog brain and aorta was carried out by using the method described previously by us.[2] In brief, in the case of brain, the brain tissue was defrosted at room temperature and minced with small scissors in 10 volumes of 0.25 M sucrose, 10 mM Tris–HCl buffer (pH 7.5) and 10 mM $MgCl_2$. The suspension was homogenized in a glass homogenizer. The homogenate was filtered through 4 layers of gauze and the filtrate was centrifuged at 40000 *g* for 30 min. However, centrifugation at 18000 *g* for 15 min was carried out to obtain the pellets for $5HT_1$ binding assay in the brain. The pellet obtained was suspended in the incubation buffer mentioned below for the radioligand binding assay.

In the case of the aorta, the frozen vessel was crushed into a fine powder using a mortar and pestle, and suspended in 10 volumes of 0.25 M sucrose, 5 mM Tris–HCl buffer, pH 7.4, containing 10 mM $MgCl_2$. The suspension was homogenized in a Polytron homogenizer (Brinkmann) for 10 s at setting 8. The homogenate was filtered through 1 layer of gauze and centrifuged at 1000 *g* for 10 min. The supernatant obtained was again centrifuged at 40000 *g* for 30 min. For the serotonin receptor ($5HT_1$ and $5HT_2$) binding assay, a portion of the pellet obtained from the aorta after 40000 *g* centrifugation and from the brain after 18000 *g* centrifugation was incubated for 10 min at 37 °C in 50 mM Tris–HCl buffer, pH 7.4, and again centrifuged at 40000 *g* for 30 min (aorta) or at 18000 *g* for 15 min (brain). Pellets obtained with and without incubation were both resuspended in incubation buffer and gently homogenized in a glass homogenizer for the radioligand binding assay.

Binding Studies——Binding studies were carried out by the displacement method. All kinetic analysis was carried out by iterative non-linear regression on an NEC PC-9801F computer system. By using the weighted sum of squares principle of Munson and Rodbard,[3] the goodness-of-fit was evaluated according to a general model for the interaction of one ligand with one class of receptor sites.

α_1-, α_2- and β-Adrenoceptor Binding Assay: The α_1-adrenoceptor binding assay with the membrane of dog aorta using 0.6 nM ^{3}H-parazosin as a radioligand was performed by the method described previously.[2] The membrane suspension (0.25 mg protein) from brain was incubated with constant shaking for 60 min at 23 °C with 0.2 nM ^{3}H-prazosin in a total volume of 1 ml containing 15 mM Tris–HCl buffer (pH 7.4), 5 mM $MgCl_2$ and the indicated concentration of unlabelled drugs. In the case of α_2-adrenoceptor binding, the concentration of ^{3}H-*p*-aminoclonidine in the incubation medium of brain and aorta was 0.6 nM. Binding of ^{3}H-DHA (1 nM) to dog brain membrane (0.25 mg) was carried out under the same conditions as described previously.[4]

Serotonergic Receptor Binding Assay: Binding of ^{3}H-serotonin (1 nM) to dog brain (0.5 mg) was determined at 37 °C for 30 min by incubation with 30 mM Tris–HCl buffer (pH 7.4), 5 mM $MgCl_2$, 2 mM $CaCl_2$, 2.85 mM ascorbic acid and 4 μM pargyline in 1.0 ml (final volume) of the reaction mixture. ^{3}H-Ketanserin binding to particulate membrane fraction (0.25 mg protein) from brain and aorta was determined at 37 °C for 30 min in an incubation medium containing 50 mM Tris–HCl buffer (pH 7.4), 2.85 mM ascorbic acid and 5 μM pargyline.

The reaction in all binding assays was started by adding the membrane suspension. After incubation, the reaction was terminated by rapid filtration under a vacuum through GF/C glass fiber filters using an automatic cell harvester (Labomash LH-101, Labo Science, Tokyo, Japan). After washing of the filters with 1 ml of the incubation medium, the radioactivity remaining in the filters was counted using a scintillation counter. The specific bindings of ^{3}H-prazosin, ^{3}H-*p*-aminoclonidine, ^{3}H-DHA, ^{3}H-serotonin and ^{3}H-ketanserin to receptors in the brain and aorta were defined as the amounts of radioligands bound in the absence of competing agent minus the amounts in the presence of 0.1 mM phentolamine (α_1-), 0.1 mM *l*-norepinephrine (α_2-), 10 μM *l*-propranolol (β-), 0.1 mM serotonin ($5HT_1$), 0.1 mM methysergide (brain $5HT_2$) and 10 μM cinanserin (aorta $5HT_2$). IC_{50} values are the concentrations of drugs inhibiting 50% of the maximal specific binding of labelled radioisotopes. Protein was determined by using the method of Lowry *et al.*[5]

Chemicals

Terazosin was kindly donated by the Mitsubishi Chemical Industries Ltd. and Dainabot Co., Ltd. Bunazosin was donated by Eisai Co., Ltd. The chemical structure of terazosin is shown in Fig. 1.

Result

Table I summarizes the IC_{50} values of terazosin derived from the displacement experiments. In the brain, the IC_{50} value of *dl*-terazosin to α_1-adrenoceptors was higher than those of bunazosin and prazosin. The IC_{50} value of *dl*-terazosin to the α_1-adrenoceptors in the dog aorta was almost the same as that of bunazosin, but was only one-tenth of that of prazosin. On the other hand, the inhibition of ^{3}H-DHA, ^{3}H-*p*-aminoclonidine, ^{3}H-serotonin and ^{3}H-ketanserin bindings to β-, α_2-, $5HT_1$ and $5HT_2$ receptors in the brain by *dl*-terazosin

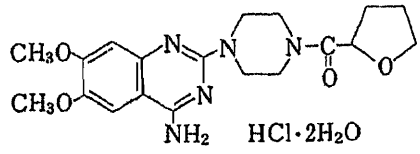

Fig. 1. Chemical Structure of Terazosin

TABLE I. Inhibitory Effects of Terazosin on ^{3}H-Prazosin, ^{3}H-*p*-Aminoclonidine, ^{3}H-DHA, ^{3}H-Serotonin and ^{3}H-Ketanserin Binding to α_1-, α_2- and β-Adrenoceptors and $5HT_1$ and $5HT_2$ Receptors in Dog Brain and Aorta

Receptors	Drugs	Brain (IC_{50}, nM)	Aorta (IC_{50}, nM)
α_1-	*dl*-Terazosin	18.1±6.2 (6)	15.1±6.2 (6)
	l-Terazosin	9.8±5.6 (4)	13.5±3.4 (5)
	d-Terazosin	26.4±20.1 (4)	36.7±15.3 (6)
	Bunazosin	2.0±0.3 (4)	15.1±7.5 (3)
	Prazosin	1.8±0.8 (5)	2.0±1.7 (5)
α_2-	*dl*-Terazosin	91500±64300 (4)	
	l-Terazosin	118000±31300 (4)	
	d-Terazosin	299000±72900 (4)	
	Bunazosin	46700±5800 (4)	
	Prazosin	55900±16700 (4)	
β-	*dl*-Terazosin	135000±59700 (4)	
	Bunazosin	812000±661000 (4)	
	dl-Propranolol	92.4±32.0 (4)	
$5HT_1$	*dl*-Terazosin	57900±49100 (3)	45000±17700 (4)
	Bunazosin	25400±4660 (4)	a)
	Ketanserin	1.70±0.44 (4)	93.4±47.9 (4)
$5HT_2$	*dl*-Terazosin	1000000> (3)	
	Bunazosin	66300±36200 (4)	
	Ketanserin	14400±10700 (4)	
	Serotonin	22.0±15.0 (4)	

Each value is the mean±S.E. Numbers in parenthesis represent the number of experiments. *a*) Not determined.

was very weak. Lower IC_{50} values of *l*-terazosin than of *dl*- and *d*-terazosin were observed in the aorta and brain.

Discussion

There is increasing evidence that the results obtained from radioligand binding assays can be used to evaluate the pharmacological potencies of newly synthesized chemicals. In fact, we reported that the potencies of α_1-blocking action of newly synthesized chemicals could be assessed from the IC_{50} values obtained by the radioligand binding assay method.[2] There is also evidence from *in vivo* studies to support the hypothesis that stimulation of both postjunctional α_1- and presynaptic α_2-adrenoceptors is involved in the regulation of blood pressure. The present study showed that terazosin inhibited only ^{3}H-prazosin binding to α_1-adrenoceptors. It is well known that prazosin and bunazosin have postsynaptic α_1-adrenoceptor blocking effects in the isolated vas deferens of the rat[6] and also have an antihypertensive effect.[7] The IC_{50} values of terazosin were almost the same as those of bunazosin. These results suggest that the antihypertensive effect of this drug may be largely due to α_1-adrenoceptors in the blood vessels, not α_2- or β-adrenoceptors.

It is known that the role of serotonin in the vasculature contributes to the development and maintenance of hypertension.[8] Ketanserin has been developed as an antihypertensive agent because this drug antagonizes the vascular effect of serotonin *in vivo*.[9] In addition, the presence of a serotonin receptor has been demonstrated in various tissues, and highly significant correlations were found between the half-maximal contraction of vessels (ED_{50}) and the affinity of serotonin for binding sites.[10] In the present study, terazosin, bunazosin

and prazosin did not inhibit the ^{3}H-serotonin and ^{3}H-ketanserin binding to $5HT_1$ and $5HT_2$ receptors in the brain. These results suggest that these drugs do not have any effect on ^{3}H-ketanserin binding sites, so that serotonergic receptors may not be an important factor in the antihypertensive effects of these drugs.

As shown in Table I, terazosin has a potent α_1-adrenoceptor blocking action. In addition, *l*-terazosin had a more potent effect on ^{3}H-prazosin binding to α_1-adrenoceptors than *d*-terazosin or *dl*-terazosin in dog brain and aorta, indicating that the α_1-adrenoceptor can differentiate the optical isomers.

References

1) J. J. Kyncl, *Am. J. Med.*, **80** (Suppl. 5B), 12 (1986).
2) T. Nagatomo, H. Tsuchihashi, S. Sasaki, Y. Nakagawa, H. Nakahara and S. Imai, *Jpn. J. Pharmacol.*, **37**, 181 (1985).
3) P. J. Munson and D. Rodbard, *Anal. Biochem.*, **107**, 220 (1980).
4) T. Nagatomo, H. Tsuchihashi, M. Sasaki, Y. Nakagawa, H. Nakahara and S. Imai, *Jpn. J. Pharmacol.*, **34**, 249 (1984).
5) O. H. Lowry, N. J. Rosebrough, A. L. Farr and R. J. Randall, *J. Biol. Chem.*, **193**, 265 (1951).
6) T. Shoji, *Jpn. J. Pharmacol.*, **31**, 361 (1981).
7) T. Kawasaki, K. Uezono, I. Abe, S. Nakamura, M. Ueno, N. Kawazoe and T. Omae, *Eur. J. Clin. Pharmacol.*, **20**, 399 (1981).
8) *a*) M. L. Cohen, R. W. Fuller and K. S. Wiley, *J. Pharmacol. Exp. Ther.*, **218**, 421 (1981); *b*) M. L. Cohen, N. Mason, K. S. Wilty and R. W. Fuller, *Biochem. Pharmacol.*, **32**, 567 (1983); *c*) P. M. Vanhoutte, *Trends Pharmacol. Sci.*, **3**, 370 (1982).
9) J. M. Van Nueten, P. A. J. Janssen, J. Vanbeek, R. Xhonneux, T. J. Verbeuren and P. M. Vanhoutte, *J. Pharmacol. Exp. Ther.*, **218**, 217 (1981).
10) J. E. Leysen, D. De Chaffoy De Courcelles, F. De Clerck, C. J. E. Niemegeers and J. M. Van Nueten, *Neuropharmacology*, **23**, 1493 (1984).

Communications to the Editor

[Chem. Pharm. Bull. 35(4)1633—1636(1987)]

KINETIC RESOLUTION OF FLUOROALKYL (E)-VINYL CARBINOL DERIVATIVES BY ASYMMETRIC EPOXIDATION WITH TITANIUM-TARTRATE CATALYSTS

Yuji Hanzawa, Kei-ichi Kawagoe, Masayuki Ito and Yoshiro Kobayashi*
Tokyo College of Pharmacy, Horinouchi, Hachioji, Tokyo 192-03, Japan

Racemic fluoroalkyl (E)-vinyl carbinols (1a-d) were kinetically resolved by Sharpless epoxidation. The optical purity of the resolved alcohols was excellent (98% ee) in mono- and difluoromethyl derivatives (1b and 1c) and moderate (60% ee) in a trifluoromethyl compound (1a).

KEYWARDS ——— kinetic resolution; asymmetric epoxidation; fluoroalkyl (E)-vinyl carbinol derivatives; absolute configuration

For many years, we have been investigating the synthesis of the fluoro analogs of bioactive compounds using a functionalized fluorine-containing molecule as a building block.[1] As reported in our recent papers on the synthesis of trifluororetinals,[2] we have prepared a trifluoromethyl (E)-vinyl carbinol derivative (1a) by reducing the trifluoromethyl alkynyl ketone (2a) with sodium borohydride followed by reduction of the triple bond with sodium bis(2-methoxyethoxy)aluminum hydride (Red-Al).

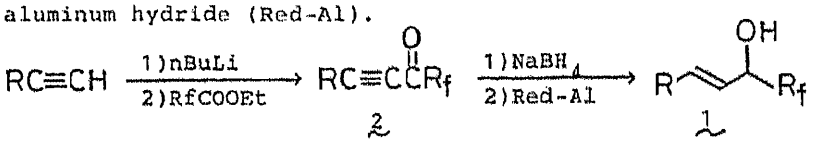

	Rf	R	2	1
a;	CF_3	nC_6H_{13}	2a 84%	1a 84%
b,	CF_2H	nC_5H_{11}	2b 79	1b 95
c;	CFH_2	nC_5H_{11}	2c 66	1c 66
d;	CF_2Et	nC_5H_{11}	2d 77	1d 78

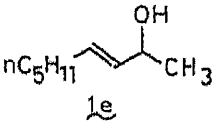

1e

Chart 1

Compounds 1 and 2 are considered very versatile building blocks for the synthesis of fluoroalkylated carbohydrate(s) and other bioactive compounds, especially when preparing compound 1 in optically active form. Recently, a microbial method for generating optically active 1 has been reported by Kitazume et al.[3] The present paper describes the results of the kinetic resolution of a series of fluoroalkyl (E)-vinyl carbinols (1) by titanium-mediated asymmetric epoxidation.[4] Unless the effects of the fluoroalkyl groups alter the enantiofacial differentiation of asymmetric epoxidation, it should be possible to predict the absolute configurations of the unreacting alcohols (1).[5]

This is one of the advantages of kinetic resolution, compared to resolution by separation of a diastereomeric mixture. It is interesting to know the effects of the fluoroalkyl groups under the asymmetric epoxidation conditions. The starting materials (1a-d) were prepared as shown in Chart 1. The results of the resolution are summarized in Table I.

Table I. Kinetic Resolution of Racemic 1[6] by Asymmetric Epoxidation

1	time[a]	recovered alcohol(%)	config.	% ee[b]	$[\alpha]_D^{25}$ /MeOH	method[c]	epoxide yield (%)	(erythro/threo)[d]
1a	5 d	46	S	60	-1.92 (c=0.31)	A	50	5/1
	3 weeks	51		47	-1.51 (c=0.59)	B	47	4.4/1
1b	4 d	31	S	97	-11.65(c=0.45)	A	59	15/1
	7 d	39		98	-11.76(c=0.68)	B	52	12/1
1c	24 h	43	S	98	-0.39 (c=0.57)	A	56	8/1
	5 d	41		93	-0.35 (c=0.56)	B	46	15/1
1d	4 d	45		14	-2.27 (c=1.32)	A	52	1.7/1
1e	24 h	40	R	98		A		
	5 d	34		97		B		

a) The reaction was followed by GLC (SE-30) analysis of the reaction mixture.
b) Determined by ^1H- and ^{19}F-NMR analysis of the (-)-MTPA ester of resolved 1.
c)

	L-(+)-DIPT	$Ti(O\text{-}iPr)_4$	TBHP	Temp.	Sol.
A:	1.2 eq.	1.0 eq.	0.55eq.	-20°C	CH_2Cl_2
B:	0.19	0.13	0.55	-20°C	CH_2Cl_2

d) Determined by integrating the ^{19}F-NMR signals of a mixture of epoxides.[7]

In a typical reaction, compound 1b was resolved as follows: A mixture of L-(+)-DIPT (405 mg, 1.73 mmol) and $Ti(OiPr)_4$ (409 mg, 1.44 mmol) in dry CH_2Cl_2 (10 ml) was stirred at -20°C for 20 min. After the mixture was coolrd at -78° C, 1b (257 mg, 1.44 mmol) was added then stirred for several minutes before adding anhydrous TBHP (0.26 ml of 3M solution in toluene). The reaction mixture was kept at -20°C for 6 d and then worked up by adding a solution of 0.3 ml of H_2O in 17 ml of acetone at -20°C. The resulting precipitate was removed by filtration through a pad of Celite and the solvent was removed in vacuo to give a crude product. The crude oil was purified by column chromatography (SiO_2, Hexane-AcOEt=10 : 1) to give two fractions. Unreacted 1b (78.7 mg, 0.44 mmol) (31%) was recovered in the first fraction. The second fraction yielded a mixture of epoxides (165 mg, 59%).

The unreacted alcohol (1a) was determined to have the S-configuration, by converting the resolved alcohol (1a) to compound 3 whose R-isomer has been prepared in high optical purity.[8] The absolute configurations of the difluoro- and monofluoromethyl compounds (1b and 1c) were confirmed by correlation with compounds which have been prepared from D-glyceraldehyde acetonide in an unambiguous way (Chart 2).

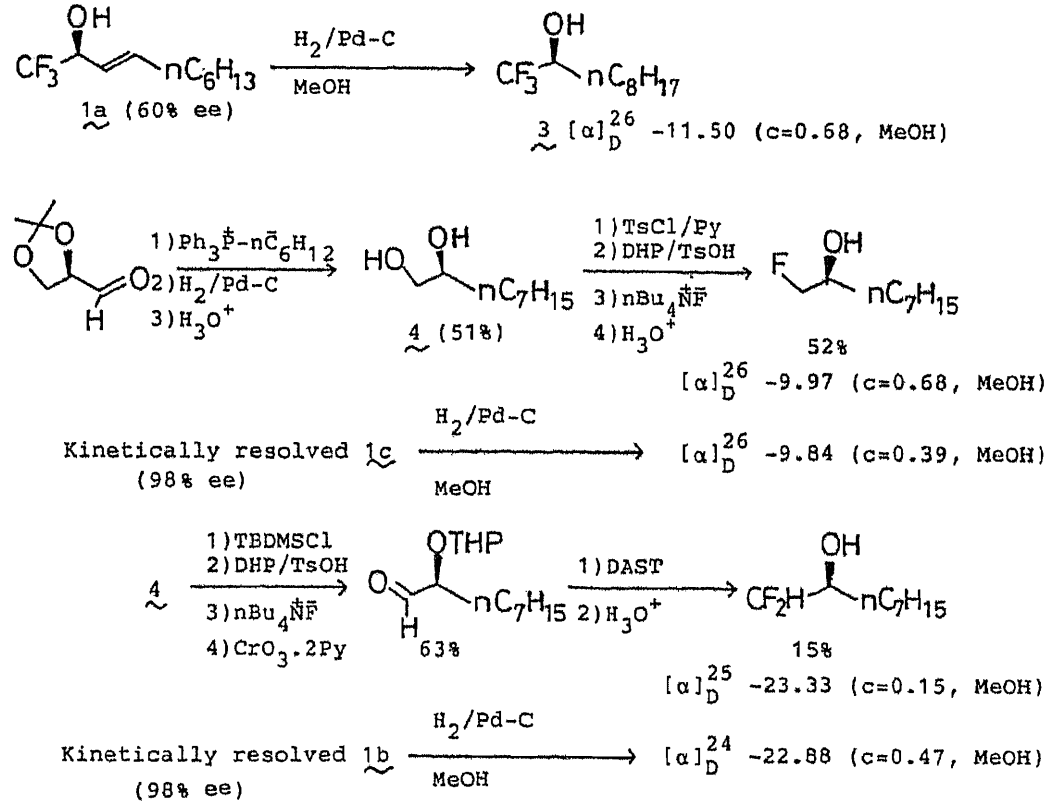

Chart 2

The fact that each resolved alcohol (1a-c) has the S-configuration indicates the kinetic preference in the asymmetric epoxidation of racemic fluoroalkyl compounds (1a-d) to be the same as that of existing examples.[5] It is worth noting that the monofluoromethyl compound (1c) behaves essentially the same as the methyl compound (1e) under the conditions of asymmetric epoxidation, with respect to the rate of epoxidation and optical purity. In difluoro- and trifluoromethyl compounds (1b and 1a), retardation of the rate or lowering of the optical purity of the recovered alcohols was observed. The poor resolution (14% ee) of 1d and moderate resolution (60% ee) of 1a compared to the excellent resolution of 1b and 1c shows that the fluoroalkyl substituents of 1a and 1d tend to be like the tertiary alkyl group in the kinetic resolution. Although the little kinetic resolution of t-butyl vinyl carbinol has been attributed to the steric effect of the large substituent,[5] the electronic effect of fluorine(s) may possibly perform an important function in the kinetic resolution of racemic 1a—1d by asymmetric epoxidation.[9] For further discussion, we should await an accumulation of more experimental results concerning the fluoroalkyl groups.

Acknowledgement: This work was supported in part by a grant from the Toray Foundation for the promotion of Science and Technics.

References and Notes

1) Y. Hanzawa, K. Inazawa, A. Kon, H. Aoki and Y. Kobayashi, Tetrahedron Lett., 28, 659 (1987).

2) Y. Hanzawa, K. Kawagoe, N. Kobayashi, T. Oshima and Y. Kobayashi, Tetrahedron Lett., 26, 2877 (1985). Y. Hanzawa, A. Yamada and Y. Kobayashi, Ibid., 26, 2881 (1985). T. Taguchi, A. Hosoda and Y. Kobayashi, Ibid., 26, 6209 (1985).

3) T. Kitazume and Y. Nakayama, J. Org. Chem., 51, 2795 (1986) and references cited therein.

4) T. Katsuki and K. B. Sharpless, J. Am. Chem. Soc., 102, 5974 (1980).

5) V. S. Martin, S. S. Woodard, T. Katsuki, Y. Yamada, M. Ikeda and K. B. Sharpless, J. Am. Chem. Soc., 103, 6237 (1981). N. C. Gonnella, K. Nakanishi, V. S. Martin and K. B. Sharpless, Ibid., 104, 3775 (1982). See also M. G. Fin, K. B. Sharpless, in "Asymmetric Synthesis" ed. by J. D. Morrison, Academic Press, Vol. 5, P 274, 1985.

6) The attempt to resolve the Z-isomer of 1 by the asymmetric epoxidation to obtain the optically active Z-isomer of 1 was without success.

7) The structures of the epoxides were estimated by the preference of erythro epoxide in Sharpless epoxidation and by comparing them with epoxides obtained from m-chloroperbenzoic acid (mcpba)-oxidation products (threo-selective) of racemic 1.

8) T. Kitazume, S. Lin and M. Asai, P84 Abstracts of the tenth fluorine symposium at Kanazawa, Japan, 1985.

9) Recently, the pseudo-π charactor of the trifluoromethyl group has been presented to explain the stereochemistry of trifluoromethylated olefin. C. L. Bumgardner, J. E. Bunch and M.-H. Whangbo, Tetrahedron Lett., 27, 1883 (1986) and references cited therein.

(Received December 17, 1986)

Communications to the Editor

Chem. Pharm. Bull. 35(4)1637—1640(1987)

SOPHORASIDE A, A NEW AROMATIC GLYCOSIDE FROM THE ROOTS OF SOPHORA JAPONICA[1)]

Yoshiaki Shirataki,* Yayoi Tagaya, Ichiro Yokoe, and Manki Komatsu
Faculty of Pharmaceutical Sciences, Josai University, 1-1 Keyakidai, Sakado, Saitama 350-02, Japan

A new aromatic glycoside, named sophoraside A (1), was isolated from the roots of Sophora japonica, together with puerol A (2) and puerol B (3). The structure of 1 was characterized as puerol B 5-O-β-D-glucopyranoside by its chemical and spectral data. These compounds have new frameworks among the naturally occurring compounds.

2 greatly inhibits ^{3}H-ethylketocycloazocine on the receptor-binding assay test.

KEYWORDS ——— Sophora japonica; Leguminosae; sophoraside A; puerol A; puerol B; 2D-NMR; analgesic

In an earlier paper,[2)] we reported the isolation and the structural elucidation of several isoflavones from the roots of Sophora japonica L. (Leguminosae), the chinese crude drug "huái-gēn". In our further studies of this drug, a new aromatic glycoside, sophoraside A (1), together with puerol A (2) and puerol B (3),[3)] which are hydrolysed products of pueroside A and pueroside B, have been isolated from the MeOH extract. In this paper, we describe the structures of these compounds.

The known compounds, 2[4)] and 3 were isolated from the ether-soluble fraction of the methanol extract. They were identified by spectroscopic analysis and comparison with authentic samples.[3)]

Sophoraside A (1), $C_{24}H_{26}O_{10}$, FAB-MS m/z: 475 $(M+H)^+$, colorless needles, mp 234-236°C, $[\alpha]_D^{25}$ +32° (c=1.0, DMSO), was obtained from the ethylacetate-soluble fraction of the methanol extract. 1 gave a pink-red color when sprayed with H_2SO_4, then heated on a TLC. The UV λ_{max}^{MeOH} nm (log ε) :218 (4.27), 288 (4.14), 314 (4.19), and IR ν_{max}^{KBr} cm^{-1}: 3200 (OH), 1700 (C=O), 1610 (arom. C=C), spectra were similar to those of 3. In this structure, the ^{1}H-NMR spectrum revealed the presence of 3 [in DMSO-d_6: δ 2.55 (1H, dd, J=14.8, 7.7 Hz, H-6_{ax}), 3.05 (1H, dd, J=14.8, 2.8 Hz, H-6_{eq}), 3.84 (3H, s, C_9-OCH_3), 6.02 (1H, br.d, J=5.9 Hz, H-5), 6.33 (1H, s, H-3), 6.62 (2H, d, J=8.5 Hz, H-3',5'), 6.72 (1H, dd, J=8.6, 1.8 Hz, H-8), 6.89 (1H, d, J=1.8 Hz, H-10), 6.95 (2H, d, J=8.5 Hz, H-2',6'), 7.56 (1H, d, J=8.6 Hz, H-7), 9.21 (1H, s, OH; exchangeable in D_2O)], and glucose [δ 5.04 (1H, d, J=7.3 Hz, glucosyl H-1)]. Acid hydrolysis of 1 gave D-glucose and enzymatic hydrolysis with β-glucosidase gave 3 ($C_{18}H_{16}O_5$, colorless plates, mp 240-242°C, $[\alpha]_D^{25}$ +87° (c=1.0, DMSO).

Accordingly, glucose must be located at position 5 or 4'. The substituted position of glucose was determined by comparison of the chemical shifts in ^{1}H-NMR spectra of 1 and pentaacetate of 1 (1a)[5] (Table I).

Table I. ^{1}H-NMR Spectral Data for 1 and Pentaacetate of 1 (1a) (in DMSO-d_6)

	1	1a	Δδ
H-3	6.33 (s)	6.22 (d,J=1.1 Hz)	-0.11
H-5	6.02 (br.d)	5.94 (m)	-0.08
H-6_{eq}	3.05 (dd)	3.16 (dd,J=14.7, 3.7 Hz)	+0.11
H-6_{ax}	2.55 (dd)	2.71 (dd,J=14.7, 7.3 Hz)	+0.16
H-7	7.56 (d,J=8.6 Hz)	7.57 (d,J=8.4 Hz)	+0.01
H-8	6.72 (dd,J=8.6, 1.8 Hz)	6.84 (dd,J=8.4, 2.2 Hz)	+0.12
H-10	6.89 (d,J=1.8 Hz)	6.90 (d, J=2.2 Hz)	+0.01
H-2',6'	6.95 (d,J=8.5 Hz)	7.11 (d,J=8.6 Hz)	+0.16
H-3',5'	6.62 (d,J=8.5 Hz)	7.02 (d,J=8.6 Hz)	+0.40

From these facts, it is clear that glucose was located at the 5 position of the aglycone. The ^{1}H-^{13}C shift correlated 2-D NMR spectrum of 1 (Fig. 1) led readily to precise assignments of the ^{13}C-signals [in DMSO-d_6: δ 38.2 (t, C-6), 55.4 (q, OCH_3), 83.6 (d, C-5), 101.2 (d, C-10), 108.5 (d, C-8), 113.3 (d, C-3), 114.8 (d, C-3',5'), 130.3 (d, C-2',6'), 131.2 (d, C-7), glucose; 60.8 (t, C-6"), 69.9 (d, C-4"), 73.0 (d, C-2"), 76.5 (d, C-3"), 77.4 (d, C-5"), 100.2 (d, C-1") at the waiting time (Δ_2) =1.79 ms, and the quaternary carbon signals δ 112.1 (s, C-6a), 126.6 (s, C-1'), 155.9 (s, C-4), 156.3 (s, C-10a), 162.9 (s, C-9), 165.9 (s, C-4'), 172.4 (s, C-2) at Δ_2=25 ms[6]].

On the basis of these NMR studies, the structure of sophoraside A has been established as follow.

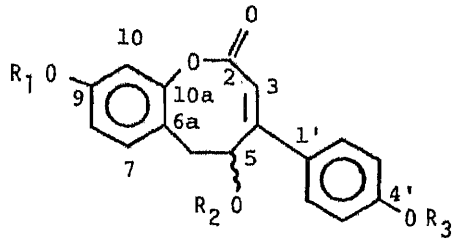

	R_1	R_2	R_3
sophoraside A (1)	Me	glc	H
puerol A (2)	H	H	H
puerol B (3)	Me	H	H

Further work is now in progress to improve the absolute configuration at C-5.

These three compounds were the first isolated natural products and have new frameworks among the naturally occurring compounds, together with pueroside A and pueroside B.

Fig. 1. ^{1}H-^{13}C Shift Correlated 2-D NMR Spectrum of 1

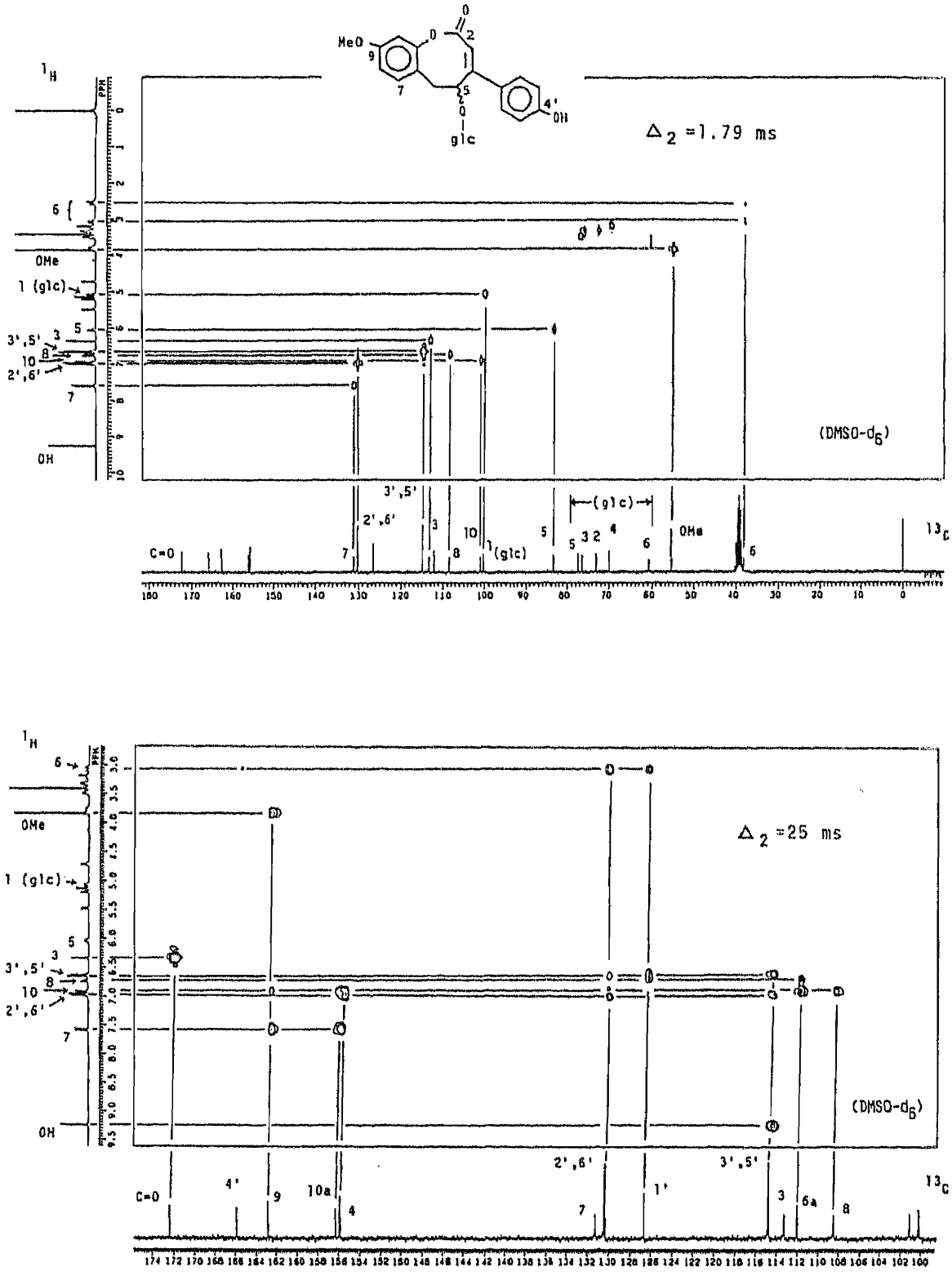

Interestingly, 2 greatly inhibits (72.8% inhibition of 0.1 mg/ml, naloxone; 79.9% inhibition of 10 μM) ^{3}H-ethylketocycloazocine on the receptor binding assay test.[7] So, 2 may be developed as a non-addictive analgesic.

ACKNOWLEDGEMENTS We are grateful to Prof. T. Nohara, Faculty of Pharmaceutical Sciences, Kumamoto University, for his kind donation of the data on puerol A and B, samples of pueroside A and B, and for useful discussion regarding the determination of these compounds. Thanks are also due to Mrs. Y. Fukuhara (née Narushima) for her helpful assistance throughout the course of this work and to Mr. S. Yamaguchi, Josai University, for the NMR spectral measurement.

REFERENCES AND NOTES

1) Part 21 in the series "Studies on the Constituents of Sophora Species." For Part 20, See Y. Shirataki et al., J. Nat. Prod., 49, 645 (1986). This paper also forms Part 2 in the series "Constituents of the Root of Sophora japonica" for Part 1, See M. Komatsu et al., 2a). This work was presented at the 33rd Annual Meeting of the Pharmacognostic Society of Japan, Saitama, October, 1986.

2) a) M. Komatsu, I. Yokoe, and Y. Shirataki, Yakugaku Zasshi, 96, 254 (1976).
b) Presented at the 96th Annual Meeting of Pharmaceutical Society of Japan, Nagoya, Paper abstract, II, 259, 1976.

3) Jun-ei Kinjo, Jun-ichi Furusawa, and Toshihiro Nohara, Tetrahedron Lett., 26, 6101 (1985).

4) The spectral data (UV, IR, MS, ^{1}H-NMR, ^{13}C-NMR) of 2 ($C_{17}H_{14}O_5$, mp 248-249°C) were almost the same as those of puerol A,[3] but this was isolated as a racemate, $[\alpha]_D^{25}$ 0° (c=1.0, MeOH).

5) Pentaacetate of 1 (1a); colorless plates, mp 154-157°C, MS m/z 684 (M^+), ^{1}H-NMR (DMSO-d_6) δ:1.85, 1.95, 1.98, 2.03, 2.25 (OAc x 5), 3.87 (C_9-OCH_3), 4.1-5.9 (glucosyl 7 protons). Others are listed in Table I.

6) ^{1}H- and ^{13}C-NMR spectra were taken on a JEOL JNM GX-270 FT NMR Spectrometer at 270 MHz and 67.8 MHz, respectively, and chemical shifts are given in δ (ppm) with TMS as an internal standard (s, singlet; d, doublet; t, triplet; q, quartet; m, multiplet; br, broad). The multiplicities (s,d,t,q) of carbon signals were determined by means of gated decoupling with NOE. ^{1}H-^{13}C shift correlated 2-D NMR spectra were obtained with the usual pulse sequence and data processing was performed with the standard JEOL software [CHSHF : PW 1=9.0 μs, PW 2=18.0 μs, PW 3=38.0 μs, (Δ_1=3.57 ms; PI 1= $1/{}^{1}J_{C-H} \times 2$, ${}^{1}J_{C-H}$ = 140 Hz), PI 2=0.17 ms, (Δ_2=1.79 ms; PI 3= $1/{}^{1}J_{C-H} \times 4$) and the case of observation of the quaternary carbon signals (Δ_2=25 ms; PI 3= $1/{}^{3}J_{C-H} \times 4$, ${}^{3}J_{C-H}$ = 10 Hz)]. The spectral widths were 3000 Hz in f_1 and 13020 Hz in f_2, giving digital resolutions of 23.4 and 25.43 Hz with a 256 x 1024 (with zero filling) data point matrix. The sample concentration was 50 mg in 0.5 ml of DMSO-d_6. Acquisition of 32 transients for each of the 128 FID's required about 3h, and processing took about 1h.

7) H. Kanatani, H. Kohda, K. Yamasaki, I. Hotta, Y. Nakata, T. Segawa, E. Yamanaka, N. Aimi, and S. Sakai, J. Pharm. Pharmacol., 37, 401 (1985).

(Received January 8, 1987)

Communications to the Editor

[Chem. Pharm. Bull. 35(4)1641 1644(1987)]

CHEMICAL MODIFICATION OF APHIDICOLIN AND THE INHIBITORY EFFECTS OF ITS DERIVATIVES ON DNA POLYMERASE α *IN VITRO*

Sayoko Hiranuma,[a] Takeshi Shimizu,[a] and Hirosuke Yoshioka*,[a]
Katsuhiko Ono,[b] Hideo Nakane,[b] and Taijo Takahashi[b]
Institute of Physical and Chemical Research,[a]
Hirosawa, Wako, Saitama 351-01, Japan and
Aichi Cancer Center Research Institute,[b]
Chikusa-ku, Nagoya 464, Japan

Various derivatives of aphidicolin (1) were prepared and their inhibitory effects on purified DNA polymerase α *in vitro* were assayed. Among these derivatives, the new 3α-, 17, 18-trihydroxyaphidicol-15-ene (24) was as inhibitory as the known 3-deoxy- and 3-oxoaphidicolins, (20) and (14). All the other derivatives with modification of any of the hydroxyl groups of 1 had no effect on the enzyme *in vitro*. The structure-activity relationships are discussed concerning functionalization on the aphidicolane ring.

KEYWORDS - aphidicolin; tetracyclic diterpene; DNA polymerase α inhibitor; aphidicolin 17-acetate; aphidicolin 17-crotonate; 16, 17, 18-trihydroxyaphidicolan-3-one; aphidicolane-16, 17, 18-triol; 3α, 17, 18-trihydroxy-aphidicol-15-ene; 16, 17, 18-trihydroxyaphidicol-2-ene

Aphidicolin (1), an antibiotic diterpene-tetraol with a tetracyclic skeleton, is a specific inhibitor of DNA polymerase α.[1] Although a limited number of its derivatives from natural sources were reported to inhibit replication of Herpes virus[2a] or HeLa cell growth[4a] in culture, there have been no reports of the structural requirements for inhibition of highly purified DNA polymerase α free from other enzyme(s) which may have metabolized the derivatives. In order to determine the essential structure-activity relationship of the hydroxyl function of 1 and the inhibition of DNA polymerase α *in vitro*, we conducted a screening study on various derivatives obtained by selective chemical transformation of the hydroxyl groups of 1. The inhibitory activities of these derivatives were assayed against DNA polymerase α purified from human KB cells under the conditions developed by Ono et al.[2c], with the following results.

Firstly, the hydroxyl groups of 1 was coupled with various protective groups such as acetyl, crotonyl, benzyl, methoxymethyl (MOM), methoxyethoxymethyl (MEM), or t-butyldimethylsilyl (TBDMS) groups by the usual procedures.[3] Among these the 17-hydroxyl group was more susceptible to the coupling reactions than the 18-hydroxyl group, and the 16-hydroxyl group was naturally the most resistant. None of

the derivatives listed in Fig. 1, whose hydroxyl groups are coupled with any of the protective groups, inhibited the purified DNA polymerase α. Although aphidicolin 17-acetate (2) was previously reported by Haraguchi et al.[4a] to inhibit DNA synthesis in cultured cells, our results indicate that 2 is inactive against the purified enzyme. We also found that the 17-crotonate (5) was inactive in our assay, whereas it inhibited HeLa cell growth in culture.[4b]

Fig. 1

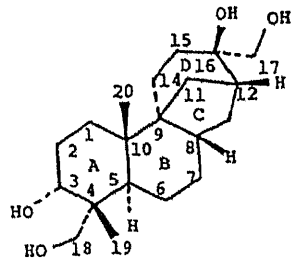

1

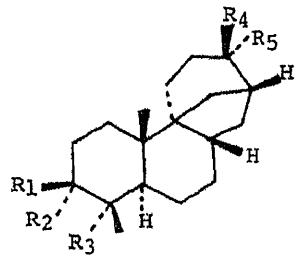

2 - 23

cpd. no.	R_n 1	2	3	4	5	ref.
2	H	OH	CH_2OH	OH	CH_2OAc	4a
3	H	OH	CH_2OAc	OH	CH_2OAc	2b
4	H	OAc	CH_2OAc	OH	CH_2OAc	2b
5	H	OH	CH_2OH	OH	CH_2OCrotonyl	7a
6	H	OH	CH_2OH	OH	CH_2OTBDMS	7b
7	H	OH	CH_2OH	OH	CH_2OBn	3
8	H	OH	CH_2OBn	OH	CH_2OBn	3
9	H	OH	CH_2OH	OMOM	CH_2OH	3
10	H	OMEM	CH_2OH	OMEM	CH_2OH	3
11	H	OH	CH_2OMEM	OMEM	CH_2OH	3
12	H	(O, O-acetonide)		OH	CH_2OH	3
13	H	OH	CH_2OH	(=O)		2b
14	(=O)		CH_2OH	OH	CH_2OH	4c
15	H	OH	CH_2OH	OH	CHO	4c
16	H	OH	CHO	OH	CHO	4c
17	H	OH	CHO	OH	COOH	7c
18	(=O)		CHO	OH	COOH	7c
19	(=O)		CH_2OH	OH	COOH	7c
20	H	H	CH_2OH	OH	CH_2OH	6
21	H	OH	CH_2OH	OH	CH_3	7d
22	H	OH	CH_3	OH	CH_2OH	7d
23	OH	H	CH_2OH	OH	CH_2OH	2b

Secondly, aphidicolin (1) and its primary derivatives were subjected to oxidation, deoxygenation, or dehydration in order to prepare another class of derivatives not containing protective groups on the oxygen atoms.

The new compounds (17), (18) and (19) containing the 17-carboxyl group were produced by oxidation of 1 with PDC in DMF. New 17- and 18-deoxy derivatives, i.e., (21) and (22), were prepared by treating an acetonide of the 16-keto derivative (13)[2b] with MeMgBr, and by reductively eliminating the 18-tosylate of 7. The C_{16} stereochemistry for 21 was postulated on the basis of preferred steric control[5] in the Grignard reaction affording 21 as a sole product. The new 15-ene derivative (24)[8] could be prepared via dehydration of the 3α, 17, 18-triacetate (4)[2b] with methanesulfonyl chloride and pyridine.

Among all the derivatives currently prepared, 3-deoxyaphidicolin (20)[6] and the 3-oxo derivative (14)[4c] had about one-third as much activity as aphidicolin in our assay (Fig. 2), and the result with 20 is consistent with that of the foregoing assays in cell culture.[4a] In contrast, neither the 2-ene (25)[6] nor the 3β-hydroxyl isomer (23)[2b] was active. Finally, the new 15-ene (24) was as active as

20 or 14, and this is the first active compound modified from 1 at the 16 position.

The following conclusions are deduced from this structure-activity study of aphidicolin and its derivatives:

1) All the hydroxyl groups of aphidicolin (1) have important parts in the *in vitro* inhibition of DNA polymerase α. Among these the 17- and 18-hydroxyl groups are particularly essential for the activity.
2) Although the 3α-hydroxyl group of 1 has a positive role in the inhibitory activity, it appears to be auxiliary since the 3-deoxy and the 3-oxo derivatives (20) and (14) still have the activity.
3) The fact that the 2-ene derivative (25) is inactive appears to contradict the deduction stated in 2). This is probably due to incorporation of the double bond in the A ring that would alter an equatorial disposition of the 18-carbon atom into a pseudo-equatorial orientation, where the 18-hydroxyl group becomes dislocated from its position in 1 (Fig. 3).
4) The negative result with the 3β-hydroxyl isomer (23) may be attributed to the 3β-hydroxyl group equatorially disposed to the A ring, which prevents the molecule from binding with the enzyme. In this connection, we assume that the 3-oxo group of 14 is pseudo-equatorially disposed so as to mimic the axial 3α-hydroxyl group of 1, or at least not to obstruct the binding to the enzyme. Besides, this conformation is favored by a hydrogen bonding of the 18-hydroxyl group to the 3-oxo group (Fig 3).
5) The 16-hydroxyl group may not be essential, since the 15-ene (24) continues to be active. In addition, we note that the 17-carbon atom equatorially disposed to the D ring in 1 seems still similarly disposed in 24 preserving a stereochemistry similar to 1 about the 17-hydroxyl group.

Fig. 2

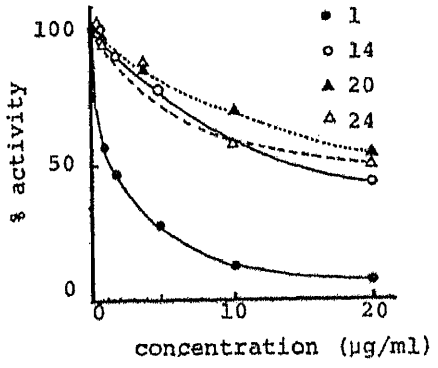

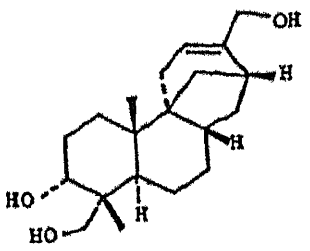

24

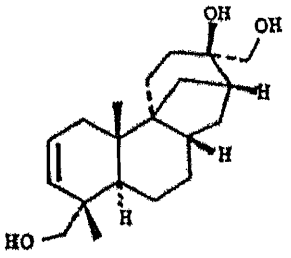

25

Fig. 3

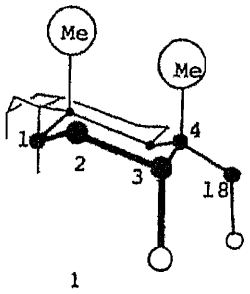

1

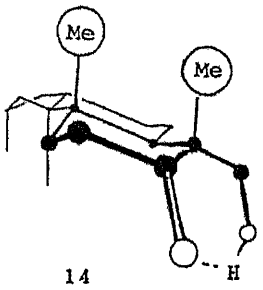

14

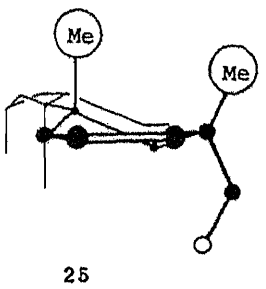

25

ACKNOWLEDGEMENTS We are thankful to Dr. H. Nagano for helpful discussions and references in bioassay. We are indebted to Mr. K. Takahashi and Mr. H. Kuramochi of Nippon Kayaku Co. Ltd. for bioassays with cancer cells in culture. We also acknowledge a Grant-in-Aid for Cancer Research from the Ministry of Education, Science and Culture, Japan and a support endowed by Nippon Kayaku Co. Ltd..

REFERENCES AND NOTES

1) a) S. Ikegami, T. Taguchi, M. Ohashi, M. Oguro, H. Nagano, and Y. Mano, Nature, 275, 458 (1978). b) J. A. Hubermann, Cell, 23, 647 (1981).

2) a) R. A. Bucknall, H. Moors, R. Simms, and B. Hesp, Antimicrobial Agents and Chemotherapy, 4, 294 (1973). b) W. Dalziel, B. Hesp, K. M. J. Stevenson, and J. A. J. Jarvis, J. Chem. Soc. Perkin I 1973, 2841. c) K. Ono, Y. Iwata, H. Nakane, Biomed. and Pharmacother., 37, 27 (1983).

3) The 17-crotonate (5), mp 158-161°C (from EtOAc), was prepared from 1 by acylation with crotonyl anhydride (1.5 eq) in pyridine at room temp. followed by TLC for separation from a dicrotonate. The 3, 18-acetonide (12) was obtained from the 17-acetate (2)[2b]. MOM or MEM group(s) was introduced after partial acetylation of 1 to give the new ether derivatives (9), (10) and (11). The new mono- and dibenzylethers, (7) and (8), could be prepared by treatment with benzyl bromide and $LiN[Si(Me)_3]_2$ in THF/HMPA followed by TLC (silica gel, n-hexane/EtOAc) separation.

4) a) T. Haraguchi, M. Oguro, H. Nagano, A. Ichihara, and S. Sakamura, Nucleic Acid Research, 11, 1197 (1983). b) K. Takahashi, and H. Kuramochi, Unpublished results. c) ICI Patent Application, Japan 59-88438.

5) R. E. Ireland, W. C. Dow, J. D. Godfrey, and S. Thaisrivongs, J. Org. Chem., 49, 1001 (1984).

6) A. Ichihara, H. Oikawa, K. Hayashi, M. Hashimoto, and S. Sakamura, R. Sakai, Agric. Biol. Chem., 48, 1687 (1984).

7) ^{1}HNMR spectra of all the compounds were recorded at 400 MHz on JEOL GX400 spectrometer in $CDCl_3$ with TMS as internal standard. Chemical shifts are given in ppm (δ). The NMR data are given below for selected compounds:
a) aphidicolin 17-crotonate (5): 0.71, 0.97(3H x 2, s), 1.90(3H, dd, J=6.8, 1.7), 3.38(1H, d, J=11.2), 3.47(1H, d, J=11.2), 3.69(1H, b), 4.00(1H, d, J=11.5), 4.07(1H, d, J=11.5), 5.89(1H, dq, J=15.6, 1.7), 7.01(1H, dq, J=15.6, 6.8).
b) [(17-t-butyldimethylsilyl)oxy]aphidicolane-3α, 16, 18-triol (6): 0.07, 0.09(3H x 2, s), 0.70(3H, s), 0.90(9H, s), 0.98(3H, s), 3.34(1H, d, J=10.8), 3.38(1H, d, J=10.0), 3.46(1H, d, J=10.8), 3.55(1H, d, J=10.0), 3.63(1H, b).
c) 3α, 16-dihydroxy-18-oxoaphidicolan-17-oic acid (17): 1.09(3H x 2, s), 3.85(1H, b), 9.57(1H, b). 16-hydroxy-3, 18-dioxoaphi-dicolan-17-oic acid (18): 1.25, 1.34(3H x 2, s), 9.37(1H, b). 16, 18-dihydroxy-3-oxoaphidicolan-17-oic acid (19): 1.03, 1.27(3H x 2, s),3.36(1H, dd, J=11.2, 6.0), 3.69(1H, dd, J=11.2, 7.8).
d) aphidicolan-3α, 16, 18-triol (21): 0.71, 0.98(3H x 2, s), 1.28(3H, s), 3.38(1H, d, J=11.5), 3.48(1H, d, J=11.5), 3.69(1H, b). aphidicolane-3α, 16, 17-triol (22): 0.70, 0.98(3H x 2, s), 1.14(3H, s), 3.38(1H, d, J=11.0), 3.47(1H, d, J=11.0), 3.69(1H, b).

8) aphidicol-15-ene-3α, 17, 18-triol (24): To a solution of aphidicolin-3α,17, 18-triacetate (4) (29 mg, 0.06 mmol) in pyridine (1ml), was added methanesulfonyl chloride (50μl), and the mixture was stirred at room temp. for 5 h. The usual working-up gave 3α, 17, 18-triacetoxyaphidicol-15-ene (19 mg, 68% yd.), which was dissolved in MeOH and aq. 1N KOH (2 ml for each) and stirred at room temp. for 15 h. The usual working-up afforded the ene-triol (24) (12 mg, 88% yd.). mp 199 - 201 °C (recryst. from EtOAc). FDMS m/z 320(M^+) calcd. for $C_{20}H_{32}O_3$, EIMS m/z 302.2253 (M^+-H_2O)) NMR: 0.72, 1.06(3H x 2, s), 3.39(1H, d, J=11.2), 3.50(1H, d, J=11.2), 3.72(1H, b), 4.01(1H, d, J=14.7), 4.05(1H, d, J=14.7), 5.32(1H, b).

(Received January 23, 1987)

Communications to the Editor

[Chem. Pharm. Bull. 35(4)1645—1648(1987)]

CHANGES CAUSED BY INCLUDED ENZYMES IN THE CONSTITUENTS OF SOLANUM NIGRUM BERRIES[1)]

Kenji Yoshida,[a] Shoji Yahara,[a] Reiko Saijo,[b] Kohtaro Murakami,[b] Toshiaki Tomimatsu[b] and Toshihiro Nohara*,[a]

Faculty of Pharmaceutical Sciences, Kumamoto University,[a] 5-1 Oe-honmachi, Kumamoto 862, Japan and Faculty of Pharmaceutical Sciences, Tokushima University,[b] 1-78 Shomachi, Tokushima 770, Japan

The uncrushed berries of Solanum nigrum L. were immersed in cold MeOH for two years. From these berries, four new steroidal alkaloids, enzymatically derived from the original constituents, were obtained.

KEYWORDS —— Solanum nigrum; Solanaceae; spirosolane derivative; oxidized solasodine derivative; enzymic oxidation

The whole plants of Solanum nigrum L. have been used traditionally[2)] as a remedy for various cancers in the Shanghai region of China. We analyzed the constituents of the immature fruits of this plant and found the steroidal glycosides, SN-0, SN-1, SN-4 together with SN-2 (solamargine) and SN-3 (solasonine).[3)] Now, we have isolated six components, SN-a - f (1 - 6), from the uncrushed berries immersed in cold MeOH for two years. Five of them have been shown to be the steroidal alkaloids oxidized selectively at C-12 and/or C-27. These are derived from solamargine and solasonine, probably by the reactions of included enzymes. Here we deals with the structural characterizations of SN-a - f (1 - 6).

The berries (3 kg) stored in MeOH were crushed and filtered. The filtrate was then evaporated to afford a residue (254 g) which was separated using a combination column chromatography with MCI-gel CHP 20P, Sephadex LH-20, silica gel and Bondapak C_{18} with various solvent systems to afford

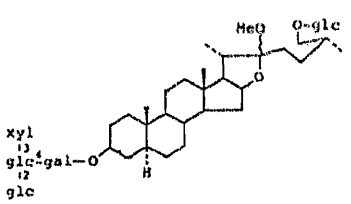

SN-0

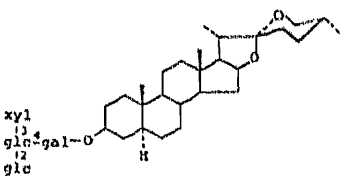

SN-1
(desgalactotigonin)

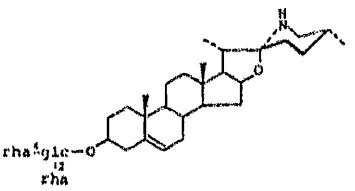

SN-2
(solamargine)

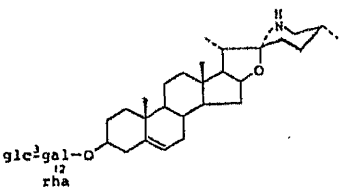

SN-3
(solasonine)

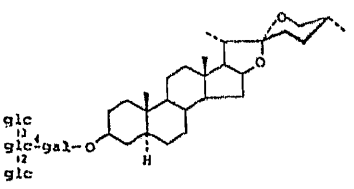

SN-4

Table I. ^{13}C-NMR Data of SN-a (1) - SN-f (6) (in Py-d_5)

	SN-a (1)	SN-b (2)	SN-c (3)	SN-d (4)	SN-e (5)			SN-f (6)		
1	37.8	37.8	37.5	37.8	37.5	gal-1	100.4	37.5	glc-1	100.3
2	32.4	32.2	32.0	32.2	30.0	2	76.2	30.1	2	78.5
3	71.3	71.2	71.3	71.3	77.6	3	84.9	76.8	3	77.6
4	43.5	43.4	43.1	43.0	38.7	4	70.1	38.9	4	78.1
5	142.0	142.0	141.8	142.0	140.9	5	74.8	140.8	5	77.8
6	121.0	121.1	121.0	121.2	121.7	6	62.5	121.7	6	62.2
7	32.6	32.5	32.5	32.5	32.2			32.9		
8	31.8	32.1	31.7	32.2	32.1	rha-1	102.0	31.9	rha-1	101.5
9	50.5	50.1	49.8	50.2	50.0	2	72.7	49.9	2	72.7
10	37.0	37.1	36.9	37.1	37.2	3	72.3	37.2	3	72.5
11	21.3	30.0	30.7	31.0	29.9	4	74.9	31.3	4	73.7
12	40.2	78.8	78.6	79.2	78.7	5	69.3	78.3	5	69.3
13	40.7	46.6	46.6	46.5	46.5	6	18.5	46.6	6	18.4
14	56.8	55.4	54.9	55.6	55.2			55.0		
15	32.6	31.6	31.7	31.6	31.3	glc-1	105.6	32.2	rha-1	102.5
16	78.8	81.3	83.2	79.2	81.4	2	74.0	83.8	2	72.8
17	63.6	62.9	61.7	63.4	62.6	3	78.3	61.2	3	72.5
18	16.6	11.2	10.9	11.3	11.0	4	71.5	11.0	4	73.8
19	19.8	19.3	19.3	19.6	19.3	5	78.1	19.3	5	70.2
20	41.6	43.0	42.5	42.6	43.0	6	62.3	42.9	6	18.5
21	15.7	14.9	14.3	14.9	14.8			14.9		
22	98.3	98.7	99.6	98.1	98.8			99.4		
23	34.7	34.0	30.8	33.9	33.8			30.9		
24	31.1	30.2	23.3	25.7	29.9			23.6		
25	31.6	31.0	36.4	43.1	30.9			36.7		
26	48.1	47.1	42.8	43.4	47.0			43.5		
27	19.6	19.6	64.3	177.2	19.2			64.5		

Table II. ^{1}H-NMR Data of SN-a - SN-d (1 - 4) (in Py-d_5) and Their Acetates (7 -9) (in $CDCl_3$)

	H-3	H-6	H-12	H-16	H-18	H-19	H-21	H-26	H-27	OAc	NAc	COOMe
SN-a(1)	3.84	5.39	*	4.42	0.90	1.05	1.09	*	0.81	-	-	-
SN-b(2)	3.81	5.41	3.61	4.92	1.07	1.13	1.56	*	0.79	-	-	-
SN-c(3)	3.51	5.34	3.62	4.71	0.89	1.04	1.34	*	-	-	-	-
SN-d(4)	3.83	5.41	3.63	4.56	1.08	1.17	1.43	3.43 3.63	-	-	-	-
7	4.61	5.37	*	4.19	0.92	1.04	1.08	*	0.93	2.03	2.20	-
8	4.57	5.38	4.63	4.19	1.01	1.05	0.98	*	0.93	2.03 2.05	2.19	-
9	4.58	5.38	4.63	4.18	1.01	1.05	0.97	*	3.90 4.03	2.03 2.05 2.06	2.21	-
10	4.51	5.37	4.62	4.11	1.00	1.05	0.99	3.47 4.18	-	2.03 2.05	2.22	3.70

* Obscured by other signals

six compounds, tentatively named SN-a - f (1 - 6), in the respective yields of 0.07, 0.10, 0.13, 0.07, 0.07 and 0.10 % based on the MeOH extractive. Since these constituents are usually absent in the fresh berries, they were apparently derived from the original ingredients.

SN-a (1), mp 202-204°C, $[\alpha]_D$ -76.4°,[4] was identified as solasodine by comapring the physicochemical data and ^{13}C-NMR spectrum[5] (Table I) of 1 and the ^{1}H-NMR spectrum (Table II) of the diacetate (7) of 1 with those of the authentic specimen.

SN-b (2), mp 226-229°C, $[\alpha]_D$ -58.2°, showed M^+ at m/z 429 and characteristic peaks[6] for the spirosolane derivatives at m/z 138 and 114 in the MS. Shifts of +8.7, +38.6, +5.9 and -5.4 ppm at C-11, 12, 13 and 18 in the ^{13}C-NMR spectrum compared with those in 1 indicated the presence of the hydroxyl groups at C-12. Its configuration was determined to be ß by the ^{1}H-NMR spectrum (12α-H: 1H, dd, J=4.6, 10.9 Hz at δ 4.63) of the triacetate (8) of 2. Therefore, 2 was assumed to be (22 R, 25R)-spirosol-5-ene-3ß,12ß-diol. This compound appears to be identical with solanaviol obtained from the leaves of mature Solanum aviculare by Kaneko, et al.[7]

SN-c (3), mp 233-237°C, $[\alpha]_D$ -54.7°, had two hydroxyl groups, one located on the A-D ring, and the other on the E or F ring, from the evidence of the MS (M^+ at m/z 445, $C_9H_{16}NO$ at m/z 154, $C_6H_{12}NO_2$ at m/z 130). Shifts were observed in the ^{13}C-NMR spectrum around C-12 as well as 2 and around C-25 (-6.9, +5.4, -4.3 and +44.7 ppm at C-24 - 27, respectively), indicating that the structure of 3 should be represented as 12ß,27-dihydroxysolasodine. The ^{1}H-NMR spectrum of the tetraacetate (9) of 3 also supported its presumptive structure.

SN-d (4), mp 276-278°C, $[\alpha]_D$ -71.2°, showed absorptions due to the carboxylate (1580 cm^{-1}) in the IR spectrum and peaks due to M^+ ($C_{27}H_{41}NO_5^+$), $C_{23}H_{33}O_3^+$, $C_{11}H_{15}NO_2^+$, $C_9H_{14}NO_2^+$, $C_7H_{10}N^+$, $C_6H_9N^+$ and $C_6H_9NO_3^+$ at m/z 459, 357, 193, 168, 108, 95 and 143 in the MS (Chart 1). Comparative studies of the ^{1}H- and ^{13}C-NMR spectra with those of 1 and 2 revealed attachments of the ß-oriented hydroxyl group at C-12 and the carboxyl group at C-25 on the solasodine skeleton. The ^{1}H-NMR spectrum of the triacetyl monomethyl ester derivative (10) of 4 was in agreement with the assignment of this structure.

SN-e (5), an amorphous powder, $[\alpha]_D$ -53.3°, and SN-f (6), an amorphous powder, $[\alpha]_D$ -64.1°, were characterized by the ^{13}C-NMR spectra as the ß-solatrioside[3,8] of 2 and the ß-chacotrioside[3,8] of 3, respectively.

It is interesting that the ingredients of the fruits with unbroken pericarps soaked in MeOH for a long time was changed by the oxidative reaction at C-12 and/or C-27 selectively on the steroidal alkaloid skeleton. This was apparently effected by the aid of enzymes included under the experimental conditions (in MeOH).

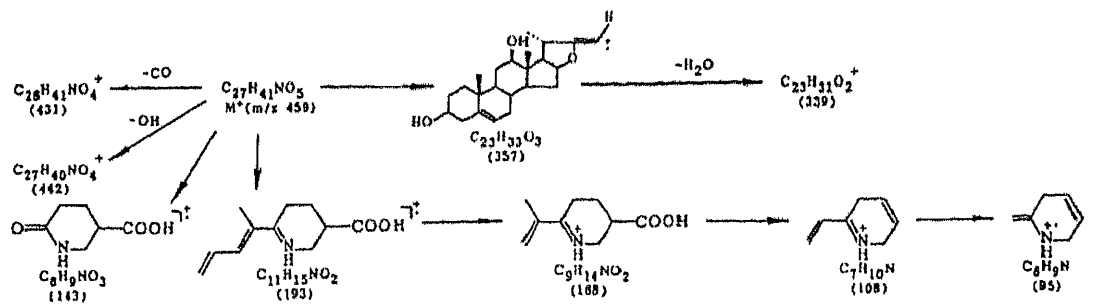

Chart 1. MS Fragmentation of SN-d (4)

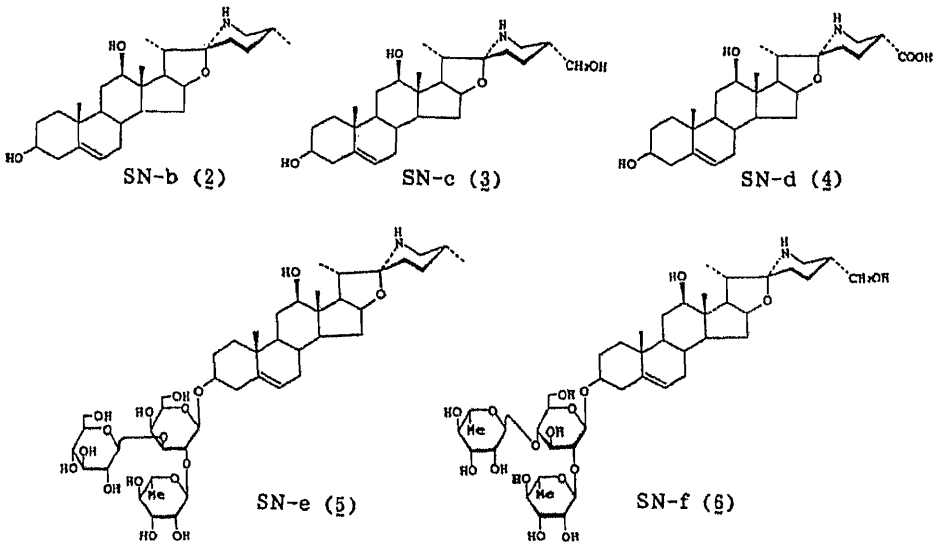

REFERENCES AND NOTES

1) Part 8 in the series "Studies on the Constituents of Solanum Plants." For Part 7: S.Yahara, M.Morooka, M.Ikeda, M.Yamasaki and T.Nohara, Planta Medica, 1986, 496.

2) Chiang Su New Medical College ed., "Dictionary of Chinese Crude Drugs", Shanghai Scientific Technologic Publisher, Shanghai, 1977, p. 630.

3) R.Saijo, K.Murakami, T.Nohara, T.Tomimatsu, A.Sato and K.Matsuoka, Yakugaku Zasshi, 102, 300 (1982).

4) Optical rotations were measured with pyridine for 1, 2, 4 - 6 and MeOH for 3.

5) R.Radeglia, G.Adam and H.Ripperger, Tetrahedron Lett., 1977, 903.

6) H.Budzikiewicz, C.Djerassi and D.H.Williams, Structure Elucidation of Natural Products by Mass Spectrometry, vol II. p. 21, Holden-Day, Inc. (1964).

7) K.Kaneko, K.Niitsu, N.Yoshida and H.Mitsuhashi, Phytochemistry, 19, 299 (1980).

8) S.B.Mahato, N.P.Sahu, A.N.Ganguly, R.Kasai and O.Tanaka, Phytochemistry, 19, 2017 (1980).

(Received February 2, 1987)

Communications to the Editor

Chem. Pharm. Bull. 35(4)1649—1652(1987)

STIMULATION OF PYRUVATE DEHYDROGENASE AND PROTEIN KINASE BY A PEPTIC FRAGMENT FROM ELASTASE

Shozo Shoji,[a] Fumiaki Haraguchi,[a] Akira Okayama,[a] Takayuki Funakoshi,[a] Yukiho Kubota,[a] and Hiroshi Ueki*,[b]
Faculty of Pharmaceutical Sciences, Kumamoto University,[a] Oe-honcho, Kumamoto 862, Japan, and Faculty of Pharmacy and Pharmaceutical Sciences, Fukuyama University,[b] Fukuyama-shi, Hiroshima 729-02, Japan

A peptic fragment from elastase was separated by affinity chromatography on an immobilized trialanine-agarose column. The fragment lost the enzymatic activity but retained the affinity for trialanyl peptide. It also stimulated pyruvate dehydrogenase activity in rat fat pads and protein kinase activity in the plasma membrane fraction of guinea-pig adipocytes.

KEYWORDS ——— elastase; biologically active fragment; affinity chromatography; pyruvate dehydrogenase; protein kinase; plasma membrane

Pancreatic elastase [EC 3.4.21.36] hydrolyzes elastin, which is not attacked by other proteases.[1] It is thought to decrease with aging and with pathological conditions, such as emphysema and arteriosclerosis.[2] We reported previously that elastase stimulated lipogenesis and pyruvate dehydrogenase activity in adipose tissues isolated from rats.[3] Other proteases, such as pronase E, subtilisin BPN', α-chymotrypsin, and trypsin also had some insulin-like effects on adipose tissues and muscles in various species.[4] It is generally thought that the insulin-like effects of these proteases are partially due to proteolytic cleavage of a limited portion of the cell surface, probably the insulin receptors.[5a,b]

This paper describes the stimulation of pyruvate dehydrogenase and protein kinase by a fragment obtained by peptic digestion of porcine elastase.

MATERIALS AND METHODS

Materials ——— Elastase (porcin pancreas, 326 EL.U/mg) was a gift from Eisai Co., Tokyo. Insulin (bovine pancreas, 24 IU/mg) and pepsin (porcin stomach mucosa, 3200 U/mg) were purchased from Sigma Chemicals Co., St. Louis. Immobilized trialanine-agarose ((Ala)$_3$-agarose) was obtained from Pierce Chemical Co.,

Rockford. Sodium [1-^{14}C] pyruvate (19.7 mCi/mmol) was purchased from New England Nuclear, Boston. [γ-^{32}P] ATP was prepared by the method of Post and Sen.[6]

Preparation of Fat pads ——— Fat pads were prepared from epididymal adipose tissue of male Wister rats weighing 100-150 g as described previously.[3]

Preparation of Plasma Membranes ——— Adipocytes were prepared by collagenase digestion of epididymal adipose tissue of male Hartley guinea-pigs weighing 400-500 g.[7] Subcellular fractions were prepared by a slight modification of the methods of Seals and Czech[8] and Kiechle et al.[9] Adipocytes were homogenized in 10 mM Tris-HCl buffer, pH 7.4, containing 0.25 M sucrose. The homogenate was then centrifuged at 28000 x g for 15 min at 4°C. The precipitate was homogenized again, layered over 32% sucrose, and centrifuged at 32000 x g for 30 min at 4°C. Plasma membrane layers were collected from the top of the sucrose layer, diluted with the Tris-HCl buffer, and centrifuged again at 28000 x g for 15 min at 4°C. The resultant precipitates were resuspended in 50 mM Tris-HCl buffer, pH 7.4. The plasma membranes were obtained with a protein yield of 0.6 mg from 22 g of the adipose tissue and were of a purity comparable to those produced by other methods, as determined by enzyme markers (data not shown).

Assay ——— The hydrolysis of N-succinyl-L-trialanine p-nitroanilide (Suc-(Ala)$_3$-pNA) was determined in 0.05 M Tris-HCl buffer, pH 8.5, as described previously.[10]

The pyruvate dehydrogenase activity was assayed by determining the rate of formation of $^{14}CO_2$ from [1-^{14}C] pyruvate using the homogenate of the pre-incubated fat pads, as described previously.[3,11]

For assay of protein kinase activity, phosphorylation of the plasma membrane and casein was determined by the incubation of [γ-^{32}P] ATP and the plasma membrane treated with samples.[12]

RESULTS AND DISCUSSION

Preparation and Properties of Peptic Fragment from Elastase

A mixture of 3 ml of elastase (26 mg) and 0.3 ml of pepsin (350 μg), dissolved in 9% formic acid, was incubated at 37°C for 20 min, diluted twice with deionized water and lyophilized. Four milligrams of the digest was dissolved in 4 ml of 10 mM NH_4HCO_3 and subjected to affinity chromatography on (Ala)$_3$-agarose (0.7 x 5 cm) with successive use of 10 and 50 mM NH_4HCO_3 as solvents. Two protein peaks were detected: The first one (P-I) passed through the column with the former solvent and the second one (P-II) was eluted with the latter solvent.

No hydrolytic activity towards Suc-(Ala)$_3$-pNA was found in any fraction. The protein yield of P-II was 9%. P-II migrated as a single band in electrophoresis on sodium dodecylsulfate-polyacrylamide gel in the absence of mercaptoethanol.[13] Its molecular weight was estimated to be less than 12000.

Biological Activities

When rat pads were incubated with P-II, the pyruvate dehydrogenase activity in the homogenate of the incubated fat pads was stimulated over a concentration

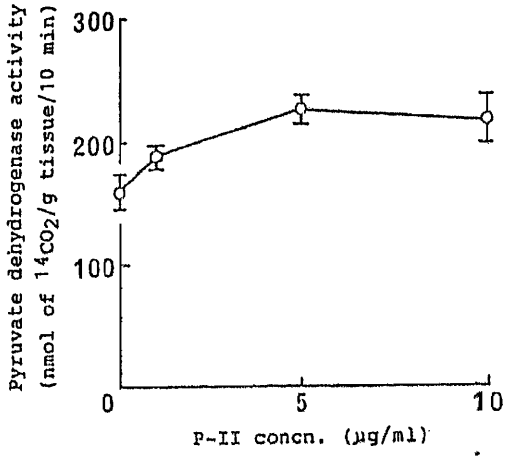

Fig 1. Dose-Response Relation for the Pyruvate Dehydrogenase-Stimulating Effect of P-II
Each point shows the mean value ± S.E. of four observations.

Table I. Effects of Insulin, Elastase, and Peptic Fragments on Protein Kinase Activity

	Protein kinase activity (%)	
	With casein	Without casein
Insulin (1 mU/ml)	164	144
Elastase(3 μg/ml)	163	131
P-I (10 μg/ml)	102	97
P-II (5 μg/ml)	159	137
(10 μg/ml)	157	130

Results are expressed as relative activity (%) with respect to the control. Each datum is the average of three observations. For the control, the plasma membrane was preincubated in the absence of samples, then assayed for protein kinase activity with or without casein.

range of 1-10 μg/ml (Fig. 1). The values obtained with P-I (10 μg/ml) and elastase (3 μg/ml) were 151±7 and 240±15 nmol of $^{14}CO_2$/g tissue/10 min, respectively.

Table I shows the effects of P-I, P-II, elastase, and insulin on protein kinase activity in the plasma membrane fraction of guinea-pig adipocytes. The activity was increased 1.6-fold with P-II, elastase, and insulin in the presence of casein which had been used as an exogenous substrate of insulin-stimulated tyrosine protein kinase.[14] In the absence of casein, the increase was 1.3-1.4-fold greater than with the control. No significant stimulation of pyruvate dehydrogenase or protein kinase activity was observed with P-I.

It has been reported that pyruvate dehydrogenase in adipocyte is activated by insulin-generated mediators from muscle extract[15] and from plasma membranes of various cells[16] and that the substances mimicking insulin effects such as concanavalin A,[17] trypsin,[5a] and vanadate[18] enhance the phosphorylation of insulin receptor by stimulating the protein kinase activity in a manner similar to but not identical to insulin. However, other details of the mechanism are still unknown.

We found that the peptic fragment from elastase lost the enzymatic activity but retained the affinity for trialanyl peptide and the biological activities.

It may stimulate pyruvate dehydrogenase and protein kinase activities by binding to the insulin receptor but not by proteolysis of the receptor. Further work, however, is required to clarify this mechanism.

REFERENCES

1) B. S. Hartley and D. M. Shotton, in "The Enzymes", Vol. III, ed. by P. D. Boyer, Academic Press, New York, 1971, pp. 323-373.
2) W. A. Loeven and M. M. Baldwin, Gerontologia, 17, 170 (1971).
3) H. Ueki, F. Haraguchi, A. Motoshima, T. Funakoshi, S. Shoji, and Y. Kubota, J. Biochem. (Tokyo), 96, 1419 (1984).
4) J. F. Kuo, C. E. Holmlund, I. K. Dill, and N. Bohonos, Arch. Biochem. Biophys., 117, 269 (1966); J. F. Kuo, I. K. Dill, and C. E. Holmlund, J. Biol. Chem., 242, 3659 (1967); L. S. Weis and H. T. Narahara, J. Biol. Chem., 244, 3084 (1969); T. Kono and F. W. Barham, ibid., 246, 6204 (1971); Y. Kubota, H. Ueki, and S. Shoji, J. Biochem. (Tokyo), 72, 235 (1972); K. Kikuchi, C. Schwartz, S. Creasy, and J. Larner, Mol. and Cell. Biochem., 37, 125 (1981).
5) a) S. Tamura, Y. Fujita-Yamaguchi, and J. Larner, J. Biol. Chem., 258, 14749 (1983); b) J. Massague, P. F. Pilch, and M. P. Czech, ibid., 256, 3182 (1981).
6) R. L. Post and A. K. Sen, in "Methods in Enzymology", Vol. X, ed. by R. W. Estabrook and M. E. Pullmann, Academic Press, New York, 1967, pp. 773-776.
7) M. Rodbell, J. Biol. Chem., 239, 375 (1964).
8) J. R. Seals and M. P. Czech, J. Biol. Chem., 256, 2894 (1981).
9) F. L. Kiechle, L. Jarett, N. Kotagal, and D. A. Popp, J. Biol. Chem., 256, 2945 (1981).
10) H. Ueki, H. Nakata, T. Funakoshi, S. Shoji, and Y. Kubota, Chem. Pharm. Bull., 27, 2959 (1979).
11) Y. Sakamoto and T. Kuzuya, Biochem. Biophys. Res. Commun., 88, 37 (1979).
12) F. Kuo and P. Greengard, J. Biol. Chem., 245, 4067 (1970); Y. Ogawa, Y. Takai, Y. Kawahara, S. Kimura, and Y. Nishizuka, J. Immunol., 127, 1369 (1981).
13) K. Weber and M. Osborn, J. Biol. Chem., 244, 4406 (1969).
14) R. A. Nemenoff, Y. C. Kwok, G. I. Shulman, P. J. Blackshear, R. Osathanondh, and J. Avruch, J. Biol. Chem., 259, 5058 (1984).
15) L. Jarett and J. R. Seals, Science, 206, 1407 (1979).
16) J. R. Seals and L. Jarett, Proc. Natl. Acad. Sci. USA, 77, 77 (1980); L. Jarett, F. L. Kiechle, D. A. Popp, N. Kotagal, and J. R. Gavin, III, Biochem. Biophys. Res. Commun., 96, 735 (1980); J. C. Parker, F. L. Kiechle, and L. Jarett, Arch. Biochem. Biophys., 215, 339 (1982).
17) R. E. Roth, D. J. Cassell, B. A. Maddux, and I. D. Goldfine, Biochem. Biophys. Res. Commun., 115, 245 (1983).
18) S. Tamura, T. A. Brown, J. H. Whipple, Y. Fujita-Yamaguchi, R. E. Dubler, K. Cheng, and J. Larner, J. Biol. Chem., 259, 6650 (1984).

(Received February 3, 1987)

Communications to the Editor

[Chem. Pharm. Bull. 35(4)1653—1655(1987)]

ALKALINE CLEAVAGE OF GINSENOSIDES

Yingjie Chen, Mitsuhiko Nose, and Yukio Ogihara*
Faculty of Pharmaceutical Sciences, Nagoya City University
Tanabe-dori, Mizuhoku, Nagoya 467, Japan

The genuine sapogenin 20(S)-protopanaxatriol (1) and its corresponding prosapogenin 20(S)-ginsenoside-Rh_1 (3) were prepared by direct treatment of the peracetate of 20(S)-ginsenoside-Rg_2 in an alcoholic alkaline solution. Two kinds of alkaline conditions were compared.

KEYWORDS--Ginsenosides; 20(S)-protopanaxatriol; 20(S)-ginsenoside-Rh_1; 20(S)-ginsenoside-Rg_2; 20(S)-ginsenoside-Re; glycosidic bond

Ginsenosides are very labile under acidic conditions. Ordinary acid hydrolysis of ginsenosides is always accompanied by many side reactions,[1,2] such as epimerization, hydroxylation and cyclization of the side chain of the sapogenins. Therefore, it is almost impossible to prepare the genuine sapogenins and their corresponding prosapogenins by acid hydrolysis of ginsenosides. The genuine sapogenins are obtained by the action of soil bacteria,[3,4] enzymes[5] and Smith's degradation,[6,7] but their yields are generally very poor. However this problem was easily resolved by using a new method described in a previous paper.[8] Recently we succeeded in preparing the genuine sapogenin 20(S)-protopanaxatriol and its corresponding prosapogenin 20(S)-ginsenoside-Rh_1 by direct treatment of the peracetate of 20(S)-ginsenoside-Rg_2 in alcoholic alkaline solutions.

A mixture of 20(S)-ginsenoside-Rg_2 and 20(R)-ginsenoside-Rg_2 (200 mg) was acetylated with acetic anhydride (5 ml) and pyridine (5 ml). The peracetates obtained were chromatographed on a column of silica gel with a mixture solvent of benzene and acetone (10:1) to give a peracetate of 20(R)-ginsenoside-Rg_2 and a peracetate of 20(S)-ginsenoside-Rg_2, respectively.[9] The latter was heated in spectroscopic butanol (10 ml) containing 0.5 g of sodium hydroxide at 80°C for 6 h to deacetylate and cleave the glycosidic bond in the same step. Then the reaction solution was moved into a separatory funnel and shaken with 20 ml of distilled water. The butanolic layer was washed three times with a little water, then chromatographed on a silica gel column with a solvent mixture of chloroform and methanol to give the genuine sapogenin 20(S)-protopanaxatriol (1) and its corresponding monoglucoside 20(S)-ginsenoside-Rh_1 (3).

Furthermore, 20(S)-ginsenoside-Re (7) was treated by method B (mentioned later) to afford pure 20(S)-protopanaxatriol (1), suggesting that no epimerization occurred at C-20 during the cleavage of the glycosidic bond.

Finally, in order to investigate the recovery of the cleavage products and compare the two kinds of alkaline condition, the mixture of 20(S)-ginsenoside-Rg_2 (5) and 20(R)-ginsenoside-Rg_2 (6) was used to perform the cleavage reaction as follows:

A) **Sodium metal method**- Sodium metal(1 g) was added to the solution of ginsenosides-Rg_2 (102 mg) in butanol (20 ml). The reaction was carried out at 80°C for 6 h. Then the reaction mixture was treated as described above to give genins (1 and 2) (18.5 mg), monoglucosides (3 and 4) (17.4 mg) and recovered ginsenosides-Rg_2 (5 and 6) (15 mg).

B) **Sodium hydroxide method**- One g of sodium hydroxide was added to the solution of ginsenosides-Rg_2 (107 mg) in butanol (20 ml) and then the reaction was carried out as described in method A to give the genuine sapogenins (1 and 2) (22.9 mg), monoglucosides (3 and 4) (23.0 mg) and recovered ginsenosides-Rg_2 (5 and 6) (4.0 mg).

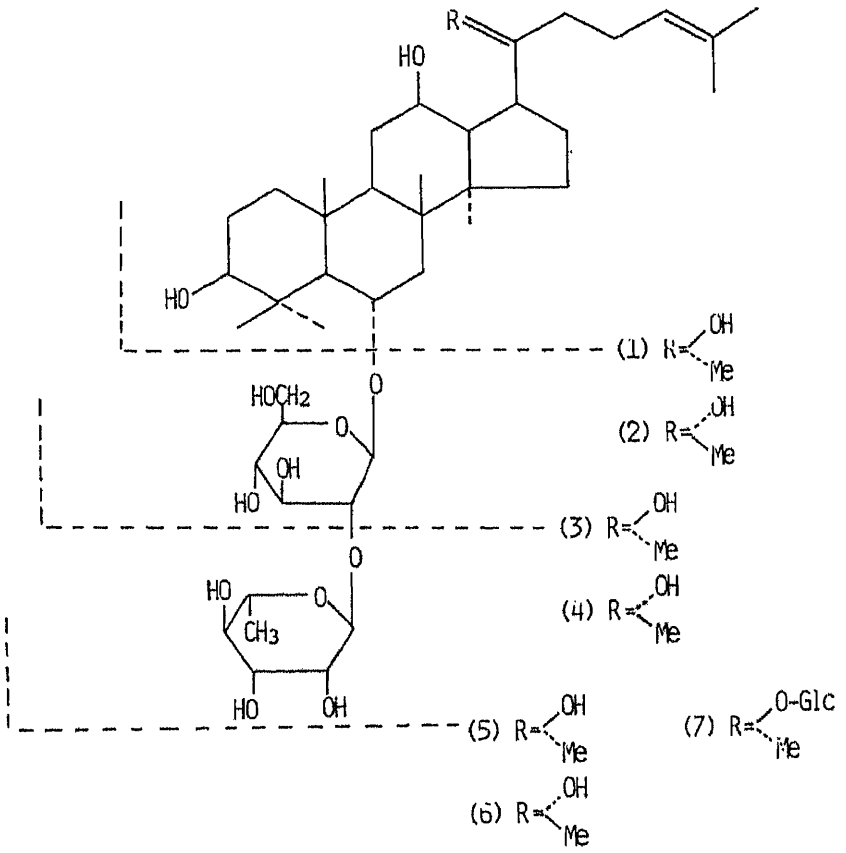

ACKNOWLEDGEMENTS We thank Professor O. Tanaka, University of Hiroshima, for his helpful suggestions and also for supplying us with precious samples.

REFERENCES

1) O. Tanaka, M. Nagai, T. Ohsawa, N. Tanaka, and S. Shibata, Chem. Pharm. Bull., 20, 1204 (1972).
2) B. H. Han, M. H. Park, Y. N. Han, L. K. Woo, U. Sankawa, S. Yahara, and O. Tanaka, Planta Medica, 44, 146 (1982).
3) I. Yoshioka, M. Fujio, M. Osamura, and I. Kitagawa, Tetrahedron Lettters, 1966, 6303.
4) I. Yoshioka, T. Sugawara, K. Imai, and I. Kitagawa, Chem. Pharm. Bull., 20, 2418 (1972).
5) H. Kohda, and O. Tanaka, Yakugaku Zasshi, 95, 246 (1975).
6) M. Nagai, T. Ando, N. Tanaka, O. Tanaka, and S. Shibata, Chem. Pharm. Bull., 20, 1212 (1972)
7) T. Ohsawa, N. Tanaka, O. Tanaka, and S. Shibata, Chem. Pharm. Bull., 20, 1890 (1972).
8) Y. Ogihara and M. Nose, Chemical communications, 1986, 1417.
9) I. Kitagawa, M. Yoshikawa, M. Yoshihara, T. Hayashi, and T. Taniyama, Yakugaku Zasshi, 103, 812 (1983).

(Received February 4, 1987)

Communications to the Editor

[Chem. Pharm. Bull. 35(4)1656—1659(1987)]

STRUCTURE OF SCUTERIVULACTONE D DETERMINED BY TWO-DIMENSIONAL NMR SPECTROSCOPY. A NEW DITERPENOID FROM A CHINESE CRUDE DRUG "BAN ZHI LIAN" (SCUTELLARIA RIVULARIS WALL.)

Haruhisa Kizu,[a] Yoshitaka Imoto,[a] Tsuyoshi Tomimori,*,[a] Koji Tsubono,[b] Shigetoshi Kadota[b] and Tohru Kikuchi*,[b]

School of Pharmacy, Hokuriku University,[a] 3 Ho, Kanagawa-machi, Kanazawa 920-11, Japan and Research Institute for Wakan-Yaku (Oriental Medicines), Toyama Medical and Pharmaceutical University,[b] 2630 Sugitani, Toyama 930-01, Japan

A new clerodane-type diterpenoid lactone, scuterivulactone D, has been isolated from the whole plants of Scutellaria rivularis Wall. and the structure has been determined by means of 2-D NMR spectroscopy including the ^{1}H-^{13}C long-range shift correlation spectrum.

KEYWORDS —— Ban Zhi Lian; Scutellaria rivularis; Labiatae; diterpenoid; clerodane; scuterivulactone D; 2-D NMR; ^{1}H-^{13}C long-range shift correlation spectrum

The ether extract from a Chinese crude drug "Ban Zhi Lian (半枝蓮)" (dried whole plants of Scutellaria rivularis Wall., Labiatae) was separated by silica gel column chromatography followed by repeated recrystallization to give five clerodane-type diterpenoid lactones, named scuterivulactone A, B, C_1 (2), C_2 (3) (isolated as the acetate) and D, together with fourteen flavonoid constituents. The structures of the flavonoid constituents and scuterivulactone C_1 (2) and C_2 (3) were reported.[1,2] This paper deals with the structure of scuterivulactone D.

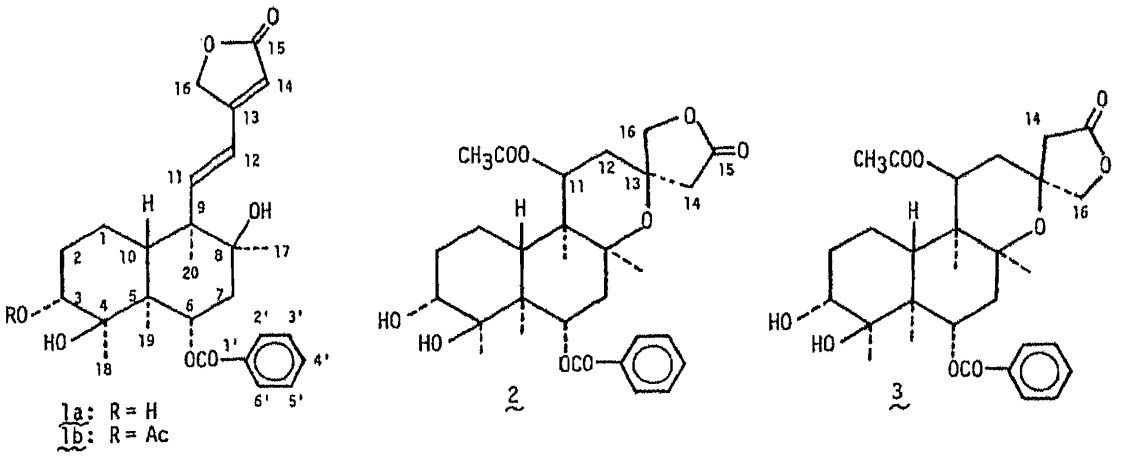

Chart 1

Scuterivulactone D (1a), $C_{27}H_{34}O_7$, was obtained as colorless needles (from acetone), mp 260 – 262°C, $[\alpha]_D^{26}$ + 57.5° (MeOH), UVλ_{max}^{MeOH}nm (log ε): 236.5 (4.30), 263 (4.44). The IR spectrum of 1a showed absorption bands at 3518 (OH), 1747 (lactone) and 1725 (sh) cm^{-1} (ester) and the EIMS exhibited the M^+ peak at m/z 470 and fragment ion peaks at m/z 452 ($M^+ - H_2O$), 434 ($M^+ - 2H_2O$), 416 ($M^+ - 3H_2O$), 348 ($M^+ - C_6H_5COOH$), 330 ($M^+ - H_2O - C_6H_5COOH$), 312 ($M^+ - 2H_2O - C_6H_5COOH$), 122 (C_6H_5COOH) and 105 (C_6H_5CO). The ^1H- and ^{13}C-NMR and ^1H-^1H COSY spectra[3] (in pyridine-d_5 and DMSO-d_6) suggested the presence of partial structures A, B and C (Fig. 1) in addition to two tert-hydroxy (δH 6.06 and 6.29) and four tert-methyl groups (δC 26.6, 25.9, 15.8 and 13.4; δH 1.30, 1.86, 1.26 and 1.94) and four quarternary carbons (δC 76.1, 74.8, 48.8 and 46.8). The ^1H-^1H COSY spectrum of 1a in pyridine-d_5 is shown in Fig. 2. Each carbon signal, except for quarternary one, was assigned based on the ^1H-^{13}C COSY spectral data.[3]

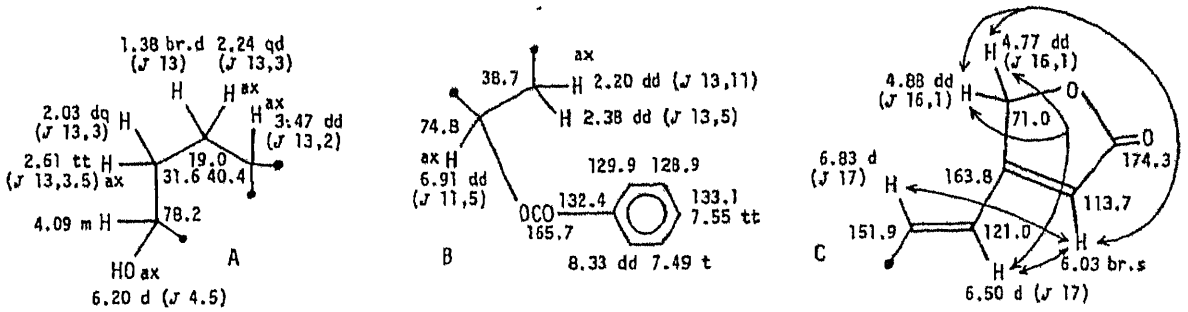

Fig. 1 Partial Structures in 1a (δ-Values in Pyridine-d_5)
(⌒ : Long-range Coupling in ^1H-^1H COSY)

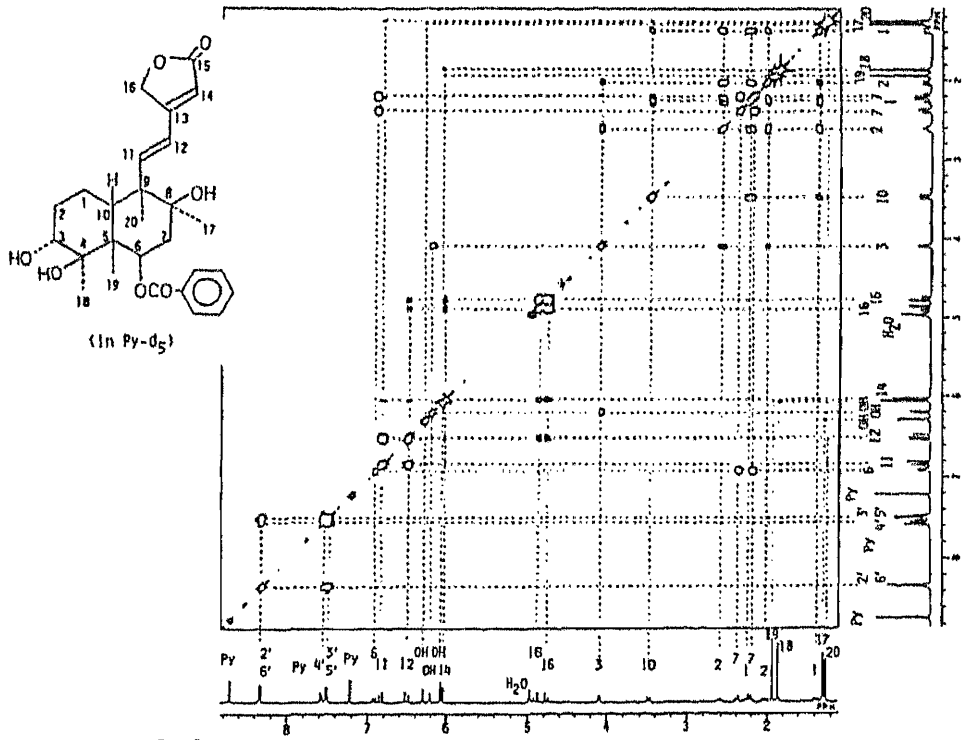

Fig. 2 ^1H-^1H Shift Correlation Spectrum of Scuterivulactone D (1a) in Pyridine-d_5

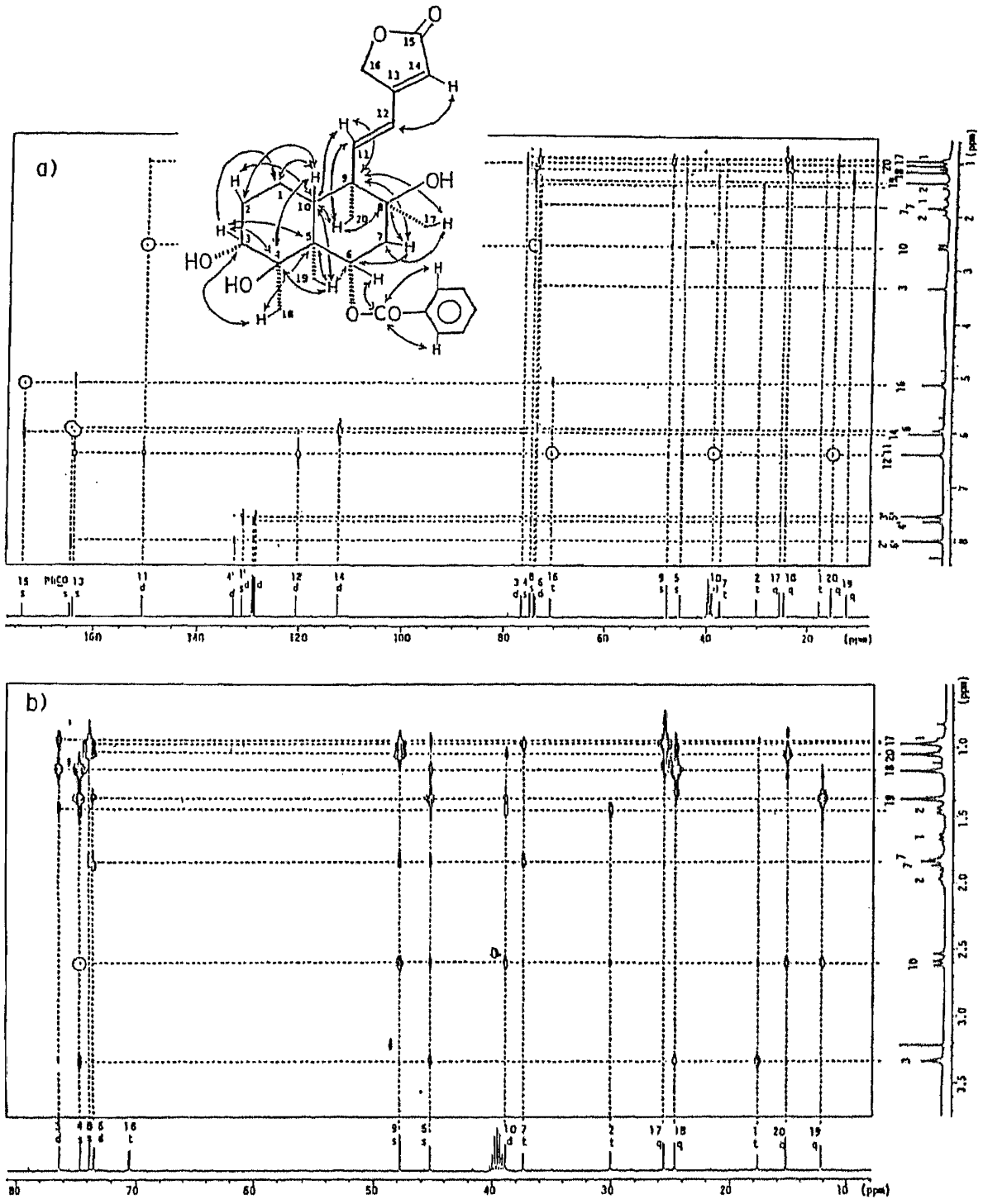

Fig. 3 ^{1}H-^{13}C Long-Range Shift Correlation Spectrum of Scuterivulactone D (1a) in DMSO-d_6: a) Whole Region, b) High Field Region (Sample: 80 mg, 40°C, J_{CH} = 12 Hz, 12 h run) Multiplicities of the carbon signals were determined by the off-resonance and DEPT methods and are indicated as s, d, t and q. Open circles indicate the correlation peaks, which are significant but weak at this threshold level.

Next, the ^{1}H-^{13}C long-range COSY spectrum of 1a was measured in order to clarify the connectivities of the partial structures and substituents groups. As shown in Fig. 3, the carbon atoms corresponding to the signals at δ 38.8 (10-C) and at δ 45.1 (5-C) are correlated with the protons corresponding to the signals at δ 1.04 (20-H_3), 1.39 (19-H_3), 1.43 (2-H) and 6.40 (11-H) and at δ 0.95 (1-H), 1.19 (18-H_3), 1.39 (19-H_3), 1.82 (7-H), 2.61 (10-H) and 3.34 (3-H), respectively. Similarly, quarternary carbons corresponding to the signals at δ 47.7 (9-C), 73.8 (8-C) and 74.6 (4-C) can be correlated with the protons indicated by arrows in the formula (Fig. 3). Also, some of significant ^{1}H-^{13}C long-range correlations observed are illustrated by arrows. These data show that the gross structure of this compound is represented by the formula 1a.

The relative stereochemistry of 1a was determined on the basis of the coupling constant of each proton and the results of NOE experiments (in benzene-d_6) using the 3-O-acetate (1b),[4] mp 242-244°C, $[\alpha]_D^{22}$ + 21.8° ($CHCl_3$), which was derived from 1a by the usual method. Irradiation at the 20-H_3 and 18-H_3 caused the increase of signal intensity of the 1α-, 7α (axial)-, 11 and 19-protons and the 3- and 19-protons, respectively, and irradiation at the 17-H_3 and 19-H_3 enhanced the signal intensity of the 7α- and 7β-protons and the 7α-, 18- and 20-protons, respectively.

On the basis of these findings, the structure of scuterivulactone D was determined to be as represented by the formula 1a. Absolute configurations of scuterivulactone C_1 (2), C_2 (3) and D (1a) and the structures of scuterivulactone A and B are currently under investigation.

ACKNOWLEDGEMENT This work was supported in part by a Grant-in-Aid for Scientific Research to T. K. and S. K. (No 61470147) from the Ministry of Education, Science and Culture, Japan.

REFERENCES AND A NOTE

1) T. Tomimori, Y. Miyaichi, Y. Imoto and H. Kizu, *Shoyakugaku Zasshi*, 38, 249 (1984); *Idem*, *Ibid.*, 40, 432 (1986).

2) T. Kikuchi, K. Tsubono, S. Kadota, H. Kizu, Y. Imoto and T. Tomimori, *Chem. Lett.*, submitted.

3) A. Bax, "Two-Dimensional NMR in Liquids," D. Reidel Publishing Co., Dordrecht, Holland, 1982; R. Benn and H. Gunther, *Angew. Chem.* Int. Ed. Engl., 22, 350 (1983).

4) 1b: ^{1}H-NMR ($CDCl_3$) δ: 1.09, 1.15, 1.20, 1.44 (each 3H, s, 20-, 17-, 18- and 19-H_3), 1.62 (1H, qd, J = 13, 3 Hz, 1α-H), 1.96 (1H, dd, J = 13, 5 Hz, 7β-H), 2.09 (3H, s, OAc), 2.10 (1H, dd, J = 13, 11 Hz, 7α-H), 4.72 (1H, m, 3-H), 6.37, 6.42 (each 1H, d, J = 17 Hz, 11- and 12-H), 5.98 (1H, dd, J = 11, 5 Hz, 6-H); ^{1}H-NMR (C_6D_6) δ: 0.83, 0.88, 1.25, 1.44 (each 3H, s, 20-, 17-, 18- and 19-H_3), 1.56 (1H, qd, J = 13, 3 Hz, 1α-H), 1.74 (3H, s, OAc), 1.80 (1H, dd, J = 13, 11 Hz, 7α-H), 1.94 (1H, dd, J = 13, 5 Hz, 7β-H), 4.91 (1H, m, 3-H), 5.91, 6.18 (each 1H, d, J = 17 Hz, 11- and 12-H), 6.23 (1H, dd, J = 11, 5 Hz, 6-H).

(Received February 5, 1987)

Communications to the Editor

[Chem. Pharm. Bull. 35(4)1660—1662(1987)]

An Antitumor Morphinane Alkaloid, Sinococuline, from Cocculus trilobus

Hideji Itokawa,*,[a] Shunji Tsuruoka,[a] Koichi Takeya,[a] Noboru Mori,[b] Toru Sonobe,[b] Seiji Kosemura[b] and Toshinori Hamanaka[b]

Tokyo College of Pharmacy,[a] Horinouchi 1432-1, Hachioji, 192-03 Tokyo, and Tobishi Pharmaceutical Co.,Ltd.,[b] Yurakucho 1, Chiyoda-ku, 100 Tokyo

An antitumor morphinane alkaloid named sinococuline was isolated from the MeOH extract of Cocculus trilobus. Its structure was determined by spectroscopic analysis.

KEYWORDS ——— Cocculus trilobus; Menispermaceae; antitumor substance; sinococuline; morphinane alkaloid; NMR spectrum

In the course of a continuing search for antitumor substances from plants,[1] a methanolic extract was prepared from Cocculus trilobus (Menispermaceae). It had a significant effect against Sarcoma 180 ascites in mice. This paper describes the isolation and structure of the active principle.

When an aqueous solution of the methanolic extract prepared from the stems and rhizomes of C. trilobus was partitioned successively with n-hexane and ethyl acetate, the anti-Sarcoma 180A effect, determined by the total packed cell volume method,[2] was concentrated in the aqueous-layer residue. The residue was subjected to Amberlite XAD-2 column chromatography eluting with H_2O-MeOH (10:0, 4:1, 1:1 and 0:10 successively). In the bioassay of each anti-Sarcoma 180A fraction in mice, the fraction eluted with H_2O exhibited strong antitumor activity. This active fraction was purified by preparative thin layer chromatography (TLC) on silica gel using a $CHCl_3$-Et_2NH (3:2) solvent system to give the alkaloid named sinococuline. This compound had the antitumor activity against Sarcoma 180A (40 mg/kg/d dose for 5 consecutive d, GR (growth ratio = T/C): 56% (+)) and P388 leukemia in mice[3] shown in Table I.

Table I Antitumor Effect of Sinococuline on P388 Leukemia

Dose (mg/kg)	Survival time (d, mean ± S.E.)	T/C (%)	BWC (g)
10	12.5 ± 0.48	154.6	+0.9
25	13.5 ± 0.34	167.0	+0.6
50	14.3 ± 0.49	177.0	-0.6
100	16.2 ± 1.92	200.0	-4.7

P388: 10^6 cells/0.1 ml, i.p., CDF1 mice (n=6).
Drug: i.p., d 1-5.

Sinococuline, amorphous powder, $[\alpha]_D^{26}$ -77° (c=0.1 in MeOH), UV λ_{max}^{EtOH}nm (ε): 234 (8000), 283 (2700) has the molecular formula $C_{18}H_{23}NO_5$ (high MS: Calcd. 333.3877, Found 333.3527) and gave a positive test for Dragendorff reagent.[4] The ^1H and

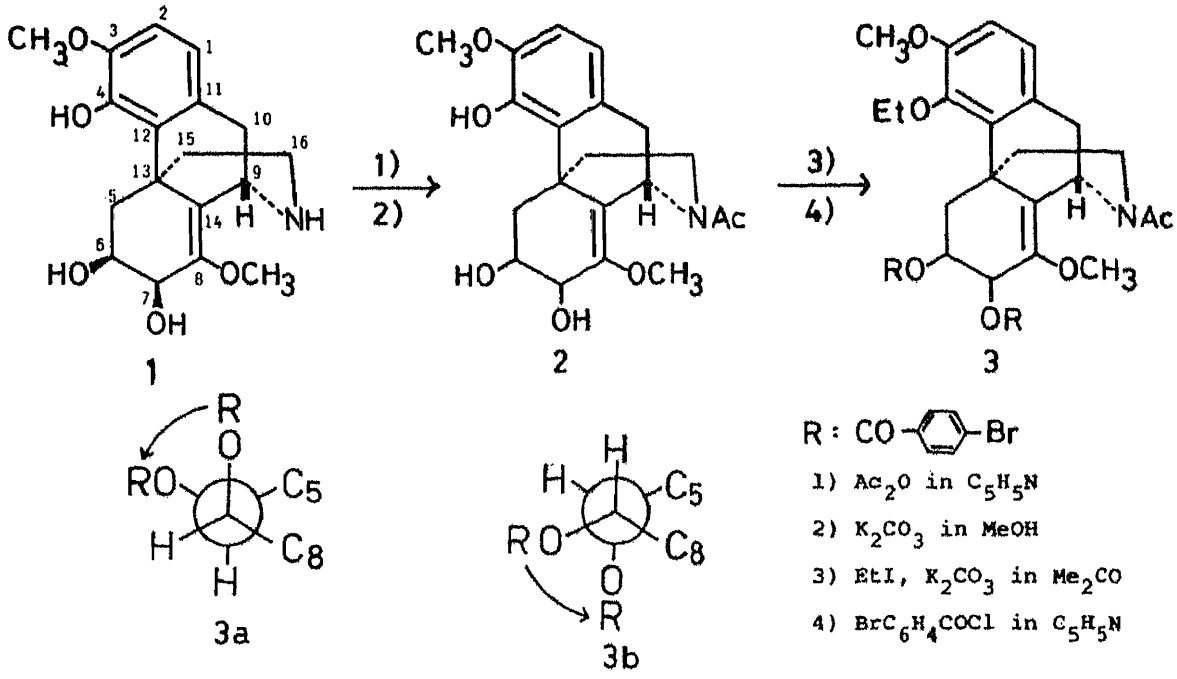

Chart 1

Table II ^{1}H and ^{13}C Chemical Shifts of Sinococuline from Cocculus trilobus

Carbon No.	^{1}H NMR	^{13}C NMR
1	6.53 (d, J=8.3Hz)	119.51(d)
2	6.75 (d, J=8.3Hz)	110.96(d)
3	-	147.61(s)*
4	-	145.72(s)
5	H 2.90 (dd, J=13.3, 3.7Hz) H 2.17 (dd, J=13.3, 13.3Hz)	36.78(t)
6	3.84 (ddd, J=13.3, 3.7, 3.5Hz)	68.57(d)
7	4.28 (d, J=3.5Hz)	66.47(d)
8	-	147.67(s)*
9	4.35 (d, J=6.1Hz)	47.15(d)
10	H 2.89 (d, J=17.7Hz) H 3.15 (dd, J=17.7, 6.1Hz)	36.09(t)
11	-	130.40(s)
12	-	121.47(s)
13	-	39.57(s)
14	-	129.95(s)
15	2.01 (dd, J=12.7, 3.4Hz) 1.88 (ddd, J=12.7, 12.5, 4.7Hz)	37.16(t)
16	2.63 (ddd, J=13.1, 12.5, 3.4Hz) 2.73 (dd, J=13.1, 4.7Hz)	41.00(t)
3-OCH_3	3.82 (3H, s)	56.95(q)
8-OCH_3	3.68 (3H, s)	57.26(q)

The measurements were made on a Bruker AM400 spectrometer in CD_3OD with TMS as an internal reference and are expressed as ppm. The assignments of* marks may be reversed.

^{13}C NMR spectral data are summarized in Table II. The NMR data indicated the presence of a 1,2,3,4-substituted benzene ring, a four-substituted double bond, vicinal two hydroxymethines, and two methoxyl groups. The ^{1}H-^{1}H COSY spectrum[5] revealed a proton sequence for H_1-H_2 on the benzene ring, $H_{5\alpha,\beta}$-H_6 (on the oxygen-containing carbon) -H_7 (on the oxygen-containing carbon), H_9 (on the carbon between olefinic carbon and nitrogen) -$H_{10\alpha,\beta}$ and H_{15}-H_{16} (on the nitrogen-containing carbon). Also, NOE appeared between 3-OCH_3 and H_2 (11%), H_1 and H_{10} (6%), H_6 and H_{15} at δ 1.88 (11%), H_7 and 8-OCH_3 (8%). Based on the above results, the structure of sinococuline was established as drawn in formula 1. It was supported by the ^{13}C chemical shifts which were assigned with ^{13}C-^{1}H COSY and DEPT techniques,[5,6] and by comparison with the ^{13}C NMR spectrum data of sinomenine.[7] Although the C_9 configuration of sinococuline was assumed to be S from the viewpoint of chemotaxonomy,[8] it was confirmed by measuring the CD spectrum (c= 9.67 x 10^{-5} in MeOH, $[\theta]^{26}$ (nm): +62100 (238), positive maximum).[9] Also, in order to determine the C_6 and C_7 configurations using the exciton chirality rule,[10] the 6,7-dibenzoate derivative[11] 3 of sinococuline was prepared as shown in Chart 1. The fact that the CD spectrum of 3 gave a negative Cotton effect (c= 3.56 x 10^{-5} in EtOH, $[\theta]^{24}$ (nm): -131900 (252), negative maximum) and the coupling constant between H_6 and H_7 was 3.5 Hz, suggested both structures 3a (6S, 7S) and 3b (6R, 7R) in Chart 1. However, the NOE between H_6 and H_{15} at δ 1.88 described above supported the structure 3a only. Consequently, both of the C_6 and C_7 configurations of sinococuline were determined to be S.

The only antitumor substance previously isolated from Cocculus plants is cocsulinine[12] which belongs to the group of bisbenzylisoquinoline alkaloids. So it is interesting that sinococuline, belonging to the morphinane alkaloids, showed antitumor activity against Sarcoma 180 ascites and P388 lymphocytic leukemia in mice.

ACKNOWLEDGEMENT We thank N.Okamura, T.Ogawa, M.Ohkoshi and K.Yamakawa of the Reasearch Laboratory of Tohbishi Pharmaceutical Co., Ltd., for their assistance. Part of this research was supported by Grants-Aid from the Ministry of Education, Science and Culture of Japan.

REFERENCES AND NOTES

1) H.Itokawa, K.Watanabe, K.Mihara and K.Takeya, Shoyakugaku Zasshi,36,145(1982).
2) A.Hoshi and K.Kuretani, Farmacia,9,464(1973).
3) R.J.Geran, N.J.Greenberg, M.M.MacDnald, A.M.Schumacher and B.J.Abbott, Cancer Chemother. Rep., Part 3,3,1(1972).
4) R.Munier, Bull. Soc. Chim. Biol.,35,1225(1953).
5) F.Inagaki and A.Abe, Yuki Gosei Kagaku Kyokai Shi,44,612(1986).
6) K.Hikichi, Kagaku Sosetsu, No.49, 17(1986).
7) Y.Terui, K.Tori, S.Maeda and Y.K.Sawa, Tetrahedron Letters,2853(1975).
8) "Alkaloidchemie" ed. by M.Hesse, Georg Thieme Verlag, Stuttgart (1978).
9) T.Kametani, M.Ihara and T.Honda, J.Chem.Soc.(C),1060(1970).
10) N.Harada and K.Nakanishi, Accounts of Chem. Res.,5,257(1972).
11) Amorphous powder ($C_{36}H_{35}NO_8Br_2$), MS m/z(%): 770(M^+,0.1), 183(100), UV λ_{max}^{EtOH}nm (ε): 243(38000), 280(3300), ^{1}H NMR δ_{ppm} in $CDCl_3$: 1.37(3H,t,J=7.0Hz), 2.06(3H, s), 3.61(3H,s), 3.85(3H,s), 4.01(2H,q,J=7.0Hz), 6.81(1H,d,J=8.3Hz), 6.84(1H, d,J=8.3Hz), 7.44, 7.53, 7.60 and 7.77(2H,d,J=8.3Hz,respectively).
12) M.Ikram, N.Shafi and M.A.Zarga, Planta Medica,45,253(1982).

(Received February 9, 1987)

Communications to the Editor

Chem. Pharm. Bull. 35(4)1663—1665(1987)

A CONVENIENT AND EFFICIENT METALLATION OF METHYLSILANE. CARBONYL METHYLENATIONS USING METALLATED (2-AMINOALKOXY)TRIMETHYLSILANE

Akira Hosomi,*[,a] Shinya Kohra,[a] Yoshinori Tominaga,[a]
Masataka Shoji,[b] and Hideki Sakurai[b]

Faculty of Pharmaceutical Sciences, Nagasaki University,[a] Nagasaki 852, Japan and Department of Chemistry, Tohoku University,[b] Sendai 980, Japan

When (2-aminoalkoxy)trimethylsilane is activated by two intramolecular heteroatoms (oxygen and nitrogen), it undergoes metallation efficiently with t-butyllithium to yield α-silyl carbanion. This process is applicable to carbonyl methylenations.

KEYWORDS —— lithiated methylsilane; α-silyl carbanion; (2-aminoalkoxy)trimethylsilane; Peterson reaction; alkene synthesis

α-Silyl carbanions are important reagents for carbonyl olefinations, well-known as the Peterson reaction.[1] Although the generation of α-silyl carbanions by way of direct deprotonation of organosilicon compounds with a base occurs when the substituent groups on the carbanion are capable of stabilizing the carbanion center, metallation of simple methylsilanes can not be satisfactorily attained even if tetramethylethylenediamine is employed as an activator of metallating base.[2] We report herein direct metallation of (2-aminoalkoxy)trimethylsilane (1) with t-butyllithium and its application to carbonyl methylenations. (Eq. 1) The results are presented in Table 1.

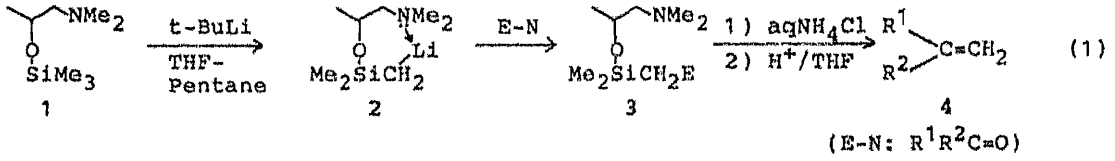

1 2 3 4 (1)

(E-N: $R^1R^2C{=}O$)

The requisite methylsilane (1),[3] prepared from readily available chlorotrimethylsilane and 1-dimethylamino-2-propanol, undergoes efficiently expeditious deprotonation with t-butyllithium, resulting in the formation of α-silyl carbanion (2) almost in quantitative yield. Thus 2 can be trapped with chlorotrimethylsilane to afford 3 (E = $SiMe_3$) in 95% yield. Moreover with benzaldehyde as an electrophile, 2-trimethylsilyl-1-phenylethanol (5) was isolated in 77% yield after treatment of 3 with methyllithium. Note that both heteroatoms, the oxygen and

Table I. Metallation of (1-dimethylamino-2-propoxy)trimethylsilane (1) with t-butyllithium[a] and subsequent reactions with electrophiles

Entry	Electrophile	Condition I[b]	Condition II[c]	Product	% Yield[d]
1	Me_3SiCl	A		$Me_2SiCH_2SiMe_3$, $OCHMeCH_2NMe_2$	95[e]
2	PhCHO	A		Me_3SiCH_2CHPh, OH[f] (5)	77
3	PhCHO	A	C	Ph, H, $C=CH_2$	75[e]
4	p-$MeOC_6H_4CHO$	A	C	p-$MeOC_6H_4$, H, $C=CH_2$	70
5	PhCOEt	A	D	Ph, Et, $C=CH_2$	100[g]
6	PhCO-i-Pr	A	D	Ph, i-Pr, $C=CH_2$	77
7	PhCOPh	A	D	Ph, Ph, $C=CH_2$	83
8	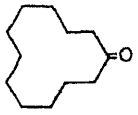	B	D	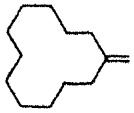	90[g]
9	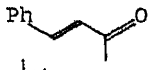	A	D	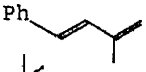	51
10	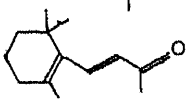	A	D	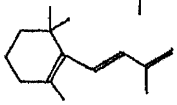	58

[a] Metallation of 1 was conducted as follows: To a solution of 1 (1 mmol) in THF (3 ml) at -78°C, t-BuLi (1.3 mmol) in pentane (1.6 M) was added from a syringe and the mixture was stirred at -78°C, -78-0°C and then 0°C for 1 h each. See also reference 5). [b] Conditions for the reaction with electrophiles. A: -78°C-rt, 3 h; B: -78°C-rt, 2h and 50°C, 1 h. [c] Conditions for hydrolysis with dilute H_2SO_4 in THF. C: rt, 1 h; D: rt, 10 h. [d] Yield after isolation by TLC. [e] Determined by GLC. [f] After treatment with MeLi at reflux for 3 h. [g] Yield based on the consumed ketone.

the oxygen and nitrogen atoms, of 1 play an important role in the prompt metallation with butyllithium. Apparently the oxygen atom participates in the increasing acidity of the methyl group due to the inductive effect, and the nitrogen atom not only activates the proton-abstracting base but also stabilizes the lithiated 2 due to chelation, since isopropoxytrimethylsilane and (3-dimethylaminopropyl)trimethylsilane, each of which contains a single heteroatom, are not metallated at all under analogous conditions. n- and s-Butyllithium prefer substitution on the silicon atom to metallation of 1.

The utility of 2 is illustrated by a series of representative carbonyl methylenations. Yields using this method are comparable to or better than reported procedures.[4] (Table 1) Thus this work demonstrates that 1 can be viewed

as a convenient and simple precursor of the α-silyl carbánion. This is applicable to carbonyl methylenations including unsaturated carbonyl compounds and further as a trimethylsilylmethyllithium equivalent. The utility of the present reaction lies mostly in the ready accessibility of the starting materials and simple manipulation of the conversion. We are currently exploring additional aspects of this class of reactions, including asymmetric induction using 2-aminoalkoxysilanes derived from optically active amino acid and stereo-controlled olefinations in the Peterson reaction. This may not actually be achieved.

Acknowledgment The work was supported in part by the Grant-in-Aids of the Ministry of Education, Japan, Yamada Science Foundation, Research Foundation of Pharmaceutical Sciences, and the Houan-sha.

REFERENCES AND NOTES

1) E. W. Colvin, "Silicon in Organic Synthesis," Butterworth, London (1981), Chap. 4 & 12; W. P. Weber, "Silicon Reagents for Organic Synthesis," Springer-Verlag, Berlin (1983), Chap. 6; D. J. Peterson, J. Org. Chem., **33**, 780 (1968); P. F. Hudrlik, J. Organomet. Chem. Library, 1, 127 (1976); T. H. Chan, Accounts Chem. Res., 10, 442 (1972); C. R. Johnson and B. D. Tait, J. Org. Chem., **52**, 281 (1987).

2) D. J. Peterson, J. Organomet. Chem., **9**, 373 (1967); R. West and G. A. Gornowicz, ibid., 28, 25 (1971).

3) 1-Dimethylamino-2-propanol (13.9 g, 0.135 mol) in ether (50 ml) was added to an ethereal solution (150 ml) of Me_3SiCl (14.6 g, 0.135 mol) and Et_3N (14.4 g, 0.142 mol) at room temperature. After stirring for 3 h at reflux, the salt was removed by filtration and the solvent was distilled. **1** (7.5 g. 0.100 mol) was obtained by distillation in 74% yield. bp 76-76.5°C (71 mmHg). Previously **1** was prepared by using $(Me_3Si)_2NH$ under more drastic conditions. See E. Lukevics and L. Liberts, Latv. PSR Zinat. Akad. Vestis, Khim. Ser., 1972, 203; C. A., 77, 75256m (1972).

4) D. E. Seitz and A. Zapata, Tetrahedron Lett., 21, 3451 (1980); T. H. Chan and E. Chang, J. Org. Chem., 39, 3264 (1974).

5) A typical experimental procedure is as follows: To a stirred solution of **1** (177 mg, 1.01 mmol) in THF (3 ml), t-butyllithium (1.34 mmol) in pentane was added slowly at -78°C. The resulting pale yellow mixture was stirred for 1 h at -78°C and warmed to 0°C during 2 h, then cooled again to -78°C . After the addition of benzophenone (170 mg, 0.93 mmol) in THF (1 ml), the reaction mixture was stirred for 3 h at -78°C-rt and hydrolyzed with saturated ammonium chloride (10 ml). Ether extraction (2 x 10 ml), drying over anhydrous magnesium sulfate and evaporation of the solvent, were conducted successively, and the residue was treated with concentrated H_2SO_4 (ca. 50 mg) in THF (2 ml) for 10 h at room temperature. After hydrolysis with saturated sodium hydrogen carbonate (10 ml), the organic layer was extracted with ether (2 x 10 ml) and the ethereal solution was dried over magnesium sulfate. The solvent was removed by evaporation and 1,1-diphenylethene (139 mg, 0.77 mmol) was isolated by preparative thin layer chromatography (TLC) using hexane as an eluent. R_f 0.90. ^{1}H-NMR (60 MHz, CCl_4) δ: 7.1-7.3 (10H, m, Ph), 5.33 (2H, s, CH_2).

(Received February 23, 1987)

Communications to the Editor

[Chem. Pharm. Bull. 35(4)1666—1669(1987)]

SYNTHESIS OF 5-FLUOROARACHIDONIC ACID AND ITS BIOTRANSFORMATION TO 5-FLUORO-12-HYDROXYEICOSATETRAENOIC ACID

Takeo Taguchi,[a] Tomoyuki Takigawa,[a] Azuma Igarashi,[a] Yoshiro Kobayashi,*[a] Yoko Tanaka,[b] William Jubiz,[b] and Robert G. Briggs[c]

Tokyo College of Pharmacy,[a] 1432-1 Horinouchi, Hachioji, Tokyo 192-03, Japan, Veterans Administration Medical Center and Department of Medicine, Albany Medical College,[b] Albany, NY 12208, USA, and Wadsworth Center for Laboratories and Research, New York State Department of Health,[c] Albany, NY 12201, USA

The synthesis of 5-fluoroarachidonic acid (1) was achieved from the intermediate (E)-5,6-dihydroxy-2-fluorohex-2-enoate 5,6-acetonide (5). Incubation of 1 with human platelets yielded 5-fluoro-12-hydroxyeicosatetraenoic acid (5F-12-HETE, 2).

KEYWORDS ——— arachidonic acid; fluoroarachidonic acid; hydroxyeicosatetraenoic acid; fluorohydroxyeicosatetraenoic acid; lipoxygenase; platelet

Incorporation of fluorine into biologically active molecules often yields compounds with enhanced, prolonged or selective activities, or with new physiological properties, probably due to the characteristics of fluorinated compounds.[1] Yet, fluorine, as the second smallest substituent, closely mimics hydrogen with respect to steric requirement at binding sites of enzymes or target tissues. Fluorinated analogs are useful tools for the pharmaco-physiological and pathophysiological studies of the natural compounds.

Eicosanoids display a wide diversity of pharmacological activities[2] and therefore study of these lipid mediators is one of the most active areas of clinical research. Although early studies of eicosanoids have been focused on cyclooxygenase products, lipoxygenase products are now emerging as topics of clinical interest. A significant number of fluorinated prostaglandins has been synthesized and many of them show increased metabolic stability or higher selectivity of action.[3] In contrast, synthesis of fluorinated lipoxygenase products has not been reported.

Biotransformation involves relatively simple techniques and short procedures, and generally, enzymic reaction proceeds in stereoselective manner. Therefore, we planned to prepare fluorinated lipoxygenase products by biotransformation of chemically synthesized fluorinated arachidonic acid. In addition to the products, this work will provide information on the effects of fluorine incorporation on enzymic reactions.

In this paper, we report the synthesis of 5-fluoro-5(E),8(Z),11(Z), 14(Z)-eicosatetraenoic acid (5F-AA, 1) and its biotransformation to 5-fluoro-12-hydroxyeicosatetraenoic acid (5F-12-HETE, 2).

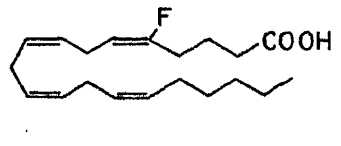

1, 5F-AA

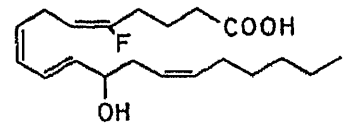

2, 5F-12-HETE

Chart 1

To synthesize fluorinated AAs including 1, ethyl (E)-5,6-dihydroxy-2-fluorohex-2-enoate 5,6-acetonide (5) obtained in high stereoselectivity was chosen as a key intermediate.

Treatment of the fluorophosphonoacetate (4)[4] with LDA in ether followed by the reaction with 3,4-dihydroxybutanal 3,4-acetonide (3)[5] (-78°C, 2 h) gave after chromatography the (E)-fluoroenoate [5, 80%; ^{1}H-nmr($CDCl_3$)δ 6.00 (dt, J=21 and 7.5 Hz, CH=CF), ^{19}F-nmr($CDCl_3$) δ -55.1 (d, J=21 Hz)][6] and the Z-isomer of 5[5%, ^{1}H-nmr ($CDCl_3$)δ 6.18 (dt, J=33 and 7.5 Hz, CH=CF), ^{19}F-nmr($CDCl_3$)δ -63 (d, J=33 Hz)]. Reduction of 5 with DIBAL-H (0.7 M hexane solution, Et_2O, -78°C, 30 min) gave the alcohol (6, 90%), which was converted to the bromide (7) by treating with butyllithium (THF, -78°C, 5 min), followed by the reaction with methanesulfonyl chloride in the presence of LiBr (THF, -78°C, 2 h) to give 7 [95%, ^{1}H-nmr($CDCl_3$)δ 5.30 (dt, J=18 and 7.5 Hz, CH=CF), ^{19}F-nmr($CDCl_3$) -36.5 (dt, J=18 and 22.5 Hz)].

The carbon chain extension reaction of the phosphate of 6 or the acetate of 6 with Grignard reagent [$BrMg(CH_2)_2CH$  , $CuBr\cdot Me_2S$][7] or lithium enolate of ethyl acetate with the bromide (7) in the presence of copper(I)[8] gave the undesired allylic rearranged products. Reaction of 7 with lithium salt derived from deprotonation of ethyl phenylthioacetate [LDA, Et_2O-HMPA (10:3), -78°C, 20 min] at room temperature for 1.5 h afforded the ester (8, 82%). Desulfurization of 8 with Raney-Ni (W-2) in acetone (9, 69%) and the subsequent reduction of 9 with DIBAL-H (Et_2O-hexane, -78°C, 1 h) afforded the alcohol (10, 93%). Conversion of the hydroxyl group to the ester group was achieved by mesylation (MsCl-Et_3N, CH_3Cl_2, -23°C), cyanation (KCN-18-crown-6, DMF, 50°C, 5 h), hydrolysis (NaOH, H_2O-MeOH, refl., 24 h then 10% HCl) followed by esterification (CH_2N_2, Et_2O) to give the methyl ester (11, 64%).

Deprotection of 11 (0.75 M HCl in 15:1 MeOH-H_2O, 1 h) gave the diol (12, 68%), which was cleaved to the corresponding β,γ-unsaturated aldehyde [1.4 equiv. $Pb(OAc)_4$, CH_2Cl_2, 10 min, -78°C].[9] This was allowed to react with the ylide derived from deprotonation of the phosphonium salt (14) [BuLi, THF-HMPA (8:1), -78°C][10] to give after chromatography methyl 5-fluoroarachidonate (15) in 24% yield. Hydrolysis of 15 [KOH, H_2O-MeOH-THF (1:4:4), r.t., 1 h] afforded 5F-AA (1) in 87% yield.[11]

Human platelets were incubated with 5F-AA (1) or AA in phosphate buffer in the presence of ionophore A23187 at 37°C for 20 min[12] followed by the reversed-phase HPLC of the extract. The reaction products from AA (Fig. 1,A) were compared with those from 5F-AA (Fig. 1,B). Compounds in (B) corresponding to those in (A) are probably non-fluorinated metabolites produced from endogenous AA released from cell membrane phospholipids[2] while peaks which appeared only in (B) are probably fluorinate compounds. The most abundant product derived from 5F-AA (Fig. 1,B, cross hatched peak) was collected, esterified (CH_2N_2) and chromatographed on a straight phase HPLC (Zorbax Sil column, Dupont; 1% 2-propanol in hexane).

UV absorption of the product showed an absorpsion maximum of 235 nm, character-

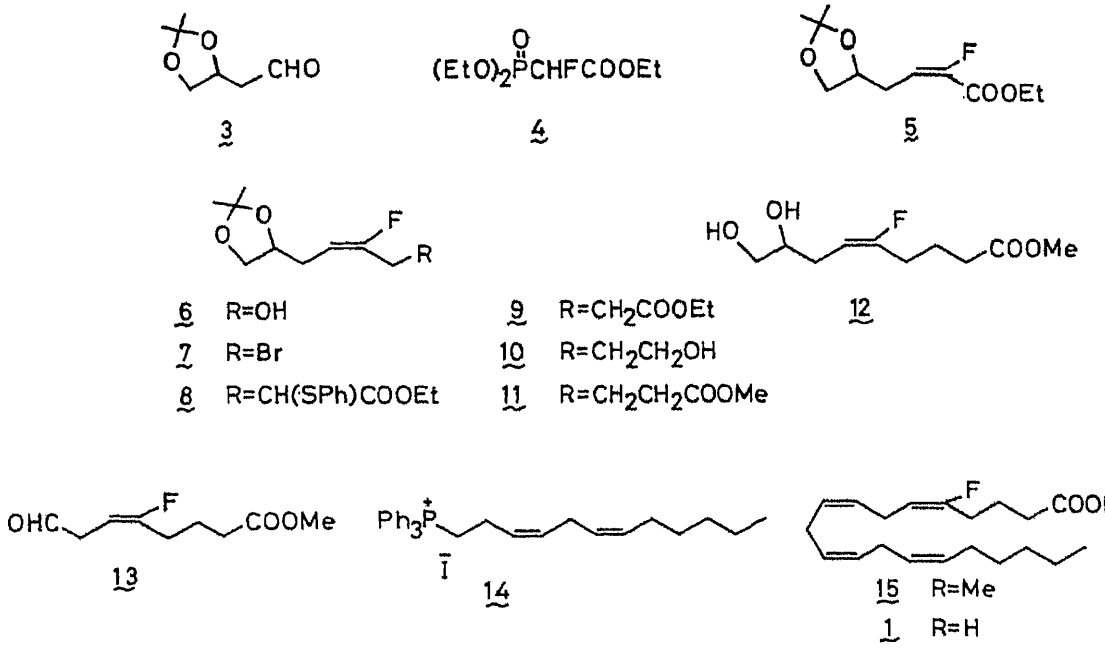

Chart 2

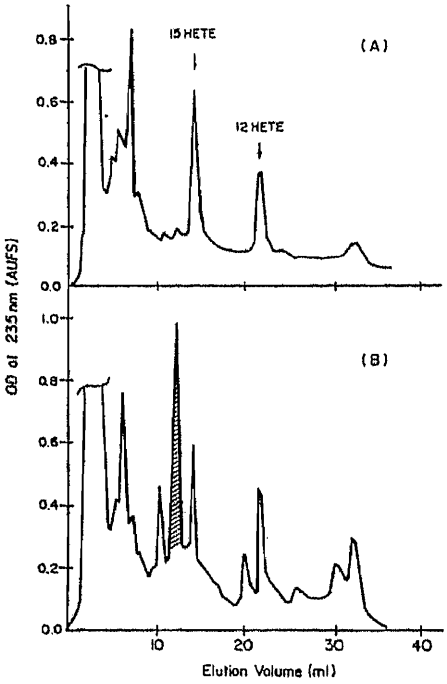

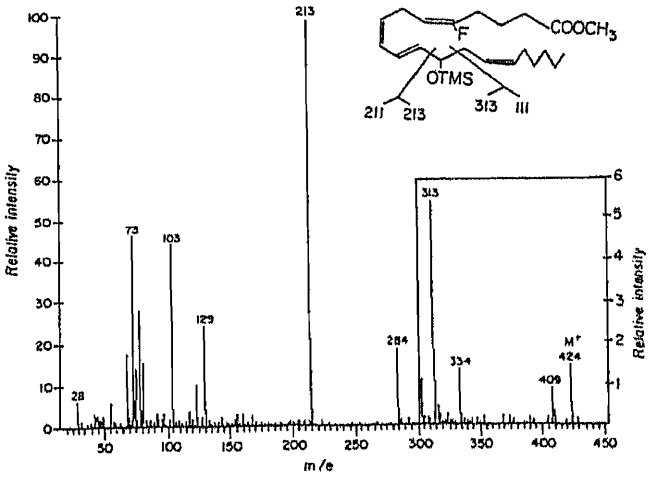

Figure 2. Mass Spectrum of the Product

Figure 1. RP-HPLC profiles of extracts of incubation media [(A) AA, (B) 5F-AA] chromatographed on a Zorbax ODS column (6.2 mm x 8 cm, Dupont) with MeOH/H_2O/acetic acid (75/25/0.01, v/v/v) at a flow rate of 2 ml/min produced by 2000 psi pressure. Arrows indicate elution position of authentic 15-HETE and 12-HETE (both purchased from Cayman Chemical, Ann Arbor, MI).

istic for HETE compounds.[13] A mass spectrum of the methylester trimethylsilylated with N,O-bis(trimethylsilyl)trifluoroacetamide showed ions at m/z 424 (M^+), 409 (M^+-15), 334 (M^+-90; loss of H+OTMS), 313 (M^+-111) and 213 (M^+-211; base peak)(Fig. 2). In comparison with that of natural 12-HETE, m/z 406 (M^+), 391 (M^+-15) and 295 (M^+-111),[13] this compound was identified as 5F-12-HETE (2). In this incubation about 11 μg of 2 was produced from 100 μg of 1. These data suggest that a significant amount of analog sufficient to perform preliminary biological assay can be produced by biotransformation.

Despite the fact that 12-HETE is the major product of AA by platelets,[13,14] its physiological significance has not been precisely defined. If a specific position of AA is substituted with fluorine(s) and incubated with platelets, 12-HETE fluorinated at the specific position can be produced. Such analogs represent new tools for investigating structure-activity relationships, and the metabolic and functional importance of natural 12-HETE.

Acknowledgements This work was supported by the Veterans Administration Medical Center, Albany, NY and in part by a grant-in aid from the Torey Foundation for the Promotion of Science and Technics. Authors thank Theresa M. Klauck and Vittoria Pascente-DiRe for their excellent technical assistances.

REFERENCES AND NOTES

1) R. Filler and S. M. Naqvi, "Biomedicinal Aspects of Fluorine Chemistry", ed. by R. Filler and Y. Kobayashi, Elsevier Biomedical Press, 1982, pp. 1-32.
2) A. J. Marcus, Am. J. Med., 78, 805(1985).
3) a) P. A. Grieco, W. Owens, C. Wang, E. Williams, and W. J. Schillinger, J. Med. Chem., 23, 1072(1980); b) J. Fried, D. K. Mitra, M. Nagarajan, and M. M. Mehrotra, ibid., 23, 234(1980); c) K. Bannai and S. Kurozumi, J. Synth. Org. Chem., Japan, 42, 794(1984).
4) a) H. Machleidt and G. Strehlke, Justus Liebigs Ann. Chem., 681, 21(1965); b) G. Etemad-Moghadam and J. Seyden-Penne, Bull. Soc. Chim. Fr., 448(1985).
5) K. Mori, T. Takigawa,and T. Matsuo, Tetrahedron, 35, 933(1979).
6) In ^{19}F-nmr, benzotrifluoride was used as an external standard.
7) J. A. Marshall and K. E. Flynm, J. Am. Chem. Soc., 105, 3360(1983).
8) I. Kuwajima and Y. Doi, Tetrahedron Lett., 1163(1973).
9) E. J. Corey and P. T. Lansbury, Jr., J. Am. Chem. Soc., 105, 4093(1983).
10) J. R. Pfister and D. V. Krishna Murthy, J. Med. Chem., 26, 1099(1983).
11) 1: ^{1}H-nmr (400 MHz; $CDCl_3$)δ 0.891 (3H, t, J=6.8 Hz, 20-H), 1.25-1.40 (6H, m, 17, 18 and 19-H), 1.868 (2H, quintet, J=7.3 Hz, 3-H), 2.055 (2H, q, J=7 Hz, 16-H), 2.328 (2H, dt, J=22.7 and 7.2 Hz, 4-H), 2.409 (2H, t, J=7.4 Hz, 2-H), 2.691 (2H, t, J=7.5 Hz), 2.807 (2H, t, J=6.4 Hz), 2.822 (2H, t, J=6.5 Hz), 5.065 (1H, dt, J=21.4 and 8 Hz, 6-H), 5.28-5.45 (6H, m, 8, 9, 11, 12 and 15-H).
12) W. F. Stenson, S. M. Precatt, and H. Spiecher, J. Biol. Chem., 259, 11784(1984).
13) M. Hamberg and B. Samuelsson, Proc. Natl. Acad. Sci. U.S.A., 71, 3400(1974).
14) P. Y. K. Wong, P. Westlund, M. Hamberg, E. Granström, P. H. W. Chao, and B. Samuelsson, J. Biol. Chem., 260, 9162(1985).

(Received February 24, 1987)

Communications to the Editor

[Chem. Pharm. Bull. 35(4)1670—1672(1987)]

THE STRUCTURES OF FOUR NEW DITERPENE ALKALOIDS, SPIRAMINES A, B, C, AND D

Xiaojiang Hao,[a] Manabu Node,[a] Tooru Taga,[b] Yoshihisa Miwa,[b]
Jun Zhou,[c] Siying Chen,[c] Kaoru Fuji*[a]

Institute for Chemical Research, Kyoto University,[a] Uji, Kyoto 611, Japan,
Faculty of Pharmaceutical Sciences, Kyoto University,[b] Kyoto 606, Japan, and
Kunming Institute of Botany, Academia Sinica,[c] Kunming, Yunnan, China

The structures of four new isoatisine-type alkaloids, spiramines A, B, C, and D, isolated from Spiraea japonica L. fil var acuminata Franch, were determined.

KEYWORDS—Spiraea japonica; spiramine A; spiramine B; spiramine C; spiramine D; X-ray analysis; diterpene alkaloid

Isomerization of the oxazolidine ring of atisine (1) into isoatisine (2) via immonium salt is well known and has been studied extensively.[1] Although the existence of epimeric mixtures at C-20 in the atisine series and at C-19 in the isoatisine series has been demonstrated by ^1H and ^{13}C NMR studies,[2,3] no epimeric pair has ever been isolated in pure form. Here we report the structures of the isoatisine-type alkaloids spiramine A (3), B (4), C (5) and D (6) isolated from Spiraea japonica L. fil var acuminata Franch, the former two and the latter two of which are epimeric at C-19, respectively.

The basic skeleton of spiramine A (3),[4] $C_{24}H_{33}NO_4$, mp 137.5 - 139°C (from hexane), $[\alpha]_D^{25}$ -103.1° (c 0.9, benzene), was established by comparing its ^{13}C NMR shift values (Table I) with the literature data.[6] Hydrolysis of spiramine A (3) afforded an approximately 2:1 mixture of spiramine C (5), $C_{22}H_{31}NO_3$, mp 167 - 169°C (from Et_2O), $[\alpha]_D^{25}$ -149.9° (c 1.0, benzene) and spiramine D (6), $C_{22}H_{31}NO_3$, mp 160 - 162°C (from Et_2O), $[\alpha]_D^{25}$ -169.0° (c 0.7, benzene), which are epimeric at C-19. Spiramine A (3) has an isoatisine-type oxazolidine ring [^1H NMR (C_6D_6): δ 3.87 (1H, s, H-19), 3.01, 3.24, 3.37, 3.81 (each 1H, m, H-21 x 2, H-22 x 2); ^{13}C NMR ($CDCl_3$): δ 51.0 (t, C-21), 63.1 (t, C-22), 95.2 (d, C-19)], an ether linkage between C-7 and C-20 [^1H NMR 3.54 (1H, d, J 5Hz, H-7), 4.47 (1H, d, J 1.8 Hz, H-20); ^{13}C NMR 74.2 (d, C-7), 85.8 (d, C-20)], a secondary acetoxy-group [ν(KBr) 1708 cm^{-1}; ^1H NMR 1.65 (3H, s), 5.46 (1H, br.s); ^{13}C NMR 20.4 (q), 170.9 (s), 69.2 (d)], and an exo methylene group [^1H NMR 5.04, 5.30 (each 1H, br. s); ^{13}C NMR 114.2 (t, C-17), 150.1 (s, C-16)]. On irradiation at 5.46, both of the signals at 5.04 and 5.30 were changed to a doublet with J = 1.8 Hz, demonstrating the location of the secondary acetoxy-group on C-15.

Reduction of spiramine A (3) with sodium borohydride afforded a triol (7), which was not identical with dihydroajaconine (8).[7] Oxidation of spiramine C (5) with manganese dioxide followed by reduction with sodium borohydride in methanol gave a triol, which was identified as dihydroajaconine (8) by spectroscopic analysis including optical rotation $[\alpha]_D^{19}$ -36.6° (c 1.2, EtOH); lit.[7]: $[\alpha]_D^{24}$ -35.5° (c 1.0, EtOH). Except for the stereochemistry at C-19, this confirmed 3 as the absolute structure for spiramine A. Three-dimensional single-crystal X-ray analysis (Fig. 1) provided the total structure for spiramine A (3) including the stereochemistry of the oxazolidine ring.[8]

Table I. ^{13}C Chemical Shifts for Spiramines A(3), B(4), C(5), and D(6).

Carbon	Spiramines A[a]	B[a]	C[a]	D[b]
1(t)	41.0	33.9	40.8	34.2
2(t)	22.9	22.9	23.0	23.0
3(t)	29.8	29.8	29.9	30.0
4(s)	35.4[c]	35.4[c]	35.4[c]	35.6[c]
5(d)	45.2	47.4	45.5	47.3
6(t)	25.2	25.3	25.2	25.5
7(d)	74.2	74.3	74.3	74.5
8(s)	40.8	41.0	41.5	41.9
9(d)	43.0	43.9	43.1	44.3
10(s)	34.2[c]	34.9[c]	34.1[c]	34.2[c]
11(t)	23.5	23.1	23.5	23.1
12(d)	36.7	36.4	37.0	37.6
13(t)	21.1[d]	21.2[d]	19.9[d]	21.3[d]
14(t)	20.9[d]	20.8[d]	20.4[d]	20.4[d]
15(d)	69.2	69.7	69.0	69.6
16(s)	150.1	150.1	155.3	156.2
17(t)	114.2	114.3	112.0	111.6
18(q)	26.0	25.9	26.4	26.9
19(d)	95.2	91.3	95.3	91.5
20(d)	85.8	83.5	85.9	83.6
21(t)	51.0	45.7	51.0	45.7
22(t)	63.1	64.9	63.1	64.9
O=C	170.9	171.1		
CH_3	20.4	20.8		

[a] In $CDCl_3$. [b] In C_6D_6. [c,d] These assignments may be interchanged in any vertical column.

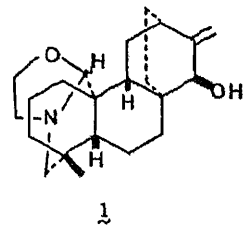

1

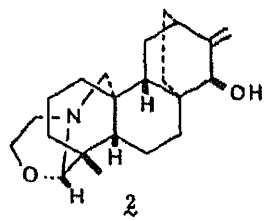

2

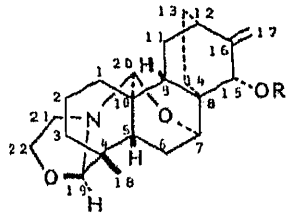

3, R=Ac
5, R=H

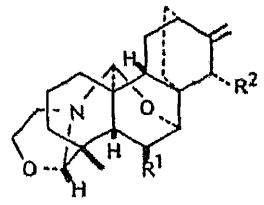

4, R^1=H, R^2=OAc
6, R^1=H, R^2=OH
9, R^1=OAc, R^2=H
10, R^1=OH, R^2=H

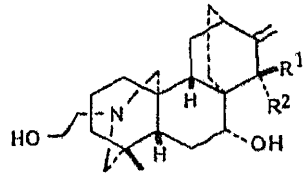

7, R^1=H, R^2=OH
8, R^1=OH, R^2=H

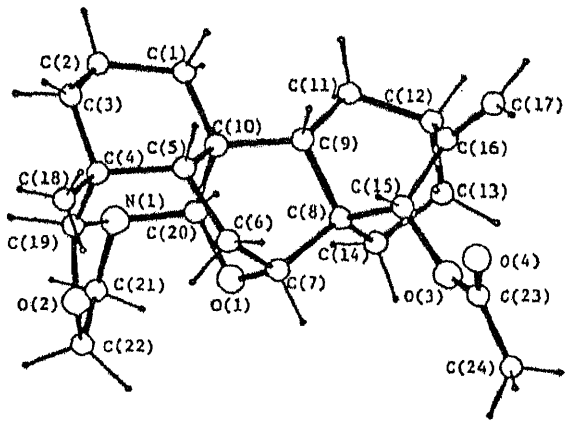

Fig. 1. The Molecular Structure of Spiramine A (3).

Spiramine B (4) $C_{24}H_{33}NO_4$, mp 129 - 131°C (from hexane), $[\alpha]_D^{25}$ -159.5° (c 0.9, benzene), epimerized at C-19 in polar solvents such as methanol to give a pair of C-19 epimers, spiramine A and B, in an approximate ratio of 1:1. Thus, structure 4 was assigned to spiramine B. A close inspection of ^{13}C chemical shifts (Table I) for the carbons of the oxazolidine ring in spiramines clearly revealed that the stereochemistries at C-19 of spiramines C and D correspond to spiramines A (3) and B (4), respectively. This suggests the structure 5 for spiramine C and 6 for spiramine D.

Two closely related alkaloids, spiradines F (9) and G (10) have been isolated from Spiraea japonica L. fil.[9] However, the corresponding epimers at C-19 have not been reported.

REFERENCES AND NOTES

1) S.M. Pelletier and N.V. Mody, "The Alkaloids," Vol. 18, ed. by R.G.A. Rodrigo, Academic Press, New York, 1981, p. 99.

2) S.W. Pelletier, N.V. Mody, H.K. Desai, J. Finer-Moore, J. Nowacki, and B.S. Joshi, J. Org. Chem., 48, 1787 (1983).

3) F. Sun, X. Liang, and D. Yu, Heterocycles, 26, 19 (1987).

4) A slight modification of dry-column flash chromatography[5] was used to isolate pure alkaloids. Thus, Kieselgel 60H (Merck) (8 g) was packed under reduced pressure in a glass filter 3 cm in diameter and 4.3 cm in height. A mixture (460 mg) of spiramine A and B in methylene chloride (1 ml) was adsorbed and elution with n-hexane-ether (3:1) afforded spiramine A (211 mg) first and then spiramine B (56 mg). This process requires about 30 min.

5) L. M. Harwood, Aldrichimica Acta, 18, 25 (1985).

6) N.V. Mody and S.W. Pelletier, Tetrahedron, 34, 2421 (1978).

7) S.W. Pelletier, R.S. Sawhney, and N. V. Mody, Heterocycles, 9, 1241 (1978).

8) Crystal data: $C_{24}H_{33}NO_4$, orthorhombic, a = 10.341 (3), b = 12.718 (7), c = 16.043 (4) Å. U = 2110 Å^3, space group $P2_12_12_1$, Z = 4, M = 399.5, D_c = 1.26 g cm^{-3}. Some 1719 independently observed reflections [$|F_o| > 3\sigma(|F_o|)$, $\theta \leq 60°$] were measured on a Rigaku AFC-5RU diffractometer (Cu-K_α radiation, graphite monochromator) using ω-2θ scans. The structure was solved by direct methods and the non-hydrogen atoms refined anisotropically to R = 0.056, R_w = 0.083. All the hydrogen atoms were located from a ΔF map and refined isotropically. The atomic co-ordinates for this work are available on request from the Director of the Cambridge Crystallographic Data Centre, University Chemical Laboratory, Lensfield Road, Cambridge, CB2 1EW.

9) M. Toda and Y. Hirata, Tetrahedron Lett., 5565 (1968).

(Received March 2, 1987)